

Inborn errors of carbohydrate metabolism

Edited by

Ivan Martinez Duncker, Ida Vanessa Doederlein Schwartz
and Jose Elias Garcia-Ortiz

Coordinated by

Melania Abreu-González

Published in

Frontiers in Genetics
Frontiers in Pediatrics
Frontiers in Pharmacology



FRONTIERS EBOOK COPYRIGHT STATEMENT

The copyright in the text of individual articles in this ebook is the property of their respective authors or their respective institutions or funders. The copyright in graphics and images within each article may be subject to copyright of other parties. In both cases this is subject to a license granted to Frontiers.

The compilation of articles constituting this ebook is the property of Frontiers.

Each article within this ebook, and the ebook itself, are published under the most recent version of the Creative Commons CC-BY licence. The version current at the date of publication of this ebook is CC-BY 4.0. If the CC-BY licence is updated, the licence granted by Frontiers is automatically updated to the new version.

When exercising any right under the CC-BY licence, Frontiers must be attributed as the original publisher of the article or ebook, as applicable.

Authors have the responsibility of ensuring that any graphics or other materials which are the property of others may be included in the CC-BY licence, but this should be checked before relying on the CC-BY licence to reproduce those materials. Any copyright notices relating to those materials must be complied with.

Copyright and source acknowledgement notices may not be removed and must be displayed in any copy, derivative work or partial copy which includes the elements in question.

All copyright, and all rights therein, are protected by national and international copyright laws. The above represents a summary only. For further information please read Frontiers' Conditions for Website Use and Copyright Statement, and the applicable CC-BY licence.

ISSN 1664-8714
ISBN 978-2-8325-5097-7
DOI 10.3389/978-2-8325-5097-7

About Frontiers

Frontiers is more than just an open access publisher of scholarly articles: it is a pioneering approach to the world of academia, radically improving the way scholarly research is managed. The grand vision of Frontiers is a world where all people have an equal opportunity to seek, share and generate knowledge. Frontiers provides immediate and permanent online open access to all its publications, but this alone is not enough to realize our grand goals.

Frontiers journal series

The Frontiers journal series is a multi-tier and interdisciplinary set of open-access, online journals, promising a paradigm shift from the current review, selection and dissemination processes in academic publishing. All Frontiers journals are driven by researchers for researchers; therefore, they constitute a service to the scholarly community. At the same time, the *Frontiers journal series* operates on a revolutionary invention, the tiered publishing system, initially addressing specific communities of scholars, and gradually climbing up to broader public understanding, thus serving the interests of the lay society, too.

Dedication to quality

Each Frontiers article is a landmark of the highest quality, thanks to genuinely collaborative interactions between authors and review editors, who include some of the world's best academicians. Research must be certified by peers before entering a stream of knowledge that may eventually reach the public - and shape society; therefore, Frontiers only applies the most rigorous and unbiased reviews. Frontiers revolutionizes research publishing by freely delivering the most outstanding research, evaluated with no bias from both the academic and social point of view. By applying the most advanced information technologies, Frontiers is catapulting scholarly publishing into a new generation.

What are Frontiers Research Topics?

Frontiers Research Topics are very popular trademarks of the *Frontiers journals series*: they are collections of at least ten articles, all centered on a particular subject. With their unique mix of varied contributions from Original Research to Review Articles, Frontiers Research Topics unify the most influential researchers, the latest key findings and historical advances in a hot research area.

Find out more on how to host your own Frontiers Research Topic or contribute to one as an author by contacting the Frontiers editorial office: frontiersin.org/about/contact

Inborn errors of carbohydrate metabolism

Topic editors

Ivan Martinez Duncker — Universidad Autónoma del Estado de Morelos, Mexico
Ida Vanessa Doederlein Schwartz — Federal University of Rio Grande do Sul, Brazil
Jose Elias Garcia-Ortiz — Centro de Investigación Biomédica de Occidente (CIBO), Mexico

Topic coordinator

Melania Abreu-González — Genos Medica, Mexico

Citation

Martinez Duncker, I., Doederlein Schwartz, I. V., Garcia-Ortiz, J. E.,
Abreu-González, M., eds. (2024). *Inborn errors of carbohydrate metabolism*.
Lausanne: Frontiers Media SA. doi: 10.3389/978-2-8325-5097-7

Dr. Abreu is the founder of Genos Medica, and Dr. Elias received financial support from Sanofi Mexico. All other Topic Editors declare no competing interests with regards to the Research Topic subject.

Table of contents

- 05 **Editorial: Inborn errors of carbohydrate metabolism**
Iván Martínez-Duncker, Ida Vanessa Doederlein-Schwartz, Melania Abreu-González and José Elías García-Ortiz
- 09 **Case report: Functional characterization of a *de novo* c.145G>A p.Val49Met pathogenic variant in a case of PIGA-CDG with megacolon**
Roberta Salinas-Marín, Yoshiko Murakami, Carlos Alberto González-Domínguez, Mario Ernesto Cruz-Muñoz, Héctor Manuel Mora-Montes, Eva Morava, Taroh Kinoshita, Susana Monroy-Santoyo and Iván Martínez-Duncker
- 16 **Case Report: The novel hemizygous mutation in the *SSR4* gene caused congenital disorder of glycosylation type iy: A case study and literature review**
Jun Wang, Xingqing Gou, Xiyi Wang, Jing Zhang, Nan Zhao and Xiaohong Wang
- 25 **Phenotypic and genetic characteristics of 130 patients with mucopolysaccharidosis type II: A single-center retrospective study in China**
Zhenjie Zhang, Mingsheng Ma, Weimin Zhang, Yu Zhou, Fengxia Yao, Lisi Zhu, Min Wei and Zhengqing Qiu
- 34 **Expanding the phenotype and metabolic basis of ATP6AP2-congenital disorder of glycosylation in a Chinese patient with a novel variant c.185G>A (p.Gly62Glu)**
Yuan Fang, Yi-Zhen Wang, Lian Chen and Xin-Bao Xie
- 46 **Molecular characterization of novel and rare DNA variants in patients with galactosemia**
Vasileios Maroulis, Andreas Agathangelidis, Anastasia Skouma, Triantafyllia Sdogou, Manoussos N. Papadakis, Evangelos Papakonstantinou, Panagiotis Girginoudis, Constantinos E. Vorgias, Vassiliki Aleporou and Panagoula Kolli
- 59 **Case report: Expanding the understanding of the adult polyglucosan body disease continuum: novel presentations, diagnostic pitfalls, and clinical pearls**
Matthew M. Gayed, Paulo Sgobbi, Wladimir Bocca Viera De Rezende Pinto, Priya S. Kishnani and Rebecca L. Koch
- 71 **An analysis of Pompe newborn screening data: a new prevalence at birth, insight and discussion**
Ryan Colburn and David Lapidus
- 87 **Identification of gene mutations associated with type 1 diabetes by next-generation sequencing in affected Palestinian families**
Abrar Bawatneh, Alaa Darwish, Hasan Eideh and Hisham M. Darwish

- 99 **Real-world outcomes from a series of patients with late onset Pompe disease who switched from alglucosidase alfa to avalglucosidase alfa**
Chris Carter, Tracy Boggs, Laura E. Case and Priya Kishnani
- 114 **Exploring the efficacy and safety of Ambroxol in Gaucher disease: an overview of clinical studies**
Fedaa E. Mohamed and Fatma Al-Jasmi
- 127 **Brain function in classic galactosemia, a galactosemia network (GalNet) members review**
Bianca Panis, E. Naomi Vos, Ivo Barić, Annet M. Bosch, Martijn C. G. J. Brouwers, Alberto Burlina, David Cassiman, David J. Coman, María L. Couce, Anibh M. Das, Didem Demirbas, Aurélie Empain, Matthias Gautschi, Olga Grafakou, Stephanie Grunewald, Sandra D. K. Kingma, Ina Knerr, Elisa Leão-Teles, Dorothea Möslinger, Elaine Murphy, Katrin Őunap, Adriana Pané, Sabrina Paci, Rossella Parini, Isabel A. Rivera, Sabine Scholl-Bürgi, Ida V. D. Schwartz, Triantafyllia Sdogou, Loai A. Shakerdi, Anastasia Skouma, Karolina M. Stepień, Eileen P. Treacy, Susan Waisbren, Gerard T. Berry and M. Estela Rubio-Gozalbo
- 138 **Efficacy and safety of enzyme replacement therapy with alglucosidase alfa for the treatment of patients with infantile-onset Pompe disease: a systematic review and meta-analysis**
A. D. Dornelles, A. P. P. Junges, B. Krug, C. Gonçalves, H. A. de Oliveira Junior and I. V. D. Schwartz
- 149 **Importance of genetic sequencing studies in managing chronic neonatal diarrhea: a case report of a novel variant in the glucose–galactose transporter SLC5A1**
Lizbeth López-Mejía, Sara Guillén-Lopez, Marcela Vela-Amieva, Rosalía Santillán-Martínez, Melania Abreu, María Dolores González-Herrera, Rubicel Díaz-Martínez and Juan Gaspar Reyes-Magaña
- 157 **Case report: Novel genotype of ALG2-CDG and confirmation of the heptasaccharide glycan (NeuAc-Gal-GlcNAc-Man2-GlcNAc2) as a specific diagnostic biomarker**
Ivan Martínez Duncker, Denisse Mata-Salgado, Ibrahim Shammas, Wasantha Ranatunga, Earnest James Paul Daniel, Mario E. Cruz Muñoz, Melania Abreu, Héctor Mora-Montes, Miao He, Eva Morava and Gildardo Zafra de la Rosa



OPEN ACCESS

EDITED AND REVIEWED BY

Alpo Juhani Vuorio,
University of Helsinki, Finland

*CORRESPONDENCE

Iván Martínez-Duncker,
✉ duncker@uaem.mx
José Elías García-Ortiz,
✉ jose.garciaor@imss.gob.mx

RECEIVED 09 May 2024

ACCEPTED 28 May 2024

PUBLISHED 20 June 2024

CITATION

Martínez-Duncker I, Doederlein-Schwartz IV,
Abreu-González M and García-Ortiz JE (2024),
Editorial: Inborn errors of
carbohydrate metabolism.
Front. Genet. 15:1430414.
doi: 10.3389/fgene.2024.1430414

COPYRIGHT

© 2024 Martínez-Duncker, Doederlein-Schwartz,
Abreu-González and García-Ortiz.
This is an open-access article distributed under
the terms of the [Creative Commons Attribution
License \(CC BY\)](#). The use, distribution or
reproduction in other forums is permitted,
provided the original author(s) and the
copyright owner(s) are credited and that the
original publication in this journal is cited, in
accordance with accepted academic practice.
No use, distribution or reproduction is
permitted which does not comply with these
terms.

Editorial: Inborn errors of carbohydrate metabolism

Iván Martínez-Duncker^{1*}, Ida Vanessa Doederlein-Schwartz²,
Melania Abreu-González³ and José Elías García-Ortiz^{4*}

¹Laboratorio de Glicobiología Humana y Diagnóstico Molecular, Centro de Investigación en Dinámica Celular, Instituto de Investigación en Ciencias Básicas y Aplicadas, Universidad Autónoma del Estado de Morelos, Cuernavaca, Mexico, ²Department of genetics, Universidade Federal do Rio Grande do Sul (UFRGS), Porto Alegre, Brazil, ³Genos Médica Centro Especializado en Genética, México. Centro Médico ABC, Mexico City, Mexico, ⁴División de Genética, Centro de Investigación Biomédica de Occidente, Centro Médico Nacional de Occidente-Instituto Mexicano del Seguro Social (CMNO-IMSS), Guadalajara, Mexico

KEYWORDS

CDG (congenital disorder of glycosylation), lysosomal storage disease, Pompe (glycogen storage disease type 2 / II), diabetes mellitus, rare disease (RD), ERT (enzyme replacement therapy), adult polyglucosan body disease (APBD), metabolism

Editorial on the Research Topic Inborn Errors of Carbohydrate Metabolism

The Inborn Errors of Carbohydrate Metabolism Research Topic offers a view on the ever-evolving field of metabolic disorders, particularly on a heterogeneous subgroup of inborn errors that are caused by pathogenic variants in human genes coding for proteins involved in catabolic and anabolic pathways of carbohydrates (Witters et al., 2021). The Research Topic includes original research articles, case reports, systematic reviews and mini-reviews, that highlight unique case reports, recent advances, innovative diagnostic techniques, and emerging therapies that are shaping the landscape of treatment. Significant challenges are addressed in terms of diagnosis, management, and therapeutic intervention of congenital disorders of glycosylation (CDGs), glucose/galactose malabsorption disorder, lysosomal storage diseases (LSDs), adult polyglucosan body disease (APBD) and diabetes mellitus type 1.

CDGs are a group of inherited metabolic diseases that disrupt glycan synthesis and thus glycoprotein and glycolipid synthesis, including glycoposphatidylinositol (GPI) anchors (Ondruskova et al., 2021). They are usually multisystemic in nature, frequently involving central nervous system disease. In this research topic, four works present molecular and clinical contributions to the comprehension of CDGs, shedding light into autosomal recessive ALG2-CDG, as well as into a small group of CDGs that are X-linked: SSR4-CDG, PIGA-CDG and ATP6AP2-CDG. In a case report and literature review Wang et al. report on the first Chinese male patient affected by an ultra-rare X-linked recessive disorder called SSR4-CDG (OMIM #300934). Whole exome sequencing (WES) revealed a novel *de novo* hemizygous variant c.269G>A (p.Trp90*) in *SSR4* that codes for a protein associated with the translocon TRAP complex, thus affecting endoplasmic reticulum protein transport and glycosylation. The patient presented psychomotor retardation, microcephaly, abnormal facial features, and nystagmus as well as an abnormal carbohydrate deficient transferrin test (CDT) (Bruneel et al., 2020). In a case report, Salinas-Marin et al. present the first Mexican male child affected with PIGA-CDG (OMIM #300868), also an X-linked recessive CDG that disrupts the initial steps of GPI-anchor biosynthesis. A novel *de novo* hemizygous variant

PIGA c.145G>A (p.Val49Met) was identified by WES and confirmed to be pathogenic through flow cytometry and complementation assays in PIGA knockout cells by measuring GPI-anchored proteins DAF and CD59. The child presented a moderate to severe phenotype characterized by neurological and gastrointestinal symptoms, including megacolon that highlights this case and that possibly results from involvement of GPI-anchored proteins in the development of the enteric nervous system. In an original research article, Fang et al. present the first Chinese male child affected by another ultra-rare X-linked hereditary condition (four patients reported worldwide) known as ATP6AP2-CDG (OMIM #301045) caused by a novel hemizygous mutation in ATP6AP2 c.185G>A (p.Gly62Glu) identified by WES. This gene codes for ATP6AP2 [ATPase H⁺ transporting accessory protein 2, also known as the (pro) renin receptor] that has a dual function, both interacting with renin or prorenin on the cell surface to affect protein activity and acting as a part of the proton pump associated with adenosine triphosphatase. The patient presented with recurrent jaundice, *cutis laxa*, cirrhosis, growth retardation, coagulopathy, anemia, and cardiomegaly. In contrast with previously reported European patients he did not present immunodeficiency and presented cardiomegaly, expanding the known phenotype of the disease. Interestingly, in a disease model using HEK293T cells, the mutation was shown to dysregulate autophagy and mTOR signaling and metabolites involved in lipid metabolism pathway were found downregulated, noting that this disease causes altered lipid metabolism in patients, particularly cholesterol. In a case report, Martínez-Duncker et al. present the first Mexican child affected by ALG2-CDG (OMIM #607906), presenting as a congenital myasthenic syndrome (Ohno et al., 2023). ALG2 encodes an α 1,3 mannosyltransferase involved in the early steps of N-glycosylation. Whole genome sequencing revealed the presence of two ALG2 variants in compound heterozygosity: a novel variant c.1055_1056delinsTGA p.(Ser352Leufs*3) and a variant of uncertain significance (VUS) c.964C>A p.(Pro322Thr). The patient presented an abnormal CDT test and interestingly, a recently reported ALG2-CDG diagnostic biomarker was found in transferrin and plasma glycoproteins, consisting of a linear heptasaccharide (Sialic acid-Galactose-N-acetylglucosamine-Mannose2-N-acetylglucosamine2), confirming its usefulness in confirming molecular diagnosis. Also included is a comparative phenotype overview of the fourteen patients reported worldwide.

Regarding the catabolic perspective of carbohydrate metabolism, LSDs encompass a group of genetic disorders characterized by lysosomal dysfunction. These disorders arise from deficiencies in specific lysosomal enzymes, membrane transporters, or lysosomal structural proteins, leading to the accumulation of undegraded substrates within lysosomes (Filocamo and Morrone, 2011). The progressive accumulation of these substrates disrupts cellular homeostasis, resulting in cellular dysfunction, tissue damage, and multi-organ pathology. LSDs typically exhibit a wide spectrum of clinical manifestations, including neurological impairment, skeletal abnormalities, hepatosplenomegaly, and cardiorespiratory complications, among others. The onset, severity, and progression of symptoms vary widely among different LSDs, influenced by factors such as the specific enzyme deficiency, the type of accumulated substrate, and the affected tissues and organs. In this Research Topic five contributions present molecular, diagnostic

and therapeutic contributions to the comprehension of lysosomal disorders including Gaucher Disease (GD), Mucopolysaccharidosis type II (MPS II) and Pompe Disease (PD).

In an original research article, Zhang et al. describe interesting data in a retrospective study in China on the clinical characteristics, genotypes, and management strategies of 130 patients with MPS II, a rare, progressive, and ultimately fatal X-linked lysosomal storage disorder caused by variants in *IDS* that encodes for the iduronate-2-sulfatase (IDS), an *exo*-sulfatase that hydrolyzes the C2-sulfate ester bond from nonreducing terminal α -L-iduronic acid residues in heparan sulfate and dermatan sulfate (OMIM# 309900). The study analyzed clinical manifestations, auxiliary examination, pathogenic gene variants, enzyme activity, and surgical history. The most common symptoms in the patients were claw-like hands, coarse facial features, birthmarks, delayed development, and inguinal or umbilical hernia. The most common cardiac manifestations were valve abnormalities, with mitral/tricuspid valve regurgitation (71.9%) and aortic/pulmonary valve regurgitation (36.8%). The study found 43 different IDS pathogenic gene variants in 55 patients, including 16 novel variants, concentrated in exon 9 (20% = 11/55), exon 3 (20% = 11/55), and exon 8 (15% = 8/55). The most common and earliest surgery was hernia repair. Three patients died of respiratory failure. The study provides additional information on the clinical, cardiac ultrasound, and surgical procedure in MPS II patients and expands the genotype spectrum of MPS II.

In an original research article, Colburn and Lapidus analyze PD newborn screening data. PD is a rare lysosomal storage disorder, is caused by genetic variants in *GAA* that encodes the acid alpha-glucosidase (GAA), an enzyme that degrades alpha-1,4 and alpha-1,6 linkages in glycogen, maltose, and isomaltose (OMIM #232300). By studying a cohort of 11.6 million newborns, the largest relevant dataset to date, they determine a new prevalence at birth of 1:18,711, with no evidence of difference across European, Latin American, or Asian ancestry. The study compares the results based on direct detection of disease and analyzed using a binomial method along with power analysis with other methods for estimating the frequency of rare genetic diseases. The study also compares these results to previous analyses to offer a framework for evaluating 'frequency' data that can be applied to other rare, genetic diseases, along with methods to assess the quality of estimates. The study demonstrates the implications of sample size and frames a discussion on its influence on the reliability of results when extrapolating to a population beyond the study dataset.

The availability of enzyme replacement therapy (ERT) with alglucosidase alfa (human recombinant GAA) has changed the natural history of PD, contributing to a longer survival, longer preserved muscle performance and increased quality of life (Kishnani et al., 2007). A systematic review and meta-analysis of 1,722 articles evaluating ERT for infantile-onset Pompe disease (IOPD) was conducted by Dornelles et al. in Brazil. The results showed that alglucosidase alfa potentially improved left ventricular mass, time to start ventilation (TSV), and survival in IOPD patients over the natural history of PD/placebo. There were no differences between the pre- and post-ERT period for myocardial function and psychomotor development. Adverse events after ERT were mild in most cases. The study concluded that alglucosidase alfa potentially improves LV mass, TSV, and survival in IOPD patients, with no

important safety issues. The authors suggest that alglucosidase alfa could be a potential treatment for PD, with no significant safety issues. The study also highlights the need for further research on the safety and efficacy of ERT in IOPD patients.

Additionally, in an original research article, [Carter et al.](#) present study findings involving patients with late-onset Pompe disease (LOPD) who switched from alglucosidase alfa to avalglucosidase alfa and that experienced significant improvements in CK, Hex4, and AST scores post-switch. The second-generation ERT avalglucosidase alfa (Nexviazyme) was designed to enhance cellular uptake via the conjugation of additional bis-mannose-6-phosphate residues ([Dhillon, 2021](#)). The study also revealed improvements in dyspnea, physical function, fatigue, and lower back pain. Avalglucosidase was well tolerated without infusion-associated reactions, and all patients on home infusions continued receiving ERT at home. Anti-drug antibodies were seen in 9/10 of patients on alglucosidase and 8/13 of those on avalglucosidase, with titers below 12,800 in a majority of patients. The study presents evidence that switching from alglucosidase to avalglucosidase may be associated with improved outcomes in certain patients with LOPD.

Gaucher disease (GD), the most prevalent lysosomal storage disorder, is a rare autosomal recessive disorder caused by genetic variations in *GBA* that encodes for the enzyme beta-glucocerebrosidase (GCase) that cleaves the beta-glucosidic linkage of glucosylceramide, an intermediate in glycolipid metabolism, leading to the toxic accumulation of sphingolipids in various organs ([OMIM #230800](#)). In a review by [Mohamed and Al-Jasmi](#) the potential of ABX as a pharmacological chaperone therapy for GD is highlighted, stressing the importance of addressing response variability in clinical studies to improve the management of this rare and complex disorder. Ambroxol (ABX) has emerged as a prospective enzyme enhancement therapy option, showing its potential to enhance mutated GCase activity and reduce glucosylceramide accumulation in GD-affected tissues of different *GBA* genotypes. The variability in response to ABX varies across different variants, highlighting the diversity in patients' therapeutic outcomes. Its oral availability and safety profile make it an attractive option, particularly for patients with neurological manifestations. Clinical trials are essential to explore further ABX's potential as a therapeutic medication for GD to encourage pharmaceutical companies' investment in its development.

In relation to APBD, the adult-onset form of glycogen storage disease type IV (GSD IV) ([OMIM #232500](#)), [Gayed et al.](#) present a case report involving the clinical course and diagnostic odyssey of a seven case series, including patients from the United States and Brazil. This disease is caused by biallelic pathogenic variants in *GBE1* which encodes the glycogen-branching enzyme (GBE) that adds branches to the growing glycogen molecule during the synthesis of glycogen, a storage form of glucose. Deficient GBE activity disrupts normal glycogen synthesis and leads to the formation of glycogen with elongated outer chains. Interestingly, the reported pathogenic variants involve a more recently identified deep intronic variant in *GBE1* as well as novel genotypes that expand our understanding of genotype-phenotype correlations. Also the results of a pilot application of patient-reported outcome measures to evaluate the domains of pain, fatigue, and quality of life are presented.

In regard to disorders affecting glucose-galactose metabolism, [López-Mejía et al.](#) present a case report that highlights the importance of Next-generation sequencing (NGS) panel in the diagnosis of the first Mexican female child reported with Congenital glucose-galactose malabsorption (CGGM; [OMIM #606824](#)), a rare autosomal recessive disorder that primarily causes chronic intractable diarrhea causing dehydration from the first day of life and that can quickly result in death. The patient presented with chronic diarrhea, anemia, jaundice, renal tubular acidosis, hyperammonemia, and initial hypertyrosinemia. A NGS panel for inborn errors of metabolism and congenital diarrhea, identified a homozygous variant in *SLC5A1* (c.1667T>C) that encodes the sodium-dependent glucose transporter-1 (SGLT-1), the primary transporter of monosaccharides in the small intestine and responsible for glucose and galactose active transport across the intestinal brush border. Introduction of galactose-glucose-free fructose-based diet led to a complete resolution of diarrhea and improved nutritional status. Also, in relation to galactose metabolism, [Maroulis et al.](#) present an original research article involving five cases of newborn patients affected by Galactosemia ([OMIM #230400](#)) identified through the National Newborn Screening program in Greece. Galactosemia is the most common and severe type of disorders related to inborn errors of galactose metabolism, caused by autosomal recessive mutations in the three genes that encode enzymes implicated in galactose catabolism (*GALT*, *GALK1*, and *GALE*) specifically in the conversion of α -D-galactose to glucose-1-phosphate. Patients were identified because of increased galactose levels. NGS identified eight rare nonsynonymous DNA variants of uncertain significance involving *GALT*, *GALK1* or *GALE*, four of them novel. Pathogenicity analysis through bioinformatic tools and *in silico* modeling as well as specific phenotypes for these cases are discussed. An additional contribution to the comprehension of galactosemia comes from a contribution by [Panis et al.](#) and members of the Galactosemia Network in a Mini Review article that presents the neurological impacts of classic galactosemia, detailing the ongoing challenges in understanding brain function associated with the disease. It discusses the role of abnormal glycosylation and myo-inositol deficiency, linking these biochemical dysfunctions to brain and neurodevelopmental issues. Treatment approaches, including dietary restrictions and emerging therapies, are examined, alongside their effectiveness in managing symptoms. Importantly, the review notes significant variability in neurological outcomes among individuals with classic galactosemia, highlighting that while some may experience worsening symptoms, many do not exhibit progressive cognitive decline.

In the more frequently studied aspect of carbohydrate metabolism [Bawatneh et al.](#) present an original research article presenting a study involving two Palestinian families affected by Diabetes Mellitus Type 1 ([OMIM #222100](#)). The use of WES allowed identification of variants, involving the *IGF1R* p.V579F variant, which follows autosomal dominant inheritance in one family and the *NEUROD1* p.P197H variant in the other family where it follows an autosomal recessive inheritance. This research marks a significant advance in understanding the genetic foundations of type 1 diabetes within this population. The study's findings also underscore the importance of tailored genetic research in diverse populations to

enhance disease understanding and management globally (Caliebe et al., 2022).

Overall, the articles in this Research Topic advance our understanding of the molecular, clinical, and therapeutic aspects of inborn errors of carbohydrate metabolism. They emphasize the importance of precision medicine, innovative diagnostics, and targeted therapies in addressing the significant challenges in diagnosis, management, and therapeutic intervention for these disorders (Might and Crouse, 2022; Trajanoska et al., 2023). It is our hope that the insights provided will inspire further research and foster collaboration to improve the lives of individuals and families affected by these metabolic diseases.

Author contributions

IM-D: Supervision, Writing–original draft, Writing–review and editing. IVD-S: Writing–original draft, Writing–review and editing. MA-G: Writing–original draft, Writing–review and editing. JG-O: Supervision, Writing–original draft, Writing–review and editing.

References

- Bruneel, A., Cholet, S., Tran, N. T., Mai, T. D., and Fenaille, F. (2020). CDG biochemical screening: where do we stand? *Biochim. Biophys. Acta Gen. Subj.* 1864 (10), 129652. doi:10.1016/j.bbagen.2020.129652
- Caliebe, A., Tekola-Ayele, F., Darst, B. F., Wang, X., Song, Y. E., Gui, J., et al. (2022). Including diverse and admixed populations in genetic epidemiology research. *Genet. Epidemiol.* 46, 347–371. Published online. doi:10.1002/gepi.22492
- Dhillon, S. (2021). Avalglucosidase alfa: first approval. *Drugs* 81 (15), 1803–1809. doi:10.1007/s40265-021-01600-3
- Filocamo, M., and Morrone, A. (2011). Lysosomal storage disorders: molecular basis and laboratory testing. *Hum. Genomics* 5 (3), 156–169. doi:10.1186/1479-7364-5-3-156
- Kishnani, P. S., Corzo, D., Nicolino, M., Byrne, B., Mandel, H., Hwu, W. L., et al. (2007). Recombinant human acid [alpha]-glucosidase: major clinical benefits in infantile-onset Pompe disease. *Neurology* 68 (2), 99–109. doi:10.1212/01.wnl.0000251268.41188.04
- Might, M., and Crouse, A. B. (2022). Why rare disease needs precision medicine-and precision medicine needs rare disease. *Cell Rep. Med.* 3 (2), 100530. doi:10.1016/j.xcrm.2022.100530
- Ohno, K., Ohkawara, B., Shen, X. M., Selcen, D., and Engel, A. G. (2023). Clinical and pathologic features of congenital myasthenic syndromes caused by 35 genes—a comprehensive review. *Int. J. Mol. Sci.* 24 (4), 3730. doi:10.3390/ijms24043730
- Ondruskova, N., Cechova, A., Hansikova, H., Honzik, T., and Jaeken, J. (2021). Congenital disorders of glycosylation: still "hot" in 2020. *Biochim. Biophys. Acta Gen. Subj.* 1865 (1), 129751. doi:10.1016/j.bbagen.2020.129751
- Trajanoska, K., Bhéer, C., Taliun, D., Zhou, S., Richards, J. B., and Mooser, V. (2023). From target discovery to clinical drug development with human genetics. *Nature* 620 (7975), 737–745. doi:10.1038/s41586-023-06388-8
- Witters, P., Morava-Kozicz, E., and Ghishan, F. K. (2021). "Inborn errors of carbohydrate metabolism," in *Liver disease in children* Editors F. J. Suchy, R. J. Sokol, and W. F. Balistreri 5 (Cambridge University Press), 455–483. doi:10.1017/9781108918978.027

Funding

The author(s) declare that no financial support was received for the research, authorship, and/or publication of this article.

Conflict of interest

The authors declare that the research was conducted in the absence of any commercial or financial relationships that could be construed as a potential conflict of interest.

Publisher's note

All claims expressed in this article are solely those of the authors and do not necessarily represent those of their affiliated organizations, or those of the publisher, the editors and the reviewers. Any product that may be evaluated in this article, or claim that may be made by its manufacturer, is not guaranteed or endorsed by the publisher.



OPEN ACCESS

EDITED BY

Daniel Grinberg,
University of Barcelona, Spain

REVIEWED BY

Mercedes Serrano,
Pediatric Research Hospital Sant Joan
de Déu, Spain
Joshi Stephen,
Baylor College of Medicine,
United States

*CORRESPONDENCE

Iván Martínez-Duncker,
duncker@uaem.mx
Susana Monroy-Santoyo,
susie@porfiriamexico.com

SPECIALTY SECTION

This article was submitted to Genetics of
Common and Rare Diseases,
a section of the journal
Frontiers in Genetics

RECEIVED 20 June 2022

ACCEPTED 23 September 2022

PUBLISHED 17 October 2022

CITATION

Salinas-Marín R, Murakami Y,
González-Domínguez CA,
Cruz-Muñoz ME, Mora-Montes HM,
Morava E, Kinoshita T,
Monroy-Santoyo S and
Martínez-Duncker I (2022), Case report:
Functional characterization of a *de novo*
c.145G>A p.Val49Met pathogenic
variant in a case of PIGA-CDG
with megacolon.
Front. Genet. 13:971473.
doi: 10.3389/fgene.2022.971473

COPYRIGHT

© 2022 Salinas-Marín, Murakami,
González-Domínguez, Cruz-Muñoz,
Mora-Montes, Morava, Kinoshita,
Monroy-Santoyo and Martínez-
Duncker. This is an open-access article
distributed under the terms of the
[Creative Commons Attribution License](https://creativecommons.org/licenses/by/4.0/)
(CC BY). The use, distribution or
reproduction in other forums is
permitted, provided the original
author(s) and the copyright owner(s) are
credited and that the original
publication in this journal is cited, in
accordance with accepted academic
practice. No use, distribution or
reproduction is permitted which does
not comply with these terms.

Case report: Functional characterization of a *de novo* c.145G>A p.Val49Met pathogenic variant in a case of PIGA-CDG with megacolon

Roberta Salinas-Marín¹, Yoshiko Murakami²,
Carlos Alberto González-Domínguez^{1,3},
Mario Ernesto Cruz-Muñoz⁴, Héctor Manuel Mora-Montes⁵,
Eva Morava^{6,7,8}, Taroh Kinoshita², Susana Monroy-Santoyo^{9*}
and Iván Martínez-Duncker^{1,8*}

¹Laboratorio de Glicobiología Humana y Diagnóstico Molecular, Centro de Investigación en Dinámica Celular, Instituto de Investigación en Ciencias Básicas y Aplicadas, Universidad Autónoma del Estado de Morelos, Cuernavaca, México, ²Research Institute for Microbial Diseases, Osaka University, Osaka, Japan, ³Instituto de Biotecnología, Universidad Nacional Autónoma de México, Cuernavaca, México, ⁴Facultad de Medicina, Universidad Autónoma del Estado de Morelos, Cuernavaca, México, ⁵Departamento de Biología, División de Ciencias Naturales y Exactas, Campus Guanajuato, Universidad de Guanajuato, Guanajuato, México, ⁶Department of Clinical Genomics, Mayo Clinic, Rochester, MN, United States, ⁷Department of Medical Genetics, University of Pecs Medical School, Pecs, Hungary, ⁸Frontiers in Congenital Disorders of Glycosylation Consortium, National Institute of Neurological Diseases and Stroke (NINDS), National Institute of Child Health and Human Development (NICHD) and the National Center for Advancing Translational Sciences (NCATS), and the Rare Disorders Clinical Research Network (RDCRN), Bethesda, MD, United States, ⁹Centro de Investigación Traslacional, Instituto Nacional de Pediatría, Secretaría de Salud, Mexico City, México

A subgroup of congenital disorders of glycosylation (CDGs) includes inherited GPI-anchor deficiencies (IGDs) that affect the biosynthesis of glycosylphosphatidylinositol (GPI) anchors, including the first reaction catalyzed by the X-linked PIGA. Here, we show the first PIGA-CDG case reported in Mexico in a male child with a moderate-to-severe phenotype characterized by neurological and gastrointestinal symptoms, including megacolon. Exome sequencing identified the hemizygous variant PIGA c.145G>A (p.Val49Met), confirmed by Sanger sequencing and characterized as *de novo*. The pathogenicity of this variant was characterized by flow cytometry and complementation assays in PIGA knockout (KO) cells.

KEYWORDS

GPI (glycosylphosphatidylinositol), CDG (congenital disorder of glycosylation), exome, PIGA, CD59 antigen

Introduction

The glycosylphosphatidylinositol (GPI) structure is ubiquitous among eukaryotes with a common minimal backbone consisting of three mannoses, one non-*N*-acetylated glucosamine (GlcN), and inositol phospholipid (PI). GPIs are attached to proteins *via* an amide bond between the C-terminal carboxyl group and an amino group of ethanolamine phosphate, and their fatty chains of PI are inserted into the outer leaflet of the plasma membrane. In this way, more than 150 different human proteins with diverse functions are anchored through GPIs (Stevens, 1995; Fujita and Kinoshita, 2012; Kinoshita and Fujita, 2016). The biosynthesis of GPIs is a stepwise sequence of 11 reactions (Kinoshita, 2020). The first reaction consists in the transference of *N*-acetylglucosamine (GlcNAc) from UDP-*N*-acetylglucosamine (UDP-GlcNAc) to the 6-position of inositol to generate GlcNAc-PI and is catalyzed by GPI *N*-acetylglucosaminyl transferase (GPI-GnT), a complex monoglycosyltransferase, consisting of seven subunits, of which the X-linked *PIGA* is a catalytic subunit (Miyata et al., 1993).

Somatic mutations in *PIGA* can occur, leading to paroxysmal nocturnal hemoglobinuria, an acquired clonal disease of hematopoietic stem cells (Takeda et al., 1993; Hill et al., 2017). Additionally, *PIGA* pathogenic germline variants have been reported in humans and are part of a subgroup of inherited GPI-anchor deficiencies (IGDs) classified as congenital disorders of glycosylation (CDGs) (Freeze et al., 2014; Tarailo-Graovac et al., 2015; Ng and Freeze, 2018). Twenty-one out of 27 genes involved in GPI biosynthesis have been reported with pathogenic germline variants, with *PIGA*-CDG being the only X-linked IGD (Kinoshita, 2020). In *PIGA*-CDG, only males have been found to be clinically affected (Tarailo-Graovac et al., 2015).

The phenotypical spectrum in *PIGA*-CDG ranges from a mild-to-moderate developmental delay (DD), treatable epilepsy, with no dysmorphic features, and no organ malformations in the milder end of the spectrum to profound DD/intellectual disability, treatment-refractory epilepsy, dysmorphic features, and multi-organ malformations in the most severe end of the spectrum (Bayat et al., 2020). We report, herein, the first Mexican child with *PIGA*-CDG presenting a previously uncharacterized novel missense *PIGA* pathogenic variant, resulting in a moderate-to-severe phenotype.

Materials and methods

Sequencing

Genomic DNA (gDNA) was extracted from the patient's saliva and enriched for targeted regions using a hybridization-based *in house* Invitae® protocol for clinical exome sequencing

(CES) analysis and sequenced (NextSeq Instrument, Illumina, San Francisco, CA, United States). Confirmation of the variant in the patient and parental screening was performed by the gDNA-based polymerase chain reaction (PCR) product covering exon 2 of *PIGA* obtained using forward primer 5'-GAGGAGGAGCTG GGAATGG -3' and reverse primer *PIGA* as 5'-CTGGTTGTA CATGACTTTCAGAG-3'. The 290-bp amplicon was isolated and sequenced using an ABI Prism 3130xl autoanalyzer (Applied Biosystems, Foster City, CA, United States), and the results were visualized using SnapGene Viewer 2.2.2 (GSL Biotech LLC, Chicago, IL, United States).

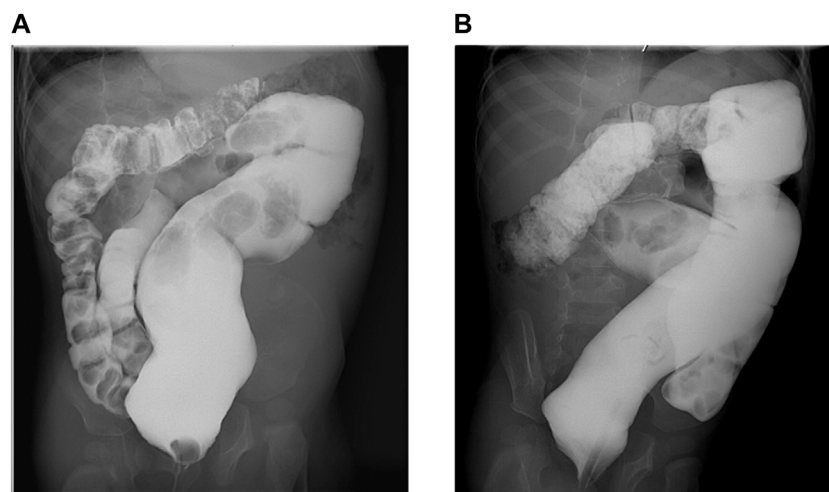
Glycophosphatidylinositol anchored protein expression and rescue analysis

The CD16 expression in granulocytes was performed on one blood sample per individual. Granulocytes were stained with 0.2 µg of phycoerythrin-anti-CD16 (CD16-PE; clone DJ130c, sc20052, Santa Cruz, United States) for 30 min at 4°C, washed three times with PBS buffer supplemented with 0.5% BSA, and stored in 2% of paraformaldehyde. The cells (20,000 events per sample) were analyzed, and fluorescence data were recorded as individual cellular events on a BD Accuri C6 Plus flow cytometer (Becton Dickinson, Franklin Lakes, NJ, United States). Data were analyzed with FlowJo software according to Neuhofer et al., (2020).

The HEK-293 *PIGA* knockout (KO) model was generated by the CRISPR/Cas9 system. HEK293 *PIGA* KO cells were transfected with wild and mutant *PIGA* cDNA driven by the weak TATA box promoter (pTA). Two days later, the surface expression of GPI-anchored proteins (GPI-APs) was determined by staining cells with mouse anti-CD59 (5H8) and anti-DAF (IA10), followed by a PE-conjugated anti-mouse IgG antibody (BD Biosciences). The cells were analyzed by a flow cytometer (MACSQuant Analyzer; Miltenyi Biotec) with Flowjo software (BD Life Sciences). Lysates from transfectants of wild and mutant pMEHA-*PIGA* were applied to SDS PAGE, and Western blotting was performed. *PIGA* proteins were detected by rabbit anti-HA polyclonal antibody (MBL), followed by HRP-conjugated anti-rabbit IgG. For the loading control, GAPDH was detected by mouse anti-GAPDH (AM4300, Invitrogen), followed by HRP-conjugated anti-mouse IgG.

Case description

The patient is the second born of a healthy, young, non-consanguineous couple; family history was unremarkable. Pregnancy and vaginal delivery at term were uneventful; birth weight was 3,500 g (Z-score = 0), height 51 cm (z-score = 0), and Apgar 9/9. At delivery, a thick and copious layer of vernix caseosa covered him. He was admitted to the NICU during his first week

**FIGURE 1**

Barium enema. (A). Anteroposterior view showing chronic megarectum. (B). Oblique view showing severe dilatation of the sigmoid and rectum with loss of haustral markings.

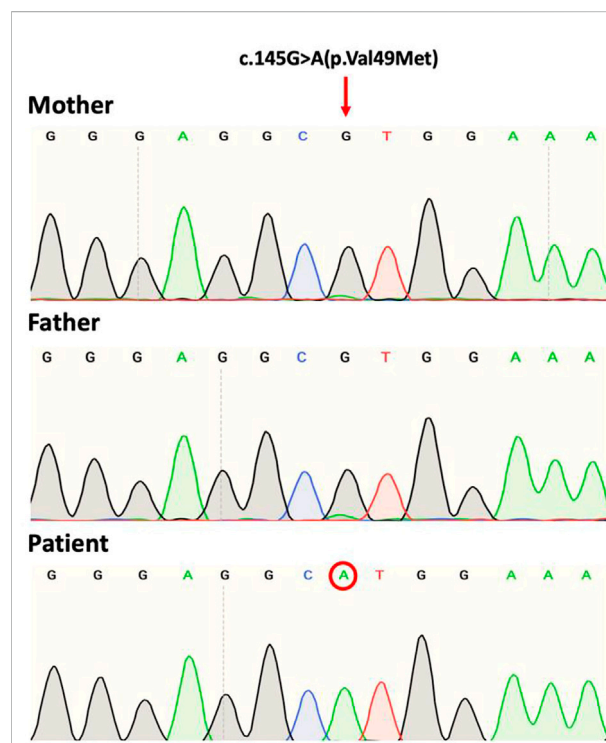
of life due to indirect hyperbilirubinemia (indirect bilirubin <20 mg/dl but >14 mg/dl), requiring three cycles of phototherapy and treatment with phenobarbital due to Crigler–Najjar syndrome suspicion. Finally, jaundice resolved when he was 3 months old, and molecular diagnosis of Gilbert's syndrome (MIM [143500]) was confirmed by identification of the TA6/TA7 genotype in the UDP glucuronosyltransferase family 1 member A1 gene (*UGT1A1*); phenobarbital was stopped, triggering seizures 4 weeks later. A cerebral MRI and two EEGs, performed at 4 and 9 months of age, respectively, revealed a normal myelination process related to the patient's age and normal cerebral electrical activity.

From 7 months of age, axial hypotonia and limb hypertonia, indifference to the environment, and severe constipation were evident; he was unable to roll over, sit independently, grab objects, and carry them to his middle line, and he only babbled occasionally. Height 73.5 cm (z-score = 2), weight 9,620 g (z-score = 2), and head circumference 45.4 cm (z-score = 1), with a broad and bulging forehead, arched eyebrows, sunken eyes, rough facies, thick and fleshy ears with “elfin” upper tip, wide mouth with thin upper vermillion, short neck, wide thorax without inverted nipples, deep palmar creases, deep-set toe nails, and skin and adipose tissue “doughy” to the touch.

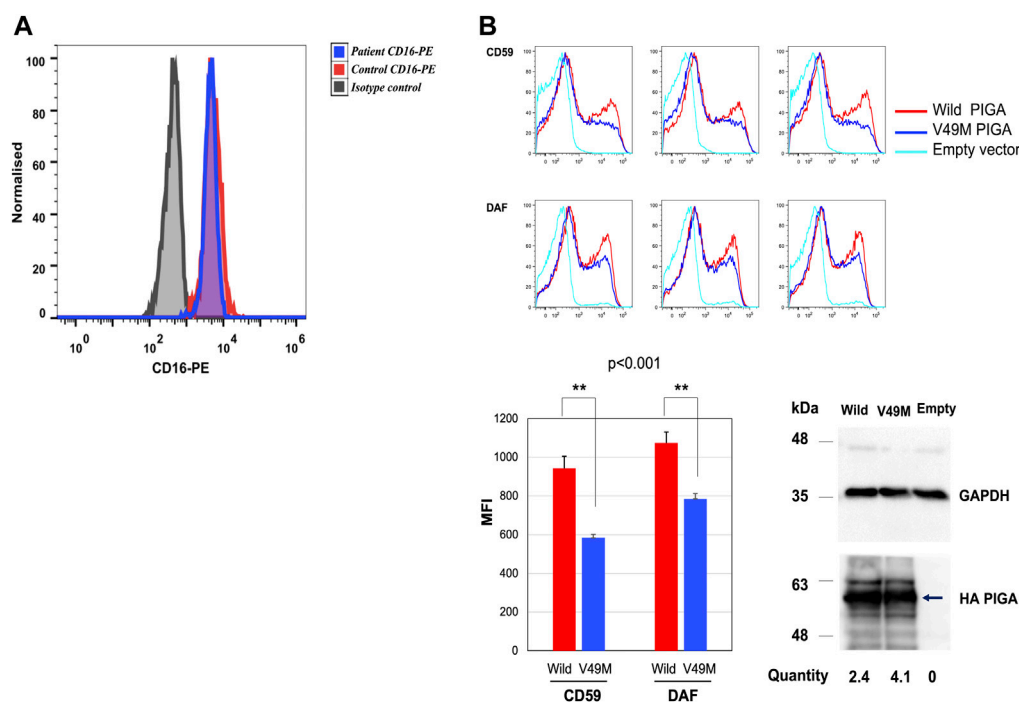
At 15 months of age, a neuropsychological evaluation was executed, using the Battelle Developmental Inventory, 2nd Edition (BDI-2), concluding a significant delay in global developmental quotient (<0.1 percentile) in relation to the patient's chronological age.

Normal audition and vision were assessed by evoked brainstem potentials. No congenital heart disease or myocardiopathy were documented. Bilateral ureterocele, predominantly right, left ureteropielectasis, and changes in the

left ureteral caliber, suggesting vesicoureteral reflux, were identified. No other malformations were reported.

**FIGURE 2**

Sanger sequence chromatograms of gDNA showing the *PIGA* variant NM_002641.4(*PIGA*):c.145G>A (p.Val49Met). The patient shows the mutation at codon position 49 of exon 2. Both mother and father are non-carriers.

**FIGURE 3**

CD16 expression in granulocytes and rescue analysis in the PIGA-KO HEK293 cells. **(A)** Histogram depicting median fluorescence intensity (MFI) of CD16-PE in granulocytes from the patient (blue histogram) and healthy control (red histogram) (healthy control MFI = 5,130 vs. patient MFI = 4,450). **(B)** Rescue of CD59 and DAF expression on the PIGA-KO HEK293 cells using a weak TATA box only promoter (pTA). The histograms represent the MFI for the rescue of CD59 and DAF expression by the wild type and Val49Met (V49M) variant using the pTA promoter. Values for three independent experiments and their statistical significance were graphed. CD59: wild type MFI = 943 vs. variant MFI = 584. DAF: wild type MFI = 1,074 vs. variant MFI = 785. Representative Western blotting of the mutant (Val49Met) and wild type (Wild) PIGA protein expression showing that the PIGA mutant protein was more expressed than the wild-type protein. (normalized with the intensities of GAPDH, the loading control, and luciferase activities used for evaluating transfection efficiencies). PIGA protein was detected by anti-His mAb (arrow), and loading control was revealed with anti-GAPDH. Empty vector = vector without insert gene. Histograms in **(A)** y axis show cell counts; the x axis shows fluorescence intensity.

Partial seizures characterized by gaze deviation to the left and motor orofacial automatisms as well as secondary generalized myoclonic seizures presented at the time of diagnosis. The EEG revealed generalized cerebral dysfunction, characterized by epileptiform paroxysms illustrated by periodic lateralized wave-spike discharges in the right and left temporal and parietal regions that tended to generalize. Treatment with levetiracetam was initiated, and later valproate was added due to partial pharmacological response; finally, clonazepam was warranted as rescue treatment in case of sudden, uncontrolled seizures. Good seizure control was achieved, but fever sensitivity and febrile-induced seizures were observed upon upper respiratory tract viral infections.

Currently, at 34 months of age, he is under neurologic and metabolic surveillance and enrolled in a physical therapy program. He still suffers from severe chronic constipation that has caused a megacolon (Figures 1A,B), requiring treatment with polyethylene glycol 3350 and/or sennosides and glycerine enemas. Other invasive procedures, such as rectal manometry and full-thickness rectal biopsy, were not performed since

Hirschsprung disease was unlikely due to response, still partial and intermittent, to laxatives and the absence of typical barium enema images, showing reduced caliber of the rectum, followed by a transition zone to an enlarged-caliber sigmoid. He has no expressive language, independent sitting or rolling over, and eye contact has slightly improved. No abnormalities in coagulation, endocrine, liver, and renal function tests have been documented. He had a mild SARS-COV-2 infection, and no seizures were triggered by a mild increase in temperature. Due to severe constipation, pyridoxine (vitamin B6) and glucosamine supplementation could not be started. Bilateral ureteroceles and ureteropielectasis remain stable. The last EEG assessment revealed a very high-voltage, asynchronous, slow wave-spike pattern consistent with hypsarrhythmia, which clinically correlated with infantile spasms illustrated by head bobbing and nystagmoid eye movements; levetiracetam was withdrawn, and vigabatrin and topiramate were started, achieving good seizure control. According to the Nijmegen Pediatric CDG Rating Scale (NPCRS) (Achouitar et al., 2011), the patient's score is 25, which scales him in the upper limit of the moderate category.

Exome sequencing of the child revealed the presence in exon 2 of the NM_002641.4(PIGA):c.145G>A (p.Val49Met) variant with genomic location X:15331786 (GRCh38). Sanger sequencing data identified that the variant is a *de novo* mutation in view that sequencing of parental gDNA showed that the mother was a non-carrier (Figure 2).

To determine the functional impact of the c.145G>A (p.Val49Met) variant, granulocyte expression of CD16 was determined by flow cytometry. CD16 is a GPI-anchored protein, considered a biomarker for IGDs (Bruneel et al., 2020). A 13% reduction in CD16 was observed in the patient compared to the healthy control (Figure 3A). This degree of reduction has been reported in other PIGA-CDG patients (Kim et al., 2016).

Additionally, a rescue analysis of DAF and CD59 expression was performed by flow cytometry in a HEK-293 PIGA KO model generated by the CRISPR/Cas9 system (Guerrero et al., 2021). DAF and CD59 are well-known GPI-anchored proteins used as biomarkers for IGDs and that are expressed in HEK-293 cells. CD16 is not expressed in this cell line.

HEK-293 PIGA KO cells were transfected with the wild type and the c.145G>A (p.Val49Met) variant, driven by the weak TATA box only promoter (pTA). Rescue of CD59 expression by the variant was found to be significantly deficient (62% of wild type; $p < 0.001$). Rescue of DAF expression was also found to be significantly deficient (73% of wild type; $p < 0.001$) (Figure 3B). Western blot from cell lysates showed similar expression of both wild type and mutant protein (Figure 3B).

Discussion and conclusion

CDGs, including IGDs, are scarcely reported from Latin America. Less than 90 cases of germline PIGA have been reported worldwide, mostly in the severe phenotype spectrum. We report the case of a male child that presented with a predominantly neurological and gastrointestinal infection, including moderate and prolonged neonatal jaundice that was associated with Gilbert's syndrome, caused by the TA6/TA7 *UGT1A1* (also named *UGT1A1*28*) polymorphism. The *UGT1A1* is related to autosomal recessive indirect hyperbilirubinemia syndromes. While some authors report the association of this polymorphism with mild-to-moderate neonatal hyperbilirubinemia (Roy-Chowdhury et al., 2002; Agrawal et al., 2009), others have failed to demonstrate its clinical significance alone on jaundice risk (Ülgenalp et al., 2003; Watchko and Lin, 2010). Nevertheless, the combination of the TA6/TA7 genotype with other icterogenic conditions, such as hemoglobinopathies, may increase the risk for hyperbilirubinemia (Watchko and Lin, 2010) and may play an additional role in the pathogenesis of hemolytic neonatal hyperbilirubinemia (Yang et al., 2021) by interfering with the bilirubin clearance pathway. Therefore, the occurrence of the

variant described previously with the *PIGA* mutation may explain the prolonged neonatal hyperbilirubinemia, which is not expected nor observed in CDG patients (Marques-da-Silva et al., 2017; Bayat et al., 2020; Lipiński et al., 2021).

Exome sequencing of the patient's gDNA revealed the presence of the variant NM_002641.4(PIGA):c.145G>A (p.Val49Met) ClinVar 623369 reported with conflicting interpretations of pathogenicity. The variant in this case is considered *de novo* as the mother was determined a non-carrier. The c.145G>A (p.Val49Met) variant has been reported in the literature in three male patients who acquired it through maternal inheritance (mothers were not reported to be affected). The first reported case was characterized by renal cysts with epileptic seizures and DD (Knaus et al., 2018); the second case showed profound DD, epileptic spasms, and focal seizures initiating at 2 months evolving to bilateral tonic-clonic seizures of intractable prognosis, with the patient dying at 12 years old suddenly and unexpectedly (Bayat et al., 2020); and the third case exhibited epileptic spasms and non-motor onset seizures with behavior arrest, myoclonic jerks, and apneas, developing pharmacoresistance with severe status epilepticus (Cabasson et al., 2020).

In contrast to the previous reports involving the 145G>A (p.Val49Met) variant, the patient exhibits a moderate neurological phenotype, perhaps related to the absence of documented brain malformations, refractory epilepsy, and multiorgan involvement. In a large number of PIGA-CDG patients, it was reported that only 10% of patients born alive belonged to the milder end of the spectrum, but only 3% of deceased patients belonged to this part of the spectrum (Bayat et al., 2021).

A distinctive feature in this case was the development of megacolon, possibly originated by a deficient development of the enteric nervous system. Reduction in the expression of GPI-linked proteins could explain gastrointestinal symptoms in PIGA-CDG, including megacolon. For example, the GPI-linked protein GFR α 1 is a co-receptor of the glial cell line-derived neurotrophic factor (GDNF) that participates in a signaling system involved in the migration of neural crest cells into the gut, as well as regulation of neuronal survival and death (Cacalano et al., 1998; Uesaka et al., 2007).

The 145G>A (p.Val49Met) variant is located in the Rossmann A fold region, a hot spot for cluster pathogenic PIGA variants (Knaus et al., 2018; Bayat et al., 2020; Cabasson et al., 2020). The Val49Met change has been predicted to be probably damaging by both PolyPhen-2 (Adzhubei et al., 2013) and SIFT (Kumar et al., 2009) assessed with 29.4 as the score using Combined Annotation-Dependent Depletion (CADD) (Bayat et al., 2020) and a REVEL score of 0.702 (likely disease-causing) (Ioannidis et al., 2016). This variant is absent from the gnomAD database.

Although the Val49Met has the lowest Grantham-score of *PIGA* variants studied in a huge number of patients (Bayat et al., 2020), the Val residue is highly conserved in *PIGA* proteins from

several organisms, which could explain the importance of this amino acid residue in *PIGA* function and the functional impact of the Val49M substitution, as was determined by the significantly reduced rescue of CD59 and DAF expression observed in the complementation assays using the HEK293 *PIGA* KO cells. Taking into consideration the experimental and theoretical data, we can conclude that the 145G>A (p.Val49Met) *PIGA* variant is pathogenic.

Unfortunately, there are no corrective treatments available for *PIGA*-CDG. Improvement has been observed in some patients upon initiation with ketogenic diets (Joshi et al., 2016), probably through stimulation of γ -amino butyric acid (GABA) production and reception, initiating an anti-epileptic effect (Daci et al., 2018), and because of their high content in omega-3 and omega-6 polyunsaturated fatty acids (PUFAs) that present modulatory effects on voltage-gated ion channels and thus a potential anti-epileptic effect (Taha et al., 2010). More recently, *PIGA* cell lines and mouse models have been used to evaluate compounds or drugs that were originally developed to address different diseases as an alternative to finding an effective treatment for *PIGA*-CDG (Olsen et al., 2017; Guerrero et al., 2021; Liu et al., 2021; Lukacs et al., 2021).

Patient perspective

The patient is currently enrolled in the Natural History Study of the Frontiers in Congenital Disorders of Glycosylation Consortium of the National Institutes of Health, United States. The parents are working with other families affected by CDG to advance diagnosis and treatment for patients in Mexico and are actively seeking clinical trials for their son to participate in.

Data availability statement

The datasets for this article are not publicly available due to concerns regarding participant/patient anonymity. Requests to access the datasets should be directed to the corresponding author.

Ethics statement

The studies involving human participants were reviewed and approved by the Ethics Committee of the National Institute of Pediatrics and the Faculty of Medicine of the Morelos State Autonomous University.

Author contributions

RS-M, SM-S, and IM-D: conceptualization. RS-M, Y-M, CAG-D, T-K, MEC-M, HMM-M, E-M, SM-S, and IM-D: investigation. RS-M, SM-S, and IM-D: data curation. RS-M, SM-S, and IM-D: writing original draft. RS-M, Y-M, CAG-D, T-K, MEC-M, HMM-M, E-M, SM-S, and IM-D: review and editing. IM-D and E-M provided project administration and funding acquisition. IM-D and SM-S: supervision and validation.

Funding

IM-D was supported by Grants 293399 Red Temática Glicociencia en Salud-CONACyT and the Sociedad Latinoamericana de Glicobiología, A.C. E-M and IM-D were supported by Frontiers in Congenital Disorders of Glycosylation (1U54NS115198-01) from the National Institute of Neurological Diseases and Stroke (NINDS), National Institute of Child Health and Human Development (NICHD) and the National Center for Advancing Translational Sciences (NCATS), and the Rare Disorders Clinical Research Network (RDCRN), at the National Institute of Health.

Acknowledgments

The authors thank Maricela Olvera and Mabel Rodríguez of the Laboratorio Nacional para la Producción y Análisis de Moléculas y Medicamentos Biotecnológicos (LAMMB) for technical support with a BD Accuri C6 Plus flow cytometer.

Conflict of interest

The authors declare that the research was conducted in the absence of any commercial or financial relationships that could be construed as a potential conflict of interest.

Publisher's note

All claims expressed in this article are solely those of the authors and do not necessarily represent those of their affiliated organizations, or those of the publisher, the editors, and the reviewers. Any product that may be evaluated in this article, or claim that may be made by its manufacturer, is not guaranteed or endorsed by the publisher.

References

- Achouitar, S., Mohamed, M., Gardeitchik, T., Wortmann, S. B., Sykut-Cegielska, J., Ensenaer, R., et al. (2011). Nijmegen paediatric CDG rating scale: A novel tool to assess disease progression. *J. Inherit. Metab. Dis.* 34, 923–927. doi:10.1007/s10545-011-9325-5
- Adzhubei, I., Jordan, D. M., and Sunyaev, S. R. (2013). Predicting functional effect of human missense mutations using PolyPhen-2. *Curr. Protoc. Hum. Genet.* Chapter 7, Unit7.20.76. doi:10.1002/0471142905.hg0720s76
- Agrawal, S. K., Kumar, P., Rath, R., Sharma, N., Das, R., Prasad, R., et al. (2009). UGT1A1 gene polymorphisms in north indian neonates presenting with unconjugated hyperbilirubinemia. *Pediatr. Res.* 65 (6), 675–680. doi:10.1203/PDR.0b013e31819ed5de
- Bayat, A., Klovgaard, M., Johannesen, K. M., Stefan Barakat, T., Kievit, A., Montomoli, M., et al. (2021). *Deciphering the premature mortality in PIGA-CDG – an untold story*. Amsterdam: Epilepsy Research, 170. doi:10.1016/j.eplepsyres.2020.106530
- Bayat, A., Knaus, A., Pendziwiat, M., Afenjar, A., Barakat, T. S., Bosch, F., et al. (2020). Lessons learned from 40 novel PIGA patients and a review of the literature. *Epilepsia* 61 (6), 1142–1155. doi:10.1111/epi.16545
- Bruneel, A., Cholet, S., Tran, N. T., Mai, T. D., and Fenaille, F. (2020). CDG biochemical screening: Where do we stand? *Biochim. Biophys. Acta. Gen. Subj.* (10), 129652. doi:10.1016/j.bbagen.2020.129652
- Cabasson, S., Van-Gils, J., Villég, F., Abi-Warde, M. T., Barcia, G., Lazaro, L., et al. (2020). Early-onset epileptic encephalopathy related to germline PIGA mutations: A series of 5 cases. *Eur. J. Paediatr. Neurol.* 28, 214–220. doi:10.1016/j.ejpn.2020.06.002
- Cacalano, G., Fariñas, I., Wang, L. C., Hagler, K., Forgie, A., Moore, M., et al. (1998). GFRalpha1 is an essential receptor component for GDNF in the developing nervous system and kidney. *Neuron* 21 (1), 53–62. doi:10.1016/s0896-6273(00)80514-0
- Daci, A., Bozalija, A., Jashari, F., and Krasniqi, S. (2018). Individualizing treatment approaches for epileptic patients with glucose transporter type1 (GLUT-1) deficiency. *Int. J. Mol. Sci.* 19, E122. doi:10.3390/ijms19010122
- Freeze, H. H., Chong, J. X., Bamshad, M. J., and Ng, B. G. (2014). *Solving glycosylation disorders: Fundamental approaches reveal complicated pathways*, 94. American Journal of Human Genetics. doi:10.1016/j.ajhg.2013.10.024
- Fujita, M., and Kinoshita, T. (2012). GPI-anchor remodeling: Potential functions of GPI-anchors in intracellular trafficking and membrane dynamics. *Biochim. et Biophys. Acta*, 1821. doi:10.1016/j.bbalip.2012.01.004
- Guerrero, P. A., Murakami, Y., Malik, A., Seeberger, P. H., Kinoshita, T., and Varón Silva, D. (2021). Rescue of glycosylphosphatidylinositol-anchored protein biosynthesis using synthetic glycosylphosphatidylinositol oligosaccharides. *ACS Chem. Biol.* 16 (11), 2297–2306. doi:10.1021/acscchembio.1c00465
- Hill, A., Dezern, A. E., Kinoshita, T., and Brodsky, R. A. (2017). *Paroxysmal nocturnal haemoglobinuria*, 3. London: Nature Reviews Disease Primers. doi:10.1038/nrdp.2017.28
- Ioannidis, N. M., Rothstein, J. H., Pejaver, V., Middha, S., McDonnell, S. K., Baheti, S., et al. (2016). Revel: An ensemble method for predicting the pathogenicity of Rare missense variants. *Am. J. Hum. Genet.* 99 (4), 877–885. doi:10.1016/j.ajhg.2016.08.016
- Joshi, C., Kolbe, D. L., Mansilla, M. A., Mason, S., Smith, R. J. H., and Campbell, C. A. (2016). Ketogenic diet – a novel treatment for early epileptic encephalopathy due to PIGA deficiency. *Brain Dev.* 38 (9), 848–851. doi:10.1016/j.braindev.2016.04.004
- Kim, Y. O., Yang, J. H., Park, C., Kim, S. K., Kim, M. K., Shin, M. G., et al. (2016). A novel PIGA mutation in a family with X-linked, early-onset epileptic encephalopathy. *Brain Dev.* 38 (8), 750–754. doi:10.1016/j.braindev.2016.02.008
- Kinoshita, T. (2020). *Biosynthesis and biology of mammalian GPI-anchored proteins*, 10. London: Open Biology. doi:10.1098/rsob.190290
- Kinoshita, T., and Fujita, M. (2016). Biosynthesis of GPI-anchored proteins: Special emphasis on GPI lipid remodeling. *J. Lipid Res.* 57, 6–24. doi:10.1194/jlr.R063313
- Knaus, A., Pantel, J. T., Pendziwiat, M., Hajjir, N., Zhao, M., Hsieh, T. C., et al. (2018). Characterization of glycosylphosphatidylinositol biosynthesis defects by clinical features, flow cytometry, and automated image analysis. *Genome Med.* 10 (1), 3. doi:10.1186/s13073-017-0510-5
- Kumar, P., Henikoff, S., and Ng, P. C. (2009). Predicting the effects of coding non-synonymous variants on protein function using the SIFT algorithm. *Nat. Protoc.* 4 (7), 1073–1081. doi:10.1038/nprot.2009.86
- Lipiński, P., Bogdańska, A., Socha, P., and Tyłki-Szymańska, A. (2021). Liver involvement in congenital disorders of glycosylation and deglycosylation. *Front. Pediatr.* 9, 696918. doi:10.3389/fped.2021.696918
- Liu, S. S., Liu, Y. S., Guo, X. Y., Murakami, Y., Yang, G., Gao, X. D., et al. (2021). A knockout cell library of GPI biosynthetic genes for functional studies of GPI-anchored proteins. *Commun. Biol.* 4 (1), 777. doi:10.1038/s42003-021-02337-1
- Lukacs, M., Blizzard, L. E., and Stottmann, R. W. (2021). CNS glycosylphosphatidylinositol deficiency results in delayed white matter development, ataxia and premature death in a novel mouse model. *Hum. Mol. Genet.* 29 (7), 1205–1217. doi:10.1093/hmg/ddaa046
- Marques-da-Silva, D., dos Reis Ferreira, V., Monticelli, M., Janeiro, P., Videira, P. A., Witters, P., et al. (2017). Liver involvement in congenital disorders of glycosylation (CDG). A systematic review of the literature. *J. Inherit. Metab. Dis.* 40, 195–207. doi:10.1007/s10545-016-0012-4
- Miyata, T., Takeda, J., Iida, Y., Yamada, N., Inoue, N., Takahashi, M., et al. (1993). The cloning of PIG-A, a component in the early step of GPI-anchor biosynthesis. *Science* 259 (5099), 1318–1320. doi:10.1126/science.7680492
- Neuhöfer, C. M., Funke, R., Wilken, B., Knaus, A., Altmüller, J., Nürnberg, P., et al. (2020). A novel mutation in PIGA associated with multiple congenital anomalies-hypotonia-seizure syndrome 2 (MCAHS2) in a boy with a combination of severe epilepsy and gingival hyperplasia. *Mol. Syndromol.* 11 (1), 30–37. doi:10.1159/000505797
- Ng, B. G., and Freeze, H. H. (2018). Perspectives on glycosylation and its congenital disorders. *Trends Genet.* 34, 466–476. doi:10.1016/j.tig.2018.03.002
- Olsen, A. K., Dertinger, S. D., Krüger, C. T., Eide, D. M., Instanes, C., Brunborg, G., et al. (2017). *The pig-a gene mutation assay in mice and human cells: A review*, 121. Basic and Clinical Pharmacology and Toxicology. doi:10.1111/bcpt.12806
- Roy-Chowdhury, N., Deocharan, B., Bejanki, H. R., Roy-Chowdhury, J., Koliopoulos, C., Petmezaki, S., et al. (2002). Presence of the genetic marker for Gilbert syndrome is associated with increased level and duration of neonatal jaundice. *Acta Paediatr.* 91, 100–101. doi:10.1080/080352502573458058
- Stevens, V. L. (1995). Biosynthesis of glycosylphosphatidylinositol membrane anchors. *Biochem. J.* 310, 361–370. doi:10.1042/bj3100361
- Taha, A. Y., Burnham, W. M. I., and Auvin, S. (2010). *Polyunsaturated fatty acids and epilepsy*, 51. Copenhagen: Epilepsia. doi:10.1111/j.1528-1167.2010.02654.x
- Takeda, J., Miyata, T., Kawagoe, K., Iida, Y., Endo, Y., Fujita, T., et al. (1993). Deficiency of the GPI anchor caused by a somatic mutation of the PIG-A gene in paroxysmal nocturnal hemoglobinuria. *Cell* 73 (4), 703–711. doi:10.1016/0092-8674(93)90250-t
- Tarailo-Graovac, M., Sinclair, G., Stockler-Ipsiroglu, S., Van Allen, M., Rozmus, J., Shyr, C., et al. (2015). The genotypic and phenotypic spectrum of PIGA deficiency. *Orphanet J. Rare Dis.* 10 (1), 23. doi:10.1186/s13023-015-0243-8
- Uesaka, T., Jain, S., Yonemura, S., Uchiyama, Y., Milbrandt, J., and Enomoto, H. (2007). Conditional ablation of GFRalpha1 in postmigratory enteric neurons triggers unconventional neuronal death in the colon and causes a Hirschsprung's disease phenotype. *Development* 134 (11), 2171–2181. doi:10.1242/dev.001388
- Ülgenalp, A., Duman, N., Schaefer, F. V., Whetsell, L., Bora, E., Gülcan, H., et al. (2003). Analyses of polymorphism for UGT1*1 exon 1 promoter in neonates with pathologic and prolonged jaundice. *Biol. Neonate* 83 (4), 258–262. doi:10.1159/000069487
- Watchko, J. F., and Lin, Z. (2010). Exploring the genetic architecture of neonatal hyperbilirubinemia. *Semin. Fetal Neonatal Med.* 15 (3), 169–175. doi:10.1016/j.siny.2009.11.003
- Yang, H., Lin, F., Chenkai, Z., Zhang, L., Xu, J. X., Wu, Y. H., et al. (2021). UGT1A1 mutation association with increased bilirubin levels and severity of unconjugated hyperbilirubinemia in ABO incompatible newborns of China. *BMC Pediatr.* 21 (1), 259. doi:10.1186/s12887-021-02726-9



OPEN ACCESS

EDITED BY

Andrea Lynne Gropman,
Children's National Hospital,
United States

REVIEWED BY

Joshi Stephen,
Baylor College of Medicine,
United States
Patrik Lipiński,
Children's Memorial Health Institute
(IPCZD), Poland

*CORRESPONDENCE

Xiaohong Wang,
wangxh99919@126.com

[†]These authors have contributed equally
to this work

SPECIALTY SECTION

This article was submitted to Genetics of
Common and Rare Diseases,
a section of the journal
Frontiers in Genetics

RECEIVED 29 May 2022

ACCEPTED 10 October 2022

PUBLISHED 26 October 2022

CITATION

Wang J, Gou X, Wang X, Zhang J, Zhao N
and Wang X (2022), Case Report: The
novel hemizygous mutation in the *SSR4*
gene caused congenital disorder of
glycosylation type iy: A case study and
literature review.
Front. Genet. 13:955732.
doi: 10.3389/fgene.2022.955732

COPYRIGHT

© 2022 Wang, Gou, Wang, Zhang, Zhao
and Wang. This is an open-access article
distributed under the terms of the
[Creative Commons Attribution License](https://creativecommons.org/licenses/by/4.0/)
(CC BY). The use, distribution or
reproduction in other forums is
permitted, provided the original
author(s) and the copyright owner(s) are
credited and that the original
publication in this journal is cited, in
accordance with accepted academic
practice. No use, distribution or
reproduction is permitted which does
not comply with these terms.

Case Report: The novel hemizygous mutation in the *SSR4* gene caused congenital disorder of glycosylation type iy: A case study and literature review

Jun Wang[†], Xingqing Gou[†], Xiyi Wang, Jing Zhang, Nan Zhao
and Xiaohong Wang*

Center for Reproductive Medicine, Department of Gynecology and Obstetrics, Tangdu Hospital, The
Air Force Military Medical University, Xi'an, Shaanxi, China

Background: Recently, the hemizygous variation of *SSR4* gene has been reported to be associated with congenital disorder of glycosylation type iy. To date, only 13 patients have been diagnosed with *SSR4*-CDG in the worldwide, but it has not been reported in the Chinese population.

Methods: Whole-exome sequencing and gene copy number variation analysis were used to genetic analysis. The mRNA expression of *SSR4* gene in blood was detected by Real-time Quantitative PCR. The clinical manifestations of all patients reported in the literature were reviewed.

Results: WES analysis identified a *de novo* hemizygous variant c.269G>A (p.Trp90*) of *SSR4* gene in the proband with psychomotor retardation, microcephaly, abnormal facial features, and nystagmus. This variant has not been reported in previous studies. The *in vivo* mRNA expression of *SSR4* gene in patient was significantly decreased. Literature review showed that all 14 patients, including our patient, presented with hypotonia, intellectual disability, developmental delay, microcephaly, and abnormal facial features, while most patients had feeding difficulties, growth retardation, and ocular abnormalities, and epilepsy and skeletal abnormalities are less common.

Conclusion: We reported the first case of *SSR4*-CDG caused by *SSR4* variant in Chinese population, expanded the clinical and mutation spectra of the disorder, clarified the genetic etiology of the patient, and offered support for the prenatal diagnosis of the index family.

KEYWORDS

SSR4 gene, congenital disorder of glycosylation, type iy, psychomotor retardation, microcephaly, X-linked *SSR4*-CDG

1 Introduction

Congenital disorders of glycosylation (CDG) belong to a group of inherited metabolic diseases caused by defects in genes that play an important role in protein and lipid glycosylation. They have high genetic and clinical heterogeneity (Ondruskova et al., 2020). Studies have reported more than 130 glycosylation-related diseases, of which more than 50 diseases involve the N-glycosylation pathway (Freeze et al., 2014), and the *PMM2*-CDG gene mutation is the most reported glycosylation disorder (Wu et al., 2015). Congenital disorder of glycosylation, type Iy (CGDIy, OMIM: 300,934) caused by *SSR4*-CDG gene mutation was first identified in a 16-year-old male patient by Losfeld et al., in 2014 (Losfeld et al., 2014).

According to the professional edition of HGMD, there have only been 13 patients with a definite genetic diagnosis of X-linked *SSR4*-CDG in the world, and most of them have *de novo* mutations. The clinical manifestations including global developmental delay, microcephaly, hypotonia, and intellectual disability, accompanied by facial and ocular abnormalities, with epilepsy and skeletal abnormalities occurring in a small number of patients (Ng et al., 2015). A recent study reported that patients with X-linked *SSR4*-CDG exhibited connective tissue disease, further expanding the phenotypic spectrum of the disease (Castiglioni et al., 2021). This study is the first report of a Chinese patient with X-linked *SSR4*-CDG caused by a nonsense variant of the *SSR4* gene, upon review of the relevant cases reported in previous literature. Our purpose is to improve clinicians' understanding of the disease, identify the cause of disease in the child from the perspective of genetics, and offer support for the prenatal diagnosis of the pedigree affected with *SSR4*-CDG.

2 Materials and methods

2.1 Patient clinical information

The patient was male and had a birth weight of 2,620 g. He was the first child of his parents (G 1P1). His parents were healthy and have no family history (Figure 1A).

At the age of 2 months, he was found to have hypotonia and difficulty in raising his head in the child healthcare department. At the age of 4 months, no disease-related chromosomal copy number variations (CNVs) or loss of heterozygosity were detected by comparing genomic hybridization (CGH) and SNP Array (4 × 180 K). As a type II atrial septal defect was detected on the heart, he was diagnosed as having congenital heart disease. At the same time, he also had retarded psychomotor development and congenital laryngeal cartilage dysplasia. At the age of 5 months and 26 days, we found he had ptosis of his left

eye, but neostigmine test was negative and he was diagnosed as having congenital ptosis of the upper eyelid of the left eye, microcephaly, large ears, and a small cleft in the left eye. At the age of 9 months, his brain MRI showed that posterior and anterior of pituitary gland has abnormal signals, and he was further diagnosed with Rathke's cleft cyst. This patient denied inherited metabolic diseases family history. He had no special body odor, there were no yellowish white skin and hair as well as denied psychomotor retardation and therefore we ruled out phenylketonuria (PKU) temporary. Since the simple physical examination of patient were normal such as daily diet, daily exercise, no abnormal distension and constipation, so we excluded the patient had Congenital Hypothyroidism (CHT). Since birth, he had no feeding difficulty, no development delay, general social interaction like smile well and newborn screening (NBS) for Methylmalonic acidemia (MMA) was normal, accordingly, the patient could be ruled out MMA. At the age of 1 year, In the physical examination, we found the patient had nystagmus and refractive error, and therefore we consulted Ophthalmologist for any relative eye diseases, he was diagnosed with horizontal nystagmus of the left eyeball, bilateral refractive errors, neck softness, and hypotonia. The patient's result of carbohydrate deficient transferrin (CDT) test (nephelometry) was abnormal elevated, and parental normal test results. At the age of 3 years, his parents planned to have another child and came to our reproductive medical center. Since the etiology of the child was unclear, whole exome sequencing (Trio-WES) of the pedigree, combined with a medical history and pedigree investigation, was recommended. According to genetic counseling, the parents were informed that it was a *de novo* variant, the chance of reoccurrence in next pregnancy was low. Natural pregnancy can be attempted. However, considering the possibility of gonad mosaicism, prenatal diagnosis is necessary in the second trimester. After careful consideration, both couples accept the plan of natural pregnancy and prenatal diagnosis in the second trimester.

This study was approved by the Ethics Committee of the Tangdu hospital of the Air Force Military Medical University, China (K202201-01). And an informed consent form was signed by the parents of the patient.

2.2 Whole exome sequencing analysis

EDTA anticoagulant tubes were used to extract 4 ml of peripheral blood from the child and his parents, respectively, and the child's whole genome DNA was extracted using QIAamp DNA Blood Mini Kit (the operation was performed according to the instructions) and stored at -2 °C for later use.

A NanoWES probe was used for hybrid capture of the whole exome DNA of the pedigree. Other tools used were the Nova Seq 6,000 platform for high-throughput sequencing, an hg38 human

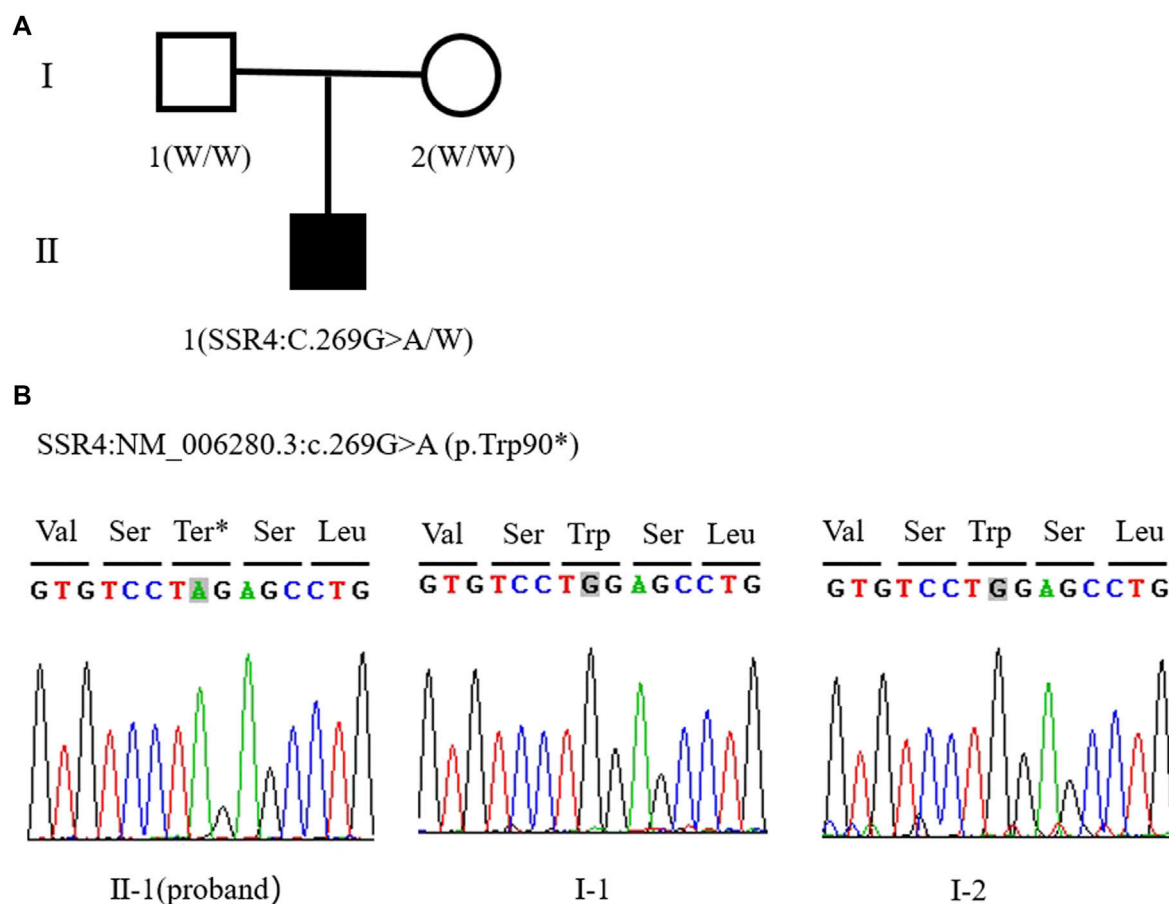


FIGURE 1

(A) Family tree of this study (W: Wild type allele). (B) Sanger sequencing peak of SSR4 gene c.269G > A mutation in proband II - one; I-1. The father of the child; I-2. The mother of the child.

genome assembly for comparison, and the Verita Trekker variant site detection system and Enliven variant site annotation interpretation system for data analysis. Mutation sites with mutation frequency greater than 1% (according to 1,000 Genomes, ExAC, gnomAD, and other databases), as well as non-functional mutation sites (such as synonymous mutation and mutation in non-coding regions), were removed. After the pathogenicity predictions were conducted in SIFT, Polyphen2, CADD, and other software, candidate gene mutation sites were screened according to clinical symptoms, related disease database queries, and literature references, and Sanger sequencing was used for pedigree verification. The primer sequences are as follows: SSR4-4F:CCAGAACATGGCTCTCTATGCT. SSR4-4R: GGGGAAAGACAGGTAGGAACAC. The pathogenicity rating of mutation sites and data interpretation rules refer to the guidelines of the American College of Medical Genetics and Genomics (ACMG) and the recommendations of the ClinGen Sequence Variant Interpretation (SVI) Working Group on the application of the guidelines (Richards et al., 2015).

2.3 RNA extraction and quantitative RT-PCR assays

2.5 ml whole blood was transferred to the blood RNA preservation tube (BioTeke (Beijing) Co., Ltd., No. st1001), fully lysed and extracted blood RNA by the blood RNA Extraction Kit (BioTeke (Beijing) Co., Ltd., No. rp4001). 1 µg RNA was used to reverse transcribe into cDNA by the reverse transcription Kit (Yeasten Biotechnology (Shanghai) Co., Ltd., No. 11123es70). Two primers for QPCR were designed using Primer five software:

SSR4-1F: CCCAGATCACCCCTTCCTAC.

SSR4-1R: CCTCGAGTGACAGGGGAATTG.

SSR4-2F: CTCAGGAAGGCTCAGAGGAA.

SSR4-2R: CGCACTGAAGGCCAAGTAGT.

(Bio-Rad, CFX connect real time system) (Figure 2A). Result of QPCR was determined by SYBR Green Master Mix (Yeasten Biotechnology (Shanghai) Co., Ltd., No.11201es03). All experiments of the three samples were repeated three times,

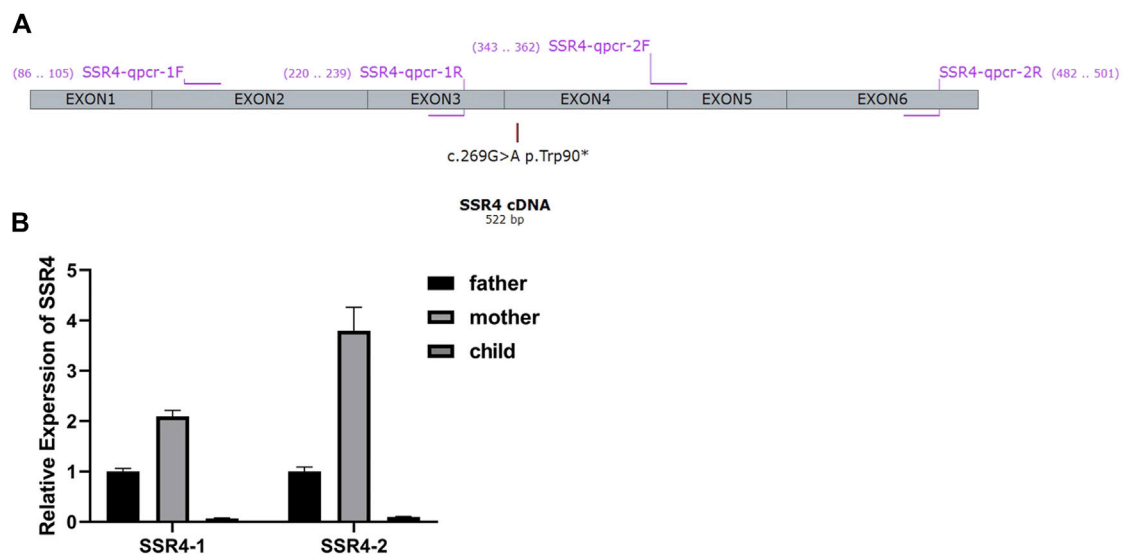


FIGURE 2

(A) Primer design for qPCR. According to the gene sequences upstream and downstream of the mutation site, two pairs of primers were designed using Primer five software. Primers specifically amplify the target region of the SSR4 gene. The length of the amplified product is in the range of 100–200bp. The product cannot form secondary structures. (B) mRNA expression. Expression levels were analyzed with normal males (father of the proband) as controls.

and the Ct values corresponding to each reaction conditions were averaged. All experiments of the three samples were repeated three times, and the Ct values corresponding to each reaction conditions were averaged. Actin gene was using as internal reference. The proband's father was selected as a normal control. The relative expression level was calculated by the comparative CT method ($\Delta\Delta\text{CT}$).

3 Results

3.1 Gene analysis results

Trio-WES showed that the patient carried hemizygous variant NM_006280.3:c.269G>A (p.Trp90*) in the SSR4 gene (chrX:153797732, hg38), his mother did not carry the variant, so the variant was confirmed as *de novo*. But the possibility that his mother carries germ cell mosaicism cannot be ruled out. The Sanger sequencing verification results were consistent with the Trio-WES (Figure 1B). p. Trp90* variant has not been included in the Exome Aggregation Consortium (ExAC), 1,000 Genomes (1000G), or Genome Aggregation Database (gnomAD). This nonsense variant p. Trp90* may produce a premature termination of protein. According to ACMG guidelines, this variant is classified as pathogenic (PVS1+PS2+PM2-Supporting). The data filtering principles are shown in Supplementary Table S1.

3.2 mRNA analysis of patient sample

Two pairs of primers SSR4-1-F/R (Upstream of variation locus) and SSR4-2-F/R (downstream of variation locus) were designed to detect the mRNA expression of the patient. $2^{-\Delta\Delta\text{Ct}}$ method was used to calculate the relative fold gene expression of samples when performing real-time polymerase chain reaction. With the expression level of father as control, SSR4-1 F/R primers test results showed that the expression level of mother was 2.09, and the expression level of patient was 0.07. SSR4-2F/R primer test results showed the expression level of the mother was 3.80 and that of the patient was 0.10 (Figure 2B). It indicated there had mRNA degradation in the patient's sample, which may result from nonsense-mediated mRNA decay (NMD).

3.3 Literature search results

"Congenital disorder of glycosylation, type Iy", "congenital deglycosylation, type Iy" and "SSR4 gene" were used as keywords to search in the China National Knowledge Infrastructure (CNKI), China Online Journals-Wanfang Data Knowledge Service Platform, and Chinese VIP Database (up to December 2021), and no case reports related to CGDIy were retrieved. "SSR4" and "Congenital disorder of glycosylation, type Iy" were used as the keywords to search in the PubMed database (up to

TABLE 1 The clinical findings and the variants in the 14 children with X-linked SSR4-CDG.

Patients	1	2	3	4	5	6	7	8	9	10	11	12	13	14	Cases
Sex	Male	Male	Male	Male	Male	Male	Male	Male	Male	Male	Male	Male	Male	Male	
Age/Origin	10years/Asian	4years/Brazilian	2years/Brazilian	4years/European	14years/Hispanic	13years/Hispanic	5years/Hispanic	NA/Hispanic	16 years/NA	16 years/NA	12 years/French	2 years 2 m/Chilean	2 y10 m/French	3years/Chinese	
Age at diagnosis	NA	NA	NA	NA	NA	NA	NA	NA	NA	NA	8 years	9 months	6 months	3years	
Variant	g.153062612_153063511del	c.358_359del, p.Arg120Glufs*2	c.358_359del, p.Arg120Glufs*2	g.153031975_153105401del	c.417 + 1G>A	c.418- 1G>C	c.418- 1G>C	c.418- 1G>C	c.317del, p.Phe106SerfsTer54	c.147_150del, p. (Phe49Leufs*6)	c.241C>T, p.Gln81*	arr [GRCh37]Xq28 (153011909_153063825)x0	arr [GRCh37]Xq28 (153060022_153063888)x0	c.269G>A p.Trp90*	
Inheritance	<i>de novo</i>	Gonadal mosaicism	Gonadal mosaicism	maternal	<i>de novo</i>	maternal	maternal	maternal	<i>de novo</i>	<i>de novo</i>	<i>de novo</i>	<i>de novo</i>	maternal	<i>de novo</i>	
Developmental retardation	+	+	+	+	+	+	+	+	+	+	+	+	+	+	14/14
Mental retardation	+	+	+	+	+	+	+	+	+	+	+	+	+	+	14/14
Microcephaly	+	+	+	+	+	+	+	+	+	+	+	+	+	+	14/14
Abnormal facial shape	+	+	+	+	+	+	+	+	+	+	+	+	+	+	14/14
Muscular hypotonia	+	+	+	+	+	+	+	+	+	+	+	+	+	+	14/14
Feeding difficulties	+	+	+	+	+	+	+	-	+	-	+	+	-	-	10/14
Abnormality of the gastrointestinal tract	+	+	+	+	+	+	+	-	Gastroesophageal reflux	-	-	Gastroesophageal reflux, gastrostomy, difficulties/ aversion to food with certain textures	Gastroesophageal reflux, no dysphagia	-	10/14
Growth retardation	+	+	+	+	-	+	+	-	+	-	+	+	+	-	10/14
Visual acuity test abnormality	-	+	+	+	+	+	+	+	-	+	+	-	+	+	11/14
Brain MRI	-	-	-	+	-	+	+	-	-	+	+	+	+	-	7/14
Skeletal Anomalies	-	-	+	+	+	-	-	-	-	-	-	Joint laxity, severe deformation of the feet in valgus, orthopedic surgery (11.5 years)	Fifth finger clinodactyly, joint laxity	Superposition of the second toe without syndactyly, joint laxity	6/14
Epilepsy	+	-	-	+	+	-	-	+	Seizure disorder was mild	Febrile	-	-	-	-	6/14
Abnormality of coagulation	+	-	-	-	-	-	-	-	Persistent bleeding and easy bruising	-	FVIII = 48% [60–150%]; vWF 34% [50–150%]	APTT = 11.2 [24.8–33.2 s]; PT = 97% [80–120%]	-	-	4/14
Cardiac anomalies	-	-	-	-	+	-	-	-	-	-	-	-	-	-	2/14
Abnormality of the kidney	-	-	-	-	+	-	-	-	-	-	-	-	-	-	1/14
References	Ng et al. (2015)	Losfeld et al. (2014)	Medrano et al. (2019)	Castiglioni et al. (2021)	This work										

Transcript, NM_006280.3. y, year. m, month.

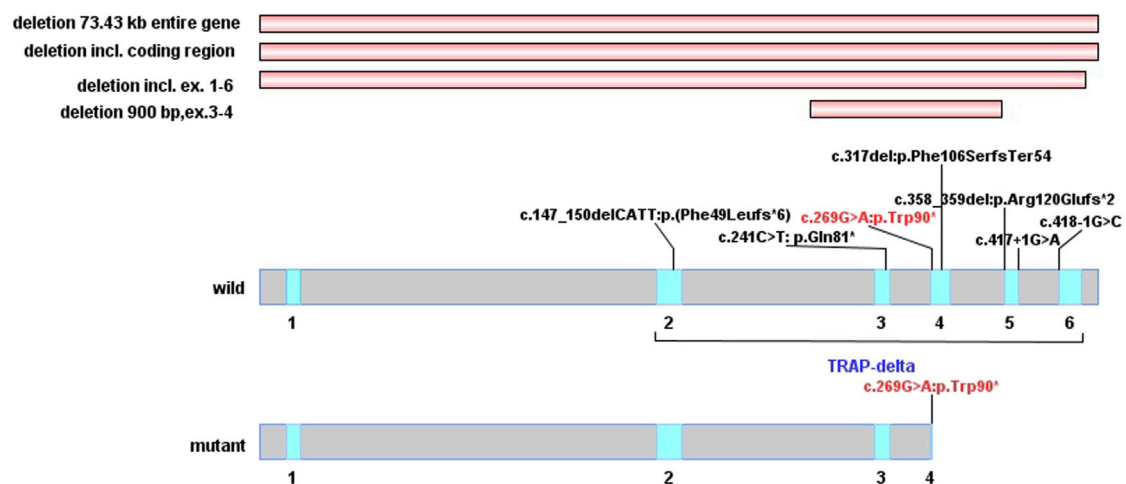


FIGURE 3

Distribution of SSR4 gene mutation. (The red horizontal stripes are the previously reported type of copy number variations. In wild-type and mutant protein domains, the red font is the variation reported in this study, and the black variations are previously reported. The blue area of delta subunit precursor (TRAP-delta) contains five exons from exon2 to exon6).

December 2021), and a total of four papers related to SSR4 gene mutation involving 13 patients were retrieved (Losfeld et al., 2014; Ng et al., 2015; Medrano et al., 2019; Castiglioni et al., 2021). All 14 patients (including the patient in this paper) are male, with clinical manifestations of developmental delay (14/14), intellectual disability (14/14), microcephaly (14/14), hypotonia (14/14), and facial abnormality (14/14). Among them, facial abnormalities mainly include a small jaw, large ears, sunken eye sockets, a large mouth, large spacing between teeth, and strabismus. Most patients have ocular abnormalities (11/14), feeding difficulties (10/14), gastrointestinal problems (10/14) in infancy, as well as postnatal growth retardation (10/14). Table 1 was summary of the clinical findings and the variants in the 14 children with X-linked SSR4-CDG. Figure 3 was drawn using IBS software according to the instruction (Liu et al., 2015).

4 Discussion

Glycosylation is one of the most common post-translational modifications of proteins and lipids, and it plays a crucial role in the growth and development of organisms (Moremen et al., 2012). -Congenital disorders of glycosylation (CDG) are a series of metabolic disorders due to defects in a complex chemical process known as glycosylation. Glycosylation involves multiple biosynthetic pathways, mainly N-glycosylation, which widely affects various systems and organs. Therefore, affected individuals have complex and diverse clinical phenotypes and are difficult to diagnose (Freeze et al., 2014; Ferreira et al., 2018; Ng and Freeze, 2018). The clinical phenotype varies depending on the organ involved, with the brain,

eyes, and bones generally being the most commonly affected (Francisco et al., 2019). The clinical manifestations are predominantly neurological, including psychomotor retardation or cognitive disorders, epilepsy, hypotonia, ataxia, polyneuropathy, and stroke-like events (Freeze et al., 2015; Gardeitchik et al., 2018; Paprocka et al., 2021). Some patients also have deformities, such as facial deformity, inverted nipples, and subcutaneous fat pads (Francisco et al., 2019).

The modes of inheritance of CDG include autosomal recessive inheritance, autosomal dominant inheritance, and X-linked recessive inheritance. The SSR4-CDG mutation reported in this study can lead to an X-linked recessive congenital disorder of glycosylation, type Iy (OMIM: 300,934). As of February 2021, 13 patients with X-linked SSR4-CDG have been included in the professional edition of HGMD. The 13 patients have five common clinical phenotypes, including psychomotor retardation, intellectual disability, facial abnormality, microcephaly, and hypotonia. Most patients (10/13) have gastrointestinal problems caused by feeding difficulties, growth retardation, and visual problems such as nystagmus and refractive errors. Half of the patients (6/13) have non-specific imaging abnormalities, including delayed myelination, corpus callosum dysplasia, decreased ventricular white matter, and absence of transparent septum. More than half of the patients have epilepsy or febrile seizures and skeletal abnormalities (skeletal deformities, scoliosis, and delayed bone age). A minority of patients have coagulation disorders, cardiac abnormalities (2/13), and renal abnormalities (1/13) (Castiglioni et al., 2021). The clinical features of the present patient are essentially consistent with the phenotypes of the X-linked SSR4-CDG patients reported in previous literature. In addition to the five typical features, he also showed obvious vision problems, nystagmus, bilateral refractive errors,

cardiac abnormalities, and special features such as high arched eyebrows and low ears. However, it is worth noting that these typical manifestations are not only limited to *SSR4* gene-related CDG patients, but also may be associated with other CDG subtypes, such as congenital disorders of glycosylation caused by *SSR3* gene variants or syndromes associated with developmental delay. For similar clinic manifestations patients, phenotypes overlap each other. Therefore, simple and economical biochemical tests, such as the determination of carbohydrate deficient transferrin (CDT), can be performed firstly, then followed by further genetic testing for accurate molecular typing. Due to the high clinical and genetic heterogeneity of glycosylation disorders, it is difficult to diagnose based on clinical manifestations alone, so genetic testing and analysis should be performed as soon as possible.

Translocon-associated protein (TRAP) is a membrane protein that is ubiquitous in all eukaryotes (Sommer et al., 2013). It is located in the endoplasmic reticulum membrane as a signal sequence receptor protein and is involved in protein transport across the endoplasmic reticulum membrane (Braunger et al., 2018). The TRAP complex consists of four signal sequence receptor proteins (*SSR1-4*), of which the *SSR4* gene encodes the delta subunit (Hartmann et al., 1993). Nagasawa et al. have confirmed that knocking out any subunit of the TRAP complex will affect the function of the entire complex (Nagasawa et al., 2007), while another study has shown that the TRAP complex binds to the oligosaccharide transferase complex and directly participates in N-glycosylation. Additionally, overexpression of the wild-type *SSR4* allele can restore the glycosylation of other members of the TRAP complex (Losfeld et al., 2014).

A recent study identified the TRAP complex as a key regulator for the maintenance of protein glycosylation modifications under conditions of cellular stress (Phoomak et al., 2021). The *SSR4* gene (NM_006280.3) consists of six exons encoding 173 amino acid residues, of which amino acids 1–23 are the signal peptide sequences of the protein and amino acids 23–173 constitute the important functional domain structure of the *SSR4* protein TRAP- δ subunit. The p. Trp90* mutation of the *SSR4* gene found in this study is located in exon 4 (Figure 3), which can cause amino acids after the 90th position of the *SSR4* protein to be unable to be translated normally. As a result, a truncated protein with only 90 amino acids is produced, the spatial structure of the protein is destroyed, and the TRAP- δ subunit becomes incomplete; which, in turn, affects the normal function of the *SSR4* subunit and is expected to affect the role of TRAP complex in endoplasmic reticulum protein transport and glycosylation modification.

A total of 10 *SSR4* gene mutations associated with CDG have been included in PubMed and HGMD databases so far, including one nonsense mutation, two splicing mutations, three frameshift mutations caused by deletions, and four large fragment deletions, with no missense mutations having been reported. Seven of these mutations are *de novo* variants, and three (c.418-1G>C, 73.43 kb

deletion, and deletion in the Xp28: 153060022–153063888 region) are inherited from mothers with mild symptoms or from asymptomatic mothers, respectively. As a haploinsufficiency of glycosylation disorder causative gene, all the reported pathogenic mutations in *SSR4* gene were loss-of-function, four of which were located in the downstream region of c.269G>A. It's predicted that they can produce shorter truncated protein and induce NMD mechanism. In this study, by detecting the mRNA expression of the *SSR4* gene in the blood, the mRNA expression of *SSR4* gene in the blood of the patient was significantly reduced than that of normal controls, which might be due to the degradation of mRNA caused by NMD. This may result in impaired protein function and lead to disease.

All the mutations are loss-of-function and there is no report on the pathogenicity of missense mutations, which may be related to the pathogenesis of the disease itself. Correlations between genotype and phenotype are difficult to establish due to the limited reported genetic mutations and few cases. This paper reports the first case of X-linked *SSR4*-CDG in China, enriches the mutation and phenotype spectra of the *SSR4* gene, improves clinicians' understanding of the disease, provides reliable genetic evidence for prenatal diagnosis of the pedigree, and lays a foundation for the follow-up study of the molecular mechanism of the disease.

At present, the whole-exome sequencing technology has been widely used in the detection of clinical genetic diseases. As the sequencing technology becomes mature and the costs reduce, more genetic diseases will be discovered, especially in children with psychomotor retardation. Genetic testing not only provides precise directions for the diagnosis and treatment of children with rare diseases but also prevents birth defects and promotes high-quality development. At present, most of the treatments for children with genetic diseases are symptomatic treatment and management. Early detection and early intervention can reduce the occurrence of complications and improve children's quality of life.

Data availability statement

The original contributions presented in the study are included in the article/Supplementary Material, further inquiries can be directed to the corresponding author.

Ethics statement

The studies involving human participants were reviewed and approved by Ethics Committee of the Tangdu hospital of the Air Force Military Medical University, China. Written informed consent to participate in this study was provided by the participants' legal guardian/next of kin. Written informed consent was obtained from the minor(s)' legal

guardian/next of kin for the publication of any potentially identifiable images or data included in this article.

Author contributions

Jun Wang wrote the manuscript and coordinated and managed the study. Xingqing Gou and Jing Zhang collected the clinical data and the phenotype of the patient. They analyzed the next-generation sequencing data. Xiyi Wang and Nan Zhao performed the Sanger sequencing data analyses and detected the mRNA expression of *SSR4* gene in blood. Xiaohong Wang revised the manuscript. The author(s) read and approved the final manuscript.

Funding

This work was supported by the Shaanxi Province Key R & D Program General Project (2021SF-012) and the National Natural Science Foundation of China (82071717).

Acknowledgments

Our sincere gratitude goes to Berry Genomics for their diagnostic reagents. We also thank the patient and his family for their participation in this study. Here, we also thank Hudson H.

References

- Braunger, K., Pfeffer, S., Shrimal, S., Gilmore, R., Berninghausen, O., Mandon, E. C., et al. (2018). Structural basis for coupling protein transport and N-glycosylation at the mammalian endoplasmic reticulum. *Science* 360 (6385), 215–219. doi:10.1126/science.aar7899
- Castiglioni, C., Feillet, F., Barnerias, C., Wiedemann, A., Muchart, J., Cortes, F., et al. (2021). Expanding the phenotype of X-linked SSR4-CDG: Connective tissue implications. *Hum. Mutat.* 42 (2), 142–149. doi:10.1002/humu.24151
- Ferreira, C. R., Altassan, R., Marques-Da-Silva, D., Francisco, R., Jaeken, J., and Morava, E. (2018). Recognizable phenotypes in CDG. *J. Inherit. Metab. Dis.* 41 (3), 541–553. doi:10.1007/s10545-018-0156-5
- Francisco, R., Marques-da-Silva, D., Brasil, S., Pascoal, C., Dos Reis Ferreira, V., Morava, E., et al. (2019). The challenge of CDG diagnosis. *Mol. Genet. Metab.* 126 (1), 1–5. doi:10.1016/j.ymgme.2018.11.003
- Freeze, H. H., Chong, J. X., Bamshad, M. J., and Ng, B. G. (2014). Solving glycosylation disorders: Fundamental approaches reveal complicated pathways. *Am. J. Hum. Genet.* 94 (2), 161–175. doi:10.1016/j.ajhg.2013.10.024
- Freeze, H. H., Eklund, E. A., Ng, B. G., and Patterson, M. C. (2015). Neurological aspects of human glycosylation disorders. *Annu. Rev. Neurosci.* 38, 105–125. doi:10.1146/annurev-neuro-071714-034019
- Gardeitchik, T., Wyckmans, J., and Morava, E. (2018). Complex phenotypes in inborn errors of metabolism: Overlapping presentations in congenital disorders of glycosylation and mitochondrial disorders. *Pediatr. Clin. North Am.* 65 (2), 375–388. doi:10.1016/j.pcl.2017.11.012
- Hartmann, E., Gorlich, D., Kostka, S., Otto, A., Kraft, R., Knespel, S., et al. (1993). A tetrameric complex of membrane-proteins in the endoplasmic-reticulum. *Eur. J. Biochem.* 214 (2), 375–381. doi:10.1111/j.1432-1033.1993.tb17933.x
- Liu, W. Z., Xie, Y., Ma, J., Luo, X., Nie, P., Zuo, Z., et al. (2015). IBS: An illustrator for the presentation and visualization of biological sequences. *Bioinformatics* 31 (20), 3359–3361. doi:10.1093/bioinformatics/btv362
- Losfeld, M. E., Ng, B. G., Kircher, M., Buckingham, K. J., Turner, E. H., Eroshkin, A., et al. (2014). A new congenital disorder of glycosylation caused by a mutation in *SSR4*, the signal sequence receptor 4 protein of the TRAP complex. *Hum. Mol. Genet.* 23 (6), 1602–1605. doi:10.1093/hmg/ddt550
- Medrano, C., Vega, A., Navarrete, R., Ecay, M. J., Calvo, R., Pascual, S. I., et al. (2019). Clinical and molecular diagnosis of non-phosphomannomutase 2 N-linked congenital disorders of glycosylation in Spain. *Clin. Genet.* 95 (5), 615–626. doi:10.1111/cge.13508
- Moremen, K. W., Tiemeyer, M., and Nairn, A. V. (2012). Vertebrate protein glycosylation: Diversity, synthesis and function. *Nat. Rev. Mol. Cell Biol.* 13 (7), 448–462. doi:10.1038/nrm3383
- Nagasawa, K., Higashi, T., Hosokawa, N., Kaufman, R. J., and Nagata, K. (2007). Simultaneous induction of the four subunits of the TRAP complex by ER stress accelerates ER degradation. *EMBO Rep.* 8 (5), 483–489. doi:10.1038/sj.embor.7400933
- Ng, B. G., and Freeze, H. H. (2018). Perspectives on glycosylation and its congenital disorders. *Trends Genet.* 34 (6), 466–476. doi:10.1016/j.tig.2018.03.002
- Ng, B. G., Raymond, K., Kircher, M., Buckingham, K. J., Wood, T., Shendure, J., et al. (2015). Expanding the molecular and clinical phenotype of SSR4-CDG. *Hum. Mutat.* 36 (11), 1048–1051. doi:10.1002/humu.22856
- Ondruskova, N., Cechova, A., Hansikova, H., Honzik, T., and Jaeken, J. (2020). Congenital disorders of glycosylation: Still "hot" in 2020. *Biochim. Biophys. Acta. Gen. Subj.* 1865 (1), 129751. doi:10.1016/j.bbagen.2020.129751
- Paprocka, J., Jezela-Stanek, A., Tylki-Szymanska, A., and Grunewald, S. (2021). Congenital disorders of glycosylation from a neurological perspective. *Brain Sci.* 11 (1), 88. doi:10.3390/brainsci11010088
- Phoomak, C., Cui, W., Hayman, T. J., Yu, S.-H., Zhao, P., Wells, L., et al. (2021). The translocon-associated protein (TRAP) complex regulates quality control of N-linked glycosylation during ER stress. *Sci. Adv.* 7 (3), eabc6364. doi:10.1126/sciadv.abc6364

Freeze and Bobby G. Ng (Human Genetics Program, Sanford Children's Health Research Center) for providing us with clinical phenotype details published in their article (10.1002/humu.22856).

Conflict of interest

The authors declare that the research was conducted in the absence of any commercial or financial relationships that could be construed as a potential conflict of interest.

Publisher's note

All claims expressed in this article are solely those of the authors and do not necessarily represent those of their affiliated organizations, or those of the publisher, the editors and the reviewers. Any product that may be evaluated in this article, or claim that may be made by its manufacturer, is not guaranteed or endorsed by the publisher.

Supplementary material

The Supplementary Material for this article can be found online at: <https://www.frontiersin.org/articles/10.3389/fgene.2022.955732/full#supplementary-material>

Richards, S., Aziz, N., Bale, S., Bick, D., Das, S., Gastier-Foster, J., et al. (2015). Standards and guidelines for the interpretation of sequence variants: A joint consensus recommendation of the American College of medical genetics and genomics and the association for molecular pathology. *Genet. Med.* 17 (5), 405–424. doi:10.1038/gim.2015.30

Sommer, N., Junne, T., Kalies, K. U., Spiess, M., and Hartmann, E. (2013). TRAP assists membrane protein topogenesis at the mammalian ER membrane.

Biochim. Biophys. Acta 1833 (12), 3104–3111. doi:10.1016/j.bbamcr.2013.08.018

Wu, R., Qiu, K., Li, D., Li, Y., Deng, B., Luo, X., et al. (2015). Analysis of PMM2 gene variant in an infant with congenital disorders of glycosylation type 1a. *Zhonghua Yi Xue Yi Chuan Xue Za Zhi* 36 (4), 314–317. doi:10.3760/cma.j.issn.1003-9406.2019.04.006



OPEN ACCESS

EDITED BY

Babak Behnam,
National Sanitation Foundation
International, United States

REVIEWED BY

Emilia Severin,
Carol Davila University of Medicine and
Pharmacy, Romania
Muhammad Umair,
King Abdullah International Medical
Research Center (KAIMRC), Saudi Arabia

*CORRESPONDENCE

Zhengqing Qiu,
✉ zhengqingqiu33@aliyun.com

SPECIALTY SECTION

This article was submitted to Genetics of
Common and Rare Diseases,
a section of the journal
Frontiers in Genetics

RECEIVED 20 November 2022

ACCEPTED 02 January 2023

PUBLISHED 13 January 2023

CITATION

Zhang Z, Ma M, Zhang W, Zhou Y, Yao F,
Zhu L, Wei M and Qiu Z (2023), Phenotypic
and genetic characteristics of 130 patients
with mucopolysaccharidosis type II: A
single-center retrospective study in China.
Front. Genet. 14:1103620.
doi: 10.3389/fgene.2023.1103620

COPYRIGHT

© 2023 Zhang, Ma, Zhang, Zhou, Yao, Zhu,
Wei and Qiu. This is an open-access article
distributed under the terms of the [Creative
Commons Attribution License \(CC BY\)](#).
The use, distribution or reproduction in
other forums is permitted, provided the
original author(s) and the copyright
owner(s) are credited and that the original
publication in this journal is cited, in
accordance with accepted academic
practice. No use, distribution or
reproduction is permitted which does not
comply with these terms.

Phenotypic and genetic characteristics of 130 patients with mucopolysaccharidosis type II: A single-center retrospective study in China

Zhenjie Zhang¹, Mingsheng Ma¹, Weimin Zhang², Yu Zhou¹,
Fengxia Yao², Lisi Zhu², Min Wei¹ and Zhengqing Qiu^{1*}

¹Department of Pediatrics, Peking Union Medical College Hospital, Chinese Academy of Medical Sciences and Peking Union Medical College, Beijing, China, ²Department of Genetics Laboratory, Peking Union Medical College Hospital, Chinese Academy of Medical Sciences and Peking Union Medical College, Beijing, China

Background: Mucopolysaccharidosis Type II (MPS II) is a rare, progressive and ultimately fatal X-linked lysosomal storage disorder caused by mutations in the iduronate-2-sulfatase (IDS) gene. This report conducted a retrospective analysis to investigate the clinical characteristics, genotypes and management strategies in a large cohort of Chinese patients with MPS II.

Methods: In this study, we explored 130 Chinese patients with MPS II between September 2008 and April 2022. Clinical manifestations, auxiliary examination, IDS pathogenic gene variants and IDS enzyme activity, surgical history were analysed in the study.

Results: A total of 130 patients were enrolled and the mean age at diagnosis was 5 years old. This study found the most common symptoms in our patients were claw-like hands, followed by coarse facial features, birthmarks (Mongolian spot), delayed development, inguinal or umbilical hernia. The most commonly cardiac manifestations were valve abnormalities, which were mitral/tricuspid valve regurgitation (71.9%) and aortic/pulmonary valve regurgitation (36.8%). We had found 43 different IDS pathogenic gene variants in 55 patients, included 16 novel variants. The variants were concentrated in exon 9 (20% = 11/55), exon 3 (20% = 11/55) and exon 8 (15% = 8/55). A total of 50 patients (38.5%) underwent surgical treatment, receiving a total of 63 surgeries. The average age of first surgery was 2.6 years, and the majority of surgery (85.7%, 54/63) was operated before 4 years old. The most common and earliest surgery was hernia repair. Three patients were died of respiratory failure.

Conclusion: This study provided additional information on the clinical, cardiac ultrasound and surgical procedure in MPS II patients. Our study expanded the genotype spectrum of MPS II. Based on these data, characterization of MPS II patients group could be used to early diagnosis and treatment of the disease.

Abbreviations: DS, Dermatan sulfate; ERT, Enzyme replacement therapy; HS, Heparan sulfate; HGMD, Human Gene Mutation Database; HOS, Hunter Outcome Survey; IDS, Iduronate-2-sulfatase; MPS II, Mucopolysaccharidosis Type II; NCBI, National Center for Biotechnology Information.

KEYWORDS

mucopolysaccharidosis type II, clinical characteristics, surgical history, genotypes, IDS gene variants

1 Introduction

Mucopolysaccharidosis type II (MPS II, Hunter Syndrome; OMIM 309900) is a rare, progressive and ultimately fatal X-linked disorder. It is caused by a deficiency of the enzyme iduronate-2-sulfatase (IDS; EC 3.1.6.13) due to the IDS gene variants (Xq28) (Clarke et al., 1992). Like all X-linked recessive disorders, MPS II affect males almost exclusively, although rare cases of MPS II in females do occur (Neufeld et al., 1977). The prevalence in European countries ranges from .13/100,000 to .71/100,000 (Khan et al., 2017), while the Asian countries is relatively higher. For example, the prevalence of live births in Korea and Japan are .74/100,000 and .84/100,000 respectively (Khan et al., 2017). MPS II accounted for approximately half (47.4%–58.0%) of all cases of mucopolysaccharidosis in Eastern Asian countries (Chen et al., 2016), compared with only 7.6% of mucopolysaccharidosis patients in the Netherlands and Portugal (Stapleton et al., 2017).

IDS deficiency leads to an accumulation of dermatan sulfate (DS) and heparan sulfate (HS) in multiple organs and tissues, resulting in progressive cell degradation and failure (Demydchuk et al., 2017). Organs implicated include the teeth, ear, nose and throat, heart and respiratory system, gastrointestinal tract and the musculoskeletal system, central nervous system (Stapleton et al., 2017). As a consequence, patients with MPS II present with multiple clinical manifestations that can include coarse facial features, hypertrophic tonsils and adenoids, claw-like hands or joint stiffness, scoliosis, otitis media, hepatosplenomegaly, abdominal or inguinal hernias (Wraith et al., 2008a; Martin et al., 2008). MPS II may also present with neurological manifestations (Wraith et al., 2008b). Patients typically have a normal appearance at birth afterwards symptoms beginning at 18 months to 4 years old (Scarpa et al., 2011). MPS II management has historically been limited to supportive and palliative treatments involving multiple clinical departments. The last decade has seen the emergence of enzyme replacement therapy (ERT), beginning with the approval of idursulfase in the United States in 2006. However, approval for MPS II ERT in China was only granted in 2019 (Kang et al., 2019). To date, more than 600 unique IDS pathogenic gene variants have been identified, with approximately half of these accounted for exonic single point variants (Human Gene Mutation Database (HGMD): IDS Gene: <http://www.hgmd.cf.ac.uk>).

Despite China's large population, and the relatively high prevalence of MPS II in Eastern Asia, there had been few reports of the clinical characteristics, genotypes or management strategies for Chinese patients with MPS II. Most published data were limited to case reports or include relatively small patient numbers. There is no newborn screening for MPS II in mainland China. A deeper understanding of the clinical characteristics and current treatment approaches for MPS II in China would be highly valuable for improving disease awareness, rates of early detection and diagnosis, supporting early initiation of palliative/supportive care and ultimately improving patients' quality of life. Therefore, we conducted a single-center retrospective study to investigate the clinical characteristics, genotypes and management strategies in a large cohort of Chinese patients with MPS II.

2 Materials and methods

2.1 Patients

This was a retrospective, single center, observational analysis of medical records for patients treated at Peking Union Medical College Hospital, Beijing, China, between September 2008 and April 2022. Eligible patients had a diagnosis of MPS II based on patient clinical presentation, laboratory examination, IDS enzyme activity in plasma and IDS gene analysis. Patients were also required to have medical records covering clinical presentation and treatment for MPS II. The study was approved by the hospital Ethics Committee and was conducted in accordance with the Helsinki Declaration ethical principles for medical research involving human subjects. Written informed consent was obtained from every patient or parents prior to inclusion in the study.

2.2 Clinical assessments

Clinical manifestations were collected by medical records. Cardiac ultrasound was used to assess for cardiac manifestations of MPS II. Brain MRI was used to evaluate cranial manifestations of MPS II.

2.3 Enzyme activity testing

IDS activity levels in plasma were determined by fluorimetric enzyme assay using 4-methylumbelliferone-labelled iduronate-2-sulfate as a substrate for IDS, as previously described (Voznyi et al., 2001). The assays were performed at the Department of Genetics laboratory, Peking Union Medical College Hospital. The normal value was 240.2–668.2 nmol/4 h/mL. MPS II could be diagnosed when the IDS enzyme activity result was less than 20 nmol/4 h/mL.

2.4 IDS genetic analysis

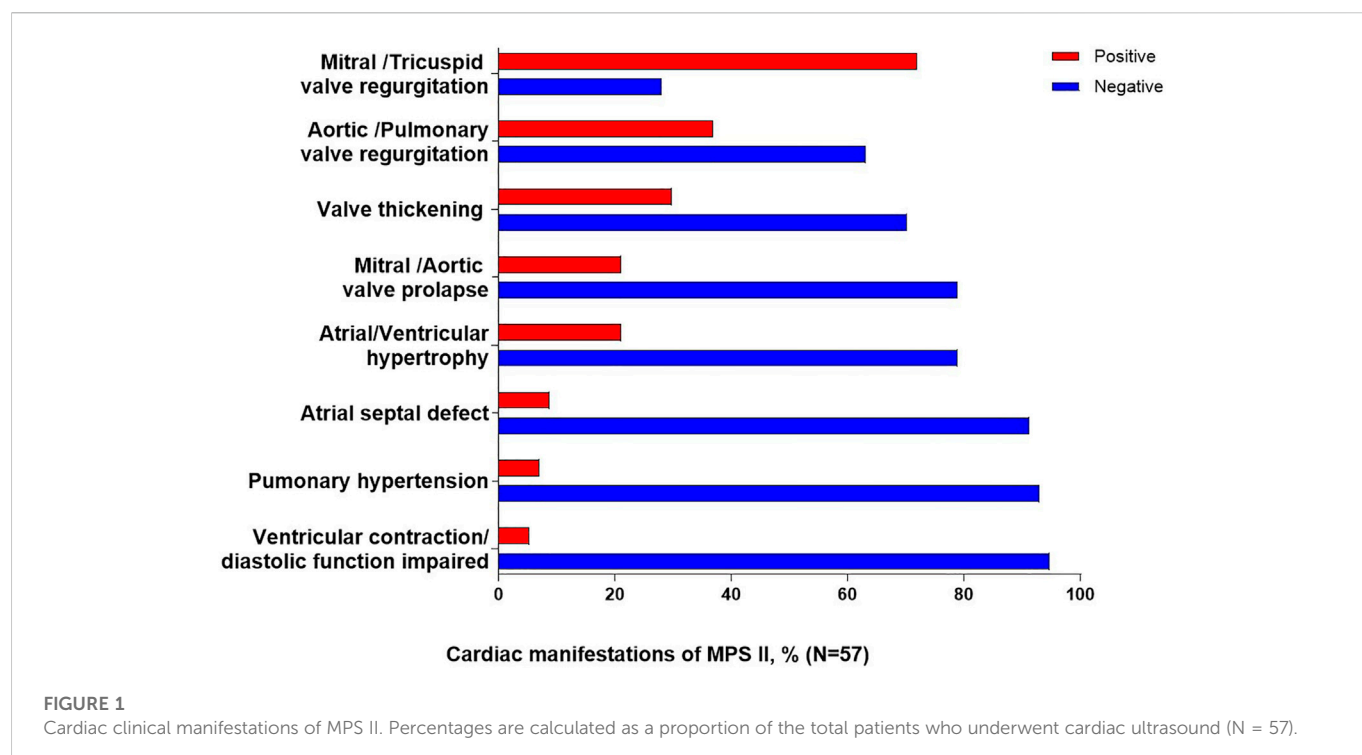
Peripheral blood was collected in EDTA tubes and genomic DNA was isolated using the QIAamp DNA Blood Midi Kit (Qiagen, Germany). DNA concentration was quantitatively isolated by NanoDrop 2000 (Thermo Fisher Scientific, MA). The exonic regions and exon-intron boundaries of the IDS gene were then amplified by PCR and sequenced using the Sanger technique and standard protocols (Kosuga et al., 2016).

2.5 *In silico* analysis

A variety of pathogenicity prediction tools were used to predict the pathogenicity potential of the novel pathogenic gene variants. Mutation Taster (<http://www.mutationtaster.org>), SIFT/PROVEAN (<http://provean.jcvi.org>) and PolyPhen-2 (<http://genetics.bwh.harvard.edu/pph2>) web software.

TABLE 1 Patient age at onset of clinical manifestations of MPS II. Percentage (Number).

	Claw-like hands	Coarse facial	Delayed development	Hernia	Sleep apnoea	Spine deformities	Deafness
<2 years old	18.8% (19)	13.1% (13)	11.2% (11)	8.1% (8)	3.9% (4)	6.9% (7)	2.0% (2)
2–4 years old	33.7% (34)	36.3% (36)	31.6% (31)	21.4% (21)	21.8% (22)	10.8% (11)	9.2% (9)
4–6 years old	29.7% (30)	31.3% (31)	23.4% (23)	28.6% (28)	20.8% (21)	13.7% (14)	6.1% (6)
6–8 years old	5.9% (6)	6.0% (6)	6.1% (6)	4.1% (4)	7.9% (8)	1.0% (1)	3.1% (3)
>8 years old	9.9% (10)	11.1% (11)	7.1% (7)	7.1% (7)	4.9% (5)	4.9% (5)	5.1% (5)
Positive	98.0% (99)	97.9% (97)	79.6% (78)	69.4% (68)	59.4% (60)	37.3% (38)	25.5% (25)
Total	100% (101)	100% (99)	100% (98)	100% (98)	100% (101)	100% (102)	100% (98)



2.6 Statistics

The quantitative data were summarized by means and standard deviations (SDs). Pathogenic gene variant types and clinical signs were represented by frequency distribution. Descriptive statistics were used to summarize data. All analyses were conducted using SPSS v19.0 (IBM, United States).

3 Results

3.1 Patients

In total, 269 patients were diagnosed with MPS II in our hospital during the study period of September 2008 to April 2022. Among them, 130 patients from 119 families had suitable medical records available and were included in the study analysis. All included patients

were male and 11 had a known family history of MPS II. The mean age at diagnosis was 5 years old ± 2.6 (range: 2 months to 22 years old).

3.2 Clinical manifestations

The most common clinical manifestations were musculoskeletal and dermatologic abnormalities. The onset age of different clinical manifestations in MPS II patients was shown in Table 1. 98.0% (99/101) patients had claw-like hands (joint stiffness), most of these patients (63.4%, 64/101) occurred between 2 and 6 years old. 97.9% (97/99) patients had coarse facial features, which also commonly occurred in patients aged 2–6 (67.6%, 67/99). In addition, 95.8% (91/95) patients had birthmarks (Mongolian spot), 79.6% (78/98) had delayed development or growth, 69.4% (68/98) had inguinal or umbilical hernia, 59.4% (60/101) had sleep apnoea, 37.3% (38/102) had spine deformities, and 25.5% (25/98) patients had deafness. It

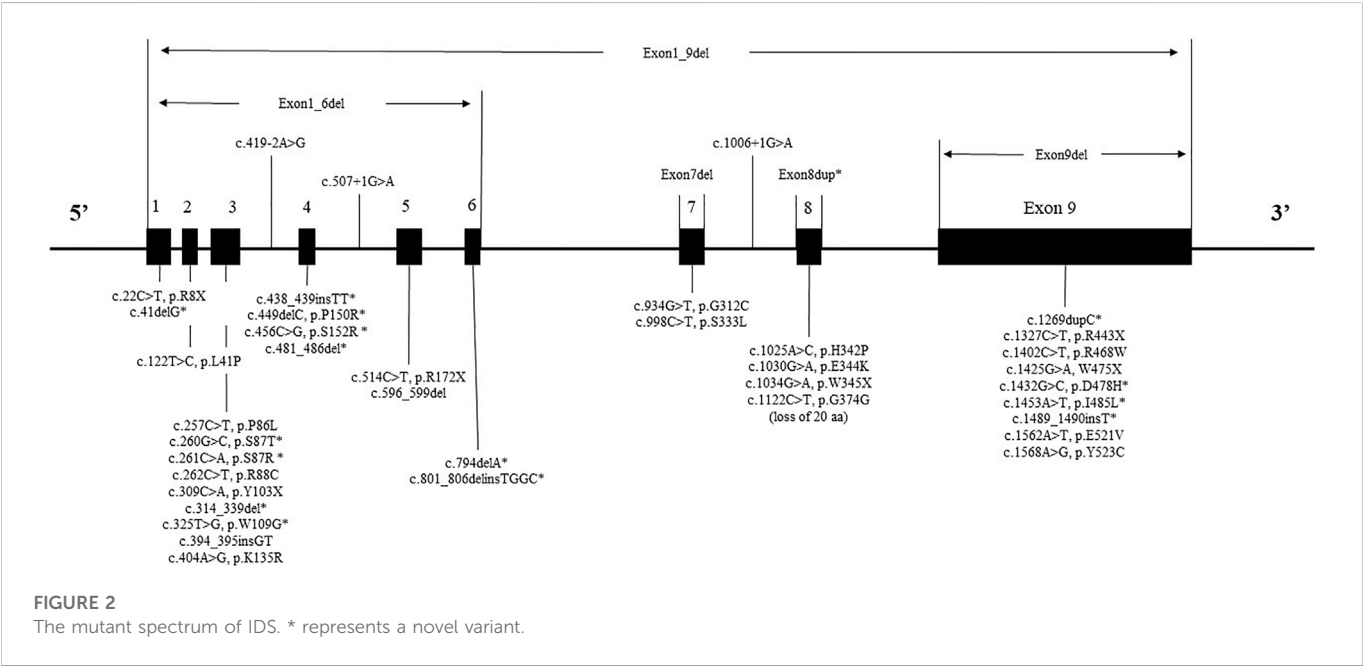
TABLE 2 The IDS variants genotype in Chinese patients with MPS II (*n* = 55).

Category	Variant	Consequence	No. of occurrences	Novel variant
Exonic point variant	c.1122C>T	p.G374G (loss of 20 aa)	4	—
	c.262C>T	p.R88C	3	—
	c.514C>T	p.R172X	3	—
	c.934G>T	p.G312C	2	—
	c.998C>T	p.S333L	2	—
	c.1402C>T	p.R468W	2	—
	c.22C>T	p.R8X	1	—
	c.122T>C	p.L41P	1	—
	c.257C>T	p.P86L	1	—
	c.260G>C	p.S87T	1	Novel
	c.261C>A	p.S87R	1	Novel
	c.309C>A	p.Y103X	1	—
	c.325T>G	p.W109G	1	Novel
	c.404A>G	p.K135R	1	—
	c.456C>G	p.S152R	1	Novel
	c.1025A>C	p.H342P	1	—
	c.1030G>A	p.E344K	1	—
	c.1034G>A	p.W345X	1	—
	c.1327C>T	p.R443X	1	—
	c.1425G>A	p.W475X	1	—
	c.1432G>C	p.D478H	1	Novel
	c.1453A>T	p.I485L	1	Novel
	c.1562A>T	p.E521V	1	—
	c.1568A>G	p.Y523C	1	—
Gross deletion	EX1_9del		1	—
	EX1_6del		1	—
	EX7del		1	—
	EX9del		1	—
Small deletion	c.449delC	p.P150R	2	Novel
	c.596_599delAACA	p.K199Rfs*13	2	—
	c.41delG	p.G14Vfs*4	1	Novel
	c.314_339del	p.F105Wfs*31	1	Novel
	c.481_486del	p.161_162del	1	Novel
	c.794delA	p.N265Tfs*15	1	Novel
Small insertion	c.394_395insGT	p.S132Cfs*82	1	—
	c.438_439insTT	p.D147Lfs*67	1	Novel
	c.1269dupC	p.V424Rfs*7	1	Novel
	c.1489_1490insT	p.Y497Lfs*2	1	Novel
Splicing	c.419–2A>G		1	—

(Continued on following page)

TABLE 2 (Continued) The IDS variants genotype in Chinese patients with MPS II (n = 55).

Category	Variant	Consequence	No. of occurrences	Novel variant
	c.507 + 1G>A		1	—
	c.1006 + 1G>A		1	—
Duplication	Exon8 duplication		1	Novel
Small indels	c.801_806delinsTGGC	p.W267Cfs*74	1	Novel



could be seen in Table 1 that the onset of all kinds of MPS II symptoms generally occurred between 2 and 6 years old.

3.3 Cardiac ultrasound and brain MRI

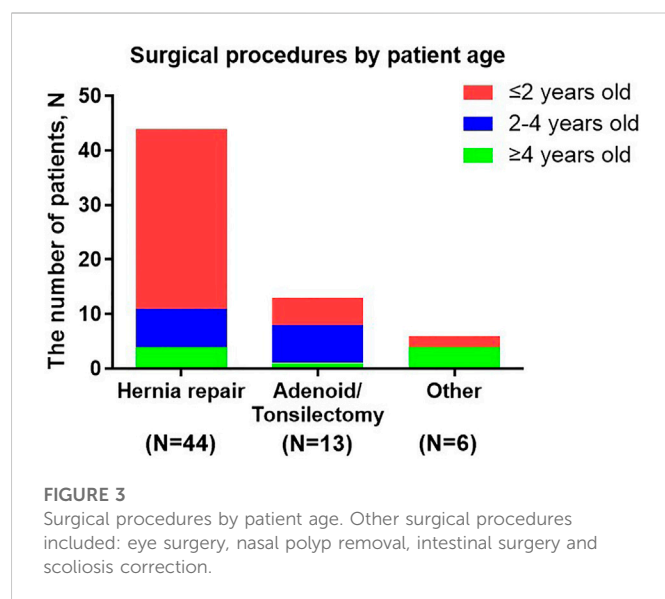
A total of 57 patients underwent cardiac ultrasound, and of these patients, valve abnormalities were the most commonly observed cardiac manifestation of MPS II (Figure 1). The most common specific manifestations observed were mitral/tricuspid valve regurgitation (41/57; 71.9%), aortic/pulmonary valve regurgitation (21/57; 36.8%), valve thickening (17/57; 29.8%), mitral/aortic valve prolapse (12/57; 21.1%) and atrial/ventricular hypertrophy (12/57; 21.1%).

A total of 30 patients checked brain MRI, of which 12 patients had abnormal results and 18 patients had normal results. Of the 12 patients with abnormalities detected on brain MRI imaging, seven patients had cystic -like brain cystic sample changes caused by widened vascular space, two patients had diffuse brain atrophy, three patients had expansion of the ventricle and hydrocephalus.

3.4 IDS pathogenic gene variants

IDS gene sequencing data was available for 59 patients, of which four patients had no pathogenic variant detected by IDS gene analysis. The IDS pathogenic gene variants of 55 patients were summarised in Table 2 (NM_000202, NM_001166550, and NM_006123). A total of 43 different variants types were detected. Of the 43 variants, 16 (37%) novel variants were detected: six exonic point variants (c.260G>C, c.261C>A, c.325T>G, c.456C>G, c.1432G>C, and c.1453A>T), three small insertions (c.438_439insTT, c.1489_1490insT, and c.1269dupC), five small deletions (c.41delG, c.314_339del, c.449delC, c.481_486del, and c.794delA), one small indels (c.801_806delinsTGGC), one duplication (Exon8 duplication).

Twenty-four exonic point variants were detected in 34 patients which were the most frequent type of variant (61.8% = 34/55). The most common point variant was c.1122C>T, which was detected in 7.3% (4/55) of patients. The second most frequent variant was c.262C>T and c.514C>T, which were detected in 5.5% (3/55) of patients separately. All three of above variants had been detected



previously in other studies of patients with MPS II. The other variant types of patients included four gross deletions, eight small deletions, four small insertions, three splicings, one duplication, one small indels variant.

The mutant spectrum of IDS could be seen in Figure 2. While variants were found in all exons, the variants of patients were concentrated in exon 9 (20% = 11/55), exon 3 (20% = 11/55) and exon 8 (15% = 8/55). The IDS gene variant had no variant hotspots, but had variant “hot exon.”

3.5 IDS enzyme activity

Data on plasma IDS enzyme activity was available for 100 patients (76.9%). IDS activity levels ranged from .0 to 11.1 nmol/4 h/mL. The mean enzyme activity was $.72 \pm .14$ nmol/4 h/mL, which was below our institution diagnosed value 20 nmol/4 h/mL.

3.6 *In silico* analysis of the novel variants

All of the novel variants in the IDS gene on protein function were indicated deleterious by the pathogenicity prediction tool Mutation Taster. Meanwhile, the novel exonic point variants were predicted damaging by the Polyphen-2 and SIFT/PROVEAN web software. This was also demonstrated by the reduced IDS enzyme activity.

3.7 Treatment

Treatment was generally supportive and palliative in nature, in line with treatment practice in China over the study period. Two patients underwent bone marrow transplant. A total of 50 patients (38.5%) underwent surgical treatment, receiving a total of 63 surgeries. Eight patients (6.2%) underwent ≥ 2 surgeries and the highest number of surgeries received by a single patient was five (including three hernia surgeries, surgeries for the adenoids and correction of congenital megacolon).

The most common palliative surgery was hernia repair (three cases of umbilical hernia and 41 inguinal hernias), which accounted for 69.8% of all surgeries received by patients, followed by 13 cases of adenoidectomy or tonsillectomy, which accounted for 20.6% of all surgeries received. Other surgical procedures included: one eye surgery, two nasal polyp removal surgeries, two intestinal surgeries and one scoliosis correction.

The average age of patients on receiving their first surgery was 2.6 years old, and the majority of surgery (85.7%, 54/63) was operated before 4 years old (Figure 3). The earliest operations were hernia repairs (at a median age of 1.8 years). 75% hernia repairs were operated before 2 years old and 90.9% were operated before 4 years old.

3.8 Morbidity and mortality

Two patients, aged 11 years and 15 years, respectively, were wheelchair-bound and one 11-year-old patient was unable to eat independently. Three patients were now known to died, aged 10, 11, and 13 years, respectively. The cause of death in all three cases was respiratory failure.

4 Discussion

This was a large scale analysis of clinical and molecular characterizations of Chinese patients with Mucopolysaccharidosis Type II. The MPS II was one of the diseases that involved multiple systems (Ullah et al., 2017; Ullah et al., 2018). The most common symptoms in our study were claw-like hands or joint stiffness, followed by coarse facial features, birthmarks (Mongolian spot), delayed growth or development, inguinal or umbilical hernia, sleep apnoea, spine deformities, deafness. The onset of MPS II symptoms generally occurred between the age of 2 and 6 years. More than one-third of the patients had surgery, the most common and earliest surgery was hernia repair. We had found 43 different IDS gene variants in 55 patients, included 16 novel variants. The variants were concentrated in exon 9, exon 3 and exon 8.

In China, MPS II was the most frequently occurring MPS (Fang et al., 2022). The median age at diagnosis in the Chinese population in this analysis was a little older than those reported previously in the global Hunter Outcome Survey (Wraith et al., 2008a) (5.0 years vs. 3.5 years) (HOS was a global multicentre registry of MPS II patients). Consistent with other findings, facial features, claw-like hands and birthmarks were the most common clinical manifestations of MPS II. The incidence rate of signs and symptoms in our study was almost same with other studies (Lin et al., 2018), claw hands (98.0% vs. 98.2%), facial features (97.9% vs. 100%).

The accumulation of GAG in cardiac valves and myocardium lead to valvular defects and cardiomyopathy (Costa et al., 2017). The mitral or aortic leaflet thickening and calcification could cause valvular stenosis and regurgitation. The deformities in cardiac structures could cause cardiac dysfunction, which could significantly increase the morbidity and mortality of affected patients (Chkioua et al., 2020). In the other study, respiratory failure was the primary cause of death (56%), followed by cardiac failure (18%) (Lin et al., 2016).

In our study, valve abnormalities were the most commonly observed cardiac manifestation of MPS II. The most common specific manifestations observed were mitral/tricuspid valve regurgitation (71.9%), aortic/pulmonary valve regurgitation (36.8%), in agreement with the report by Lin et al. (2021). Therefore, echocardiography should be checked regularly (Scarpa et al., 2011).

IDS gene sequencing data was available for 55 patients and 43 different variants types were detected. In this study, sixteen novel variants (37%) were detected, the rate of discovery of novel genes was consistent with another study from China (32.7%) (Zhang et al., 2019). It had been reported that, variants tend to be more frequent in exons 3, 7, 8, and 9 (Rathmann et al., 1996; Agrawal et al., 2022). As expected, in our sample, the highest frequency of variant exons were 9, 3, and 8. Consistent with data from other Chinese study, exons 9 and 3 had comparatively more variants (Zhang et al., 2011).

In our study, the most common variant identified was c.1122C>T, in codon 374, constituting about 7.3% (4/55) of all variants. This was also the most frequent variant of the IDS gene in Spain, Portugal and Latin American patients, which more than 30 patients had been reported (Brusius-Facchin et al., 2014). Other two studies from China reported the codon 468 position could be a “hot” spot, which five patients showed variants from 63 patients and 38 patients, respectively (Zhang et al., 2011; Zhang et al., 2019). In our study, we found two patients had variants with p.R468W.

This analysis was one of the largest studies about surgical records in Chinese MPS II patients. A total of 50 patients (38.5%) in this analysis had undergone surgical treatment, while the occurrence rate of surgical treatment in HOS was more than three-quarters (Mendelsohn et al., 2010). The age at first surgery in Chinese patients was almost the same as the global HOS population (2.6 years) and the vast majority of surgeries was undergone before 4 years old. The earliest operations to be performed were hernia repairs. However, some surgeries prevalence in our study had a little different from the global HOS population (Mendelsohn et al., 2010): hernia repair (69.8% vs. 50.1%), adenoidectomy or tonsillectomy (20.6% vs. 85.0%). Clinicians and caregivers in China may had different perceptions of the need for MPS II surgery compared with other countries, which might explain these differences in the frequency of surgery among Chinese patients and HOS population. The other studies showed tympanostomy (placement of ear-drum ventilating tubes) were commonly performed operations and the incidence rate was 51.4% and 27.9% (Mendelsohn et al., 2010; Lin et al., 2018). However, few patients in our study performed this surgery. It indicated that hearing screening at follow-up was important.

The knowledge gained from this study broadens the list of indicators of MPS II to include early and repeated surgical intervention. Some of the symptoms associated with hernias and adenoid/tonsillectomy might suggest that the patient had MPS II, which could be helpful for early diagnosis of the disease. Early diagnosis permitted early initiation of ERT, which could decrease complications, particularly before organ damage becoming

irreversible (Scarpa et al., 2011). Prompt diagnosis might also mean that complications during surgical intervention could be avoided.

Usually, the main criterion for severity relies on the degree of intellectual disability. But intellectual disability was not the main cause of death in MPS II, most patients died of respiratory failure and cardiac failure in our study and other studies (Lin et al., 2016). The intellectual disability could reduce the quality of life, but it did not affect longevity. We believed that cardiopulmonary function was the main cause of death in the disease, therefore, it was more appropriate to distinguish between mild and severe subtype by whether cardiopulmonary function was affected or not. According to the cardiopulmonary function, a standard scoring system was recommended, which could evaluate the patient's survival time and prognosis.

Since MPS II was an X-linked genetic disease, molecular diagnosis was important for carrier detection and prenatal diagnosis. The other studies identified carrier status in 70%–72% of the mothers of the probands (Agrawal et al., 2022). Parenteral diagnosis could play a major role in reducing the burden of such severe disorders.

It was important to consider the limitations of this study. As a retrospective and single-center study, some medical records were missing and not available at the time of this study. This study did not analysis the genotype–phenotype correlations in MPS II. MPS II genetic heterogeneity represents a major difficulty in establishing genotype–phenotype correlations. The problem was complicated by the lack of a standardized scoring index of severity in clinical evaluation and the comparison of clinical phenotypes was difficult and subjective. Therefore, a greater number of patients and longer follow-up would be needed to investigate.

Despite these limitations, this was one of the largest studies of clinical presentations and surgical histories in Chinese patients. By continuously recording and analyzing clinical and laboratory data of various patients, we would deepen our understanding of MPS II in China. Understanding surgical history patterns in patients with MPS II would help improve diagnosis, disease management, prospective guidance, and quality of life. Analysis of longitudinal surgical data from a large number of Chinese patients provided unique insights into the surgical history of MPS II patients. Furthermore, the disease was complex, and management was often challenging and required a multidisciplinary approach.

5 Conclusion

In conclusion, this paper provided additional information on the clinical, cardiac ultrasound and surgical procedure in MPS II patients. This analysis found that claw-hands, birthmarks and facial features were the most common symptoms. The valve abnormalities were the most commonly cardiac manifestation of MPS II, which were mitral/tricuspid valve regurgitation and aortic/pulmonary valve regurgitation. Our study expanded the spectrum of genotype of MPS II. We had found 43 different IDS gene variants in 55 patients, included 16 novel variants. The variants were concentrated in exon 9, 3 and 8. A total of 38.5% of the patients

underwent a surgical procedure. The most common and earliest surgery was hernia repair. Our study expanded the genotype spectrum of MPS II. Based on these data, characterization of MPS II patients group could be used to early diagnosis and treatment of the disease.

Data availability statement

The original contributions presented in the study are included in the article/supplementary material, further inquiries can be directed to the corresponding author.

Ethics statement

The study was approved by the hospital Ethics Committee and was conducted in accordance with the Helsinki Declaration ethical principles for medical research involving human subjects. Written informed consent was obtained from every patient or parents prior to inclusion in the study.

Author contributions

ZZ (Formal analysis; Investigation; Methodology; Writing—original draft). MM (Conceptualization; Investigation;

Resources). WZ (Experimental detection). YZ (Data curation; Formal analysis; Investigation). FY (Experimental detection). LZ (Experimental detection). MW (Data curation; Formal analysis). ZQ (Funding acquisition; Conceptualization; Resources; Writing—review).

Funding

This work was supported by the CAMS Innovation Fund for Medical Sciences (CIFMS 2021-I2M-1-003).

Conflict of interest

The authors declare that the research was conducted in the absence of any commercial or financial relationships that could be construed as a potential conflict of interest.

Publisher's note

All claims expressed in this article are solely those of the authors and do not necessarily represent those of their affiliated organizations, or those of the publisher, the editors and the reviewers. Any product that may be evaluated in this article, or claim that may be made by its manufacturer, is not guaranteed or endorsed by the publisher.

References

- Agrawal, N., Verma, G., Saxena, D., Kabra, M., Gupta, N., Mandal, K., et al. (2022). Genotype-phenotype spectrum of 130 unrelated Indian families with Mucopolysaccharidosis type II. *Eur. J. Med. Genet.* 65 (3), 104447. doi:10.1016/j.ejmg.2022.104447
- Brusius-Facchin, A. C., Schwartz, I. V. D., Zimmer, C., Ribeiro, M. G., Acosta, A. X., Horovitz, D., et al. (2014). Mucopolysaccharidosis type II: Identification of 30 novel mutations among Latin American patients. *Mol. Genet. Metabolism* 111 (2), 133–138. doi:10.1016/j.ymgme.2013.08.011
- Chen, X., Qiu, W., Ye, J., Han, L., Gu, X., and Zhang, H. (2016). Demographic characteristics and distribution of lysosomal storage disorder subtypes in Eastern China. *J. Hum. Genet.* 61 (4), 345–349. doi:10.1038/jhg.2015.155
- Chkioua, L., Grissa, O., Leban, N., Gribaa, M., Boudabous, H., Turkia, H. B., et al. (2020). The mutational spectrum of hunter syndrome reveals correlation between biochemical and clinical profiles in Tunisian patients. *BMC Med. Genet.* 21 (1), 111. doi:10.1186/s12881-020-01051-9
- Clarke, J. T., Wilson, P. J., Morris, C. P., Hopwood, J. J., Richards, R. I., Sutherland, G. R., et al. (1992). Characterization of a deletion at Xq27-q28 associated with unbalanced inactivation of the nonmutant X chromosome. *Am. J. Hum. Genet.* 51 (2), 316–322.
- Costa, R., Urbani, A., Salvalaio, M., Bellesso, S., Cieri, D., Zancan, I., et al. (2017). Perturbations in cell signaling elicit early cardiac defects in mucopolysaccharidosis type II. *Hum. Mol. Genet.* 26 (9), 1643–1655. doi:10.1093/hmg/ddx069
- Demydchuk, M., Hill, C. H., Zhou, A., Bunkoczi, G., Stein, P. E., Marchesan, D., et al. (2017). Insights into Hunter syndrome from the structure of iduronate-2-sulfatase. *Nat. Commun.* 8, 15786. doi:10.1038/ncomms15786
- Fang, X., Zhu, C., Zhu, X., Feng, Y., Jiao, Z., Duan, H., et al. (2022). Molecular analysis and novel variation identification of Chinese pedigrees with mucopolysaccharidosis using targeted next-generation sequencing. *Clin. Chim. Acta* 524, 194–200. doi:10.1016/j.cca.2021.11.019
- Kang, Q., Hu, J., Yang, N., He, J., Yang, Y., Tang, M., et al. (2019). Marketing of drugs for rare diseases is speeding up in China: Looking at the example of drugs for mucopolysaccharidosis. *Intractable Rare Dis. Res.* 8 (3), 165–171. doi:10.5582/irdr.2019.01090
- Khan, S. A., Peracha, H., Ballhausen, D., Wiesbauer, A., Rohrbach, M., Gautschi, M., et al. (2017). Epidemiology of mucopolysaccharidoses. *Mol. Genet. Metab.* 121 (3), 227–240. doi:10.1016/j.ymgme.2017.05.016
- Kosuga, M., Mashima, R., Hirakiyama, A., Fuji, N., Kumagai, T., Seo, J., et al. (2016). Molecular diagnosis of 65 families with mucopolysaccharidosis type II (Hunter syndrome) characterized by 16 novel mutations in the IDS gene: Genetic, pathological, and structural studies on iduronate-2-sulfatase. *Mol. Genet. Metabolism* 118 (3), 190–197. doi:10.1016/j.ymgme.2016.05.003
- Lin, H., Chen, M., Lee, C., Lin, S., Hung, C., Niu, D., et al. (2021). Natural progression of cardiac features and long-term effects of enzyme replacement therapy in Taiwanese patients with mucopolysaccharidosis II. *Orphanet J. Rare Dis.* 16 (1), 99. doi:10.1186/s13023-021-01743-2
- Lin, H., Chuang, C., Chen, M., Lin, S. J., Chiu, P. C., Niu, D., et al. (2018). Clinical characteristics and surgical history of Taiwanese patients with mucopolysaccharidosis type II: Data from the hunter Outcome Survey (HOS). *Orphanet J. Rare Dis.* 13 (1), 89. doi:10.1186/s13023-018-0827-1
- Lin, H., Chuang, C., Huang, Y., Tu, R., Lin, F., Lin, S. J., et al. (2016). Causes of death and clinical characteristics of 34 patients with Mucopolysaccharidosis II in Taiwan from 1995–2012. *Orphanet J. Rare Dis.* 11 (1), 85. doi:10.1186/s13023-016-0471-6
- Martin, R., Beck, M., Eng, C., Giugliani, R., Harmatz, P., Munoz, V., et al. (2008). Recognition and diagnosis of mucopolysaccharidosis II (Hunter syndrome). *Pediatrics* 121 (2), e377–e386. doi:10.1542/peds.2007-1350
- Mendelsohn, N. J., Harmatz, P., Bodamer, O., Burton, B. K., Giugliani, R., Jones, S. A., et al. (2010). Importance of surgical history in diagnosing mucopolysaccharidosis type II (hunter syndrome): Data from the hunter Outcome Survey. *Genet. Med.* 12 (12), 816–822. doi:10.1097/GIM.0b013e3181f6e74d
- Neufeld, E. F., Liebaers, I., Epstein, C. J., Yatziv, S., Milunsky, A., and Migeon, B. R. (1977). The hunter syndrome in females: Is there an autosomal recessive form of iduronate sulfatase deficiency? *Am. J. Hum. Genet.* 29 (5), 455–461.
- Rathmann, M., Bunge, S., Beck, M., Kresse, H., Tylki-Szymanska, A., and Gal, A. (1996). Mucopolysaccharidosis type II (hunter syndrome): Mutation "hot spots" in the iduronate-2-sulfatase gene. *Am. J. Hum. Genet.* 59 (6), 1202–1209.
- Scarpa, M., Almassy, Z., Beck, M., Bodamer, O., Bruce, I. A., De Meirleir, L., et al. (2011). Mucopolysaccharidosis type II: European recommendations for the diagnosis and multidisciplinary management of a rare disease. *Orphanet J. Rare Dis.* 6, 72. doi:10.1186/1750-1172-6-72
- Stapleton, M., Kubaski, F., Mason, R. W., Yabe, H., Suzuki, Y., Orii, K. E., et al. (2017). Presentation and treatments for mucopolysaccharidosis type II (MPS II; hunter syndrome). *Expert Opin. Orphan Drugs* 5 (4), 295–307. doi:10.1080/21678707.2017.1296761

- Ullah, A., Khalid, M., Umair, M., Khan, S. A., Bilal, M., Khan, S., et al. (2018). Novel sequence variants in the MKKS gene cause Bardet-Biedl syndrome with intra- and inter-familial variable phenotypes. *Congenit. Anom. (Kyoto)* 58 (5), 173–175. doi:10.1111/cga.12264
- Ullah, A., Umair, M., Yousaf, M., Khan, S. A., Nazim-Ud-Din, M., Shah, K., et al. (2017). Sequence variants in four genes underlying Bardet-Biedl syndrome in consanguineous families. *Mol. Vis.* 23, 482–494.
- Voznyi, Y. V., Keulemans, J. L., and van Diggelen, O. P. (2001). A fluorimetric enzyme assay for the diagnosis of MPS II (Hunter disease). *J. Inherit. Metab. Dis.* 24 (6), 675–680. doi:10.1023/a:1012763026526
- Wraith, J. E., Beck, M., Giugliani, R., Clarke, J., Martin, R., Muenzer, J., et al. (2008a). Initial report from the hunter Outcome Survey. *Genet. Med.* 10 (7), 508–516. doi:10.1097/gim.0b013e31817701e6
- Wraith, J. E., Scarpa, M., Beck, M., Bodamer, O. A., De Meirleir, L., Guffon, N., et al. (2008b). Mucopolysaccharidosis type II (hunter syndrome): A clinical review and recommendations for treatment in the era of enzyme replacement therapy. *Eur. J. Pediatr.* 167 (3), 267–277. doi:10.1007/s00431-007-0635-4
- Zhang, H., Li, J., Zhang, X., Wang, Y., Qiu, W., Ye, J., et al. (2011). Analysis of the IDS gene in 38 patients with hunter syndrome: The c.879G>A (p.Gln293Gln) synonymous variation in a female create exonic splicing. *PLoS One* 6 (8), e22951. doi:10.1371/journal.pone.0022951
- Zhang, W., Xie, T., Sheng, H., Shao, Y., Lin, Y., Jiang, M., et al. (2019). Genetic analysis of 63 Chinese patients with mucopolysaccharidosis type II: Functional characterization of seven novel IDS variants. *Clin. Chim. Acta* 491, 114–120. doi:10.1016/j.cca.2019.01.009



OPEN ACCESS

EDITED BY

Javier Corral,
University of Murcia, Spain

REVIEWED BY

Patryk Lipiński,
Children's Memorial Health Institute
(IPCZD), Poland
Ivan Martinez Duncker,
Universidad Autónoma del Estado de
Morelos, Mexico

*CORRESPONDENCE

Lian Chen,
✉ doctchenlian@163.com
Xin-Bao Xie,
✉ xxb116@163.com

[†]These authors have contributed equally
to this work and share first authorship

RECEIVED 04 August 2023

ACCEPTED 31 October 2023

PUBLISHED 22 November 2023

CITATION

Fang Y, Wang Y-Z, Chen L and Xie X-B
(2023), Expanding the phenotype and
metabolic basis of ATP6AP2-congenital
disorder of glycosylation in a Chinese
patient with a novel variant
c.185G>A (p.Gly62Glu).
Front. Genet. 14:1264237.
doi: 10.3389/fgene.2023.1264237

COPYRIGHT

© 2023 Fang, Wang, Chen and Xie. This is
an open-access article distributed under
the terms of the [Creative Commons
Attribution License \(CC BY\)](#). The use,
distribution or reproduction in other
forums is permitted, provided the original
author(s) and the copyright owner(s) are
credited and that the original publication
in this journal is cited, in accordance with
accepted academic practice. No use,
distribution or reproduction is permitted
which does not comply with these terms.

Expanding the phenotype and metabolic basis of ATP6AP2-congenital disorder of glycosylation in a Chinese patient with a novel variant c.185G>A (p.Gly62Glu)

Yuan Fang^{1†}, Yi-Zhen Wang^{1†}, Lian Chen^{2*} and Xin-Bao Xie^{3*}

¹Department of Pathology, Anhui Provincial Children's Hospital, Hefei, China, ²Department of Pathology, Children's Hospital of Fudan University, Shanghai, China, ³Department of Hepatology, Children's Hospital of Fudan University, Shanghai, China

Background: A rare X-linked hereditary condition known as ATP6AP2-congenital disorder of glycosylation (ATP6AP2-CDG) is caused by pathogenic variants in *ATP6AP2*, resulting in autophagic misregulation with reduced signaling of mammalian target of rapamycin (mTOR) that clinically presents with aberrant protein glycosylation, hepatosteatosis, immunodeficiency, cutis laxa, and psychomotor dysfunction. To date, only two missense mutations have been reported in three patients from two unrelated families.

Methods: In order to extend the profiles of phenotype and genotype associated with ATP6AP2-CDG, we assessed the clinical history, whole exome sequencing (WES), and liver histology as well as immunohistochemistry in a Chinese patient, and performed quantitative real-time polymerase chain reaction (qRT-PCR), Western blotting and untargeted metabolomics in genetic exogenously constructed cells.

Results: The 11-month-old Chinese boy presented with recurrent jaundice, cutis laxa, cirrhosis, growth retardation, coagulopathy, anemia, and cardiomegaly, and underwent liver transplantation. A novel mutation, c.185G>A (p.Gly62Glu), was identified in exon 3 of *ATP6AP2*. The expression of ATP6AP2 was observed to remain unchanged in the liver sample of the patient as well as in HEK293T cells harboring the p.Gly62Glu. This missense mutation was found to dysregulate autophagy and mTOR signaling. Moreover, metabolomics analysis revealed that the exogenously introduced Gly62Glu mutant resulted in the downregulation of numerous metabolites involved in lipid metabolism pathway.

Conclusion: This study may enable a more detailed exploration of its precise pathogenesis and potential therapeutic interventions.

KEYWORDS

ATP6AP2, congenital disorders of glycosylation, X-linked, hereditary, cirrhosis

Introduction

There is a group of Mendelian diseases, congenital disorders of glycosylation (CDGs), affecting the glycosylation of proteins or lipids, which is a post-translational modification to acquire complete biological function. Defective glycosylation involved in CDGs includes disruption of N-linked glycosylation, O-linked glycosylation, glycosylphosphatidylinositol anchor biosynthesis, multiple glycosylation pathways, and others (Ondruskova et al., 2021). According to the isoelectrofocusing (IEF) of serum transferrin, CDGs are classified into type I and type II patterns. While a type II pattern (increased trisialo- and monosialotransferrin) suggests a remodeling problem, a type I pattern (decreased tetrasialotransferrin, increased disialo- and asialotransferrin) indicates an assembly flaw or a defect in the transfer to the peptide chain (Peanne et al., 2018).

Since the first CDG was reported in 1980, more than 170 types of CDG have been identified with the development of genetic testing approaches. Recently, a new subtype ATP6AP2-CDG (OMIM: 301045) was reported in three patients from two unrelated families (Rujano et al., 2017). Patients presented with hepatosteatorrhea, immunodeficiency, cutis laxa, and psychomotor impairment. Serum transferrin glycosylation profiles were consistent with a type II transferrin IEF pattern. *In vitro* and *in vivo* experiments validated the mutations leading to the hypoglycosylation in a pathogenetic cascade, including degradation of misfolded proteins in the ER, impairment of interaction with the assembly factor ATP6AP1, defective lysosomal acidification, downregulation of mammalian target of rapamycin (mTOR) signaling, and induction of autophagy defection.

In this study, we identified the first Chinese patient diagnosed with ATP6AP2-CDG, presenting with recurrent jaundice, cutis laxa, cirrhosis, growth retardation, coagulopathy, anemia, and cardiomegaly. Whole exome sequencing (WES) revealed a hemizygous variant, the c.185G>A (p.Gly62Glu) mutation in exon 3 of *ATP6AP2*, which has not been previously reported. The expression of *ATP6AP2* in the liver was normal as well as in HEK293T cells harboring p.Gly62Glu. Furthermore, in HEK293T cells, the missense mutation dysregulated autophagy and mTOR signaling. Metabolomics analysis in HEK293T cells indicated that in the exogenously introduced Gly62Glu mutant, most metabolites were downregulated and involved in the pathway of lipid metabolism.

Materials and methods

Subject

The clinical data of a patient with ATP6AP2-CDG was gathered at the Children's Hospital of Fudan University. This study was approved by the Ethics Committee of Children's Hospital of Fudan University (No. FELL-2020-402). Any potentially identifiable photographs or data were published with the parents' written informed consent.

Liver sample and immunohistochemistry

The material was removed from the liver transplant procedure, fixed in 10% buffered formalin, dried in varying degrees of ethyl alcohol,

and then embedded in paraffin. Hematoxylin and eosin (HE) staining was followed by periodic acid Schiff (PAS) with and without diastase, Masson, reticulin, copper, and iron special staining.

Additional 4 μ m sections were deparaffinized, rehydrated, and pretreated with 3% H₂O₂ to eliminate endogenous peroxidase activity. Besides, the sections were heat-mediated antigen-retrieved with EDTA (pH 9) or citrate buffer (pH 6) before immunohistochemical staining was undertaken. A variety of antibodies were used as primary antibodies, including ATP6AP2 (purchased from www.ptgcn.com, catalog number 10926-1-AP, 1:50 dilution), LC3A/B (purchased from www.affbiotech.com, catalog number AF5402, 1:100 dilution), and mTOR (purchased from www.affbiotech.com, catalog number AF6308, 1:100 dilution). After incubating overnight at 4°C, the sections were incubated at room temperature for an hour with the general secondary antibody. Then, the sections were developed with DAB and counterstained with hematoxylin. To serve as a control, we used a normal liver sample donated by a surgical patient.

Genetic analysis

We collected the patient's and his parents' EDTA-anticoagulated whole blood specimens to perform WES004 (Human All Exon V4) using the Illumina HiSeq X ten platform by MyGenostics (a commercial genetic testing company). Using the TruSeq DNA Library Preparation Kit, DNA libraries were created. The raw data were aligned to the reference human genome (GRCh37/hg19). For variation calling to compile single nucleotide variations (SNVs) and indels, the Genome Analysis Toolkit (GATK) (<https://gatk.broadinstitute.org>) was applied. The annotation and interpretation processes used ANNOVAR software and the Enliven® Variants Annotation Interpretation System. Data were filtered in 1,000 Genome (www.1000genomes.org), NHLBI Exome Sequencing Project (ESP6500) (<https://esp.gs.washington.edu>), Genome Aggregation Database (gnomAD) (<https://gnomad.broadinstitute.org>), dbSNP152 (<https://www.ncbi.nlm.nih.gov/snp>), and Exome Aggregation Consortium (ExAC) (<http://exac.broadinstitute.org>). In order to score the genetic variants and further compare them, damage prediction was conducted using Combined Annotation Dependent Depletion (CADD) (<https://cadd.gs.washington.edu>) and Mutation Significance Cutoff (MSC) (<https://lab.rockefeller.edu/casanova/MSC>). With a 99% confidence level and HGMD and ClinVar as the database sources, the MSC server was deployed to CADD, PolyPhen 2 (<http://genetics.bwh.harvard.edu/pph2>), and SIFT (https://sift.bii.a-star.edu.sg/www/SIFT_indels2.html). For analysis based on variant-disease and gene-disease relationships, Genomics England PanelApp, a crowdsourcing tool, was used (<https://panelapp.genomicsengland.co.uk>). The HGMD database, Online Mendelian Inheritance in Man (OMIM), and Human Phenotype Ontology (HPO) were utilized to correlate phenotype descriptions with variant and gene prioritization results. Genetic variants were categorized into five categories by the American College of Medical Genetics and Genomics (ACMG): pathogenic, likely pathogenic, variant of uncertain significance (VUS), likely benign, and benign. Following that, a VUS of *ATP6AP2* was discovered in the patient with the transcript NM_005765, the mutation site was confirmed by Sanger sequencing in his parents.

MutationTaster (<http://www.mutationtaster.org>) predicted the toxicity of the amino acid shift brought on by the gene mutation. In

addition, the conservation of the mutation site was analyzed among multiple species. We modeled the protein using SWISS-model (<https://www.swissmodel.expasy.org>) with the UniProtKB code O75787, and PyMol (<http://www.pymol.org>) was used to analyze and visualize the altered structure.

Cell culture and plasmids transfection

HEK293T cells were cultured in high-glucose DMEM (Gibco) supplemented with 10% fetal bovine serum and 1% penicillin/streptomycin at 37°C under 5% CO₂. The cDNA of *ATP6AP2* was generated by gene synthesis (www.generalbiol.com) and cloned into pcDNA3.1 with an N-terminal FLAG-tagged version. The original plasmid was used as a template to introduce the site mutation *ATP6AP2*^{Gly62Glu} by homologous recombination. All constructs were confirmed by DNA sequencing. The plasmids were chemically transformed into competent DH5α *E. coli* (TIANGEN). Individual colonies were selected, and plasmid DNAs were extracted using OMEGA Endo-Free Plasmid Midi Kit D6915. Then, Beyotime Lipo8000™ Transfection Reagent was used for plasmid DNA transfection following the manufacturer's instructions.

RNA extraction, reverse transcription, and quantitative real-time PCR

Total RNA was extracted using AG RNAex Pro Reagent. Reverse transcription of the total RNA into cDNA was carried out using Evo M-MLV RT Premix (Accurate Biotechnology). The relative expression of endogenous, wild-type, and mutant *ATP6AP2* was determined by quantitative real-time polymerase chain reaction (qRT-PCR) using SYBR Green Premix Pro Taq HS Kit (Accurate Biotechnology) on a Bio-Rad system. The forward primer sequence is 5'CTGCATTGTCCATGGGCTTC3', and the reverse primer sequence is 5'AACAGGTTACCCACTGCGAG3'.

Western blotting

Cells were harvested in 100 μL RIPA buffer supplemented with 1 μL phenylmethanesulfonyl fluoride lysed on ice for 30 min. The lysates were then centrifuged at 12,000 rpm for 20 min at 4°C. The supernatant was measured for the protein concentration using the Pierce BCA Protein Assay Kit (Thermo Fisher Scientific) and was denatured with 1× SDS-PAGE Sample Loading Buffer (Beyotime) at 100°C for 10 min. We measured 10 μg total protein of each aliquot, and it was analyzed by SDS-PAGE and immunoblotted to a hydrophobic polyvinylidene fluoride membrane. After 1 h of milk blocking, the membranes were incubated with primary antibodies at 4°C overnight followed by second antibodies. Bands signal was detected by Tanon 5,200 automatic chemiluminescence image analysis system, and the relative expression was calculated by ImageJ software.

The following antibodies were used: *ATP6AP2* (purchased from www.ptgcn.com, catalog number 10926-1-AP, 1:1,000 dilution), LC3A/B (purchased from www.affbiotech.com, catalog number AF5402, 1:1,000 dilution), mTOR (purchased from www.affbiotech.com, catalog number AF6308, 1:1,000 dilution), FLAG tag (purchased from www.huabio.cn, catalog number HA601080, 1:5,000 dilution) and GAPDH (purchased from Zsbio, catalog number TA-08, 1:2000 dilution). HRP-labeled Goat Anti-Rabbit (purchased from www.beyotime.com, catalog number A0208, 1:20000 dilution) and HRP-labeled Goat Anti-Mouse IgG (purchased from www.beyotime.com, catalog number A0216, 1:20000 dilution) were used as second antibodies.

affbiotech.com, catalog number AF6308, 1:1,000 dilution), FLAG tag (purchased from www.huabio.cn, catalog number HA601080, 1:5,000 dilution) and GAPDH (purchased from Zsbio, catalog number TA-08, 1:2000 dilution). HRP-labeled Goat Anti-Rabbit (purchased from www.beyotime.com, catalog number A0208, 1:20000 dilution) and HRP-labeled Goat Anti-Mouse IgG (purchased from www.beyotime.com, catalog number A0216, 1:20000 dilution) were used as second antibodies.

Untargeted metabolomics

HEK293T cells harboring *ATP6AP2*^{WT} and *ATP6AP2*^{Gly62Glu} were cultured in 10 cm dishes. Each group of six samples was extracted with extractant containing internal standard (methanol: acetonitrile:water = 2:2:1, V/V/V) for metabolite extraction. Metabolomic data analyses were conducted using non-targeted metabolomic profiling by Biomarker Co., Ltd. The Waters Acquity I-Class PLUS ultra-high performance liquid tandem mass spectrometer and the Waters Xevo G2-XS QToF high-resolution mass spectrometer made up the LC/MS equipment used for the metabolomics investigation. The column used was purchased from Waters Acquity UPLC HSS T3 column (1.8 μm 2.1×100 mm). Based on the Progenesis QI software's online METLIN database and Biomark's own self-built library for identification, the raw data collected using MassLynx V4.2 were processed by Progenesis QI software for peak extraction, peak alignment, and other data processing operations. At the same time, theoretical fragment identification and mass deviation were both within 100 ppm. The follow-up study was carried out after the first peak area data was normalized with the total peak area. In order to assess the repeatability of the samples within the group and the quality control samples, principal component analysis and Spearman correlation analysis were utilized. The KEGG, HMDB, and lipid mapping databases were examined for classification and route information pertaining to the discovered chemicals. The OPLS-DA modeling was carried out using the R language package, and the model's dependability was examined using 200 permutations.

Statistical analysis

Data were analyzed using SPSS 20.0 and statistical plotting was performed using GraphPad Prism 8.0 software. Metric data were expressed in (mean ± standard deviation, ± s). A parametric *t*-test was used for comparisons of metric data that followed a normal distribution, and a nonparametric *t*-test was used when the normal distribution was not followed. Statistics were considered significant for *p*-values under 0.05.

Results

Clinical description

The boy was born to healthy non-consanguineous parents and was delivered by a full-term cesarean section with a birth weight of

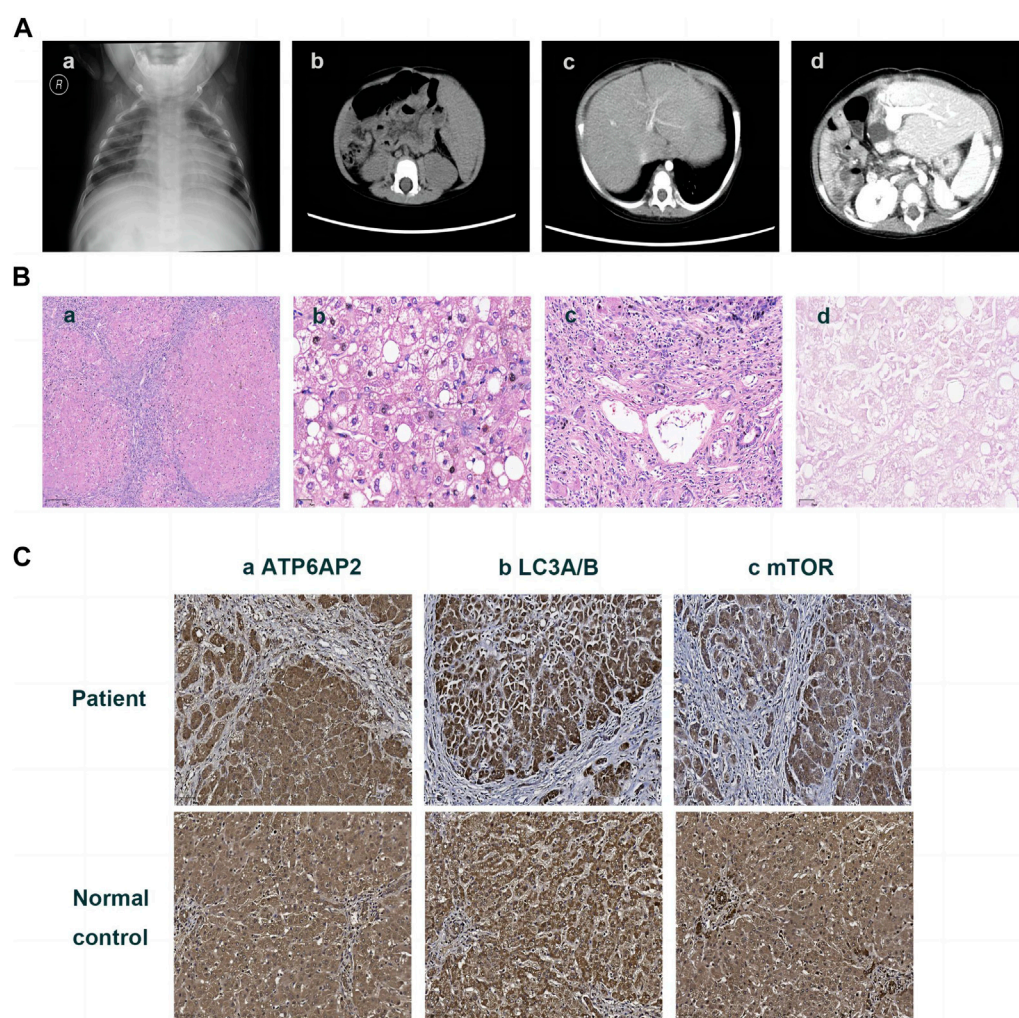


FIGURE 1

Imaging and pathologic findings of the patient. An enlarged heart shadow was displayed in X-ray (A)-a. CT showed multiple hepatic hypointensive foci and splenomegaly (A)-b and revealed portal hypertension and lateral branch circulation formation as well (A)-c. Portal anastomotic stenosis was present after liver transplantation (A)-d. HE staining showed the distorted architecture of liver lobules and the morphology of pseudo-lobules (B)-a $\times 40$, hepatic cells with finely granular cytoplasm and clear cell membrane, along with obvious vesicular steatosis in the portal area (B)-b $\times 200$, and lymphocytic infiltration in the portal area (B)-c 100. PAS staining identified various sizes of vacuoles in partial hepatocytes (B)-d $\times 200$. Immunohistochemistry on the liver showed hepatocytes positive for ATP6AP2 (C)-a $\times 100$, LC3A/B (C)-b $\times 100$ and mTOR (C)-c $\times 100$, without obvious differences in expression compared to the normal control.

3.5 kg. From 3 days to 2 months age, he was hospitalized three times for jaundice. During routine blood tests, remarkably elevated total bilirubin, direct bilirubin, alanine aminotransferase, aspartate aminotransferase, γ -glutamyl transferase, total cholesterol, low-density lipoprotein (LDL) cholesterol, international normalized ratio, prolonged prothrombin time, and decreased serum ceruloplasmin were noticed. There was no hepatosplenomegaly, no significant anemia, no elevated reticulocytes, and no hemolytic manifestations. The patient was discharged after the condition improved, followed by treatment with ursodeoxycholic acid (UDCA), compound glycyrrhizin tablets, and traditional Chinese medicine (details are not available). However, the hyperbilirubinemia, hypertransaminasemia, coagulopathy, and decreased serum ceruloplasmin persisted, and massive ascites emerged during the approximate 9-month follow-up. Besides, alpha-fetoprotein (AFP) (1,395 ng/mL, reference range 0–8.1 ng/mL)

was elevated at 10 months of age, which might result from his young age and liver impairment.

Then the 11-month-old boy was admitted to our hospital for further therapy. Physical examination showed that his height was 70 cm (<3rd percentile by the WHO standard) and weight was 7.4 kg (<3rd percentile). There was mild yellowing of the sclera and skin throughout the body without rash or bleeding points. Cutis laxa was noticed in the patient. There was an II/VI murmur of the heart at the left sternal border. Abdominal distention was present. The liver was located 3.5–4 cm below the xiphoid process, with a tough texture. The spleen was located reaching the iliac fossa below the left costal, and right to the midline, with a diameter of 9–10 cm. No anomalies were discovered during the nervous system evaluation. Echocardiography and X-ray revealed cardiomegaly (Figure 1A-a). Normal cardiac function was assessed since a normal left ventricular ejection fraction without manifestations of left or right ventricular

TABLE 1 Predominant changes in laboratory investigations of the current patient.

Age (m, month)		2 m	4 m	10 m	11 m	12 m	13 m	14 m	16 m	17 m	20 m	21 m
Serum biochemistry (reference range)	Albumin (35–55 g/L)	NA	NA	NA	23.49	43.99	26.84	28.20	37.95	39.96	35.71	37.23
	Globulin (20–30 g/L)	NA	NA	NA	NA	24.41	16.56	NA	NA	16.10	16.49	17.07
	Alanine aminotransferase (0–40 IU/L)	68.72	26.00	47.00	NA	21.00	44.40	46.91	15.69	32.76	37.91	15.22
	Aspartate aminotransferase (0–40 IU/L)	166.13	112.00	241.00	161.00	61.00	131.25	139.61	27.07	58.28	75.81	37.14
	γ-glutamyl transferase (7–50 IU/L)	125.18	180.00	409.00	NA	48.00	40.73	31.94	27.82	15.93	22.54	20.31
	Total bilirubin (5.1–17.1 μmol/L)	233.85	88.00	190.00	71.00	107.30	119.80	165.10	9.20	15.50	11.30	8.30
	Direct bilirubin (0–6 μmol/L)	13.88	4.80	44.90	34.99	37.10	54.00	89.20	3.30	6.30	3.70	3.60
	Total bile acid (0–10 μmol/L)	NA	NA	NA	NA	15.70	123.30	371.30	2.90	5.20	7.10	11.70
	Alkaline phosphatase (42–383 IU/L)	NA	NA	NA	NA	593.00	1,100.88	NA	NA	91.07	390.66	245.09
	Ammonia (10–47 μmol/L)	NA	NA	NA	NA	66.00	119.00	110.00	92.00	105.00	NA	NA
	Total cholesterol (3.1–5.2 mmol/L)	7.24	NA	NA	2.87	1.46	1.55	NA	NA	NA	NA	NA
	LDL-cholesterol (1.30–3.90 mmol/L)	5.12	NA	NA	2.04	NA	NA	NA	NA	NA	NA	NA
	HDL-cholesterol (0.91–2.05 mmol/L)	1.53	NA	NA	1.01	NA	NA	NA	NA	NA	NA	NA
	Triglyceride (0.56–1.70 mmol/L)	1.30	NA	NA	0.68	0.39	0.44	NA	NA	NA	NA	NA
	Ceruloplasmin (0.22–0.58 g/L)	<0.02	NA	NA	0.08	0.17	NA	NA	NA	NA	NA	NA
Blood coagulation profiles (reference range)	Activated partial thromboplastin time (28.0–44.5 s)	NA	NA	NA	NA	62.40	71.40	77.80	47.50	NA	NA	NA
	D-dimer (0–0.3 mg/L)	NA	NA	NA	NA	2.09	1.00	0.97	1.95	NA	NA	NA
	Fibrinogen (2–4 g/L)	NA	NA	NA	0.97	1.57	0.76	0.95	2.77	NA	NA	NA
	International normalized ratio (0.8–1.2)	1.63	NA	NA	2.10	2.10	3.00	3.20	1.75	NA	NA	NA
	Prothrombin time (12.0–14.8 s)	30.60	NA	NA	NA	24.00	31.80	33.50	20.00	NA	NA	NA
	Prothrombin time activity (80%–100%)	NA	NA	NA	30.40	35.00	24.00	NA	NA	NA	NA	NA
Complete blood count (reference range)	Red blood cell (3.5–5.6 × 10 ¹² /L)	NA	NA	NA	NA	2.11	2.45	2.41	4.09	3.76	3.99	3.87
	White blood cell (5.6–14.5 × 10 ⁹ /L)	NA	NA	NA	8.07	5.19	6.29	7.17	5.71	5.27	8.46	8.85
	Hemoglobin (99–196 g/L)	NA	NA	NA	79	67	72	71	NA	102	97	93
	Platelet (203–653 × 10 ⁹ /L)	NA	NA	NA	69	57	78	66	207	145	129	128
	Reticulocyte percentage (0.82%–2.25%)	NA	NA	NA	NA	4.0	5.1	NA	3.5	NA	4.0	4.9

NA: not available.

insufficiency. The patient did not present with hypertrophic cardiomyopathy as well. Abdominal ultrasonography indicated multiple hepatic focal lesions and splenomegaly; the former presented as an enhancement on computed tomography (CT) (Figure 1A-b). CT showed portal hypertension and lateral branch circulation formation as well (Figure 1A-c). The development screening test (DST) showed growth retardation of the patient. The majority of biochemical liver test results were abnormal,

including low albumin, elevated aspartate aminotransferase, γ -glutamyl transferase, alkaline phosphatase, creatine kinase isoenzyme, total bilirubin, direct bilirubin, and total bile acid. Prolonged activated partial thromboplastin time and prothrombin time, increased international normalized ratio and D-dimer, and decreased fibrinogen were present. Complete blood count demonstrated anemia and thrombocytopenia without immunodeficiency. The patient's primary laboratory investigations at various stages are summarized in Table 1. Symptomatic treatment was then carried out by albumin and fibrinogen infusion, oral administration of D-galactose, UDCA, and vitamin D/AD/E/K1 supplements. Among them, D-galactose was administered to correct abnormal glycosylation metabolic pathway in purpose. Due to chronic liver failure with life-threatening decompensated cirrhosis and an increased risk of transplantation as his physical condition deteriorated, the patient underwent living-related liver (donated by his mother) transplantation at that time. At subsequent follow-up, ultrasound and CT showed portal anastomotic stenosis (Figure 1A-d). Liver function parameters gradually normalized, and cutis laxa also improved post transplantation. Tacrolimus was given to control the graft versus host reaction. The patient has been followed through 1 year postoperatively and recovered well.

Histology and immunohistochemistry of the liver

The liver specimen resected from transplantation surgery showed distorted architecture of liver lobules and morphology of pseudo-lobule (Figure 1B-a). High power displayed hepatic cells with finely granular cytoplasm and clear cell membrane, as well as obvious vesicular steatosis in the portal area rather than around the central vein (Figure 1B-b). The portal area was enlarged with infiltration of a lot of lymphocytes (Figure 1B-c). PAS staining identified various sizes of vacuoles in the hepatocytes with steatosis (Figure 1B-d); while staining for PAS with diastase, copper and iron were negative. The liver lobules were divided by hyperplastic fibrous tissue in the portal area, which created pseudo-lobules and bridging-like fibrosis that were identified by Masson staining. Reticulin staining revealed preserved reticular scaffold structure. According to the Ishak staging system (Ishak et al., 1995), it was diagnosed as stage 6 cirrhosis.

Immunohistochemical staining of the patient's liver showed a cytoplasmic positive pattern in hepatocytes for ATP6AP2 (Figure 1C-a), as well as LC3A/B (Figure 1C-b) and mTOR (Figure 1C-c). Compared with the healthy control, there were no obvious alterations observed.

A novel germline mutation in ATP6AP2

WES identified a hemizygous variation c.185G>A in ATP6AP2 exon 3. The c.185G>A was inherited from the healthy mother (Figure 2A), leading to a change of glycine to glutamic acid at the amino acid position 62 (p.Gly62Glu), which was not reported in the HGMD. The amino acid residue of the site mutation was fairly well conserved (Figure 2B), which might

be important for the protein's function. The CADD score of c.185G>A was 27.9, predicted as deleterious. According to the ACMG guidelines, the variant was initially determined as clinically insignificant (uncertain) PM2: the mutation frequency was 0 in the general population database; there were no reports in the literature; comprehensive bioinformatic predictions indicated that it was harmful; and it was verified through family analysis. The Human Genome Variation Society (HGVS; <http://www.hgvs.org/varnomen>) guidelines served as the foundation for the nomenclature of variants. Wild-type and mutated ATP6AP2 were modeled by PyMol (<http://www.pymol.org>), which showed that the non-polar aliphatic amino acid glycine was substituted by acidic amino acid glutamic acid with altered polar contact with Arg31 and Trp60 (Figure 2C). The absence of a side chain in the wild-type glycine increases the flexibility of the protein at this site. The variant residue glutamic acid has a negatively charged side chain, making it hydrophilic and resulting in it preferring the surface of the protein to its interior. The glycine to glutamic acid residue change had a high "disease propensity" value of 1.67 (Figure 2D). Figure 2E illustrates the ATP6AP2 protein domains and location of amino acid changes of the reported variants in CDG so far.

Expression of ATP6AP2^{Gly62Glu} and regulation of autophagy and mTOR signaling

In HEK293T cells, qRT-PCR showed mRNA of ATP6AP2 was slightly increased in mutant rather than in wild type exogenous constructs (Figure 3A), but the difference was not statistically significant ($p = 0.1000$). Western blotting (Figure 3B) revealed that ATP6AP2 protein (Figure 3C) was also increased without significant difference ($p = 0.0563$). Whereas the expression of FLAG (Figure 3D) tagged in the N-terminal of ATP6AP2 confirmed the elevated level in mutant cells ($p < 0.001$). The autophagosome marker, LC3A/B (Figure 3E), was upregulated without significant difference ($p = 0.5053$). And mTOR signaling (Figure 3F) was significantly upregulated ($p < 0.05$).

Metabolomics signature of ATP6AP2^{Gly62Glu} mutant

In HEK293T cells, a total of 5,225 peaks were detected, of which 943 metabolites were annotated. Compared with the wild-type group, there were 66 differential metabolites, containing 29 ups and 37 downs. As shown by volcano plot, metabolite downregulation was more pronounced (Figure 4A). The difference in metabolism between wild types and mutants is depicted in a heat map as well (Figure 4B). It was observed that the top 10 metabolites with the smallest p -value were significantly lower in ATP6AP2^{Gly62Glu} than in ATP6AP2^{WT}: tyr-pro-phe-pro-gly-pro-ile, 7-[(6-Hydroxy-3,7-dimethyl-2,7-octadienyl)oxy]-2H-1-benzopyran-2-one, testosterone, corticosterone acetate, narbomycin, 9(S)-HPOT, oleandomycin, praziquantel, phenylalanyl-leucyl-leucyl-arginyl-asparagine, and antibiotic JI-20B (Figure 4C). In organisms, different metabolites interact to

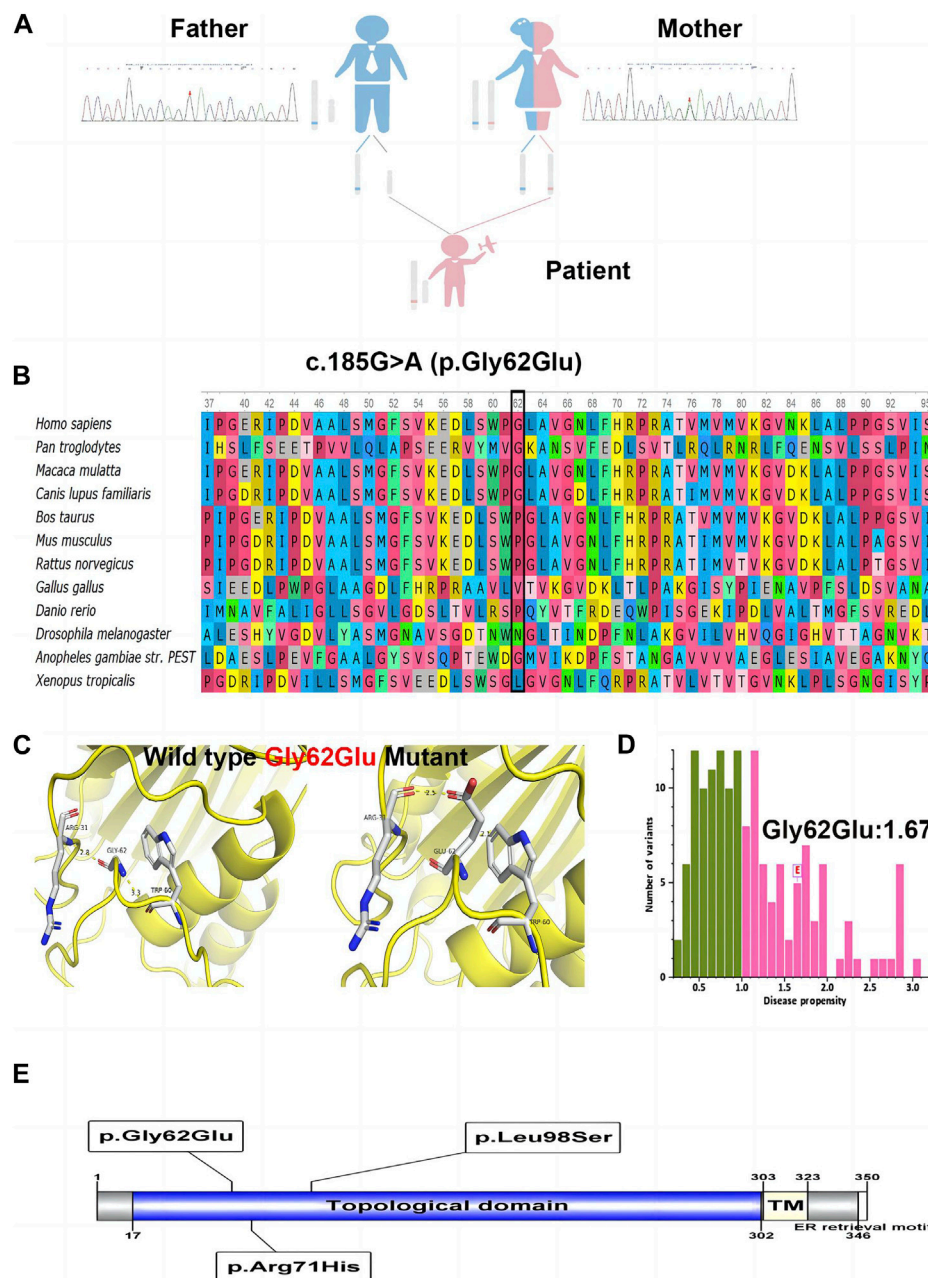


FIGURE 2

The identified c.185G>A (p.Gly62Glu) in *ATP6AP2*. Genetic genealogy diagram and Sanger sequencing confirmation in the parents (A). Conservation status of amino acid residue of the variant across various species (B). Wild and mutant type of the p. Gly62Glu variant compared by PyMol (C). The variant of interest, Gly62Glu, had a disease propensity of 1.67, and was marked on the histogram with a boxed label (D). Illustration of *ATP6AP2* protein domains, location of amino acid changes of the reported variants in CDG so far (E).

create various pathways. The KEGG database was used to annotate the differential metabolites, and the top 20 entries with the most differential metabolites in the pathway were selected. A summary bar chart and annotation category are illustrated in Figure 4D. The most involved metabolic pathway was steroid hormone biosynthesis, steroid biosynthesis, and arachidonic acid metabolism in lipid metabolism. Metabolism of terpenoids and polyketides as well as the endocrine system were involved. The enrichment netplot shows similar results (Figure 4E).

Discussion

ATP6AP2-CDG is a rare glycosylation defective disorder, which results from mutations in the X-linked *ATP6AP2*. To date, only three European (Germany and Portugal) patients with *ATP6AP2*-CDG have been described (Rujano et al., 2017). Incorporating the current patient, there are four reported cases of *ATP6AP2*-CDG, whose main manifestations were listed in Table 2. European patients were all males (3/3) with a current age range of 10 months–21 years,

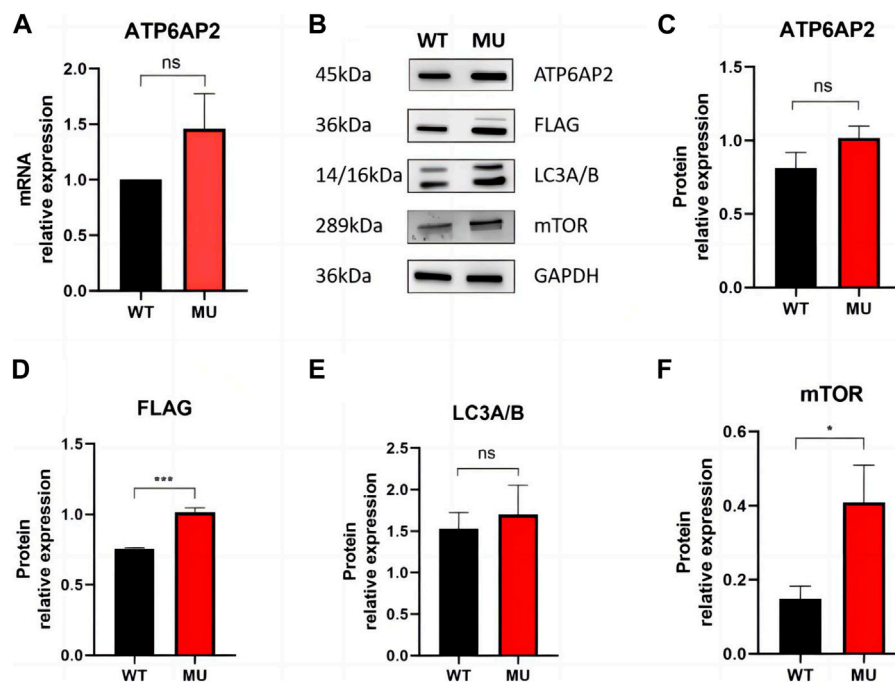


FIGURE 3

Expression of ATP6AP2, FLAG, LC3A/B and mTOR in HEK293T cells harboring wild type and mutant. mRNA of ATP6AP2 was slightly increased in mutant rather than in wild-type exogenous constructs, without significant difference (A). Western blotting showed alterations of the proteins (B). ATP6AP2 was increased without significant difference (C), while the expression of FLAG confirmed the elevated level in the mutant (D). LC3A/B was upregulated without significant difference (E). But mTOR signaling was significantly upregulated (F). ns represents no statistical significance, * represents $p < 0.05$, and *** represents $p < 0.001$.

two of whom were from the same family. Patients had disease onset since birth (2/3). Clinical manifestations included neonatal icterus (2/3), mild to moderate or pronounced cutis laxa (3/3), mild cognitive impairment (2/3), ataxic gait (1/3), and dysmorphic features (2/3). The gender, age, onset symptoms, and main presentations of the Chinese patient were consistent with the Europeans. In addition, he presented with growth retardation, cardiomegaly, anemia, and thrombocytopenia. For laboratory test results, European patients presented high fluctuating levels of alanine aminotransferase and aspartate aminotransferase (3/3) as well as elevated cholesterol and LDL cholesterol (2/3). Reduced coagulation factors, prolonged activated partial thromboplastin time and prothrombin time, increased D-dimer and international normalized ratio, and decreased fibrinogen and prothrombin time activity indicated coagulation dysfunction in them (3/3). The Chinese patient also had hypertransaminasemia, hypercholesterolemia, and coagulopathy but with a low level of serum ceruloplasmin. The European patients presented with immunodeficiency (3/3), suffering recurrent infections; this was not present in the Chinese patient. To understand the severity of liver damage, European patients underwent histological examination of the liver (2/3). Morphological features were consistent with micronodular hepatic cirrhosis (2/2), accompanied by moderate macro- and microvesicular steatosis (1/2). Transmission electron microscopy revealed lipid deposition and increased vacuolar structures inside hepatocytes (1/3). There were no other findings on liver histology in the Chinese patient. Generally, ATP6AP2-CDG mainly affects the liver and the nervous

system, though the immune and lymphatic hematopoietic system may be involved as well. WES demonstrated hemizygous missense mutations in ATP6AP2 in European patients (3/3), including c.212G>A (p.Arg71His) and c.293C>T (p.Leu98Ser). The Chinese patient had a hemizygous missense mutation in novel c.185G>A (p.Gly62Glu) in ATP6AP2. ATP6AP2 (NM_005765, ENST00000636580.2) is located on chromosome Xp11.4 (chrX: 40,580,970-40,606,848) and contains nine exons encoding a protein of 350 amino acids. The encoded ATP6AP2 [ATPase H⁺ transporting accessory protein 2, also known as the (pro) renin receptor] interacts with renin or prorenin on the cell surface to affect protein activity in one way, and acts as a part of the proton pump associated with adenosine triphosphatase (ATPase) in the other way (Wendling et al., 2017; Guida et al., 2018). Acidification of intracellular compartments, secondary active transport, energy conservation, and cellular pH regulation are all important functions of proton-translocating ATPases (Nelson et al., 2000; Scarborough, 2000; Tomashek and Brusilow, 2000). ATPases can be divided into the F, P, and V classes. The transmembrane proton-conducting sector V0 and the extramembrane catalytic sector V1 are both present in vacuolar (V-type) ATPases (Forgac, 2007). It has been discovered that ATP6AP2 is connected to the V0 sector of the V-type ATPases (Guida et al., 2018). Patients with mutation of c.185G>A (p.Gly62Glu), c.212G>A (p.Arg71His), or c.293C>T (p.Leu98Ser) presented a glycosylation disorder with predominant liver disease, immunodeficiency, and developmental delays. ATP6AP2 ablation affects multiple organs in adult mice (Wendling et al., 2017), providing the supporting basis. The

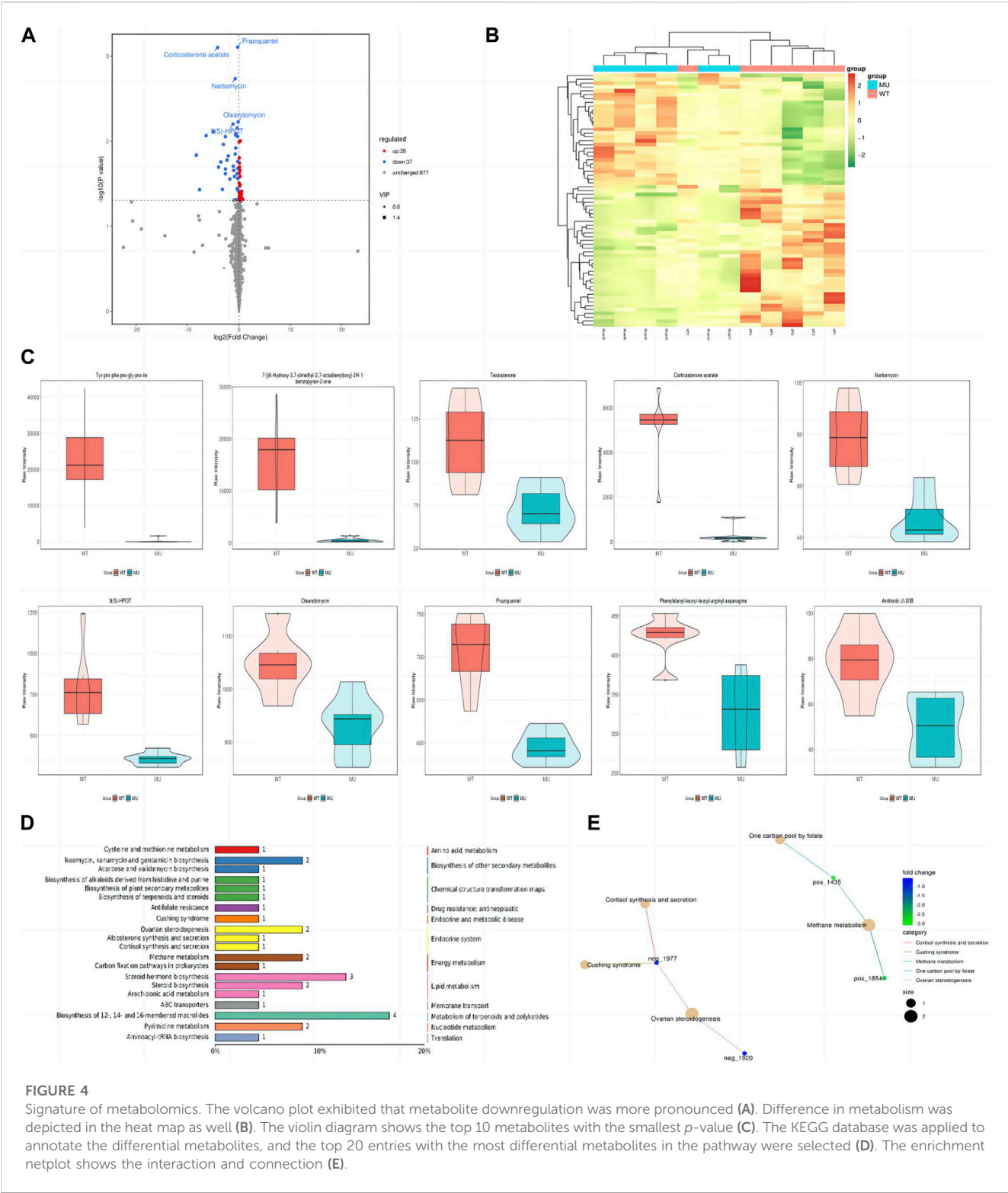


FIGURE 4 Signature of metabolomics. The volcano plot exhibited that metabolite downregulation was more pronounced (A). Difference in metabolism was depicted in the heatmap as well (B). The violin diagram shows the top 10 metabolites with the smallest *p*-value (C). The KEGG database was used to annotate the differential metabolites, and the top 20 entries with the most differential metabolites in the pathway were selected (D). The enrichment netplot shows the interaction and connection (E).

cardiomegaly in the Chinese patient might be associated with the ATP6AP2 variation, indicating the importance of cardiac evaluation and follow-up in these patients. In cardiomyocytes, ATP6AP2 is essential for vacuolar H⁺-ATPase assembly, and the loss-of-function could result in lethal heart failure (Kinouchi et al., 2010; Li et al., 2022). Mutations in TMEM199 (Vma12) and CCDC115 (Vma22), another two human homologues of yeast, could result in the similar

main clinical phenotypes (Jansen et al., 2016a; Jansen et al., 2016b; Fang et al., 2022). Therefore, V0 mis-assembly is speculated to be the common pathogenic process in these syndromes. In the previous study (Rujano et al., 2017), the mRNA level of the mutant Arg71His not Leu98Ser was elevated, while the level of both mutant proteins was decreased. A cycloheximide chase assay uncovered a shorter half-life in both mutant proteins. It indicated that disease-associated

TABLE 2 Main findings of the four patients with ATP6AP2-CDG.

Patient	Patient 1	Patient 2	Patient 3	Patient 4
	Family 1			
Reference	Rujano et al. (2017)	Rujano et al. (2017)	Rujano et al. (2017)	Current study
Gender	Male	Male	Male	Male
Current age	21 years	10 months	17 years	21 months
Onset of symptoms	Directly after birth	Directly after birth	5 months	Directly after birth
Country of origin	Germany	Germany	Portugal	China
Neonatal icterus	Absent	Present	Present	Present
Cutis laxa	Pronounced, improvement over time	Pronounced	Mild to moderate	Pronounced, improvement after liver transplantation
Developmental abnormalities	Ataxic gait, mild cognitive impairment	Normal	Mild cognitive impairment	Growth retardation
Other manifestation	Low-set ears, micrognathia, a flat and wide-set chest, laterally facing nipples, and hypospadias	NA	Mild dysmorphic features	Cardiomegaly, anemia and thrombocytopenia
Elevated transaminases	ALT 59 IU/L; AST 92–135 IU/L	AST 100–160 IU/L	ALT 51 IU/L; AST 61 IU/L	ALT 15.22–68.72 IU/L; AST 27.07–241.00 IU/L
Serum lipids	LDL cholesterol: 149 (reference: 50–130 md/dL)	Cholesterol: 254 (reference: 81–147 mg/dL)	Normal	Total cholesterol: 7.24 (reference: 3.1–5.2 mmol/L) LDL-cholesterol: 5.12 (reference: 1.30–3.90 mmol/L)
Ceruloplasmin (0.22–0.58 g/L)	NA	NA	NA	<0.02–0.17
Coagulation parameters	Low factor XI and free Protein S	Low factors II, V, VII, IX, and XI	Low factor V and VII	Prolonged APTT and PT, increased D-dimer and INR, and decreased fibrinogen and PTA
Infection	Recurring pulmonary and upper respiratory tract infections	Recurring upper respiratory tract infections	Recurrent sepsis and peritonitis	Absent
Liver histology	NA	Diffuse micronodular hepatic cirrhosis	Micronodular hepatic cirrhosis with moderate macro- and microvesicular steatosis	Micronodular hepatic cirrhosis with moderate macro- and microvesicular steatosis
Hepatic ultrastructure	NA	Accumulations of autolysosomes	NA	NA
Zygosity	Hemizygous	Hemizygous	Hemizygous	Hemizygous
Mutation sites	c.212G>A	c.212G>A	c.293C>T	c.185G>A
Amino acid change	p.Arg71His	p.Arg71His	p.Leu98Ser	p.Gly62Glu
Glycosylation studies	Abnormal N-glycosylation	Abnormal N-glycosylation	Abnormal N-glycosylation	NA
Treatment	IgG substitution for immunodeficiency	NA	Weekly subcutaneous Ig for immunodeficiency	Living related liver transplantation for chronic liver failure

NA: not available.

mutations targeted ATP6AP2 for degradation. In addition, the p.Leu98Ser mutation led to developmental defects, protein instability, and lipid homeostasis impairment in functional experiments. The previous study also found that the missense mutations impaired the interaction between ATP6AP2 and other V-ATPase assembly factors, which generally formed a complex (Rujano et al., 2017). For the current identified p.Gly62Glu mutation, immunohistochemistry detected no obvious expression changes of ATP6AP2 in the patient's liver sample. Then we introduced an exogenous mutant into HEK293T cells, which did

not show increased mRNA or protein expression of ATP6AP2 in Gly62Glu mutant cells with respect to wild type, indicating that c.185G>A (p.Gly62Glu) in ATP6AP2 had no influence on its expression. Our predicted protein model displayed that the non-polar aliphatic amino acid glycine was substituted by acidic amino acid glutamic acid with altered polar contact with around Arg31 and Trp60. Because there is no side chain on the glycine in the wild type, the protein is more flexible at this point. While the variant residue glutamic acid has a negatively charged side chain, making it hydrophilic to prefer the surface of the protein to its interior. It

suggests that the p.Gly62Glu mutation may have different effects on protein function, though there is a lack of direct evidence. Further research is needed to investigate the influence and association with the patient's presentation.

Autophagy is a lysosomal breakdown process that controls the homeostasis of proteins and organelles, and it is essential for maintaining a healthy liver and regulating hepatic physiology and metabolism (Ke, 2019). Since ATP6AP2-CDG causes liver disease mainly, autophagy flux was explored in those patients. In Rujano et al. (2017) study, autophagosome markers p62 and Atg8a/LC3 were increased in ATP6AP2^{Leu98Ser} animals, suggesting increased autophagosome formation and/or decreased autophagic degradation. The enlarged autophagosomes were observed with undegraded content (lipid droplets) under electron microscopy. Meanwhile, LC3A/B was not elevated in the current patient's liver but increased in the HEK293T cells with a p.Gly62Glu mutation. As the last step of autophagic breakdown is typically dependent on V-ATPase-mediated acidification, the decrease in V-ATPase activity caused by ATP6AP2 mutations induces an autophagy defect. Notably, it is well known that the mTOR pathway is essential for the regulation of autophagy (Wang et al., 2019). mTOR recruits two different signaling complexes, mTOR complex 1 (mTORC1) and mTOR complex 2 (mTORC2). In ATP6AP2^{Leu98Ser} animals, mTOR signaling was reduced in agreement with the proposed role of the V-ATPase in mTORC1 activation at the lysosomal-membrane (Rujano et al., 2017). The mTORC1 has been clarified to negatively regulate autophagy in multiple pathways (Kim et al., 2011; Martina et al., 2012; Park et al., 2016). However, it is unclear how exactly mTORC2 controls autophagy. The current finding of dysregulated autophagy and mTOR signaling seems to be consistent with previous knowledge.

The deficiency caused by c.212G>A (p.Arg71His) and c.293C>T (p.Leu98Ser) in ATP6AP2 was proved to result in hypoglycosylation of serum proteins in patients and mice (Rujano et al., 2017). The prior patients showed aberrant tetrasialotransferrin and tri-, di-, and monosialotransferrin glycosylation patterns, which indicated N-Glycosylation disorder. The mice model treated with adeno-CRE induced liver-specific acute ATP6AP2 decrease; consequently, the liver enzymes and lipid parameters were elevated, which illustrated that ATP6AP2 defect could lead to liver damage and metabolic abnormalities. Transferrin evaluation, the main biomarker of CDG, was not possible in this patient because of the liver transplantation. In this study, the metabolomics signature of ATP6AP^{Gly62Glu} mutant introduced into HEK293T cells elucidated that most metabolites were downregulated and involved in the pathway of lipid metabolism. The patient carrying c.185G>A (p.Gly62Glu) presented with severe liver impairment (cirrhosis and steatosis) with elevated serum lipids before liver transplantation. Considering the obvious growth retardation as well, we speculate that the patient has metabolic dysfunction of lipids, which accumulate in the liver and cannot be transported, utilized, and energy supplied normally. Nevertheless, there were limitations of untargeted metabolomics and metabolomics itself, thus abnormalities in glucose metabolism were not detected. In addition, as the patient-derived live cells were not available, the metabolomics in this study is not sufficient to recapitulate the patient's real situation, which will facilitate the initiation of our further study.

Optional treatments are limited in CDGs, including substrate supplementation, cofactor supplementation, pharmaceutical chaperons, non-causative, and other treatment (Park and Marquardt, 2021). In addition, organ transplantation, such as liver transplantation for end-stage cirrhosis, was recommended recently. Successful liver transplantation was reported in ATP6AP1-CDG, MPI-CDG, and PMM2-CDG (Janssen et al., 2014; Alharbi et al., 2023; Semanova et al., 2023; Tahata et al., 2023). After liver transplantation in the patients, not only the specific clinical presentation was improved, but the abnormal glycosylation was also restored. It demonstrated that liver transplantation could be a curative option for certain CDG patients with late course of hepatopathy. However, no treatment and prognosis has been described for ATP6AP2-CDG previously. The Chinese patient was treated with albumin and fibrinogen infusion, oral administration of D-galactose, UDCA, and vitamin D/AD/E/K1 supplements. Yet liver transplantation was performed eventually because of chronic liver failure with decompensated cirrhosis at a high death risk. Liver function parameters gradually normalized, and cutis laxa also improved post transplantation. These observations illustrated the current effectiveness of liver transplantation. Although the patient presented no significant disease progression during 1 year follow-up, long-term surveillance is still necessary. Subsequent *in vitro* and *in vivo* trials will be conducted to further investigate the pathogenicity of the novel c.185G>A (p.Gly62Glu) in ATP6AP2 and potentially effective therapeutic strategies.

Conclusion

This work presents the first Chinese patient with additional growth retardation, cardiomegaly, anemia and thrombocytopenia, and the c.185G>A (p.Gly62Glu) mutation in ATP6AP2 exon 3, expanding the phenotypic and genotypic profile of ATP6AP2-CDG. The missense mutation dysregulated autophagy and mTOR signaling. The majority of metabolites were downregulated and implicated in the pathway of lipid metabolism in the exogenous Gly62Glu mutant. It establishes the groundwork for future investigations into the pathogenesis of ATP6AP2-CDG.

Data availability statement

The data presented in this study is included in the article/supplementary material. The datasets are not readily available due to privacy restrictions, further inquiries should be directed to the corresponding authors.

Ethics statement

The studies involving humans were approved by Children's Hospital of Fudan University. The studies were conducted in accordance with the local legislation and institutional requirements. Written informed consent for participation in this study was provided by the participants' legal guardians/next of kin. Written informed consent was obtained from the minor(s)' legal guardian/next of kin for the publication of any potentially identifiable images or data included in this article.

Author contributions

YF: Data curation, Formal Analysis, Investigation, Writing—original draft. Y-ZW: Data curation, Formal Analysis, Investigation, Writing—original draft. LC: Conceptualization, Writing—review and editing. X-BX: Conceptualization, Investigation, Writing—review and editing.

Funding

The author(s) declare that no financial support was received for the research, authorship, and/or publication of this article.

References

- Alharbi, H., Daniel, E. J. P., Thies, J., Chang, I., Goldner, D. L., Ng, B. G., et al. (2023). Fractionated plasma N-glycan profiling of novel cohort of ATP6AP1-CDG subjects identifies phenotypic association. *J. Inherit. Metab. Dis.* 46 (2), 300–312. doi:10.1002/jimd.12589
- Fang, Y., Abuduxikuer, K., Wang, Y. Z., Li, S. M., Chen, L., and Wang, J. S. (2022). TMEM199-Congenital disorder of glycosylation with novel phenotype and genotype in a Chinese boy. *Front. Genet.* 13, 833495. doi:10.3389/fgene.2022.833495
- Forgac, M. (2007). Vacuolar ATPases: rotary proton pumps in physiology and pathophysiology. *Nat. Rev. Mol. Cell Biol.* 8 (11), 917–929. doi:10.1038/nrm2272
- Guida, M. C., Hermle, T., Graham, L. A., Hauser, V., Ryan, M., Stevens, T. H., et al. (2018). ATP6AP2 functions as a V-ATPase assembly factor in the endoplasmic reticulum. *Mol. Biol. Cell* 29 (18), 2156–2164. doi:10.1091/mbc.E18-04-0234
- Ishak, K., Baptista, A., Bianchi, L., Callea, F., Groote, J. D., Gudat, F., et al. (1995). Histological grading and staging of chronic hepatitis. *J. Hepatol.* 22 (6), 696–699. doi:10.1016/0168-8278(95)80226-6
- Jansen, J. C., Cirak, S., van Scherpenzeel, M., Timal, S., Reunert, J., Rust, S., et al. (2016a). CCDC115 deficiency causes a disorder of golgi homeostasis with abnormal protein glycosylation. *Am. J. Hum. Genet.* 98 (2), 310–321. doi:10.1016/j.ajhg.2015.12.010
- Jansen, J. C., Timal, S., van Scherpenzeel, M., Michelakakis, H., Vicogne, D., Ashikov, A., et al. (2016b). TMEM199 deficiency is a disorder of golgi homeostasis characterized by elevated aminotransferases, alkaline phosphatase, and cholesterol and abnormal glycosylation. *Am. J. Hum. Genet.* 98 (2), 322–330. doi:10.1016/j.ajhg.2015.12.011
- Janssen, M. C. H., de Kleine, R. H., van den Berg, A. P., Heijdra, Y., van Scherpenzeel, M., Lefeber, D. J., et al. (2014). Successful liver transplantation and long-term follow-up in a patient with MPI-CDG. *Pediatrics* 134 (1), e279–e283. doi:10.1542/peds.2013-2732
- Ke, P. Y. (2019). Diverse functions of autophagy in liver physiology and liver diseases. *Int. J. Mol. Sci.* 20 (2), 300. doi:10.3390/ijms20020300
- Kim, J., Kundu, M., Viollet, B., and Guan, K. L. (2011). AMPK and mTOR regulate autophagy through direct phosphorylation of Ulk1. *Nat. Cell Biol.* 13 (2), 132–141. doi:10.1038/ncb2152
- Kinouchi, K., Ichihara, A., Sano, M., Sun-Wada, G. H., Wada, Y., Kurauchi-Mito, A., et al. (2010). The (pro)renin receptor/ATP6AP2 is essential for vacuolar H⁺-ATPase assembly in murine cardiomyocytes. *Circ. Res.* 107 (1), 30–34. doi:10.1161/CIRCRESAHA.110.224667
- Li, L., Cui, Y. J., Liu, Y., Li, H. X., Su, Y. D., Li, S. N., et al. (2022). ATP6AP2 knockdown in cardiomyocyte deteriorates heart function via compromising autophagic flux and NLRP3 inflammasome activation. *Cell Death Discov.* 8 (1), 161. doi:10.1038/s41420-022-00967-w
- Martina, J. A., Chen, Y., Gucek, M., and Puertollano, R. (2012). MTORC1 functions as a transcriptional regulator of autophagy by preventing nuclear transport of TFEB. *Autophagy* 8 (6), 903–914. doi:10.4161/auto.19653
- Nelson, N., Perzov, N., Cohen, A., Hagai, K., Padler, V., and Nelson, H. (2000). The cellular biology of proton-motive force generation by V-ATPases. *J. Exp. Biol.* 203 (Pt 1), 89–95. doi:10.1242/jeb.203.1.89
- Ondruskova, N., Cechova, A., Hansikova, H., Honzik, T., and Jaeken, J. (2021). Congenital disorders of glycosylation: still "hot" in 2020. *Biochim. Biophys. Acta Gen. Subj.* 1865 (1), 129751. doi:10.1016/j.bbagen.2020.129751
- Park, J. H., and Marquardt, T. (2021). Treatment options in congenital disorders of glycosylation. *Front. Genet.* 12, 735348. doi:10.3389/fgene.2021.735348
- Park, J. M., Jung, C. H., Seo, M., Otto, N. M., Grunwald, D., Kim, K. H., et al. (2016). The ULK1 complex mediates MTORC1 signaling to the autophagy initiation machinery via binding and phosphorylating ATG14. *Autophagy* 12 (3), 547–564. doi:10.1080/15548627.2016.1140293
- Peanne, R., de Lonlay, P., Foulquier, F., Kornak, U., Lefeber, D. J., Morava, E., et al. (2018). Congenital disorders of glycosylation (CDG): *quo vadis?* *Eur. J. Med. Genet.* 61 (11), 643–663. doi:10.1016/j.ejmg.2017.10.012
- Rujano, M. A., Cannata Serio, M., Panasyuk, G., Peanne, R., Reunert, J., Rymen, D., et al. (2017). Mutations in the X-linked ATP6AP2 cause a glycosylation disorder with autophagic defects. *J. Exp. Med.* 214 (12), 3707–3729. doi:10.1084/jem.20170453
- Scarborough, G. A. (2000). The plasma membrane proton-translocating ATPase. *Cell Mol. Life Sci.* 57 (6), 871–883. doi:10.1007/PL00000730
- Semenova, N., Shatokhina, O., Shchagina, O., Kamenec, E., Marakhonov, A., Degtyareva, A., et al. (2023). Clinical presentation of a patient with a congenital disorder of glycosylation, type IIa (ATP6AP1), and liver transplantation. *Int. J. Mol. Sci.* 24 (8), 7449. doi:10.3390/ijms24087449
- Tahata, S., Weckwerth, J., Ligezka, A., He, M., Lee, H. E., Heimbach, J., et al. (2023). Liver transplantation recovers hepatic N-glycosylation with persistent IgG glycosylation abnormalities: three-year follow-up in a patient with phosphomannomutase-2-congenital disorder of glycosylation. *Mol. Genet. Metab.* 138 (4), 107559. doi:10.1016/j.ymgme.2023.107559
- Tomashek, J. J., and Brusilow, W. S. (2000). Stoichiometry of energy coupling by proton-translocating ATPases: a history of variability. *J. Bioenerg. Biomembr.* 32 (5), 493–500. doi:10.1023/a:1005617024904
- Wang, H., Liu, Y., Wang, D., Xu, Y., Dong, R., Yang, Y., et al. (2019). The upstream pathway of mTOR-mediated autophagy in liver diseases. *Cells* 8 (12), 1597. doi:10.3390/cells8121597
- Wendling, O., Champy, M. F., Jaubert, S., Pavlovic, G., Dubos, A., Lindner, L., et al. (2017). Atp6ap2 ablation in adult mice impairs viability through multiple organ deficiencies. *Sci. Rep.* 7 (1), 9618. doi:10.1038/s41598-017-08845-7

Conflict of interest

The authors declare that the research was conducted in the absence of any commercial or financial relationships that could be construed as a potential conflict of interest.

Publisher's note

All claims expressed in this article are solely those of the authors and do not necessarily represent those of their affiliated organizations, or those of the publisher, the editors and the reviewers. Any product that may be evaluated in this article, or claim that may be made by its manufacturer, is not guaranteed or endorsed by the publisher.



OPEN ACCESS

EDITED BY

Ivan Martinez Duncker,
Universidad Autónoma del Estado de
Morelos, Mexico

REVIEWED BY

Duangrurdee Wattanasirichaigoon,
Mahidol University, Thailand
Alireza Tafazoli,
Medical University of Bialystok, Poland

*CORRESPONDENCE

Panagoula Kollia,
✉ pankollia@biol.uoa.gr

RECEIVED 24 July 2023

ACCEPTED 06 November 2023

PUBLISHED 27 November 2023

CITATION

Maroulis V, Agathangelidis A, Skouma A,
Sdogou T, Papadakis MN,
Papakonstantinou E, Girginoudis P,
Vorgias CE, Aleporou V and Kollia P
(2023), Molecular characterization of
novel and rare DNA variants in patients
with galactosemia.
Front. Genet. 14:1266353.
doi: 10.3389/fgene.2023.1266353

COPYRIGHT

© 2023 Maroulis, Agathangelidis,
Skouma, Sdogou, Papadakis,
Papakonstantinou, Girginoudis, Vorgias,
Aleporou and Kollia. This is an open-
access article distributed under the terms
of the [Creative Commons Attribution
License \(CC BY\)](https://creativecommons.org/licenses/by/4.0/). The use, distribution or
reproduction in other forums is
permitted, provided the original author(s)
and the copyright owner(s) are credited
and that the original publication in this
journal is cited, in accordance with
accepted academic practice. No use,
distribution or reproduction is permitted
which does not comply with these terms.

Molecular characterization of novel and rare DNA variants in patients with galactosemia

Vasileios Maroulis¹, Andreas Agathangelidis¹, Anastasia Skouma²,
Triantafyllia Sdogou², Manoussos N. Papadakis³,
Evangelos Papakonstantinou³, Panagiotis Girginoudis²,
Constantinos E. Vorgias⁴, Vassiliki Aleporou¹ and
Panagoula Kollia^{1*}

¹Department of Genetics and Biotechnology, Faculty of Biology, School of Physical Sciences, National and Kapodistrian University of Athens, Athens, Greece, ²Department of Newborn Screening, Institute of Child Health, Athens, Greece, ³Neolab SA, Athens, Greece, ⁴Department of Biochemistry and Molecular Biology, Faculty of Biology, School of Physical Sciences, National and Kapodistrian University of Athens, Athens, Greece

Introduction: Galactosemia is an inherited disorder caused by mutations in the three genes that encode enzymes implicated in galactose catabolism. Currently, the only available treatment for galactosemia is life-long dietary restriction of galactose/lactose, and despite treatment, it might result in long-term complications.

Methods: Here, we present five cases of newborn patients with elevated galactose levels, identified in the context of the newborn screening program. Genetic analysis concerned a next generation sequencing (NGS) methodology covering the exons and adjacent splice regions of the *GALT*, *GALK1*, and *GALE* genes.

Results: Our approach led to the identification of eight rare nonsynonymous DNA variants. Four of these variants, namely, p.Arg204Gln and p.Met298Ile in *GALT*, p.Arg68Leu in *GALK1*, and p.Ala180Thr in *GALE*, were already recorded in relevant databases, yet their clinical significance is uncertain. The other four variants, namely, p.Phe245Leu in *GALT*, p.Gly193Glu in *GALK1*, and p.Ile266Leu and p.Ala216Thr in the *GALE* gene, were novel. *In silico* analysis of the possible effect of these variants in terms of protein function and stability was performed using a series of bioinformatics tools, followed by visualization of the substituted amino acids within the protein molecule. The analysis revealed a deleterious and/or destabilizing effect for all the variants, supported by multiple tools in each case.

Discussion: These results, given the extreme rarity of the variants and the specific phenotype of the respective cases, support a pathogenic effect for each individual variant. Altogether, our study shows that targeted NGS methodologies may offer a time- and cost-effective approach for the genetic investigation of galactosemia and can assist in elucidating the complex genetic background of this disorder.

KEYWORDS

galactosemia, newborn screening, next-generation sequencing, genetics, molecular analysis, mutation

1 Introduction

Hereditary galactosemia is the most common and severe type of disorders related to inborn errors of galactose metabolism. More specifically, the disease is caused by a functional impairment in any of the three enzymes responsible for the conversion of α -D-galactose to glucose-1-phosphate (Holden et al., 2003). These three enzymes constitute the “Leloir pathway” and include galactokinase (GALK, EC:2.7.1.6), galactose-1-phosphate uridylyltransferase (GALT, EC 2.7.7.12), and UDP-galactose 4-epimerase (GALE, EC 5.1.3.2). Defects in any of these enzymes are directly linked to the onset of galactosemia, which is inherited in an autosomal recessive manner. GALT deficiency or classic galactosemia (OMIM 230400) caused by mutations in the *GALT* gene emerges during the neonatal period and presents with feeding problems, liver dysfunction, lethargy, bleeding diathesis, growth failure, and sepsis (Berry et al., 2000; Demirbas et al., 2018). Duarte galactosemia is characterized by the presence of a typical *GALT* mutation and the Duarte-2 allele. The latter is associated with the presence of the p.Asn314Asp variant occurring in *cis* configuration with three intronic variants (namely, c.378–27G>C, c.507 + 62G>A, and c.508–24G>A) and a deletion at the *GALT* gene promoter ((c.-119_116delGTCA). Individuals with Duarte galactosemia exhibit lower GALT activity (15%–35% compared to the germline allele), a moderate increase in blood galactose, and are usually asymptomatic (Demirbas et al., 2018). GALK deficiency or galactosemia II (OMIM 230200) is caused by mutations in the *GALK1* gene, with its main clinical presentation concerning the formation of cataracts due to galactitol accumulation in the lens (Sangiulio et al., 2004; Demirbas et al., 2018). GALE deficiency (OMIM 230350) is caused by mutations in the *GALE* gene and presents with similar symptoms as those of classic galactosemia, including feeding problems, hypotonia, jaundice, and liver dysfunction (Alano et al., 1998; Demirbas et al., 2018). The prevalence of classic galactosemia is estimated to be 1:40,000–60,000 in Europe and the United States (Berry et al., 2000; Demirbas et al., 2018), while the disease incidence in Greece is estimated to be 1:51,000 (Schulpis et al., 2016). The incidence of GALK deficiency ranges between 1:150,000 and 1:1,000,000 (Sangiulio et al., 2004), while the frequency of GALE deficiency varies from 1:6,200 to 1:64,800 depending on the ethnic background (Alano et al., 1998). Currently, the only available treatment for all three types of galactosemia is lifelong galactose-/lactose-restricted diet. Despite the application of this treatment, the majority of patients with classic galactosemia have long-term complications including cognitive and/or behavioral problems, speech and motor delay, and premature ovarian insufficiency (Fridovich-Keil et al., 2011). In contrast, the formation of cataracts due to GALK deficiency is usually preventable with diet, while long-term effects have not been observed in the case of GALE deficiency (Cerone and Rios, 2019).

Overall, the increased frequency of galactosemia, its variability in terms of clinical effects, and the lifelong nature of the only available treatment have attracted the interest of researchers in the genetic investigation of the disease. In this context, the

integration of galactosemia genetic markers in screening programs was important in the continuous effort for the identification of novel mutations in relevant genes. In Greece, the Institute of Child Health (ICH) is responsible for newborn screening (NS) for the metabolic disorders of phenylketonuria and galactosemia. To date, 363 variants of the *GALT* gene have been recorded in the Associated Regional and University Pathologists (ARUP) database (Calderon et al., 2007), of which 300 variants have been characterized as mutations, with nine of those (3%) being found in Greece (Schulpis et al., 2017). Furthermore, the number of recorded mutations for the *GALK1* and *GALE* genes in ClinVar is 60 and 17, respectively (Landrum et al., 2018).

In the current study, we present five cases of newborn patients with elevated galactose levels identified in the context of the NS program. The application of a targeted re-sequencing approach for the three pathogenic genes, namely, *GALT*, *GALK1*, and *GALE*, led to the identification of four novel and four rare DNA variants.

2 Materials and methods

2.1 Study group

Five galactosemia patients (2 with *GALT*, 2 with *GALE*, and 1 with *GALK* deficiency) were identified through the National Newborn Screening (NBS) program. Patients' follow-up was performed by the clinical department of the Greek Institute of Child Health in compliance with the European Guidelines for Classical Galactosemia (Welling et al., 2017). All procedures were performed in accordance with the ethical standards of the responsible committee on human experimentation in our department and with the Helsinki Declaration of 1975 as revised in 2008.

2.2 Study subjects

Patient M1 was a female neonate born to a primigravida mother at full term (after 40 weeks) by cesarean section. Neonatal screening indicated a high level of galactose in the blood (36.4 mg/dL). The patient was admitted to the hospital in good general condition, with jaundice (bilirubin levels of 10.56 mg/dL) and cortical cataract. According to her family history, her maternal grandmother was epileptic for which she received medical treatment. Her *GALT* enzyme activity was normal (9.5 U/g Hb). She was immediately started on a galactose-free diet and received vitamin D supplementation. Patient M1 maintained normal levels of galactose without psychomotor retardation. During her more recent follow-up, the patient was 4 years old, had no cataract, and did not present with any learning difficulties at the nursery school. Her results of blood biochemical test and ultrasound of abdomen were normal. Finally, the galactose follow-up level on a dried blood spot (DBS) was below 10 mg/dL, while the more recent measurement of galactose was 2.1 mg/dL. She continues the galactose-restricted diet.

Patient T1 was a male neonate born after 39 weeks of gestation via normal delivery. Neonatal screening indicated a high level of galactose in the blood (>50 mg/dL). The patient was admitted to the

hospital without any clinical symptoms or cataract. Yet, the patient presented with increased bilirubin levels (16.99 mg/dL) and increased liver function; regarding the latter, both the serum glutamic-oxaloacetic transaminase (SGOT) and serum glutamic pyruvic transferase (SGPT) tests showed elevated levels (>120 IU/dL). GALT enzyme activity was equivocal (3 U/g Hb), and therefore analysis of genes implicated in galactosemia could assist in patient diagnosis. The patient started a galactose-free diet, preserving normal psychomotor development. In his clinical follow-up at the age of 4 years, he presented with normal blood biochemistry, normal eye examination, no psychomotor retardation, and displayed normal learning ability at the nursery school. His weight and height were normal for his age, and he still followed a galactose-restricted diet. The more recent assessment of his galactose level was normal (1.5 mg/dL).

Patient L1 was a female neonate born after 37 weeks of gestation by normal delivery. Neonatal screening indicated a high level of galactose in the blood (64.5 mg/dL). She had only bilateral cataract with no other symptoms and received galactose-free diet and iron supplementation. Her GALT activity was normal, with the GALT measurement at birth being 24 μ mol/h/g Hb (normal rate 20–35). Her clinical follow-up remained uneventful with normal galactose levels. The most recent galactose measurement was 2 mg/dL. Eye examination showed that she still has cataract, without any other abnormality. No abnormality was found later during her menstrual period, which started without the need of any hormone supplement. She is now 15 years old, without any difficulties in concentration, yet she has disease phobia and receives regular psychological support. In terms of learning capacity, she is a good student but a very introvert person. She also has anemia and was started on iron supplements. The abdominal ultrasound and bone density test (DXA) results were normal.

Patient D1 was a female neonate born after 39 weeks of gestation by normal delivery. Neonatal screening indicated mildly elevated galactose levels in the blood (15.8 mg/dL), and she was admitted to the hospital to perform the galactosemia diagnostic work-up, where she remained clinically normal and was started on a galactose-free diet. Her GALT activity was normal and psychomotor development was normal on clinical follow-up. Eventually, the special diet was discontinued due to the Duarte mild mutation. She is 4 and a half years old and is currently on a normal diet. Her blood biochemical tests were normal, with no evidence of mental retardation. Galactose levels were normal, with no visual defects. Her growth charts are normal for her age, with the weight being at the 85–97th percentile and the height at the 50th percentile. The most recent measurement showed a galactose level of 1.15 mg/dL.

Patient K1 was a female neonate born after 40 weeks of gestation by normal delivery. Neonatal screening indicated a blood galactose level of 20.4 mg/dL. During hospitalization, the patient displayed normal levels of the relevant liver enzymes without any specific clinical symptoms. GALT activity was estimated at 5.9 U/g Hb, while the ophthalmological examination result was also normal. Nevertheless, she was started on a galactose-free diet, yet for the last 2 years, she has been on a diet with normal galactose levels. She is now 4 and half years old, and besides being on regular galactose diet, the blood biochemical tests were normal, with no evidence of cataract. Despite her good clinical condition, she is hesitant to communicate and needs psychological support. The most recent measurement of galactose was 1.3 mg/dL.

2.3 Quantification of galactose levels

Screening procedures have been described in detail previously (Sanguolo et al., 2004). In brief, total galactose was measured from dried blood spots using enzymatic DELFIA methods with the PerkinElmer GSP analyzer. The cutoff/normal level of total blood galactose was 20 mg/dL, while the measurement of GALT activity was the second-tier test in the diagnostic algorithm.

2.4 GALT activity assay

GALT activity was measured using an assay; specifically, GALT in the blood sample catalyzed a reaction between galactose-1-phosphate and uridine diphosphoglucose contained in the assay substrate reagent. In the course of further reactions, nicotinamide adenine dinucleotide phosphate (NADP) also contained in the assay substrate reagent was reduced to NADPH, a fluorescent substance that was measured via excitation at 355 nm and emission detection at 460 nm. Values over 3.5 (U/g Hb) corresponded to normal GALT activity, while values between 2.5 and 3.5 corresponded to equivocal GALT activity. Finally, values below 2.5 corresponded to abnormal GALT activity, which alludes to a pathogenic galactose metabolism. Therefore, the estimation of GALT activity was used as a second-tier test in the galactosemia algorithm.

2.5 Genomic analysis

Genomic DNA was extracted from whole blood using the NucleoSpin® Blood mini kit (Macherey-Nagel GmbH, Germany). The quantity of DNA samples was measured using a Qubit® 2.0 fluorometer (Thermo Fisher Scientific, MA, United States). In terms of next-generation sequencing (NGS) analysis, a custom Ion AmpliSeq™ panel was designed, covering the exons, adjacent splice regions, and parts of the 5' and 3' UTRs of the *GALT*, *GALK1*, and *GALE* genes. Library preparation was performed using the Ion AmpliSeq™ Library Kit 2.0 (Thermo Fisher Scientific, MA, United States) according to the manufacturer's instructions. Emulsion PCR was performed using the Ion OneTouch™ 2 system (Thermo Fisher Scientific, MA, United States), and the libraries were sequenced on an Ion Torrent PGM sequencer (Thermo Fisher Scientific, MA, United States). NGS raw data were analyzed using Torrent Suite Software (Thermo Fisher Scientific, MA, United States), while the visualization of results was performed using the Integrative Genomics Viewer (IGV) (<http://software.broadinstitute.org/software/igv/>) (Robinson et al., 2011). Genetic analysis of parents toward identifying the configuration of coexisting variants (either in *trans* or in *cis*) was only feasible for patient M1 and was performed with Sanger sequencing.

2.6 *In silico* prediction analysis

Evaluation of the possible impact of gene DNA variants on protein function and stability was performed with a series of purpose-built bioinformatics tools. More specifically, the

pathogenicity of the variants in terms of protein function was analyzed with the SIFT, Polyphen-2, PROVEAN, Mutation Taster, and CADD tools. In addition, the effect on protein stability was investigated with the Site Directed Mutator (SDM), mCSM, MUpro, and CUPSAT prediction tools. The selection of multiple tools was based on the fact that these tools are among the most widely used and also based on very distinct methodologies, and their performances may vary depending on the setting.

Analysis of the variant effect on protein function with SIFT was based on sequence homology and led to the calculation of a score ranging from 0 to 1. Substitutions with a score of <0.05 are characterized as deleterious, while those with a score of ≥ 0.05 are considered tolerated (Kumar et al., 2009). Polyphen-2 uses sequence-based and structure-based features to classify variants. The Polyphen-2 score represents the probability of a substitution to be damaging; scores between 0 and 0.15 are associated with benign variants, while scores between 0.15 and 1 are assigned to possibly damaging variants (Adzhubei et al., 2010). PROVEAN performs an alignment of the query sequence with related protein sequences and calculates an alignment score. If the score is equal or below a certain threshold (by default 2.5), the variant is predicted to be deleterious; otherwise, it is considered neutral (Choi and Chan, 2015). Mutation Taster classifies variants by incorporating data from common polymorphisms and known mutations extracted from relevant databases and the literature, as well as conservation data from the alignment of nucleotide and amino acid sequences with the respective sequences of ten other species. The tool provides a prediction together with its probability; a score close to 1 indicates a high probability (Schwarz et al., 2010). Finally, CADD compares real against simulated variants and integrates multiple annotations into one metric, the C-score. The C-score is strongly correlated with pathogenicity, with a value of 10 indicating that the variant is among the 10% of most deleterious nucleotide changes in the human genome. For the identification of deleterious variants, the default cutoff is set between 10 and 20 (Rentzsch et al., 2019). For these reasons, the cutoff for the detection of relevant variants in the present study was set to 15.

SDM uses environment-specific substitution tables (ESSTs) to calculate the difference in stability between the wild-type and mutated proteins. ESSTs are calculated for each family of proteins and provide the probability that an amino acid substitution may occur in a specific local structural environment that is defined by main-chain conformational angles and secondary structures, relative solvent accessibility, and hydrogen bonding patterns (Pandurangan et al., 2017). mCSM uses a graph-based approach where the amino acid environment is defined by atoms within a certain distance. Distance patterns are then extracted from the pairwise distances of the atoms as feature vectors called mCSM signatures. mCSM signatures and vectors that represent the difference between the reference and replacement amino acids are then used to train predictive models for protein stability and protein interactions (Pires et al., 2014). MUpro uses support-vector machines (SVMs) trained in a dataset of 1,615 single-site mutations from 42 proteins extracted from the thermodynamic database for proteins and mutants ProTherm (Gromiha et al., 2000) to predict the stability changes caused by mutations (Cheng et al., 2006). CUPSAT predicts changes in protein stability due to point mutations using a prediction model based on atom potentials

and torsion angle potentials derived from a set of 4,024 protein structures. The tool also incorporates information regarding the secondary structure and solvent accessibility (Parthiban et al., 2006). Visualization of the three-dimensional structure of the protein and the respective residues was performed using Visual Molecular Dynamics (Humphrey et al., 1996).

2.7 *In silico* structural analysis

In silico protein structural analysis was employed for the assessment of the impact of the identified variants on protein structure. The applied methodology can be categorized in three main levels: (i) primary sequence collection, (ii) modeling of the three-dimensional (3D) protein structures, and (iii) 3D protein structure comparison.

The first step concerned the collection of sequences of the *GALT*, *GALE*, and *GALK1* genes with or without the identified variants (germline/wildtype form); given the inability to assess whether concurrent variants in the same gene were present in *cis* or *trans* configuration, all possible combinations of variants were taken into account. In particular, the *GALT* sequence dataset included the germline sequence as well as sequences carrying the individual Arg204Gln, Met298Ile, Asn314Asp, and Phe245Leu variants as well as the combinations of Arg204Gln/Met298Ile and Asn314Asp/Phe245Leu. In the case of the *GALE* gene, the germline sequence as well as sequences carrying the Ala216Thr, Ala180Thr, and Ile266Leu variants were included in the analysis. Regarding the *GALK1* gene, sequence collection involved the germline counterpart as well as those sequences carrying the Arg68Leu and Gly193Glu variants and their combination.

This set of 15 protein amino acid sequences were transformed to 3D protein models, using the SWISS-MODEL protein structure prediction tool (<https://swissmodel.expasy.org/>), which represents a fully automated protein structure homology-modeling analyzer. This process resulted in a set of protein models in PDB format. Structural alignment was performed between the germline form of each gene and all its respective variants using the PDBeFold tool, and the structural similarity score that corresponds to the overall root mean standard deviation (RMSD) was computed. The RMSD metric is well-established for the comparison of protein structures, while it is also a reliable indicator of variability when applied to very similar proteins. Finally, differences were visualized using the PyMOL tool.

3 Results

In total, five cases of patients presenting with clinical and biochemical indices of galactosemia were examined. Overall, the genetic investigation of the *GALT*, *GALK1*, and *GALE* genes led to the identification of eight DNA variants, which were either novel or had an unknown effect; detailed information regarding these variants is given in Table 1.

Concerning classical galactosemia (*GALT* deficiency), three cases (namely, D1, K1, and L1) were found to carry five variants in the *GALT* gene, four of which were unique (the Duarte-2 variant was identified in cases D1 and L1). The analysis of the individual *GALT* variants showed that three of them were either novel

TABLE 1 Detailed characterization of identified DNA variants in the *GALT*, *GALK1*, and *GALE* genes.

Case ID	Sex	Allele 1				Allele 2				Allele 3			
		Gene	Variant at protein level	Variant at cDNA level	Population frequency	Gene	Variant at protein level	Variant at cDNA level	Population frequency	Gene	Variant at protein level	Variant at cDNA level	Population frequency
D1	F	<i>GALT</i>	p.Phe245Leu	c.735C>G	Absent from population databases	<i>GALT</i>	p.Asn314Asp	Duarte-2 (c.-119_-116delGTCA, c.940A>G)	4.6% gnomAD	-	-	-	-
K1	F	<i>GALT</i>	p.Arg204Gln	c.611G>A	0.005% gnomAD	<i>GALT</i>	p.Met298Ile	c.894G>A	0.005% ALPHA	-	-	-	-
M1	F	<i>GALE</i>	p.Ile266Leu	c.796A>C rs758252537	Absent from population databases	<i>GALE</i>	p.Ala180Thr	c.538G>A	0.003% gnomAD	-	-	-	-
T1	M	<i>GALE</i>	p.Ala216Thr	c.646G>A	Absent from population databases	<i>GALE</i>	p.Ala216Thr	c.646G>A	Absent from population databases	-	-	-	-
L1	F	<i>GALK1</i>	p.Gly193Glu	c.578G>A	Absent from population databases	<i>GALK1</i>	p.Arg68Leu	c.203G>T	0.001% gnomAD	<i>GALT</i>	p.Asn314Asp	Duarte-2 (c.-119_-116delGTCA, c.940A>G)	4.6% gnomAD

(p.Phe245Leu) or rare (p.Arg204Gln and p.Met298Ile). Variant p.Arg204Gln was recorded in dbSNP and gnomAD, while it was also recorded in ClinVar as of uncertain significance. The other previously described *GALT* variant (p.Met298Ile) was identified in two siblings and two other independent cases with classic galactosemia (Schulpis et al., 2017) and was recorded in the dbSNP and ALPHA databases; no record of this variant was found in ClinVar.

Three novel variants were also identified in the *GALE* (namely, p.Ile266Leu and p.Ala216Thr) and *GALK1* genes (p.Gly193Glu). These variants were not present in any of the dbSNP, gnomAD, and ClinVar databases. In contrast, variants p.Ala180Thr and p.Arg68Leu identified in the *GALE* and *GALK1* genes, respectively, were previously recorded in dbSNP and/or gnomAD. Moreover, the *GALK1* p.Arg68Leu variant was recorded in ClinVar as of uncertain significance.

The genotypes of the individual cases of the present study were as follows: (i) *GALT*: Phe245Leu/Duarte-2 either in *cis* or *trans* configuration (case D1), (ii) *GALT*: p.Arg204Gln/p.Met298Ile either in *cis* or *trans* configuration (case K1), (iii) *GALE*: Ile266Leu/Ala180Thr in *trans* configuration (case M1), (iv) *GALE*: Ala216Thr/Ala216Thr with the possibility of a deletion in *trans* configuration (case T1), and (v) *GALK1*: Gly193Glu/Arg68Leu either in *cis* or *trans* configuration and *GALT*: Duarte-2/N1 (case L1).

3.1 Analysis of variants in the *GALT* gene

The novel amino acid change of Phe at position 245 for Leu (Phe245Leu) corresponded to an important physicochemical alteration of the R-amino acid group. *In silico* analysis led to its characterization as pathogenic (Table 2) by all applied functional prediction tools, while two out of the four stability prediction tools predicted a destabilizing effect, with CUPSAT also predicting unfavorable torsion angles. The *GALT* enzyme is an obligate dimer also requiring zinc for its function. Phe245 is located at a loop of the amino acid chain away from the active site or the zinc-binding site of the *GALT* enzyme (Figure 1), but in close proximity (<5 angstroms) with three amino acid residues (at positions 117, 118, and 119) located within a beta sheet of the other subunit. Hence, the p.Phe245Leu variant may affect subunit interaction, although such a role has not been extensively documented (McCorvie et al., 2016). The analysis of the rare amino acid change p.Arg204Gln showed contradictory results (Table 2), with Mutation Taster and CADD characterizing it as deleterious and the rest of the tools as neutral, even though this substitution led to a clear change in terms of polarity. Regarding protein stability, three out of the four stability prediction tools predicted a destabilizing effect, with only CUPSAT predicting favorable torsion angles. Arg204 is located away from the active site or the zinc binding site of the enzyme (Figure 1), within an alpha helix in the exterior of the molecule with no indications that this region may be implicated in subunit interaction.

The variant p.Met298Ile was considered deleterious after the *in silico* analysis by all functional prediction tools, even though both amino acids involved in the substitution are large and hydrophobic. Two out of the four stability prediction tools predicted a destabilizing effect, with CUPSAT also predicting unfavorable torsion angles. Met298 is located within a beta sheet in the

TABLE 2 *In silico* data analysis for the functional and stability effects of each variant at the protein level.

Gene	Variant at protein level	SIFT prediction score	Polyphen-2 prediction score	PROVEAN prediction score	Mutation taster prediction	CADD Phred score	SDM prediction	mCSM prediction	MUpro prediction	CUPSAT prediction	
										Stability	Torsion
GALT	p.Phe245Leu	Damaging	Possibly damaging	Deleterious	Disease causing	24,9	Increased stability	Destabilizing	Decrease stability	Stabilizing	Unfavorable
		000.002	0.763	−4.23							
GALT	p.Arg204Gln	Tolerated	Benign	Neutral	Disease causing	21,7	Increased stability	Destabilizing	Decrease stability	Destabilizing	Favorable
		000.321	0.007	−0.97							
GALT	p.Met298Ile	Damaging	Probably damaging	Deleterious	Disease causing	29,3	Increased stability	Destabilizing	Decrease stability	Stabilizing	Unfavorable
		000.001	1.0	−3.76							
GALE	p.Ile266Leu	Tolerated	Benign	Neutral	Disease causing	22,6	Reduced stability	Destabilizing	Decrease stability	Stabilizing	Favorable
		000.071	0.003	−1.37							
GALE	p.Ala180Thr	Damaging	Probably damaging	Neutral	Disease causing	25,9	Reduced stability	Destabilizing	Decrease stability	Destabilizing	Unfavorable
		000.021	0.96	−0.35							
GALE	p.Ala216Thr	Damaging	Probably damaging	Deleterious	Disease causing	28	Reduced stability	Destabilizing	Decrease stability	Stabilizing	Unfavorable
		0.0	1.0	−3.70							
GALK1	p.Gly193Glu	Damaging	Probably damaging	Deleterious	Disease causing	23,7	Reduced stability	Destabilizing	Decrease stability	Destabilizing	Unfavorable
		000.002	0.999	−6.58							
GALK1	p.Arg68Leu	Tolerated	Benign	Neutral	Polymorphism	15,41	Reduced stability	Destabilizing	Decrease stability	Destabilizing	No change
		000.705	0.009	−1.48							

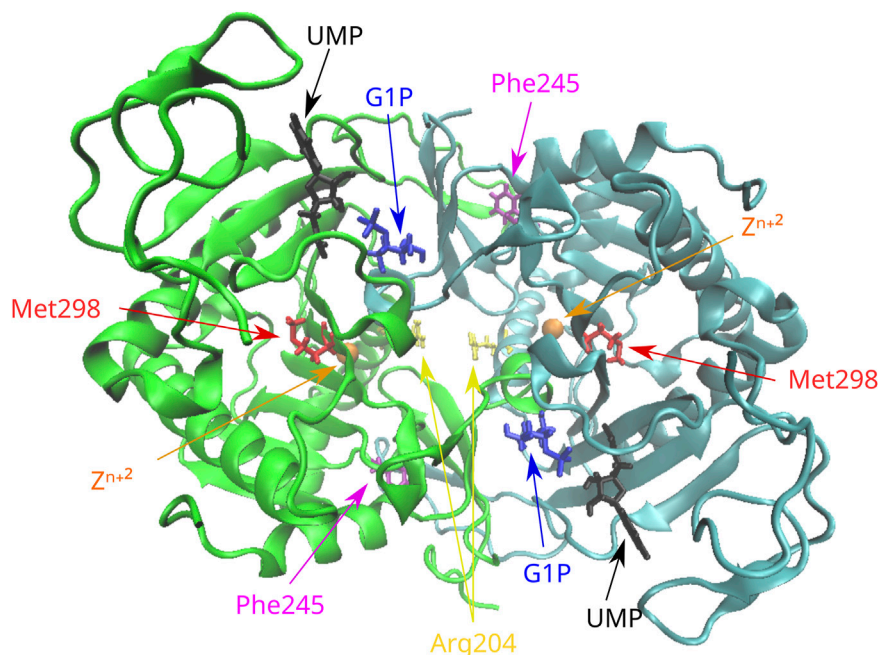


FIGURE 1

Position of the missense variants in the 3D structure of the GALT dimer. Phe245 is located in a loop of the molecule in proximity with residues of the other subunit. Arg204 is located in an alpha helix in the exterior of the molecule. Met298 is located in a beta sheet in the interior of the molecule. G1P, glucose-1-phosphate; UMP, uridine monophosphate.

interior of the molecule (Figure 1) and is not associated with either the active and zinc-binding sites of the enzyme or with subunit interaction.

3.2 Analysis of variants in the *GALE* gene

The novel variant p.Ile266Leu, which was located at exon 10, did not concern a significant change in the polarity of the amino acid R-group since both implicated amino acids are aliphatic. In terms of functional prediction, only Mutation Taster and CADD characterized this variant as deleterious. Three out of the four stability prediction tools predicted a destabilizing effect, while only CUPSAT predicted a stabilizing effect as well as favorable torsion angles (Table 2). The *GALE* enzyme also functions as a dimer, and Ile266 is located at the C-terminal domain of the subunits within a beta strand. This beta strand forms a parallel beta sheet with six other beta strands from the N-terminal domain (Figure 2), which is responsible for the positioning of NAD⁺. Yet Ile266 is not proximal to the active site nor is implicated in subunit interactions (Thoden et al., 2000).

The rare variant p.Ala180Thr resulted in a significant change from a hydrophobic to a polar R-group. As probably expected, all function prediction tools employed in the *in silico* analysis characterized the variant as deleterious, with the exception of PROVEAN. Likewise, all stability prediction tools predicted a destabilizing effect with unfavorable torsion angles. Ala180 is located at a beta strand of the N-terminal domain of the enzyme, which forms the same seven-stranded beta sheet responsible for the positioning of NAD⁺, although again the

residue is located away from the active site and is not implicated in subunit interactions.

The novel *GALE* variant p.Ala216Thr leads to a change of the hydrophobic R-group of alanine to the polar R-group of threonine. *In silico* analysis showed pathogenic predictions by all functional prediction tools. In line with this, all stability prediction tools reported a destabilizing effect. The only exception was CUPSAT, which predicted an overall stabilizing effect but unfavorable torsion angles. Ala216 is located at the C-terminal domain at one end of an alpha helix, which is not proximal to the active site of *GALE*. Of relevance, the other end of the helix is proximal enough to form interactions with the substrate. Again, there are no indications that this residue is implicated in subunit interactions.

3.3 Analysis of variants in the *GALK1* gene

The novel variant p.Gly193Glu concerns an amino acid change from the polar R-chain of glycine to the negatively charged R-chain of glutamate; a prediction of pathogenicity was supported by the *in silico* analysis with all aforementioned functional prediction tools. Furthermore, a destabilizing effect with unfavorable torsion angles was also supported by all stability prediction tools (Table 2). It has been suggested that the *GALK* enzyme functions as a dimer (Thoden et al., 2005); although Gly193 is not proximal to its active site, it is located at a loop of the molecule (Figure 3) that belongs to the subunit–subunit interface.

In the case of the rare variant p.Arg68Leu, the positively charged R-chain of arginine is replaced by the hydrophobic R-group of leucine. All *in silico* functional prediction tools classified this variant

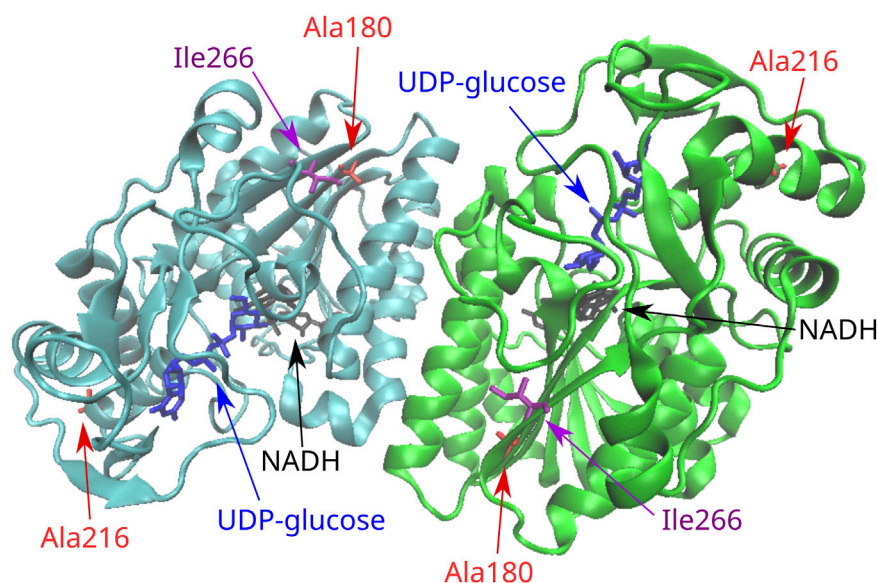


FIGURE 2

Position of the missense variants in the 3D structure of the GALE dimer. Ala216 is located in one end of an alpha helix in the C-terminal domain of the molecule. Ile266 is located in the C-terminal domain in a beta strand that forms a parallel beta sheet with six other beta strands from the N-terminal domain. This seven-stranded beta sheet is responsible for the positioning of NAD⁺. Ala180 is located in a beta strand of the N-terminal domain that forms the same seven-stranded beta sheet.

as neutral; in contrast, all stability prediction tools showed a destabilizing effect, with CUPSAT predicting no change in torsion angles. Arg68 is located at the N-terminal region of the molecule within a six-stranded beta sheet that is distal to the active site. Furthermore, there are no indications for the implication of this residue in subunit interactions.

3.4 Assessment of variant impact on protein structure

Given the fact that our genetic analysis in the *GALE*, *GALK1*, and *GALT* genes revealed the presence of either individual variants or, at most, combinations of two variants in each patient, the overall impact on the protein structure was, as expected, rather minor. However, different findings were evident depending on the gene; in the case of the *GALE* gene, the effect of the Ala180Thr and Ile266Leu variants was quite minor (range of overall RMSD: 0.02–0.05), while in contrast, the effect of the Ala216Thr variant had an almost 10-fold stronger impact (Figure 4A). The results were largely different when focusing on the *GALK1* gene variants; more specifically, both the Arg68Leu and Gly193Glu variants displayed a considerable effect on protein structure with an RMSD value of 0.44 and 0.443 (Figure 4B), respectively. However, these variants were shown to neutralize each other since their combination showed a significantly lower overall RMSD value (0.08) than that of the protein structure encoded by the germline *GALK1* gene. Finally, the Arg204Gln variant of the *GALT* gene displayed a significantly stronger impact on the protein structure than the Met298Ile (overall RMSD of 0.134 versus only 0.012). As expected, their combination had an overall RMSD value similar to that of the former variant (0.135), indicating its impact (Figure 4C). In regard to the Asn314Asp and Phe245Leu variants,

they both displayed a significant effect on the protein structure of the *GALT* gene, with an overall RMSD value of 0.134 in both cases. Yet, as in the case of the *GALK1* variants, the combination of variants (Asn314Asp/Phe245Leu) led to an overall protein structure that was very similar to the germline (overall RMSD of 0.007). The overall RMSD distance values for individual variants as well as variant combinations for the *GALE*, *GALK1*, and *GALT* genes are given in Table 3.

4 Discussion

To date, a large number of mutations have been recorded in the *GALT* gene, with the respective numbers being considerably smaller for the *GALK1* and *GALE* genes (Cooper et al., 1998). The existence of this largely heterogeneous genetic background suggests that it may affect, at least in part, the phenotypic variability of the disease. Within this complex genetic background, there are some mutations that predominate; more specifically, p.Gln188Arg is the most frequent *GALT* mutation and together with p.Lys285Asn, p.Ser135Leu, and p.Leu195Pro was reported to account for up to more than 70% of the mutated *GALT* alleles in certain population studies (Tyfield et al., 1999; Boutron et al., 2012). In terms of phenotypic impact, the p.Gln188Arg, p.Lys285Asn, and p.Leu195Pro *GALT* mutations have been associated with a more severe phenotype, whereas the p.Ile32Asn, p.Thr138Met, p.Thr350Ala, p.Arg259Trp, and p.Ala330Val mutations have been associated with a milder one (Tyfield et al., 1999). The very common Duarte-2 *GALT* variant, characterized by a population frequency of 4%, has a mild effect with homozygotes, displaying 50% of the normal enzyme activity (Elsas et al., 1994). In regard to *GALE* mutations, the p.Val94Met variant is associated with the more

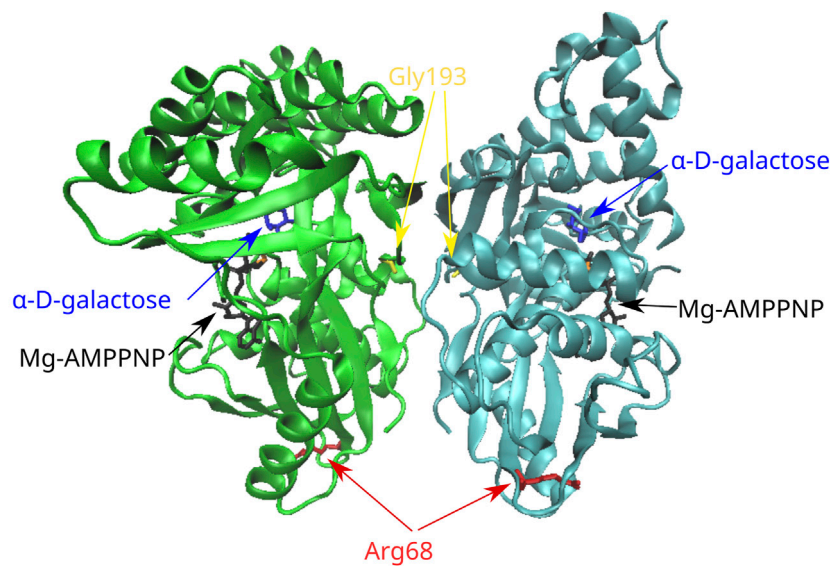


FIGURE 3

Position of the missense variants in the 3D structure of the GALK dimer. Gly193 is located in a loop of the molecule that belongs to the subunit–subunit interface. Arg68 is located in a six-stranded beta sheet in the N-terminal region of the molecule. AMPPNP, adenylyl imidodiphosphate (an ATP analog).

severe, generalized form of the disease (Timson, 2006). Overall, reports on the association between genotype and phenotype are relatively scarce; of interest, patients with identical genotypes and biochemical features may demonstrate high variability in terms of the clinical phenotype (Elsas and Lai, 1998; Welsink-Karssies et al., 2020).

In the present study, we analyzed five cases with galactosemia diagnosed in the context of the Greek National NS program for galactosemia. Genetic analysis of the galactosemia genes, namely, *GALT*, *GALE*, and *GALK1*, led to the identification of four novel and four rare variants of uncertain significance. Two of the cases, namely, M1 and K1, were heterozygotes for either a novel and a rare variant or two rare variants in the *GALE* and *GALT* genes, respectively. Case T1 was a homozygote for a novel variant in the *GALE* gene, whereas case D1 was a heterozygote for a novel variant and an established mild mutation in the *GALT* gene (Duarte-2). Finally, case L1 was a heterozygote for a novel and a rare variant in the *GALK1* gene and also a heterozygote for the mild mutation Duarte-2 in the *GALT* gene. Genetic analysis of the parents to confirm the *trans/cis* status of concurrent variants was feasible only in the case of patient M1, which showed that the implicated variants were present in *trans* configuration. Therefore, for the rest of the cases, the configuration of coexisting variants was not assessed. The small size of our cohort was due to a strict selection of cases with particular clinical and biochemical features. Hence, the results of this study, even though largely informative, might not fully capture the genetic background of the Greek galactosemia population and its mutational spectrum.

According to the *in silico* variant analysis, all or at least the majority of functional prediction tools assigned a deleterious effect to *GALT* variants p.Phe245Leu and p.Met298Ile, *GALE* variants p.Ala180Thr and p.Ala216Thr, as well as the *GALK1* variant p.Gly193Glu. For the variants p.Arg204Gln and p.Ile266Leu of

the *GALT* and *GALE* genes, respectively, predictions were contradictory; more specifically, Mutation Taster and CADD predicted a deleterious effect for both variants, contrasting the prediction of the rest of the tools that characterized them as neutral. Finally, the *GALK1* variant p.Arg68Leu was predicted to be neutral by all tools.

Regarding protein stability, *GALK1* variants p.Arg68Leu and p.Gly193Glu as well as the *GALE* variant p.Ala180Thr were predicted to have a destabilizing effect by all bioinformatics tools, while the *GALE* variants p.Ala216Thr and p.Ile266Leu and the *GALT* variant p.Arg204Gln were predicted to have a destabilizing effect by the majority of the tools. For the rare and novel *GALT* variants p.Met298Ile and p.Phe245Leu, respectively, protein stability predictions were contradictory. Notably, all aforementioned variants were predicted to have at least a deleterious or a destabilizing effect by the majority of the bioinformatics tools.

Finally, the analysis of the impact of the identified *GALE*, *GALK1*, and *GALT* gene variants on protein structure led to quite variant results depending on the gene and the variants. Of importance, the results from the *in silico* 3D protein structure analysis showed a good level of concordance with those of the aforementioned analyses on protein function and stability, at least in most cases, strengthening the relevance of our findings. Concerning the *GALE* gene, the strongest impact on protein structure was evident for the Ala216Thr variant followed by the Ala180Thr variant; both of these variants were also shown to significantly affect the function and stability of the protein. In terms of the *GALK1* gene, the Gly193Glu and Arg68Leu variants were shown to be the most impactful at the level of protein structure; the former was also characterized by a significant effect on protein function and stability, whereas the latter was characterized by a protein destabilizing effect. A similar scenario was observed for the Phe245Leu and Arg204Gln variants of the *GALT* gene, both

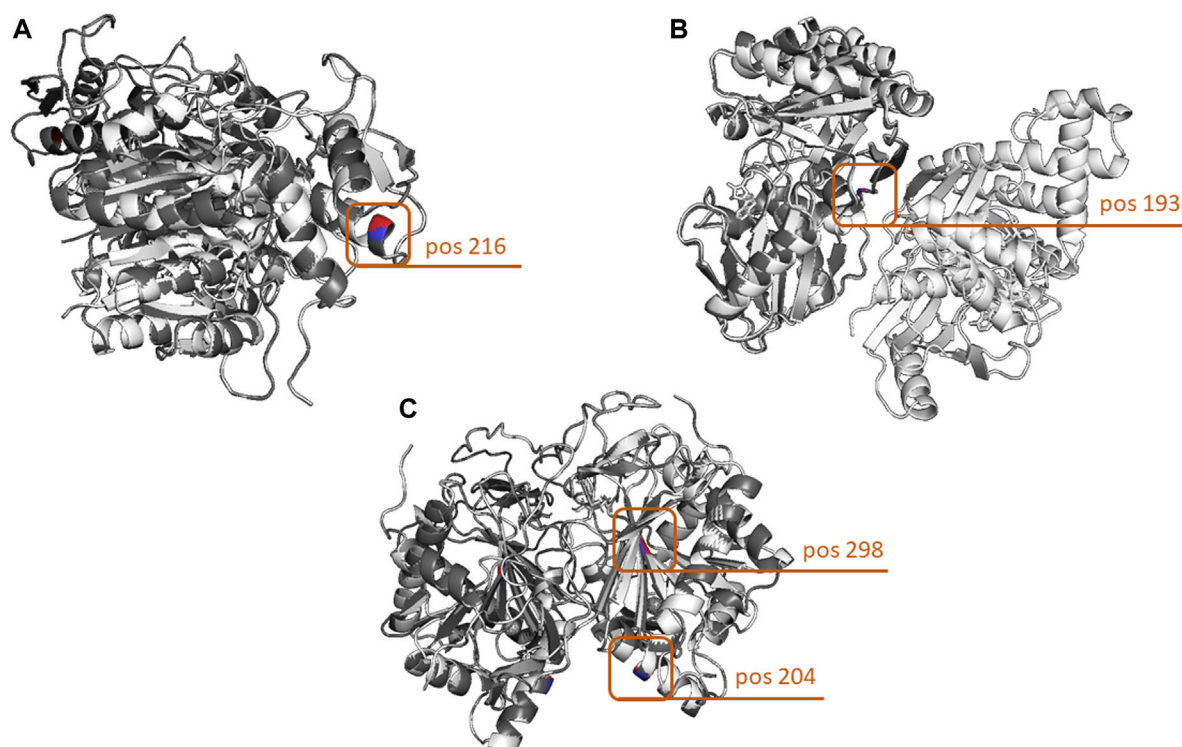


FIGURE 4

Three-dimensional comparison of the *GALE*, *GALK*, and *GALT* protein structures encoded by the germline versions of the genes and the variants with the highest structural impact. (A) In the case of the *GALE* gene, the highest structural impact was evidenced by the change of Ala to Thr at amino acid position 216. (B) In terms of protein structure, the most impactful *GALK1* variant leads to the change of Gly to Glu at amino acid position 193. (C) Finally, the strongest effect in the structure of the *GALT* protein was evidenced by the combination of two variants leading to the Arg204Gln and Met298Ile amino acid changes. Protein structures were loaded and aligned using the PyMOL tool. The amino acid chains of the germline forms of the proteins are depicted in white, whereas those carrying the variants are depicted in gray. In terms of the amino acid positions carrying the variants, the germline-encoded amino acid is depicted in red, and that encoded by the variant in blue.

being characterized by a strong impact on protein structure; the former was also associated with a strong impact on protein function, while the latter displayed a significant impact on protein stability. The only case of disagreement between the *in silico* analyses on protein function/stability and structure concerned the *GALT* Asn314Asp and the Met298Ile variants; the Asn314Asp variant was characterized by a strong impact on protein structure yet displayed no effect on function and stability, while the Met298Ile variant was associated only with an effect on protein function without affecting the structure and stability of the molecule.

Patient D1 harbored the novel *GALT* p.Phe245Leu variant together with the mild Duarte-2 variant. The mild biochemical and clinical features of this case are consistent with the identification of the Duarte-2 variant, although it cannot be excluded that variant p.Phe245Leu may also have a mild effect. The latter was predicted to be pathogenic by all functional prediction tools, while two out of four stability prediction tools showed a destabilizing effect. Due to its position in the 3D structure of the enzyme, there is a possibility that the Phe245 residue is implicated in the subunit interaction of the *GALT* dimer. Interestingly, an amino acid change at the adjacent amino acid position (p.Phe244Ser) was previously described in a case with classic galactosemia in combination with a common *GALT* mutation (Viggiano et al., 2015), indicating that this region may be important for the

function of the molecule. According to the ACMG guidelines (Richards et al., 2015), p.Phe245Leu is classified as a variant of uncertain significance (PM2, PP3, and PP4).

Patient K1 carried the rare p.Met298Ile and p.Arg204Gln variants in the *GALT* gene, which were related to a milder increase in galactose levels compared to the other cases, suggesting that either one of these variants or both of them may have a mild effect. Variant Met298Ile was predicted as pathogenic by all functional prediction tools, while two out of four of the stability prediction tools showed a destabilizing effect. This variant has already been described in cases with classic galactosemia of Greek origin, where in combination with known *GALT* mutations it resulted in a typical galactosemia phenotype (Schulpis et al., 2017). Functional predictions in the case of the variant p.Arg204Gln were contradictory, yet the majority of the stability prediction tools predicted a destabilizing effect. Of relevance, a different variant at the same position (p.Arg204Pro) was identified at the gnomAD database at a very low prevalence (0.005%, 7/140230 alleles), which was characterized as pathogenic (Zekanowski et al., 1999). There is no evidence that either of these variants is implicated either in the function of the enzyme, due to their positioning away from the active site, or in its subunit interactions. Finally, both the p.Met298Ile and p.Arg204Gln variants have a very low population frequency (0.005% in

TABLE 3 Assessment of comparison and 3D alignment of protein structures between the germline configuration and all possible variants of the *GALT*, *GALE*, and *GALK1* genes.

Gene	Variant	Overall RMSD distance
<i>GALT</i>	Arg204Gln	0.134
	Met298Ile	0.012
	Arg204Gln/Met298Ile	0.135
	Asn314Asp	0.134
	Phe245Leu	0.134
	Asn314Asp/Phe245Leu	0.007
<i>GALE</i>	Ala216Thr	0.048
	Ala180Thr	0.005
	Ile266Leu	0.002
<i>GALK1</i>	Arg68Leu/Gly193Glu	0.08
	Arg68Leu	0.44
	Gly193Glu	0.443

ALPHA and gnomAD databases for both variants), another feature compatible with their probable pathogenic effect. According to the ACMG guidelines, both the p.Met298Ile (PP3, PP4, PP5, and PS4 as moderate due to the rarity of the variant) and p.Arg204Gln (PP4) variants are classified as variants of uncertain significance.

Patient M1 was a compound heterozygote for the novel p.Ile266Leu and the rare p.Ala180Thr *GALE* variants. The biochemical and clinical features of this case were typical, including elevated galactose and bilirubin levels in the blood along with cataract development. Function predictions concerning p.Ile266Leu were contradictory, while the majority of stability prediction tools supported a destabilizing effect. Regarding the p.Ala180Thr variant, the majority of the function predictions supported a deleterious effect, whereas all the stability predictions supported a destabilizing effect. There is no evidence that either of these residues may be implicated in the function of the active site or the subunit interactions of the enzyme. The highly specific phenotype in combination with the *in silico* predictions, the novelty of p.Ile266Leu, and the very low population frequency of p.Ala180Thr (0.003% in gnomAD) support a causative effect for the combination of these variants. According to the ACMG guidelines, p.Ile266Leu (PM2, PP4) and p.Ala180Thr (PP3, PP4) are classified as variants of uncertain significance.

Patient T1 was homozygous for the novel p.Ala216Thr variant in the *GALE* gene. The patient presented with typical biochemical and clinical features. The variant p.Ala216Thr was predicted to be pathogenic by all the functional prediction tools, whereas the majority of the stability tools predicted a destabilizing effect. In terms of impact, there was not sufficient evidence that this residue has any implication in the active site or the subunit interactions of the enzyme. Interestingly, another variant at the same amino acid position (p.Ala216Val) in compound heterozygosity with another variant of uncertain clinical significance was described in a case with elevated galactose level (37.6 mg/dL) suspected of *GALE* deficiency. Of importance, *GALE* activity in the patients' erythrocytes was

reduced to only 0.5% of the control mean (Li et al., 2014). Thus, the *in silico* predictions in combination with the absence of the p.Ala216Thr variant from population databases support the probable pathogenicity of this variant. According to ACMG guidelines, p.Ala216Thr is classified as a variant of uncertain significance (PM2, PP3, and PP4).

Finally, patient L1 who presented with typical biochemical and clinical features of *GALK* deficiency was a compound heterozygote for the novel variant p.Gly193Glu and the rare variant p.Arg68Leu, both in the *GALK1* gene. Variant p.Gly193Glu was predicted to have a deleterious effect as well as a destabilizing effect by all prediction tools, while p.Arg68Leu was predicted to be neutral by all functional prediction tools, yet destabilizing by all stability prediction tools. Regarding their relative position in the 3D structure of the enzyme, there was no evidence that Arg68 is implicated either in the active site or subunit interactions of the enzyme, even though Gly193 is located at a loop of the molecule that belongs to the interface of the enzyme subunits. These features in combination with the highly specific and typical phenotype, the novelty of p.Gly193Glu, and the low population frequency of p.Arg68Leu (0.001% in gnomAD) support a causative effect for the combination of these variants. Interestingly enough, this patient also harbored the known, mild Duarte-2 mutation in the *GALT* gene. This highlights the notion that the genetic basis of galactosemia disorders can be rather complex, underlining the importance of genetic testing in the characterization of these cases. According to ACMG guidelines, p.Gly193Glu (PM2, PP3, and PP4) and p.Arg68Leu (PP4) are classified as variants of uncertain significance.

Galactosemia testing was incorporated in the Greek NS programs to provide early diagnosis of the disorder and prevent any dangerous neonatal complications through a galactose-restricted diet. Most of the cases in our study presented with a typical biochemical and clinical galactosemia phenotype, and the *in silico* analysis of the identified variants together with their absence or very low frequency in population databases supports a pathogenic effect for these variants. In the cases with a milder biochemical and clinical phenotype, this could be attributed to either the presence of a known mild variant (case D1) or to a possible mild effect of the newly identified variants (case K1). Our results show that the application of NGS methods offers a time- and cost-effective approach for the comprehensive genetic investigation of all three genes implicated in galactosemia. This can, in turn, lead to the identification of novel and rare variants as well as assist in the elucidation of the complex genetic background of this disorder.

Data availability statement

The datasets for this article are not publicly available due to concerns regarding patient anonymity. Requests to access the datasets should be directed to the corresponding author.

Ethics statement

The studies involving humans were approved by the Ethics Committee of the Department of Biology, National and

Kapodistrian University of Athens. The studies were conducted in accordance with the local legislation and institutional requirements. Written informed consent for participation in this study was provided by the participants' legal guardians/next of kin.

Author contributions

VM: data curation, formal analysis, funding acquisition, investigation, methodology, validation, visualization, writing—original draft, and writing—review and editing. AA: investigation, supervision, visualization, writing—original draft, and writing—review and editing. AS: investigation, resources, supervision, and writing—review and editing. TS: data curation, investigation, resources, writing—original draft, and writing—review and editing. MP: investigation, methodology, validation, writing—original draft, and writing—review and editing. EP: investigation, resources, and writing—review and editing. PG: investigation, resources, and writing—review and editing. CV: investigation, supervision, and writing—review and editing. VA: investigation, supervision, and writing—review and editing. PK: conceptualization, funding acquisition, investigation, supervision, and writing—review and editing.

References

- Adzhubei, I. A., Schmidt, S., Peshkin, L., Ramensky, V. E., Gerasimova, A., Bork, P., et al. (2010). A method and server for predicting damaging missense mutations. *Nat. Methods* 7 (4), 248–249. doi:10.1038/nmeth0410-248
- Alano, A., Almashanu, S., Chinsky, J. M., Costeas, P., Blitzer, M. G., Wulfsberg, E. A., et al. (1998). Molecular characterization of a unique patient with epimerase-deficiency galactosaemia. *J. Inherit. Metab. Dis.* 21 (4), 341–350. doi:10.1023/a:1005342306080
- Berry, G. T. (2000). "Classic galactosemia and clinical variant galactosemia," in *GeneReviews*. Editors M. P. Adam, G. M. Mirzaa, R. A. Pagon, S. E. Wallace, L. J. H. Bean, K. W. Gripp, et al. (Seattle (WA): University of Washington, Seattle), 1993–2023. [updated 2021 Mar 11]. Available at: <https://www.ncbi.nlm.nih.gov/books/NBK1518/>.
- Boutron, A., Marabotti, A., Facchiano, A., Cheillan, D., Zater, M., Oliveira, C., et al. (2012). Mutation spectrum in the French cohort of galactosemic patients and structural simulation of 27 novel missense variations. *Mol. Genet. Metab.* 107 (3), 438–447. doi:10.1016/j.ymgme.2012.07.025
- Calderon, F. R., Phansalkar, A. R., Crockett, D. K., Miller, M., and Mao, R. (2007). Mutation database for the galactose-1-phosphate uridylyltransferase (GALT) gene. *Hum. Mutat.* 28 (10), 939–943. doi:10.1002/humu.20544
- Cerone, J., and Rios, A. (2019). Galactosemia. *Pediatr. Rev.* 40 (Suppl. 1), 24–27. doi:10.1542/pir.2018-0150
- Cheng, J., Randall, A., and Baldi, P. (2006). Prediction of protein stability changes for single-site mutations using support vector machines. *Proteins* 62 (4), 1125–1132. doi:10.1002/prot.20810
- Choi, Y., and Chan, A. P. (2015). PROVEAN web server: a tool to predict the functional effect of amino acid substitutions and indels. *Bioinformatics* 31 (16), 2745–2747. doi:10.1093/bioinformatics/btv195
- Cooper, D. N., Ball, E. V., and Krawczak, M. (1998). The human gene mutation database. *Nucleic Acids Res.* 26 (1), 285–287. doi:10.1093/nar/26.1.285
- Demirbas, D., Coelho, A. I., Rubio-Gozalbo, M. E., and Berry, G. T. (2018). Hereditary galactosemia. *Metabolism* 83, 188–196. doi:10.1016/j.metabol.2018.01.025
- Elsas, L. J., 2nd, and Lai, K. (1998). The molecular biology of galactosemia. *Genet. Med.* 1 (1), 40–48. doi:10.1097/00125817-199811000-00009
- Elsas, L. J., Dembure, P. P., Langley, S., Paulk, E. M., Hjelm, L. N., and Fridovich-Keil, J. (1994). A common mutation associated with the Duarte galactosemia allele. *Am. J. Hum. Genet.* 54 (6), 1030–1036.
- Fridovich-Keil, J. L., Gubbels, C. S., Spencer, J. B., Sanders, R. D., Land, J. A., and Rubio-Gozalbo, E. (2011). Ovarian function in girls and women with GALT-deficiency galactosemia. *J. Inherit. Metab. Dis.* 34 (2), 357–366. doi:10.1007/s10545-010-9221-4
- Gromiha, M. M., An, J., Kono, H., Oobatake, M., Uedaira, H., Prabakaran, P., et al. (2000). ProTherm, version 2.0: thermodynamic database for proteins and mutants. *Nucleic Acids Res.* 28 (1), 283–285. doi:10.1093/nar/28.1.283
- Holden, H. M., Rayment, I., and Thoden, J. B. (2003). Structure and function of enzymes of the Leloir pathway for galactose metabolism. *J. Biol. Chem.* 278 (45), 43885–43888. doi:10.1074/jbc.R300025200
- Humphrey, W., Dalke, A., and Schulten, K. (1996). VMD: visual molecular dynamics. *J. Mol. Graph* 14 (1), 33–38. doi:10.1016/0263-7855(96)00018-5
- Kumar, P., Henikoff, S., and Ng, P. C. (2009). Predicting the effects of coding non-synonymous variants on protein function using the SIFT algorithm. *Nat. Protoc.* 4 (7), 1073–1081. doi:10.1038/nprot.2009.86
- Landrum, M. J., Lee, J. M., Benson, M., Brown, G. R., Chao, C., Chitipiralla, S., et al. (2018). ClinVar: improving access to variant interpretations and supporting evidence. *Nucleic Acids Res.* 46 (D1), D1062–D1067. doi:10.1093/nar/gkx1153
- Li, Y., Huang, X., Harmonay, L., Liu, Y., Kellogg, M. D., Fridovich-Keil, J. L., et al. (2014). Liquid chromatography-tandem mass spectrometry enzyme assay for UDP-galactose 4'-epimerase: use of fragment intensity ratio in differentiation of structural isomers. *Clin. Chem.* 60 (5), 783–790. doi:10.1373/clinchem.2013.219931
- McCorvie, T. J., Kopec, J., Pey, A. L., Fitzpatrick, F., Patel, D., Chalk, R., et al. (2016). Molecular basis of classic galactosemia from the structure of human galactose 1-phosphate uridylyltransferase. *Hum. Mol. Genet.* 25 (11), 2234–2244. doi:10.1093/hmg/ddw091
- Pandurangan, A. P., Ochoa-Montaño, B., Ascher, D. B., and Blundell, T. L. (2017). SDM: a server for predicting effects of mutations on protein stability. *Nucleic Acids Res.* 45 (W1), W229–W235. doi:10.1093/nar/gkx439
- Parthiban, V., Gromiha, M. M., and Schomburg, D. (2006). CUPSAT: prediction of protein stability upon point mutations. *Nucleic Acids Res.* 34, W239–W242. doi:10.1093/nar/gkl190
- Pires, D. E., Ascher, D. B., and Blundell, T. L. (2014). mCSM: predicting the effects of mutations in proteins using graph-based signatures. *Bioinformatics* 30 (3), 335–342. doi:10.1093/bioinformatics/btt691
- Rentsch, P., Witten, D., Cooper, G. M., Shendure, J., and Kircher, M. (2019). CADD: predicting the deleteriousness of variants throughout the human genome. *Nucleic Acids Res.* 47 (D1), D886–D894. doi:10.1093/nar/gky1016
- Richards, S., Aziz, N., Bale, S., Bick, D., Das, S., Gastier-Foster, J., et al. (2015). Standards and guidelines for the interpretation of sequence variants: a joint consensus recommendation of the American college of medical genetics and genomics and the association for molecular pathology. *Genet. Med.* 17 (5), 405–424. doi:10.1038/gim.2015.30

Funding

The author(s) declare that financial support was received for the research, authorship, and/or publication of this article. The research work was supported by the Hellenic Foundation for Research and Innovation (HFRI) and the General Secretariat for Research and Technology (GSRT), under the HFRI PhD Fellowship grant (GA. no. 2556).

Conflict of interest

The authors declare that the research was conducted in the absence of any commercial or financial relationships that could be construed as a potential conflict of interest.

Publisher's note

All claims expressed in this article are solely those of the authors and do not necessarily represent those of their affiliated organizations, or those of the publisher, the editors, and the reviewers. Any product that may be evaluated in this article, or claim that may be made by its manufacturer, is not guaranteed or endorsed by the publisher.

- Robinson, J. T., Thorvaldsdóttir, H., Winckler, W., Guttman, M., Lander, E. S., Getz, G., et al. (2011). Integrative genomics viewer. *Nat. Biotechnol.* 29 (1), 24–26. doi:10.1038/nbt.1754
- Sangiulio, F., Magnani, M., Stambolian, D., and Novelli, G. (2004). Biochemical characterization of two GALK1 mutations in patients with galactokinase deficiency. *Hum. Mutat.* 23 (4), 396. doi:10.1002/humu.9223
- Schulpis, K., Kalogerakou, M., and Monopolis, I. (2016). Incidence of galactose metabolic disorders in Greece. *Minerva Pediatr.* 68 (6), 505–507.
- Schulpis, K. H., Thodi, G., Iakovou, K., Chatzidaki, M., Dotsikas, Y., Molou, E., et al. (2017). Mutational analysis of GALT gene in Greek patients with galactosaemia: identification of two novel mutations and clinical evaluation. *Scand. J. Clin. Lab. Invest.* 77 (6), 423–427. doi:10.1080/00365513.2017.1334262
- Schwarz, J. M., Rödelberger, C., Schuelke, M., and Seelow, D. (2010). MutationTaster evaluates disease-causing potential of sequence alterations. *Nat. Methods* 7 (8), 575–576. doi:10.1038/nmeth0810-575
- Thoden, J. B., Timson, D. J., Reece, R. J., and Holden, H. M. (2005). Molecular structure of human galactokinase: implications for type II galactosemia. *J. Biol. Chem.* 280 (10), 9662–9670. doi:10.1074/jbc.M412916200
- Thoden, J. B., Wohlers, T. M., Fridovich-Keil, J. L., and Holden, H. M. (2000). Crystallographic evidence for Tyr 157 functioning as the active site base in human UDP-galactose 4-epimerase. *Biochemistry* 39 (19), 5691–5701. doi:10.1021/bi000215l
- Timson, D. J. (2006). The structural and molecular biology of type III galactosemia. *IUBMB Life* 58 (2), 83–89. doi:10.1080/15216540600644846
- Tyfield, L., Reichardt, J., Fridovich-Keil, J., Croke, D. T., Elsas, L. J., Strobl, W., et al. (1999). Classical galactosemia and mutations at the galactose-1-phosphate uridyl transferase (GALT) gene. *Hum. Mutat.* 13 (6), 417–430. doi:10.1002/(SICI)1098-1004(1999)13:6<417::AID-HUMU1>3.0.CO;2-0
- Viggiano, E., Marabotti, A., Burlina, A. P., Cazzorla, C., D'Apice, M. R., Giordano, L., et al. (2015). Clinical and molecular spectra in galactosemic patients from neonatal screening in northeastern Italy: structural and functional characterization of new variations in the galactose-1-phosphate uridyltransferase (GALT) gene. *Gene* 559 (2), 112–118. doi:10.1016/j.gene.2015.01.013
- Welling, L., Bernstein, L. E., Berry, G. T., Burlina, A. B., Eyskens, F., Gautschi, M., et al. (2017). International clinical guideline for the management of classical galactosemia: diagnosis, treatment, and follow-up. *J. Inherit. Metab. Dis.* 40 (2), 171–176. doi:10.1007/s10545-016-9990-5
- Welsink-Karssies, M. M., Ferdinandusse, S., Geurtsen, G. J., Hollak, C. E. M., Huidekoper, H. H., Janssen, M. C. H., et al. (2020). Deep phenotyping classical galactosemia: clinical outcomes and biochemical markers. *Brain Commun.* 2 (1), fcaa006. doi:10.1093/braincomms/fcaa006
- Zekanowski, C., Radomyska, B., and Bal, J. (1999). Molecular characterization of Polish patients with classical galactosaemia. *J. Inherit. Metab. Dis.* 22 (5), 679–682. doi:10.1023/a:1005511020607



OPEN ACCESS

EDITED BY

Ivan Martinez Duncker,
Universidad Autónoma del Estado de
Morelos, Mexico

REVIEWED BY

Patryk Lipiński,
Children's Memorial Health Institute
(IPCZD), Poland
Alice Barbara Schindler,
National Institute of Neurological
Disorders and Stroke (NIH), United States

*CORRESPONDENCE

Priya S. Kishnani,
✉ priya.kishnani@duke.edu

[†]These authors have contributed equally
to this work and share last authorship

RECEIVED 24 August 2023

ACCEPTED 26 September 2023

PUBLISHED 18 December 2023

CITATION

Gayed MM, Sgobbi P, Pinto WBVD, Kishnani PS and Koch RL (2023), Case report: Expanding the understanding of the adult polyglucosan body disease continuum: novel presentations, diagnostic pitfalls, and clinical pearls. *Front. Genet.* 14:1282790. doi: 10.3389/fgene.2023.1282790

COPYRIGHT

© 2023 Gayed, Sgobbi, Pinto, Kishnani and Koch. This is an open-access article distributed under the terms of the [Creative Commons Attribution License \(CC BY\)](#). The use, distribution or reproduction in other forums is permitted, provided the original author(s) and the copyright owner(s) are credited and that the original publication in this journal is cited, in accordance with accepted academic practice. No use, distribution or reproduction is permitted which does not comply with these terms.

Case report: Expanding the understanding of the adult polyglucosan body disease continuum: novel presentations, diagnostic pitfalls, and clinical pearls

Matthew M. Gayed¹, Paulo Sgobbi²,
Wladimir Bocca Viera De Rezende Pinto², Priya S. Kishnani^{1*†} and
Rebecca L. Koch^{1†}

¹Division of Medical Genetics, Department of Pediatrics, Duke University Medical Center, Durham, NC, United States, ²Division of Neuromuscular Diseases, Department of Neurology and Neurosurgery, University of São Paulo (UNIFESP), São Paulo, Brazil

Introduction: Adult polyglucosan body disease (APBD) has long been regarded as the adult-onset form of glycogen storage disease type IV (GSD IV) and is caused by biallelic pathogenic variants in *GBE1*. Advances in the understanding of the natural history of APBD published in recent years have led to the use of discrete descriptors ("typical" versus "atypical") based on adherence to traditional symptomatology and homozygosity for the p.Y329S variant. Although these general descriptors are helpful in summarizing common findings and symptoms in APBD, they are inherently limited and may affect disease recognition in diverse populations.

Methods: This case series includes three American patients (cases 1–3) and four Brazilian patients (cases 4–7) diagnosed with APBD. Patient-reported outcome (PRO) measures were employed to evaluate pain, fatigue, and quality of life in cases 1–3.

Results: We describe the clinical course and diagnostic odyssey of seven cases of APBD that challenge the utility and efficacy of discrete descriptors. Cases 1–3 are compound heterozygotes that harbor the previously identified deep intronic variant in *GBE1* and presented with "typical" APBD phenotypically, despite lacking two copies of the pathogenic p.Y329S variant. Patient-reported outcome measures in these three cases revealed the moderate levels of pain and fatigue as well as an impacted quality of life. Cases 4–7 have unique genotypic profiles and emphasize the growing recognition of presentations of APBD in diverse populations with broad neurological manifestations.

Conclusion: Collectively, these cases underscore the understanding of APBD as a spectrum disorder existing on the GSD IV phenotypic continuum. We draw attention to the pitfalls of commonly used genetic testing methods when diagnosing APBD and highlight the utility of patient-reported outcome questionnaires in managing this disease.

KEYWORDS

adult polyglucosan body disease, glycogen storage disease type IV, whole exome sequencing, patient-reported outcome, polyglucosan body neuropathy

1 Introduction

Adult polyglucosan body disease (APBD) is the adult-onset form of glycogen storage disease type IV (GSD IV) and is caused by biallelic pathogenic variants in *GBE1* which encodes the glycogen-branching enzyme (GBE) (Robitaille et al., 1980; Mochel et al., 2012; Souza et al., 2021). Reduced or deficient GBE activity disrupts normal glycogen synthesis and leads to the formation of glycogen with elongated outer chains resembling plant amylopectin (polyglucosan) (Koch et al., 2023). The polyglucosan aggregates and accumulates in various tissues, including the central nervous system, peripheral nervous system, skeletal muscle, heart, and lungs (Peress et al., 1979; Robitaille et al., 1980; Postler et al., 2002; Sindern et al., 2003; Dainese et al., 2013; Sullivan et al., 2019). Characteristic symptoms of APBD include progressive neurogenic bladder, spastic paraparesis, and sensorimotor axonal peripheral neuropathy, with the typical onset between the fourth and sixth decades of life (Robitaille et al., 1980; Mochel et al., 2012; Koch et al., 2023). While formal epidemiological studies categorizing the number of patients affected globally are yet to be conducted, it has been established that the pathogenic missense variant, NM_000158.4(*GBE1*):c.986A>C (p.Tyr329Ser; p.Y329S) (National Center for Biotechnology Information, 2023a), occurs with greater frequency in patients with Ashkenazi Jewish ancestry (estimated carrier rate 1:35–1:48) (Bao et al., 1996; Hussain et al., 2012; Schwartz et al., 2020).

APBD was first described by Robitaille et al. (1980) and Mochel et al. (2012) published the first natural history study in a cohort of 50 patients with APBD. This foundational work detailed APBD symptomatology and common misdiagnoses, as well as described the characteristic findings on magnetic resonance imaging (MRI): hyperintense white matter abnormalities predominant in the periventricular region, as well as medullary and spinal atrophy, on T2-weighted/fluid-attenuated inversion recovery (FLAIR) imaging (Mochel et al., 2012). The investigation was conducted primarily in patients homozygous for the p.Y329S variant but also included a subset of heterozygote patients without a known second variant (Mochel et al., 2012). Shortly thereafter, Akman et al. (2015) identified a novel pathogenic deep intronic variant, NM_000158.4(*GBE1*):c.2053-3358_2053-3350delinsTGTTTTTTACATGACAGGT (National Center for Biotechnology Information, 2023b) (herein referred to as the identified deep intronic variant), in symptomatic patients heterozygous for the p.Y329S variant without a previously known second mutation. Since the discovery of this identified deep intronic variant, there have not been extensive, longitudinal phenotypic descriptions of patients confirmed to have this intronic variant (Akman et al., 2015; Grunseich et al., 2021). Although clinical heterogeneity has been acknowledged, more recent work in 2021 sought to delineate APBD into categories of “typical” versus “atypical” on the basis of adherence to the aforementioned traditional symptomatology and homozygosity for the p.Y329S variant (Souza et al., 2021). Yet, APBD has been reported in a variety of patients of various ages, with or without Ashkenazi Jewish ancestry, and there continues to be additional phenotypes reported through multiple case series since the initial characterizations of the disorder (Ferguson et al., 1983; Bruno et al., 1993; Ziemssen et al., 2000; Klein et al., 2004; Billot et al., 2013; Souza et al., 2021).

Due to symptoms overlapping with other neurological disorders, APBD is frequently misdiagnosed; the most common misdiagnoses include multiple sclerosis, cerebral small vessel disease, peripheral neuropathy, amyotrophic lateral sclerosis, and benign prostatic hypertrophy in men (Hellmann et al., 2015). As a result, APBD patients often face prolonged diagnostic delays and may undergo unnecessary and potentially invasive procedures (Hellmann et al., 2015). Delay in diagnosing APBD is likely complicated by a number of factors including lack of awareness regarding the disorder and its associated presentations (Mochel et al., 2012; Hellmann et al., 2015). Collective understanding also continues to be hindered by a lack of longitudinal, comprehensive clinical history data in the medical literature, particularly for those with uncommon genotypes or presenting in earlier life. To address this, we present the clinical history and diagnostic odyssey for multiple patients with APBD receiving care in the United States and Brazil.

We describe three patients from the United States who are compound heterozygotes for the identified deep intronic variant in *GBE1* and utilize patient-reported outcome (PRO) measures to shed light on quality of life as well as other functional limitations: fatigue and pain. In addition, we detail four cases from Brazil with novel *GBE1* genotypes not previously described in patients with APBD and with broad neurological presentations.

2 Materials and methods

2.1 Chart review and case descriptions

As part of an international collaboration, patients with a confirmed diagnosis of APBD were included for participation in a longitudinal, retrospective natural history study (Duke University Institutional Review Board Pro00060753, ClinicalTrials.gov Identifier: NCT02683512). All available paper and electronic medical records were reviewed for participants who consented to the study. Collaborating institutions managing patients with APBD for whom direct consent was not possible submitted de-identified participant data using a targeted, study-specific spreadsheet. Participant data were entered into REDCap electronic data capture tools hosted at Duke University. Ages reported in this study represent available information in patient records and an estimation when exact ages were not available.

2.2 Patient-reported outcome measures

To evaluate symptoms of pain and fatigue as well as health-related quality of life, patients were asked to complete a series of validated PRO surveys. Due to institution research ethics restrictions, only United States-based participants were eligible to complete the survey (patients 1–3). The details of each validated survey and scoring are provided in [Supplementary Material](#). Surveys were distributed and returned in April 2023. The results represent one time point ([Supplementary Table S1](#)). Survey scoring and selection details are provided in [Supplementary Material](#).

Aspects of pain and its interference with daily life were measured using the Brief Pain Inventory (BPI) (Cleeland and Ryan, 1994; Tan et al., 2004; Güngör et al., 2013) and the Patient-Reported Outcomes

Measurement Information System (PROMIS) Short Form v1.1—Pain Interference 8a (PI-8a) (Amtmann et al., 2010; Cella et al., 2010; Rothrock et al., 2010). Fatigue and its impact on quality of life were measured using the Brief Fatigue Inventory (BFI) (Mendoza et al., 1999; Shahid et al., 2012; Liu et al., 2022; Ritchie et al., 2023) and the PROMIS Short Form v1.0—Fatigue 13a (FACIT-Fatigue) (Lai et al., 2011; Cella et al., 2016). Here, pain and fatigue as measured by the BPI and BFI, respectively, were defined as no interference (0), mild (1–3), moderate (4–6), and severe (7–10) (Serlin et al., 1995; Mendoza et al., 1999; Li et al., 2007; Deandrea et al., 2008; Shahid et al., 2012; Güngör et al., 2013; Liu et al., 2022; Ritchie et al., 2023). PI-8a and FACIT-Fatigue T-scores were calculated using HealthMeasures Scoring Service, powered by Assessment Center (https://www.assessmentcenter.net/ac_scoringervice), and cut-offs for normal, mild, moderate, and severe pain interference were defined as >55, 55 to >60, 60 to >70, and >70, respectively (Cella et al., 2010; Rothrock et al., 2010; HealthMeasures, 2023).

Quality of life was measured using the EuroQol Research Foundation EQ-5D-5L (Janssen et al., 2013; Devlin et al., 2018; Janssen et al., 2018; Pickard et al., 2019) survey and the RAND Corporation 36-Item Health Survey 1.0 (SF-36) (Ware and Sherbourne, 1992; RAND Corporation, 2023). The EQ-5D-5L measures the quality of life across five dimensions: mobility, self-care, usual activities, pain/discomfort, and anxiety/depression; health states were then converted into a utility index value for each participant (Janssen et al., 2013; Devlin et al., 2018; Janssen et al., 2018; EuroQol Research Foundation, 2019; Pickard et al., 2019). The SF-36 assesses quality of life in eight domains: physical functioning, role limitations due to physical health, role limitations due to emotional problems, energy/fatigue, emotional wellbeing, social functioning, pain, and general health (Ware and Sherbourne, 1992; RAND Corporation, 2023). Individual patient utility index values (EQ-5D-5L) and health scores (SF-36) were then compared to published norm values (Jiang et al., 2021; RAND Corporation, 2023).

3 Results

3.1 Cases of APBD with the identified deep intronic variant in *GBE1* underscore the pitfalls of common genetic testing methods

3.1.1 Case 1

Case 1 is a White American male with known Ashkenazi Jewish ancestry who initially presented at age 51.4 years due to fecal incontinence and urinary retention. He reported to the emergency department due to an episode of sudden, forceful loss of fecal contents. Preliminary abdominal X-ray imaging returned benign, and he was recommended to begin fiber supplementation. Of note, he was also found to be retaining urine at this visit. At age 52.6 years following multiple subsequent episodes of fecal incontinence, he was evaluated by the gastroenterology department and anorectal manometry was performed, revealing sphincter dysfunction. MRI of the lumbar spine at 52.7 years did not reveal a cause for the fecal incontinence or sphincter dysfunction. MRI of the brain without contrast, followed by MRA (magnetic resonance angiography) of the head and,

subsequently, MRI of the brain with and without contrast and of the cervical, thoracic, and lumbar spine were performed together, revealing evidence of leukodystrophy with findings of white matter abnormalities, cerebral and cerebellar volume loss, spinal cord atrophy, and vascular anomalies (Table 1). Evaluation by the neurology department at age 53.3 years disclosed a history of bladder dysfunction and erectile dysfunction from age 44.5 years, as well as gait abnormalities starting at age 49.6 years. Bladder dysfunction was diagnosed as benign prostatic hypertrophy, although a review of records showed resistance to multiple medications. He was noted to have bilateral pes cavus, ataxic gait, and abnormal reflexes (increased knee jerk, decreased ankle jerk, and upgoing plantar reflex bilaterally). A leukodystrophy gene panel returned without notable findings. At age 53.5 years, he underwent cystoscopy, showing urethral obstruction (Table 2), and had a prostatic urethral lift procedure at age 54.0 years. Despite this procedure, he continued to develop symptoms of urinary retention and elevated post void residuals. To further evaluate gait disturbances, he underwent the electromyography and nerve conduction velocity test (EMG/NCS) at age 54.4 years, showing a length-dependent sensorimotor axonal neuropathy in the right lower extremity (Table 3).

At age 54.6 years, he was formally diagnosed with APBD after research reanalysis of the prior leukodystrophy panel identified NM_000158.4(*GBE1*):c.760A>G (p.Thr254Ala; p.T254A)—a variant with conflicting interpretations of pathogenicity (National Center for Biotechnology Information, 2023d)—and the identified deep intronic variant. At age 54.7 years, he underwent repeat EMG, confirming length-dependent, axonal, sensorimotor peripheral neuropathy (Table 3) and, subsequently, began clean intermittent catheterizations due to urinary retention. He was evaluated at the Duke Metabolic Genetics clinic at age 55.5 years and reported ongoing symptoms of bladder dysfunction and gait instability, as well as intermittent episodes of fecal incontinence at least once every 6 months. During that visit, he reported an overall improvement of bladder control with clean intermittent catheterizations and has not had any resultant infections. However, he disclosed experiencing increased fatigue, noting that he was no longer able to walk distances greater than a mile due to sensation of muscle weakness as well as profound tiredness following meals. Muscle weakness was further evaluated using muscle ultrasound, with findings suggestive of myopathy in conjunction with an elevated creatine kinase level (516 U/L). Case 1 has no known liver or cardiac manifestations of GSD IV; routine echocardiograms and electrocardiograms performed between ages 47.6 and 54.7 years were normal, and alanine transaminase (ALT) levels have always been within normal limits, most recently measured at age 56.0 years.

3.1.2 Case 2

Case 2 is a White American female with Ashkenazi Jewish ancestry, who presented at age 61.9 years to an orthopedist with symptoms of worsening gait, frequent falls, poor hand dexterity, and paresthesia and pain in the proximal left lower extremity initially thought to be due to worsening of longstanding kyphoscoliosis. On further review, postural changes and gait instability began as early as ages 45 and 55 years, respectively. MRI of the spine at age 62.0 years revealed atrophy of the cerebellum, cervical, and thoracic spinal cord (Table 1). EMG/NCS performed at age 62.2 years also displayed evidence of polyneuropathy (Table 3).

TABLE 1 Results of MRI in cases with APBD.

Case	Age (years)	Image location	Summary of MRI findings
Case 1	52.7	Lumbar spine	Multilevel discogenic and facet hypertrophic degenerative change with mild central canal and foraminal stenosis
	53.2	Brain	Moderate diffuse cerebral volume loss and marked diffuse cerebellar volume loss. Diffuse confluent signal abnormality in the supratentorial white matter, brainstem, middle cerebellar peduncles, and bilateral cerebral hemispheres with signal abnormalities extending into the cervical spine. Prominent linear susceptibility artifact in right greater than left cerebral peduncles
	53.2	Brain MRA	Infundibulum at the origin of the left inferolateral trunk. Subtle contour irregularity of the vertical portion of the left vertebral artery at the C2 level
	53.2	Brain	Stable diffuse severe FLAIR hyperintensity throughout supratentorial and infratentorial white matter. Abnormal T2/FLAIR signals in the brainstem most pronounced at the cerebral peduncles and centrally within the medulla and pyramids. Mild supratentorial volume loss and severe cerebellar and brainstem volume loss
	53.2	Cervical spine	Small spinal cord with signal abnormalities. Disc herniation causing narrowing of the canal at C6–C7. Abnormal tortuous vasculature in dorsal paraspinal soft tissue
	53.2	Thoracic spine	Diffusely small spinal cord with abnormal signals. Hemangiomas within multiple vertebral bodies. Abnormal tortuous vasculature of the paraspinal soft tissues
	53.2	Lumbar spine	Multilevel degenerative change most prominent at L3–L4 and L4–L5. Large extraspinal synovial cysts at L3–L4 larger than those reported in prior studies
Case 2	62.0	Cervical spine	Mild cervical spondyloarthropathy at C4–C5 and C5–C6. Atrophy of the brainstem, cerebellum, and cervical cord
	62.0	Thoracic spine	Moderately severe S-shaped scoliosis and moderate generalized atrophy of the thoracic cord
	62.0	Lumbar spine	Moderate dextrorotatory scoliosis of the mid-to-upper lumbar spine. Multilevel lumbar disc desiccation and degeneration. Small L3–L4 and L5–S1 disc protrusions contributing to foraminal stenosis. Small posterior central L5–S1 disc protrusion
	63.9	Brain	Confluent T2/FLAIR hyperintensities throughout the supratentorial and infratentorial white matter, extending to the juxtacortical regions including the anterior temporal lobes. Severe atrophy of the midline cerebellum with milder cerebellar atrophy. Atrophy of the midbrain/medulla with relative sparing of the pons. Cervical spinal cord atrophy as previously demonstrated. Moderate diffuse cortical atrophy. Hemosiderin signals in the bilateral pallidum, red nucleus, and dentate nuclei
	64.7	Brain	Extensive confluent signal abnormality in bilateral cerebral white matter with volume loss. No significant change from prior studies. T1 hypointensity in bilateral parietal and occipital white matter and along the cortical spinal tracts. Moderate atrophy of cerebral and cerebellar hemispheres. Disproportionate atrophy of the brainstem and cerebellar vermis
Case 3	60.6	Brain	Severe patchy and confluent T2/FLAIR hyperintensities in the periventricular, deep, and subcortical white matter bilaterally with involvement of the pons. Parenchymal volume loss with enlargement of the ventricles greater than sulci
	60.9	Brain	Extensive signal abnormality in bilateral cerebellar hemispheres, mostly confluent, but also more focal areas of signal abnormality. Some are associated with cystic changes. The region of the cerebellar dentate nuclei is markedly abnormal. Marked atrophy of the cervical spinal cord, cerebellar vermis and tonsils, medulla, and portions of the cerebellar hemispheres
	60.9	Cervical and thoracic spine	Marked spinal cord thinning. Mild spondylosis. Lumbar scoliosis
	63.0	Pelvis	No pathology
	64.4	Right hip	Degenerative anterior superior and superior labral tear. Partial tear of the gluteus minimus tendon. Hamstring tendinosis
	64.4	Cervical, thoracic, and lumbar spine	Diffuse atrophy of the spinal cord, slightly progressive from prior studies. Severe atrophy of the medulla. Multilevel degenerative changes in the cervical spine with mild canal narrowing and right foramen at the C5–C6 level. Multilevel degenerative changes in the lumbar spine
Case 4	31.0	Brain	Small hyperintense foci in the subcortical and periventricular areas on T2/FLAIR
Case 5	50.0	Brain	Severe patchy and confluent T2/FLAIR hyperintensities in the periventricular, deep, and subcortical white matter bilaterally with involvement of the pons. Parenchymal volume loss with the enlargement of the ventricles greater than sulci
Case 6	47.0	Brain	Periventricular white matter abnormalities characterized by confluent T2/FLAIR hyperintensities throughout the supratentorial compartment with cerebellar atrophy predominantly on vermis and thin corpus callosum

(Continued on following page)

TABLE 1 (Continued) Results of MRI in cases with APBD.

Case	Age (years)	Image location	Summary of MRI findings
Case 7	72.0	Brain and spine	Diffuse, confluent, and multifocal leukoencephalopathy with profound periventricular predominance sparing U-fibers with moderate atrophy of the brainstem with hummingbird sign and global cerebellar atrophy

MRA, magnetic resonance angiography.

TABLE 2 Results of bladder studies in cases with APBD.

Case	Age (years)	Procedure type	Summary of bladder study findings
Case 1	49.6	Cystoscopy and urodynamic studies	Circumferential narrowing of the bladder neck with mild visual obstruction. Bladder with trabeculation. Normal bladder capacity and compliance. Detrusor pressure relatively weak and non-sustained. Incomplete emptying
	53.5	Cystoscopy and transurethral ultrasound	Bilobar enlargement of the prostate with visible obstruction of the bladder neck. Diffuse trabeculation of the bladder with multiple wide caliber diverticula
	53.9	Cystoscopy and urodynamic studies	Moderate capacity. Uninhibited bladder contractions with urge urinary incontinence. Low-to-moderate flow and slightly low pressure
	54.3	Cystoscopy	Bladder trabeculation. No obstruction of the prostatic urethra. Improved flow following prostatic urethral lift procedure. Filling phase without uninhibited contractions and urge urinary incontinence as previously observed. Capacity improved
	54.7	Urodynamic studies	Elevated post-void residual with low Qmax
Case 3	*	Cystoscopy and urodynamic studies	Inflamed bladder with diverticula, trabeculation, and cellule formation on cystoscopy. Urodynamic evidence of overactivity, reduced capacity, and high-pressure phasic contractions
	61.9	Cystoscopy	Neurogenic trabeculated bladder with evidence of phasic instability
	65.1	CT abdomen and pelvis	Moderate bladder wall thickening and pelvic floor laxity

*Represents result at an undisclosed age prior to initial clinical evaluation.

TABLE 3 Results of EMG/NCS in cases with APBD.

Case	Age (years)	Summary of EMG/NCS findings
Case 1	54.4	Length-dependent motor greater than sensory axonal neuropathy with chronic neurogenic changes in the right lower extremity
	54.7	Length-dependent, axonal, sensorimotor peripheral neuropathy
Case 2	62.2	Moderately severe, predominantly axonal, sensorimotor polyneuropathy without evidence of lumbosacral radiculopathy
	64.7	Severe axonal neuropathy in the legs with chronic neurogenic changes in the needle EMG to the proximal and distal leg muscles. Carpal tunnel in the right hand as well as mild ulnar sensory neuropathy
Case 3	*	Generalized axonal sensorimotor polyneuropathy with L4–5 radiculopathy
	61.2	Motor-predominant axonal polyneuropathy vs. radiculopathy. Abnormal conduction in descending corticospinal tracts
Case 4	31.0	Length-dependent motor and sensory axonal neuropathy with chronic neurogenic changes involving the lower limbs
Case 5	50.0	Length-dependent, moderate axonal sensorimotor peripheral neuropathy involving the lower and upper limbs
Case 6	47.0	Length-dependent, mild axonal sensorimotor peripheral neuropathy with motor predominance involving the lower and upper limbs
Case 7	71.0	Length-dependent, mild axonal sensorimotor peripheral neuropathy with sensory predominance involving the lower and upper limbs

*Represents result at an undisclosed age prior to initial clinical evaluation available for review.

At age 62.7 years, she was evaluated by the neurology department, at which time she endorsed muscle tightness/stiffness as well as cramping of the right hand, rollator use from approximately age 60 years, as well as long-standing bladder dysfunction from as early as age 49 years beginning initially as urgency and progressing to incontinence requiring the use of pads. An ataxia gene panel and subsequent whole exome sequencing on

the same sample were performed at age 63.6 years and returned negative; notably, *GBE1* analysis was not performed on the ataxia panel nor was it commented on in the whole exome sequencing report. Following undiagnostic genetic testing results, MRI of the brain was performed at age 63.9 years, revealing white matter hyperintensities as well as cortical, midbrain, and midline cerebellar atrophy (Table 1). At age

64.0 years, mitochondrial gene testing and targeted *FMRI* testing were performed and returned negative. She had worsening symptoms including deteriorating balance, weakness of the right leg, and frequent falls. On examination, she was noted to have abnormal reflexes, abnormal gait, and paratonia in the lower extremities. At subsequent evaluations, she reported increased dependency on a rollator for mobility and increasing difficulties with daily life activities.

She was referred for a neurological specialty evaluation at age 64.7 years at which point she reported the continuing progression of symptoms including lower extremity stiffness and weakness as well as bilateral foot drop and progression of bladder dysfunction, with excessive straining to urinate. EMG/NCS indicated severe axonal neuropathy in the lower extremities, in addition to incidental carpal tunnel syndrome in the right arm. Repeat MRI of the brain again showed extensive white matter signal abnormalities as well as cerebral, brainstem, and cerebellar atrophy. Reanalysis of molecular testing was performed at age 65.2 years, detecting the p.Y329S and identified deep intronic variants in *GBE1*.

Case 2 was reported to have a history of anxiety and was subjectively reported to have declining short-term memory throughout the diagnostic work up period without formal cognition evaluations. She has no known cardiac or hepatic manifestations of GSD IV; ALT levels most recently measured at age 64.7 years were within normal limits.

3.1.3 Case 3

Case 3 is a White American female with known Ashkenazi Jewish ancestry who initially presented to a specialty multiple sclerosis clinic at age 60.9 years with bladder and bowel dysfunction and increasing difficulty with balance and gait. Bladder dysfunction manifested at approximately age 51 years as increased urgency and later progressed to incontinence and extensive urinary tract infections. Gait instability also began at approximately age 51 years with worsening of coordination and balance over time. She also reported a history of bowel dysfunction marked by constipation and fecal incontinence. Prior to initial evaluation, peripheral neuropathy was noted on EMG/NCS and extensive non-enhancing leukodystrophy on brain MRI (Table 1). Urodynamic studies and cystoscopy revealed reduced bladder capacity and overactivity in addition to bladder wall trabeculation and cellule formation (Table 2).

She was reevaluated at age 61.2 years for adult-onset leukodystrophy. At this visit, she further reported significant fatigue with the onset as early as age 59 years accompanied by frequent headaches and neck pain. She also noted the limited intermittent use of a wheelchair due to gait instability. Physical examination revealed diminished reflexes accompanied by a positive Babinski sign and an unsteady, wide-based gait. Repeat EMG/NCS disclosed prolonged central motor conduction times, indicating abnormal conduction in the descending corticospinal tracts in addition to a motor-predominant axonal polyneuropathy versus polyradiculopathy (Table 3). Mitochondrial DNA testing and whole exome sequencing were performed, and both returned as non-diagnostic. Because of the clinical suspicion for APBD, further evaluation and subsequent gene sequencing of the *GBE1* gene led to a diagnosis of APBD at age 62.1 years. She had two pathogenic *GBE1* variants (p.Y329S and the identified deep intronic variant) as well as GBE activity less than 10% compared to normal in skin fibroblasts.

Case 3 experienced ongoing deterioration since the time of diagnosis characterized by worsening bladder dysfunction, pain, gait instability, and

cognition. Repeat cystoscopy at age 61.9 years again demonstrated neurogenic bladder dysfunction (Table 2). A trial of desmopressin (DDAVP) and pelvic floor physical therapy did not alleviate the symptoms. At age 65.1 years, a CT scan of the abdomen and pelvis revealed moderate bladder wall thickening and pelvic floor laxity/cystocele. She continues to have difficulty with urinary incontinence, voiding, urinary stream strength, recurrent UTIs, and perineal irritation.

Case 3 reports a significant history of pain throughout her disease course. At age 62.1 years, she began experiencing neuropathic, burning pain in the lower extremities up to the level of the thighs. Bladder/pelvic/perineal pain was reported as early as 62.8 years. Due to the unremitting, disabling nature of her pain, case 3 has trialed a number of therapies, such as a vibration table, duloxetine, transcranial magnetic stimulation, spinal procedures (selective nerve root blocks and pulsed radiofrequency ablations), and scrambler therapy—none of which alleviated her pain.

She has noted worsening gait instability and progressed from using a cane to a walker at age 64.3 years and then an increased reliance on a wheelchair by age 64.9 years. Despite regular physical therapy, her condition continues to deteriorate. Case 3 has no known cardiac or hepatic manifestations of GSD IV; she had a normal abdominal CT scan at age 65.1 years, and ALT levels most recently measured at 61.2 years old were within normal limits. Notably, she has a history of acute adjustment disorder with anxiety and insomnia.

3.2 PRO measures: pain, fatigue, and quality of life

PROs were used to further evaluate the health statuses for cases 1–3 across a series of domains including fatigue, pain, and quality of life (Table 4). On the BPI, averaged scores for pain severity and pain interference were 5.5 (moderate) and 6.1 (moderate), respectively. The mean T-score for the PI-8a was 62.7 (moderate pain interference). On the BFI, the average global fatigue score was 6.5 (moderate); the greatest impacted domain on average was walking ability. The mean T-score for the FACIT-Fatigue was 60.0 (moderate fatigue). Average scores for quality of life domains as measured by the SF-36 were lower than the established national averages, reflecting a significant impact on quality of life. Lastly, EQ-5D-5L assessed quality of life, and the health profiles were 32,233 (case 1), 54,532 (case 2), and 42,442 (case 3); these equate to utility index values of 0.5, 0.048, and 0.044, respectively. When compared to the US national mean utility index value (mean = 0.851, SD = 0.205), case 1 has an index value falling to approximately 1.7 SD from the mean, and cases 2 and 3 have index values falling to 3.9 SD from the mean.

3.3 Expanding our understanding of the APBD continuum: novel genotypes and earlier clinical presentation

3.3.1 Case 4

Case 4 is a White Brazilian female with no known Ashkenazi Jewish ancestry. She presented with urinary urgency beginning at age 26 years, followed by frequent urinary tract infections at age 28 years. Bladder dysfunction was notable for urgency and difficulty in emptying. At age 30 years, she experienced muscle cramping in

TABLE 4 Results of PRO measures from patients with APBD.

Pain		
BPI	Average value (n = 3)	
Pain severity	5.5 (3.5–7)	
Pain interference	6.1 (4.0–8.7)	
PI-8a	Average value (n = 3)	Standard deviation*
T-score	62.7 (55.9–70.7)	1.3
Fatigue		
BFI	Average value (n = 3)	
Current fatigue	6.3	
Usual fatigue	6.7	
Worst fatigue	8.7	
General activity	6.3	
Mood	5.7	
Walking ability	8.0	
Normal work	6.7	
Relations with others	4.7	
Enjoyment	5.7	
Global fatigue score	6.5	
FACIT-Fatigue	Average value (n = 3)	Standard deviation*
T-score	60.0 (55.3–66.5)	1.0
Quality of life		
SF-36	Average value (n = 3)	Standard deviation*
Physical functioning	23.3	1.7
Role functioning/physical	25.0	0.7
Role functioning/emotional	55.6	0.3
Energy/fatigue	20.0	1.4
Emotional wellbeing	56.0	0.7
Social functioning	25.0	2.1
Pain	40.8	1.2
General health	21.7	1.7
EQ-5D-5L	Utility index	Standard deviation*
Patient 1	0.5	1.7
Patient 2	0.048	3.9
Patient 3	0.044	3.9

*Represents standard deviations from the population mean value.

Validated PRO measures assessed pain, fatigue, and quality of life in patients 1–3. Pain and its interference with daily life were assessed using Brief Pain Inventory (BPI) and the Patient-Reported Outcomes Measurement Information System (PROMIS) Short Form v1.1—Pain Interference 8a (PI-8a). The most common pain descriptors on BPI were aching, gnawing, exhausting, tiring, penetrating, nagging, and miserable. Fatigue and its impact on quality of life were measured using the Brief Fatigue Inventory (BFI) and the PROMIS Short Form v1.0—Fatigue 13a (FACIT-Fatigue). Quality of life was measured using the EuroQol Research Foundation EQ-5D-5L survey and the RAND 36-Item Health Survey 1.0 (SF-36). Scores reported are averaged, and ranges are provided within parentheses for pain, fatigue, and SF-36.

the lower extremities (peroneal muscle group bilaterally) and small-fiber neuropathy symptoms in the distal lower extremities characterized by sensations of burning and tingling. At age 31 years, she exhibited muscle wasting, muscle weakness, easy fatigability, and pain in the lower limb muscle groups as well as peripheral neuropathy characterized by hyperesthesia and paresthesia. At this time, NCS was performed, which disclosed sensorimotor axonal neuropathy (Table 3). Brain imaging revealed small foci of hyperintensity in the subcortical and periventricular areas on FLAIR and T2-weighted imaging (Table 1). At age 31 years, she underwent gene panel testing for inherited peripheral neuropathies which revealed homozygosity for NM_000158.4(GBE1):c.292G>C (p.Val98Leu; p.V98L), interpreted as a variant of uncertain significance (VUS) in ClinVar (National Center for Biotechnology Information, 2023e). She was not reported to have an unsteady or spastic gait or any cognitive deficits as of age 31 years.

3.3.2 Case 5

Case 5 is a White Brazilian male with no known Ashkenazi ancestry presenting with numbness and paresthesia in the lower limbs. At age 30, he reported experiencing symptoms of small-fiber neuropathy characterized by burning and tingling in the distal lower extremities. Between age 30 and 50 years, he was misdiagnosed and symptomatically treated for sporadic and idiopathic small-fiber neuropathy with pregabalin without resolution. Evaluation at age 50 years also reported diffuse muscle pain involving the quadriceps femoris muscles and the gastrocnemii bilaterally not associated with exercise. He also had symptoms of peripheral neuropathy, and NCS confirmed moderate axonal sensorimotor polyneuropathy involving the lower and upper limbs (Table 3). He began experiencing bladder dysfunction at age 50 years marked by increased urgency. Physical examination revealed decreased strength in hip extensors, hip flexors, and ankle plantar flexion. Brain MRI revealed periventricular white matter hyperintensities and parenchymal volume loss (Table 1). Genetic testing with a multigene panel for inherited neuropathies at age 50 years revealed homozygosity for NM_000158.4(GBE1):c.534G>C (p.Trp178Cys; p.W178C), interpreted as a VUS (National Center for Biotechnology Information, 2023f).

3.3.3 Case 6

Case 6 is a White Brazilian female with no known Ashkenazi ancestry who presented with bradykinesia and spastic paraparesis since age 35 years. There was an initial clinical suspicion for juvenile monogenic Parkinson's disease or neurotransmitter disorders such as Segawa syndrome; a further review of history revealed good clinical improvement with low doses of levodopa. Previous medical history detailed bladder dysfunction beginning at age 32 years, including urinary incontinence and frequent urinary tract infections, as well as constipation beginning at age 44 years. She began using a cane at age 45 years and reported frequent daily falls and continuing unsteady gait on evaluation at age 47 years. NCS performed at 45 years revealed mild axonal sensorimotor polyneuropathy involving the upper and lower limbs (Table 3). At age 47 years, brain MRI identified cerebellar atrophy with periventricular white matter abnormalities (Table 1), and gene panel testing for neurodegenerative disorders identified p.V98L and NM_000158.4(GBE1):c.1909C>T (p.Arg637Ter; p.R637*), the

latter interpreted as pathogenic/likely pathogenic (National Center for Biotechnology Information, 2023c). Physical examination from the time of diagnosis revealed preserved muscle strength and normal deep tendon reflexes with bradykinesia, mild spasticity in the lower limbs, and postural instability as well as cognitive impairment [Montreal Cognitive Assessment (MoCA): 22/30] and major depressive disorder.

3.3.4 Case 7

Case 7 is a Black Brazilian male with no known Ashkenazi Jewish ancestry presenting with constipation, bladder dysfunction, erectile dysfunction, muscle cramping, spasticity, and unsteady gait. Of note, family history is positive for consanguinity as parents are first-degree cousins. The onset of constipation occurred at age 60 years. Bladder dysfunction was characterized by incontinence accompanied by frequent urinary tract infections starting at age 65 years, and EMG/NCS at age 71 years confirmed axonal sensorimotor polyneuropathy (Table 3). At age 72 years, physical examination revealed overall brisk tendon reflexes and reduced strength in hip flexion and extension bilaterally. Brain and spine MRI at age 72 years revealed evidence of leukoencephalopathy with periventricular predominance and atrophy of the brainstem and cerebellum (Table 1). A gene panel for neurodegenerative disorders at age 72 years revealed homozygosity for NM_000158.4(GBE1):c.929A>C (p.Tyr310Ser; p.Y310S). This variant has not been previously reported in the literature in an individual with APBD or entered in ClinVar, nor is it present in the population database gnomAD. Currently, there is limited information on this variant, and thus it is classified as a VUS. As of age 73 years, he began experiencing frequent falls and used a walker for mobility. A review of medical records further revealed history of misdiagnosis with Parkinson's disease and normal pressure hydrocephalus.

4 Discussion

Through our work, we present the detailed, longitudinal clinical history of seven patients with APBD, with the goal of expanding the collective understanding of the phenotypic presentation of APBD.

We began by describing in detail the clinical course of three cases confirmed to have the identified deep intronic variant in *GBE1*, for which longitudinal descriptions in the medical literature have thus far been limited (Akman et al., 2015; Grunseich et al., 2021). The clinical course and phenotypic presentation of these three cases followed the well-documented pattern of APBD progression previously established largely in populations homozygous for the *GBE1* p.Y329S variant (Mochel et al., 2012; Hellmann et al., 2015). Case 1 is the first known case to be reported harboring the identified deep intronic variant without concomitantly harboring the p.Y329S variant in *GBE1*. This patient presented with bladder dysfunction at age 44 years, followed by gait abnormalities at 49 years, fecal incontinence at 54 years, and progressive fatigue at 55 years. Case 2 developed postural changes at age 45 years, followed by bladder dysfunction at age 49 years, gait instability at 55 years, and peripheral neuropathy at 62 years. Case 3 presented with bladder and bowel dysfunction as well as gait instability at age 51 years; these symptoms were followed by pain resistant to treatment, affecting various parts of the body including the neck, back, legs, and perineal

region in the groin. Previous work has suggested defining cases of APBD as “typical” versus “atypical,” largely based on genotype by grouping “typical” cases with homozygosity for the p.Y329S variant in *GBE1* (Souza et al., 2021). Cases 1–3 described here displayed features associated with “typical” APBD, despite not harboring homozygosity for the p.Y329S variant. Based on this and other cases in the literature, we suggest avoiding the use of these dichotomous descriptors and instead recommend using the term “APBD” to describe all patients with this diagnosis regardless of genotypic/phenotypic presentation.

We then presented three patients that expanded our understanding of the phenotypic presentation of APBD. Clinically, cases 4–6 represent individuals with APBD in Brazil who are not of Ashkenazi Jewish descent and presented with “traditional” symptoms in early adulthood. Case 4 presented with bladder dysfunction starting at age 26 years, followed by neuropathy and muscle cramping at age 30 years. Case 5 presented with symptoms of small-fiber neuropathy at age 30 years and was diagnosed with APBD at age 50 years, by which time he was also experiencing muscle pain and bladder dysfunction. Case 6 reported bladder dysfunction at age 32 years, gait difficulties marked by bradykinesia and spastic paraparesis at age 35 years, and bowel dysfunction at age 44 years. These cases add to the growing body of evidence of APBD in younger, diverse populations, suggesting that greater attention should be paid to patients of all ages and demographics (Ferguson et al., 1983; Bruno et al., 1993; Ziemssen et al., 2000; Klein et al., 2004; Billot et al., 2013; Souza et al., 2021). We encourage clinicians to maintain high clinical suspicion and to not rule out an APBD diagnosis solely based on ancestry or age of onset. With continued use and improvements in whole exome sequencing and whole genome sequencing technologies, we expect that the diagnosis of GSD IV, including APBD, and our understanding of its natural history will improve.

All phenotypes on the GSD IV continuum, including APBD, are caused by deficiency in functional GBE activity. The genotypic profiles of cases 4–7, when evaluated in combination with their clinical presentation, extend the insight that APBD exists on the GSD IV clinical spectrum. Cases 4 and 6 harbored p.R637* and p.V98L in *GBE1*, which have previously been reported in patients with pediatric-onset GSD IV presenting with hepatic and/or neuromuscular involvement (Bruno et al., 2004; Janecke et al., 2004; Bruno et al., 2007; Li et al., 2010; Beyzaei et al., 2021). The p.V98L variant was previously reported in ClinVar in a patient with APBD, but no phenotypic information was available. Case 5 presented as homozygous for c.534G>C (p.W178C), a variant that has been reported in ClinVar in a patient with GSD IV but for which no phenotypic presentations have been published. The c.929A>C (p.Y310S) variant detected in case 7 was not previously reported in ClinVar or in the published literature and, therefore, was considered to be novel. Recent work has sought to establish that GSD IV symptomatology and presentation exist on a continuum with overlapping and multisystem involvement, rather than previously defined discrete hepatic or neuromuscular categories (Kiely et al., 2022). Our cases show that recognizing the presence of these variants in combination with the reported symptoms is important for understanding how APBD exists on the GSD IV continuum and for future phenotype–genotype correlations to improve genetic and prognostic counseling. Future work should

focus on elucidating the multifaceted symptomatology of GBE deficiency, which has implications on management plans including long-term follow up and counseling.

In presenting a series of patients with APBD representing diverse phenotypic and genotypic presentations, we further suggest the broader inclusion of *GBE1* analysis on relevant gene testing panels. The diagnostic pathways for cases 1–3 provide particularly unique insights into the pitfalls of common genetic testing methods. Case 1 underwent genetic testing with a targeted leukodystrophy gene panel which initially returned negative. After strong clinical suspicion, subsequent research re-evaluation of the data from the test nearly 1.3 years later confirmed the diagnosis of APBD. Similarly, case 2 faced a prolonged time for diagnosis after initially receiving negative results on an ataxia gene panel and whole exome sequencing. Moreover, whole exome sequencing also proved undiagnostic for case 3; yet, because of strong clinical suspicion, her providers pursued GBE activity testing and targeted gene re-evaluation that led to her diagnosis. These patients frequently underwent numerous diagnostic studies and evaluations before diagnosis, resulting in increased patient burden and overall costs to healthcare systems. Although we continue to believe that genetic testing is the gold standard, first-line option for diagnosing patients with APBD, our cases demonstrate the common limitations and pitfalls of these methods. To this regard, with the broad phenotypic, genotypic, and radiographic presentation of APBD becoming increasingly well-characterized (Mochel et al., 2012; De Winter et al., 2022), the inclusion of *GBE1* testing on relevant gene panels, including those for leukodystrophy, ataxia, and peripheral neuropathy, is critical. For those that undergo whole exome sequencing, the limitations of this method have previously been described (Mori et al., 2017; Burdick et al., 2020) and may result in a missed diagnosis—as in cases 1–3. Therefore, until the current pitfalls with whole exome sequencing are resolved, we argue that clinicians should not be completely reliant on negative results from whole exome sequencing. Additionally, the utility of measuring GBE activity testing should not be understated. GBE activity testing can help diagnose APBD and can be conducted using cultured skin fibroblasts, skeletal muscle, leukocytes, and other tissues; diagnosis guidelines previously published include considerations when interpreting GBE activity in different tissues and cells (Koch et al., 2023). For those that are found to have decreased GBE activity and/or be a carrier of a pathogenic *GBE1* variant, re-evaluation of genetic data and targeted follow-up testing with the intent of assessing for the presence of commonly missed variants, including the identified deep intronic variant (Koch et al., 2023), is warranted.

Lastly, in light of the increasing number of therapeutic options in development for the treatment of APBD (Kakhlon et al., 2013; Kakhlon et al., 2018; Gumusgoz et al., 2021; Gentry et al., 2022; Gumusgoz et al., 2022) and recently published consensus guidelines (Koch et al., 2023), we piloted the use of PRO surveys to evaluate the domains of pain, fatigue, and quality of life in United States-based patients (cases 1–3). As a conglomerate, the surveys disclosed impairment in all assessed domains. Averaged scores revealed a moderate level of pain severity and pain interference on the BPI; these results were mirrored by responses on the PI-8a, which also indicated a moderate level of interference caused by pain on daily functioning. Regarding fatigue, averaged scores showed moderate

levels of fatigue on both the BFI as well as the FACIT-Fatigue compared to the general population. Regarding quality of life, averaged results on the SF-36 showed lower quality of life scores in every domain assessed compared to the general population. The EQ-5D-5L again identified significant impairments in quality of life, with cases 1–3 harboring health index scores ranging from 1.7 to 3.9 and standard deviations lower than population normative values. While the PROs provided useful insights into functional impairment in aggregate, they showed perhaps a greater value at the individual level. Upon review of available medical records, pain was poorly characterized for cases 1 and 2. However, the use of PROs better elucidated this symptom. Similarly, fatigue was a poorly characterized symptom throughout the medical records for all surveyed patients, but the dual use of fatigue-related PROs revealed impairment. To the best of our knowledge, this is the first published implementation of PROs in patients with APBD. Given our limited sample size, our implementation of PROs was intended to be an initial proof of concept to establish use within this patient population, providing preliminary evidence to support the United States Food and Drug Administration guidance regarding the use of PROs to support clinical trials (Food and Drug Administration, 2020). Longitudinal data should be collected and analyzed to further evaluate the true utility of PROs in this population more broadly. In the future, we strongly encourage the use of PROs both in the setting of clinic visits as well the clinical trial space. These metrics provide an opportunity for an enhanced personalized medicine approach for symptom management and can serve as trackable outcomes to monitor therapeutic interventions.

The interdisciplinary, multicentered, retrospective nature of this study inherently has limitations. Over the last decade, MRI of the brain and spinal cord has proven essential in the evaluation and eventual diagnosis of individuals with APBD. Characteristic imaging findings were first described in 2012 (Mochel et al., 2012) and recently expanded on in 2022 (De Winter et al., 2022). While we provided herein the radiological findings reported by the various institutions at which our cases received care, we were unable to independently evaluate primary imaging. Future work should prospectively investigate imaging findings and symptomatology in individuals with APBD from a wide variety of genotypic backgrounds. Moreover, our ability to assess systemic manifestations of disease in our cohort was limited; our cases underwent limited to no evaluation for hepatic or cardiac involvement. Future work should aim to provide a more dedicated analysis of systemic manifestations in APBD. Lastly, the presented data on PROs represent one time point and serve as initial evidence for PRO use in this population while also highlighting their utility in understanding individual disease burden. Longitudinal data across multiple time points will prove essential in the validation of these surveys for APBD.

5 Conclusion

We describe in detail the clinical course of three compound heterozygotes harboring the identified deep intronic variant in *GBE1* as well as four cases from Brazil with unique genotypic profiles. We emphasize the growing presentation of APBD in diverse populations, requiring heightened awareness to ensure

proper diagnosis and intervention, and suggest discontinuing the use of discrete classification categories. Lastly, we present the proof-of-concept use of PRO questionnaires to further describe the clinical states of APBD.

Data availability statement

The datasets for this article are not publicly available due to concerns regarding participant/patient anonymity. Requests to access the datasets should be directed to the corresponding author.

Ethics statement

The studies involving humans were approved by the Duke University Health System Institutional Review Board Pro00060753. The study was conducted in accordance with the local legislation and institutional requirements. Cases 1–3 provided their written informed consent to participate in the study and for publication of information and data in the study. Due to language barriers, Cases 4–7 could not provide written informed consent and therefore de-identified data was contributed for them by their care providers in accordance with Federal University of Sao Paulo ethics and privacy policies and the Pro00060753 study protocol. The Federal University of Sao Paulo research ethics committee did not require additional informed written consent from Cases 4–7 to publish de-identified data for this type of scientific report.

Author contributions

MG: conceptualization, data curation, writing—original draft, and writing—review and editing. PS: data curation and writing—review and editing. WP: data curation and writing—review and editing. PK: conceptualization, data curation, supervision, and writing—review and editing. RK: conceptualization, data curation, supervision, and writing—review and editing.

Funding

The authors declare that no financial support was received for the research, authorship, and/or publication of this article.

Acknowledgments

The authors wish to acknowledge the YT and Alice Chen Pediatric Genetics and Genomics Research Center for its encouragement of this work. The authors thank all patients who participated in this study and their families for their ongoing support, time, and commitment to advancing the field of medicine by enrolling in this study. The authors thank Leticia Flores, Erin Huggins, Tracy Boggs, Dr. Lisa Hobson-Webb, and Dr. Mark Waters for their efforts in the implementation of this project. The authors also thank the numerous care teams that have worked tirelessly to improve the lives of patients with APBD.

Conflict of interest

The authors declare that the research was conducted in the absence of any commercial or financial relationships that could be construed as a potential conflict of interest.

Publisher's note

All claims expressed in this article are solely those of the authors and do not necessarily represent those of their affiliated

organizations, or those of the publisher, the editors, and the reviewers. Any product that may be evaluated in this article, or claim that may be made by its manufacturer, is not guaranteed or endorsed by the publisher.

Supplementary material

The Supplementary Material for this article can be found online at: <https://www.frontiersin.org/articles/10.3389/fgene.2023.1282790/full#supplementary-material>

References

- Akman, H. O., Kakhlon, O., Coku, J., Peverelli, L., Rosenmann, H., Rozenstein-Tsalkovich, L., et al. (2015). Deep intronic GBE1 mutation in manifesting heterozygous patients with adult polyglucosan body disease. *JAMA Neurol.* 72 (4), 441–445. doi:10.1001/jamaneurol.2014.4496
- Amtmann, D., Cook, K. F., Jensen, M. P., Chen, W.-H., Choi, S., Revicki, D., et al. (2010). Development of A Promis Item Bank to Measure Pain Interference. *Pain* 150 (1), 173–182. doi:10.1016/j.pain.2010.04.025
- Bao, Y., Kishnani, P., Wu, J. Y., and Chen, Y. T. (1996). Hepatic and neuromuscular forms of glycogen storage disease type IV caused by mutations in the same glycogen-branching enzyme gene. *J. Clin. Investigation* 97 (4), 941–948. doi:10.1172/JCI118517
- Bezaei, Z., Ezgu, F., Geramizadeh, B., Imanieh, M. H., Haghighat, M., Dehghani, S. M., et al. (2021). Clinical and genetic spectrum of glycogen storage disease in Iranian population using targeted gene sequencing. *Sci. Rep.* 11, 7040. doi:10.1038/s41598-021-86338-4
- Billot, S., Hervé, D., Akman, H. O., Froissart, R., Baussan, C., Claeys, K. G., et al. (2013). Acute but transient neurological deterioration revealing adult polyglucosan body disease. *J. Neurological Sci.* 324 (1–2), 179–182. doi:10.1016/j.jns.2012.10.015
- Bruno, C., Cassandrini, D., Assereto, S., Akman, H. O., Minetti, C., and Di Mauro, S. (2007). Neuromuscular forms of glycogen branching enzyme deficiency. *Acta Myologica myopathies cardiomyopathies official J. Mediterr. Soc. myology* 26 (1), 75–78.
- Bruno, C., Servidei, S., Shanske, S., Karpatis, G., Carpenter, S., McKee, D., et al. (1993). Glycogen branching enzyme deficiency in adult polyglucosan body disease. *Ann. Neurology* 33 (1), 88–93. doi:10.1002/ana.410330114
- Bruno, C., van Diggelen, O. P., Cassandrini, D., Gimpelev, M., Giuffrè, B., Donati, M. A., et al. (2004). Clinical and genetic heterogeneity of branching enzyme deficiency (glycogenosis type IV). *Neurology* 63 (6), 1053–1058. doi:10.1212/01.wnl.0000138429.11433.0d
- Burdick, K. J., Cogan, J. D., Rives, L. C., Robertson, A. K., Koziura, M. E., Brokamp, E., et al. (2020). Limitations of exome sequencing in detecting rare and undiagnosed diseases. *Am. J. Med. Genet. A* 182 (6), 1400–1406. doi:10.1002/ajmg.a.61558
- Cella, D., Lai, J.-S., Jensen, S. E., Christodoulou, C., Junghaenel, D. U., Reeve, B. B., et al. (2016). PROMIS Fatigue Item Bank had Clinical Validity across Diverse Chronic Conditions. *J. Clin. Epidemiol.* 73, 128–134. doi:10.1016/j.jclinepi.2015.08.037
- Cella, D., Riley, W., Stone, A., Rothrock, N., Reeve, B., Yount, S., et al. (2010). The Patient-Reported Outcomes Measurement Information System (PROMIS) developed and tested its first wave of adult self-reported health outcome item banks: 2005–2008. *J. Clin. Epidemiol.* 63 (11), 1179–1194. doi:10.1016/j.jclinepi.2010.04.011
- Cleeland, C. S., and Ryan, K. M. (1994). Pain assessment: global use of the Brief Pain Inventory. *Ann. Acad. Med. Singap.* 23 (2), 129–138.
- Dainese, L., Monin, M. L., Demeret, S., Brochier, G., Froissart, R., Spraul, A., et al. (2013). Abnormal glycogen in astrocytes is sufficient to cause adult polyglucosan body disease. *Gene* 515 (2), 376–379. doi:10.1016/j.gene.2012.12.065
- De Winter, J., Cypers, G., Jacobs, E., Bossche, S. V., Deconinck, T., De Ridder, W., et al. (2022). Distinct features in adult polyglucosan body disease: a case series. *Neuromuscul. Disord.* 33 (2), 148–152. doi:10.1016/j.nmd.2022.12.016
- Deandrea, S., Montanari, M., Moja, L., and Apolone, G. (2008). Prevalence of undertreatment in cancer pain. A review of published literature. *Ann. Oncol.* 19 (12), 1985–1991. doi:10.1093/annonc/mdn419
- Devlin, N., Brazier, J., Pickard, A. S., and Stolk, E. (2018). 3L, 5L, What the L? A NICE Conundrum. *Pharmacoeconomics* 36 (6), 637–640. doi:10.1007/s40273-018-0622-9
- EuroQol Research Foundation, (2019). *EQ-5D-5L user Guide*. Rotterdam, Netherlands: EuroQol Research Foundation.
- Ferguson, I. T., Mahon, M., and Cumming, W. J. K. (1983). An adult case of Andersen's disease - type IV glycogenosis. A clinical, histochemical, ultrastructural and biochemical study. *J. Neurological Sci.* 60 (3), 337–351. doi:10.1016/0022-510X(83)90144-2
- Food and Drug Administration, (2020). "Patient-Reported Outcome Measures: use in medical product development to support labeling claims," in *FDA guidance documents* (Oak, Maryland: Food and Drug Administration).
- Gentry, M. S., Markussen, K. H., and Donohue, K. J. (2022). Two Diseases—One Preclinical Treatment Targeting Glycogen Synthesis. *Neurotherapeutics* 19 (3), 977–981. doi:10.1007/s13311-022-01240-9
- Grünseich, C., Sarkar, N., Lu, J., Owen, M., Schindler, A., Calabresi, P. A., et al. (2021). Improving the efficacy of exome sequencing at a quaternary care referral centre: novel mutations, clinical presentations and diagnostic challenges in rare neurogenetic diseases. *J. Neurology, Neurosurg. Psychiatry* 92 (11), 1186–1196. doi:10.1136/jnnp-2020-325437
- Gumusgoz, E., Guisso, D. R., Kasiri, S., Wu, J., Dear, M., Verhalen, B., et al. (2021). Targeting Gys1 with AAV-SaCas9 Decreases Pathogenic Polyglucosan Bodies and Neuroinflammation in Adult Polyglucosan Body and Lafora Disease Mouse Models. *Neurother. J. Am. Soc. Exp. Neurother.* 18 (2), 1414–1425. doi:10.1007/s13311-021-01040-7
- Gumusgoz, E., Kasiri, S., Guisso, D. R., Wu, J., Dear, M., Verhalen, B., et al. (2022). AAV-Mediated Artificial miRNA Reduces Pathogenic Polyglucosan Bodies and Neuroinflammation in Adult Polyglucosan Body and Lafora Disease Mouse Models. *Neurother. J. Am. Soc. Exp. Neurother.* 19 (3), 982–993. doi:10.1007/s13311-022-01218-7
- Güngör, D., Schober, A. K., Kruijshaar, M. E., Plug, I., Karabul, N., Deschauer, M., et al. (2013). Pain in adult patients with Pompe disease: a cross-sectional survey. *Mol. Genet. Metabolism* 109 (4), 371–376. doi:10.1016/j.ymgme.2013.05.021
- HealthMeasures, (2023). HealthMeasures PROMIS® Score Cut Points. Available: <https://www.healthmeasures.net/score-and-interpret/interpret-scores/promis/promis-score-cut-points> (Accessed May 11, 2023).
- Hellmann, M. A., Kakhlon, O., Landau, E. H., Sadeh, M., Giladi, N., Schlesinger, I., et al. (2015). Frequent misdiagnosis of adult polyglucosan body disease. *J. Neurology* 262 (10), 2346–2351. doi:10.1007/s00415-015-7859-4
- Hussain, A., Armistead, J., Gushulak, L., Kruck, C., Pind, S., Triggs-Raine, B., et al. (2012). The adult polyglucosan body disease mutation GBE1 c.1076A>C occurs at high frequency in persons of Ashkenazi Jewish background. *Biochem. Biophys. Res. Commun.* 426 (2), 286–288. doi:10.1016/j.bbrc.2012.08.089
- Janecke, A. R., Dertinger, S., Ketelsen, U.-P., Bereuter, L., Simma, B., Müller, T., et al. (2004). Neonatal type IV glycogen storage disease associated with "null" mutations in glycogen branching enzyme 1. *J. Pediatr.* 145 (5), 705–709. doi:10.1016/j.jpeds.2004.07.024
- Janssen, M. F., Bonsel, G. J., and Luo, N. (2018). Is EQ-5D-5L Better Than EQ-5D-3L? A Head-to-Head Comparison of Descriptive Systems and Value Sets from Seven Countries. *Pharmacoeconomics* 36 (6), 675–697. doi:10.1007/s40273-018-0623-8
- Janssen, M. F., Pickard, A. S., Golicki, D., Gudex, C., Niewada, M., Scalone, L., et al. (2013). Measurement properties of the EQ-5D-5L compared to the EQ-5D-3L across eight patient groups: a multi-country study. *Qual. Life Res.* 22 (7), 1717–1727. doi:10.1007/s11136-012-0322-4
- Jiang, R., Janssen, M. F. B., and Pickard, A. S. (2021). US population norms for the EQ-5D-5L and comparison of norms from face-to-face and online samples. *Qual. Life Res.* 30 (3), 803–816. doi:10.1007/s11136-020-02650-y
- Kakhlon, O., Ferreira, I., Solmesky, L. J., Khazanov, N., Lossos, A., Alvarez, R., et al. (2018). Guaiacol as a drug candidate for treating adult polyglucosan body disease. *JCI insight* 3 (17), e99694–e99694. doi:10.1172/jci.insight.99694
- Kakhlon, O., Glickstein, H., Feinstein, N., Liu, Y., Baba, O., Terashima, T., et al. (2013). Polyglucosan neurotoxicity caused by glycogen branching enzyme deficiency can be reversed by inhibition of glycogen synthase. *J. Neurochem.* 127 (1), 101–113. doi:10.1111/jnc.12277

- Kiely, B. T., Koch, R. L., Flores, L., Burner, D., Kaplan, S., and Kishnani, P. S. (2022). A novel approach to characterize phenotypic variation in GSD IV: reconceptualizing the clinical continuum. *Front. Genet.* 13, 992406. doi:10.3389/fgene.2022.992406
- Klein, C. J., Boes, C. J., Chapin, J. E., Lynch, C. D., Campeau, N. G., Dyck, P. J. B., et al. (2004). Adult polyglucosan body disease: case description of an expanding genetic and clinical syndrome. *Muscle Nerve* 29 (2), 323–328. doi:10.1002/mus.10520
- Koch, R. L., Soler-Alfonso, C., Kiely, B. T., Asai, A., Smith, A. L., Bali, D. S., et al. (2023). Diagnosis and management of glycogen storage disease type IV, including adult polyglucosan body disease: A clinical practice resource. *Mol. Genet. Metabolism* 138 (3), 107525. doi:10.1016/j.ymgme.2023.107525
- Lai, J.-S., Cella, D., Choi, S., Junghaenel, D. U., Christodoulou, C., Gershon, R., et al. (2011). How Item Banks and Their Application Can Influence Measurement Practice in Rehabilitation Medicine: A PROMIS Fatigue Item Bank Example. *Archives Phys. Med. Rehabilitation* 92 (10), S20–S27. doi:10.1016/j.apmr.2010.08.033
- Li, K. K., Harris, K., Hadi, S., and Chow, E. (2007). What Should be the Optimal Cut Points for Mild, Moderate, and Severe Pain? *J. Palliat. Med.* 10 (6), 1338–1346. doi:10.1089/jpm.2007.0087
- Li, S.-C., Chen, C.-M., Goldstein, J. L., Wu, J.-Y., Lemyre, E., Burrow, T. A., et al. (2010). Glycogen storage disease type IV: novel mutations and molecular characterization of a heterogeneous disorder. *J. Inher. Metabolic Dis.* 33 (3), S83–S90. doi:10.1007/s10545-009-9026-5
- Liu, D., Weng, J.-S., Ke, X., Wu, X.-Y., and Huang, S.-T. (2022). The relationship between cancer-related fatigue, quality of life and pain among cancer patients. *Int. J. Nurs. Sci.* 10 (1), 111–116. doi:10.1016/j.ijnss.2022.12.006
- Mendoza, T. R., Wang, X. S., Cleeland, C. S., Morrissey, M., Johnson, B. A., Wendt, J. K., et al. (1999). The rapid assessment of fatigue severity in cancer patients: use of the Brief Fatigue Inventory. *Cancer* 85 (5), 1186–1196. doi:10.1002/(SICI)1097-0142(19990301)85:5<1186::AID-CNCR24>3.0.CO;2-N
- Mochel, F., Schiffmann, R., Steenweg, M. E., Akman, H. O., Wallace, M., Sedel, F., et al. (2012). Adult polyglucosan body disease: natural history and key magnetic resonance imaging findings. *Ann. Neurology* 72 (3), 433–441. doi:10.1002/ana.23598
- Mori, M., Haskell, G., Kazi, Z., Zhu, X., DeArmy, S. M., Goldstein, J. L., et al. (2017). Sensitivity of whole exome sequencing in detecting infantile- and late-onset Pompe disease. *Mol. Genet. Metab.* 122 (4), 189–197. doi:10.1016/j.ymgme.2017.10.008
- National Center for Biotechnology Information, (2023a). VCV000002777.46 - ClinVar - NCBI. Available: <https://www.ncbi.nlm.nih.gov/clinvar/variation/2777/> (Accessed August 17, 2023).
- National Center for Biotechnology Information, (2023b). VCV000225145.6 - ClinVar - NCBI. Available: <https://www.ncbi.nlm.nih.gov/clinvar/variation/225145/> (Accessed August 17, 2023).
- National Center for Biotechnology Information, (2023c). VCV000346785.11 - ClinVar - NCBI. Available: <https://www.ncbi.nlm.nih.gov/clinvar/variation/346785/> (Accessed August 17, 2023).
- National Center for Biotechnology Information, (2023d). VCV000374517.33 - ClinVar - NCBI. Available: <https://www.ncbi.nlm.nih.gov/clinvar/variation/374517/> (Accessed August 17, 2023).
- National Center for Biotechnology Information, (2023e). VCV000520678.12 - ClinVar - NCBI. Available: <https://www.ncbi.nlm.nih.gov/clinvar/variation/520678/> (Accessed August 17, 2023).
- National Center for Biotechnology Information, (2023f). VCV002152670.1 - ClinVar - NCBI. Available: <https://www.ncbi.nlm.nih.gov/clinvar/variation/2152670/> (Accessed August 17, 2023).
- Peress, N. S., DiMauro, S., and Roxburgh, V. A. (1979). Adult polysaccharidosis. Clinicopathological, ultrastructural, and biochemical features. *Arch. Neurol.* 36 (13), 840–845. doi:10.1001/archneur.1979.00500490054009
- Pickard, A. S., Law, E. H., Jiang, R., Pullenayegum, E., Shaw, J. W., Xie, F., et al. (2019). “United States Valuation of EQ-5D-5L Health States Using an International Protocol,” in *Value in Health* (Boston, MA, USA: ISPOR-The Professional Society for Health Economics and Outcomes Research).
- Postler, E., Sindern, E., Vorgerd, M., Schmitz, I., Malin, J. P., and Müller, K. M. (2002). Fatal cardiomyopathy in adult in polyglucosan body disease. *Pathologie* 23 (3), 229–234. doi:10.1007/s00292-002-0533-5
- Rand Corporation, (2023). RAND Corporation 36-Item Short Form Survey (SF-36) Scoring Instructions. Available: https://www.rand.org/health-care/surveys_tools/mos/36-item-short-form/scoring.html (Accessed April 29, 2023).
- Ritchie, E. K., Cella, D., Fabbiano, F., Pigneux, A., Kanda, Y., Ivanescu, C., et al. (2023). Patient-reported outcomes from the phase 3 ADMIRAL trial in patients with FLT3-mutated relapsed/refractory AML. *Leukemia Lymphoma* 64, 938–950. doi:10.1080/10428194.2023.2186731
- Robitaille, Y., Carpenter, S., Karpati, G., and DiMauro, S. D. (1980). A distinct form of adult polyglucosan body disease with massive involvement of central and peripheral neuronal processes and astrocytes: a report of four cases and a review of the occurrence of polyglucosan bodies in other conditions such as Lafora's disease and normal ageing. *Brain* 103 (2), 315–336. doi:10.1093/brain/103.2.315
- Rothrock, N. E., Hays, R. D., Spritzer, K., Yount, S. E., Riley, W., and Cella, D. (2010). Relative to the General US Population, Chronic Diseases are Associated with Poorer Health-Related Quality of Life as Measured by the Patient-Reported Outcomes Measurement Information System (PROMIS). *J. Clin. Epidemiol.* 63 (11), 1195–1204. doi:10.1016/j.jclinepi.2010.04.012
- Schwartz, L. R., Lu, Q., Liu, R., Kornreich, R., Edelman, L. L., Birch, A. H., et al. (2020). Estimating the Prevalence of the Adult Polyglucosan Body Disease at the Gene Level for Ashkenazi Jews in the United States. *Am. J. Rare Disord. Diagnosis Ther.* 3 (1), 004–008. doi:10.37871/ajrddt.id17
- Serlin, R. C., Mendoza, T. R., Nakamura, Y., Edwards, K. R., and Cleeland, C. S. (1995). When is cancer pain mild, moderate or severe? Grading pain severity by its interference with function. *Pain* 61 (2), 277–284. doi:10.1016/0304-3959(94)00178-H
- Shahid, A., Wilkinson, K., Marcu, S., and Shapiro, C. (2012). *STOP, THAT, and one hundred other Sleep Scales*. Berlin, Germany: Springer.
- Sindern, E., Ziemssen, F., Ziemssen, T., Podskarbi, T., Shin, Y., Brasch, F., et al. (2003). Adult polyglucosan body disease: A postmortem correlation study. *Neurology* 61 (2), 263–265. doi:10.1212/01.WNL.0000073144.96680.CB
- Souza, P. V. S., Badia, B. M. L., Farias, I. B., Pinto, W. B. V. D. R., Oliveira, A. S. B., Akman, H. O., et al. (2021). GBE1-related disorders: adult polyglucosan body disease and its neuromuscular phenotypes. *J. Inher. Metabolic Dis.* 44 (3), 534–543. doi:10.1002/jimd.12325
- Sullivan, M. A., Nitschke, S., Skwara, E. P., Wang, P., Zhao, X., Pan, X. S., et al. (2019). Skeletal Muscle Glycogen Chain Length Correlates with Insolubility in Mouse Models of Polyglucosan-Associated Neurodegenerative Diseases. *Cell Rep.* 27, 1334–1344. doi:10.1016/j.celrep.2019.04.017
- Tan, G., Jensen, M. P., Thornby, J. I., and Shanti, B. F. (2004). Validation of the brief pain inventory for chronic nonmalignant pain. *J. Pain* 5 (2), 133–137. doi:10.1016/j.jpain.2003.12.005
- Ware, J. E., and Sherbourne, C. D. (1992). The MOS 36-Item Short-Form Health Survey (SF-36): I. Conceptual Framework and Item Selection. *Med. Care* 30 (6), 473–483. doi:10.1097/00005650-199206000-00002
- Ziemssen, F., Sindern, E., Schröder, J. M., Shin, Y. S., Zange, J., Kilimann, M. W., et al. (2000). Novel missense mutations in the glycogen-branching enzyme gene in adult polyglucosan body disease. *Ann. neurology* 47 (4), 536–540. doi:10.1002/1531-8249(200004)47:4<536::aid-ana22>3.0.co;2-k



OPEN ACCESS

EDITED BY

Ivan Martinez Duncker,
Universidad Autónoma del Estado de Morelos,
Mexico

REVIEWED BY

Charles Marques Lourenco,
Faculdade de Medicina de São José do Rio
Preto, Brazil
Amy Gaviglio,
Centers for Disease Control and Prevention
(CDC), United States

*CORRESPONDENCE

Ryan Colburn
✉ ryan.colburn@odimm.com

RECEIVED 18 May 2023

ACCEPTED 10 November 2023

PUBLISHED 08 January 2024

CITATION

Colburn R and Lapidus D (2024) An analysis of
Pompe newborn screening data: a new
prevalence at birth, insight and discussion.
Front. Pediatr. 11:1221140.
doi: 10.3389/fped.2023.1221140

COPYRIGHT

© 2024 Colburn and Lapidus. This is an open-
access article distributed under the terms of the
Creative Commons Attribution License (CC BY).
The use, distribution or reproduction in other
forums is permitted, provided the original
author(s) and the copyright owner(s) are
credited and that the original publication in this
journal is cited, in accordance with accepted
academic practice. No use, distribution or
reproduction is permitted which does not
comply with these terms.

An analysis of Pompe newborn screening data: a new prevalence at birth, insight and discussion

Ryan Colburn^{1*} and David Lapidus²

¹odimm inc., Los Angeles, CA, United States, ²LapidusData Inc., Oklahoma City, OK, United States

This study includes over 11.6M newborns screened (NBS) for Pompe Disease (PD) from 29 distinct universal screening programs across 8 countries and 4 continents. The birth prevalence of PD is 1:18,711, with no evidence of difference across populations of European, Latin American, or Asian ancestry, though differences may exist for PD subtypes. This study also compares these results, based on direct detection of disease and analyzed using a binomial method along with power analysis, with other methods for estimating the 'frequency' of rare genetic diseases (such as utilizing Hardy-Weinberg equilibrium on allele frequency and confidence interval analysis). This comparison demonstrates the implications of sample size and frames a discussion on its influence on the reliability of results when extrapolating to a population beyond the study dataset.

Objectives: Primary: Establish a new figure for prevalence at birth for Pompe disease by collecting and analyzing the largest relevant dataset to date and using that result to project population prevalence at birth in a novel way. Secondary: Compare these results to previous analyses to offer a framework for evaluating 'frequency' data that can be applied to other rare, genetic diseases, along with methods to assess quality of estimates.

KEYWORDS

Pompe (glycogen storage disease type 2/II), rare disease epidemiology, newborn screening (NBS), lysosomal storage disorder/disease (LSD), autosomal recessive inheritance, genetic prevalence, gnomAD, diagnosis/diagnostic yield

Introduction and background

Pompe disease (PD), also known as glycogen storage disease type II, is a rare genetic disorder with an autosomal recessive inheritance pattern and a metabolic consequence. The acid alpha glucosidase (GAA) gene on chromosome 17 codes for production of the acid alpha glucosidase (GAA) enzyme/protein which is responsible for a step in the process of breaking down stored energy in the lysosome on its way to a usable form (energy stored as glycogen breaks down into glucose). Single or multi-nucleotide sequence variants within this gene can have a range of impact on the resultant enzyme produced: from minimal functional change to decreased functionality of the enzyme to reduced quantity of functional enzyme produced (as low as zero). When function- or quantity-limiting variants are present on both inherited GAA alleles, leading to sufficiently reduced GAA enzyme activity, Pompe disease is diagnosed. With decreased functional enzyme, glycogen or partially broken-down glycogen accumulates in the lysosome, initiating a metabolic cascade which eventually leads to cellular damage. While nearly every cell contains lysosomes which have the potential to be impacted by this disorder, cell damage is primarily observed in specific cells which rely on this stored energy more heavily (for example proximal skeletal muscle). Within the 18,000+ nucleotide long GAA gene, hundreds of variants have been established as pathogenic (1) for PD thus far. There is

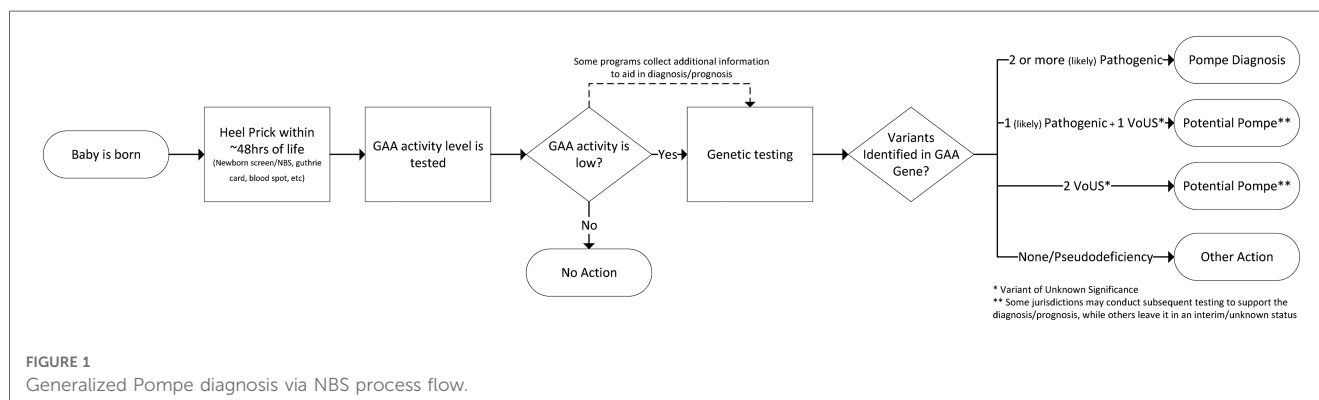
some ability to predict the impact on GAA enzyme based on the variant type and location. Historically, the disease has been categorized into subgroups based on an “age of onset” classification: initially as infantile, juvenile, and adult subgroups and more recently, an infantile onset form (IOPD) and a late onset form (LOPD). These age-of-onset based classification systems can be misleading as even persons diagnosed as late onset may have (had) detectable disease features in infancy. A 2010 analysis detected enlarged lysosomes in a one-month-old “asymptomatic” newborn who had been diagnosed via newborn screening (NBS) with “milder late-onset” genetic variants (2). A 2017 study of seven infants diagnosed with LOPD via NBS concluded that all seven patients demonstrated Pompe specific signs of motor involvement by age six months (3). Of note, four of the seven were identified as having a homozygous c.-32-13T>G genotype, which is predicted to have the “mildest” associated PD phenotype. A more-recent 2022 study of 20 infants diagnosed with LOPD via NBS also found that the entire cohort had detectable features of Pompe within the first years of life—including the four (20%) homozygous c.-32-13T>G participants (4). These observations reinforce the importance of considering an alternate basis for a classification system. A diagnosis of Pompe disease, having a spectrum of progression, may be sufficient, with a severe subcategory as a pragmatic distinction for cases with uniquely urgent sensitivity to starting treatment. This severe PD subset would encompass the generalized description of IOPD as those with zero or near-zero GAA enzyme function, who may have cardiac involvement, as there is an expectation of rapid accumulation of potentially irreversible

progression in such cases where treatment is unavailable or delayed. That notwithstanding, this study uses the IOPD and LOPD distinctions as provided by the contributing NBS programs, while the discussion considers the generalizations as described.

Understanding disease frequency¹ (incidence² and prevalence³) has important implications. These values inform public health impact, assist in identification of affected communities, and support the development of disease-specific therapies. Because of the importance of epidemiology to rare diseases, estimates must be generated, revisited, and challenged. In the case of Pompe disease, increasing adoption of NBS affords us an opportunity to improve estimates of PD birth prevalence.

This paper uses the diagnosis criteria of the NBS programs that supplied the data which represents a diagnostic threshold of both a biochemical screen and a molecular (genetic) confirmation. Summarily, individuals included in the analysis have been assigned a diagnosis of PD based on low GAA enzyme activity *and* two (or more) identified pathogenic or likely pathogenic variants to the GAA gene. Because the diagnostic algorithms used in NBS provide visibility into the biochemical consequence of the detected variants already, testing to determine configuration of the variants (trans vs. cis) is not routine for diagnosis. There are circumstances where additional testing may be prudent. While each screening jurisdiction has its own detailed NBS workflow, a generalized process flow for diagnosis of Pompe via NBS is shown in Figure 1.

A general example of sources of variability for the NBS data used in this study is provided in Figure 2.

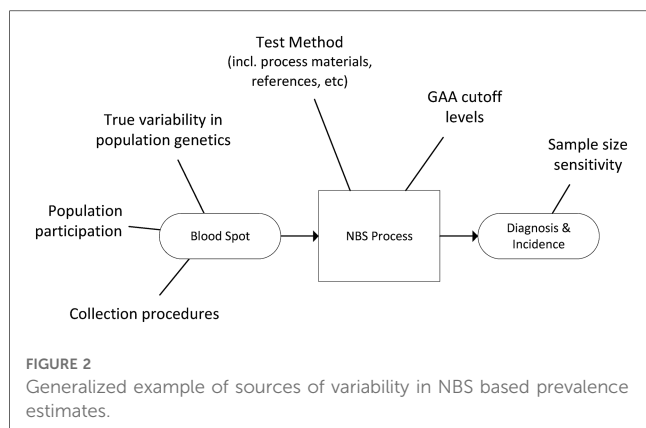


¹Frequency is a catch-all term that captures any measure of disease occurrence in a population.

²Incidence measures the number of new cases that occur in a specified time period (e.g., cases per year). Colloquially, it is often used to mean “prevalence at birth”. However, prevalence at birth is not actually a measure of incidence because this metric is independent of time (e.g., cases per 100,000 births).

³Prevalence measures the number of affected persons among a broader population. For example, birth prevalence measures the

number of affected newborns out of the total newborn population. A related metric is prevalence at conception (familiar as the result of the Hardy–Weinberg formula). It differs from birth prevalence as some pregnancies do not reach term. Compared to birth prevalence, total population prevalence may be lower due to disease-related mortality. As mortality decreases (e.g., from timely access to quality treatment), prevalence converges towards birth prevalence.



Methods

Data collection

A literature review of available NBS data accounted for approximately 4 million newborns universally screened for PD (i.e., not selectively screened or high risk). To estimate the completeness of these published figures, a comparison was made against the estimated number of births in jurisdictions that have described their NBS programs, factoring in the time frame for active screening and birthrates for that jurisdiction. This analysis suggested that results for fewer than half of total Pompe screened births had been published. To resolve this gap, and improve the size and representativeness of the analysis, an attempt was made to collect the missing US data from the publicly funded NewSTEPs data repository, but the data were not made available for this study. As a result, individual states and countries (departments of health, newborn screening programs, etc.) were contacted by one of this paper's authors (RC), to gather additional data as well as verify previously published data. Each program provided the following variables which were included in the analysis: date range, birth count, diagnosed count and any sub or adjacent category of diagnosed count (e.g.: IOPD, LOPD, unknown disposition). These efforts increased the dataset to over 11.6M newborns.

Analysis

The initial analysis uses the traditional approach of using a 95% confidence interval (CI) to estimate birth prevalence from individual and aggregate datasets - in this case, specifically the Wilson methodology which is appropriate for very small proportions (frequencies of occurrence). A limitation of this approach is that it considers only the sample size and proportion of occurrence for the discrete set of data used. For epidemiological analyses, it can be useful to consider clusters of discrete data or subsets of general data, which are intended to represent a hypothesized feature of interest, for example geography (by region, continent, etc.). With a traditional 95% CI approach, it is necessary to do this by creating subsets and groupings of the data (for example, different geographical

regions)⁴. In this approach, these aggregate datasets contain all the elements of the source datasets, but any unique characteristics (such as birth prevalence for an individual contributing jurisdiction) become indistinguishable when aggregated. This approach becomes challenging as the amount and diversity of data, or number of clusters of interest, increases. It becomes difficult to interpret the discrete analytical outputs, and more data preparation is required. These factors may discourage the kind of exploration that drives the development of new knowledge.

This paper uses a methodology that can address these limitations. We recognize a benefit to retaining the unique features of a source dataset (in this case birth prevalence within an NBS jurisdiction), but also acknowledge heredity as a process common to all humans, albeit with potential factors that may differentially impact sub-populations. We maintain both features by utilizing a binomial methodology, a technique often used in the field of process analysis, which has mathematical terms that factor both individual/contributing datasets and the total dataset in a single analytical output. Additional detail on the supporting calculations can be found in [Appendix A](#).

A visual comparison of the two approaches (Wilson 95% CI and binomial) is shown in the Results section. The birth prevalence value is the same for both approaches⁵, but the organization of the binomial model yields additional observations which will be covered in the Discussion section.

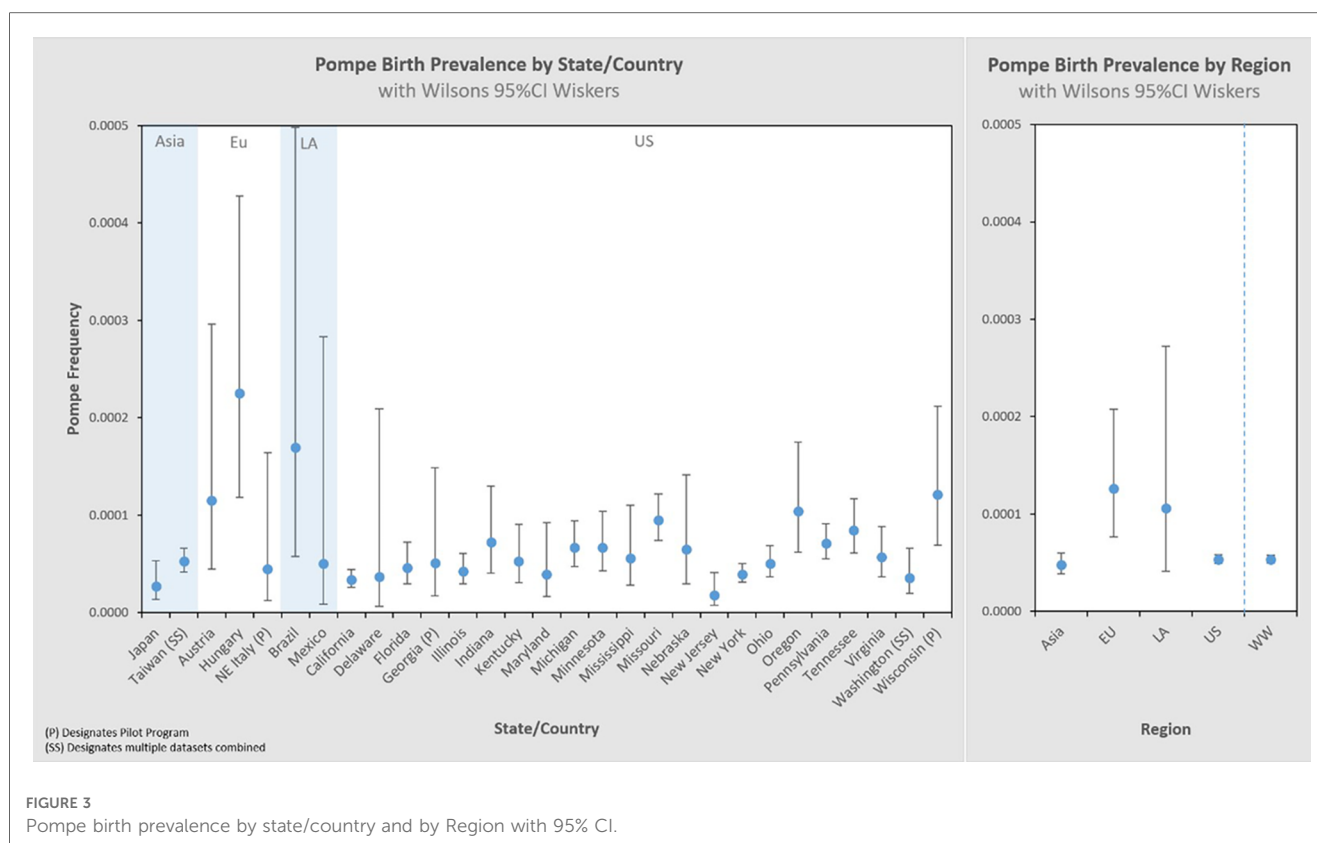
Results

Pompe disease birth prevalence is 1:18,711 births (5.3 per 100,000 births) in this dataset of over 11.6M newborns screened for Pompe across 22 states and 8 countries on 4 continents between 2010 and 2022.

Of the 11,619,662 screened newborns included in this analysis and the 621 total Pompe diagnoses, 91 were classified by their NBS programs as IOPD (1:126,118 or 7.9 per 1M births), and 524 as LOPD (1:21,902 or 45.6 per 1M births), while 6 were only classified generally as PD without subtype distinction (5 from Taiwan, 1 from Mexico). These figures exclude an additional 120 newborns who were flagged as having low GAA enzyme activity and identified GAA variants, but with interim "unknown" dispositions. These are potentially LOPD or pseudodeficiency cases, but with previously uncharacterized genetic variants, or cases awaiting further reporting at the time of data collection. When states/countries identified an "unknown" diagnosis, these specific counts were not included in

⁴To consider relationships between regional datasets, one would compile several aggregate datasets (i.e., sample 1, and separately a dataset of sample 1 + sample 2, and separately still a dataset of sample 1 + sample 2 + ... + sample *n*).

⁵The projected uncertainty ranges are different (but concentric). They are calculated differently, with different specific meanings in each approach, but can generically be interpreted as a "variability figure".



the analysis, but they're noted in the data table which can be found in [Appendix B](#). If any of the 120 “unknown” cases are ultimately diagnosed as PD, then the true birth prevalence of PD is higher than the 1:18,711 reported here⁶. These additional cases are not likely to be severe PD, because the very low-to-no enzyme activity and typical cardiac involvement associated are identifiable features that can support an IOPD diagnosis. Among the sources of variability summarized in [Figure 2](#), there are two noteworthy examples that further suggest this analysis as an underestimate of birth prevalence: Some cases have been lost to or refused follow up, and some NBS jurisdictions use enzyme activity cut-offs that are too low to identify all cases of PD⁷ (5). The approach of this paper, to only use cases diagnosed by NBS, is conservative as the examples of excluded uncertainty above can only increase the prevalence of Pompe as they would add, not subtract cases. The resultant birth

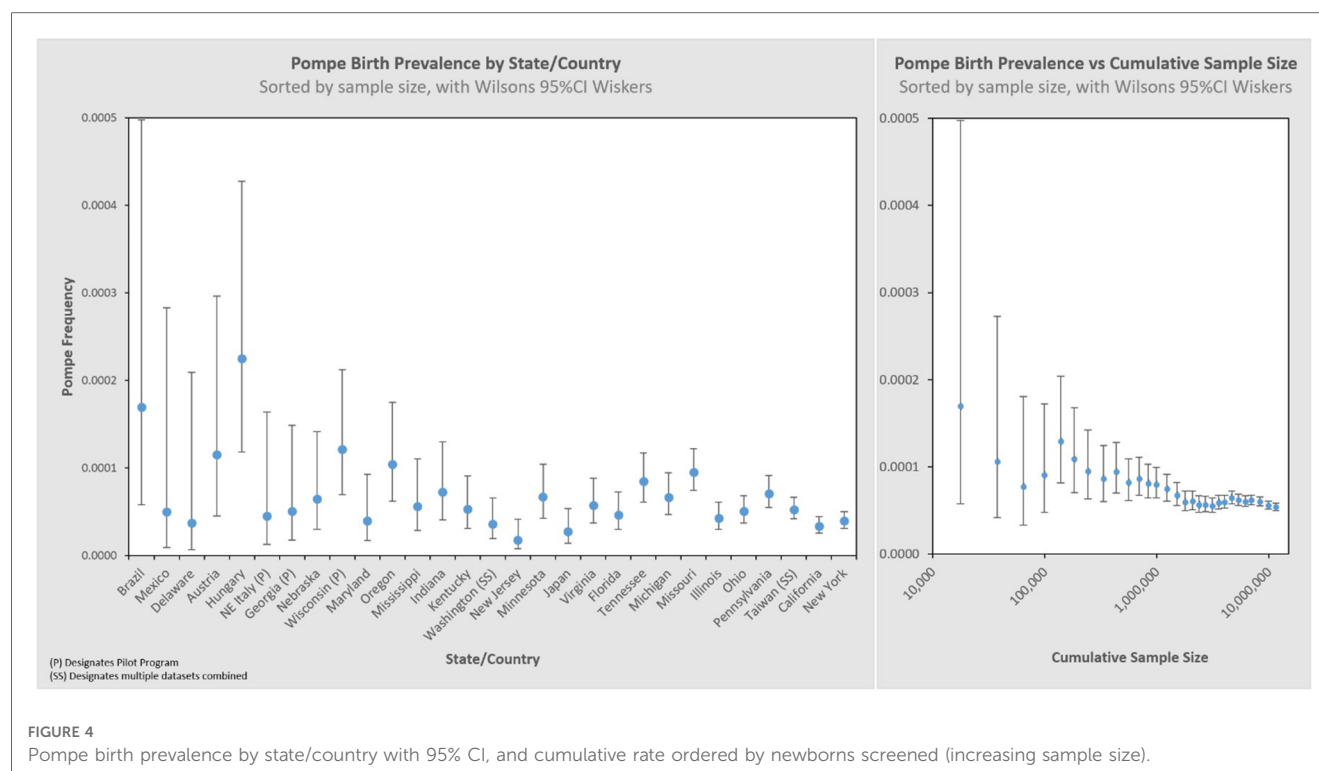
prevalence value is therefore confidently a minimum estimate, i.e., the true birth prevalence is at least 1:18,711.

[Figure 3](#) presents these results in a typical format for “frequency” analyses. Each jurisdiction's observed birth prevalence is shown along with a 95% CI, as well as several regional groupings [Asia, Europe (Eu), Latin America (LA), United States (US), and worldwide (WW) aggregate]. In each of these figures, birth prevalence is shown as a point, and the confidence interval shown as whiskers. When comparing each value with another, the more the confidence interval (whiskers) overlaps, the lower the statistical likelihood that a difference exists between them.

Larger data sets have greater statistical precision (narrower whiskers), which is one characteristic by which to judge the reliability of the result. We can visualize this by organizing the same dataset by sample size, shown in the left panel of [Figure 4](#). The sample size increases from left to right on the x-axis, and the corresponding 95% CI decreases (narrower whiskers). Another way to visualize this is on the right panel which cumulatively aggregates the birth prevalence results by jurisdictions of increasing newborns screened. When only the smallest data sets are considered (~10k newborns) the calculated birth prevalence is so imprecise as to be barely usable for public health purposes. The addition of increasingly larger samples (moving along the x-axis to over 10M newborns) quickly leads to leaps in precision. This can be seen in this figure where the upper bound value of the 95% CI range on the left is 8.6× the lower bound value of the 95% CI range, while on the right it is only 1.2×. It is also notable that there are diminishing returns along the x-axis—after a certain point, even hundreds of

⁶If all 120 Unknown cases resolved in a diagnosis of Pompe, then the birth prevalence for this dataset would be 1:15,681 (63.8 per 1M births).

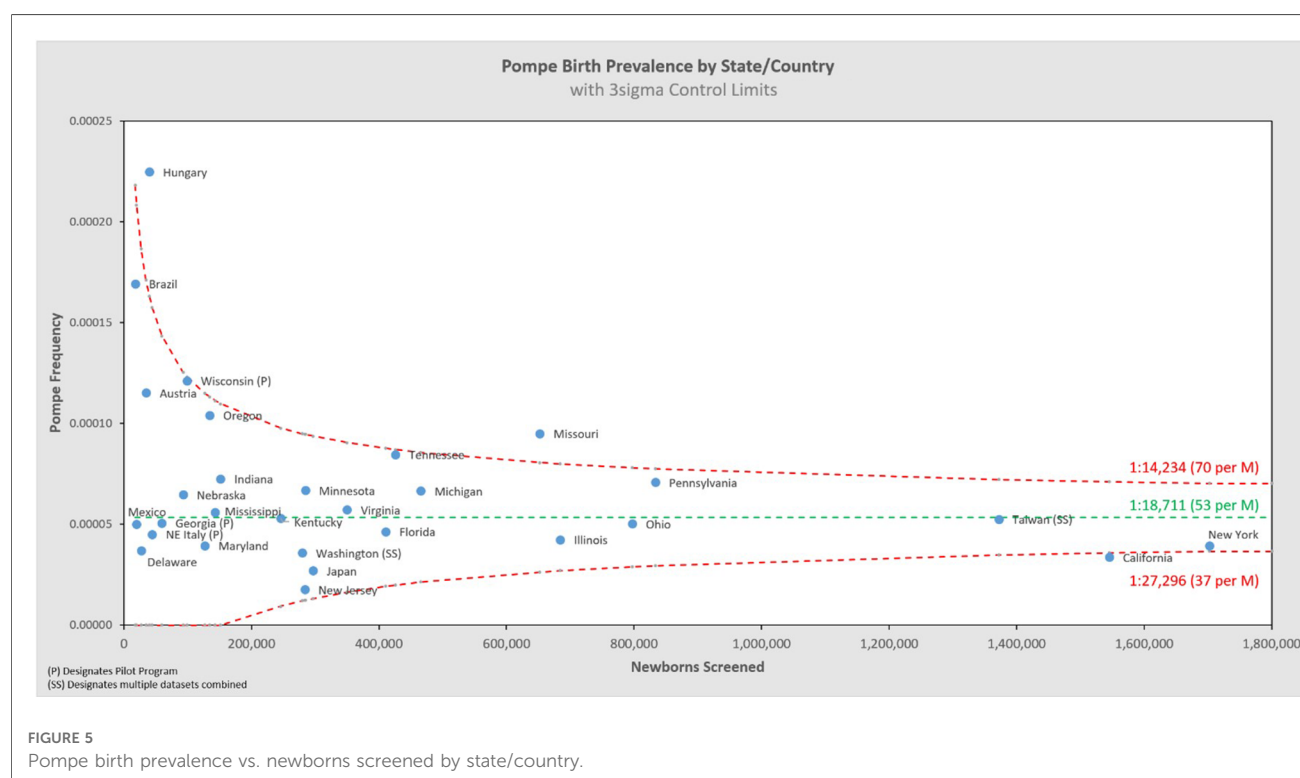
⁷For example: Between 8/1/17 and 7/31/21, Minnesota Department of Health had one case lost to follow up which it considers to be LOPD, but is not included, and two confirmed LOPD cases which were not identified by NBS due to low screening cutoffs. They were instead identified as a result of familial testing after a later-born sibling was identified. These cases were not included in this study. Differences in enzyme activity thresholds may also explain some variability between jurisdictions.

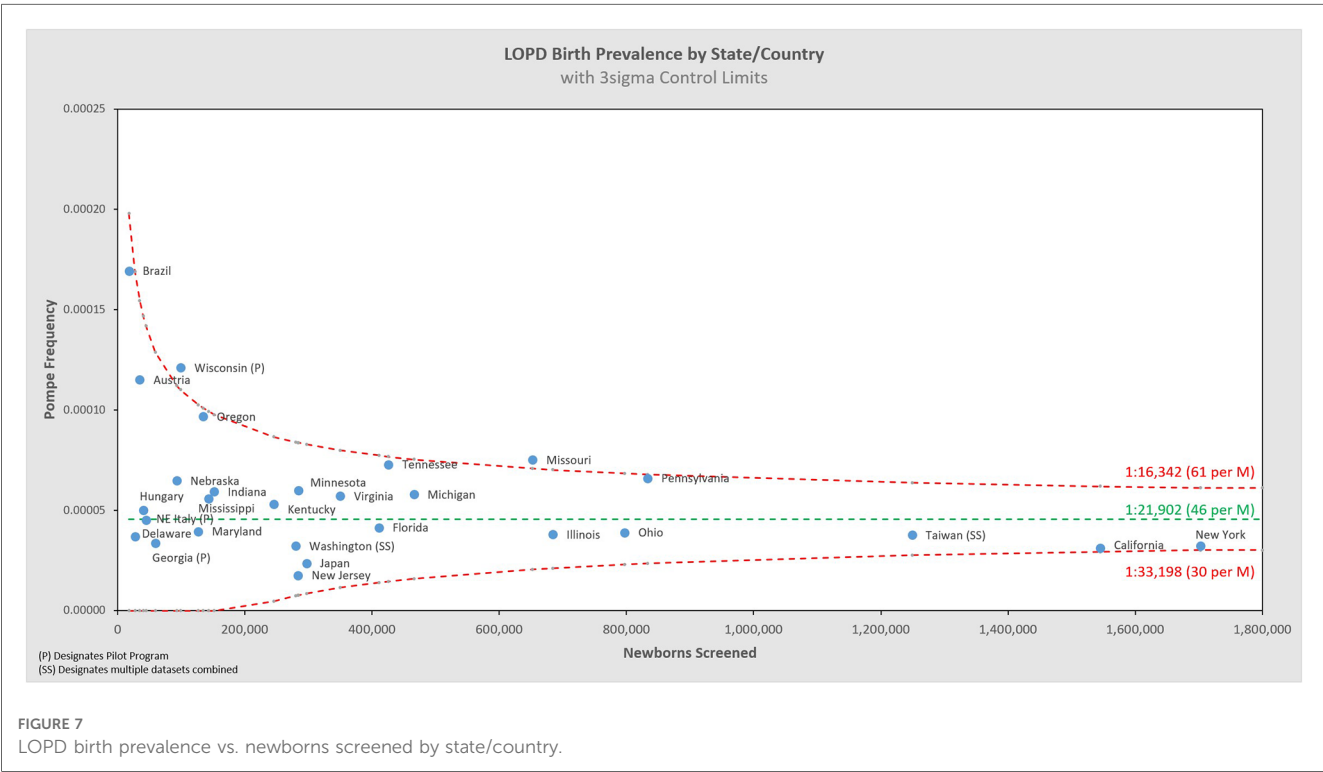
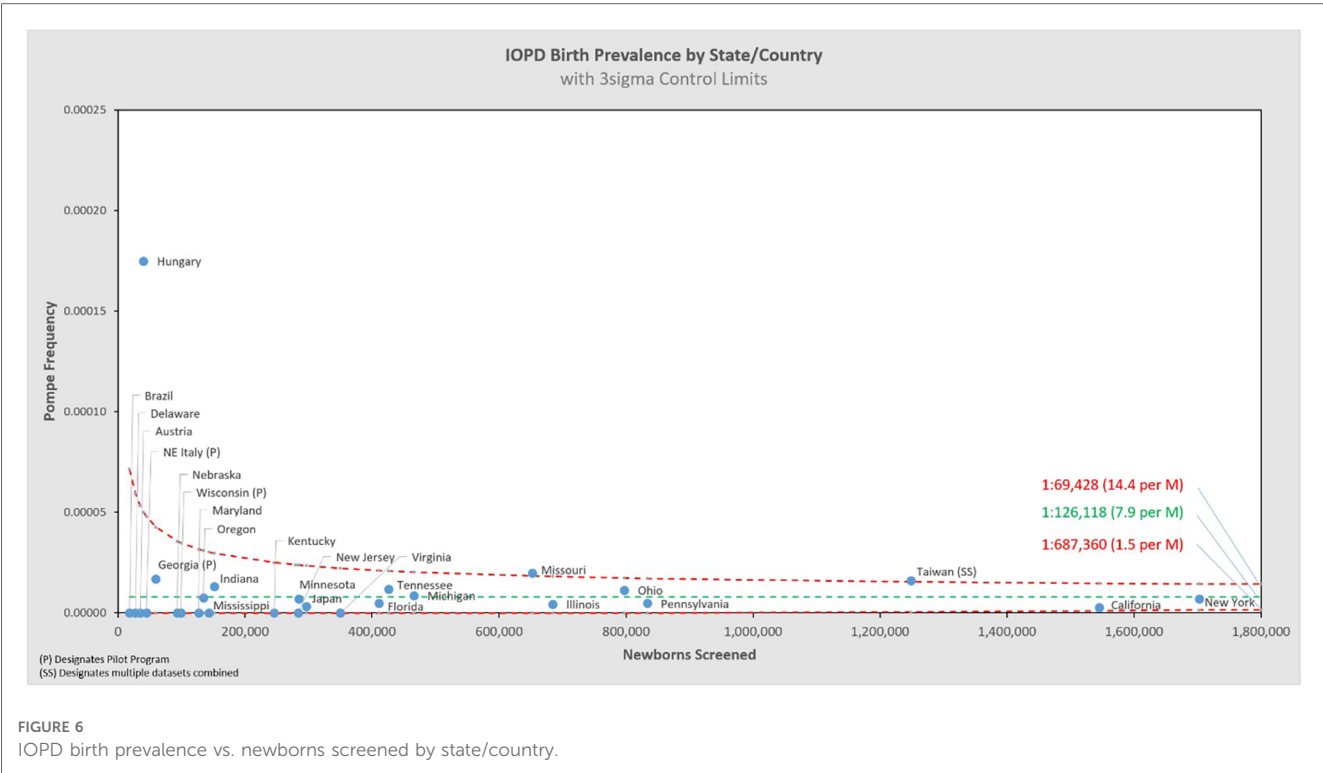


thousands of additional newborns have little impact on precision (the spread of the whiskers).

Figure 5 shows the same data analyzed using a binomial model, and Figures 6, 7 break out IOPD and LOPD respectively. In each of these figures, birth prevalence is shown as a point and the uncertainty figures ($\pm 3\sigma$ control limits that consider both the individual point as well as the entire dataset)

are shown as connected lines through this value for each point. With this analysis one can visualize the number of newborns screened, the birth prevalence, and individual uncertainty relative to the entire dataset for each individual jurisdiction. Adherence of each jurisdiction to the narrowing uncertainty range suggests a convergence of birth prevalence as sample size increases.





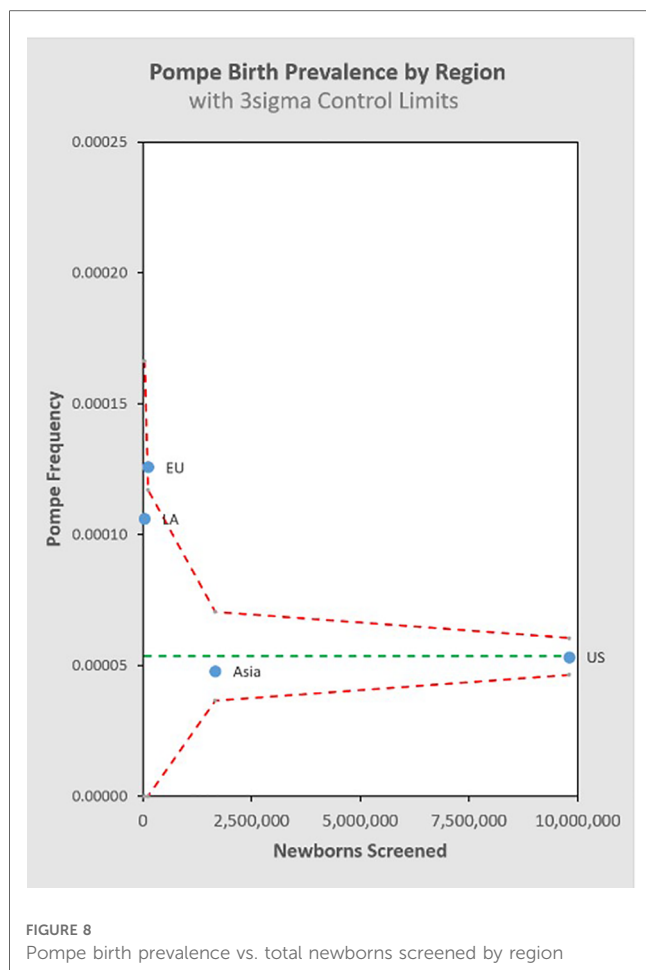


FIGURE 8
Pompe birth prevalence vs. total newborns screened by region

Figure 8 groups the State/Country data by common regional groupings.

Discussion

The birth prevalence of PD for the 11,619,662 newborns screened included in this dataset is shown in Table 1, along with population birth prevalence projection ranges produced through two different analytic approaches. The birth prevalence value is the same in each method, but each has a different uncertainty

TABLE 1 Measured Pompe birth prevalence with two projections for population birth prevalence range.

	Measured birth prevalence	Projected population birth prevalence	
	Direct detection	Wilson's 95% CI	$\pm 3\sigma$ control limit convergence
Total Pompe	1:18,711 ^a 53.4 per 1M births	1:20,242 , 1:17,296 49.4–57.8 per 1M births	1:27,296 , 1:14,234 36.6–70.2 per 1M births
IOPD	1:126,118 7.9 per 1M births	1:154,829 , 1:102,731 6.5–9.7 per 1M births	1:687,360 , 1:69,428 1.5–14.4 per 1M births
LOPD	1:21,902 45.6 per 1M births	1:23,859 , 1:20,105 41.9–49.7 per 1M births	1:33,198 , 1:16,342 30.1–61.2 per 1M births

^aUsing the Hardy–Weinberg principle, this projects that 1:68.9 people are carriers of a Pompe contributing genetic variant.

range due to slightly different techniques for incorporating statistical uncertainty. An additional note on the standard values used: $\pm 3\sigma$ is a higher statistical threshold (inclusive of more possible outcomes) accounting for 99.7% of observed normal variation, which is more rigorous than the 95% confidence interval, hence the broader range than the 95% CI.

This study is the most comprehensive examination of birth prevalence to date, and its results address the question of whether there are significant differences in prevalence across different ancestry groups: there is little evidence to support that significant differences in total PD birth prevalence exist across the jurisdictions included. It remains possible that differences may emerge with even larger and broader data sets, but in the absence of further evidence, it is appropriate to apply the results from this study for total PD birth prevalence to any given population.

The direct detection of PD biomarkers used in the NBS diagnosis process offers a significant step forward for estimating PD birth prevalence compared to data collected via indirect methods, such as carrier screening which estimates prevalence at conception. Additionally, this dataset is 3–4 orders of magnitude larger than the indirect datasets previously used, and it is generated from more a broadly representative population. There is still inherent bias to this dataset, which will be discussed below, but on balance this dataset represents a major advance in Pompe disease epidemiology. These factors favor the total PD birth prevalence from this study as the basis for population-wide prevalence projections as a replacement for previous estimates.

Reflections on previous work and responsibility in interpretation

Groft & de la Paz (6) give an overview of the impact that epidemiological data can have on evolving knowledge, enabling movement from misperceptions and myths toward scientific realities. They describe the importance and implications of accurate epidemiological data for the study of rare diseases. The data used in this study represent progress toward a true PD prevalence, along with a statistical model which can gauge whether a given data set is sufficiently large to represent true population prevalence. We further propose the use of statistical power⁸ as a tool to estimate the strength a given study relative to the misperception/myth vs. scientific realities/truth continuum.

The development of new knowledge around a topic is fundamentally iterative. It is essential to regularly revisit and challenge the assumptions, foundations and context from which early knowledge and conclusions are derived.

⁸In Statistics, Power (β) is the probability of avoiding a Type II error—i.e., correctly rejecting the null hypothesis. It can be used to assess how confident one can be based on the input parameters available by providing the probability of correctly detecting a difference from a projected prevalence based on how big that difference is.

TABLE 2 Comparison of multiple datasets to project prevalence of PD.

Year / Method	Sample size	Variants covered	Effect measured?	Direct/indirect	Projection	$\alpha = 5\%$ (95% CI)	$\beta = 80\%$ power range (with $\alpha = 5\%$)
1998 / Martiniuk	928	7	N	Indirect	1:32,189 ^a 31.1 per 1M births	1:278,014 , 1:3,758 3.6–266.6 per 1M births	– , 1:1,137 (0)–879.2 per 1M births
1999 / Ausems	3,043	3	N	Indirect	1:40,059 ^a 24.9 per 1M births	1:115,325 , 1:13,886 8.7–72.0 per 1M births	– , 1:2,209 (0)–452.6 per 1M births
1999 / Ausems (2022 updated assumptions)	3,043	3	N	Indirect	1:28,138 ^a 35.5 per 1M births	1:76,270 , 1:10,294 13.1–97.1 per 1M births	– , 1:1,859 (0)–538.0 per 1M births
1999 / Ausems (Martiniuk approach)	3,043	3	N	Indirect	1:15,298 ^a 65.4 per 1M births	1:30,743 , 1:7,631 32.5–131.0 per 1M births	– , 1:1,395 (0)–716.6 per 1M births
2021 / Park	141,456	154	N	Indirect	1:23,177 ^a 43.1 per 1M births	1:25,368 , 1:21,176 39.4–47.2 per 1M births	1:232,558 , 1:10,030 4.3–99.7 per 1M births
2022 / NBS_Direct	11,619,662	Any/all ^b	Y (enzyme activity)	Direct	1:18,711 53.4 per 1M births	1:20,242 , 1:17,296 49.4–57.8 per 1M births	1:21,053 , 1:16,779 47.5–59.6 per 1M births

^aNote these figures are different than reported in their respective papers. They are recalculations based on the inputs provided in those papers.

^bBounded by gene sequencing method and procedures of the responsible lab.

Two commonly referenced studies of Pompe frequency, from 1998 and 1999, use the carrier-frequency method, based on allelic prevalence, to estimate Pompe prevalence at conception (7, 8). Both estimate prevalence at 1:40,000 as an update from an even older 1:100,000 estimate. Martiniuk et al. analyzed 928 randomly selected individuals from New York to establish a carrier frequency of 7 known pathogenic variants in the GAA gene, with these variants seen in 29% of a diagnosed reference dataset. In a separate effort, Ausems et al. analyzed 3,043 randomly selected blood spot cards from various regions of the Netherlands to establish a carrier frequency of three known pathogenic variants in the GAA gene. These three variants were seen in 63% of the then diagnosed Dutch PD population. Ausems et al. stated that their higher variant representation (63% vs. 29%) led to ‘extrapolations that were considerably more accurate’ than the approach of Martiniuk et al., and that it was merely coincidence that both studies estimate the same point value for disease frequency.

Both papers noted the limitations of their estimates, including the statistical uncertainty inherent in their small sample sizes. Despite this acknowledged uncertainty, let alone the still-unknown uncertainty, the cross-validation effect of these two studies has led to a broad, highly entrenched adoption of 1:40,000 as a projection of Pompe prevalence that continues to be widely circulated.

In 2021, Dr. Park published an analysis (9) that applied the same carrier-frequency method to a much larger and more broadly representative dataset. She also considered a larger set of PD variants. Park’s dataset includes over 140,000 genetic screens, with sample diversity across eight identified demographic groups, and considers 154 pathogenic or likely pathogenic variants. Using this dataset, Park projects a prevalence (at conception) of 1:23,232; which is notably close to this paper’s measured value for birth prevalence of 1:18,711.

The implications of Park’s result being in proximity to the result of this study may be impactful for gaining further understanding of PD, as well as for the broader rare disease community.

With hindsight, it is clear that the two early studies were not so different as they must have seemed at the time, and the underlying strength of their datasets was weaker than the 20+ years of use would suggest. A power analysis, using only information available at the time of each study (namely sample size and an estimation of proportion/frequency of occurrence), provides a confidence figure

for the results of these two studies. Table 2 shows a summary of inputs and the results from a power analysis, along with the more recent Park study, and this paper. The associated power curves for each study, along with a visual comparison of the uncertainty ranges from Table 2, are shown in Appendix C. In addition, rows three and four revisit assumptions made in the Ausems paper for additional perspective:

- Row 3: The original Ausems analysis excluded homozygosity of a mild variant (c.-32-13T>G) it considered on the grounds that it probably did not give rise to Pompe. The cited studies by Rairikar et al. and Huggins et al. compel a reversal of this exclusion, which is reflected in row three.
- Row 4: Ausems’ original analysis used separate calculations for IOPD and LOPD carriers, whereas Martiniuk considered carriers of any pathogenic variant as a single cohort without a homozygous mild variant exception. Applying Martiniuk’s approach that includes scaling for the variant coverage estimate of the time, stated at 63% for Ausems, yields the projection provided in row four.

The utility of a power calculation is to show how narrowly a range can be defined while remaining confident that we do not exclude the truth from that range. As applied here, the calculation is based on the sample size of a given study, the observed prevalence in that study, and a power value, β , that can be selected for the purpose (common values for β are 0.8 or 0.9). The calculation yields a “power curve,” which illustrates a range of possible results for which the study is adequately powered to reject that the true prevalence is outside of this range with a likelihood of β (for example, 0.8 or 80%). In simpler terms, if a study were performed 100 times with the same parameters, these power ranges are the narrowest 95% CI range that 80 of those 100 repeats would fall into.

Accelerating learning | reflections on effort, building momentum and a validated reference concept

The analytic approach used in this study could be applied to other conditions, but the process for collecting the data is not

scalable in a reasonable timeframe. While it is currently time consuming to gather NBS data, the real challenge is the massive undertaking required to implement NBS for a condition. As evidence of this point, PD was first submitted for consideration on the Recommended Uniform Screening Panel (RUSP) in the US in 2006, but it wasn't included on the RUSP until nine years later when it was approved in 2015. As of September 2023, 45 states (including DC) accounting for approximately 87% of US births had initiated a Pompe NBS program, while just over 2% of worldwide births have programmatic/universal NBS for Pompe. It is not tenable to expect a 15+ year process for each of the projected 10,000+ rare diseases (10) to get to the point of having reliable epidemiological data—our approach to these challenges must evolve.

The availability of increasingly large genetic datasets that are publicly accessible (for free), such as that used by Park⁹, point the way forward for some diseases. The convergence of Park's estimate (using expanding broad general open access datasets), towards this study's result (using data from a major effort specific to a single disease) is exciting because it supports the use of genetic databases where NBS data are not available. It suggests that publicly available genetic data may have sufficient sample size and diversity to be useful for other conditions. Replicating these two studies for other conditions where NBS is already in place can further delineate the strengths and weaknesses for use of publicly available data. This validation approach can cut years, if not decades, from the process of generating quality epidemiological insight for other diseases. It is worth emphasizing that this type of progress acceleration depends on the availability of datasets.

It is important to highlight some key considerations and limitations of this approach that could affect other diseases¹⁰:

- The disease considered here is monogenic with an autosomal recessive inheritance pattern.
- Some knowledge of pathogenic variants is established (or can be reasonably projected).
- Appropriate sample size is determined by rarity, so conditions that are rarer than PD will have lower statistical power. This improves as genetic databases increase in size.
- The genetics of the sample population may be a source of bias. For this analysis of PD, both the NBS dataset and the publicly available genetic datasets may not necessarily represent the population of interest for all research questions. This factor improves as datasets increase in diversity and representation.

Possible regional variation in PD subtypes

In general, we can look at the R-Value of a linear regression of sample size vs. birth prevalence for the regions included in the

analysis to suggest that this single variable model explains as much as 81.6% of the observed variability between the individual screening jurisdictions (Appendix D). This metric shows that differences between regions are small relative to the effect of sample size itself for the NBS programs considered in this analysis. It is interesting to note that while the total birth prevalence seems to converge towards single figure globally, there does appear to be a meaningful difference in the IOPD/LOPD breakdown in specific regions. In the US, 12% of NBS cases are diagnosed as IOPD and 88% LOPD (this likely underestimates the share of LOPD, as “unknown” cases are expected to skew towards LOPD). By contrast, in Asia (primarily Taiwanese data) the diagnoses are 28% IOPD and 72% LOPD. One possible explanation is the “mild” c.-13-32T>G variant that is common in the US population, but not in the Taiwanese population. It is considered a “rescue” variant because it results in enzyme with enough function to shift towards a LOPD phenotype even when paired with a severe variant that would otherwise suggest IOPD. This observation that total PD birth prevalence is generally similar across populations, while the distribution of IOPD vs. LOPD differs, may be of interest in an investigation of survivability and modifiers for propagation of recessive conditions on an evolutionary scale. Additionally, while the data considered in this analysis suggests convergence of total PD birth prevalence, even across diverse populations, the authors note that data from the two most populous countries (China and India) are not directly represented, which may be a source of variability when projecting global prevalence.

An example of applied insight towards the topic of diagnosis timelines and diagnostic delay

It is clearly desirable to diagnose people who have a potentially severe yet treatable condition such as PD in a timely manner. For many rare diseases, the term “odyssey” is applied because it can take years or even decades to get a diagnosis, as noted by Groft and de la Paz. Surveys are often used as a retrospective estimate of time-to-diagnose as a performance metric for the clinical diagnosis process. This study offers insight on this same concept in a less subjective way: In April 2022, Sanofi presented to the AMDA (Acid Maltase Deficiency Association) that the Pompe Registry had 819 PD diagnosed participants in North America (an alternate, more conservative figure for this is 343 provided by Reuser et al. (11)) — not a perfect estimate of diagnosed prevalence, but, reasonable as an order of magnitude estimate. We can compare this with an estimated North American prevalence of over 23,000 (using LOPD birth prevalence only, as a simplification based on high mortality in undiagnosed/untreated severe PD) to show that <5% of the Pompe population are represented in the registry. While some diagnosed people do not participate in the registry, the rest of the gap must be due to under/misdiagnosis. This suggests that a small fraction of the global Pompe population has been diagnosed. This helps quantify the inefficiency of the clinical diagnosis process for this treatable condition, with the suggestion that those with public health or commercial interests should consider strategies that increase

⁹The exception in her study is Pompe Registry data (used as a part the variant cross-checking process she described), some of which is available through publication, but is ultimately owned and siloed by the pharmaceutical sponsor.

¹⁰This is an incomplete list of limitations to consider.

emphasis on higher-yield diagnostic processes, such as NBS. The implications of a strategy to improve diagnostic yield would be impactful on further development of knowledge, through study participation, participant/spectrum diversity, business case justification, etc.

Post Factum

While working through publication of this manuscript, additional data were published about incidence of PD in Italy (12), as well as updated data made available by the Tennessee Department of Health NBS program, and data shared by both Colorado newborn screening program and North Carolina department of health and human services via posters at the APHL/ISNS NBS Symposium in Sacramento, October 15–19, 2023. An updated binomial analysis, inclusive of this additional data is available in [Appendix E](#). In short, these additional data fit very well within the model presented. Summary stats with this additional data included: 12,060,529 newborns screened for PD with a birth prevalence of 1:18,698.

Data availability statement

The original contributions presented in the study are included in the article/Supplementary Material, further inquiries can be directed to the corresponding author.

Ethics statement

Ethical approval was not required for the study involving humans in accordance with the local legislation and institutional requirements. Written informed consent to participate in this study was not required from the participants or the participants' legal guardians/next of kin in accordance with the national legislation and the institutional requirements.

Author contributions

RC: conceptualization, methodology, validation, formal analysis, investigation, resources, data curation, writing – original

draft, writing – review & editing, visualization, supervision, project administration, funding acquisition DL: conceptualization, methodology, validation, formal analysis, writing – review & editing. All authors contributed to the article and approved the submitted version.

Funding

Support for this study was provided by Rare Crossroads.

Acknowledgments

Thank you to the representatives from each NBS program that contributed data and fielded questions to clarify nuance in each dataset. The public good that your work in Newborn Screening does is clear in the lives that are positively impacted and saved through NBS. It has the potential to go even farther if there is a greater emphasis on *using* the data collected to develop new understanding—thank you for allowing the authors to try to show this.

Thank you to Dr. Arnold Reuser for the guidance, support and encouragement throughout this study.

Conflict of interest

RC was employed by odimm inc., DL was employed by LapidusData Inc.

The Rare Crossroads fund for community led Initiatives in Pompe is managed by RC and has received contributions from M6P Therapeutics, Askbio, Astellas Gene Therapies, Maze Therapeutics, and contributors from the Pompe community.

Publisher's note

All claims expressed in this article are solely those of the authors and do not necessarily represent those of their affiliated organizations, or those of the publisher, the editors and the reviewers. Any product that may be evaluated in this article, or claim that may be made by its manufacturer, is not guaranteed or endorsed by the publisher.

References

1. Available at: <http://www.pompevariantdatabase.nl/>
2. Raben N, Ralston E, Chien YH, Baum R, Schreiner C, Hwu WL, et al. Differences in the predominance of lysosomal and autophagic pathologies between infants and adults with Pompe disease: implications for therapy. *Mol Genet Metab.* (2010) 101(4):324–31. doi: 10.1016/j.ymgme.2010.08.001
3. Rairikar MV, Case LE, Bailey LA, Kazi ZB, Desai AK, Berrier KL, et al. Insight into the phenotype of infants with Pompe disease identified by newborn screening with the common c.-32-13T>G “late-onset” GAA variant. *Mol Genet Metab.* (2017) 122(3):99–107. doi: 10.1016/j.ymgme.2017.09.008
4. Huggins E, Holland M, Case LE, Blount J, Landstrom AP, Jones HN, et al. Early clinical phenotype of late onset Pompe disease: lessons learned from newborn screening. *Mol Genet Metab.* (2022) 135(3):179–85. doi: 10.1016/j.ymgme.2022.01.003
5. Pillai NR, Fabie NAV, Kaye TV, Rosendahl SD, Ahmed A, Hietala AD, et al. *Newborn screening experience and outcome from Minnesota Pompe disease consortium. Poster presented at WORLDSymposium*; February 7–11, 2022; San Diego, CA, USA
6. Groft SC, de la Paz MP. Rare diseases—avoiding misperceptions and establishing realities: the need for reliable epidemiological data. In: Posada de la Paz M, Groft S. editors. *Rare diseases epidemiology. Advances in experimental*

medicine and biology, vol 686. Dordrecht: Springer (2010). p. 3–14. doi: 10.1007/978-90-481-9485-8_1

7. Martiniuk F, Chen A, Mack A, Arvanitopoulos E, Chen Y, Rom WN, et al. Carrier frequency for glycogen storage disease type II in New York and estimates of affected individuals born with the disease. *Am J Med Genet.* (1998) 79(1):69–72. doi: 10.1002/(sici)1096-8628(19980827)79:1<69::aid-ajmg16>3.0.co;2-k

8. Ausems MG, Verbiest J, Hermans MP, Kroos MA, Beemer FA, Wokke JH, Sandkuijl LA, Reuser AJ, van der Ploeg AT. Frequency of glycogen storage disease type II in The Netherlands: implications for diagnosis and genetic counselling. *Eur J Hum Genet.* (1999) 7(6):713–6. doi: 10.1038/sj.ejhg.5200367

9. Park KS. Carrier frequency and predicted genetic prevalence of Pompe disease based on a general population database. *Mol Genet Metab Rep.* (2021) 27:100734. doi: 10.1016/j.ymgmr.2021.100734

10. Available at: <https://rare-x.org/wp-content/uploads/2022/05/be-counted-052722-WEB.pdf>

11. Reuser A, van der Ploeg AT, Chien YH, Llerena J Jr, Abbott MA, Clemens PR, et al. GAA variants and phenotypes among 1,079 patients with Pompe disease: data from the Pompe registry. *Hum Mutat.* (2019) 40(11):2146–64. doi: 10.1002/humu.23878

12. Gragnaniello V, Pijnappel PWWM, Burlina AP, In 't Groen SLM, Gueraldi D, Cazzorla C, et al. Newborn screening for Pompe disease in Italy: long-term results and future challenges. *Mol Genet Metab Rep.* (2022) 33:100929. doi: 10.1016/j.ymgmr.2022.100929

Appendix A

Equations used in the Wilsons CI analysis

Each Plotted point represents the proportion of occurrence for the specified cluster

$$p_c = \frac{x_i + \dots + x_n}{n_i + \dots + n_n}$$

Where,

p_c is the proportion of occurrence for the cluster

x_i is the count of occurrence for the subgroup

n_i is the size of the subgroup

Each Plotted whisker represents the CI range for the specified cluster

$$CI = \frac{p_c + \frac{z^2}{2n_c}}{1 + \frac{z^2}{n_c}} \pm \frac{z}{1 + \frac{z^2}{n_c}} \sqrt{\frac{p_c(1 - p_c)}{n_c} + \frac{z^2}{4n_c^2}}$$

Where,

p_c is the proportion of occurrence for the cluster

z is the z -score associated with the desired CI For a 95% CI, a z score of 1.96 is used.

n_c is the size of the cluster

Equations used in the binomial analysis¹¹

Each plotted point represents the proportion of occurrence for the specified subgroup

$$p_i = \frac{x_i}{n_i}$$

Where,

p_i is the proportion of occurrence for the subgroup

x_i is the count of occurrence for the subgroup

n_i is the size of the subgroup

The centerline represents the average proportion of occurrence for the entire dataset

$$\bar{p} = \frac{\sum x_i}{\sum n_i}$$

Where,

\bar{p} is the calculated average proportion for the entire dataset used

x_i is the count of occurrence for the subgroup

n_i is the size of the subgroup

The Control Limits (CL), or expected range, are shown as connected lines through each individual subgroups $\pm 3\sigma$ proportion of occurrence

$$CL_i = \bar{p} \pm k \sqrt{\frac{\bar{p}(1 - \bar{p})}{n_i}}$$

Where,

\bar{p} is the calculated average proportion for the entire dataset used

k is sigma value (3 is commonly used)

n_i is the size of the subgroup

Note: lower control limit proportions are bound at 0, while upper control limits are bound at 1

¹¹Adapted from <https://support.minitab.com/en-us/minitab-express/1/help-and-how-to/control-charts/how-to/attribute-control-charts/p-chart/methods-and-formulas/methods-and-formulas/>

Appendix B

Table of input figures for each contributing region, along with source citation and date range references.

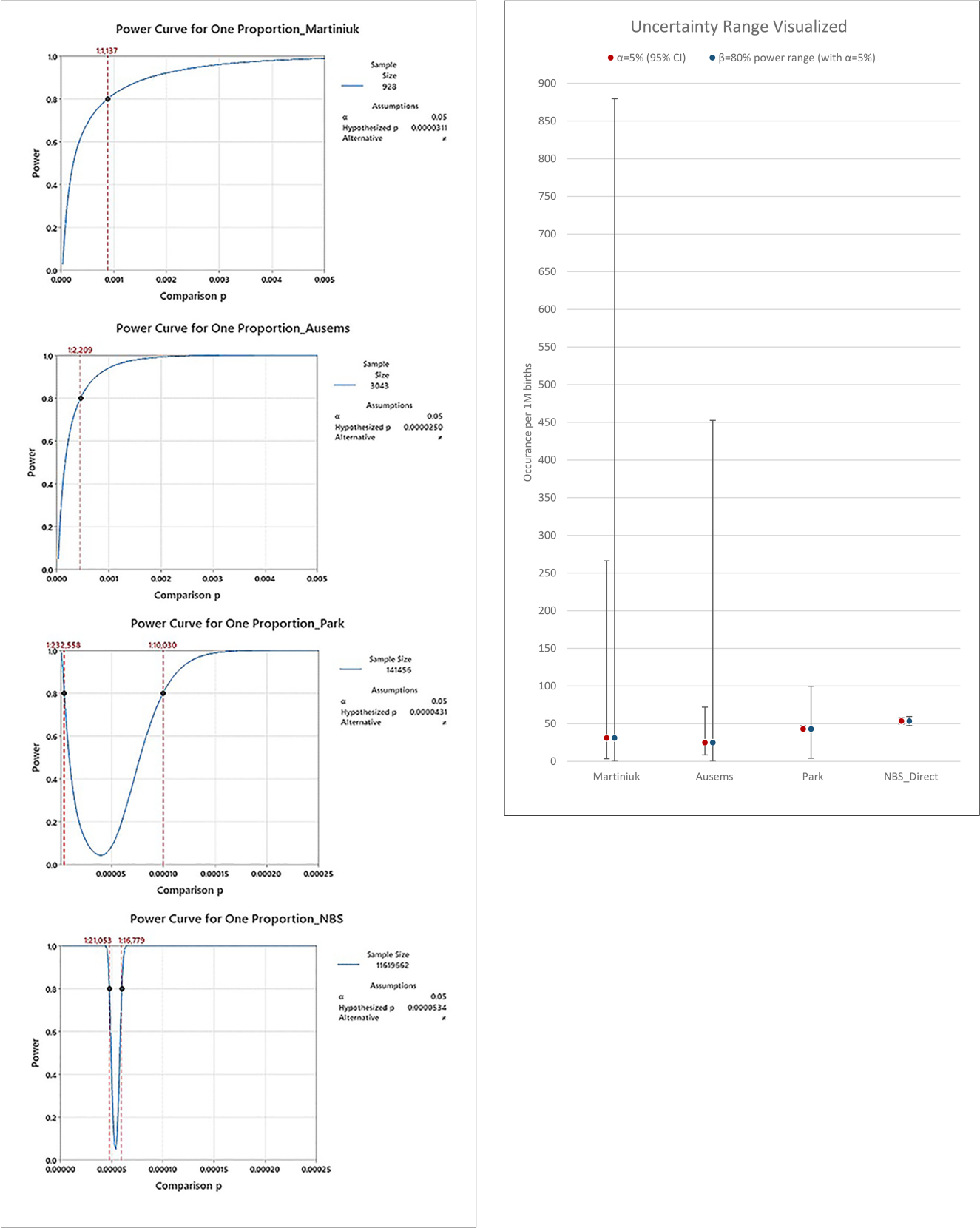
Region	State/Country	N	Unknown	IOPD	LOPD	Total Pompe	Total Incl. unknown	IOPD Prevalence _{birth} (1x)	LOPD Prevalence _{birth} (1x)	Total PD Prevalence _{birth} (1x)	% IOPD	% LOPD	Data source	Published date	Data start date	Data end date
US	Illinois	684,290	8	3	26	29	37	228,097	26,319	23,596	10%	90%	Int. J. Neonatal Screen. 2020; 6, 4, doi:10.3390/ijns6010004	21-Jan-20	3-Nov-14	30-Sep-19
US	California	1,545,100		4	48	52	52	386,275	32,190	29,713	8%	92%	Genetic Disease Screening Program, California Department of Public Health	11-Jun-22	29-Aug-18	1-Mar-22
US	Wisconsin (P)	99,018		0	12	12	12		8,252	8,252	0%	100%	https://www.wiaap.org/pompe-pilot-conclusion-wi-state-laboratory-of-hygiene/	Mar-19	14-Jul-17	31-Jan-19
US	New York	1,702,482	55	12	55	67	122	141,874	30,954	25,410	18%	82%	New York State Newborn Screening Program	29-Jun-21	1-Oct-14	27-May-22
US	Missouri	652,374		13	49	62	62	50,183	13,314	10,522	21%	79%	Missouri Department of Health, Jefferson City, MO	17-Aug-22	Jan-13	Dec-21
US	Georgia (P)	59,332	1	1	2	3	4	59,332	29,666	19,777	33%	67%	Int J Neonatal Screen. 2020 March; 6(1). doi:10.3390/ijns6010002	1-Mar-20		
US	Ohio	797,109	6	9	31	40	46	88,568	25,713	19,928	23%	78%	Ohio Newborn Screening Program	29-Jun-22	1-Jul-16	25-Jun-22
Asia	Taiwan (SS)	1,371,857	0	20	47	72	72	62,446	26,573	19,054	28%	65%	NTUH Newborn Screening Program (unpublished), doi.org/10.1016/j.cca.2014.01.030, doi:10.1016/j.ymgme.2012.04.013, doi: 10.3390/ijns6020030	Various	Various	Various
Eu	Austria	34,736		0	4	4	4		8,684	8,684	0%	100%	DOI:10.1016/S0140-6736(11)61266-X	30-Nov-11	Jan-10	Jul-10
Eu	Hungary	40,024	3	7	2	9	12	5,718	20,012	4,447	78%	22%	DOI 10.1007/8904_2012_130	21-Mar-12		
Asia	Japan	296,759		1	7	8	8	296,759	42,394	37,095	13%	88%	https://doi.org/10.1186/s13023-021-02146-z	18-Dec-21	Apr-13	Oct-20
Eu	NE Italy (P)	44,411		0	2	2	2		22,206	22,206	0%	100%	https://doi.org/10.1007/s10545-017-0098-3	15-Nov-17	Sep-15	Jan-17
LA	Mexico	20,018			1	1	1		20,018	20,018			http://dx.doi.org/10.1016/j.ymgme.2017.03.001	9-Mar-17	Jul-12	Apr-16
LA	Brazil	17,716		0	3	3	3		5,905	5,905	0%	100%	Unpublished data from Brazil (Dr. Roberto Glugiani and Dr. Francyne Kubaski)	Mar-21	Jan-19	Feb-21
US	Minnesota	284,372		2	17	19	19	142,186	16,728	14,967	11%	89%	Minnesota Department of Health, St. Paul, MN	13-Jun-22	1-Aug-17	31-Dec-21
US	Kentucky	245,637		0	13	13	13		18,895	18,895	0%	100%	Kentucky Newborn Screening Program	23-Dec-20	Feb-16	Jul-20
US	Michigan	465,703		4	27	31	31	116,426	17,248	15,023	13%	87%	Michigan Newborn Screening Program, 2017-2021	17-Jun-22	Aug-17	Dec-21
US	Tennessee	425,700		5	31	36	36	85,140	13,732	11,825	14%	86%	Tennessee Department of Health, Newborn Screening Program	8-Jul-22	1-Jul-17	31-May-22
US	Pennsylvania	833,413	40	4	55	59	99	208,353	15,153	14,126	7%	93%	Pennsylvania Department of Health, Harrisburg, PA	10-Jun-22	1-Feb-16	30-Apr-22
US	Delaware	27,051		0	1	1	1		27,051	27,051	0%	100%	Delaware Division of Public Health Newborn Screening Program	29-Jun-22	1-Jan-20	15-Jun-22
US	Florida	410,681	7	2	17	19	26	205,341	24,158	21,615	11%	89%	Florida Department of Health, Newborn Screening Program, Public Records Request	29-Jun-22	3-Feb-20	31-Dec-21
US	Oregon	134,432		1	13	14	14	134,432	10,341	9,602	7%	93%	Oregon Newborn Screening Program	8-Jul-22	1-Oct-18	31-Dec-21
US	Maryland	126,762		0	5	5	5		25,352	25,352	0%	100%	Maryland Department of Health, Division of Newborn Screening	18-Mar-21	17-Jun-19	15-Mar-21
US	Virginia	350,000		0	20	20	20		17,500	17,500	0%	100%	Virginia Department of Health, Newborn Screening Program	29-Jun-22	Jan-19	Jun-22
US	Mississippi	143,219		0	8	8	8		17,902	17,902	0%	100%	MS Newborn Screen 3.0 Access Database	7-Apr-21	Jul-16	Dec-20
US	Nebraska	92,747		0	6	6	6		15,458	15,458	0%	100%	Nebraska Newborn Screening Program	29-Jun-22	1-Jul-18	31-Mar-22
US	Indiana	151,682		2	9	11	11	75,841	16,854	13,789	18%	82%	Indiana Department of Health, Newborn Screening Reports	9-Jun-22	1-Jul-20	31-May-22
US	New Jersey	283,493		0	5	5	5		56,699	56,699	0%	100%	New Jersey Department of Health	12-Jul-22	22-Jul-19	12-Jul-22
US	Washington (SS)	279,544		1	9	10	10	279,544	31,060	27,954	10%	90%	Washington State Department of Health, NBS program and pilot study data (doi:10.1016/j.jpeds.2013.01.031 & doi:10.1016/j.ymgme.2016.05.015.)	Various	Various	Various

Region	State/Country	N	Unknown	IOPD	LOPD	Total Pompe	Total Incl. unknown	IOPD Prevalence _{birth} (1x)	LOPD Prevalence _{birth} (1x)	Total PD Prevalence _{birth} (1x)	% IOPD	% LOPD	Comment
US	US	9,794,141	117	63	459	522	639	155,463	21,338	18,763	12%	88%	
Asia	Asia	1,668,616	0	21	54	80	80	73,604	28,624	20,858	28%	72%	Excludes Taiwan subset 1 from IOPD, LOPD prevalence and % - data not discretized
Eu	Eu	119,171	3	7	8	15	18	17,024	14,896	7,945	47%	53%	
LA	LA	37,734	0	0	3	4	4		5,905	9,434	0%	100%	Excludes Mexico from IOPD, LOPD prevalence and % - data not discretized
All	Global	11,619,662	120	91	524	621	741	126,118	21,902	18,711	15%	85%	Excludes Mexico from IOPD, LOPD prevalence and % - data not discretized

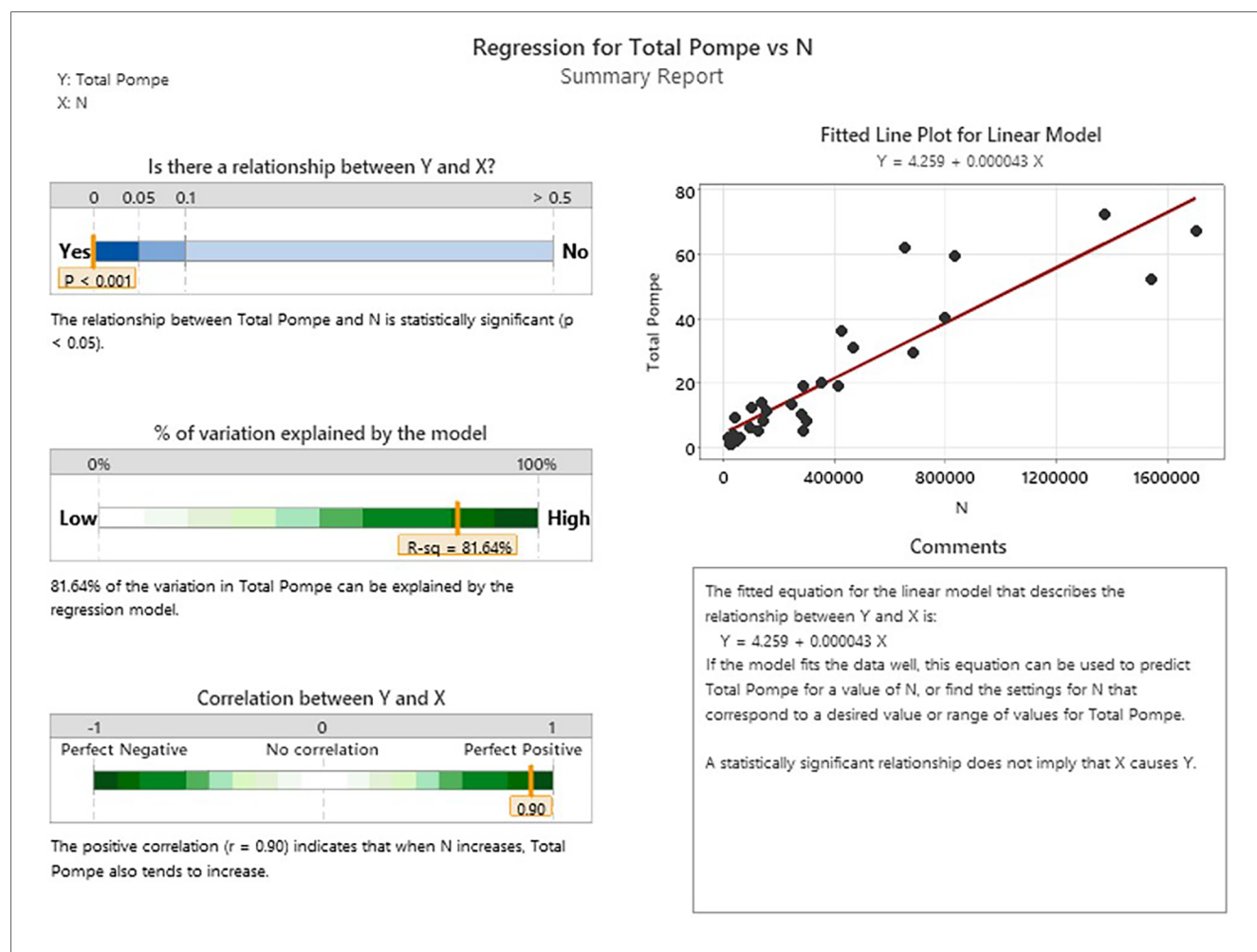
Appendix C

Note, the scale for comparison proportion (x axis) is 20× “zoomed out” for the earlier analysis (Martiniuk, Ausems) vs. the additional resolution possible for the more recent ones (Park, NBS).

A visualization of the uncertainty range results in table 2:

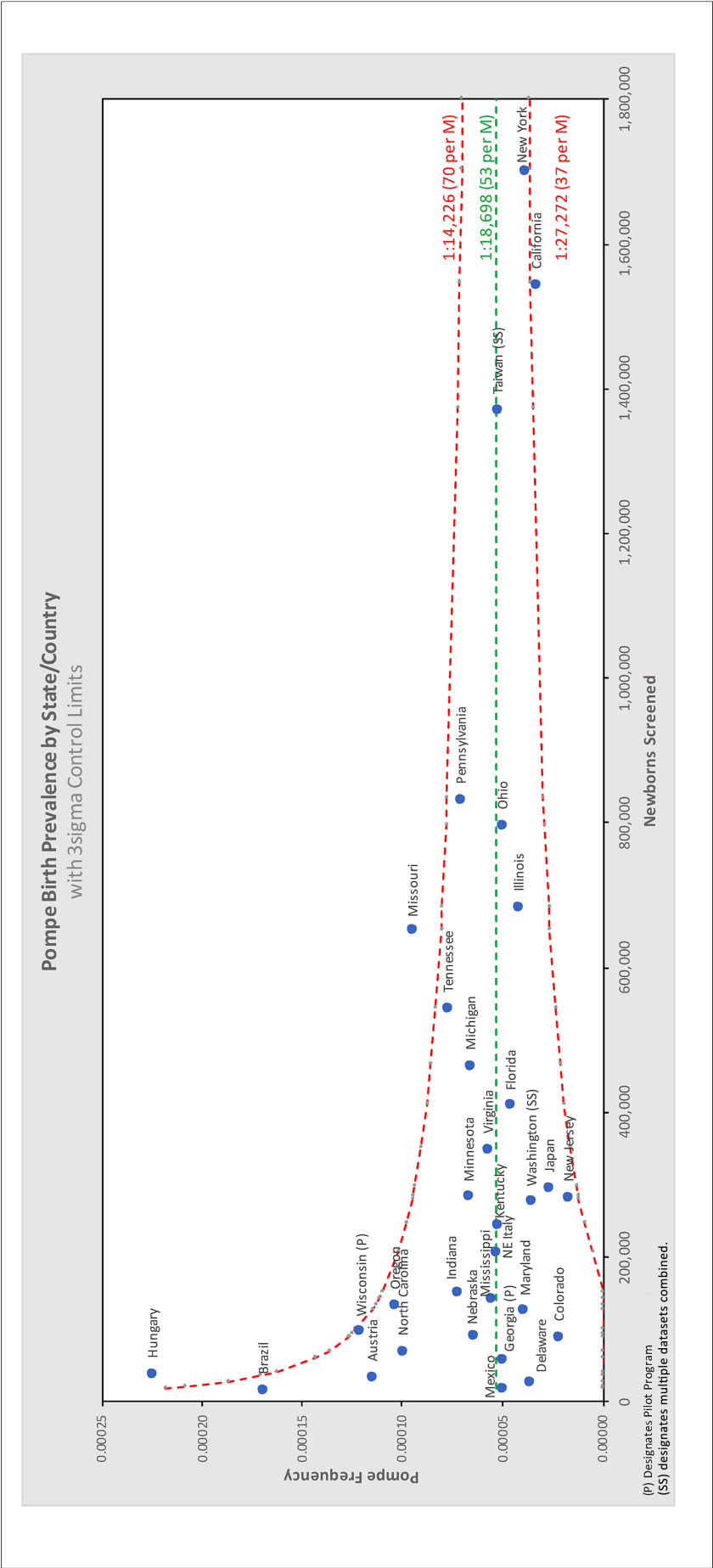


Appendix D



Appendix E

Updated binomial analysis of 12,060,529 newborns screened for PD with a birth prevalence of 1:18,698.





OPEN ACCESS

EDITED BY

Ivan Martinez Duncker,
Universidad Autónoma del Estado de
Morelos, Mexico

REVIEWED BY

Angélica G. Martínez-H,
National Institute of Genomic Medicine
(INMEGEN), Mexico
Yinan Jiang,
University of Pittsburgh, United States

*CORRESPONDENCE

Hisham M. Darwish,
✉ hisham.darwish@aaup.edu

RECEIVED 10 September 2023

ACCEPTED 04 December 2023

PUBLISHED 11 January 2024

CITATION

Bawatneh A, Darwish A, Eideh H and
Darwish HM (2024), Identification of gene
mutations associated with type 1 diabetes
by next-generation sequencing in
affected Palestinian families.
Front. Genet. 14:1292073.
doi: 10.3389/fgene.2023.1292073

COPYRIGHT

© 2024 Bawatneh, Darwish, Eideh and
Darwish. This is an open-access article
distributed under the terms of the
[Creative Commons Attribution License
\(CC BY\)](https://creativecommons.org/licenses/by/4.0/). The use, distribution or
reproduction in other forums is
permitted, provided the original author(s)
and the copyright owner(s) are credited
and that the original publication in this
journal is cited, in accordance with
accepted academic practice. No use,
distribution or reproduction is permitted
which does not comply with these terms.

Identification of gene mutations associated with type 1 diabetes by next-generation sequencing in affected Palestinian families

Abrar Bawatneh¹, Alaa Darwish², Hasan Eideh³ and
Hisham M. Darwish^{1,4*}

¹Molecular Genetics and Genetics Toxicology Program, Faculty of Graduate Studies, Arab American University, Jenin, Palestine, ²Faculty of Health Professions, AlQuds University, Jerusalem, Palestine, ³Layan Medical Center, Ramallah, Palestine, ⁴Faculty of Allied Medical Sciences, Arab American University, Jenin, Palestine

Introduction: Diabetes Mellitus is a group of metabolic disorders characterized by hyperglycemia secondary to insulin resistance or deficiency. It is considered a major health problem worldwide. T1DM is a result of a combination of genetics, epigenetics, and environmental factors. Several genes have been associated with T1DM, including *HLA*, *INS*, *CTLA4*, and *PTPN22*. However, none of these findings have been based on linkage analysis because it is rare to find families with several diabetic individuals. Two Palestinian families with several afflicted members with variations in the mode of inheritance were identified and selected for this study. This study aimed to identify the putative causative gene(s) responsible for T1DM development in these families to improve our understanding of the molecular genetics of the disease.

Methods: One afflicted member from each family was selected for Whole-Exome Sequencing. Data were mapped to the reference of the human genome, and the resulting VCF file data were filtered. The variants with the highest phenotype correlation score were checked by Sanger sequencing for all family members. The confirmed variants were analyzed *in silico* by bioinformatics tools.

Results: In one family, the *IGF1R* p.V579F variant, which follows autosomal dominant inheritance, was confirmed and segregated in the family. In another family, the *NEUROD1* p.P197H variant, which follows autosomal recessive inheritance, was positively confirmed and segregated.

Conclusion: *IGF1R* p.V579F and *NEUROD1* p.P197H variants were associated with T1DM development in the two inflicted families. Further analysis and functional assays will be performed, including the generation of mutant model cell systems, to unravel their specific molecular mechanism in the disease development.

KEYWORDS

type diabetes genetics, gene function, molecular genetic, WES, in born errors of metabolism

1 Introduction

Diabetes mellitus is a group of metabolic disorders characterized by the presence of hyperglycemia secondary to insulin resistance or deficiency, and it is associated with abnormalities in lipid and protein metabolism and electrolyte disturbances (Kharroubi and Darwish, 2015). Diabetes is considered a great health problem worldwide, with about

425 million adults having been recorded as affected in 2017 (Tremblay and Hamet, 2019). Diabetes mellitus can be classified into type 1 diabetes (T1D), which is characterized by insulin deficiency, type 2 diabetes (T2D), which is characterized by resistance to the action of insulin, gestational diabetes, which develops in women during pregnancy, and Maturity-Onset Diabetes of the Young (MODY), which is characterized by autosomal dominant inheritance and non-dependence on insulin (Anik et al., 2015). The annual health report in Palestine in 2018 reported diabetes health complications as the fifth-ranked cause of death (about 7.5% of all deaths). In 2018, the incidence rate of diabetes mellitus in the West Bank region was reported as 210.7 cases per 100,000 people. There were 2,420 cases among males and 3,135 among females. The mortality rate was 20.4 per 100,000 people (Health annual Palestine report, 2018).

T1D is an autoimmune disease in which insulin is deficient due to the destruction of pancreatic beta cells. There are two forms of T1DM: type 1A, which results from cell-mediated attack and is characterized by the presence of autoantibodies to beta cells, and type 1B, which results from unknown causes and includes unmeasurable autoantibodies or monogenic diabetes (Nyaga et al., 2018; Giwa et al., 2020). Patients are diagnosed in the first few months after birth based on the absence of insulin, detection of C-peptide, and presence of antibodies in the serum. These patients will be treated for life without interruption by insulin and are monitored for several metabolic indicators. T1D is the most common form in children and white persons, accounting for 80% of childhood diabetes in the United States (Redondo et al., 2017). The risk of the disease increases in relatives and siblings and exceeds 70% in identical twins (Bradfield et al., 2011). This clearly implies that T1D is associated with genetic factors. Overall, T1D represents a multifactorial disease that develops from the interplay of genetic, epigenetic, and environmental factors, and it can be affected by age, ethnicity, race, geography, and socioeconomic status (Tremblay and Hamet, 2019).

Genetics are responsible for 80% of hereditary T1D; the HLA region on chromosome 6p21 accounts for 40%–50% of familial T1D. Variation in this region is correlated with the role of autoimmunity in T1D development and can increase its risk or be protective. HLA DR and DQ (part of MCH class II) form alpha-beta heterodimer cell surface antigens and have the strongest association with T1D. The Type 1 Diabetes Genetics Consortium showed that DRB1*0301-DQA1*0501-DQB1*0201, DRB1*0405-DQA1*0301-DQB1*0302, and DRB1*0401-DQA1*0301-DQB1*0302 are the most susceptible haplotypes. Whereas, DRB1*1501-DQA1*0102-DQB1*0602, DRB1*1401-DQA1*0101-DQB1*0503, and DRB1*0701-DQA1*0201-DQB1*0303 are the most protective haplotypes (Erlich et al., 2013).

The insulin gene region on chromosome 11 (locus 11p15) constituted the next strongest genetic factor in T1D, and the third associated locus was the cytotoxic T lymphocyte-associated protein 4 (*CTLA4*) gene (Cronin et al., 2017). The protein tyrosine phosphatase non-receptor type 22 (*PTPN22*) gene was reported to be the fourth identified locus in 2004 (Bottini et al., 2004). Later, the interleukin 2 receptor alpha (*IL2RA*) gene (Vella et al., 2005) and the interferon-induced helicase C domain 1 (*IFIH1*) gene on chromosome 2q24.3 (Smyth et al., 2006) were reported as the fifth and sixth associated loci, respectively. In a Japanese study,

the *FOX3P* gene, which plays a role in the regulation of T-cell differentiation, was also found to be associated with T1D (Bassuny et al., 2003). Genome-wide association studies were later started to search for further loci associated with T1D (Bakay et al., 2019). They confirmed previous loci and showed evidence of new loci on chromosomes 16p13, 12q13, 12q24, and 18p11. The 16p13 region contains the *KIAA0350* gene, which lies within a 233 kb LD block and is suspected to produce a sugar-binding C-type lectin (Hakonarson et al., 2007; Todd et al., 2007; Concannon et al., 2008). Regions like 12q13 and 12q24 contain many genes in which some of these loci play a role in immune signaling and insulin production, and they are evidenced to be associated with T1D genes such as *ERBB3*, *CYP27B1*, and *SH2B3* (Cooper et al., 2012; Groop and Pociot, 2014). The 18p11 region contains the *PTPN2* gene, which has a function in the immune system and cytokine-induced apoptosis (Groop and Pociot, 2014; Pociot, 2017). Other groups conducted their investigation on 2,496 families inflicted with T1D genotyped with a panel of 6,090 SNPs and reported additional T1D-dependent loci on 21q22.3 in the *UBASH3A* locus (Concannon et al., 2008).

Arab countries have one of the highest incidence and prevalence rates of T1D, which varies from low prevalence (2.54/100,000) in Oman to significantly higher values in Saudi Arabia (29/100,000) (Zayed, 2016). The DRB1*030101-DQB1*0201 haplotypes increased the risk of T1D in Tunisia, Lebanon, and Bahrain, whereas the DRB1*040101-DQB1*0302 haplotype was highly associated with Tunisia and Bahrain but is protective among the Lebanese population (Al-Jenaidi et al., 2005; Stayoussef et al., 2009). The most common HLA haplotypes in Egypt were DRB1*0301-DRB3*0201-DQA1*0501-DQB1*0201 and DRB1*04:02-DQA1*03-DQB1*03:02, while the protective one was DRB1*04:03-DQA1*03DQB1*03:02 (El-Amir et al., 2015). Studies from Morocco showed that Moroccans share some susceptible and protective haplotypes with other populations, such as those from Tunisia, Algeria, Spain, and France, including DRB1*08-DQA1*0401-DQB1*0402 and DRB1*07-DQA1*0201-DQB1*020 haplotypes, respectively (Nadia et al., 2012). Concerning non-HLA genes, several studies reported T1D in Arabs was associated with *PTPN22*, *CTLA4*, *IL15*, *ZAP70*, *CD3z*, *CD28*, *TCRβ*, and *BANK1* (Zayed, 2016). However, no previous studies on the molecular genetics of T1D in Palestine have been reported. We have identified two Palestinian families with several affected members with clear variations in the inheritance pattern of the disease. We hypothesized the presence of putative gene mutations that have a direct role in developing T1DM in these families. Therefore, the objective of this study was to investigate the molecular genetics of T1D development in these families using WES technology. Such genes will provide valuable information to increase our understanding of the molecular genetics basis of Type 1 diabetes and provide tools for early diagnosis and clinical intervention to improve the survival and life quality of these patients before severe complications develop in these individuals.

2 Materials and methods

2.1 Characteristics of study subjects

Two Palestinian families inflicted with Type 1 diabetes mellitus were included in this study and referred to us by a

specialized local Medical Center (Layan Center) in Ramallah, Palestine. They were confirmed to have T1DM based on specific parameters including high serum glucose (above 350 g/dL), high levels of HbA1C (>7%), Low levels of C peptide, the presence of autoantibodies, and insulin dependence. Family I was composed of diabetic parents, six diabetic offspring, and one non-diabetic daughter, indicating the presence of a potentially dominant gene factor. Family II was composed of non-diabetic parents, three diabetic offspring, and a non-diabetic daughter, indicating the presence of a potentially recessive gene mutation. Figure 1 shows the pedigree of both families. Written informed consent was obtained from all participants.

2.2 DNA purification

Genomic DNA was extracted from peripheral blood samples according to a commercially available kit (Master Pure™ Genomic DNA Purification Kit, Epicenter Technology Co. Cat.No.MG71100) (Mcd, 2012). Extracted DNA was checked for purity, concentration size, and integrity using Nanodrop spectrophotometer and Agarose Gel Electrophoresis and stored at -30°C .

2.3 Library preparation and exome sequencing

Samples were subjected to whole-exome sequencing using Illumina Nextseq550 according to the manufacturer's instructions (Illumina, 2021).

2.4 NGS data analysis

Fastq paired-end reads were mapped to the reference human genome version GRCh38 using the Burrows-Wheeler Alignment Tool with the BWA-MEM algorithm. The mapped reads in the bam file were filtered for the following two criteria; first, we retained only paired reads for which both the forward and the reverse read have been mapped to the reference successfully using Samtools. Second, PCR duplicates were removed using the RmDup tool. Filtered mapped reads were then used to call the variants using the FreeBayes variant detector to identify SNPs (single-nucleotide polymorphisms) and indels (insertions and deletions). The list of variants produced in a VCF format were filtered and prioritized with

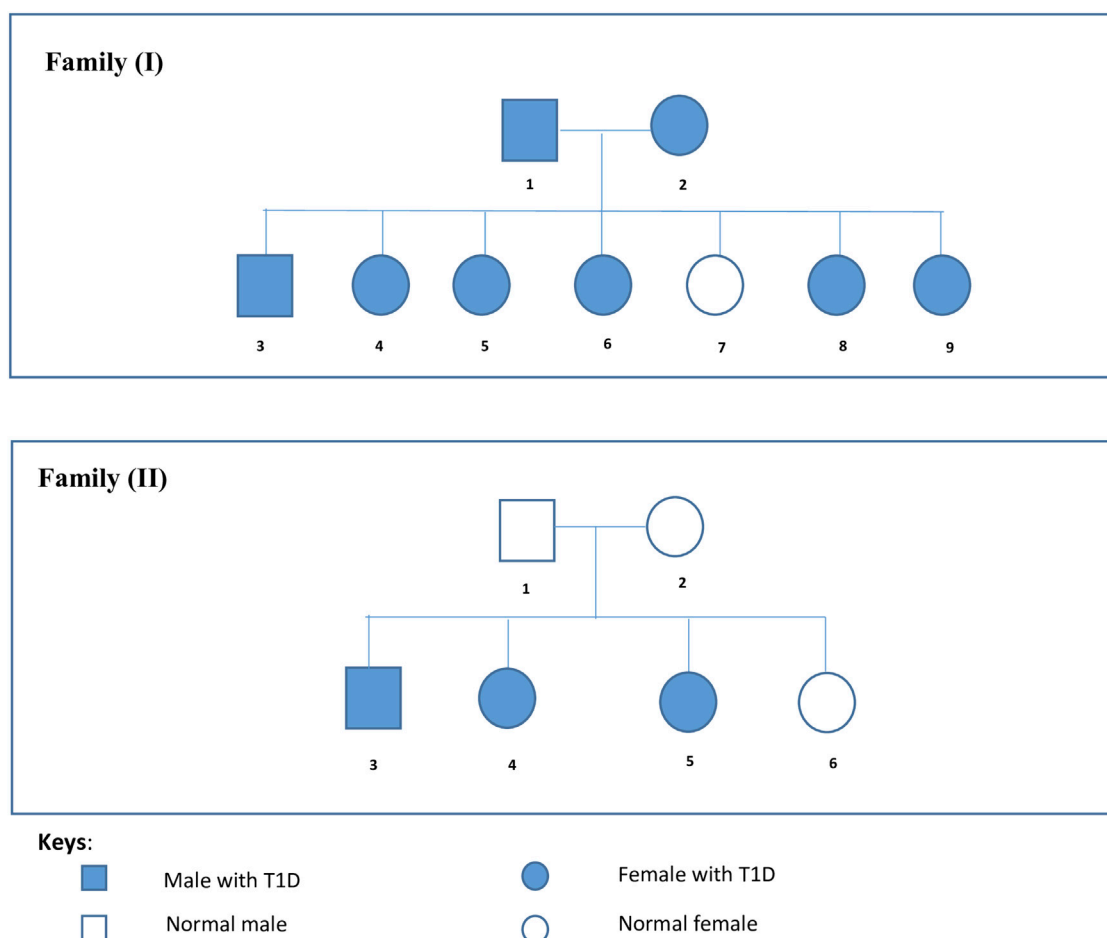


FIGURE 1

Families' Pedigrees. Family I is composed of diabetic parents, six diabetic offspring, and one non-diabetic daughter. Family II is composed of non-diabetic parents, three diabetic offspring, and a non-diabetic daughter.

respect to their potential relevance for features that have been used, and a VCF file containing annotations of variant effects was produced. Finally, we filtered out variants that are unlikely to have a pathogenic effect like variants in UTRs, those upstream/downstream of the gene, deep intronic variants (but we leave variants that affect splice sites), and other non-coding variants. In addition, we filtered out variants that are common in population databases such as Gnomad. Furthermore, we prioritized variants that have been reported as pathogenic in databases like Clinvar. The aligned data were deposited in the SRA database under the accession number SRR26632668.

2.5 Selection of candidate variants

We focused on non-synonymous exonic variants with high correlation scores present in the affected family members and not present in the unaffected family members.

2.6 Primers design

Primer 3 web (<https://primer3.ut.ee/>) was used to design the primers listed in Table 1 below for PCR amplification and direct sanger sequencing of selected regions in the indicated genes with the identified potential mutant variants.

2.7 Sanger sequencing

Samples were sequenced using the BigDye™ Terminator Cycle Sequencing Kit and Applied Biosystems Genetic Analyzer according to the manufacturer's instructions (Thermo Fisher Scientific, 2015).

2.8 In-silico analysis

The Mutation Mapper tool of cBioPortal was used to map mutations on proteins and their domains. The conservation of the variant locus was detected using the COBALT Alignment tool. Several prediction tools were used to predict the impact of amino acid substitution on protein structure and function, including PolyPhen-2, PROVEAN, FATHMM, SIFT, Mutation Taster, GVG, and LIST-S2. The HaploR tool from R package was used to analyze motif changing.

2.9 Ethics

Ethical approval for this study was provided. A written informed consent form was obtained from all participating subjects in the study. Written informed consent was obtained from the individuals for the publication of any potentially identifiable images or data included in this article.

3 Results

3.1 Family I

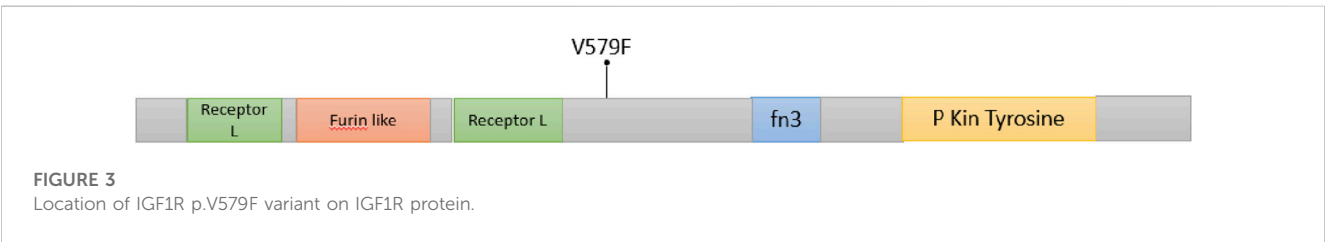
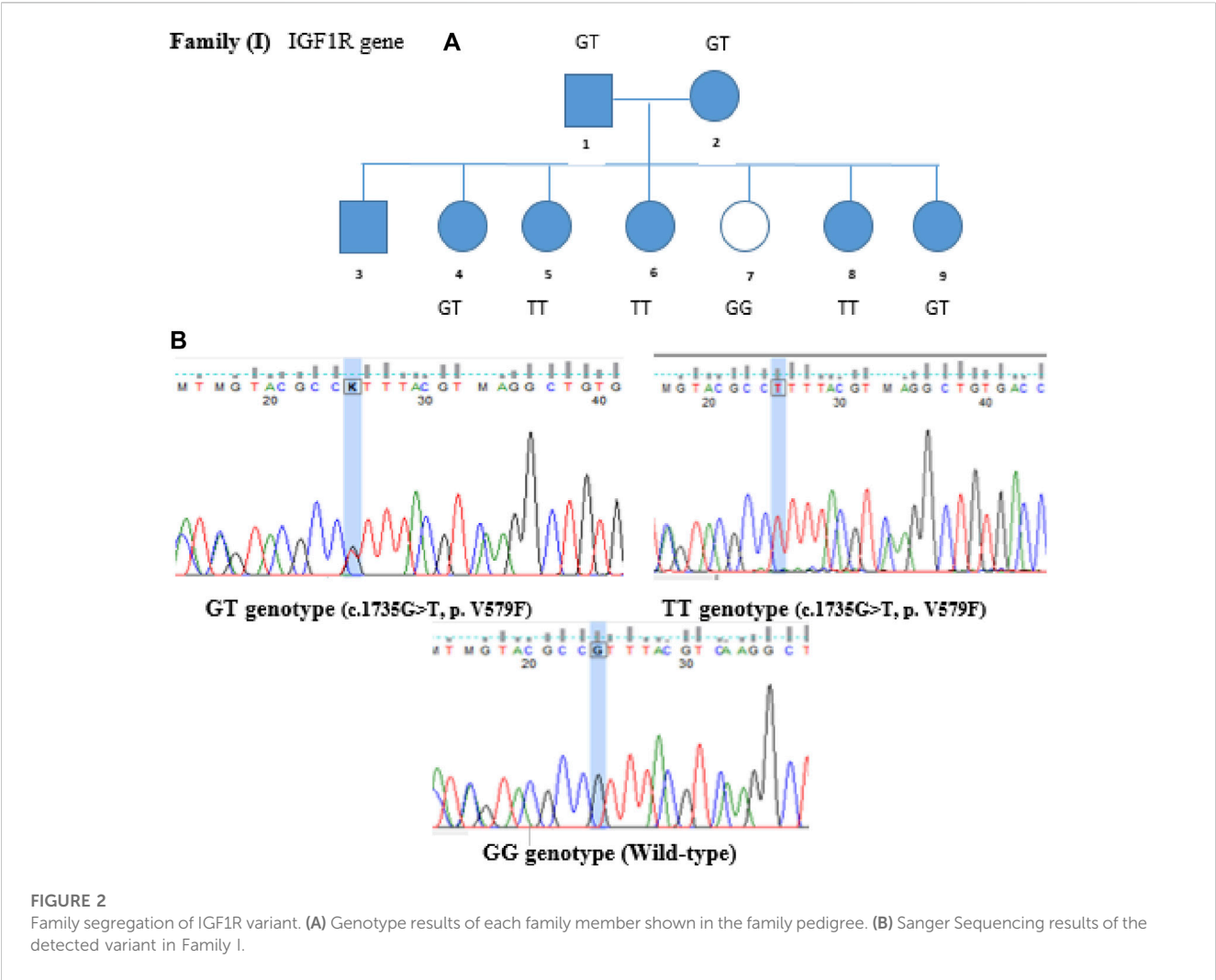
Variants of the *INS*, *HNF1A*, *KCNJ11*, and *IGF1R* genes were found to have high correlation based on data analysis. The first three variants were tested by Sanger sequencing but showed no segregation in the family because both diabetic patients and non-diabetic individuals have similar genotypes.

Variants of the *IGF1R* gene were identified in T1DM patients but not in non-diabetic ones. The *IGF1R* gene is located on chromosome 15, and the identified variant was a missense mutation where Guanine is replaced by Thymidine at position 1735 (c.1735G>T), leading to replacing Valine with Phenylalanine at codon number 579. This variant was confirmed by Sanger sequencing and segregated in the family (genotypes match the phenotype). Members I-1, I-2, I-4, and I-9 are heterozygous GT, non-diabetic member I-7 is wild-type GG, and members I-5, I-6, I-8 are homozygous TT, as shown in Figure 2.

Mutation conservation, functional location, and pathogenicity were further investigated. The IGF1R protein is composed of five domains: two Receptor-L domains, a Furin-like cysteine-rich region, a Fibronectin type III domain, and a Protein tyrosine kinase domain. IGF1R p.V579F is located between the Receptor-L domain and Fibronectin type III domain, as shown in Figure 3. This region is highly conserved, as shown in Figure 4. Several prediction tools were used to investigate whether the IGF1R p.V579F variant has an impact on the biological function and structure of the protein. The variant is predicted to be neutral and tolerated according to PROVEAN and SIFT tools. It is also predicted to be benign by the PolyPhen-2 tool. Based on the FATHMM prediction tool, IGF1R p.V579F will be tolerated. However, according to the FATHMM-MKL and LIST-S2 tools, it is predicted to be damaging. The IGF1R p.V579F variant is disease-causing based on the Mutation Taster tool and is classified in the C45 class of Align-GVG classes, which means it is pathogenic.

TABLE 1 The sequences and characteristics of the variants' primers.

Gene name	Coordinates	Sequence of primer	Primer length	GC% content	Tm °C
<i>NEUROD1</i>	chr2:181,678,194-181,678,370	Forward: ACTGGTAGGAGTAGGGGTGT	20	55	56.9
		Reverse: ACCTGGTCTCCTTCGTTTCAG	20	55	56.4
<i>IGF1R</i>	chr15:98,913,141-98,913,328	Forward: GAGCCCGGCATCTTACTACA	20	55	56
		Reverse: TTGCGAAGAAGTGTGGATGC	20	55	56



3.2 Family II

In the second family, we identified variants in the *ABCC8*, *RYR1*, *CTRC*, and *NEUROD1* genes. The first three variants were tested by Sanger sequencing but showed no segregation in the family. However, a variant in the *NEUROD1* gene that is located on chromosome 2 was segregated. The identified variant c.590G>T is a missense mutation where Guanine is replaced by Thymidine at position 590 replacing Proline with Histidine. This variant was validated by Sanger sequencing and segregated in Family II, as shown in Figure 5. Members II-1 and II-2 (Parents) have heterozygous GT genotypes, whereas members

II-3, II-4, and II-5 (diabetic offspring) have homozygous TT genotypes. The non-diabetic daughter (member II-6) has a wild-type GG genotype. Therefore, the segregation matches the observed expression of the disease.

The *NEUROD1* protein is composed of two domains: the helix loop helix domain and the transactivation domain. The *NEUROD1* p.P197H variant is located at the transactivation domain of the *NEUROD1* protein (Figure 6) in a highly conserved region, as shown in Figure 7. The *NEUROD1* p.P197H variant is predicted to be damaging according to the PROVEAN, LIST-S2, and FATHMM-XF tools. It is also predicted to be possibly damaging according to the PolyPhen-2

H. sapiens	P08069.1	560	KDVEPGILLHGLKPWTQYAVYKAVT	LMVENDHIRGAKSEILYIRTNASVPSIPLDVLSASNSSSQLIVKWNPPSLPNG	639
M. morax	KAH8214489.1	560	KDVEPGILLHGLKPWTQYAVYKAVT	LMVENDHIRGAKSEILYIRTNASVPSIPLDVLSASNSSSQLIVKWNPPSLPNG	639
H. sapiens	P08069.1	560	KDVEPGILLHGLKPWTQYAVYKAVT	LMVENDHIRGAKSEILYIRTNASVPSIPLDVLSASNSSSQLIVKWNPPSLPNG	639
B. taurus	NP_001231541.1	560	KDVEPGILLHGLKPWTQYAVYKAVT	LMVENDHIRGAKSEILYIRTNASVPSIPLDVLSASNSSSQLIVKWNPPSLPNG	639
M. musculus	NP_034643.2	561	KEGEPGILLHGLKPWTQYAVYKAVT	LMVENDHIRGAKSEILYIRTNASVPSIPLDVLSASNSSSQLIVKWNPPSLPNG	640
S. scrofa	NP_999337.1	560	KDVEPGILLHGLKPWTQYAVYKAVT	LMVENDHIRGAKSEILYIRTNASVPSIPLDVLSASNSSSQLIVKWNPPSLPNG	639
C. canadensis	JAV39572.1	561	KDKEPGILLHGLKPWTQYAVYKAVT	LMVENDHIRGAKSEILYIRTNASVPSIPLDVLSASNSSSQLIVKWNPPSLPNG	640
M. meles	XP_045863984.1	560	KDVEPGILLHGLKPWTQYAVYKAVT	LMVENDHIRGAKSEILYIRTNASVPSIPLDVLSASNSSSQLIVKWNPPSLPNG	639
M. angustirostris	XP_045755443.1	560	KDVEPGILLHGLKPWTQYAVYKAVT	LMVENDHIRGAKSEILYIRTNASVPSIPLDVLSASNSSSQLIVKWNPPSLPNG	639

FIGURE 4
Conservation analysis of IGF1R V579 locus using COBALT alignment tool.

Family (II)

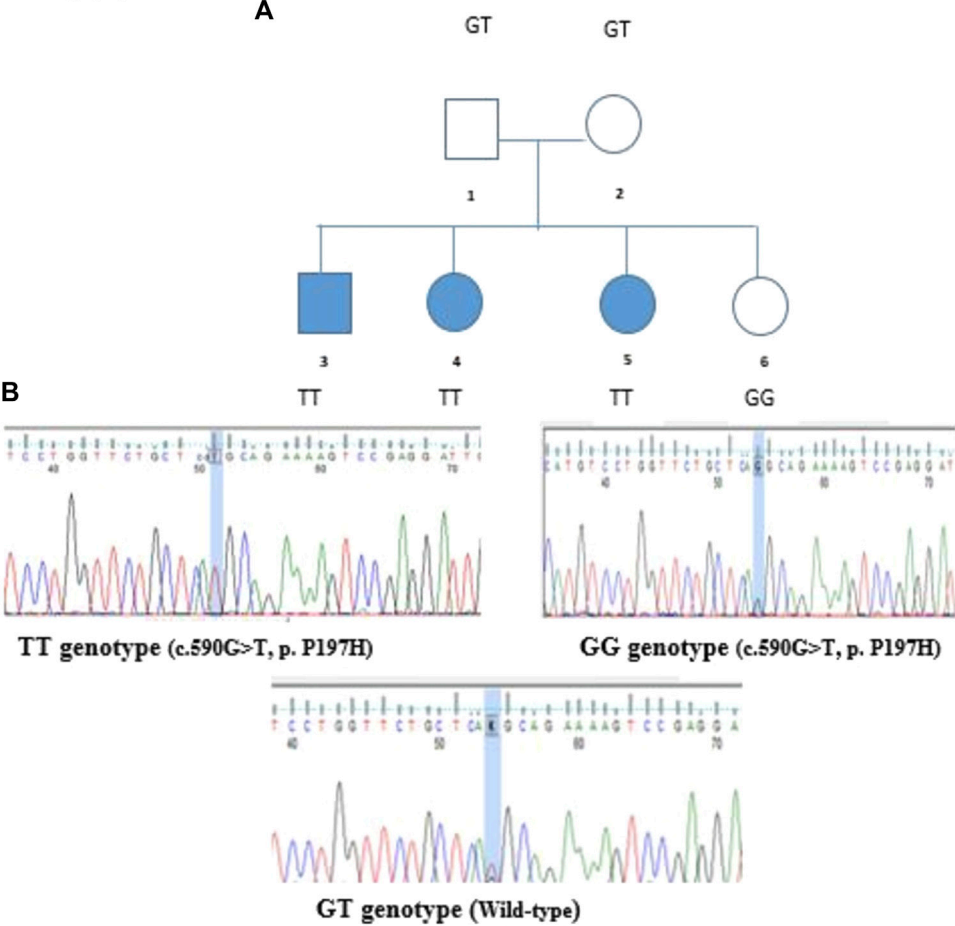
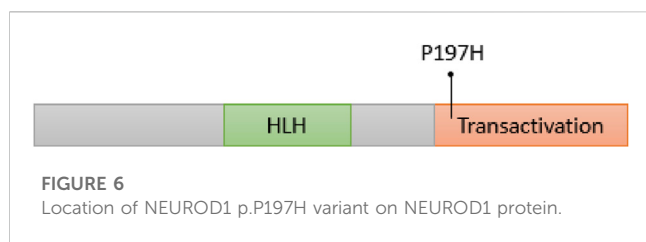


FIGURE 5
Family segregation of NEUROD1 variant. (A) Genotype results of each family member shown in the family pedigree. (B) Sanger Sequencing results of the detected variant in Family II.



tool. The variant was predicted to be disease-causing by the GVG tool and pathogenic by the Mutation Taster tool. On the other hand, the *NEUROD1* p.P197H variant is predicted to be tolerated according to the FATHMM and FATHMM-MKL tools.

To detect whether the *NEUROD1* p.P197H variant affects the binding motif of any transcription factor, the HaploR tool was used. Figure 8 shows the variant is located within the PAX motif.

The indicated variants in the *IGF1R* and *NEUROD1* genes were tested in genomic DNA samples from 80 non-familial T1D patients available in our laboratory. The results showed these variants are unique mutations found in the study's two families.

4 Discussion

Despite several gene mutations having been linked with type 1 diabetes mellitus, the molecular mechanisms of the disease are not fully understood. This hampers the presence of specific genetic factors that require increased efforts to unravel the transmittance of the disease within generations. This work was initiated to study two families with T1DM inherited between consecutive generations. Two putative candidate variants were prioritized and were checked for confirmation by Sanger sequencing and family segregation.

In the first family, T1D follows autosomal dominant inheritance; the *IGF1R* p.V579F variant was associated with T1DM in the family confirmed by Sanger sequencing and segregated in the family with the phenotype. This variant showed uncertain significance according to ACMG classification (The American College of Medical Genetics). No previous studies reported the association between this variant and T1DM or other diseases. However, the Val579 residue is highly conserved, indicating its importance in the protein with potential pathogenicity. This was confirmed with several *in silico* prediction tools, including FATHMM-MKL, LIST-S2, GVG, and Mutation Taster, which predicted the variant to be damaging and disease-causing. Other tools predicted the variant to be benign, including PolyPhen-2, SIFT,

H. sapiens	P08069.1	560	KDVEPGILLHGLKPWTQYAVYKAVT	TVENDHIRGAKSEILYIRTNASVPSIPLDVL	SASNSSQLIVKWNPPSLPNG	639
M. morax	KAH8214489.1	560	KDVEPGILLHGLKPWTQYAVYKAVT	TVENDHIRGAKSEILYIRTNASVPSIPLDVL	SASNSSQLIVKWNPPSLPNG	639
H. sapiens	P08069.1	560	KDVEPGILLHGLKPWTQYAVYKAVT	TVENDHIRGAKSEILYIRTNASVPSIPLDVL	SASNSSQLIVKWNPPSLPNG	639
B. taurus	NP_001231541.1	560	KDVEPGILLHGLKPWTQYAVYKAVT	TVENDHIRGAKSEILYIRTNASVPSIPLDVL	SASNSSQLIVKWNPPSLPNG	639
M. musculus	NP_034643.2	561	KEGEPGILLHGLKPWTQYAVYKAVT	TVENDHIRGAKSEILYIRTNASVPSIPLDVL	SASNSSQLIVKWNPPSLPNG	640
S. scrofa	NP_999337.1	560	KDVEPGILLHGLKPWTQYAVYKAVT	TVENDHIRGAKSEILYIRTNASVPSIPLDVL	SASNSSQLIVKWNPPSLPNG	639
C. canadensis	JAV39572.1	561	KDKEPGILLHGLKPWTQYAVYKAVT	TVENDHIRGAKSEILYIRTNASVPSIPLDVL	SASNSSQLIVKWNPPSLPNG	640
M. meles	XP_045863984.1	560	KDVEPGILLQGLKPWTQYAVYKAVT	TVENDHIRGAKSEILYIRTNASVPSIPLDVL	SASNSSQLIVKWNPPSLPNG	639
M. angustirostris	XP_045755443.1	560	KDVEPGILLHGLKPWTQYAVYKAVT	TVENDHIRGAKSEILYIRTNASVPSIPLDVL	SASNSSQLIVKWNPPSLPNG	639

FIGURE 7
Conservation analysis of *IGF1R* V579 locus using COBALT alignment tool.

Regulatory motifs altered

Position Weight Matrix ID (Library from Kheradpour and Kellis, 2013)	Strand	Ref	Alt	Match on:
Pax-8_1	-	7.2	10.1	Ref: GGTGGGGGGCATGCTCTGTTCTGCTCAGGCAGAAAAGTCCGAGGATTGAGTTGCAGG Alt: GGTGGGGGGCATGCTCTGTTCTGCTCAGCAGAAAAGTCCGAGGATTGAGTTGCAGG
Pax-8_2	-	7.7	10	BDNHICAYKCDMNDVDSH DHYCAYBCDDNDNDV

FIGURE 8
In silico analysis of *NEUROD1* p.P197H variant by HaploR tool (motifs alteration).

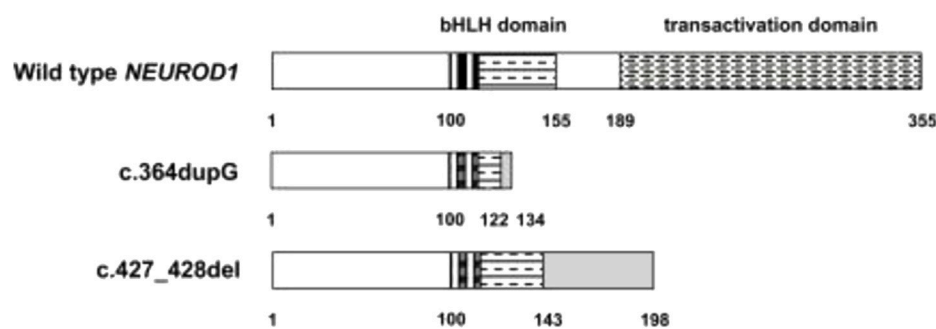


FIGURE 9
The effects of c.364dupG and c.427_428del mutations on NEUROD1 protein structure.

and PROVEAN. This shows the necessity for further analysis and studies, including studies on the effects of the *IGF1R* p.V579F variant on the 3D structure of the protein and its functional implications. The *IGF1R* gene is located in chromosome 15, which encodes the insulin growth factor 1 receptor that binds with high affinity to insulin growth factor (IGF1) and with lower affinity to insulin. The structure of IGF1R and insulin receptors are very similar. Both receptors consist of a tetramer of two α subunits representing the extracellular ligand-binding domain and two β subunits representing the transmembrane domain with tyrosine kinase activity. The two subunits are linked with disulfide bonds (Hakuno and Takahashi, 2018). The IGF1 binds to the α subunits of IGF1R, causing conformational changes and stimulation of β subunit activity. This leads to autophosphorylation and transphosphorylation of tyrosine (especially tyrosine 1131, 1135, 1136, and 1221), increasing its kinase activity and thus activating and recruiting the insulin receptor substrate (IRS), CT10 regulator of kinase (CRK), and Src homology and Collagen (SHC) adaptor proteins. The latter will transduce and activate downstream signaling pathways, including the MAPK/RasRaf-Erk pathway, phosphatidylinositol-3-kinase/AKT/mTOR (PI3K/AKT) pathway, Janus kinase/signal transducer, and activator of transcription (JAK/STAT) pathway, resulting in stimulation cell proliferation, survival, and differentiation (Arnaldez and Helman, 2012). Moreover, activated AKT can activate mTOR and inhibit *FOXO1* and GSK3 downstream molecules involved in cellular processes and glucose homeostasis, resulting in gluconeogenesis inhibition and increasing glycogen and protein synthesis (Jung and Suh, 2015).

The *IGF1R* gene is highly expressed in 9% of cancer cells, including lung adenocarcinoma, cutaneous melanoma, breast cancer, and colon adenocarcinoma (Farabaugh et al., 2015). It plays an important role in phenotypic and oncogenic transformation by activating signaling pathways downstream. *IGF1R* can then interact with oncogenes such as *RAS*, *c-MYC*, and epidermal growth factor receptor (*EGFR*), causing an increase in cell migration, invasion, poor prognosis, and shorter survival rate (Sun et al., 2017).

Several studies suggest a close link between *IGF1R* function and glucose metabolism. It plays several physiological roles in glucose metabolism and tissue development including growth, heart ventricular development, neutrophils differentiation, and brain development (Wit and Walenkamp, 2013; Moody et al., 2014;

Yuan et al., 2018; Jin et al., 2019). Mouse models with *IGF1R* knockout showed a significant decrease in their weight after birth. These animals suffer from reduced glucose tolerance in addition to several organ failures, leading to earlier death (Hakuno and Takahashi, 2018). The significant association between *IGF1R* expression and diabetes is evident (Fowlkes et al., 2012). One previous study found that the absence of *IGF1R* in beta cells in mice caused glucose intolerance and deficiency in insulin secretion (Xuan et al., 2002). Another study showed that the loss of one allele of *IGF1R* is associated with glucose intolerance and later insulin resistance, resulting in low birth weight and growth (Garg et al., 2011). Additionally, osteopathy defects, which are serious complications of T1DM and T2DM, result from interruption of insulin and *IGF1R* (Fowlkes et al., 2012). Noncoding RNAs (lncRNA and Micro RNAs) have a major role in disease development, including diabetes and cancer, through the regulation of *IGF1R* or other IGF signaling molecules (Chen et al., 2019). Interestingly, knockout of miR-375 in mice model revealed insulin resistance and decreased glucose homeostasis, leading to diabetes, an effect that was associated with upregulation of *IGF1R* (Kumar et al., 2021). The *IGF1R* p.V579F is predicted to be a loss-of-function mutation affecting insulin release from beta cells. The significant association between *IGF1R* and cancer results from *IGF1R* gain-of-function mutations. Therefore, diabetic patients from Family I are not expected to develop cancer due to this variant. In contrast, we cannot exclude the possibility that some *IGF1R* gain-of-function mutations are associated with diabetes as previous studies showed (Engberding et al., 2009; Kumar et al., 2021). One possible explanation is that upregulated *IGF1R* may suppress insulin signaling through a direct effect on the insulin receptor itself or its signaling mechanisms. Therefore, the collective indication of these studies and the present study indicate a significant correlation between the *IGF1R* signaling pathway and disruption in glucose metabolism leading to diabetes.

In the family with autosomal recessive inheritance, the *NEUROD1* p.P197H variant was found to be associated with T1DM. This was a missense mutation where Guanine is replaced by Thymidine at position 590 resulting in Histidine replacing Proline at codon 197. This exchange can lead to a major change in the protein structure since the variant is located in the Neuronal helix-loop-helix transactivation domain and its locus is well

conserved, indicating this residue has functional significance. It is predicted to have deleterious functional consequences by several prediction tools, including PolyPhen-2, PROVEAN, SIFT, GVG, LIST-S2, and FATHMM-XF.

The neurogenic differentiation 1 (*NEUROD1*) gene is located in chromosome 2 and encodes the basic helix-loop-helix (bHLH) transcription factor. These factors regulate the expression of genes through binding to a consensus sequence CANNTG, known as E-box. *NEUROD1* combines with E2A-encoded proteins and HEB-encoded proteins. The HLH region of *NEUROD1* is responsible for the dimerization between the bHLH protein and the basic region, mediating protein–DNA interactions. The *NEUROD1* gene is expressed in the intestine, pituitary gland, some central and peripheral nerves, and pancreatic islet cells. In the intestine, it stimulates the release of secretin hormone (Ray and Leiter, 2007). In the pituitary gland, it regulates the expression of proopiomelanocortin (POMC), which is a precursor of some important hormones (Parvin et al., 2017). In the nervous system, it motivates the formation of neurites, and its name is derived from this activity. This gene is also known as *BETA2* due to its function in activating the insulin gene in beta cells. Moreover, it has an important role in the development of the pancreas (Sharma et al., 1999). A previous study showed that mice lacking *NEUROD1* $-/-$ exhibited serious complications of the pancreas, which causes a decline in beta cells, leading to severe diabetes (Naya et al., 1997).

NEUROD1 forms a heterodimer with a bHLH transcription factor called E4, which binds to the E-box binding site in the promoter region of insulin (*INS*), glucokinase (*GCK*), sulfonylurea receptor 1 (*SUR1*), Paired box (*PAX*), and islet-specific glucose-6-phosphatase catalytic subunit-related protein (*IGRP*) genes and activates their expression (Rubio-Cabezas et al., 2010). These genes are known to play important roles in glucose homeostasis besides differentiation and development of pancreatic cells (Panneerselvam et al., 2019). This explains the connection between the *NEUROD1* gene and diabetes. *NEUROD1* is also involved in beta cell dysfunction during chronic hyperglycemia through two mechanisms. First, high glucose concentration will activate the expression of a small heterodimer partner (*SHP*) gene, which in turn inhibits p300-mediated pancreatic duodenal homeobox factor 1 (*PDX1*) and *NEUROD1*, resulting in insulin gene downregulation. Second, a decreased protein phosphatase 2 (PP2A) level will activate cyclic AMP-responsive element-binding protein (CREB), leading to *NEUROD1* and *INSULIN* repression (Horikawa and Enya, 2019; Bohuslavova et al., 2021). The detected *NEUROD1* P197H variant is found within a motif sequence specific to the *PAX* transcription factor. This can explain its role in developing diabetes. Further validation can be tested using CHIP-sequencing.

The *NEUROD1* gene has two exons; the first one is not translated while the second encodes for a protein with several motifs. Four variants have been identified in exon 2. One variant is p.Ala45Thr, the second one is p.Pro197His, and the third one is p.Arg111Leucine, which is located in the proximal basic portion of the basic HLH domain. The fourth variant is an insertion of cytosine in codon 206, defined as c.206 + C, leading to nonsense mutation and a premature stop codon. Malecki M. et al. studied these variants in autosomal dominant families inflicted with T2DM.

The first two variants, p.Ala45Thr and p.Pro197His, were not associated with T2DM, whereas the latter two variants, p.Arg111Leu and c.206 + C, were associated with T2DM development by affecting the ability of *NEUROD1* to bind E-box and active CBP/p300, respectively (Malecki et al., 1999; Malecki et al., 2003).

Previous studies reported that the *NEUROD1* p.Ala45Thr variant was associated with T1DM but not T2DM (Iwata et al., 1999; Hansen et al., 2000). In another Japanese case-control study, the researchers hypothesized that the *NEUROD1* gene can affect the development and onset of T1DM since it acts on initial islet precursors (Yamada et al., 2001). They studied *NEUROD1* polymorphisms in 105 T1DM patients and 122 nondiabetic controls, and the diabetic patients were classified into groups according to their onset pattern. Interestingly, a significant difference in *NEUROD1* polymorphisms between cases and the control was detected in the acute-onset group (Yamada et al., 2001). This revealed the clear association of the *NEUROD1* gene with T1DM development. A study in 2010, aimed to examine the effect of *NEUROD1* mutations on patients with permanent monogenic neonatal diabetes (PNDM), found two rare homozygous mutations. The first was a duplication of a single base pair (c.364dupG), while the second was a deletion of two base pairs CT (c.427_428del)^x. Both mutations lead to the absence of the transactivation domain from the protein due to premature truncation of the C terminus (p.Asp122Glyfs*12 and p.Leu143Alafs*55, respectively) as shown in Figure 9. These two indicated patients had some neurological abnormalities, including weakening of vision and hearing, cerebellar hypoplasia, and development delay. This leads to the conclusion that *NEUROD1* plays an important role in the pancreas as well as in the nervous system (Rubio-Cabezas et al., 2010).

In maturity-onset diabetes of the youth (MODY), several studies demonstrated some *NEUROD1* candidate mutations, including *NEUROD1* p.Pro197His, p.Asp202Glu, p.Leu157Arg, and p.Arg103Pro (Ang et al., 2016; Ağladioğlu et al., 2016; Szopa et al., 2016; Horikawa et al., 2018; Demirci et al., 2021). Recently, another heterozygous mutation, *NEUROD1* p.Met114Leu (c.340A > C), was reported in an Italian patient with MODY6 (Brodosi et al., 2021). This variant is predicted to be pathogenic based on many prediction tools and was later confirmed in a French family (Bouillet et al., 2020). In Latin America, a novel frameshift deletion (p.Phe256Leufs*2) in *NEUROD1* was reported in the MODY6 family (Abreu et al., 2019). Horikawa Y. and Enya H. concluded that heterozygous mutations in the *NEUROD1* gene are associated with MODY6 whereas homozygous mutations cause neonatal diabetes (Horikawa and Enya, 2019; Oliveira et al., 2020). The Diabetic members of Family II (II-2, II-3, and II-4) did not have neurological disorders. Similarly, some patients in previous studies have homozygous mutations in the *NEUROD1* gene with no neurological abnormalities (Wang et al., 2015). The reasons for this are not clear; however, one possibility suggests that the missense mutations P197H do not affect the domain needed for neurological functions.

A previous study aimed to determine if genetic variation in MODY genes can affect the response to insulin-sensitizing interventions. The study included individuals with a high risk of developing diabetes (high fasting glucose, being overweight, etc.). These subjects were divided into

three groups; the first group took a placebo, the second group took a metformin drug twice a day, and the third group experienced lifestyle intervention. Different variants in several MODY genes, including *HNF4A*, *GCK*, *HNF1A*, *PDX1*, *HNF1B*, and *NEUROD1*, were genotyped in all participants. There was a significant association between *HNF4A*, *HNF1B*, and *NEUROD1* variants and treatment response to metformin and lifestyle intervention. One minor allele (rs6719578) in the *NEUROD1* gene showed an increase in insulin secretion in the metformin group (Billings et al., 2017). Therefore, *NEUROD1* variants can also be used in treatment programming. Its genotypes can predict the treatment response, thus it affects the selection of the drug and the doses given.

In conclusion, *NEUROD1* p.P197H and *IGF1R* p.V579F constitute high susceptibility mutations for T1DM development. Further studies should be done to confirm their causative relationship in T1DM and its mechanisms. One approach is to develop human *in vitro* modeling system(s) using selected cells in culture transformed with the mutation by CRISPR-CAS9 technology and study various responses, including glucose-stimulated insulin secretion, and the expression and activity of several genes involved in glucose metabolism. The data generated from these studies can be extended to the development of mouse models for long-term studies. These investigations will help to extend our understanding of the pathogenesis of T1D for early diagnoses and more effective clinical intervention.

Data availability statement

The original contributions presented in the study are publicly available. This data can be found here: <https://www.ncbi.nlm.nih.gov/sra/SRR26632668>.

Ethics statement

Written informed consent was obtained from the individuals for the publication of any potentially identifiable images or data included in this article.

References

- Abreu, G. de M., Tarantino, R. M., Cabello, P. H., Zembruski, V. M., da Fonseca, A. C. P., Rodacki, M., et al. (2019). The first case of NEUROD1-MODY reported in Latin America. *Mol. Genet. Genomic Med.* 7, e989. doi:10.1002/mgg3.989
- Agladioglu, S. Y., Aycan, Z., Cetinkaya, S., Baş, V. N., Önder, A., Peltek Kendirci, H. N., et al. (2016). Maturity onset diabetes of youth (MODY) in Turkish children: sequence analysis of 11 causative genes by next generation sequencing. *J. Pediatr. Endocrinol. Metab.* 29, 487–496. doi:10.1515/jpem-2015-0039
- Al-Jenaidi, F. A., Wakim-Ghorayeb, S. F., Al-Abbasi, A., Arekat, M. R., Irani-Hakime, N., Najm, P., et al. (2005). Contribution of selective HLA-DRB1/DQB1 alleles and haplotypes to the genetic susceptibility of type 1 diabetes among Lebanese and Bahraini Arabs. *J. Clin. Endocrinol. Metab.* 90, 5104–5109. doi:10.1210/jc.2005-1166
- Ang, S. F., Lim, S. C., Tan, C. S., Fong, J. C., Kon, W. Y., Lian, J. X., et al. (2016). A preliminary study to evaluate the strategy of combining clinical criteria and next generation sequencing (NGS) for the identification of monogenic diabetes among multi-ethnic Asians. *Diabetes Res. Clin. Pract.* 119, 13–22. doi:10.1016/j.diabres.2016.06.008
- Anik, A., Çatli, G., Abacı, A., and Böber, E. (2015). Maturity-onset diabetes of the young (MODY): an update. *J. Pediatr. Endocrinol. Metabolism* 28, 251–263. doi:10.1515/jpem-2014-0384
- Arnaldes, F. I., and Helman, L. J. (2012). "Targeting the insulin growth factor receptor 1," in *Hematology/oncology clinics of north America* (Berlin, Germany: Springer). doi:10.1016/j.hoc.2012.01.004
- Bakay, M., Pandey, R., Grant, S. F. A., and Hakonarson, H. (2019). The genetic contribution to type 1 diabetes. *Curr. Diab. Rep.* 19, 116. doi:10.1007/s11892-019-1235-1
- Bassuny, W. M., Ihara, K., Sasaki, Y., Kuromaru, R., Kohno, H., Matsuura, N., et al. (2003). A functional polymorphism in the promoter/enhancer region of the FOXP3/Scurfin gene associated with type 1 diabetes. *Immunogenetics* 55, 149–156. doi:10.1007/s00251-003-0559-8
- Billings, L. K., Jablonski, K. A., Warner, A. S., Cheng, Y. C., McAteer, J. B., Tipton, L., et al. (2017). Variation in maturity-onset diabetes of the young genes influence response to interventions for diabetes prevention. *J. Clin. Endocrinol. Metab.* 102, 2678–2689. doi:10.1210/jc.2016-3429
- Bohuslavova, R., Smolik, O., Malfatti, J., Berkova, Z., Novakova, Z., Saudek, F., et al. (2021). Neurod1 is required for the early α and β endocrine differentiation in the pancreas. *Int. J. Mol. Sci.* 22, 6713. doi:10.3390/ijms22136713
- Bottini, N., Musumeci, L., Alonso, A., Rahmouni, S., Nika, K., Rostamkhani, M., et al. (2004). A functional variant of lymphoid tyrosine phosphatase is associated with type 1 diabetes. *Nat. Genet.* 36, 337–338. doi:10.1038/ng1323
- Bouillet, B., Crevisy, E., Baillot-Rudoni, S., Gallegarin, D., Jouan, T., Duffourd, Y., et al. (2020). Whole-exome sequencing identifies the first French MODY 6 family with a new mutation in the NEUROD1 gene. *Diabetes Metab.* 46, 400–402. doi:10.1016/j.diabet.2020.03.001

Author contributions

AB: Data curation, Formal Analysis, Validation, Writing—original draft. AD: Formal Analysis, Software, Conceptualization, Visualization, Writing—review and editing. HE: Conceptualization, Data curation, Resources, Writing—review and editing. HD: Conceptualization, Formal Analysis, Funding acquisition, Project administration, Resources, Supervision, Writing—review and editing, Data curation, Investigation, Visualization.

Funding

The author(s) declare that no financial support was received for the research, authorship, and/or publication of this article.

Acknowledgments

The authors are grateful to the faculty of graduate studies at the Arab American University for providing support for this study.

Conflict of interest

The authors declare that the research was conducted in the absence of any commercial or financial relationships that could be construed as a potential conflict of interest.

Publisher's note

All claims expressed in this article are solely those of the authors and do not necessarily represent those of their affiliated organizations, or those of the publisher, the editors and the reviewers. Any product that may be evaluated in this article, or claim that may be made by its manufacturer, is not guaranteed or endorsed by the publisher.

- Bradfield, J. P., Qu, H. Q., Wang, K., Zhang, H., Sleiman, P. M., Kim, C. E., et al. (2011). A genome-wide meta-analysis of six type 1 diabetes cohorts identifies multiple associated loci. *PLoS Genet.* 7, e1002293. doi:10.1371/journal.pgen.1002293
- Brodosi, L., Baracco, B., Mantovani, V., and Pironi, L. (2021). NEUROD1 mutation in an Italian patient with maturity onset diabetes of the young 6: a case report. *BMC Endocr. Disord.* 21, 202. doi:10.1186/s12902-021-00864-w
- Chen, B., Li, J., Chi, D., Sahnoune, I., Calin, S., Girnita, L., et al. (2019). Non-coding RNAs in IGF-1R signaling regulation: the underlying pathophysiological link between diabetes and cancer. *Cells* 8, 1638. doi:10.3390/cells8121638
- Concannon, P., Onengut-Gumuscu, S., Todd, J. A., Smyth, D. J., Pociot, F., Bergholdt, R., et al. (2008). A human type 1 diabetes susceptibility locus maps to chromosome 21q22.3. *Diabetes* 57, 2858–2861. doi:10.2337/db08-0753
- Cooper, J. D., Howson, J. M. M., Smyth, D., Walker, N. M., Stevens, H., Yang, J. H. M., et al. (2012). Confirmation of novel type 1 diabetes risk loci in families. *Diabetologia* 55, 996–1000. doi:10.1007/s00125-012-2450-3
- Cronin, R., Dias, N., and Yung Peng, R. K. (2017). 乳鼠心肌提取 HHS public access. *Physiol. Behav.* 176, 139–148.
- Demirci, D. K., Darendeliler, F., Poyrazoglu, S., Al, A. D. K., Gul, N., Tutuncu, Y., et al. (2021). Monogenic childhood diabetes: dissecting clinical heterogeneity by next-generation sequencing in maturity-onset diabetes of the young. *Omi. A J. Integr. Biol.* 25, 431–449. doi:10.1089/omi.2021.0081
- El-Amir, M. I., El-Feky, M. A., Laine, A. P., Härkönen, T., El-Badawy, O., Eltayeb, A. A., et al. (2015). Risk genes and autoantibodies in Egyptian children with type 1 diabetes - low frequency of autoantibodies in carriers of the HLA-DRB1*04:05-DQA1*03:01-DQB1*02 risk haplotype. *Diabetes. Metab. Res. Rev.* 31, 287–294. doi:10.1002/dmrr.2609
- Engberding, N., San Martín, A., Martín-Garrido, A., Koga, M., Pounkova, L., Lyons, E., et al. (2009). Insulin-like growth factor-1 receptor expression masks the antiinflammatory and glucose uptake capacity of insulin in vascular smooth muscle cells. *Arterioscler. Thromb. Vasc. Biol.* 29, 408–415. doi:10.1161/ATVBAHA.108.181727
- Erlich, H. A., Valdes, A. M., McDevitt, S. L., Simen, B. B., Blake, L. A., McGowan, K. R., et al. (2013). Next generation sequencing reveals the association of DRB3*02:02 with type 1 diabetes. *Diabetes* 62, 2618–2622. doi:10.2337/db12-1387
- Farabaugh, S. M., Boone, D. N., and Lee, A. V. (2015). Role of IGF1R in breast cancer subtypes, stemness, and lineage differentiation. *Front. Endocrinol.* 6, 59. doi:10.3389/fendo.2015.00059
- Fowlkes, L., Bunn R. C., and Thraikill, K. M. (2012). Contributions of the insulin/insulin-like growth factor-1 Axis to diabetic osteopathy. *J. Diabetes Metab.* 1, S1-003. doi:10.4172/2155-6156.s1-003
- Garg, N., Thakur, S., Alex McMahan, C., and Adamo, M. L. (2011). High fat diet induced insulin resistance and glucose intolerance are gender-specific in IGF-1R heterozygous mice. *Biochem. Biophys. Res. Commun.* 413, 476–480. doi:10.1016/j.bbrc.2011.08.123
- Giwa, A. M., Ahmed, R., Omidian, Z., Majety, N., Karakus, K. E., Omer, S. M., et al. (2020). Current understandings of the pathogenesis of type 1 diabetes: genetics to environment. *World J. Diabetes* 11, 13–25. doi:10.4239/wjdv11.i1.13
- Groop, L., and Pociot, F. (2014). Genetics of diabetes - are we missing the genes or the disease? *Mol. Cell. Endocrinol.* 382, 726–739. doi:10.1016/j.mce.2013.04.002
- Hakonarson, H., Grant, S. F. A., Bradfield, J. P., Marchand, L., Kim, C. E., Glessner, J. T., et al. (2007). A genome-wide association study identifies KIAA0350 as a type 1 diabetes gene. *Nature* 448, 591–594. doi:10.1038/nature06010
- Hakuno, F., and Takahashi, S. I. (2018). 40 years of IGF1: IGF1 receptor signaling pathways. *J. Mol. Endocrinol.* 61, T69–T86. doi:10.1530/JME-17-0311
- Hansen, L., Jensen, J. N., Urioste, S., Petersen, H. V., Pociot, F., Eiberg, H., et al. (2000). NeuroD/BETA2 gene variability and diabetes: no associations to late-onset type 2 diabetes but an A45 allele may represent a susceptibility marker for type 1 diabetes among Danes. Danish Study Group of Diabetes in Childhood, and the Danish IDDM Epidemiology and Genetics Group. *Diabetes* 49, 876–878. doi:10.2337/diabetes.49.5.876
- Health annual Palestine report, (2018). Health annual Palestine report. https://healthclusterpt.org/admin/file_manager/uploads/files/1/Health%20Annual%20Report%20Palestine%202018.pdf.
- Horikawa, Y., and Enya, M. (2019). Genetic dissection and clinical features of MODY6 (NEUROD1-MODY). *Curr. Diabetes Rep.* 19, 12. doi:10.1007/s11892-019-1130-9
- Horikawa, Y., Enya, M., Mabe, H., Fukushima, K., Takubo, N., Ohashi, M., et al. (2018). NEUROD1-deficient diabetes (MODY6): identification of the first cases in Japanese and the clinical features. *Pediatr. Diabetes* 19, 236–242. doi:10.1111/pedi.12553
- Illumina, (2021). Illumina DNA prep with enrichment reference guide. https://support.illumina.com/content/dam/illumina-support/documents/documentation/chemistry_documentation/illumina_prep/illumina-dna-prep-with-enrichment-reference-guide-1000000048041-07.pdf.
- Iwata, I., Nagafuchi, S., Nakashima, H., Kondo, S., Koga, T., Yokogawa, Y., et al. (1999). Association of polymorphism in the neuroD/BETA2 gene with type 1 diabetes in the Japanese. *Diabetes* 48, 416–419. doi:10.2337/diabetes.48.2.416
- Jin, J., Ravindran, P., Meo, D. Di, and Püschel, A. W. (2019). Igf1R/InsR function is required for axon extension and corpus callosum formation. *PLoS One* 14, e0219362. doi:10.1371/journal.pone.0219362
- Jung, H. J., and Suh, Y. (2015). Regulation of IGF -1 signaling by microRNAs. *Front. Genet.* 5, 472. doi:10.3389/fgene.2014.00472
- Kharroubi, A. T., and Darwish, H. M. (2015). Diabetes mellitus: the epidemic of the century. *World J. Diabetes* 6, 850–867. doi:10.4239/wjdv6.i6.850
- Kumar, A., Ren, Y., Sundaram, K., Mu, J., Sriwastva, M. K., Dryden, G. W., et al. (2021). miR-375 prevents high-fat diet-induced insulin resistance and obesity by targeting the aryl hydrocarbon receptor and bacterial tryptophanase (tnaA) gene. *Theranostics* 11, 4061–4077. doi:10.7150/thno.52558
- Malecki, M. T., Cyganek, K., Klupa, T., and Sieradzki, J. (2003). The Ala45Thr polymorphism of BETA2/NeuroD1 gene and susceptibility to type 2 diabetes mellitus in a Polish population. *Acta Diabetol.* 40, 109–111. doi:10.1007/s005920300015
- Malecki, M. T., Jhala, U. S., Antonellis, A., Fields, L., Doria, A., Orban, T., et al. (1999). Mutations in NEUROD1 are associated with the development of type 2 diabetes mellitus. *Nat. Genet.* 23, 323–328. doi:10.1038/15500
- Mcd, C. N. MasterPure™ DNA purification kit. <https://shop.biosearchtech.com/dna-rna-extraction-and-purification-kits/dna-and-rna-purification-kits-and-reagents/masterpure-complete-dna-and-rna-purification-kit>. (2012).
- Moody, G., Beltran, P. J., Mitchell, P., Cajulis, E., Chung, Y. A., Hwang, D., et al. (2014). IGF1R blockade with ganitumab results in systemic effects on the GH-IGF axis in mice. *J. Endocrinol.* 221, 145–155. doi:10.1530/JOE-13-0306
- Nadia, B., Chehrzade, B., Ouafa, A., Asmaa, D. B., Ouadghiri, S., and Malika, E. (2012). Human leukocyte antigen (HLA) polymorphism and type 1 diabetes in the Moroccan population. *Afr. J. Biotechnol.* 11, 16126–16131. doi:10.5897/ajb12.1863
- Naya, F. J., Huang, H. P., Qiu, Y., Mutoh, H., DeMayo, F. J., Leiter, A. B., et al. (1997). Diabetes, defective pancreatic morphogenesis, and abnormal enteroendocrine differentiation in BETA2/NeuroD-deficient mice. *Genes Dev.* 11, 2323–2334. doi:10.1101/gad.11.18.2323
- Nyaga, D. M., Vickers, M. H., Jefferies, C., Perry, J. K., and O'Sullivan, J. M. (2018). The genetic architecture of type 1 diabetes mellitus. *Mol. Cell. Endocrinol.* 477, 70–80. doi:10.1016/j.mce.2018.06.002
- Oliveira, S. C., Neves, J. S., Pérez, A., and Carvalho, D. (2020). Maturity-onset diabetes of the young: from a molecular basis perspective toward the clinical phenotype and proper management. *Endocrinol. Diabetes Nutr.* 67, 137–147. doi:10.1016/j.endinu.2019.07.012
- Panneerselvam, A., Kannan, A., Mariajoseph-Antony, L. F., and Prahalathan, C. (2019). PAX proteins and their role in pancreas. *Diabetes Res. Clin. Pract.* 155, 107792. doi:10.1016/j.diabres.2019.107792
- Parvin, R., Saito-Hakoda, A., Shimada, H., Shimizu, K., Noro, E., Iwasaki, Y., et al. (2017). Role of NeuroD1 on the negative regulation of Pomc expression by glucocorticoid. *PLoS One* 12, e0175435. doi:10.1371/journal.pone.0175435
- Pociot, F. (2017). Type 1 diabetes genome-wide association studies: not to be lost in translation. *Clin. Transl. Immunol.* 6, e162–e167. doi:10.1038/cti.2017.51
- Ray, S. K., and Leiter, A. B. (2007). The basic helix-loop-helix transcription factor NeuroD1 facilitates interaction of Sp1 with the secretin gene enhancer. *Mol. Cell. Biol.* 27, 7839–7847. doi:10.1128/mcb.00438-07
- Redondo, M. J., Oram, R. A., and Steck, A. K. (2017). Genetic risk scores for type 1 diabetes prediction and diagnosis. *Curr. Diab. Rep.* 17, 129. doi:10.1007/s11892-017-0961-5
- Rubio-Cabezas, O., Minton, J. A. L., Kantor, I., Williams, D., Ellard, S., and Hattersley, A. T. (2010). Homozygous mutations in NEUROD1 are responsible for a novel syndrome of permanent neonatal diabetes and neurological abnormalities. *Diabetes* 59, 2326–2331. doi:10.2337/db10-0011
- Sharma, A., Moore, M., Marcora, E., Lee, J. E., Qiu, Y., Samaras, S., et al. (1999). The NeuroD1/BETA2 sequences essential for insulin gene transcription colocalize with those necessary for neurogenesis and p300/CREB binding protein binding. *Mol. Cell. Biol.* 19, 704–713. doi:10.1128/mcb.19.1.704
- Smyth, D. J., Cooper, J. D., Bailey, R., Field, S., Burren, O., Smink, L. J., et al. (2006). A genome-wide association study of nonsynonymous SNPs identifies a type 1 diabetes locus in the interferon-induced helicase (IFIH1) region. *Nat. Genet.* 38, 617–619. doi:10.1038/ng1800
- Stayousssef, M., Benmansour, J., Al-Irhayim, A. Q., Said, H. B., Rayana, C. B., Mahjoub, T., et al. (2009). Autoimmune type 1 diabetes genetic susceptibility evoked by human leukocyte antigen DRB1 and DQB1 genes in Tunisia. *Clin. Vaccines Immunol.* 16, 1146–1150. doi:10.1128/CI.100105-09
- Sun, Y., Sun, X., and Shen, B. (2017). Molecular imaging of IGF-1R in cancer. *Mol. Imaging* 16, 1536012117736648. doi:10.1177/1536012117736648
- Szopa, M., Ludwig-Galezowska, A. H., Radkowski, P., Skupien, J., Machlowska, J., Klupa, T., et al. (2016). A family with the Arg103Pro mutation in the NEUROD1 gene detected by next-generation sequencing - clinical characteristics of mutation carriers. *Eur. J. Med. Genet.* 59, 75–79. doi:10.1016/j.ejmg.2016.01.002
- Thermo Fisher Scientific, (2015). U. BigDye exp. guide. https://assets.thermofisher.com/TFS-Assets/LSG/manuals/4337035_BDTv31CycSqKt_RUO_UG.pdf.

- Todd, J. A., Walker, N. M., Cooper, J. D., Smyth, D. J., Downes, K., Plagnol, V., et al. (2007). Robust associations of four new chromosome regions from genome-wide analyses of type 1 diabetes. *Nat. Genet.* 39, 857–864. doi:10.1038/ng2068
- Tremblay, J., and Hamet, P. (2019). Environmental and genetic contributions to diabetes. *Metabolism* 100, 153952–153956. doi:10.1016/j.metabol.2019.153952
- Vella, A., Cooper, J. D., Lowe, C. E., Walker, N., Nutland, S., Widmer, B., et al. (2005). Localization of a type 1 diabetes locus in the IL2RA/CD25 region by use of tag single-nucleotide polymorphisms. *Am. J. Hum. Genet.* 76, 773–779. doi:10.1086/429843
- Wang, F., Li, H., Xu, M., Li, H., Zhao, L., Yang, L., et al. (2015). A homozygous missense mutation in NEUROD1 is associated with nonsyndromic autosomal recessive retinitis pigmentosa. *Investig. Ophthalmol. Vis. Sci.* 56, 150–155. doi:10.1167/iovs.14-15382
- Wang, F., Stewart, M., McDermott, S., Kazanjian, A., Vissandjee, B., DesMeules, M., et al. (2012). Migration and diabetes in British Columbia and Quebec: prevalence and health service utilization. *Can. J. Public Heal* 103, 59–64. doi:10.1007/bf03404070
- Wit, J. M., and Walenkamp, M. J. (2013). Role of insulin-like growth factors in growth, development and feeding. *World Rev. Nutr. Dietetics* 106, 60–65. doi:10.1159/000342546
- Xuan, S., Kitamura, T., Nakae, J., Politi, K., Kido, Y., Fisher, P. E., et al. (2002). Defective insulin secretion in pancreatic β cells lacking type 1 IGF receptor. *J. Clin. Invest.* 110, 1011–1019. doi:10.1172/jci15276
- Yamada, S., Motohashi, Y., Yanagawa, T., Maruyama, T., Kasuga, A., Hirose, H., et al. (2001). NeuroD/BETA2 gene G→A polymorphism may affect onset pattern of type 1 diabetes in Japanese. *Diabetes Care* 24, 1438–1441. doi:10.2337/diacare.24.8.1438
- Yuan, J., Yin, Z., Tao, K., Wang, G., and Gao, J. (2018). Function of insulin-like growth factor 1 receptor in cancer resistance to chemotherapy. *Oncol. Lett.* 15, 41–47. doi:10.3892/ol.2017.7276
- Zayed, H. (2016). Genetic epidemiology of type 1 diabetes in the 22 Arab countries. *Curr. Diab. Rep.* 16, 37. doi:10.1007/s11892-016-0736-4



OPEN ACCESS

EDITED BY

Ivan Martinez Duncker,
Universidad Autónoma del Estado de Morelos,
Mexico

REVIEWED BY

Jose Elias Garcia-Ortiz,
Centro de Investigación Biomédica de
Occidente (CIBO), Mexico
Stephan Wenninger,
Ludwig Maximilian University of Munich,
Germany

*CORRESPONDENCE

Priya Kishnani,
✉ priya.kishnani@duke.edu

RECEIVED 07 October 2023

ACCEPTED 04 January 2024

PUBLISHED 19 January 2024

CITATION

Carter C, Boggs T, Case LE and Kishnani P
(2024), Real-world outcomes from a series of
patients with late onset Pompe disease who
switched from alglucosidase alfa to
avalglucosidase alfa.
Front. Genet. 15:1309146.
doi: 10.3389/fgene.2024.1309146

COPYRIGHT

© 2024 Carter, Boggs, Case and Kishnani. This is
an open-access article distributed under the
terms of the [Creative Commons Attribution
License \(CC BY\)](#). The use, distribution or
reproduction in other forums is permitted,
provided the original author(s) and the
copyright owner(s) are credited and that the
original publication in this journal is cited, in
accordance with accepted academic practice.
No use, distribution or reproduction is
permitted which does not comply with these
terms.

Real-world outcomes from a series of patients with late onset Pompe disease who switched from alglucosidase alfa to avalglucosidase alfa

Chris Carter¹, Tracy Boggs², Laura E. Case^{1,3} and Priya Kishnani^{1*}

¹Division of Medical Genetics, Department of Pediatrics, Duke University Health System, Durham, NC, United States, ²Department of Rehabilitation Services, Duke University Health System, Durham, NC, United States, ³Doctor of Physical Therapy Division, Department of Orthopaedics, Duke University School of Medicine, Durham, NC, United States

Introduction: Pompe disease is an inherited, progressive neuromuscular disorder caused by deficiency of lysosomal acid α -glucosidase and accumulation of glycogen in tissues, resulting in cellular dysfunction, muscle damage, and functional disabilities. Enzyme replacement therapy with alglucosidase alfa (Myozyme/Lumizyme) has led to better outcomes, but many patients have plateaued or declined despite treatment. The second-generation ERT avalglucosidase alfa (Nexvazyme) was designed to have enhanced cellular uptake via the conjugation of additional bis-mannose-6-phosphate residues. There have been trials comparing the efficacy of alglucosidase and avalglucosidase, but there remains a need for more real-world data on patients who switched from alglucosidase to avalglucosidase.

Methods: A chart review was conducted on $n = 15$ patients with late-onset Pompe disease followed at a single center who switched from alglucosidase to avalglucosidase and continued for at least 6 months.

Results: A total of $n = 8/15$ patients received alglucosidase for more than 3 years prior to switching, and $n = 7/15$ received it for more than 5 years prior to switching. There were statistically significant improvements in CK, Hex4, and AST with mean differences of -104.8 U/L, -3.0 mmol/molCr, and -14.7 U/L, respectively, post-switch. 6-Minute Walk Test; comfortable gait speed; Gait, Stairs, Gower, Chair; and Quick Motor Function Test scores improved or stabilized in most patients post-switch ($n = 8/12$, $n = 11/12$, $n = 9/12$, $n = 7/11$, respectively). Of $n = 7$ patients with pulmonary function testing, $n = 4/7$ had improved upright FVC. Patient-reported outcomes revealed improvements in dyspnea ($n = 4/4$), physical function ($n = 3/4$), fatigue ($n = 2/3$), and lower back pain ($n = 3/3$). Avalglucosidase was well tolerated without infusion-associated reactions, and all $n = 7$ patients on home infusions continued receiving ERT at home. Anti-drug antibodies were seen in $n = 9/10$ of patients on alglucosidase and $n = 8/13$ of those on avalglucosidase, with titers below 12,800 in a majority of patients. We also present the first outcome data for a patient with LOPD who is non-ambulatory and a full-time wheelchair user; she demonstrated meaningful improvements in quality of life and motor function with the switch.

Discussion: In summary, improved outcomes were seen in most patients, with a subset whose decline persisted. This study presents evidence that switching from alglucosidase to avalglucosidase may be associated with improved outcomes in certain patients with LOPD.

KEYWORDS

glycogen storage disease type 2, lysosomal storage disease (LSD), alglucosidase alfa, avalglucosidase alfa, late-onset Pompe disease (LOPD), enzyme replacement therapy

Introduction

Pompe disease, also known as glycogen storage disease type II (OMIM #232300), is an inherited, progressive neuromuscular disorder caused by deficiency of lysosomal acid α -glucosidase (GAA) and accumulation of glycogen in various tissues, resulting in cellular dysfunction, progressive muscle damage, and functional disabilities.

Broadly, there are two categories based on age of onset and symptomatology: classic infantile-onset Pompe disease (IOPD) and late-onset Pompe disease (LOPD). IOPD is the most severe and rapidly progressive form of Pompe disease. Patients present with cardiomyopathy in the first year of life, and without treatment, fatal cardiorespiratory failure ensues with death in the first 1–2 years of life. Over the last few decades, prognoses have improved dramatically with the advent of newborn screening for Pompe disease and prompt initiation of treatment, preferably before the onset of severe signs and symptoms of the disease (Kishnani et al., 2021; Huggins et al., 2022). In contrast, LOPD includes cases of Pompe disease in which the age of onset is after 12 months, as well as those in which the age of onset is before 12 months who do not develop cardiomyopathy in the first year of life. Patients with LOPD experience progressive weakness in skeletal muscles including the diaphragm and other respiratory muscles, and consequently, respiratory failure remains the principal cause of death in LOPD (Toscano et al., 2019; Dimachkie et al., 2022).

LOPD may manifest in a wide spectrum of clinical presentations with varying ages of onset and rates of progression. The clinical diversity in LOPD can largely be explained by variable amounts of residual enzyme activity, considerable genotypic variability, and modifying factors that may have a sizeable effect on phenotype even among patients with the same variant (Toscano et al., 2019; Diaz-Manera et al., 2021).

Enzyme replacement therapy (ERT) with alglucosidase alfa was approved in 2006 as the first treatment for Pompe disease. Administering exogenous recombinant human GAA provides patients with an alternate means of cleaving glycogen, thus reducing accumulation and slowing disease progression. In IOPD and LOPD populations, ERT has remarkably improved both survival and quality of life (Schoser et al., 2017). For many years after its approval, alglucosidase alfa remained the standard of care for patients with Pompe disease. However, many patients on alglucosidase alfa infusions plateau or decline while on treatment, an indication that there remained an unmet need in the management of Pompe disease. This disease progression despite treatment has been partly attributed to suboptimal uptake of ERT into skeletal muscle (Diaz-Manera et al., 2021; Dimachkie et al., 2022).

A second-generation ERT, avalglucosidase alfa, was approved by the FDA in August 2021 for the treatment of patients 1 year of age

and older with LOPD as well as by the European Commission in June 2022 for the treatment of both LOPD and IOPD. Avalglucosidase alfa has ~15-fold more bis-mannose-6-phosphate (M6P) residues per enzyme molecule than alglucosidase alfa. This enhances uptake and trafficking to the lysosome via the cation independent M6P receptor, resulting in increased delivery, improved glycogen clearance, and better outcomes compared to alglucosidase alfa. In preclinical models, avalglucosidase alfa exhibited as much as five-times greater glycogen clearance compared to an equivalent dose of alglucosidase alfa (Zhu et al., 2009; Kishnani et al., 2021; Sanofi Genzyme, 2021).

According to the package insert, an avalglucosidase dosage of 20 mg/kg q2w is the standard recommendation for patients 30 kg or more, while 40 mg/kg q2w is recommended for those less than 30 kg (Sanofi Genzyme, 8/2021). This higher dose has also previously been shown in clinical trials (Mini COMET) to be safe and beneficial for patients with IOPD who showed clinical decline or a suboptimal response to alglucosidase alfa. Given the safety and efficacy of higher dosages in the IOPD population, some patients with LOPD who continued to decline despite 20 mg/kg q2w of avalglucosidase or were previously on 40 mg/kg/week of alglucosidase alfa were treated with 40 mg/kg q2w in this study. Further research into the safety and efficacy of increasing avalglucosidase dosage beyond standard recommendations is still needed.

Patients may develop antidrug antibodies (ADAs) against their ERT medications. These have long been associated with worse outcomes in IOPD, including declines in muscle strength, pulmonary function, and overall survival. There have also been reports of clinical decline in LOPD (de Vries et al., 2010; Desai et al., 2019; Kim et al., 2023). In general, persistent titers greater than or equal to 12,800 are viewed as clinically significant. Titers are monitored regularly, and patients with high and persistent titers often require immunomodulation (Sanofi Genzyme, 2010; Desai et al., 2019; Sanofi Genzyme, 2021; Kim et al., 2023).

In the real-world setting since the approval of avalglucosidase alfa, patients often switch from alglucosidase alfa to avalglucosidase alfa with the goal of improving clinical outcomes or preventing further decline. The difference in outcomes between these agents has been the subject of several studies with strict inclusion criteria and an emphasis on treatment-naïve patients (see Table 1), and there remains a paucity of evidence on the real-world results of switching from first-generation to second-generation ERT (Pena et al., 2019; Kishnani et al., 2021; Kishnani et al., 2023). Moreover, the switch data has been mostly limited to patients switching after relatively short durations of alglucosidase alfa; switch data from long-term ERT-experienced patients is scarce (Diaz-Manera et al., 2021; Dimachkie et al., 2022). Specifically, the COMET trial included $n = 49$ patients who switched after 49 weeks on alglucosidase alfa,

TABLE 1 Avalglucosidase in the literature. Notable studies comparing the efficacy of avalglucosidase alfa and alglucosidase alfa.

Study	Population, dosages	Results
Long-Term Safety and Efficacy of Avalglucosidase Alfa in Patients with Late-Onset Pompe Disease. Dimachkie, Mazen M., et al. (2022)	$n = 7$ treatment naïve, $n = 10$ switch patients (who received alglucosidase alfa for 0.9–7 years), all adults with LOPD. Doses of 5, 10, or 20 mg/kg q2w for 32–45 months and then 20 mg/kg q2w for all	Upright FVC and 6MWT distance remained stable in most participants, and improvements in 6MWT distance were observed in most participants <45 years at enrollment in both the naïve and switch groups
Safety and efficacy of avalglucosidase alfa versus alglucosidase alfa in patients with late-onset Pompe disease (COMET): a phase 3, randomised, multicentre trial. Diaz-Manera et al. (2021) , Kishnani et al. (2023)	Patients ≥ 3 years of age with LOPD. $n = 51$ patients on avalglucosidase alfa, $n = 49$ on alglucosidase alfa in primary period. All on avalglucosidase alfa in extension. Doses of 20 mg/kg q2w	Outcomes at the primary endpoint of 49 weeks showed an increased mean improvement in percent predicted upright FVC on avalglucosidase alfa compared to alglucosidase alfa. This was sufficient to meet noninferiority criteria, but it narrowly missed the threshold for superiority ($p = 0.063$). Other findings include a greater increase in 6MWT distance on avalglucosidase alfa versus alglucosidase alfa. In the 49-week extension period, the results were consistent with the original findings demonstrating maintenance of positive clinical outcomes
Mini-Comet: Individual-Level Treatment Responses in Infantile-Onset Pompe Disease Participants Receiving Avalglucosidase Alfa or Alglucosidase Alfa Who Previously Received Alglucosidase Alfa. Kishnani, Priya, et al. (2021)	$n = 22$ patients with IOPD. Doses of 20 and 40 mg/kg q2w	Exploratory efficacy outcomes (6MWT, GMFM-88, QMFT, Pompe-PEDI, ptosis, and LVM z-score) improved or stabilized with avalglucosidase alfa at 40 mg/kg q2w, whereas these parameters stabilized or declined with 20 mg/kg q2w or on alglucosidase alfa

and [Dimachkie et al., 2022](#) included $n = 10$ patients who switched after 0.9–7 years and met criteria for inclusion. This study seeks to evaluate the clinical outcomes of patients who switched from alglucosidase alfa at various doses and variable durations to avalglucosidase alfa across a variety of outcome measures.

Materials and methods

Study design and population

This study was approved by the Duke Institutional Review Board under IRB number Pro00010830.

This study is a retrospective, longitudinal case series of patients seen at the Duke University metabolic clinic with a diagnosis of LOPD confirmed by molecular testing. Fifteen patients were identified who switched treatment from alglucosidase alfa to avalglucosidase alfa and continued for at least 6 months after the transition with varying amounts of post-switch clinical data. Patients, including patient 10, were excluded if they had no available follow-up data from at least 6 months after switching.

Data collection

Data collection began from the first date in which the patient was seen in the Duke Health System and included all subsequent encounters prior to August 2023. Physical therapy (PT) data was collected through 11/13/2023. Information collected included demographics, medical history, and disease course, incorporating laboratory markers, antidrug antibodies, PT metrics, pulmonary function testing, and patient-reported outcomes. All data extracted from the medical record was compiled into a spreadsheet for analysis.

Patient-reported outcomes (PROs) were collected for Dyspnea (PROMIS Short Form v1.0–Dyspnea Severity–10a 01 August 2016),

Physical Function (PROMIS Short Form v2.0–Physical Function 20a 29 November 2016), Fatigue (PROMIS Short Form v1.0–Fatigue–8a 16 March 2020), and Oswestry Low Back Pain Disability ([Fairbank et al., 1980](#)).

Physical therapy outcome measures

All of the following outcome measures were performed by physical therapists experienced in neuromuscular disorders and the data obtained via chart review was evaluated by an experienced PT. The Six-Minute Walk Test (6MWT) was conducted to measure walking endurance per American Thoracic Society guidelines ([ATS Committee on Proficiency Standards for Clinical Pulmonary Function Laboratories, 2002](#)). Percent of predicted distance was calculated in accordance with norms established for age, gender, and height ([Enright and Sherrill, 1998](#); [Li et al., 2007](#)). The Gait, Stairs, Gower, Chair (GSGC) test was used to measure motor function as previously described ([Angelini et al., 2012](#); [Khan et al., 2020a](#)); GSGC scores range from 4 to 27, with a score of 4 indicating normal function. Patients were categorized into three degrees of impairment based on their GSGC score prior to the switch: mild (4–11), moderate (12–19), or severe (20–27). The Gross Motor Function Measure (GMFM-88) was used to test motor skills, with scores ranging from 0% to 100%, with 100% indicating normal function, which should be achieved by 5 years of age in those with typical function ([Russell et al., 1989](#)). The Quick Motor Function Test (QMFT), developed from the GMFM and validated in Pompe disease, has scores ranging from 0–64 with a score of 64 indicating normal function ([van Capelle et al., 2012](#)). Two subtests on the Bruininks-Oseretsky Test of Motor Proficiency Second Edition (BOT-2) were utilized: running speed and agility (subtest 6) and strength (subtest 8) ([Deitz et al., 2007](#)). For the patient who was non-ambulatory, the 9-Hole Peg Test (9-HPT) was used to measure hand dexterity ([Wang et al., 2015](#)), and lateral (key) pinch was used to assess strength as previously described ([Paschall et al., 2021](#)).

TABLE 2 Summary of cohort characteristics. Note that patient 10 was excluded from the study due to a lack of data.

Patient/Sex	GAA genotype	Onset age (y)	Diagnosis age (y)	Primary symptoms
1/F	c.-32-13T>G	48	56	Muscle weakness, atrophy, myalgia, gait disturbance, poor endurance
	c.1796C>A			
2/F	c.-32-13T>G	32	34	Muscle weakness, myalgia, dyspnea, gait disturbance, fatigue, dysphagia
	c.1445C>G			
3/F	c.2481 + 110_2646 + 39del	40	43	Muscle weakness, atrophy, fatigue, dyspnea, lower back pain
	c.2294A>G			
4/M	c.-32-13T>G	20	77	Muscle weakness, gait disturbance, loss of agility, fatigue
	c.1655T>C			
5/F	c.-32-13T>G	30	48	Muscle weakness, loss of balance, hypophonia, fatigue, dysphagia
	c.1548G>A			
6/F	c.-32-13T>G	51	71	Muscle weakness, dyspnea, gait disturbance, loss of balance, fatigue
	c.1943G>A			
7/F	c.525delT	47	67	Muscle weakness, dyspnea, fatigue, dysphagia
	c.336-13T>G			
8/M	c.-32-13T>G	27	44	Muscle weakness, dyspnea, gait disturbance, scoliosis, fatigue
	c.1827delC			
9/M	c.-32-13T>G	43	43	Muscle weakness, lower back pain, fatigue
	c.1143delC			
11/F	c.-32-13T>G	16	16	Muscle weakness, myalgia
	c.2236T>C			
12/F	c.-32-13T>G	49	49	Muscle weakness, dyspnea, gait disturbance, scoliosis, dysphagia
	c.1572C>A			
13/F	c.1655T>C	<1	1.75	Delayed motor milestones, poor head control, low tone, wheelchair and ventilator dependence
	c.896T>G			
14/M	c.-32-13T>G	15	46	Muscle weakness, myalgia, lower back pain, fatigue
	c.1942G>A			
15/M	c.-32-13T>G	2	2.5	Muscle weakness, myalgia, gait disturbance, delayed motor skills, fatigue
	c.1051delG			
16/M	c.-32-13T>G	2	2	Muscle weakness, gait disturbance, delayed motor skills, scoliosis
	c.2501_2502delCA			

Analysis

Descriptive analysis was used to summarize the baseline patient characteristics, treatments, and endpoints: Hex4, AST, CK, antidrug antibody titers, percent predicted forced vital capacity, PT outcome measures, and patient-reported outcomes. Statistical analysis and figure design were performed in GraphPad Prism 9. Paired t-tests were used in the analysis of laboratory markers between timepoints. For PT data, Intellectus Statistics (Intellectus Statistics 2019, Clearwater, Florida) was used to perform paired t-tests for

examination of trends and to analyze differences between the pre- and post-switch assessments.

Results

Description of cohort and ERT history

Fifteen patients with LOPD were included in the study. GAA variants differed among the cohort, but the c.-32-13T>G variant

TABLE 3 Treatment history. All dosages are 20 mg/kg q2w unless otherwise specified.

Patient/ Sex	Age at ERT initiation (y)	Time on alglucosidase (mo)	Age at ERT switch (y)	Time on avalglucosidase (mo)	Notes
1/F	57	30	59	19	
2/F	42	121 (20 mg/kg q2w)	58	18	
		23 (30 mg/kg q2w)			
		37 (40 mg/kg q2w)			
3/F	43	7	44	21	
4/M	77	12 (20 mg/kg q2w)	82	23 (40 mg/kg q2w)	17 months VAL-1221 after 12 months on al
		1 (40 mg/kg q2w)			
		33 (40 mg/kg q1w)			
5/F	48	12	49	6 (5 mg/kg q2w)	
				113 (20 mg/kg q2w)	
6/F	71	72	77	16	
7/F	67	12	68	41 (20 mg/kg q2w)	
				19 (40 mg/kg q2w)	
8/M	44	85 (20 mg/kg q2w)	53	16 (40 mg/kg q2w)	
		24 (40 mg/kg q2w)			
9/M	45	81 (20 mg/kg q2w)	58	12	21 months VAL-1221 after 81 months on al
		30 (20 mg/kg q2w)			16 months ACTUS-101 before switch
11/F	16	2.3	16	22	
12/F	51	11	52	29 (20 mg/kg q2w)	3 months stopped ERT after 29 months on aval
				16 (20 mg/kg q2w)	
13/F	7	175 (20 mg/kg q2w)	25	18 (40 mg/kg q2w)	
		24 (40 mg/kg q2w)			
		30 (40 mg/kg q1w)			
14/M	46	9	47	17	
15/M	2.5	75	9	21	
16/M	2	146	14	10	

predominated and was present in 12/15 patients in heterozygosity. The average age of onset in this cohort (Mean ± SD) was 27.75 ± 17.97, ranging from <1 year to 51 years of age. Muscle weakness was the most common presenting symptom. Fatigue, dyspnea, and myalgia were also frequently reported. *n* = 14/15 patients were ambulatory; patient 13 used both a power wheelchair and ventilator full-time. The median interval from symptom onset to diagnosis was 5.1 years (range 2.4 months–57 years). A full list of patient genotypes and other characteristics is included in Table 2.

Median interval from diagnosis to ERT initiation was 2.5 months (range 0.3 months–8 years). Patients received alglucosidase alfa for periods ranging from 2.3 months to 19.1 years with a median duration of 3.8 years. A total of *n* = 8/15 patients received alglucosidase alfa for more than 3 years, and *n* = 7/15 received it for more than 5 years. Patients 2, 4, 8, and

13 underwent dosage increases during their time on alglucosidase alfa. At the time of switching to avalglucosidase alfa, patients were on alglucosidase alfa dosages ranging from 20 mg/kg q2w to 40 mg/kg q1w.

Median age of switch was 52 years. *n* = 11 patients started avalglucosidase alfa at 20 mg/kg q2w, *n* = 3 (patients 4, 8, and 13) started at 40 mg/kg q2w, and *n* = 1 (patient 5) started at 5 mg/kg q2w as part of the COMET trial before increasing to 20 mg/kg q2w. Patient 7 had an avalglucosidase alfa dose increase during her treatment from 20 to 40 mg/kg q2w. At the time of database lock, all patients continued to receive avalglucosidase alfa and have received it for durations ranging from 10 months to 9.9 years (median 18.9 months).

Patients 4 and 9 stopped alglucosidase therapy for 17 and 21 months, respectively, while participating in the VAL-1221

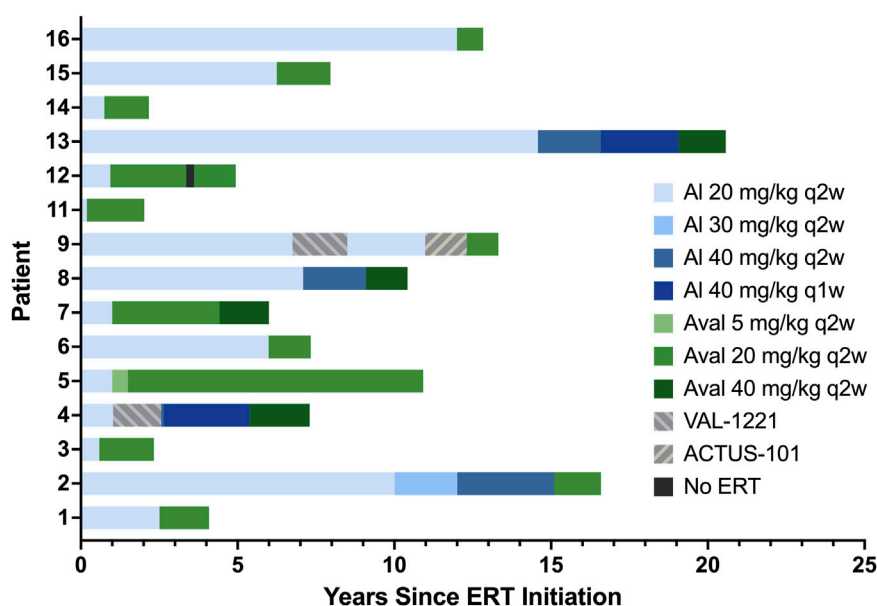


FIGURE 1
ERT history. Alglucosidase regimens are indicated by shades of blue, avalglucosidase regimens are indicated by shades of green, and other regimens are indicated by patterned gray bars.

clinical trial. Both of them withdrew due to a lack of clinical benefit and resumed alglucosidase therapy for 34 and 30 months, respectively, before switching to avalglucosidase. Patient 9 also stopped receiving alglucosidase to participate in a gene therapy trial for 16 months; after withdrawing from that study due to lack of clinical benefit, he switched to avalglucosidase therapy. Finally, patient 12 stopped avalglucosidase therapy for 3 months mid-treatment due to insurance issues. Full treatment history is detailed in Table 3 and depicted in Figure 1.

Laboratory markers

When available, urinary Hex4 (Glc4) and serum CK, AST, and ALT values were obtained via chart review at three time points: at baseline prior to ERT initiation, while on alglucosidase prior to ERT switch, and while on avalglucosidase at the most recent assessment. These values were compared to all other timepoints to ensure that they were representative of overall trends. Trends are depicted in Figure 2 and full data is available in Supplementary Tables S1, S2; Supplementary Figure S1.

From baseline to alglucosidase alfa, all patients showed a reduction or stabilization across all biomarkers. Average differences (Mean \pm SD) in CK, AST, ALT, and Hex4 were -266.5 ± 301.2 U/L, -60.3 ± 98.40 U/L, -51.9 ± 74.78 , and -2.449 ± 1.876 mmol/mol Cr, respectively. Changes in CK and Hex4 were statistically significant ($p = 0.0149$ and $p = 0.0077$, respectively). Expressed as a percent drop from baseline to ERT with alglucosidase alfa, the changes were -44% (CK), -56% (AST), -49% (ALT), and -10% (Hex4).

A further reduction or stabilization in CK, AST, ALT, and Hex4 was seen from alglucosidase alfa to avalglucosidase alfa in all patients. Average differences from alglucosidase to avalglucosidase (Mean \pm SD) in CK, AST, ALT, and Hex4 were -104.8 ± 89.01 U/L,

-14.7 ± 14.58 U/L, -22.1 ± 26.55 U/L, and -2.998 ± 4.811 mmol/mol Cr, respectively. Changes in all four biomarkers were statistically significant ($p = 0.0011$ for CK, $p = 0.0023$ for AST, $p = 0.0083$ for ALT, and $p = 0.0364$ for Hex4). Expressed as a percent drop from pre- to post-switch, the changes were -40% (CK), -39% (AST), -43% (ALT), and -56% (Hex4).

Across all biomarkers, there was also a considerable increase in the number of values that fell below the upper limit of normal. This was the case when comparing values prior to starting any ERT to those while on alglucosidase, as well as comparing values on alglucosidase to those on avalglucosidase. Across the three timepoints, the number of CK values less than 220 U/L increased from 0 to 5 to 11. The same trend was seen with AST, from 1 to 6 to 12 values less than 41 U/L, and ALT, from 2 to 6 to 13 values less than 40 U/L. Finally, this was also the case with Hex4, which went from 1 to 4 to 11 values that fell below 3.0 mmol/mol Cr.

Physical therapy measures

Thirteen of the 15 patients in this study had PT data available from before and after the switch to avalglucosidase alfa: 12 were ambulatory (patients 1–7, 9, 12, 14–16) and one was non-ambulatory (patient 13, discussed separately below). Differences between the last pre-switch assessment and the most recent assessment were analyzed for each performance metric. An overview of PT outcomes with patients categorized into groups of severity is included in Table 4.

6MWT

At the most recent post-switch assessment, there were no trends or statistically significant differences in the mean distance walked for

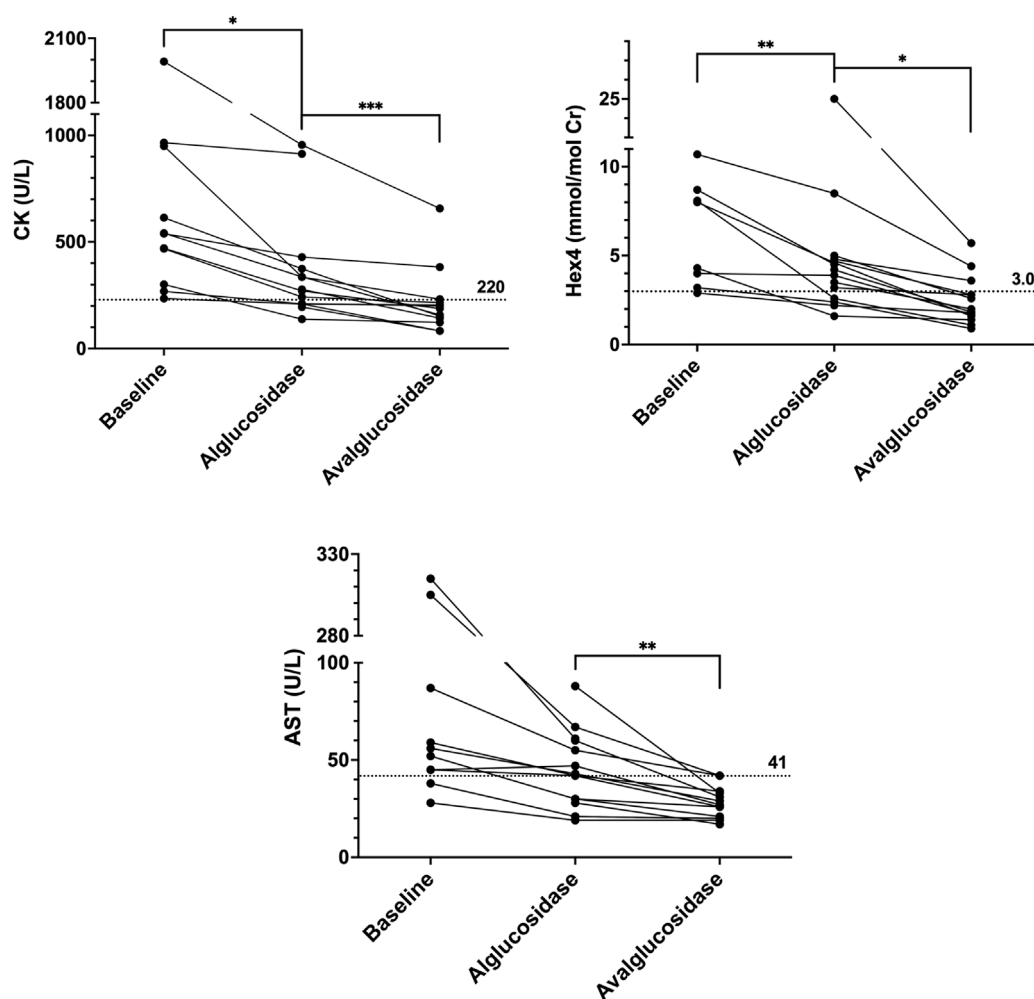


FIGURE 2

CK, Hex4, and AST trends. Baseline values are the last known values prior to initiating ERT. Alglucosidase values are the last known values prior to the switch. Avalglucosidase values are the most recent values available in patient's chart. Dotted horizontal lines are upper limits of normal.

the 6MWT or in the percent predicted, whether analyzed as a group or by level of severity.

However, looking at individual 6MWT performances at the most recent visit, 8/12 (67%) did show an increase in distance walked (mean increase 39.4, range 2.4–80.2 m) while 4/12 (33%) showed a decrease in distance walked (mean decrease –72.7, range –84.3 to –50.0 m). Using a minimal detectable change (MDC) cutoff of 5% change in distance walked for the 6MWT (Claeys et al., 2022), 5/12 patients (41.7%) showed an increase greater than the MDC, 3/12 (25%) showed improvements that did not meet the MDC, and 4/12 (33.3%) had a decrease greater than the MDC.

To look at clinically significant changes on the 6MWT at the individual level, a minimal clinically important difference (MCID) of 30 m was used, as suggested for adults with neuromuscular disorders (but not Pompe-specific) (van der Ploeg et al., 2010; Bohannon and Crouch, 2017). At the most recent visit, 5/12 participants (41.7%) showed a clinically important increase in distance walked (mean increase 60.5, range 33.6–80.2 m), while 3/12 (25%) improved but did not show a clinically important difference (mean increase 18.4, range 2.4–21.6 m), and 4/12 (33.3%) showed a

clinically important decrease in distance walked (mean decrease –72.7, range –84.3 to –50.0 m).

Full 6MWT trends are included in [Supplementary Figure S2](#).

GSGC

For the total GSGC (qualitative) score, 2/12 (16.7%) showed improvement (both by 2 points), 7/12 (58.3%) remained stable (no change in score), and 3/12 (25%) declined (by an average of 1.25, range 1–3) at their most recent visit. Full GSGC trends are included in [Supplementary Figure S3](#). While most patients showed stability in overall GSGC score at each of the post-switch time points, there were notable trends of improvement in the time it took to walk 10 m (Gait). At the most recent visit, there were no statistically significant changes (alpha of 0.05) in the Stairs, Gowers, or Chair quantitative (timed) scores.

There is no published MDC or MCID for gait speed in Pompe, but using an MDC of 0.15 m/s (Middleton et al., 2015) as a cutoff, comfortable (self-selected) gait speed improved in 5/12 (41.7%)

TABLE 4 PT outcomes at most recent visit. Patients were categorized based on GSGC score prior to the switch as having mild (GSGC 4–11, green), moderate (GSGC 12–19, yellow), or severe (GSGC 20–27, red) impairment. Notably, patients who declined on avalglucosidase were more likely to be those with severe impairments, while those with moderate and mild impairments were generally more likely to stabilize or improve. An MDC of 5% was used to qualify as a change in 6MWT distance, and an MCID of 18.9% change was used for gait speed. Patients with any increase in QMFT, GMFM, and BOT2 were placed in the improved category, and any decrease in score was considered a decline. For GSGC, any increase in score was considered a decline, and any decrease in score was considered improved.

	6MWT	GSGC	Comfortable gait speed	QMFT	GMFM	BOT2
Improved	3F, 9M, 16M	15M	15M, 16M	1F, 15M, 16M	15M	16M
	5F	12F	2F, 5F	2F		
	4M		4M, 6F	12F		
Stable	1F, 14M	1F, 3F, 9M, 16M	1F, 3F, 9M, 14M	3F, 9M	9M, 16M	–
	2F	2F	12F			
		4M, 6F				
Declined	15M	14M	7F	14M	–	–
	6F, 7F, 12F	5F		6F, 4M, 7F		
		7F				

patients (mean improvement 0.33, range 0.24–0.47 m/s), remained stable in 7/12 (58.3%) (mean change 0.04, range –0.12–0.14 m/s), and declined in none at their most recent visit. When applying the gait speed cutoffs for Duchenne muscular dystrophy, given its similar gait presentation to Pompe, 6/12 patients met the lower MCID of 18.9% of baseline indicating clinically significant improvement, and 4/12 met the higher bar of 31.1% (McDonald et al., 2013). Two patients (P4, P7) had changes that were significant using both MCID cutoffs, but their baseline walking speeds were low enough that these cutoffs were lower than the MDC of 0.15 m/s. Patient 4 had significant improvement (+0.10 m/s) and patient 7 had a significant decline (–0.12 m/s).

For the whole group, both the mean comfortable gait speed and mean fast gait speed were faster at the most recent visit post-switch, showing statistical significance at an alpha level of 0.05 (comfortable gait speed pre-switch mean 0.90, range 0.32–1.36 m/s, most recent mean 1.05, range 0.20–1.41 m/s; fast gait speed pre-switch mean 2.13 m/s, range 1.49–2.76, most recent mean 2.48 m/s, range 1.61–3.73). See Supplementary Figures S4, S5 and Supplementary Table S7 for full comfortable and fast gait speed data.

QMFT

Eleven of the twelve patients had QMFT data; of these, 5/11 (45%) had improved scores, 2/11 (18%) remained stable with no change in score, and 4/11 (36%) had scores that declined at their most recent visit. The average increase in those who improved was 5 points (range 1–11), while the average decrease in decliners was –2.75 points (range –5 to –1). No MDC has been established for the QMFT. Full QMFT data including individual item response is detailed in Supplementary Table S5.

GMFM and BOT-2

Only three patients (P9, P15, P16) had GMFM data, and all were seen only once after the switch. The total GMFM score improved

from 98.86% to 100% for one patient and remained unchanged for the other two. One patient (P16) had BOT-2 scores and his score improved on the running speed/agility scale score from 12 to 14, improved on the strength and agility standard score from 43 to 46 (24th to 35th percentile), and remained unchanged on the strength scale score at 11. For both of these subtests, he placed in the “average” descriptive category before and after the switch.

Pulmonary function testing

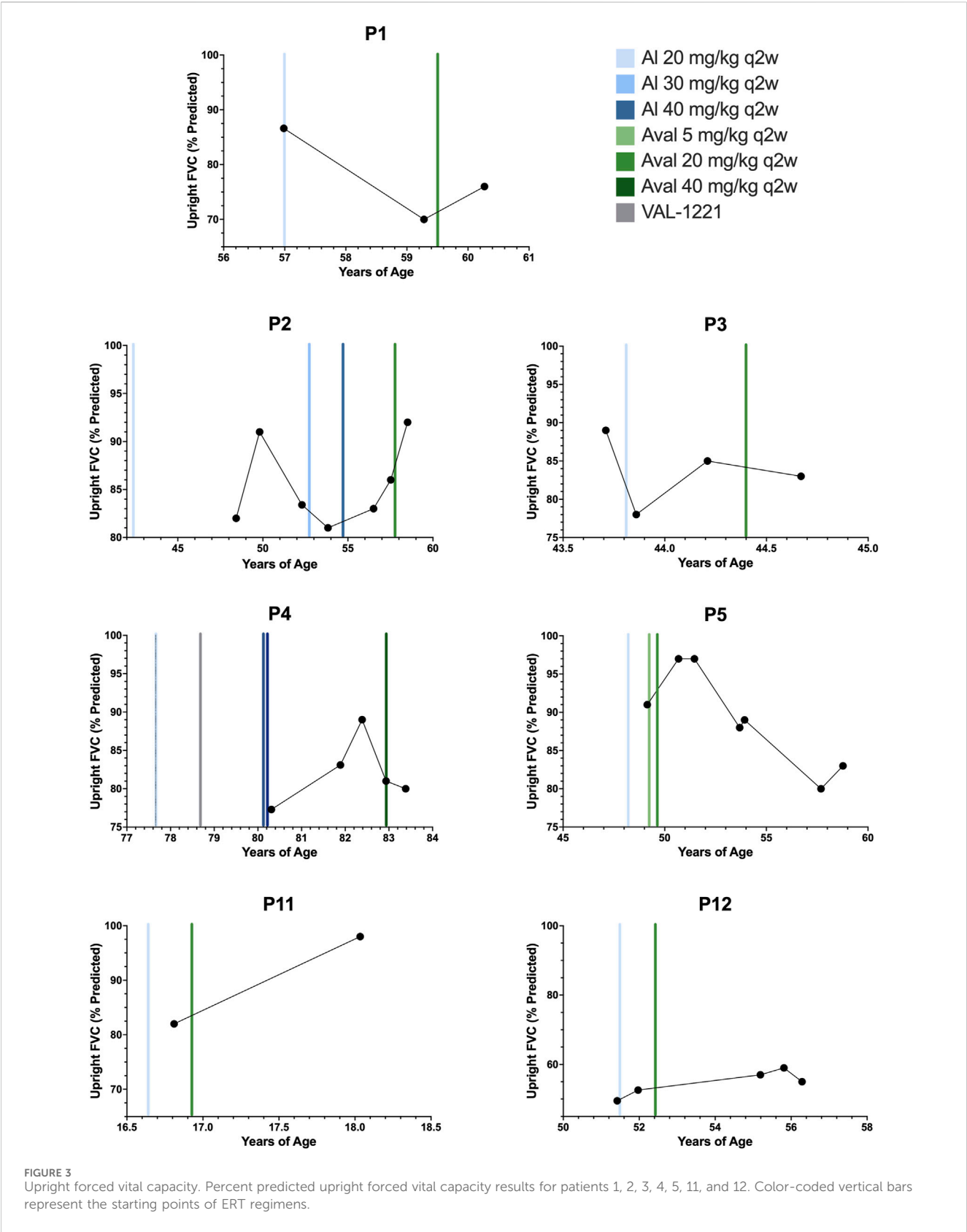
Longitudinal pulmonary function test (PFT) data was available for *n* = 7 patients (P1-5, P11, P12) and is depicted in Figure 3. To our knowledge, no specific minimal clinically important change (MCIC) for PFTs in Pompe disease has been established (Lachmann and Schoser, 2013).

Of *n* = 7 patients, *n* = 4/7 (P1, P2, P11, P12) experienced improvement in percent predicted upright forced vital capacity (FVC) after switching to avalglucosidase alfa with an average improvement (Mean ± SD) of +7.6% ± 5.9%. The remaining *n* = 3/7 patients (P3, P4, P5) experienced decreases. The average decrease was –3.7% ± 3.8%. Overall, the mean change in percent predicted FVC was +2.7 ± 7.6%. The median interval between baseline PFT testing on alglucosidase and most recent evaluation on avalglucosidase was 12 months, ranging from 5.4 months to 9.6 years. Notably, one patient who declined (P5) did demonstrate improvements in FVC for over 2 years and peaked at 97% before declining through her most recent evaluation to 83% at 9.6 years post-switch.

Patient-reported outcomes

Patient-reported outcome (PRO) data was available for *n* = 4 patients (P2, P3, P6, and P9). All PRO data for dyspnea, physical function, fatigue, and lower back pain is depicted in Figure 4.

Dyspnea is reported on a scale from 0 to 99 with higher scores indicating increased severity of dyspnea with common daily



activities. Dyspnea improved in $n = 4/4$ patients with an average (Mean \pm SD) difference of -7.00 ± 4.08 . Physical function is reported on a scale from 20 to 99 with higher scores indicating increased physical function and ability to carry out daily life activities. Physical function improved in $n = 3/4$ patients with an average difference of 1.25 ± 2.36 . Fatigue is reported on a scale from 8 to 40 with higher

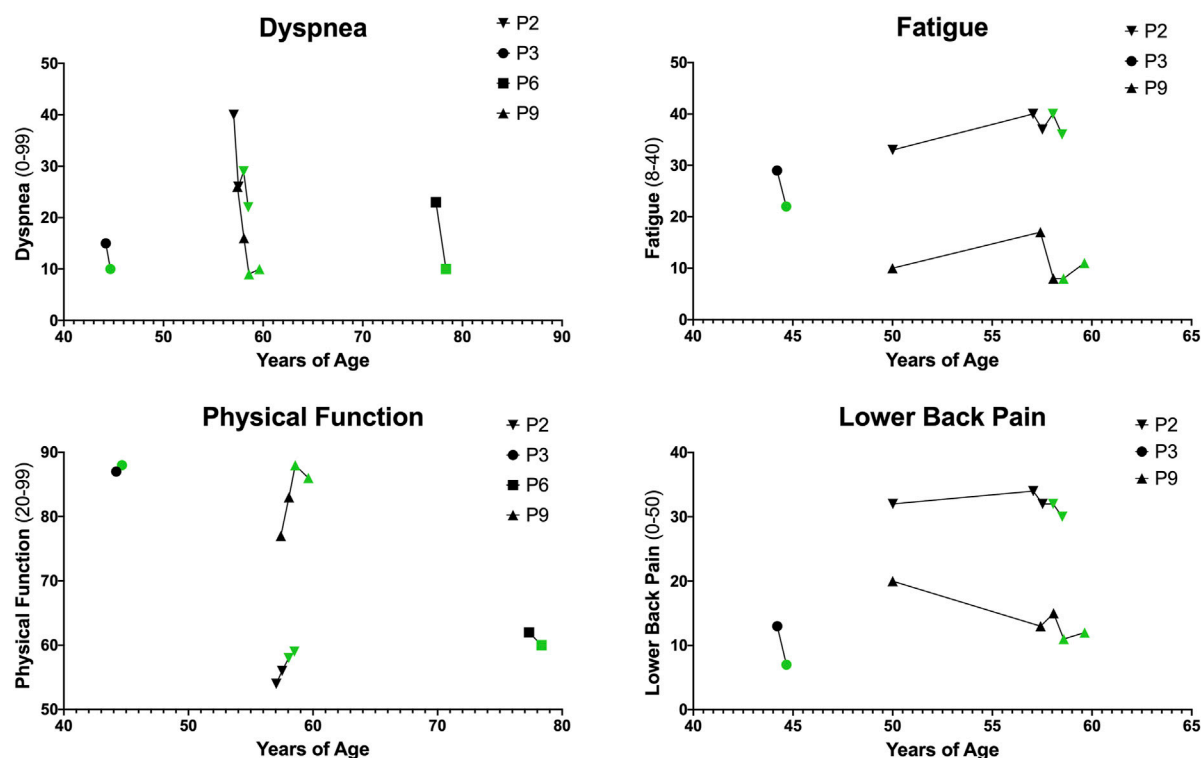


FIGURE 4

Patient-Reported Outcomes (PROs). PROs for dyspnea, physical function, fatigue, and lower back pain. Higher dyspnea scores (range 0–99) indicate increased severity of dyspnea with common daily activities. Higher physical function scores (range 20–99) indicate increased physical function and ability to carry out daily life activities. Higher fatigue scores (range 8–40) indicate increased fatigue on average over the past week. Higher lower back pain scores (range 0–50) indicate greater severity of lower back pain and impact on life.

scores indicating increased fatigue on average over the past week. Fatigue improved in $n = 2/3$ patients and with an average difference of -1.67 ± 5.03 . Lower back pain, reported via the Oswestry Disability Index, ranges from 0 to 50 with higher scores indicating greater severity of lower back pain and disability. In this cohort, $n = 3/3$ patients reported improved back pain with an average difference of -3.67 ± 2.08 .

Safety outcomes and antidrug antibodies

There were five reports of infusion reactions while receiving alglucosidase alfa. Patient 2 reported experiencing intermittent diarrhea with infusions. Patient 6 reported an event in which she experienced epigastric pain, tongue swelling, and uncontrollable salivation during an alglucosidase infusion. This resolved with diphenhydramine. Patient 13 reported repeated episodes in which she experienced a full-body rash, emotional difficulties, bloating, body pain, hand/body tremors, nausea, and fatigue. These were associated with the switch to more frequent (weekly) and longer (7–7.5 h) alglucosidase alfa infusions, and they resolved with the switch to avalglucosidase alfa. Finally, patients 7 and 12 reported mild reactions of chills and itching, respectively. There was one report of infusion reaction in this cohort after the change to avalglucosidase alfa; patient 11 reported two episodes of fever associated with infusions. All $n = 7$ patients on home infusions

of alglucosidase alfa were able to continue home infusions for avalglucosidase alfa, and $n = 3$ additional patients switched to home infusions after switching ERT.

Most recent and peak ADA titers for all patients are listed in [Supplementary Tables S3, S4](#), and full titer history for each patient is detailed in [Supplementary Figure S1](#). Out of $n = 10$ patients with data available while on alglucosidase alfa, $n = 9/10$ had positive ADA titers. All positive titers fell below 12,800 except for patients 6 and 9, who both peaked at 12,800. Patient 9 only reached this level at one timepoint, while patient 6 reached this level three times over the course of 5 years. At the time of switching, P6 had a titer of 12,800 and P9 had a titer of 200.

Out of $n = 13$ patients with ADA data available while on avalglucosidase alfa, $n = 8/13$ had positive titers. Notably, patient 6 had negative titers while on avalglucosidase. All positive titers fell below 12,800 except for patients 11 and 14, who peaked at 102,400 and 25,600, respectively. Patient 11 has three ADA data points while on avalglucosidase alfa, and these are trending downward (102,400, 51,200, 25,600), most recently 20.34 months post-switch. Patient 14 had two ADA data points (12,800 and 25,600) since switching to avalglucosidase alfa, most recently 12.39 months post-switch.

Patient 11 was on alglucosidase for 2.3 months prior to switching, and she had no ADA titer data from this period. Since the switch, she has shown an increase in percent predicted FVC of 16%, though this is limited to two available time points. Her biomarkers showed improvements of 11% in CK and AST, both

of which normalized, as well as an improvement of 63% in Hex4, which has remained within normal limits. She has had no infusion-associated reactions. Patient 14 was on alglucosidase for 9 months prior to switching and had titers of 6,400 at 3.71 months before switching. For patient 14, PT assessment showed stability in 6MWT and gait speed with a worsening of GSGC and QMFT by one point each. Biomarkers in this patient showed improvements of 31% in CK, 56% in Hex4, and 24% in AST. CK (657 U/L) and AST (42 U/L) remained above the upper limit of normal, while Hex4 normalized. He has also had no infusion-associated reactions. Overall, limited post-switch data in patients 11 and 14 present a mixed bag of outcomes, and the impact of these elevated titers is unclear at this time. Continued close follow-up is necessary to evaluate their effects.

Patient 13: non-ambulatory case

Patient 13 represents the first reported case of a patient with LOPD who is non-ambulatory and switched from alglucosidase alfa to avalglucosidase alfa. She was diagnosed at age 21 months and retrospectively reported symptom onset within the first year of life without cardiomyopathy. Her initial symptoms were low tone, decreased head control, and delayed achievement of motor milestones. From a motor standpoint, she was able to independently drive her motorized wheelchair using a joystick at her most recent assessment, but she has been dependent for all functional mobility since 3 years of age and requires full-time care. She was initially managed with nasal intermittent positive pressure ventilation but progressed to tracheostomy tube and ventilator dependence by age 4. Her past medical history is also significant for T4-sacral posterior spinal fusion surgery, oral-maxillary reconstructive surgery, history of fractures secondary to severe osteoporosis, and severe recurrent kidney stones secondary to poor water intake. She received alglucosidase alfa infusions for 19 years, up to a maximum dose of 40 mg/kg q1w. Due to a combination of lack of response to alglucosidase, infusion-associated reactions (full-body rash, emotional difficulties, myalgias, nausea, fatigue), and prolonged infusion time (7–7.5 h), she switched to avalglucosidase alfa at 40 mg/kg q2w. From her perspective, she reported improvements on avalglucosidase that far outweigh the minimal, if any, improvements that she noted on alglucosidase alfa.

Her hand dexterity was measured using the 9-HPT by her local occupational therapist. She was unable to complete the standard 9-HPT prior to switching but was able to complete a modified version using easy grip pegs. She was making improvements prior to the switch and demonstrated continued improvements in her right hand after the switch, from 110 s prior to switch to 87 s on day 12 and 57 s on day 286. She also demonstrated continued improvements in her left hand, from 162 s prior to the switch to 110 s on day 12 and 59 s on day 286. Furthermore, by day 286, she had also improved enough to complete the standard 9-HPT with her right hand, improving from 98 s on day 286 to 58 s on day 518 (norm is 16.04 s \pm 1.82) (Oxford Grice et al., 2003). She was able to complete the task with her left hand by day 356, but a time was not documented. She was only able to complete part of the test with her left hand on day 433, which was attributed to edema and pain noted in her arm, but by day 518, she was again able to complete it with her left hand in 116 s. Full 9-HPT details are available in [Supplementary Table S6](#). She did not have baseline pinch data, but when tested, she demonstrated improved lateral pinch from day 290 to

day 465 from 3.83 to 4.0 lbs on right and from 2.77 to 3.17 lbs on left, respectively (right hand norm 17.7 \pm 2.1 lbs and left hand norm 16.6 \pm 2.1 lbs) (Mathiowetz et al., 1985).

Subjectively, she and her mother reported improvements in hand function, head control, breathing, and endurance, all substantiated by her local OT and PT. Her reported fatigue with school activities and transfers decreased from 9/10 to 5/10. She reported an improved ability to raise a utensil to her mouth, move her cell phone from her lap to her armrest, use a keyboard, and flip her notebook. Remarkably, she also reported being able to chew longer without fatigue, suck through a straw, and blow out her birthday candles for both birthdays since switching. She also reported being able to breathe for 5 min off of her ventilator, which she has not been able to do for 12–13 years. Overall, she reported having more energy, less brain fog, and feeling happier.

Discussion

For many years after its approval, alglucosidase alfa remained the standard of care for patients with Pompe disease. The treatment has been lifesaving, but many patients on alglucosidase alfa infusions continue to decline while on treatment and require increased dosages, an indication that there remained an unmet need in the management of Pompe disease (Khan et al., 2020b; Diaz-Manera et al., 2021; Dimachkie et al., 2022). Second-generation ERT with avalglucosidase alfa was designed to exhibit enhanced uptake in target cells, thereby improving clinical response. Over the last few years, several studies have provided evidence of improved outcomes with avalglucosidase, though these studies used strict inclusion criteria and focused primarily on treatment-naïve patients. The COMET trial included $n = 49$ patients who switched after just 49 weeks on alglucosidase alfa, and Dimachkie et al., 2022 included $n = 10$ patients who switched after 0.9–7 years (Diaz-Manera et al., 2021; Kishnani et al., 2021; Dimachkie et al., 2022). This study describes real-world experiences in patients with LOPD, including $n = 8$ on alglucosidase alfa for more than 3 years, $n = 7$ for more than 5 years. The data generated provides additional evidence that switching from alglucosidase alfa to avalglucosidase alfa may lead to better outcomes across a variety of measures.

Our cohort of fifteen patients includes a diversity of genotypes and presentations, incorporating patients across a wide age range and broad spectrum of severity. We report data across a variety of measures and discuss the first report of outcomes when switching from alglucosidase to avalglucosidase in a patient with LOPD who uses a power wheelchair and ventilator full-time. Dosages and durations of ERT regimens varied widely among the cohort. $n = 8/15$ patients received alglucosidase alfa for greater than 3 years before switching, and $n = 7/15$ received it for greater than 5 years. Notably, we present four patients (P4, P7, P8, P13) receiving avalglucosidase at doses of 40 mg/kg q2w. We also present one patient (P2) who switched from alglucosidase alfa at a dose of 40 mg/kg q2w to avalglucosidase alfa at 20 mg/kg q2w and demonstrated improvement. Patients 4, 9, and 12 also stood out from the others, as patients 4 and 9 have a history of enrollment in clinical trials, and patient 12 stopped ERT for 3 months due to insurance issues. Enrollment in these clinical trials did not appear to have any positive impact on the clinical course of these patients; both

TABLE 5 Overall outcome heat map. Changes in all outcomes organized by disease severity and color-coded (improvement in green, stability in blue, decline in red). Number of months on alglucosidase and avalglucosidase (at any dose) included. Laboratory values that remain elevated beyond the reference range after the switch to avalglucosidase have been bolded.

Severity		P1	P3	P9	P11	P14	P15	P16	P2	P5	P4	P6	P7	P8	P12	P13
		Mild	Mild	Mild	Mild	Mild	Mild	Mild	Mod	Mod	Sev	Sev	Sev	Sev	Sev	Sev
Al. Months		30	7	111	2.3	9	75	146	181	12	46	72	12	109	11	229
Aval. Months		15	17	8	18	13	17	6	14	115	19	12	56	12	41	14
Labs	CK (%)	-53	-11	-31	-11	-31	-31	-	-49	-59	-11	-57	-5	-2	-60	-
	Hex4 (%)	-56	-58	-13	-63	-56	-48	-13	-40	-65	-18	-43	-25	-	-48	-77
	AST (%)	-33	-19	-13	-11	-24	-37	-	-30	-48	-5	-39	-63	-43	0	-5
PT Metrics	6MWT Dist. (%)	+4.4	+16.3	+7.6	-	+1.9	-14.0	+12.9	-0.6	+8.8	+74.3	-34.7	-50.0	-	-39.7	-
	GSGC	0	0	0	-	1	-2	0	0	3	0	0	1	-	-2	-
	Gait (m/s)	+0.14	+0.04	+0.06	-	-0.09	+0.36	+0.28	+0.24	+0.31	+0.10	+0.47	-0.12	-	+0.04	-
	QMFT	+2	0	0	-	-1	+11	+5	+1	-	-5	-2	-3	-	+6	-
	GMFM (%)	-	-	0	-	-	+1.43	0	-	-	-	-	-	-	-	-
	BOT-2	-	-	-	-	-	-	+3	-	-	-	-	-	-	-	-
PFTs	FVC (%)	+6	-2	-	+16	-	-	-	+6	-8	-1	-	-	-	+2.4	-
PROs	Dyspnea	-	-5	-6	-	-	-	-	-4	-	-	-13	-	-	-	-
	Fatigue	-	-7	+3	-	-	-	-	-1	-	-	-	-	-	-	-
	PF	-	+1	+3	-	-	-	-	+3	-	-	-2	-	-	-	-
	LBP	-	-6	-3	-	-	-	-	-2	-	-	-	-	-	-	-

continued to decline and withdrew from the trials before 2 years of enrollment. Despite all of these differences in ERT regimens, these patients demonstrated improvement across most outcomes (see overview of outcomes in Table 5).

In particular, we highlight patient 13, who exhibited severe, progressive disease despite receiving 19 years of alglucosidase therapy up to a maximum dose of 40 mg/kg q1w, which she received for 2.5 years. She has now been on avalglucosidase alfa at 40 mg/kg q2w for a total of 18 months. Although she was not able to undergo the standard PT assessments, she demonstrated continued objective improvements in 9-HPT time and lateral pinch strength after switching to avalglucosidase. She also showed substantial improvement in her Hex4 biomarker. She noted considerable improvement of her motor function, breathing ability, endurance, and overall quality of life, as well as resolution of the infusion-associated reactions that she experienced while on alglucosidase. She has had physical and occupational therapy on and off throughout her life and was participating in both while on avalglucosidase; thus, it cannot be determined how much of her improvement was due to switching ERT and how much was due to PT/OT interventions. This is the first outcome data in a non-ambulatory Pompe patient with the switch from alglucosidase to avalglucosidase.

Some patients in this cohort with particularly severe clinical manifestations appeared to benefit from a higher dosage of avalglucosidase at 40 mg/kg q2w. P4, P8, and P13 transitioned to this dose directly from 40 mg/kg alglucosidase, at either q1w or q2w, and P7 increased to 40 mg/kg q2w after demonstrating a suboptimal

response to 20 mg/kg q2w. In the management of patients with Pompe disease, there is often a need to utilize dosing beyond that recommended by the package insert to maximize benefit to the patient. These four patients showed improvement in clinical status without any adverse effects or safety concerns from the higher dosage. Further research into the safety and efficacy of increasing avalglucosidase dosage beyond standard recommendations is needed.

Laboratory markers (CK, Hex4, AST, ALT) improved in all patients at statistically significant levels from alglucosidase alfa to avalglucosidase alfa. Notably, while laboratory values did decrease substantially from baseline to alglucosidase alfa, a majority of those values remained above the upper limit of normal. Switching to avalglucosidase alfa was associated with further decreases in biomarkers, more than doubling the number that fell within the reference range for normal. These improvements in biomarkers were accompanied by evidence of improvement in clinical function measured in physical therapy metrics, PFTs, and PROs.

Improvement in motor and pulmonary function is a much sought-after outcome in the treatment of Pompe disease, and in this cohort, $n = 4/7$ patients had improvements in percent predicted upright FVC, while $n = 3/7$ showed a decline in percent predicted upright FVC. Unfortunately, without a true established MCIC for upright FVC in Pompe disease, interpretation of these changes is challenging. PFT data was limited, and patient 11 in particular only had two data values and no true historical baseline was able to be established for her. Notably, patient 5, the one patient with a decline in FVC, experienced an early improvement in percent predicted

FVC from 91% to 97%, recorded around 18 months after switching. This improvement persisted at 28 months after the switch. However, the next set of PFTs at 54 months post-switch showed a decline, which progressed for the rest of her treatment history arriving at her most recent value of 83%. Her supine values followed a similar trend, decreasing from 67% pre-switch to 47% at most recent evaluation. Upon chart review, no direct cause for this decline could be identified. Despite worsening in PFTs, patient 5 did show improvement in laboratory markers and PT assessments.

Notably, those with mild-to-moderate functional impairments were the most likely to show improvement or stabilization in their PT scores, suggesting that the individuals with less established muscle damage retained greater capacity for functional improvement. A majority ($n = 8/12$) of patients have improved or remained stable in 6MWT distance since the switch. Of the four that did decline, three were among those with the most impaired gait, and one was a ten-year-old with low effort during the test (2/10 on the self-reported effort scale and minimal change in heart rate during the test, from 84 to 86 bpm).

Most ($n = 9/12$) patients stabilized or improved on the GSGC at their most recent visit, with additional positive trends noted in the timed functional sub-components of the GSGC. There were statistically significant improvements in comfortable and fast gait speed, while supine-to-stand (Gowers) and sit-to-stand (Chair) showed trends toward improvement that were not statistically significant. For gait speed, there were meaningful clinical improvements or stability for all but one patient at all time points after the switch. Gait speed is associated with various outcomes and functional categories (Middleton et al., 2015), thus stability or improvement in speed is important for functional capacity. A speed below 0.8 m/s is clinically significant, as it indicates that the patient may be categorized functionally as a limited community ambulator, while speeds below 0.42 m/s indicate that they are more likely a household only ambulator (Perry et al., 1995). Patients with severe functional impairments had the slowest walking speeds, yet one moved from the household-only ambulator category to limited-community ambulator (P6). The two patients in the moderately impaired group (P2, P5) had gait speeds between the mild and severe groups, and both made gains which placed them more firmly in the community ambulator category. All of the mildly impaired patients had gait speeds placing them in the community ambulator group, and they remained stable or improved.

QMFT scores also improved or stabilized in a majority ($n = 7/11$) of patients, with increases ranging from +1 to +11. No MCID has been established for the QMFT, limiting interpretation of the clinical significance of these data. GMFM and BOT-2 were available for fewer patients ($n = 3$ and $n = 1$, respectively), and they showed improvement or stabilization in all cases.

Finally, although PRO data was limited in this cohort, the majority of patients that had data at multiple timepoints showed improvements in dyspnea ($n = 4/4$), physical function ($n = 3/4$), fatigue ($n = 2/3$), and lower back pain ($n = 3/3$).

There were five reports of infusion reactions while receiving alglucosidase alfa and one report of infusion reactions after the switch to avalglucosidase alfa. While on alglucosidase alfa, $n = 9/10$ patients had positive ADA titers ranging from 400 to 12,800. While on avalglucosidase alfa, $n = 8/13$ patients had positive ADA titers

ranging from 400 to 102,400. ADA peak titers $\geq 12,800$ have been associated with an increased risk of infusion-associated reactions and a trend toward decreased pharmacodynamic response as measured by percent change in urinary Hex4 (Sanofi Genzyme, 8/2021). Two patients (patients 11 and 14) had sustained titers above 12,800.

Patient 11 has three ADA data points while on avalglucosidase alfa, and these are trending downward (102,400, 51,200, 25,600). Assessments in this patient since switching include PFTs and biomarkers. On PFTs, she was limited to two data points without a clear baseline, increasing from 82% to 98%. Biomarkers showed improvements of 11% in CK and AST, both of which normalized, as well as an improvement in Hex4, which has remained within normal limits. Other than two episodes of fever associated with infusions, she has had no infusion-associated reactions.

Patient 14 had two ADA data points (12,800 and 25,600) since switching to avalglucosidase alfa. Initial follow-up data in this patient includes PT assessments and biomarkers. He showed stability in 6MWT and gait speed, with a worsening of GSGC and QMFT by one point each. Biomarkers in this patient showed improvements of 31% in CK, 56% in Hex4, and 24% in AST. CK (657 U/L) and AST (42 U/L) remain above the upper limit of normal, while Hex4 normalized. He has had no infusion-associated reactions.

Overall, initial post-switch assessments in patients 11 and 14 present a mixed bag of outcomes, and there is no clear clinical impact of these elevated titers as of yet. Continued close follow-up is necessary to evaluate their effects.

Limitations of this study include its relatively small cohort ($n = 15$) and short follow-up period. Many of the patients did not complete all of the evaluations used therein, and consequently some draw upon limited amounts of data. For instance, longitudinal PRO outcomes were only available in $n = 4$ patients; this was largely due to a lack of consistent data obtainable during the COVID-19 pandemic. Moreover, the selection of patients took place via convenience sampling, utilizing patients at the Duke metabolic clinic who met the inclusion criteria of switching ERT regimens. While this sample included a variety of patients, it may not be statistically representative of the general population of patients with LOPD. Despite thorough and comprehensive review of patient charts for the abstraction of data, it is possible that some data was missing from the chart or otherwise unavailable for use in this study. Future studies should be oriented toward substantiating these findings across a larger cohort of patients and with stricter control of confounding variables. The short follow-up periods resulted in data from only a few follow-up visits after the switch. This was especially apparent with patient 16, who had PT follow up only at 72-days post-switch. Continued follow-up is necessary to fully understand how patients are faring. This study also applied the MCID from other chronic pulmonary diseases to FVC results in LOPD, a common but imperfect practice that may not adequately reflect the pathological process in Pompe disease (Lachmann and Schoser, 2013). Finally, it should be noted that many of the PT evaluations were performed by different PTs. Although all examiners were experienced with Pompe disease, some discrepancies between scores, especially QMFT, were seen between different evaluators, reflecting the potentially decreased inter-rater reliability in a real-world clinical setting compared to a research setting.

In conclusion, many patients in this cohort stabilized or improved after the switch from alglucosidase alfa to avalglucosidase alfa. A subset of patients with particularly severe manifestations appeared to show more persistent decline. Stabilization already represents a much-improved outcome compared to the well-documented natural history of progressive decline in LOPD, but many patients in this cohort also showed tangible improvements after the switch (Hagemans et al., 2005; Winkel et al., 2005; Dimachkie et al., 2022). Overall, stabilization or improvement was seen across several different outcome metrics, including laboratory markers ($n = 15/15$), PT evaluations ($n = 8/12$ in 6MWT, $n = 9/12$ in GSGC, $n = 11/12$ in gait speed, and $7/12$ in QMFT), PFTs ($n = 4/7$), and PROs ($n = 3/4$ in physical function or $n = 4/4$ in dyspnea, fatigue, and back pain). This study presents additional evidence that switching from alglucosidase to avalglucosidase may be associated with improved outcomes in a subset of patients with LOPD.

Data availability statement

The original contributions presented in the study are included in the article/Supplementary Material, further inquiries can be directed to the corresponding author.

Ethics statement

The studies involving humans were approved by the Duke University Health System Institutional Review Board. The studies were conducted in accordance with the local legislation and institutional requirements. Written informed consent for participation in this study was provided by the participants' legal guardians/next of kin. Written informed consent was obtained from the individual(s), and minor(s)' legal guardian/next of kin, for the publication of any potentially identifiable images or data included in this article.

Author contributions

CC: Data curation, Formal Analysis, Investigation, Methodology, Project administration, Software, Visualization, Writing—original draft, Writing—review and editing. TB: Data curation, Formal Analysis, Visualization, Investigation, Writing—original draft, Writing—review and editing. LC: Formal Analysis, Methodology, Validation, Visualization, Writing—review and editing. PK: Conceptualization, Supervision, Writing—review and editing.

Funding

The author(s) declare that no financial support was received for the research, authorship, and/or publication of this article.

Acknowledgments

The authors would like to thank Caitlin Williams and Mary McGann for their assistance in coordinating care for these patients as well as Stephanie DeArme and Seung-Hye Jung for their assistance with data collection. The authors would also like to thank the Emerson & Barbara Kampen Foundation, Judy and Monty Frost, Abigail and JB Spaulding, and Marshall's Mountain for their generous contributions to research efforts in Pompe disease.

Conflict of interest

PK has received research/grant support from Sanofi Genzyme and Amicus Therapeutics. PK has received consulting fees and honoraria from Sanofi Genzyme, Amicus Therapeutics, Maze Therapeutics, Bayer and Asklepios Biopharmaceutical, Inc. (AskBio). PK is a member of the Pompe and Gaucher Disease Registry Advisory Board for Sanofi Genzyme, Pompe Disease Advisory Board for Amicus Therapeutics, and Advisory Board for Baebies. PK has equity with Maze Therapeutics and has held equity in Asklepios Biopharmaceuticals, and may receive milestone payments related to that equity in the future. TB has participated in research funded by Sanofi Genzyme, Amicus Therapeutics and Asklepios Biopharmaceutical, Inc. (AskBio). TB is a member of the Pompe Physical Therapy Advisory Board for Sanofi Genzyme, and 2021 Pompe Disease Advisory Board for Sanofi Genzyme. LC has received honoraria from Genzyme Corporation of Sanofi, Pfizer, and Sarepta for presentations given; has participated in research funded by Amicus, AskBio, AveXis, Biogen, Genzyme Corporation of Sanofi, NS Pharma, Pfizer, PTC Therapeutics, Reveragen, and TRiNDS (Therapeutic Research in Neuromuscular Disorders Solutions); and is a member of the North American Pompe Registry Board of Advisors.

The remaining author declares that the research was conducted in the absence of any commercial or financial relationships that could be construed as a potential conflict of interest.

Publisher's note

All claims expressed in this article are solely those of the authors and do not necessarily represent those of their affiliated organizations, or those of the publisher, the editors and the reviewers. Any product that may be evaluated in this article, or claim that may be made by its manufacturer, is not guaranteed or endorsed by the publisher.

Supplementary material

The Supplementary Material for this article can be found online at: <https://www.frontiersin.org/articles/10.3389/fgene.2024.1309146/full#supplementary-material>

References

- Angelini, C., Semplicini, C., Ravaglia, S., Moggio, M., Comi, G. P., Musumeci, O., et al. (2012). New motor outcome function measures in evaluation of late-onset Pompe disease before and after enzyme replacement therapy. *Muscle Nerve* 45, 831–834. doi:10.1002/mus.23340
- ATS Committee on Proficiency Standards for Clinical Pulmonary Function Laboratories (2002). ATS statement: guidelines for the six-minute walk test. *Am. J. Respir. Crit. Care Med.* 166, 111–117. doi:10.1164/ajrccm.166.1.at1102
- Bohannon, R. W., and Crouch, R. (2017). Minimal clinically important difference for change in 6-minute walk test distance of adults with pathology: a systematic review. *J. Eval. Clin. Pract.* 23, 377–381. doi:10.1111/jep.12629
- Clayes, K. G., D'hondt, A., Fache, L., Peers, K., and Depuydt, C. E. (2022). Six-Minute walk distance is a useful outcome measure to detect motor decline in treated late-onset Pompe disease patients. *Cells* 11, 334. doi:10.3390/cells11030334
- Deitz, J. C., Kartin, D., and Kopp, K. (2007). Review of the bruininks-oseretsky test of motor proficiency, second edition (BOT-2). *Phys. Occup. Ther. Pediatr.* 27, 87–102. doi:10.1300/j006v27n04_06
- Desai, A. K., Li, C., Rosenberg, A. S., and Kishnani, P. S. (2019). Immunological challenges and approaches to immunomodulation in Pompe disease: a literature review. *Ann. Transl. Med.* 7, 285. doi:10.21037/atm.2019.05.27
- De Vries, J. M., Van Der Beek, N. A., Kroos, M. A., Ozkan, L., Van Doorn, P. A., Richards, S. M., et al. (2010). High antibody titer in an adult with Pompe disease affects treatment with alglucosidase alfa. *Mol. Genet. Metab.* 101, 338–345. doi:10.1016/j.ymgme.2010.08.009
- Diaz-Manera, J., Kishnani, P. S., Kushlaf, H., Ladha, S., Mozaffar, T., Straub, V., et al. (2021). Safety and efficacy of avalglucosidase alfa versus alglucosidase alfa in patients with late-onset Pompe disease (COMET): a phase 3, randomised, multicentre trial. *Lancet Neurol.* 20, 1012–1026. doi:10.1016/S1474-4422(21)00241-6
- Dimachkie, M. M., Barohn, R. J., Byrne, B., Goker-Alpan, O., Kishnani, P. S., Ladha, S., et al. (2022). Long-term safety and efficacy of avalglucosidase alfa in patients with late-onset Pompe disease. *Neurology* 99, e536–e548. doi:10.1212/WNL.000000000000200746
- Enright, P. L., and Sherrill, D. L. (1998). Reference equations for the six-minute walk in healthy adults. *Am. J. Respir. Crit. Care Med.* 158, 1384–1387. doi:10.1164/ajrccm.158.5.9710086
- Fairbank, J. C., Couper, J., Davies, J. B., and O'Brien, J. P. (1980). The Oswestry low back pain disability questionnaire. *Physiotherapy* 66, 271–273.
- Hagemans, M. L., Winkel, L. P., Van Doorn, P. A., Hop, W. J., Loonen, M. C., Reuser, A. J., et al. (2005). Clinical manifestation and natural course of late-onset Pompe's disease in 54 Dutch patients. *Brain* 128, 671–677. doi:10.1093/brain/awh384
- Huggins, E., Holland, M., Case, L. E., Blount, J., Landstrom, A. P., Jones, H. N., et al. (2022). Early clinical phenotype of late onset Pompe disease: lessons learned from newborn screening. *Mol. Genet. Metab.* 135, 179–185. doi:10.1016/j.ymgme.2022.01.003
- Khan, A. A., Boggs, T., Bowling, M., Austin, S., Stefanescu, M., Case, L., et al. (2020a). Whole-body magnetic resonance imaging in late-onset Pompe disease: clinical utility and correlation with functional measures. *J. Inherit. Metab. Dis.* 43, 549–557. doi:10.1002/jimd.12190
- Khan, A. A., Case, L. E., Herbert, M., Dearnley, S., Jones, H., Crisp, K., et al. (2020b). Higher dosing of alglucosidase alfa improves outcomes in children with Pompe disease: a clinical study and review of the literature. *Genet. Med.* 22, 898–907. doi:10.1038/s41436-019-0738-0
- Kim, K. H., Desai, A. K., Vucko, E. R., Boggs, T., Kishnani, P. S., and Burton, B. K. (2023). Development of high sustained anti-drug antibody titers and corresponding clinical decline in a late-onset Pompe disease patient after 11+ years on enzyme replacement therapy. *Mol. Genet. Metab. Rep.* 36, 100981. doi:10.1016/j.ymgmr.2023.100981
- Kishnani, P., Broomfield, A., Davison, J., Labarthe, F., Brassier, A., Hahn, S., et al. (2021). Mini-COMET: individual-level treatment responses in infantile-onset Pompe disease participants receiving avalglucosidase alfa or alglucosidase alfa who previously received alglucosidase alfa. *Mol. Genet. Metabolism* 132, S75–S76. doi:10.1016/s1096-7192(21)00195-5
- Kishnani, P. S., Diaz-Manera, J., Toscano, A., Clemens, P. R., Ladha, S., Berger, K. I., et al. (2023). Efficacy and safety of avalglucosidase alfa in patients with late-onset Pompe disease after 97 Weeks: a phase 3 randomized clinical trial. *JAMA Neurol.* 80, 558–567. doi:10.1001/jamaneurol.2023.0552
- Lachmann, R., and Schoser, B. (2013). The clinical relevance of outcomes used in late-onset Pompe disease: can we do better? *Orphanet J. Rare Dis.* 8, 160. doi:10.1186/1750-1172-8-160
- Li, A. M., Yin, J., Au, J. T., So, H. K., Tsang, T., Wong, E., et al. (2007). Standard reference for the six-minute-walk test in healthy children aged 7 to 16 years. *Am. J. Respir. Crit. Care Med.* 176, 174–180. doi:10.1164/rccm.200607-883OC
- Mathiowetz, V., Kashman, N., Volland, G., Weber, K., Dowe, M., and Rogers, S. (1985). Grip and pinch strength: normative data for adults. *Arch. Phys. Med. Rehabil.* 66, 69–74.
- Mcdonald, C. M., Henricson, E. K., Abresch, R. T., Florence, J., Eagle, M., Gappmaier, E., et al. (2013). The 6-minute walk test and other clinical endpoints in duchenne muscular dystrophy: reliability, concurrent validity, and minimal clinically important differences from a multicenter study. *Muscle Nerve* 48, 357–368. doi:10.1002/mus.23905
- Middleton, A., Fritz, S. L., and Lusardi, M. (2015). Walking speed: the functional vital sign. *J. Aging Phys. Act.* 23, 314–322. doi:10.1123/japa.2013-0236
- Oxford Grice, K., Vogel, K. A., Le, V., Mitchell, A., Muniz, S., and Vollmer, M. A. (2003). Adult norms for a commercially available Nine Hole Peg Test for finger dexterity. *Am. J. Occup. Ther.* 57, 570–573. doi:10.5014/ajot.57.5.570
- Paschall, A., Khan, A. A., Enam, S. F., Boggs, T., Hijazi, G., Bowling, M., et al. (2021). Physical therapy assessment and whole-body magnetic resonance imaging findings in children with glycogen storage disease type IIIa: a clinical study and review of the literature. *Mol. Genet. Metab.* 134, 223–234. doi:10.1016/j.ymgme.2021.10.002
- Pena, L. D. M., Barohn, R. J., Byrne, B. J., Desnuelle, C., Goker-Alpan, O., Ladha, S., et al. (2019). Safety, tolerability, pharmacokinetics, pharmacodynamics, and exploratory efficacy of the novel enzyme replacement therapy avalglucosidase alfa (neoGAA) in treatment-naïve and alglucosidase alfa-treated patients with late-onset Pompe disease: a phase 1, open-label, multicenter, multinational, ascending dose study. *Neuromuscul. Disord.* 29, 167–186. doi:10.1016/j.nmd.2018.12.004
- Perry, J., Garrett, M., Gronley, J. K., and Mulroy, S. J. (1995). Classification of walking handicap in the stroke population. *Stroke* 26, 982–989. doi:10.1161/01.str.26.6.982
- Russell, D. J., Rosenbaum, P. L., Cadman, D. T., Gowland, C., Hardy, S., and Jarvis, S. (1989). The gross motor function measure: a means to evaluate the effects of physical therapy. *Dev. Med. Child. Neurol.* 31, 341–352. doi:10.1111/j.1469-8749.1989.tb04003.x
- Sanofi Genzyme (2010). *Lumizyme (alglucosidase alfa) [package insert]*. U.S. Food and Drug Administration website. Available at: https://www.accessdata.fda.gov/drugsatfda_docs/label/2010/125291bl.pdf (Accessed April 2023).
- Sanofi Genzyme (2021). *Nexviazyme (avalglucosidase alfa-ngpt) [package insert]*. U.S. Food and Drug Administration website. Available at: https://www.accessdata.fda.gov/drugsatfda_docs/label/2021/761194s000bl.pdf (Accessed April 2023).
- Schoser, B., Stewart, A., Kanter, S., Hamed, A., Jansen, J., Chan, K., et al. (2017). Survival and long-term outcomes in late-onset Pompe disease following alglucosidase alfa treatment: a systematic review and meta-analysis. *J. Neurol.* 264, 621–630. doi:10.1007/s00415-016-8219-8
- Toscano, A., Rodolico, C., and Musumeci, O. (2019). Multisystem late onset Pompe disease (LOPD): an update on clinical aspects. *Ann. Transl. Med.* 7, 284. doi:10.21037/atm.2019.07.24
- Van Capelle, C. I., Van Der Beek, N. A., De Vries, J. M., Van Doorn, P. A., Duivenvoorden, H. J., Leshner, R. T., et al. (2012). The quick motor function test: a new tool to rate clinical severity and motor function in Pompe patients. *J. Inherit. Metab. Dis.* 35, 317–323. doi:10.1007/s10545-011-9388-3
- Van Der Ploeg, A. T., Clemens, P. R., Corzo, D., Escolar, D. M., Florence, J., Groeneveld, G. J., et al. (2010). A randomized study of alglucosidase alfa in late-onset Pompe's disease. *N. Engl. J. Med.* 362, 1396–1406. doi:10.1056/NEJMoa0909859
- Wang, Y. C., Bohannon, R. W., Kapellusch, J., Garg, A., and Gershon, R. C. (2015). Dexterity as measured with the 9-Hole Peg Test (9-HPT) across the age span. *J. Hand Ther.* 28, 53–59. doi:10.1016/j.jht.2014.09.002
- Winkel, L. P., Hagemans, M. L., Van Doorn, P. A., Loonen, M. C., Hop, W. J., Reuser, A. J., et al. (2005). The natural course of non-classic Pompe's disease; a review of 225 published cases. *J. Neurol.* 252, 875–884. doi:10.1007/s00415-005-0922-9
- Zhu, Y., Jiang, J. L., Gumlaw, N. K., Zhang, J., Bercury, S. D., Ziegler, R. J., et al. (2009). Glycoengineered acid alpha-glucosidase with improved efficacy at correcting the metabolic aberrations and motor function deficits in a mouse model of Pompe disease. *Mol. Ther.* 17, 954–963. doi:10.1038/mt.2009.37



OPEN ACCESS

EDITED BY

Jose Elias Garcia-Ortiz,
Centro de Investigación Biomédica de
Occidente (CIBO), Mexico

REVIEWED BY

Neal Weinreb,
University of Miami, United States
Margarita Ivanova,
Lysosomal and Rare Disorders Research and
Treatment Center, United States
Patryk Lipiński,
Children's Memorial Health Institute (IPCZD),
Poland

*CORRESPONDENCE

Fatma Al-Jasmi,
✉ aljasmif@uaeu.ac.ae

RECEIVED 08 November 2023

ACCEPTED 17 January 2024

PUBLISHED 13 February 2024

CITATION

Mohamed FE and Al-Jasmi F (2024), Exploring the efficacy and safety of Ambroxol in Gaucher disease: an overview of clinical studies.
Front. Pharmacol. 15:1335058.
doi: 10.3389/fphar.2024.1335058

COPYRIGHT

© 2024 Mohamed and Al-Jasmi. This is an open-access article distributed under the terms of the [Creative Commons Attribution License \(CC BY\)](#). The use, distribution or reproduction in other forums is permitted, provided the original author(s) and the copyright owner(s) are credited and that the original publication in this journal is cited, in accordance with accepted academic practice. No use, distribution or reproduction is permitted which does not comply with these terms.

Exploring the efficacy and safety of Ambroxol in Gaucher disease: an overview of clinical studies

Feda E. Mohamed^{1,2} and Fatma Al-Jasmi ^{1,2,3*}

¹Department of Genetics and Genomics, College of Medicine and Health Sciences, United Arab Emirates University, Al Ain, United Arab Emirates, ²ASPIRE Precision Medicine Research Institute Abu Dhabi, United Arab Emirates University, Abu Dhabi, United Arab Emirates, ³Department of Pediatrics, Tawam Hospital, Al Ain, United Arab Emirates

Gaucher disease (GD) is mainly caused by glucocerebrosidase (GCase) enzyme deficiency due to genetic variations in the *GBA1* gene leading to the toxic accumulation of sphingolipids in various organs, which causes symptoms such as anemia, thrombocytopenia, hepatosplenomegaly, and neurological manifestations. GD is clinically classified into the non-neuronopathic type 1, and the acute and chronic neuronopathic forms, types 2 and 3, respectively. In addition to the current approved GD medications, the repurposing of Ambroxol (ABX) has emerged as a prospective enzyme enhancement therapy option showing its potential to enhance mutated GCase activity and reduce glucosylceramide accumulation in GD-affected tissues of different *GBA1* genotypes. The variability in response to ABX varies across different variants, highlighting the diversity in patients' therapeutic outcomes. Its oral availability and safety profile make it an attractive option, particularly for patients with neurological manifestations. Clinical trials are essential to explore further ABX's potential as a therapeutic medication for GD to encourage pharmaceutical companies' investment in its development. This review highlights the potential of ABX as a pharmacological chaperone therapy for GD and stresses the importance of addressing response variability in clinical studies to improve the management of this rare and complex disorder.

KEYWORDS

Gaucher disease, inborn error of metabolism, sphingolipidoses, Ambroxol, pharmacological chaperones, glucocerebrosidase enzyme, enzyme enhancement therapy, drug repurposing

1 Introduction

1.1 Overview of Gaucher disease

Gaucher disease (GD, OMIM #230800) is the second most prevalent disease among lysosomal storage disorders with a worldwide incidence of about 1:40,000 to 1:60,000 births (Stirnemann et al., 2017). It is a rare autosomal recessive disorder caused by genetic variations in the *GBA1* gene leading to the expression of defective glucocerebrosidase (GCase, EC: 4.2.1.25) enzyme mainly characterized by low residual activity in affected tissues (Hruska et al., 2008). To date, there have been more than 690 different variants reported in the *GBA1* gene according to the Human Gene Mutation Database of which the majority are from the missense type (Stenson et al., 2020). Abnormal low GCase enzymatic activity consequently accumulates its glucosylceramide (GlcCer) substrate in affected

organs like bone marrow, the spleen, and the liver. GlcCer accumulation may also occur in bone and neuronal tissues in different forms of the disease. Therefore, GD is subclinically categorized into types I, II, and III, considering factors such as the nature of the genetic variant, levels of residual activity, neuronal involvement, disease severity, and prognosis. Based on neuronal involvement, type I is named non-neuronopathic GD while types II and III are neuronopathic-GD (nGD) (Sidransky, 2004).

GD presents a wide range spectrum of clinical manifestations. GD type I (GD1, non-neuronopathic GD, MIM 230800) is the most common form of the disease and is primarily distinguished by the absence of neurological impairment (Linari and Castaman, 2015). The average age of onset is 10–20 years old, although milder manifestations in early childhood might be downplayed or ignored. Clinical manifestations often affect the patient's quality of life but nowadays, when patients are usually treated, GD1-associated mortality is rare (Charrow et al., 2000). The primary clinical features of this form include splenomegaly, hepatomegaly, fatigue, gallstone formation, anemia, and thrombocytopenia. Bone involvement, seen in approximately 80% of GD1 cases due to bone marrow infiltration, can present as acute painful bone crises or chronic pain, which is assessed using tools like the Visual Analog Scale (VAS) or Numerical Rating Scale (NRS) (Wenstrup et al., 2002; Chis et al., 2021). The intensity of the pain varies, potentially influencing functional prognosis. Assessing skeletal manifestations in GD involves a combination of clinical evaluations, laboratory tests, and imaging techniques such as Magnetic Resonance Imaging (MRI) and Dual-energy X-ray absorptiometry (DEXA) (Hughes et al., 2019). While type I GD is typically considered the non-neuronopathic form of the disease, initial investigations into individual cases of GD1 patients have suggested a significantly higher risk of developing Parkinson's disease (PD) (Biegstraaten et al., 2010). Bultron et al.'s study (2010) involving a cohort of 444 GD1 patients demonstrated that these individuals face an approximately 20-fold increased lifetime risk of developing PD compared to the general population (Bultron et al., 2010). Recent data further underscores a substantial correlation between *GBA1* variants (approximately 130 variants) and the onset of PD (Zhang et al., 2018; Riboldi and Di Fonzo, 2019). GD type III (GD3, also known as subacute or juvenile neuronopathic GD, MIM 231000) patients are similarly affected with the visceral symptoms mentioned in GD1 but neurological involvement has been reported before the age of 20 years in most of the cases (Stirnemann et al., 2017). Patients who are affected by this condition generally survive into their mid to early adulthood although, with treatment for the systemic manifestations some patients are now in their sixties. Systemic features include enlarged liver and spleen, anemia, thrombocytopenia, bone abnormalities, and early-onset horizontal supranuclear gaze palsy (Schwartz et al., 2017). Neurological symptoms range from cognitive impairment, saccadic eye movement abnormalities, myoclonus, seizures, dementia, ocular muscle apraxia, and muscle weakness (Schwartz et al., 2017). The disease prognosis exhibits considerable variation, as certain patients may undergo a relatively stable clinical course, whereas others may encounter more pronounced neurological manifestations (Stone et al., 2023). Clinical studies have shown that there is heterogeneity in the reported neurological impairments among patients with GD3 (Tylki-Szymańska et al., 2010). While

some patients may show only mild systemic involvement, with horizontal ophthalmoplegia being their sole neurological symptom, others may experience more severe forms of the disease (Stirnemann et al., 2017). Lung involvement with interstitial lung disease has been seen in a substantial percentage of reported GD3 patients and some present with retroperitoneal lymphadenopathy that often fails to respond to the available medications (Linari and Castaman, 2015). GD patients with saposin C (GCCaseactivator protein) deficiency are mostly presented with neurological manifestations comparable to that observed in the GD3 form of the disease (Mohamed et al., 2022). Technically, however, they are no longer classified as having GD as the causative mutations are in *PSAP* rather than in *GBA1* (Mohamed et al., 2022).

GD type II (GD2, known as infantile or acute neuronopathic GD, MIM 230900) is the rarest and most severe form of the disease. It typically onset at 1–6 months of age and has a mean survival age of 11.7 months (Mignot et al., 2006). In addition to visceral symptoms, neurological impairments appear initially as oculomotor abnormalities followed by brainstem involvement which may include psychomotor development delay, seizures, growth retardation, and apnea (Stirnemann et al., 2017). The fetal form of GD2 usually results in intrauterine fetal demise or early neonatal death mainly due to hydrops fetalis (Mignot et al., 2003). Overall, the clinical classification of nGD patients is complex as the symptoms may overlap between GD2 and GD3. In some instances, it is unclear if all the associated neurological symptoms are directly caused by the enzyme deficiency or if they arise as secondary effects that emerge as a consequence of the primary manifestations of the underlying GD (Sidransky, 2004). For example, neurological symptoms may arise in GD1 patients due to spinal compression fractures although type I GD is considered non-neuronopathic (Roshan Lal and Sidransky, 2017). Also, GD3 patients with neurological findings restricted to mild eye movement abnormalities may be misclassified as having GD1 whereas patients with genotypes usually predictive for GD3 may never have CNS manifestations. The challenge lies in distinguishing between symptoms directly attributable to the enzyme deficiency and those arising as a cascade of complications triggered by the fundamental aspects of Gaucher disease.

1.2 Current medicational options for GD

To date, there are two categories of clinically approved medications available for the management of GD symptoms, to improve the patient's quality of life while also preventing irreversible damage. These categories include Enzyme Replacement Therapy (ERT) and Substrate Reduction Therapy (SRT). ERT involves the administration of recombinant enzymes to patients to replace the deficient enzyme in the body, while SRT focuses on reducing the production of the accumulated substrate that leads to GD symptoms. Despite their reported limitations and side effects, ERT and SRT are effective for ameliorating GD manifestations, and are currently considered standard treatments for this condition. ERT augments low-activity mutant GCCase with a recombinant form of the normal human enzyme (Van Rossum and Holsopple, 2016). This allows the body to break down the accumulated

glucocerebroside in affected organs and bone marrow. Patients receive ERT via intravenous (IV) infusion about every 2 weeks (1–2 h per session) usually taking place at an infusion center or home infusion. Imiglucerase, velaglucerase alfa, and taliglucerase alfa are the current approved medications for the treatment and management of GD within the ERT medication class (Sam et al., 2021; National Gaucher Foundation, 2023). Generally, both pediatric and adult patients with GD1 respond well to the mentioned ERT options, which significantly ameliorates the underlying clinical manifestation (Gupta and Pastores, 2018). Although it is rare, hypersensitivity reactions due to ERT drugs have been reported (Turgay Yagmur et al., 2020). Slowing the infusion rate and using the appropriate premedication will usually solve the issue, alternatively adjusting the dose, or switching to another ERT medication (Revel-Vilk et al., 2018).

SRT compounds have been introduced in the therapy of multiple lysosomal storage disorders including GD by targeting the glucocerebroside substrate synthesis pathway in the cell (Gupta and Pastores, 2018). These compounds reduce the workload on the mutated GCase by decreasing the amount of glucocerebroside for it to break down, enabling the patient's remaining residual activity to address the accumulated substrates and prevent additional accumulation (Sam et al., 2021). SRT compounds are small molecular weight compounds that are orally administered. Eliglustat and miglustat are currently the only clinically approved oral SRT drugs for patients with GD (McCormack and Goa, 2003; National Gaucher Foundation, 2023). SRTs are not approved for use in individuals under 18 or women who are breastfeeding, pregnant, or trying to become pregnant, or in patients with nGD. Miglustat has significant gastrointestinal side effects while eliglustat has the potential for dose-limiting interactions with other drugs that are metabolized by CYP-2D6 or CYP-3A (Bennett and Mohan, 2013). Clinical trials (#NCT02843035) are currently ongoing for Venglustat (Genzyme) to overcome the former SRT compounds' lack of efficacy for nGD patients. Venglustat can penetrate the blood-brain barrier (BBB) and could specifically be useful in GD3 (Genzyme and a Sanofi Company, 2023).

The use of small chemical chaperones is a promising approach for the treatment of diseases caused by improperly folded proteins like GD in which the majority of the reported disease-causing *GBA1* genetic variants are missense mutations (Jung et al., 2016). They are small molecular weight compounds that are designed to selectively bind to a specific target protein, facilitating its folding and stabilization, as well as promoting lysosomal translocation (Maegawa et al., 2009; Parenti et al., 2015). In the case of lysosome-resident enzymes, genetic mutations can lead to misfolding and subsequent degradation in the proteasome, preventing the enzyme from reaching its intended destination in the lysosome. Chaperone therapy can increase enzyme stability, catalytic activity, and lysosomal translocation, thus restoring normal cellular function (Parenti et al., 2015). However, it is important to note that the presence of the enzyme is required for chaperones to be effective, as these molecules physically bind to the target protein (Muntau et al., 2014). Overall, the development of chaperones represents a promising avenue for the treatment of a range of diseases caused by improperly folded proteins like GD (Liguori et al., 2020). While chaperoning compounds offer hope for

stabilizing misfolded proteins in genetic diseases like Gaucher's, their effectiveness is unfortunately limited by mutation-specificity (Mohamed et al., 2017). The variable efficacy of this compound across different mutations exposes a critical gap in available treatment options for the extensive range of genetic variants in this condition. Therefore, discovering a broader spectrum of chaperone compounds with wider effectiveness across mutations is an urgent priority. Screening chemical libraries consisting of Food and Drug Administration (FDA) and clinically approved compounds has demonstrated practicality and success in identifying small molecules that can function as enzyme enhancement therapy (EET) agents for specific lysosomal enzymes deficient in lysosomal storage disorders. Since ongoing trials for EET or SRT synthesized compounds are still in the early stages of development, and considering the challenges associated with enrolling patients with rare diseases, it is anticipated that market authorization may not be obtained for at least 5–10 years from the present day. In such circumstances, patients with significant nGD features involving the CNS may seek alternative solutions, one of which is repurposing already approved drugs.

In this context, Ambroxol (ABX) has been identified as an EET agent for rescuing misfolded GCase enzymes of different genotypes (Maegawa et al., 2009). In the initial *in vitro* characterization, ABX exhibited a maximal inhibition at a neutral pH (characteristic of the endoplasmic reticulum) and almost undetectable inhibition at the acidic pH found within lysosomes (Maegawa et al., 2009). ABX's pH-dependent interaction involves binding and stabilizing the misfolded GCase enzyme in the ER to prevent its recognition via the ER quality control machinery. This process facilitates the enzyme's trafficking to the lysosomes, where ABX dissociates, allowing the mutated GCase enzyme to remain unbound and effectively engage in the breakdown of accumulated substrates (Liguori et al., 2020). Using patient fibroblast cells, treatment with ABX showed promising enzymatic enhancement in various missense variants through direct binding, folding alteration, and the subsequent trafficking correction of the ER-retained ones (Bendikov-Bar et al., 2011; Bendikov-Bar et al., 2013; Kopytova et al., 2021). Modulation and structural analysis showed that ABX interacts with both the enzyme active and allosteric site residues. Based on this discovery, several clinical and pilot studies have been conducted to evaluate the efficacy and safety of ABX as an alternative and/or adjunct therapy in GD patients of different forms (Istaiti et al., 2021; Zhan et al., 2023). Although ABX is well tolerated in most patients, the findings obtained from these studies showed a wide response variability even in cases with similar genotypes (Table 1). Therefore, this review aims to comprehensively explore and summarize all the available clinical findings regarding the use of ABX as a potential therapeutic agent in GD patients of different forms. The focus will be on evaluating the response variability observed in clinical studies to assess the potential of ABX in improving the management of GD.

2 Ambroxol as a potential pharmacological chaperone therapy in GD

ABX is an oral mucolytic drug available over the counter since many years as a cough medicine in various countries with the exception of the United States (Cazan et al., 2018). It has been

TABLE 1 Summary of the clinical studies performed to evaluate the effectiveness and safety of ABX in Gaucher Disease treatment.

Genotype	Patients number	Phenotype	Adjunct treatments	ABX dosage	Assessment parameters	Improvements	Adverse effects (AEs)	Year and ethnicity	Ref
Different combinations of variants	32	29 GD1	Did not afford treatments	12.7 ± 3.9 mg/kg/day (0.5–6.5 years)	Chitotriosidase activity, glucosylsphingosine level, liver and spleen volumes, and hematologic parameters	More significant among milder and younger cases	Safe (only 3 cases encountered mild and temporary AEs)	2023 China	Zhan et al. (2023)
		1 GD2-3							
		2 GD3							
N370S/N370S N370S/other	40 (16 fully completed the trial)	GD1 (26:ERT, 2:SRT, and 12:Stopped ERT or SRT)	Poor response to ERT or SRT	600 mg/day (12 months)	Platelet counts, lumbar spine T-score, and LysoGb1 levels	- >20% increase in platelet counts and reduction in LysoGb1 - >0.2 improvement in lumbar spine T-score	-no severe AEs –13 patients reported mild AEs	2023 Israel	Istaiti et al. (2023)
R398L/R398L	1	GD2	In combination with ERT	25 mg/kg/day (Initiated at the age of 15 months)	Blood and CSF LysoGb1, neurocognitive and motor development	- Improved visceral and neurological symptoms	no side effects or signs of toxicity	2022 Turkey	Aries et al. (2022)
						–20-fold increase in GCase activity			
V414L/S235P	1	GD1	Never treated	660 mg/day for 2 years	GCase activity and liver assessment	- Significant reduction of hepatic fibrosis	NA	2022 China	Zhang et al. (2022)
						-Enhanced GCase activity			
Different combinations of variants	41	11:GD1 (4 with PD)	In combination with ERT (only 4 were not exposed to ERT)	75–1,485 mg/day (1–76 months)	Demographics, GD type, GD therapy, history of splenectomy, and AEs	25 patients showed enhanced neurological status, physical activity, and reduced fatigue	No severe AEs reported but 12 patients reported mild AEs	2021 Israel	Istaiti et al. (2021)
		27:nGD							
		3:PD							
L444P/H225Q; D409H	2	GD3	Combined with ERT	25 mg/kg/day (Older and younger siblings started at ages 5 years and 7 weeks, respectively)	LysoGb1, GCase activity, CSF CHT activity, neurological assessment	ABX early initiation delayed or halted neurological manifestations prognosis in the younger sibling	No severe AEs reported	2021 Croatia	Ramadža et al. (2021)
L444P/RecNcil	1	nGD	Combined with ERT	30 mg/kg/day (Started at 8 months of age)	LysoGb1, Plasma CHT	Slow progress in the neurological involvement	NA	2020 Taiwan	Chu et al. (2020)
L483P/L483P*	1	GD3	Combined with ERT	7.5 mg/kg/day	Numerical Rating Scale (NRS)	potent analgesic effect with chronic pain that was resistant to standard therapy	No AEs reported	2020 China	Pawlinski et al. (2020)
P1: N188S/ IVS2+1G>A	2	nGD	Combined with ERT	25 mg/kg/day	GCase and CHT activities, LysoGb1 levels	P1: LysoGb1 levels, CHT activity, and seizure frequency decreased	No AEs reported	2020 Italy	Ciana et al. (2020)

(Continued on following page)

TABLE 1 (Continued) Summary of the clinical studies performed to evaluate the effectiveness and safety of ABX in Gaucher Disease treatment.

Genotype	Patients number	Phenotype	Adjunct treatments	ABX dosage	Assessment parameters	Improvements	Adverse effects (AEs)	Year and ethnicity	Ref
P2: L444P/L444P						P2: no effects were observed (ABX was started at 60 years)			
L356Wfs*8/R392W	1	GD1	Never exposed to ERT or SRT	10 mg/kg/day increased to 15 mg/kg/day after 6 months for up to 2.5 years	Skeletal imaging assessment, CHT, platelet count, hematological workup	Improved skeletal manifestations as both femoral heads showed significant improvement in sphericity and reshaping	No AEs reported	2019 China	Jiang et al. (2020)
N227S/R296Q	4	nGD	Combined with ERT for 4.5 years	1.5–27 mg/kg/day	GCase activity, biochemical, safety, and neurocognitive findings	Seizure frequencies markedly decreased; neurocognitive function was improved, and LysoGb1 levels were normalized	High-dose ABX was well-tolerated with no severe AEs	2019 Korea	Kim et al. (2020)
N227S/V211Ffs									
F252I/L483P*									
G377S/G195E	2	GD3	Combined with ERT	25 mg/Kg/day	LysoGb1 levels and neurological status	Improvement in ambulation, and LysoGb1 levels	No AEs reported	2019 Canada	Charkhand et al. (2019)
N188S/R463H						Lower seizure duration in one patient only			
N188S/G193W	5	nGD	Combined with ERT	25 mg/kg/day	GCase activity, LysoGb1 levels, Neurological assessment	Myoclonus, seizures, and pupillary light reflex dysfunction markedly improved in all patients and two were able to walk again	No serious AEs reported	2015 Japan	Narita et al. (2016)
N188S/?									
F213I*/RecNciI									
D409H/IVS10-1									
N370S/N370S N370S/84GG	12	GD1	Unable or unwilling to receive ERT	2 capsules of 75 mg/day (6–12 months)	Liver and spleen volumes, platelet count, hemoglobin, and CHT activity	ABX stabilized and enhanced the clinical status of GD1 patients not receiving ERT.	Two patients dropped out due to hypersensitivity reactions. No other AEs	2013 Israel	Zimran et al. (2013)

*L483P, F252I, and N409S are alternate nomenclatures for L444P, F213I, and N409S respectively due to the use of different *GBA1* transcripts.

demonstrated to be highly effective as an expectorant, anti-inflammatory, and antioxidant agent due to its extensive history of human use in treating airway mucus hypersecretion diseases such as chronic bronchitis, asthma, and cystic fibrosis (Ollier et al., 2020). Moreover, ABX has been employed as an alternative preventive therapy for hyaline membrane disease in newborns by enhancing the secretion of surfactant in the lungs (Ollier et al., 2020). ABX showed an anesthetic effect in several studies which is mainly due to its inhibitory effects towards Na^+ channels, Ca^{2+} channels, and glutamate receptors (AMPA type) effectively suppressing symptoms of chronic, inflammatory, and neuropathic pain *in vivo* (Jarvis et al., 2007; Weiser, 2008). Unlike other blockers, ABX CNS-related toxicity and adverse effects were mainly reported with very high doses (Istaiti et al., 2021). ABX is available in multiple prescription formulations. ABX immediate-release oral form (tablets, soft pastilles, granules, syrup, and oral solution) with a half-life of ≈ 10 h which is prescribed twice per day (Cazan et al., 2018). The ABX extended-release formulations on the other hand have a longer half-life that maintains the drug levels in the blood over 24 h reducing the frequency of administration to once per day. Beyond its chaperone activity, previous data indicate that ABX possesses additional anti-inflammatory and antioxidant properties (Bianchi et al., 1990; Kantar et al., 2020). This suggests broader therapeutic potential for ABX in lysosomal storage diseases (LSDs), including GD, by targeting additional aspects of their pathogenesis.

To establish the potential use of ABX as an EET for GD treatment, several studies have been conducted. Using patients' derived cells, cellular assessment of ABX's chaperoning activity demonstrated positive enhancement in mutated GCase expression, residual activity, and/or glucosylceramide accumulation for different GD disease-causing variants, including N370S, L444P, N227S, F213I, G232W, R159W, and G241R (Maegawa et al., 2009; Bendikov-Bar et al., 2011; Narita et al., 2016; Kim et al., 2020). In GD3 fibroblast cells with L444P (the second most prevalent following F213I) variant, ABX helps to release ER-retained enzymes to lysosomes, resulting in a noticeable increase in residual activity (Ivanova et al., 2021). Notably, the observed impact was not universally present in cells derived from L444P homozygous patients, with some displaying no discernible positive response (Bendikov-Bar et al., 2011). Cells from GD1 patients carrying L444P genotypes in a compound heterozygous state with another *GBA1* variant exhibited a more significant overall improvement compared to L444P homozygous forms (Kopytova et al., 2021). This indicates that there is a certain level of response variability towards ABX even with the same genotype. Protein modeling studies have shown that ABX interacts with both active and non-active site residues of the GCase enzyme, which is consistent with its mixed-type response in different cells (Maegawa et al., 2009). ABX's mechanism of restoring GCase levels and function may involve direct binding for enzyme stabilization, upregulation of expression through the activation of the transcription factor Nrf2, changes in lysosomal pH to enhance enzymatic activity, and induction of GCase expression through TFEB-mediated lysosomal regulation (Sardiello, 2016; Kopytova et al., 2021). Additionally, ABX significantly enhances both trafficking and activity of ER-retained GCase in patients' fibroblast cells for various GD variants and

disease forms. It is noteworthy that the level of improvement varies among the variants; hence, the chaperoning effect of ABX is variant-dependent (Bendikov-Bar et al., 2013; Luan et al., 2013; Suzuki et al., 2013). Therefore, clearing the ER compartment from the retained mutated GCase through ABX ameliorates the ongoing ER stress resulting from the underlying accumulation. Data from different studies have shown that ABX has the potential to promote proper protein folding, reduce the accumulation of misfolded proteins, and enhance the ER-associated degradation (ERAD) pathway (Remondelli and Renna, 2017). It also plays a significant role in ER stress relieve as evident from Unfolded Protein Response (UPR) markers reduction in the 18-day-old ABX-treated *Gdrosophila* model (Cabasso et al., 2019). The treatment significantly lowers the dihydroethidium marker of oxidative stress in cultured fibroblast cells carrying various *GBA1* mutations (homozygous and heterozygous) (McNeill et al., 2014). In normal mice, ABX showed elevated GCase activity in various tissues, including the spleen, heart, and brain, without causing any severe adverse effects indicating its wide range of tissue bioavailability (Luan et al., 2013). ABX's capability of crossing the BBB was further supported in healthy nonhuman primates (Migdalska-Richards et al., 2017). Besides its chaperoning effect, ABX also affects lysosomal biogenesis, autophagy, secretory pathways, and mitochondrial function (Ambrosi et al., 2015; Fois et al., 2015; Magalhaes et al., 2018; Ivanova et al., 2021; Kopytova et al., 2021). ABX has been discovered to boost lysosomal activity and facilitate the removal of protein aggregates in different neurological-related disorders including GD (Bonam et al., 2019). Autophagy was found to respond differently to ABX treatment as it influences the redirection of the accumulated cellular cargo toward the secretory pathway (exocytosis) by blocking autophagy in primary cortical *GBA1*^{-/-} mouse neurons (Magalhaes et al., 2018). On the other hand, autophagy was activated in human iPSC differentiated neurons obtained from PD cells carrying *GBA1* mutation through elevated LC3-II and p62 expression upon ABX treatment (Yang et al., 2017). ABX was shown to target lysosomal dysfunctions in human *GBA1* mutated fibroblasts through Cathepsin D, LIMP2, and Sap C modulation, facilitating GCase folding and proper trafficking (Ambrosi et al., 2015). ABX facilitates lysosomal-autophagosomal fusion, enhancing protein degradation and potentially reducing ER stress and lysosomal dysfunction for improved protein folding and clearance (Magalhaes et al., 2018). Additionally, ABX induces mitochondrial activation, evidenced by an augmentation in both mitochondrial mass and density, along with the activation of mitochondrial membrane potential as demonstrated in GD2-3 fibroblast cells (Ivanova et al., 2021). Mitochondrial content and lysosomal biogenesis are also enhanced by ABX through peroxisome proliferator-activated receptor gamma coactivator 1- α (PGC1- α) and TFEB, respectively (Magalhaes et al., 2018). The compound has a significant potential in the treatment of PD and neuronopathic GD by reducing both α -synuclein and phosphorylated α -synuclein levels in vivo transgenic murine models (Migdalska-Richards et al., 2016).

Given ABX's over-the-counter availability and oral formulation, its effectiveness for certain GD manifestations could offer significant benefits, particularly for patients encountering challenges with their current treatment regimens, especially those with neurological

symptoms. Although they have a lower prevalence, the nGD subtypes are more prevalent in developing countries of the middle east and Asia-Pacific (Al-Jasmi et al., 2013; Roshan Lal and Sidransky, 2017; Fateen and Abdallah, 2019; Castillon et al., 2022). Providing a cheaper therapeutic option like ABX can solve the limited availability of ERT and SRT expensive medications to this group of patients. As the doses needed to maintain the pharmacological chaperone (PC) effect of ABX are significantly higher compared to over-the-counter doses (the highest: 75 mg/tablet) available in the market, ABX formulations are limited to lower concentrations. This may result in the need for consuming multiple capsules or a large amount of syrup daily, in adults and children, respectively (Istaiti et al., 2021). Further research and clinical studies investigating the chaperoning effect of ABX in treating GD can help encourage pharmaceutical companies to develop appropriate formulations and dosage regimens for the drug in the market. Unfortunately, the exclusive patent (European Patent Office Register Application number: EP3145491) for this drug was granted to a small company that lacks the financial resources to conduct a clinical trial for its potential use as a treatment for GD (European Patent Register, 2023). Furthermore, larger pharmaceutical companies have not expressed interest in this drug, partly due to the abundance of generic versions available for purchase online (Istaiti et al., 2021).

3 Clinical studies on Ambroxol

3.1 Gaucher disease assessment parameters and monitoring

To date, there is no conclusive biomarker that can reliably predict the risk associated with all aspects of GD morbidity. Although several potential biomarkers have been recognized, each comes with inherent limitations, making clinical parameters the primary method for establishing treatment objectives and evaluating outcomes. Clinicians must rely on their expertise to determine the most effective monitoring protocol that is tailored to each case based on the GD form presented and the treatment type. Over the duration of any therapeutic intervention, patients undergo standard clinical monitoring that includes regular clinical status evaluation, radiological evaluations, hemogram, enzymatic activity, and different disease biomarkers (Stirnemann et al., 2017).

Since ABX binds directly to the mutated GCase enzyme, assessing the enzymatic activity is a key indicator to determine the effectiveness of the ABX treatment and whether the mutated enzyme function is improving during the treatment period (Han et al., 2020). This information can help clinicians adjust the drug dosage based on the rate of increase in residual enzymatic measurement. The test can be performed regularly using a fresh peripheral blood leukocytes sample (Hurvitz et al., 2019; Dardis et al., 2022). As previously mentioned above, ABX additionally modifies the enzyme conformation through an allosteric site interaction which its enhancement effect might not be detected directly through enzymatic activity measurement (Maegawa et al., 2009). Therefore, other biomarkers like substrate accumulation parameters can be measured. While the impairment of GCase enzyme in GD patients results in the accumulation of its GlcCer

substrate, several additional lipids like glucosylsphingosine (LysoGb1, derived by ceramidase deacylation of GlcCer) are enriched in GD patient samples (Dekker et al., 2011). The quantification of LysoGb1 through liquid chromatography-mass spectrometry in patient plasma, dried blood, and cerebrospinal fluid (CSF) samples represents the most sensitive approach. This analytical method is highly effective, and accurate that has the potential to provide valuable insights into GD therapeutic monitoring including ABX treatment (Hurvitz et al., 2019). To obtain a comprehensive understanding of a patient's clinical progress, it is essential to consider multiple other biomarkers in the clinical assessment. Studies have shown that the enzyme chitotriosidase (CHT) and the chemokine CCL1811 are produced by Gaucher cells and released into the patient's circulation (Hollak et al., 1994). These two proteins are potential biomarkers because their plasma levels are significantly elevated in GD patients, and change as the disease progresses as well as after a treatment intervention like ABX (Zhan et al., 2023).

Platelet count monitoring is crucial for GD management and treatment evaluation as more than 90% of affected patients suffer from thrombocytopenia due to bone marrow infiltration and splenic sequestration (Hollak et al., 2012). Although it is less common, anemia and hemoglobin level measurement in 50% of the cases can help in assessing the efficacy of the ongoing treatment (Charrow et al., 2000). Abdominal magnetic resonance imaging (MRI) is used to measure the dimensions of the liver and spleen, to evaluate their volume and morphology to assess the progression of hepatosplenomegaly. The decrease in organ volumes as a result of treatments is usually a slow process and should be monitored as a long-term effect (Elstein et al., 2011). Improvement of bone abnormalities is best followed through radiology via bone MRI to check for bone marrow infiltration (Bone Marrow Burden score), bone infarction, avascular necrosis, and osteoarthritis (Vom Dahl et al., 2006). Bone densitometry is measured via X-ray imaging to diagnose and monitor osteopenia/osteoporosis in adults and older children affected with GD. Patients with nGD forms require additional neurological monitoring. The combination of electroencephalogram (EEG) recording and brain MRI is regularly performed to evaluate the improvement or progression speed of nGD-associated CNS symptoms along any therapeutic intervention. The tests mainly check for brainstem-evoked potential, swallowing studies, and neuro-ophthalmologic evaluation should be done at regular intervals (Stone et al., 2023). The frequency of clinical examination is mostly decided by the patient's clinician, but it is advisable to run full laboratory tests and imaging when required every 6 months for pediatric GD patients as a function of disease progression and drug monitoring.

3.2 Ambroxol effectiveness and response variability in Gaucher disease patients

Ever since its discovery as a chaperone in 2009, ABX repurposing efficacy in the treatment of GD patients of different forms has been evaluated in a total of 14 clinical trials and studies summarized in Table 1 (Maegawa et al., 2009). The positive responses reported in these published data have encouraged physicians and patients to consider the off-label use of ABX for

GD in combination with the currently available ERT/SRT treatments or as an alternative when such solutions fail to induce any clinical improvement. Also, it has been an option when ERT or SRT is not available or affordable for some patients. The majority of the trials conducted on ABX have reported it to be safe and well-tolerated in most cases even during long-term treatments. However, understanding the reported adverse effects in detail is key to minimizing their impact and preventing future occurrences. Among the 14 reported trials, 4 extensive primary studies explored ABX's impact on a large cohort of GD patients (Zimran et al., 2013; Istiti et al., 2021; Istiti et al., 2023; Zhan et al., 2023). Notably, 3 of these studies took place in Israel, reflecting its higher GD prevalence compared to other populations (Zimran et al., 2013; Istiti et al., 2021; Istiti et al., 2023).

In an observational data involving a cohort of 28 GD patients representing the three clinical forms who completed the proposed treatment, ABX (administered over 2.6 ± 1.7 years) successfully improved the overall clinical status in most of the enrolled patients including reduced fatigue, more energy, fewer nosebleeds, and disappearance of petechia on the skin (Zhan et al., 2023). Patients with nGD experienced stable or improved neurological manifestations during the treatment. Hematological levels were enhanced within the first year of the treatment at which 76.2% and 23.8% of the participants met the hemoglobin and platelet count goals, respectively. Improvements in platelet count were the hardest to achieve mainly due to the associated spleen enlargement. Among the eight patients who were assessed for hepatosplenomegaly, seven patients achieved the spleen volume goal, and six reached the desired liver volume, resulting in an average reduction rate of 29.5% and 21.1% respectively. A decrease in the primary GD biomarkers (LysoGb1 and CHT) levels was observed and consistently maintained throughout the treatment period in 76.9% of the patients with elevated LysoGb1 (26 patients) and 93.8% of those with elevated CHT (16 patients). Eleven patients of the cohort who underwent a prolonged (>4.5 years) ABX treatment exhibited more substantial reductions in CHT (77.8%) and LysoGb1 levels (52.8%). A strong response to ABX treatment was observed in splenectomized patients who showed decreased LysoGb1 and CHT levels ranging from 16.9% to 77.9% and 24.2%–55.4%, respectively (Zhan et al., 2023). ABX may require an extended duration to reverse the pathological glycosphingolipids accumulation which was observed in two patients who had a stable clinical course with no significant improvement detected during the early stages of the treatment, but after the continuous administration for 4 years eventually led to a significant reduction in LysoGb1 and CHT levels.

In parallel to the previously mentioned trial, a prospective open-label clinical trial (investigator-initiated research) was conducted to assess the application of high-dose ABX in treating two subgroups of GD1 patients; those who exhibited no response to ERT and/or SRT, and patients who had never been exposed to any of the available therapies (Istiti et al., 2023). Out of the forty patients enrolled, sixteen completed the study of which ten were on ERT, one on SRT, and five never had a treatment adjunct to the given ABX protocol. The study proposed the partial potential of high ABX dosage in improving platelet count (5/16), LysoGb1 (3/16), and lumbar spine T-score (measurement of bone densitometry) (6/16) with a success rate ranging from ~20% to 40% encouraging further studies (Istiti

et al., 2023). Notably, four patients experienced a notable decrease in LysoGb1 levels after 1 month of ABX treatment, but unfortunately, these levels subsequently increased over time failing to meet the desired outcome by the end of the study. The same group conducted an earlier observational study from a cohort of 41 GD patients (GD1: 11, nGD:27) exposed to off-label ABX (Istiti et al., 2021). Patient data were collected from 13 different centers to establish an investigator-initiated registry II-Reg, which was registered on [ClinicalTrials.gov](https://clinicaltrials.gov) (ID: NCT04388969) (Istiti et al., 2021). Although, 12 patients reported mild adverse effects, clinical benefits of the underlying ABX (75–1,485 mg/day) treatment were observed in 25 patients, leading to stable or improved neurological status, enhanced physical activity, and reduced fatigue. Among the GD1 group, 6 out of 11 patients showed overall wellbeing improvement, with some exhibiting enhanced LysoGb1 levels (an 85% reduction in one patient) and increased platelet counts. In contrast, patients with nGD demonstrated a more favorable response (20/27) towards ABX treatment with 16 patients experiencing stabilized or improved neurological status, along with improvements in physical activity, LysoGb1 levels, and reduced pain (3 out of 27). The seven patients who did not show improvement mainly discontinued ABX due to adverse effects or medication reimbursement issues, with one patient, unfortunately, passing away due to deteriorating clinical status. In summary, this study underscores the potential of ABX in improving the clinical manifestations of GD patients when used alongside their existing ERT medications.

Shaare Zedek Medical Center's Gaucher Unit tested ABX as a possible EET treatment in the first clinical trial with a cohort of GD1 patients who had never been on ERT (Zimran et al., 2013). They received an off-label ABX dosage of 150 mg/day for 6 months. During the study, one patient demonstrated a significant improvement in hemoglobin levels and platelet counts, with increases of 16.2% and 32.9%, respectively. His spleen and liver volumes decreased by 2.9% and 14.4%. Alongside this patient, two others continued ABX treatment for an additional 6 months. During this period, all three patients experienced ongoing reductions in spleen volume, ranging from 6.4% to 23.4%. Their hemoglobin levels and liver volumes remained stable, while the patient who initially responded well recorded a further increase in platelet counts by 52.6%. The substantial clinical impact on this patient initiated subsequent investigations, with a specific focus on potential adjustments to the ABX dosage, particularly considering the responsive patient's low BMI (17.1) compared to the other participants.

Like CNS-related manifestations, improvement of skeletal symptoms and complications is limited with the current approved GD therapies due to the inability of ERT enzymes to reach affected tissues in optimal concentrations (Jiang et al., 2020). A clinical case study of a GD1 patient who underwent a gradual ABX dose escalation revealed a significant therapeutic impact on the bilateral aseptic necrotic lesions linked to his presented phenotype (Jiang et al., 2020). The 5-year-old patient was suffering from severe pain in the bilateral lower extremities, restraining her from walking independently due to the aseptic necrosis detected in the bilateral femoral head of her hip. As neither ERT nor SRT was applicable, she was enrolled in a clinical protocol under compassionate use, receiving an initial 10 mg/kg/day dosage of ABX for 6 months to

assess her tolerance, followed by an extended treatment period of 2 years at a dosage of 15 mg/kg/day. Three years post-treatment, the patient maintained a remarkable recovery of the femoral head sphericity and reshaping that is primarily attributed to the prevention of further progression of ischemic lesions in the femoral head's epiphysis, which has contributed to the maintenance of remodeling and nearly normal growth in the femoral heads.

Clinical data suggests that ABX when added to standard therapy, can effectively manage pain associated with GD. This allows patients to rely less on traditional pain medications and improves their quality of life. ABX has shown analgesic properties by inhibiting calcium channels, which reduces the transmission of sensory signals from primary afferent neurons to the dorsal spinal cord. This mode of action was found to relieve the pain in a 38-year-old GD3 female patient who suffered from chronic soreness around the lumbar part of her spine and pelvis, which worsened during more intensive physical activity (Pawlinski et al., 2020). Despite undergoing various painkiller treatments, the pain persisted until ABX was incorporated into her treatment plan. Initially, she was given a dose of 150 mg/day, which was gradually increased to 450 mg/day. Over several months, her need for painkillers significantly decreased, and her pain levels became more manageable at which the pain intensity decreased from NRS 7 to below 3. Subsequent attempts to reduce the ABX dosage resulted in the return of the pain.

The last two studies referenced above emphasize ABX's potential to cross the blood-brain barrier and access hard-to-reach tissues, such as bone. This was initially administered to patients who were unresponsive to ERT/SRT and presented with CNS-related GD symptoms. Administering ABX, particularly at high dosages, to individuals with nGD (GD2 and GD3) has been shown to significantly improve their condition (Narita et al., 2016; Charkhand et al., 2019; Chu et al., 2020; Ciana et al., 2020; Kim et al., 2020; Pawlinski et al., 2020; Ramadža et al., 2021). It exerts a neuroprotective impact by slowing down the progression of the affected tissue in the brain by reducing the build-up of the accumulated substrates which is evident in decreased levels of LysoGb1 biomarker in patients' both plasma and CSF samples. As a result, nGD patients have reported improvements in seizure frequency and duration, motor function, cognitive abilities, and quality of life at various degrees following ABX treatment. Myoclonus in affected patients showed progressive improvements with increasing doses of ABX where they were able to regain their ability to stand steadily, maintain balance, and either walk again or experience improved ambulation (Narita et al., 2016; Charkhand et al., 2019). The most favorable improvements were witnessed in younger patients even with known responsive genotypes like L444P (Ciana et al., 2020). The patient was in his 60s when he started taking ABX and showed no phenotypic enhancement of any level even with increasing the drug dosage. Early initiation of ABX treatment at a younger age showed more substantial improvements by postponing or averting neurological progression in nGD patients (Ramadža et al., 2021). In Ramadža et al. report, two GD3 siblings were administered a combination of ABX and ERT medication at varying stages of their disease (Ramadža et al., 2021). The older sibling, diagnosed at 4.5 years with severe neurological symptoms, experienced substantial improvement and stability with ABX treatment. In contrast, the younger sibling, who started treatment

at just 7 weeks old, exhibited cognitive challenges without the development of other neurological symptoms his brother suffered from. This suggests that there may be a threshold in the progression of GD beyond which ABX therapy might not be effective, particularly in cases of advanced disease stages, therefore, initiating ABX treatment early in the disease course could be critical for its effectiveness.

3.3 The significance of Ambroxol dosage and its role as a supplementary treatment

A major limitation in these clinical trials is the selection of the proper ABX dosage. The choice of the amount of the drug given to patients might seem somewhat random, and the selected dosage in the reported data may be either too much or too little. The clinical data presented in this review article suggests that ABX has a greater chaperoning effect in GD patients when used at high dosages rather than over-the-counter use. In the first pilot study conducted on GD1 patients, where ERT was not an option, the dosage administered was kept low due to safety concerns. However, it is possible that the dosage was too low as patients with low BMI showed better measurable improvements and the thinnest patient (BMI = 17.1) among the recruited cohort had a robust response in all disease parameters tested (Zimran et al., 2013).

In Istaiti et al. study (2023), most patients who were exposed to lower doses did not show clear benefits except for a few who had low LysoGb1 biomarkers from the start before drug administration (Istaiti et al., 2023). This suggests that the given 600 mg/day dose might be necessary for most affected patients included in the study, even though some studies in the past hinted at the use of lower doses. Unlike data obtained from nGD trials, the authors suggested that higher doses are probably unnecessary in GD1 patients as there is no need to cross BBB (Narita et al., 2016; Istaiti et al., 2021). To reach a responsive high ABX dosage, patients will need to take a lot of capsules daily (8 per day for the 600 mg/day) which is another limiting factor and cause for dropout in some studies. As previously mentioned above, ABX was given as a pain relief medication at 450 mg/day over several months which was effective in reducing the underlying chronic pain but the subsequent attempts to reduce the ABX dosage resulted in the return of the pain (Pawlinski et al., 2020).

ABX has been initially identified to target patients who did not benefit from the current therapeutic protocols or those who suffer from neurological manifestations that do not respond well to such treatments. However, ABX also has been investigated as a potential complementary therapy for GD patients, particularly those with neurological involvement. These patients often receive standard treatments like ERT or SRT alongside ABX, as part of clinical trials or under compassionate use protocols. In a 2016 pilot study, five patients with GD were included, four of whom were diagnosed with an nGD form and received high-dose ABX treatment in combination with ERT. Apart from its tolerability and wide distribution into affected tissues including the brain, the results showed significant response as concluded from the enhanced GCase activity, LysoGb1 levels, and overall physical and neurological wellbeing of the patients (Narita et al., 2016). As indicated in previous studies, a notable reduction in LysoGb1 levels was reported among GD1 patients who received

ERT or SRT treatments (Zhan et al., 2023). In patients who completed 209 weeks of Velaglucerase alfa treatment, the median substrate accumulation reduction exhibited an impressive 85.7% reduction. Similarly, for GD1 patients undergoing eliglustat therapy for 8 years, LysoGb1 levels decreased by approximately 60% from baseline after just 1 year followed by a remarkable 92% reduction after 8 years of treatment indicating that better responses in ABX-treated patients are associated with long-term ERT. These findings highlight the potential of ABX to provide supplementary benefits in further improving the overall management of GD.

3.4 Preclinical assessment

Variants such as R392W, F76V, N227S, R87W, M75V, R159W, L188F, L303I, V414L, and R502C have previously been associated with a late-onset and milder GD phenotypes. Patients harboring either two mild variants or one in association with another variant (L444P, RecNcil, R535C, R202X, N227S, N227K, and V230G) linked to more severe phenotype responded well to ABX compared to those patients carrying two severe variants (Zhan et al., 2023). Given that, it has been observed that the response to the ABX chaperoning effect is not only specific to mutations but also varies among patients. Even patients with the same genotype may respond differently to ABX treatment, requiring dosage optimization or displaying varying degrees of phenotypical enhancement. To address this issue, preclinical assessment has been suggested, wherein ABX treatment can be tested and optimized using the patient's cells, such as fibroblast cells and peripheral blood mononuclear cells (PBMC) derived cells, *in vitro* (Bendikov-Bar et al., 2011; Kopytova et al., 2021). The L444P missense variant variable response to ABX is the best example to support the stated point. The mutation is the second most frequent mutation identified in nGD patients and has been reported in GD1 patients when inherited in a heterozygous state (Ciana et al., 2020).

Although the initial *in vitro* evaluation of ABX's effect on L444P genotype demonstrated no positive enhancement, a significant increase in GCase activity was observed in patient's cells harboring the compound heterozygous genotype of L444P (Maegawa et al., 2009). Despite that, computational and docking studies have demonstrated a strong binding affinity of ABX towards L444P mutated GCase (Thirumal Kumar et al., 2019). In animal studies, oral administration of 4 mM ABX for 12 days showed a significant increase in the GCase activity in different brain tissues of L444P/+ transgenic mice (Migdalska-Richards et al., 2016). On the other hand, the data at the clinical level was highly varied showing contradictory results for this variant. In a 2021 clinical investigation of ABX effect on 41 GD patients carrying different GD variants of which 10 with the homozygous state of L444P and 7 were in a compound heterozygous state with other variants (Istaiti et al., 2021). Among the L444P homozygous patients, ABX was able to enhance the neurological status of two patients and arrest the neurological progression in five other patients without any noticeable improvements. It also managed to improve the overall physical status of another two patients and decrease their complaints of underlying pain. Of the seven patients with the compound heterozygous variants with L444P, three showed improvements in their neurological status while two patients did not show any

further deterioration. It is worth noting that the patient carrying the null GD variant (L444P/IVS2+1) showed significant neurological enhancement also (Istaiti et al., 2021). In Croatian GD3-affected siblings (L444P/H225Q; D409H), ABX showed rapid improvement in neurological manifestations and later stabilized the older sibling's clinical condition (Ramadža et al., 2021). However, the younger sibling, who started the ABX protocol at 7 weeks of age, did not exhibit any severe neurological symptoms indicating that ABX delayed or even halted the evolution of neurological manifestations regardless of the underlying genotype. Also, both *in vitro* (using his fibroblast cells) and clinical investigations of ABX therapy in an Italian 60-year-old nGD patient carrying the L444P/L444P genotype showed no effect (Ciana et al., 2020). The patient was undertaking ERT medication but due to the worsening of the neurological involvement he began on high ABX dosage for 4 months with no success. This is another case that may support the importance of the early administration of ABX as an EET medication in GD especially with patients presented with neurological crises with irreversible consequences. It appears that factors other than the patient's genotype could affect their response to ABX. One such factor is the patient's age, especially if they are experiencing severe neurological or skeletal crises that EET cannot reverse. Additionally, polymorphisms or genetic modifiers may have some influence as well. Since L444P affects the folding and trafficking of the mutated GCase, individual differences in the ER quality control machinery components involved in proteostasis likely play a major role in this process (Bendikov-Bar et al., 2011). Therefore, it is highly recommended to test the response to ABX *in vitro* before initiating chaperone therapy, even in patients with responsive variants.

Chu et al. clinical report has also demonstrated that the *in vitro* ABX pre-assessment may not apply to all patients (Chu et al., 2020). Although it was previously reported as an unfavorable variant via *in vitro* analysis, an nGD infant carrying L444P/RecNcil variant followed a high ABX dosage started at the age of 6 months showed significant clinical enhancements with no further regression. The obtained outcome might be a result of the early initiation of the therapeutic intervention (ERT and ABX) when the patient's condition was less severe compared to progressive cases reported in older patients carrying the same genotype and did not benefit from ABX.

3.5 Safety and adverse effects

ABX treatment has generally been considered safe in most of the reported clinical studies, with limited adverse effects or severe cutaneous adverse reactions (SCARs). Most patients tolerate ABX well, and it is often used as an over-the-counter mucolytic agent (Cazan et al., 2018). Adverse effects are typically mild and transient, including issues like gastrointestinal discomfort with symptoms like nausea, vomiting, or stomach upset which mostly tend to resolve on their own or with dose adjustments (Zhou et al., 2022). However, the safety and adverse effects may vary among individuals and require careful monitoring, especially with long-term administration and high dosages (>120 mg/day). ABX dosage has been thoroughly evaluated in preclinical studies involving patients with diverse medical conditions to determine its safety profile. These studies

have yielded promising results, highlighting the potential of high-dosage ABX in managing various medical conditions. For example, a study involving pregnant women experiencing premature labor or premature rupture of membranes showed that intravenous administration of 1,000 mg of ABX for 4 hours daily over 3 days significantly reduced the incidence of infant respiratory distress syndrome (IRDS) and perinatal morbidity and mortality, without any adverse effects (Laoag-Fernandez et al., 2000). In two distinct studies, ABX has exhibited its capacity as an antiallergic agent and a local anesthetic, and notably, no toxicity was reported in either case (Fischer et al., 2002; Gibbs, 2009). Similarly, intravenous administration of high-dose ABX at 990 mg/day for five consecutive days after cervical spinal cord injury surgery has been shown to enhance oxygenation and prevent postoperative respiratory complications with limited adverse effects (Li et al., 2012).

In the context of GD, out of all the ABX-treated patients followed in the clinical trials summarized in Table 1, only two were reported to develop hypersensitivity reactions and discontinued the treatment (Zimran et al., 2013). It is worth noting that these two patients were not eligible for ERT treatment due to similar reactions and the developed hypersensitivity is not only developed due to ABX treatment. In the latest clinical trial involving a high ABX dosage (12.7 ± 3.9 mg/kg/day) administered over a duration spanning from 6 months to 6.5 years to 28 GD patients representing all three forms of GD, only a minor subset of three patients encountered mild and temporary adverse events, including nausea, salivation, diarrhea, and rash providing additional evidence of the long-term safety of high ABX dosage (Zhan et al., 2023). Despite its reported excellent safety profile, 13 ABX-treated patients (600 mg/day) dropped out of a clinical study involving 40 candidates due to the development of mild adverse events associated with the treatment (Istaiti et al., 2023). During the treatment, there were some reported side effects such as cough, nausea, abdominal pain, diarrhea, and headache. However, none of these side effects were severe and they were mostly resolved once the treatment was discontinued. One patient had a temporary asymptomatic rise of the liver enzymes, but it rapidly resolved upon the termination of the ABX treatment. Additionally, eight cases of hypouricemia were observed, but they were transient and resolved on their own. While twelve patients out of the initial 41 participants encountered similar mild adverse events, only eight dropped out (two due to ABX-unrelated death) from the study which was primarily established to initiate a registry of ABX treatment in GD in 2021 (Istaiti et al., 2021). The other conducted trials did not report any further severe adverse effects with the administered dosages of ABX (Table 1). However, like any medication, individual responses may vary, and careful monitoring is essential. Further research and long-term studies are needed to comprehensively assess the safety and potential adverse effects of ABX, especially in various clinical contexts and patient populations.

4 Conclusion

An invited commentary article was recently published, in which the authors examined the use of ABX treatment in GD (Weinreb and

Goker-Alpan, 2023). They noted that while the treatment may be regarded as ambitious, it is also associated with a sense of ambivalence, owing to the lingering uncertainty surrounding several critical clinical issues. The unresolved nature of these issues makes it difficult to fully endorse the use of ABX in the treatment of GD. Concerns lie around potential safety issues, the lack of official data, and the absence of standardized treatment protocols. Despite its potential therapeutic effect seen in many cases, the lack of ABX pharmacokinetic data to adjust the appropriate responsive dosage limits the ability of clinicians to prescribe GD patient-specific prescription (dose and formula). Beyond the associated *GBA1* genotype, patients response to ABX may be influenced by other factors like different genetic modifiers, epigenetics, and drug metabolism (Davidson et al., 2018). In addition, major GD registries (International Collaborative Gaucher Group and Gaucher Outcome Survey), holding thousands of patient records and data, have not recognized ABX as a valid treatment, further contributing to the ongoing hesitation (Istaiti et al., 2021). To bridge this gap and facilitate data collection, collaborative efforts between clinical research entities and the International Gaucher Alliance are needed to support clinical studies like the ones mentioned in this review article that involve the recruitment of more patients of all representations (ethnicities, genotypes, clinical phenotypes, and treatment options).

Author contributions

FM: Conceptualization, Writing—original draft, Writing—review and editing. FA-J: Funding acquisition, Supervision, Writing—review and editing.

Funding

The author(s) declare financial support was received for the research, authorship, and/or publication of this article. This research is supported by ASPIRE, the technology program management pillar of Abu Dhabi's Advanced Technology Research Council (ATRC), via the ASPIRE Precision Medicine Research Institute Abu Dhabi (ASPIREPMRIAD) award grant number VRI-20-10.

Conflict of interest

The authors declare that the research was conducted in the absence of any commercial or financial relationships that could be construed as a potential conflict of interest.

Publisher's note

All claims expressed in this article are solely those of the authors and do not necessarily represent those of their affiliated organizations, or those of the publisher, the editors and the reviewers. Any product that may be evaluated in this article, or claim that may be made by its manufacturer, is not guaranteed or endorsed by the publisher.

References

- Al-Jasmi, F. A., Tawfig, N., Berniah, A., Ali, B. R., Taleb, M., Hertecant, J. L., et al. (2013). Prevalence and novel mutations of lysosomal storage disorders in United Arab Emirates: LSD in UAE. *JIMD Rep.* 10, 1–9. doi:10.1007/8904_2012_182
- Ambrosi, G., Ghezzi, C., Zangaglia, R., Levandis, G., Pacchetti, C., and Blandini, F. (2015). Ambroxol-induced rescue of defective glucocerebrosidase is associated with increased LIMP-2 and saposin C levels in GBA1 mutant Parkinson's disease cells. *Neurobiol. Dis.* 82, 235–242. doi:10.1016/j.nbd.2015.06.008
- Aries, C., Lohmöller, B., Tiede, S., Täuber, K., Hartmann, G., Rudolph, C., et al. (2022). Promising effect of high dose ambroxol treatment on neurocognition and motor development in a patient with neuropathic gaucher disease 2. *Front. Neurol.* 13, 13. doi:10.3389/fneur.2022.907317
- Bendikov-Bar, I., Maor, G., Filocamo, M., and Horowitz, M. (2013). Ambroxol as a pharmacological chaperone for mutant glucocerebrosidase. *Blood Cells Mol. Dis.* 50, 141–145. doi:10.1016/j.bcmd.2012.10.007
- Bendikov-Bar, I., Ron, I., Filocamo, M., and Horowitz, M. (2011). Characterization of the ERAD process of the L444P mutant glucocerebrosidase variant. *Blood Cells Mol. Dis.* 46, 4–10. doi:10.1016/j.bcmd.2010.10.012
- Bennett, L. L., and Mohan, D. (2013). Gaucher disease and its treatment options. *Ann. Pharmacother.* 47, 1182–1193. doi:10.1177/1060028013500469
- Bianchi, M., Mantovani, A., Erroi, A., Dinarello, C. A., and Ghezzi, P. (1990). Ambroxol inhibits interleukin 1 and tumor necrosis factor production in human mononuclear cells. *Agents Actions* 31, 275–279. doi:10.1007/BF01997619
- Biegstraaten, M., Mengel, E., Maródi, L., Petakov, M., Niederau, C., Giraldo, P., et al. (2010). Peripheral neuropathy in adult type 1 Gaucher disease: a 2-year prospective observational study. *Brain J. Neurol.* 133, 2909–2919. doi:10.1093/brain/awq198
- Bonam, S. R., Wang, F., and Muller, S. (2019). Lysosomes as a therapeutic target. *Nat. Rev. Drug Discov.* 18, 923–948. doi:10.1038/s41573-019-0036-1
- Bultron, G., Kacena, K., Pearson, D., Boxer, M., Yang, R., Sathe, S., et al. (2010). The risk of Parkinson's disease in type 1 Gaucher disease. *J. Inherit. Metab. Dis.* 33, 167–173. doi:10.1007/s10545-010-9055-0
- Cabasso, O., Paul, S., Dorot, O., Maor, G., Krivoruk, O., Pasmanik-Chor, M., et al. (2019). *Drosophila melanogaster* mutated in its GBA1b ortholog recapitulates neuronopathic gaucher disease. *J. Clin. Med.* 8, 1420. doi:10.3390/jcm8091420
- Castillon, G., Chang, S.-C., and Moride, Y. (2022). Global incidence and prevalence of gaucher disease: a targeted literature review. *J. Clin. Med.* 12, 85. doi:10.3390/jcm12010085
- Cazan, D., Klimek, L., Sperl, A., Plomer, M., and Kölsch, S. (2018). Safety of ambroxol in the treatment of airway diseases in adult patients. *Expert Opin. Drug Saf.* 17, 1211–1224. doi:10.1080/14740338.2018.1533954
- Charkhand, B., Scantlebury, M. H., Narita, A., Zimran, A., and Al-Hertani, W. (2019). Effect of Ambroxol chaperone therapy on Glucosylsphingosine (Lyso-Gb1) levels in two Canadian patients with type 3 Gaucher disease. *Mol. Genet. Metab. Rep.* 20, 100476. doi:10.1016/j.ymgmr.2019.100476
- Charrow, J., Andersson, H. C., Kaplan, P., Kolodny, E. H., Mistry, P., Pastores, G., et al. (2000). The Gaucher registry: demographics and disease characteristics of 1698 patients with Gaucher disease. *Arch. Intern. Med.* 160, 2835–2843. doi:10.1001/archinte.160.18.2835
- Chis, B. A., Chis, A. F., and Dumitrascu, D. L. (2021). Gaucher disease – bone involvement. *Med. Pharm. Rep.* 94, S61–S63. doi:10.15386/mpr-2233
- Chu, S.-Y., Chien, C.-C., Hwu, W.-L., Wang, P.-J., and Chien, Y.-H. (2020). Early initiation of high-dose oral ambroxol in combination with enzyme replacement therapy in a neuropathic Gaucher infant. *Blood Cells Mol. Dis.* 81, 102402. doi:10.1016/j.bcmd.2019.102402
- Ciana, G., Dardis, A., Pavan, E., Riolo, R. M. D., Biasizzo, J., Ferino, D., et al. (2020). *In vitro* and *in vivo* effects of Ambroxol chaperone therapy in two Italian patients affected by neuronopathic Gaucher disease and epilepsy. *Mol. Genet. Metab. Rep.* 25, 100678. doi:10.1016/j.ymgmr.2020.100678
- Dardis, A., Michelakakis, H., Rozenfeld, P., Fumic, K., Wagner, J., Pavan, E., et al. (2022). Patient centered guidelines for the laboratory diagnosis of Gaucher disease type 1. *Orphanet J. Rare Dis.* 17, 442. doi:10.1186/s13023-022-02573-6
- Davidson, B. A., Hassan, S., Garcia, E. J., Tayebi, N., and Sidransky, E. (2018). Exploring genetic modifiers of gaucher disease: the next horizon. *Hum. Mutat.* 39, 1739–1751. doi:10.1002/humu.23611
- Dekker, N., van Dussen, L., Hollak, C. E. M., Overkleeft, H., Scheij, S., Ghauharali, K., et al. (2011). Elevated plasma glucosylsphingosine in Gaucher disease: relation to phenotype, storage cell markers, and therapeutic response. *Blood* 118, e118–e127. doi:10.1182/blood-2011-05-352971
- Elstein, D., Tiomkin, M., Hadas-Halpern, I., and Zimran, A. (2011). Organ volume by computed tomography correlates with longitudinal axis on ultrasound in patients with Gaucher disease. *Ultrasound Q.* 27, 225–228. doi:10.1097/RUQ.0b013e318239c5eb
- European Patent Register (2023). Register EPO. Available at: <https://register.epo.org/application?number=EP15723930> (Accessed December 30, 2023).
- Fateen, E., and Abdallah, Z. Y. (2019). Twenty-five years of biochemical diagnosis of Gaucher disease: the Egyptian experience. *Heliyon* 5, e02574. doi:10.1016/j.heliyon.2019.e02574
- Fischer, J., Pschorn, U., Vix, J.-M., Peil, H., Aicher, B., Müller, A., et al. (2002). Efficacy and tolerability of ambroxol hydrochloride lozenges in sore throat. Randomised, double-blind, placebo-controlled trials regarding the local anaesthetic properties. *Arzneimittelforschung* 52, 256–263. doi:10.1055/s-0031-1299889
- Fois, G., Hobi, N., Felder, E., Ziegler, A., Miklavc, P., Walther, P., et al. (2015). A new role for an old drug: ambroxol triggers lysosomal exocytosis via pH-dependent Ca²⁺ release from acidic Ca²⁺ stores. *Cell Calcium* 58, 628–637. doi:10.1016/j.ceca.2015.10.002
- Genzyme, a Sanofi Company (2023). *A 4-part, open-label, multicenter, multinational study of the safety, tolerability, pharmacokinetics, pharmacodynamic, and exploratory efficacy of Venglustat in combination with cerezyme in adult patients with gaucher disease type 3 with Venglustat monotherapy extension*. clinicaltrials.gov.
- Gibbs, B. F. (2009). Differential modulation of IgE-dependent activation of human basophils by ambroxol and related secretolytic analogues. *Int. J. Immunopathol. Pharmacol.* 22, 919–927. doi:10.1177/039463200902200407
- Gupta, P., and Pastores, G. (2018). Pharmacological treatment of pediatric Gaucher disease. *Expert Rev. Clin. Pharmacol.* 11, 1183–1194. doi:10.1080/17512433.2018.1549486
- Han, T.-U., Sam, R., and Sidransky, E. (2020). Small molecule chaperones for the treatment of gaucher disease and GBA1-associated Parkinson disease. *Front. Cell Dev. Biol.* 8, 271. doi:10.3389/fcell.2020.00271
- Hollak, C. E., van Weely, S., van Oers, M. H., and Aerts, J. M. (1994). Marked elevation of plasma chitotriosidase activity. A novel hallmark of Gaucher disease. *J. Clin. Invest.* 93, 1288–1292. doi:10.1172/JCI117084
- Hollak, C. E. M., Belmatoug, N., Cole, J. A., Vom Dahl, S., Deegan, P. B., Goldblatt, J., et al. (2012). Characteristics of type 1 Gaucher disease associated with persistent thrombocytopenia after treatment with imiglucerase for 4–5 years. *Br. J. Haematol.* 158, 528–538. doi:10.1111/j.1365-2141.2012.09175.x
- Hruska, K. S., LaMarca, M. E., Scott, C. R., and Sidransky, E. (2008). Gaucher disease: mutation and polymorphism spectrum in the glucocerebrosidase gene (GBA). *Hum. Mutat.* 29, 567–583. doi:10.1002/humu.20676
- Hughes, D., Mikosch, P., Belmatoug, N., Carubbi, F., Cox, T., Goker-Alpan, O., et al. (2019). Gaucher disease in bone: from pathophysiology to practice. *J. Bone Min. Res.* 34, 996–1013. doi:10.1002/jbmr.3734
- Hurvitz, N., Dinur, T., Becker-Cohen, M., Cozma, C., Hovakimyan, M., Oppermann, S., et al. (2019). Glucosylsphingosine (lyso-Gb1) as a biomarker for monitoring treated and untreated children with gaucher disease. *Int. J. Mol. Sci.* 20, 3033. doi:10.3390/ijms20123033
- Istaiti, M., Frydman, D., Dinur, T., Szer, J., Revel-Vilk, S., and Zimran, A. (2023). High-dose ambroxol therapy in type 1 gaucher disease focusing on patients with poor response to enzyme replacement therapy or substrate reduction therapy. *Int. J. Mol. Sci.* 24, 6732. doi:10.3390/ijms24076732
- Istaiti, M., Revel-Vilk, S., Becker-Cohen, M., Dinur, T., Ramaswami, U., Castillo-Garcia, D., et al. (2021). Upgrading the evidence for the use of ambroxol in Gaucher disease and GBA related Parkinson: investigator initiated registry based on real life data. *Am. J. Hematol.* 96, 545–551. doi:10.1002/ajh.26131
- Ivanova, M. L., Dao, J., Kasaci, N., Adewale, B., Nazari, S., Noll, L., et al. (2021). Cellular and biochemical response to chaperone versus substrate reduction therapies in neuropathic Gaucher disease. *PLOS ONE* 16, e0247211. doi:10.1371/journal.pone.0247211
- Jarvis, M. F., Honore, P., Shieh, C.-C., Chapman, M., Joshi, S., Zhang, X.-F., et al. (2007). A-803467, a potent and selective Nav1.8 sodium channel blocker, attenuates neuropathic and inflammatory pain in the rat. *Proc. Natl. Acad. Sci. U. S. A.* 104, 8520–8525. doi:10.1073/pnas.0611364104
- Jiang, W., Yi, M., Maegawa, G. H. B., and Zhang, H. (2020). Ambroxol improves skeletal and hematological manifestations on a child with Gaucher disease. *J. Hum. Genet.* 65, 345–349. doi:10.1038/s10038-019-0704-3
- Jung, O., Patnaik, S., Marugan, J., Sidransky, E., and Westbroek, W. (2016). Progress and potential of non-inhibitory small molecule chaperones for the treatment of Gaucher disease and its implications for Parkinson disease. *Expert Rev. Proteomics* 13, 471–479. doi:10.1080/14789450.2016.1174583
- Kantar, A., Klimek, L., Cazan, D., Sperl, A., Sent, U., and Mesquita, M. (2020). An overview of efficacy and safety of ambroxol for the treatment of acute and chronic respiratory diseases with a special regard to children. *Multidiscip. Respir. Med.* 15, 511. doi:10.4081/mrm.2020.511
- Kim, Y.-M., Yum, M.-S., Heo, S. H., Kim, T., Jin, H. K., Bae, J.-S., et al. (2020). Pharmacologic properties of high-dose ambroxol in four patients with Gaucher disease and myoclonic epilepsy. *J. Med. Genet.* 57, 124–131. doi:10.1136/jmedgenet-2019-106132
- Kopytova, A. E., Rychkov, G. N., Nikolaev, M. A., Baydakova, G. V., Cheblov, A. A., Senkevich, K. A., et al. (2021). Ambroxol increases glucocerebrosidase (GCase) activity and restores GCase translocation in primary patient-derived macrophages in Gaucher

- disease and Parkinsonism. *Park. Relat. Disord.* 84, 112–121. doi:10.1016/j.parkreldis.2021.02.003
- Laoa-Fernandez, J. B., Fernandez, A. M., and Maruo, T. (2000). Antenatal use of ambroxol for the prevention of infant respiratory distress syndrome. *J. Obstet. Gynaecol. Res.* 26, 307–312. doi:10.1111/j.1447-0756.2000.tb01327.x
- Li, Q., Yao, G., and Zhu, X. (2012). High-dose ambroxol reduces pulmonary complications in patients with acute cervical spinal cord injury after surgery. *Neurocrit. Care* 16, 267–272. doi:10.1007/s12028-011-9642-4
- Liguori, L., Monticelli, M., Allocca, M., Hay Mele, B., Lukas, J., Cubellis, M. V., et al. (2020). Pharmacological chaperones: a therapeutic approach for diseases caused by destabilizing missense mutations. *Int. J. Mol. Sci.* 21, 489. doi:10.3390/ijms21020489
- Linari, S., and Castaman, G. (2015). Clinical manifestations and management of Gaucher disease. *Clin. Cases Min. Bone Metab.* 12, 157–164. doi:10.11138/ccmbm/2015.12.2.157
- Luan, Z., Li, L., Higaki, K., Nanba, E., Suzuki, Y., and Ohno, K. (2013). The chaperone activity and toxicity of ambroxol on Gaucher cells and normal mice. *Brain Dev.* 35, 317–322. doi:10.1016/j.braindev.2012.05.008
- Maegawa, G. H. B., Tropak, M. B., Buttner, J. D., Rigat, B. A., Fuller, M., Pandit, D., et al. (2009). Identification and characterization of ambroxol as an enzyme enhancement agent for gaucher disease. *J. Biol. Chem.* 284, 23502–23516. doi:10.1074/jbc.M109.012393
- Magalhaes, J., Gegg, M. E., Migdalska-Richards, A., and Schapira, A. H. (2018). Effects of ambroxol on the autophagy-lysosome pathway and mitochondria in primary cortical neurons. *Sci. Rep.* 8, 1385. doi:10.1038/s41598-018-19479-8
- McCormack, P. L., and Goa, K. L. (2003). Miglustat. *Drugs* 63, 2427–2434. doi:10.2165/00003495-200363220-00006
- McNeill, A., Magalhaes, J., Shen, C., Chau, K.-Y., Hughes, D., Mehta, A., et al. (2014). Ambroxol improves lysosomal biochemistry in glucocerebrosidase mutation-linked Parkinson disease cells. *Brain* 137, 1481–1495. doi:10.1093/brain/awu020
- Migdalska-Richards, A., Daly, L., Bezard, E., and Schapira, A. H. V. (2016). Ambroxol effects in glucocerebrosidase and α -synuclein transgenic mice. *Ann. Neurol.* 80, 766–775. doi:10.1002/ana.24790
- Migdalska-Richards, A., Ko, W. K. D., Li, Q., Bezard, E., and Schapira, A. H. V. (2017). Oral ambroxol increases brain glucocerebrosidase activity in a nonhuman primate. *Synapse*. N. Y. N. 71, e21967. doi:10.1002/syn.21967
- Mignot, C., Doummar, D., Maire, I., De Villemeur, T. B., and French Type 2 Gaucher Disease Study Group (2006). Type 2 Gaucher disease: 15 new cases and review of the literature. *Brain Dev.* 28, 39–48. doi:10.1016/j.braindev.2005.04.005
- Mignot, C., Gelot, A., Bessières, B., Daffos, F., Voyer, M., Menez, F., et al. (2003). Perinatal-lethal gaucher disease. *Am. J. Med. Genet. A* 120A, 338–344. doi:10.1002/ajmg.a.20117
- Mohamed, F. E., Al-Gazali, L., Al-Jasmi, F., and Ali, B. R. (2017). Pharmaceutical chaperones and proteostasis regulators in the therapy of lysosomal storage disorders: current perspective and future promises. *Front. Pharmacol.* 8, 448. doi:10.3389/fphar.2017.00448
- Mohamed, F. E., Ali, A., Al-Tenaiji, A., Al-Jasmi, A., and Al-Jasmi, F. (2022). A type 3 gaucher-like disease due to saposin C deficiency in two Emirati families caused by a novel splice site variant in the PSAP gene. *J. Mol. Neurosci.* MN 72, 1322–1333. doi:10.1007/s12031-022-01987-y
- Muntau, A. C., Leandro, J., Staudigl, M., Mayer, F., and Gersting, S. W. (2014). Innovative strategies to treat protein misfolding in inborn errors of metabolism: pharmacological chaperones and proteostasis regulators. *J. Inherit. Metab. Dis.* 37, 505–523. doi:10.1007/s10545-014-9701-z
- Narita, A., Shirai, K., Itamura, S., Matsuda, A., Ishihara, A., Matsushita, K., et al. (2016). Ambroxol chaperone therapy for neuronopathic Gaucher disease: a pilot study. *Ann. Clin. Transl. Neurol.* 3, 200–215. doi:10.1002/acn.3.292
- National Gaucher Foundation (2023). Natl gauch found. Available at: <https://www.gaucherdisease.org/> (Accessed December 29, 2023).
- Ollier, C., Sent, U., Mesquita, M., and Michel, M. C. (2020). Pharmacokinetics of ambroxol sustained release (Mucosolvan® retard) compared with other formulations in healthy volunteers. *Pulm. Ther.* 6, 119–130. doi:10.1007/s41030-020-00116-7
- Parenti, G., Andria, G., and Valenzano, K. J. (2015). Pharmacological chaperone therapy: preclinical development, clinical translation, and prospects for the treatment of lysosomal storage disorders. *Mol. Ther.* 23, 1138–1148. doi:10.1038/mt.2015.62
- Pawlinski, L., Krawczyk, M., Fiema, M., Tobor, E., and Kiec-Wilk, B. (2020). Dual-action ambroxol in treatment of chronic pain in Gaucher Disease. *Eur. J. Pain* 24, 992–996. doi:10.1002/ejp.1538
- Ramadža, D. P., Zekušić, M., Žigman, T., Škaričić, A., Bogdanić, A., Mustać, G., et al. (2021). Early initiation of ambroxol treatment diminishes neurological manifestations of type 3 Gaucher disease: a long-term outcome of two siblings. *Eur. J. Paediatr. Neurol.* EJPN Off. J. Eur. Paediatr. Neurol. Soc. 32, 66–72. doi:10.1016/j.ejpn.2021.03.013
- Remondelli, P., and Renna, M. (2017). The endoplasmic reticulum unfolded protein response in neurodegenerative disorders and its potential therapeutic significance. *Front. Mol. Neurosci.* 10, 187. doi:10.3389/fnmol.2017.00187
- Revel-Vilk, S., Szer, J., Mehta, A., and Zimran, A. (2018). How we manage Gaucher Disease in the era of choices. *Br. J. Haematol.* 182, 467–480. doi:10.1111/bjh.15402
- Riboldi, G. M., and Di Fonzo, A. B. (2019). GBA, gaucher disease, and Parkinson's disease: from genetic to clinic to new therapeutic approaches. *Cells* 8, 364. doi:10.3390/cells8040364
- Roshan Lal, T., and Sidransky, E. (2017). The spectrum of neurological manifestations associated with gaucher disease. *Diseases* 5, 10. doi:10.3390/diseases5010010
- Sam, R., Ryan, E., Daykin, E., and Sidransky, E. (2021). Current and emerging pharmacotherapy for Gaucher disease in pediatric populations. *Expert Opin. Pharmacother.* 22, 1489–1503. doi:10.1080/14655666.2021.1902989
- Sardiello, M. (2016). Transcription factor EB: from master coordinator of lysosomal pathways to candidate therapeutic target in degenerative storage diseases. *Ann. N. Y. Acad. Sci.* 1371, 3–14. doi:10.1111/nyas.13131
- Schwartz, I. V. D., Göker-Alpan, Ö., Kishnani, P. S., Zimran, A., Renault, L., Panahloo, Z., et al. (2017). Characteristics of 26 patients with type 3 Gaucher disease: a descriptive analysis from the Gaucher Outcome Survey. *Mol. Genet. Metab. Rep.* 14, 73–79. doi:10.1016/j.ymgmr.2017.10.011
- Sidransky, E. (2004). Gaucher disease: complexity in a “simple” disorder. *Mol. Genet. Metab.* 83, 6–15. doi:10.1016/j.ymgme.2004.08.015
- Stenson, P. D., Mort, M., Ball, E. V., Chapman, M., Evans, K., Azevedo, L., et al. (2020). The Human Gene Mutation Database (HGMD®): optimizing its use in a clinical diagnostic or research setting. *Hum. Genet.* 139, 1197–1207. doi:10.1007/s00439-020-02199-3
- Stirnermann, J., Belmatoug, N., Camou, F., Serratrice, C., Froissart, R., Caillaud, C., et al. (2017). A review of gaucher disease pathophysiology, clinical presentation and treatments. *Int. J. Mol. Sci.* 18, 441. doi:10.3390/ijms18020441
- Stone, W. L., Basit, H., and Master, S. R. (2023). *Gaucher disease. StatPearls, treasure island (FL)*. United States: StatPearls Publishing.
- Suzuki, T., Shimoda, M., Ito, K., Hanai, S., Aizawa, H., Kato, T., et al. (2013). Expression of human Gaucher disease gene GBA generates neurodevelopmental defects and ER stress in *Drosophila* eye. *PLoS One* 8, e69147. doi:10.1371/journal.pone.0069147
- Thirumal Kumar, D., Iyer, S., Christy, J. P., Siva, R., Tayubi, I. A., George Priya Doss, C., et al. (2019). A comparative computational approach toward pharmacological chaperones (NN-DNJ and ambroxol) on N370S and L444P mutations causing Gaucher's disease. *Adv. Protein Chem. Struct. Biol.* 114, 315–339. doi:10.1016/bs.apcsb.2018.10.002
- Turgay Yagmur, I., Unal Uzun, O., Kucukcongur Yavas, A., Kulhas Celik, I., Toyran, M., Gunduz, M., et al. (2020). Management of hypersensitivity reactions to enzyme replacement therapy in children with lysosomal storage diseases. *Ann. Allergy Asthma Immunol.* 125, 460–467. doi:10.1016/j.anai.2020.07.010
- Tylki-Szymańska, A., Vellodi, A., El-Beshlawy, A., Cole, J. A., and Kolodny, E. (2010). Neuronopathic gaucher disease: demographic and clinical features of 131 patients enrolled in the international collaborative gaucher group neurological outcomes subregistry. *J. Inherit. Metab. Dis.* 33, 339–346. doi:10.1007/s10545-009-9009-6
- Van Rossum, A., and Holsopple, M. (2016). Enzyme replacement or substrate reduction? A review of gaucher disease treatment options. *Hosp. Pharm.* 51, 553–563. doi:10.1310/hpj5107-553
- Vom Dahl, S., Poll, L., Di Rocco, M., Ciana, G., Denes, C., Mariani, G., et al. (2006). Evidence-based recommendations for monitoring bone disease and the response to enzyme replacement therapy in Gaucher patients. *Curr. Med. Res. Opin.* 22, 1045–1064. doi:10.1185/030079906X104623
- Weinreb, N. J., and Goker-Alpan, O. (2023). Ambroxol as therapy for gaucher disease—ambitious but ambivalent. *JAMA Netw. Open* 6, e2319336. doi:10.1001/jamanetworkopen.2023.19336
- Weiser, T. (2008). Ambroxol: a CNS drug? *CNS Neurosci. Ther.* 14, 17–24. doi:10.1111/j.1527-3458.2007.00032.x
- Wenstrup, R. J., Roca-Espiau, M., Weinreb, N. J., and Bembi, B. (2002). Skeletal aspects of Gaucher disease: a review. *Br. J. Radiol.* 75, A2–A12. doi:10.1259/bjr.75.suppl_1.750002
- Yang, S.-Y., Beavan, M., Chau, K.-Y., Taanman, J.-W., and Schapira, A. H. V. (2017). A human neural crest stem cell-derived dopaminergic neuronal model recapitulates biochemical abnormalities in GBA1 mutation carriers. *Stem Cell Rep.* 8, 728–742. doi:10.1016/j.stemcr.2017.01.011
- Zhan, X., Zhang, H., Maegawa, G. H. B., Wang, Y., Gao, X., Wang, D., et al. (2023). Use of ambroxol as therapy for gaucher disease. *JAMA Netw. Open* 6, e2319364. doi:10.1001/jamanetworkopen.2023.19364
- Zhang, P., Zheng, M.-F., Cui, S.-Y., Zhang, W., and Gao, R.-P. (2022). Ambroxol chaperone therapy for gaucher disease type I-associated liver cirrhosis and portal hypertension: a case report. *Endocr. Metab. Immune Disord. Drug Targets* 22, 658–662. doi:10.2174/187153032166621119145230
- Zhang, Y., Shu, L., Zhou, X., Pan, H., Xu, Q., Guo, J., et al. (2018). A meta-analysis of GBA-related clinical symptoms in Parkinson's disease. *Park Dis.* 2018, 3136415. doi:10.1155/2018/3136415
- Zhou, X., Jin, X., Yang, L., and Wei, X. (2022). Efficacy and safety of ambroxol hydrochloride in the treatment of secretory otitis media: a systematic review and meta-analysis. *Ann. Transl. Med.* 10, 142. doi:10.21037/atm-22-237
- Zimran, A., Altarescu, G., and Elstein, D. (2013). Pilot study using ambroxol as a pharmacological chaperone in type 1 Gaucher disease. *Blood Cells Mol. Dis.* 50, 134–137. doi:10.1016/j.bcmd.2012.09.006



OPEN ACCESS

EDITED BY

Pranoot Tanpaiboon,
Quest Diagnostics, United States

REVIEWED BY

Andrea Lynne Gropman,
Children's National Hospital, United States

*CORRESPONDENCE

M. Estela Rubio-Gozalbo,
✉ estela.rubio@mumc.nl

[†]These authors have contributed equally to this work and share first authorship

[‡]These authors share senior authorship

RECEIVED 14 December 2023

ACCEPTED 24 January 2024

PUBLISHED 15 February 2024

CITATION

Panis B, Vos EN, Barić I, Bosch AM, Brouwers MCGJ, Burlina A, Cassiman D, Coman DJ, Couce ML, Das AM, Demirbas D, Empain A, Gautschi M, Grafakou O, Grunewald S, Kingma SDK, Knerr I, Leão-Teles E, Möslinger D, Murphy E, Öunap K, Pané A, Paci S, Parini R, Rivera IA, Scholl-Bürgi S, Schwartz IVD, Sdogou T, Shakerdi LA, Skouma A, Stepien KM, Treacy EP, Waisbren S, Berry GT and Rubio-Gozalbo ME (2024), Brain function in classic galactosemia, a galactosemia network (GalNet) members review. *Front. Genet.* 15:1355962. doi: 10.3389/fgene.2024.1355962

COPYRIGHT

© 2024 Panis, Vos, Barić, Bosch, Brouwers, Burlina, Cassiman, Coman, Couce, Das, Demirbas, Empain, Gautschi, Grafakou, Grunewald, Kingma, Knerr, Leão-Teles, Möslinger, Murphy, Öunap, Pané, Paci, Parini, Rivera, Scholl-Bürgi, Schwartz, Sdogou, Shakerdi, Skouma, Stepien, Treacy, Waisbren, Berry and Rubio-Gozalbo. This is an open-access article distributed under the terms of the [Creative Commons Attribution License \(CC BY\)](https://creativecommons.org/licenses/by/4.0/). The use, distribution or reproduction in other forums is permitted, provided the original author(s) and the copyright owner(s) are credited and that the original publication in this journal is cited, in accordance with accepted academic practice. No use, distribution or reproduction is permitted which does not comply with these terms.

Brain function in classic galactosemia, a galactosemia network (GalNet) members review

Bianca Panis^{1,2,3†}, E. Naomi Vos^{1,2,3,4,5†}, Ivo Barić⁶, Annet M. Bosch^{2,3,7}, Martijn C. G. J. Brouwers^{2,8}, Alberto Burlina^{2,9}, David Cassiman¹⁰, David J. Coman¹¹, María L. Couce^{2,12}, Anibh M. Das^{2,13}, Didem Demirbas¹⁴, Aurélie Empain^{2,15}, Matthias Gautschi¹⁶, Olga Grafakou^{2,17}, Stephanie Grunewald¹⁸, Sandra D. K. Kingma^{2,19}, Ina Knerr²⁰, Elisa Leão-Teles^{2,21}, Dorothea Möslinger^{2,22}, Elaine Murphy²³, Katrin Öunap^{2,24}, Adriana Pané^{2,25}, Sabrina Paci^{2,26}, Rossella Parini^{2,27}, Isabel A. Rivera²⁸, Sabine Scholl-Bürgi²⁹, Ida V. D. Schwartz³⁰, Triantafyllia Sdogou^{2,31}, Loai A. Shakerdi³², Anastasia Skouma^{2,31}, Karolina M. Stepien³³, Eileen P. Treacy³⁴, Susan Waisbren¹⁴, Gerard T. Berry^{14*} and M. Estela Rubio-Gozalbo^{1,2,3,4,5*‡}

¹Department of Pediatrics, MosaKids Children's Hospital, Maastricht University Medical Centre, Maastricht, Netherlands, ²European Reference Network for Hereditary Metabolic Disorders (MetabERN) Member, Padova, Italy, ³United for Metabolic Diseases (UMD), Amsterdam, Netherlands, ⁴Department of Clinical Genetics, Maastricht University Medical Centre, Maastricht, Netherlands, ⁵GROW School for Oncology and Reproduction, Faculty of Health, Medicine and Life Sciences, Maastricht University, Maastricht, Netherlands, ⁶Department of Pediatrics, University Hospital Center Zagreb, Croatia, and School of Medicine, University of Zagreb, Zagreb, Croatia, ⁷Department of Pediatrics, Division of Metabolic Diseases, Emma Children's Hospital, Amsterdam University Medical Center, Amsterdam Gastroenterology Endocrinology Metabolism, Inborn Errors of Metabolism, Amsterdam, Netherlands, ⁸Department of Internal Medicine, Division of Endocrinology and Metabolic Disease, Maastricht University Medical Centre, Cardiovascular Research Institute Maastricht (CARIM), Maastricht University, Maastricht, Netherlands, ⁹Division of Inherited Metabolic Diseases, Reference Centre Expanded Newborn Screening, University Hospital Padova, Padova, Italy, ¹⁰Laboratory of Hepatology, Department of Chronic Diseases, Metabolism and Ageing, Faculty of Medicine, KU Leuven, Leuven, Belgium, ¹¹Queensland Children's Hospital, Children's Health Queensland, Brisbane, QLD, Australia, ¹²Department of Pediatrics, Diagnosis and Treatment Unit of Congenital Metabolic Diseases, University Clinical Hospital of Santiago de Compostela, IDIS-Health Research Institute of Santiago de Compostela, CIBERER, RICORS Instituto Salud Carlos III, Santiago de Compostela, Spain, ¹³Department of Paediatrics, Pediatric Metabolic Medicine, Hannover Medical School, Hannover, Germany, ¹⁴Division of Genetics and Genomics, Boston Children's Hospital, Harvard Medical School, Manton Center for Orphan Disease Research, Boston, MA, United States, ¹⁵Department of Paediatrics, Metabolic and Nutrition Unit, Division of Endocrinology, Diabetes and Metabolism, University Hospital for Children Queen Fabiola, Bruxelles, Belgium, ¹⁶Department of Paediatrics, Institute of Clinical Chemistry, Inselspital, Bern University Hospital, Swiss Reference Centre for Inborn Errors of Metabolism, Site Bern, Division of Pediatric Endocrinology, Diabetes and Metabolism, University of Bern, Bern, Switzerland, ¹⁷IEM Clinic, Arch Makarios III Hospital,

Abbreviations: AR, aldose reductase; CG, classic galactosemia; CNS, central nervous system; ER, endoplasmic reticulum; Gal-1-P, galactose-1-phosphate; GALDH, galactose dehydrogenase; GALE, UDP-galactose 4'-epimerase; GALK1, galactokinase; GalNet, Galactosemia Network; GALT, galactose-1-phosphate uridylyltransferase; GALM, galactose mutarotase; IQ, intelligence quotient; MRI: magnetic resonance imaging; NDI, neurite density index; NMJ: neuromuscular junction; NODDI, neurite orientation dispersion and density imaging; ODI, orientation dispersion index; PIQ, performance IQ; PSPC, purple sweet potato color; TIQ, total IQ; UDP, Uridine diphosphate; UGP2, UDP-glucose pyrophosphorylase 2; VIQ, verbal component IQ.

Nicosia, Cyprus, ¹⁸Metabolic Unit Great Ormond Street Hospital and Institute for Child Health, University College London, London, United Kingdom, ¹⁹Centre for Metabolic Diseases, University Hospital Antwerp, University of Antwerp, Antwerp, Belgium, ²⁰National Centre for Inherited Metabolic Disorders, Children's Health Ireland at Temple Street, University College Dublin, Dublin, Ireland, ²¹Reference Centre of Inherited Metabolic Diseases, Centro Hospitalar Universitário São João, Porto, Portugal, ²²Department of Paediatrics and Adolescent Medicine, Medical University of Vienna, Vienna, Austria, ²³Charles Dent Metabolic Unit, National Hospital for Neurology and Neurosurgery (NHN), London, United Kingdom, ²⁴Genetics and Personalized Medicine Clinic, Faculty of Medicine, Tartu University Hospital, Institute of Clinical Medicine, University of Tartu, Tartu, Estonia, ²⁵Endocrinology and Nutrition Department, Hospital Clínic de Barcelona, Centro de Investigación Biomédica en Red de la Fisiopatología de la Obesidad y Nutrición (CIBEROBN), Instituto de Salud Carlos III (ISCIII), Madrid, Spain, ²⁶Inborn Errors of Metabolism, Clinical Department of Pediatrics, San Paolo Hospital - ASST Santi Paolo e Carlo, University of Milan, Milan, Italy, ²⁷Rare Diseases Unit, Department of Internal Medicine, San Gerardo Hospital IRCCS, Monza, Italy, ²⁸Med.U.Lisboa-Instituto de Investigação do Medicamento, Faculdade de Farmácia, Universidade de Lisboa, Lisboa, Portugal, ²⁹Department of Child and Adolescent Health, Division of Pediatrics I-Inherited Metabolic Disorders, Medical University Innsbruck, Innsbruck, Austria, ³⁰Medical Genetics Service, Hospital de Clinicas de Porto Alegre, Porto Alegre, Brazil, ³¹Newborn Screening Department, Institute of Child Health, Athens, Greece, ³²Adult Metabolics/Genetics, National Centre for Inherited Metabolic Disorders, The Mater Misericordiae University Hospital, Dublin, Ireland, ³³Salford Royal Organisation, Northern Care Alliance NHS Foundation Trust, Salford, United Kingdom, ³⁴School of Medicine, Trinity College Dublin, National Rare Diseases Office, Mater Misericordiae University Hospital, Dublin, Ireland

Classic galactosemia (CG, OMIM #230400, ORPHA: 79,239) is a hereditary disorder of galactose metabolism that, despite treatment with galactose restriction, affects brain function in 85% of the patients. Problems with cognitive function, neuropsychological/social emotional difficulties, neurological symptoms, and abnormalities in neuroimaging and electrophysiological assessments are frequently reported in this group of patients, with an enormous individual variability. In this review, we describe the role of impaired galactose metabolism on brain dysfunction based on state of the art knowledge. Several proposed disease mechanisms are discussed, as well as the time of damage and potential treatment options. Furthermore, we combine data from longitudinal, cross-sectional and retrospective studies with the observations of specialist teams treating this disease to depict the brain disease course over time. Based on current data and insights, the majority of patients do not exhibit cognitive decline. A subset of patients, often with early onset cerebral and cerebellar volume loss, can nevertheless experience neurological worsening. While a large number of patients with CG suffer from anxiety and depression, the increased complaints about memory loss, anxiety and depression at an older age are likely multifactorial in origin.

KEYWORDS

classic galactosemia, brain, galactose, cognitive problems, neurodevelopment, movement disorders, neuropsychiatry

1 Galactose metabolism

Galactose is a natural aldohexose that exists as free galactose and as a component of complex carbohydrates, glycoproteins and glycolipids. Together with glucose, galactose forms lactose, a disaccharide abundantly present in dairy products. Among other functions, it serves as a key source of energy in infants and is important for galactosylation of complex molecules such as galactocerebroside in myelin. On average, 88% of galactose is retained in the liver (Coelho et al., 2015a; Conte et al., 2021).

The Leloir pathway is the main pathway of galactose metabolism and consists of four steps, consecutively mediated by galactose mutarotase (GALM EC 5.1.3.3), galactokinase (GALK1 EC 2.7.1.6), galactose-1-phosphate uridylyltransferase (GALT, EC 2.7.7.12) and UDP-galactose 4'-epimerase (GALE,

EC 5.1.3.7) (Figure 1A). Galactose entering the Leloir pathway either becomes a precursor for glycosylation (as UDP-galactose) or is used in glycolysis and glycogen synthesis pathways (as UDP-glucose) (Conte et al., 2021).

In Classic Galactosemia (CG), severe deficiency of GALT (<1% residual activity) fuels several alternative galactose disposal routes. Firstly, aldose reductase (AR, EC 1.1.1.21) converts α -D-galactose into galactitol in a NADPH-dependent reaction. Secondly, galactose is oxidized to galactonate by galactose dehydrogenase (GALDH, EC 1.1.1.48), producing NADH. Galactonate is excreted from the body or converted to D-xylulose 5-phosphate to enter the pentose phosphate pathway (Coelho et al., 2015a; Conte et al., 2021). Lastly, although a poor substrate (low affinity), Gal-1-P can be converted to UDP-galactose by UDP-glucose pyrophosphorylase 2 (UGP2, EC 2.7.7.9) (Coelho et al., 2015a).

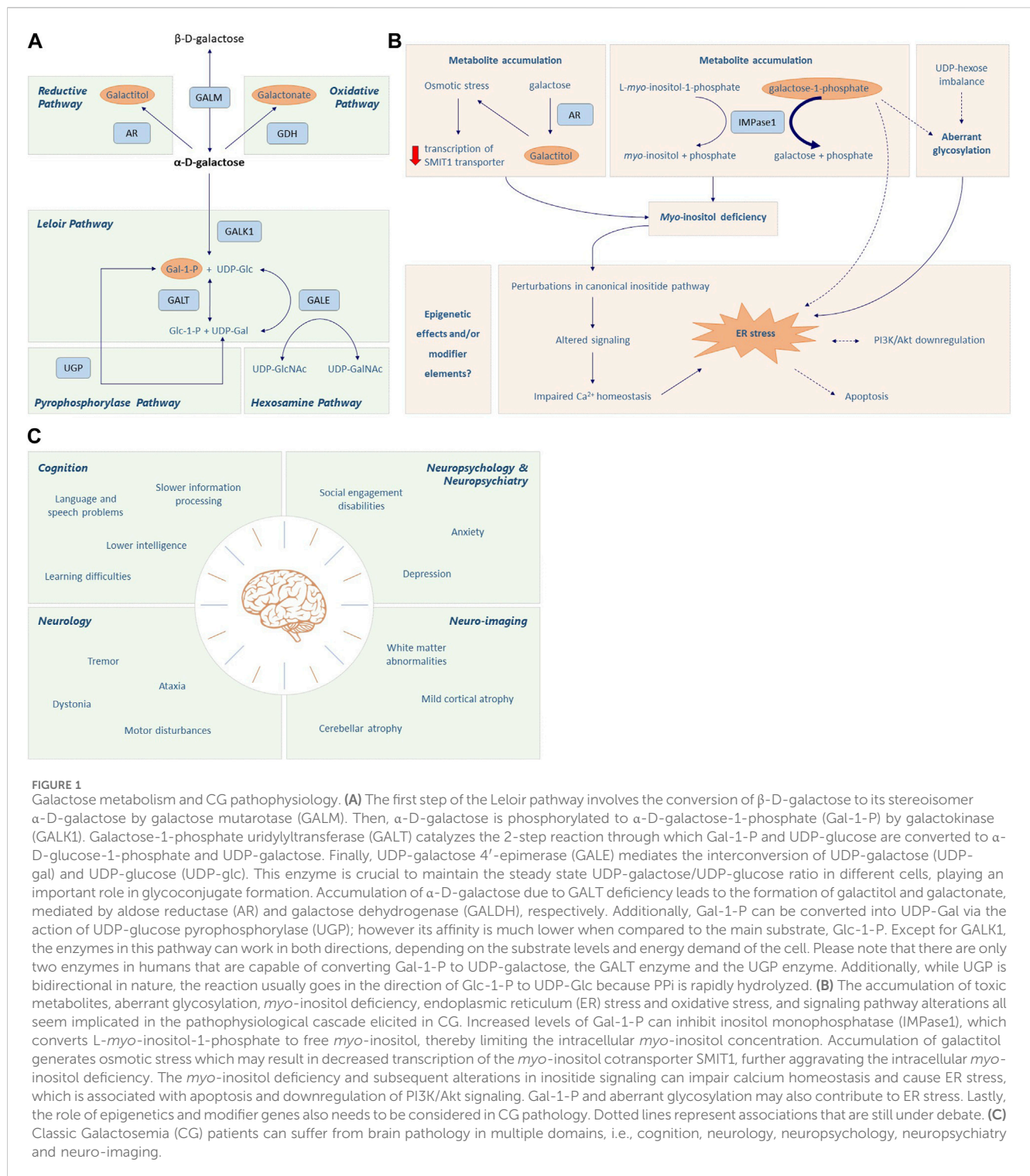


FIGURE 1

Galactose metabolism and CG pathophysiology. **(A)** The first step of the Leloir pathway involves the conversion of β-D-galactose to its stereoisomer α-D-galactose by galactose mutarotase (GALM). Then, α-D-galactose is phosphorylated to α-D-galactose-1-phosphate (Gal-1-P) by galactokinase (GALK1). Galactose-1-phosphate uridylyltransferase (GALT) catalyzes the 2-step reaction through which Gal-1-P and UDP-glucose are converted to α-D-glucose-1-phosphate and UDP-galactose. Finally, UDP-galactose 4'-epimerase (GALE) mediates the interconversion of UDP-galactose (UDP-gal) and UDP-glucose (UDP-glc). This enzyme is crucial to maintain the steady state UDP-galactose/UDP-glucose ratio in different cells, playing an important role in glycoconjugate formation. Accumulation of α-D-galactose due to GALT deficiency leads to the formation of galactitol and galactonate, mediated by aldose reductase (AR) and galactose dehydrogenase (GALDH), respectively. Additionally, Gal-1-P can be converted into UDP-Gal via the action of UDP-glucose pyrophosphorylase (UGP); however its affinity is much lower when compared to the main substrate, Glc-1-P. Except for GALK1, the enzymes in this pathway can work in both directions, depending on the substrate levels and energy demand of the cell. Please note that there are only two enzymes in humans that are capable of converting Gal-1-P to UDP-galactose, the GALT enzyme and the UGP enzyme. Additionally, while UGP is bidirectional in nature, the reaction usually goes in the direction of Glc-1-P to UDP-Glc because PPI is rapidly hydrolyzed. **(B)** The accumulation of toxic metabolites, aberrant glycosylation, myo-inositol deficiency, endoplasmic reticulum (ER) stress and oxidative stress, and signaling pathway alterations all seem implicated in the pathophysiological cascade elicited in CG. Increased levels of Gal-1-P can inhibit inositol monophosphatase (IMPase1), which converts L-myo-inositol-1-phosphate to free myo-inositol, thereby limiting the intracellular myo-inositol concentration. Accumulation of galactitol generates osmotic stress which may result in decreased transcription of the myo-inositol cotransporter SMIT1, further aggravating the intracellular myo-inositol deficiency. The myo-inositol deficiency and subsequent alterations in inositide signaling can impair calcium homeostasis and cause ER stress, which is associated with apoptosis and downregulation of PI3K/Akt signaling. Gal-1-P and aberrant glycosylation may also contribute to ER stress. Lastly, the role of epigenetics and modifier genes also needs to be considered in CG pathology. Dotted lines represent associations that are still under debate. **(C)** Classic Galactosemia (CG) patients can suffer from brain pathology in multiple domains, i.e., cognition, neurology, neuropsychology, neuropsychiatry and neuro-imaging.

2 Clinical spectrum

The first description of an infant with galactosemia dates from 1908 (von Reuss, 1908). In the following years, more patients were described with hypergalactosemia and neonatal illness, including hepatocellular damage, renal tubular disease, *Escherichia coli* sepsis, encephalopathy and cataract (Göppert, 1917; Mason and Turner, 1935). A well-recognized phenomenon is brain edema, also called

'pseudotumor cerebri', leading to increased intracranial pressure and bulging of the fontanel (Wells et al., 1965; Quan-Ma et al., 1966; Huttenlocher et al., 1970; Belman et al., 1986; Berry et al., 2001). A galactose-restricted diet resolves the acute neonatal symptoms but is insufficient to prevent long-term complications, which have the same prevalence in patients with and without neonatal illness.

Brain impairments occur in 85% of CG patients despite diet (Rubio-Gozalbo et al., 2019) (Figure 1C; Supplementary Table S1).

Cognitive problems frequently experienced are global developmental delay and language delay (Komrower and Lee, 1970; Fishler et al., 1980; Waisbren et al., 1983; Waggoner et al., 1990; Schweitzer et al., 1993; Kaufman et al., 1995a; Hansen et al., 1996; Robertson et al., 2000; Antshel et al., 2004; Bosch et al., 2004; Potter et al., 2008; Hughes et al., 2009; Hoffmann et al., 2011; Potter, 2011; Timmers et al., 2011; Timmers et al., 2012; Waisbren et al., 2012; Potter et al., 2013; Demirbas et al., 2019; Kuiper et al., 2019; Welsink-Karssies et al., 2020a; Welsink-Karssies et al., 2020b; Hermans et al., 2023), with a below average mean total intelligence quotient (IQ) of 87 (Coss et al., 2013; Welling et al., 2017a). The language and speech impairments cannot solely be explained by lower cognitive abilities (Waisbren et al., 1983; Waggoner et al., 1990; Schweitzer et al., 1993; Kaufman et al., 1995a; Robertson et al., 2000; Antshel et al., 2004; Potter et al., 2008; Hughes et al., 2009; Potter, 2011; Timmers et al., 2011; Timmers et al., 2012; Waisbren et al., 2012; Potter et al., 2013; Kuiper et al., 2019). Expressive language is mainly affected, with receptive language and comprehension being relatively preserved (Potter et al., 2008; Timmers et al., 2011). Among the speech disorders are verbal dyspraxia (23.5%) and dysarthria (19.9%) (Nelson et al., 1991; Potter et al., 2008; Potter, 2011; Kuiper et al., 2019). Patients require more time to prepare and finish the utterances and make more errors (Timmers et al., 2012), and also recruit additional and more extensive brain regions than control participants (Timmers et al., 2015a).

Approximately half of the CG patients suffer from neurological complications, the most prevalent being tremor (31.0%), which may affect daily life in some cases (Rubio-Gozalbo et al., 2019). Other complications include general motor abnormalities, ataxia, dystonia and epilepsy (Jan and Wilson, 1973; Lo et al., 1984; Bohles et al., 1986; Friedman et al., 1989; Waggoner et al., 1990; Koch et al., 1992; Schweitzer et al., 1993; Robertson et al., 2000; Arn, 2003; Antshel et al., 2004; Martins et al., 2004; Ridel et al., 2005; Potter et al., 2008; Hughes et al., 2009; Shah and Kuchhai, 2009; Waisbren et al., 2012; Rubio-Agusti et al., 2013; Demirbas et al., 2019; Kuiper et al., 2019; Rubio-Gozalbo et al., 2019; Welling et al., 2019; Özgün et al., 2019; Welsink-Karssies et al., 2020a; MacWilliams et al., 2021). Epilepsy is not frequently reported (Friedman et al., 1989; Aydin-Ozemir et al., 2014) and may be the result of brain damage occurring in the neonatal period, or the consequence of unrelated genetic predisposition. Psychiatric and behavioral problems such as depression and anxiety disorder are reported in 44.4% of the patients (Rubio-Gozalbo et al., 2019). Most have a shy and reserved personality (Antshel et al., 2004) and achieve fewer social developmental milestones when compared to healthy controls, which is postulated to be intrinsic to the disease rather than a result of the burden of a chronic disease or lifelong dietary restrictions (Bosch et al., 2009; Gubbels et al., 2011).

Numerous central nervous system (CNS) grey and white matter abnormalities have been reported in CG (Crome, 1962; Haberland et al., 1971; Lo et al., 1984; Choulot et al., 1991; Koch et al., 1992; Nelson et al., 1992; Kaufman et al., 1995b; Hughes et al., 2009; Timmers et al., 2015b; Timmers et al., 2016; Özgün et al., 2019; Ahtam et al., 2020; Welsink-Karssies et al., 2020a; Welsink-Karssies et al., 2020c). Magnetic resonance imaging (MRI) in a cohort of 67 patients showed cerebral and cerebellar atrophy in 22 and 8 patients, respectively, as well as white matter abnormalities in 11 patients (Nelson et al., 1992). In a study that

assessed the integrity of myelinated networks, abnormal somatosensory evoked potentials were present in 17 (28%) of 60 CG patients who had electrophysiological testing of the median nerve, and in 26 (77%) of 34 CG patients who had the posterior tibial nerve tested (Kaufman et al., 1995b). Neurite orientation dispersion and density imaging (NODDI) revealed a lower neurite density index (NDI) in bilateral anterior areas and increased orientation dispersion index (ODI) mainly in the left hemisphere (Timmers et al., 2015b). More recent studies showed lower white matter volume and impaired microstructure in the whole brain, especially in the corticospinal tract (Welsink-Karssies et al., 2020c), as well as the left cerebellum, bilateral putamen and left superior temporal sulcus (Ahtam et al., 2020). Additional disturbances in grey matter density have also been described (Nelson et al., 1992; Dubroff et al., 2008; Timmers et al., 2016; Ahtam et al., 2020).

Several studies have attempted to correlate the grey and white matter abnormalities with clinical outcome. The severity of symptoms at the age of diagnosis was associated with abnormal somatosensory evoked potentials (Kaufman et al., 1995b). Additionally, neurocognitive outcome was linked to patients' resting-state brain connectivity patterns (van Erven et al., 2017), and grey matter density disturbances associated with later initiation of dietary intervention (Timmers et al., 2016). Furthermore, patients with a tremor and/or dystonia had smaller white matter volume, more impaired white matter microstructure and less myelin compared to patients without movement disorders. Patients with IQ < 85 had grey and white matter abnormalities, as well as lower cerebral and cerebellar volume (Welsink-Karssies et al., 2020c). Lastly, language difficulties were correlated with abnormal diffusivity values of the bilateral dorsal and ventral language networks (Ahtam et al., 2020).

Although the aforementioned abnormalities could help explain the neurocognitive profile, the possibility of a coexistent disorder should always be considered, especially in case of unexpected symptoms (Papachristoforou et al., 2014; Neville et al., 2016; Boca and Whone, 2017; Rossi-Espagnet et al., 2021).

3 Proposed disease mechanisms

Toxic metabolites, aberrant glycosylation, *myo*-inositol deficiency, endoplasmic reticulum (ER) stress and oxidative stress, signaling pathway alterations, and structural impairment of GALT, all seem implicated in the pathophysiological cascade elicited in CG (Haskovic et al., 2020) (Figure 1B). Additionally, the role of epigenetics and modifier genes needs to be considered. Different mechanisms could be acting synergistically, depending on the tissue type and developmental stage.

3.1 Metabolite toxicity

Despite diet, the levels of galactose metabolites are persistently increased due to endogenous production of galactose, which is mainly derived from lysosomal hydrolysis of glycolipids, glycoproteins and proteoglycans (Berry et al., 1995a; Berry et al., 1997). The rate of galactose production is higher in infants and children and decreases until adulthood (Berry et al., 2004; Schadewaldt et al., 2004).

Gal-1-P is deemed one of the key pathogenic agents of CG (Gitzelmann, 1995; Leslie, 2003; Lai et al., 2009). Toxicity has been ascribed to the inhibition of enzymes like UGP, phosphoglucomutase, glycogen phosphorylase and inositol monophosphatase, but convincing evidence is still lacking (Gitzelmann, 1995; Lai et al., 2009). Notably, GALK1 deficiency, which causes accumulation of the galactose metabolites except Gal-1-P, does not give rise to the brain and ovarian complications seen in CG (Tang et al., 2010).

Galactitol excretion in urine can be elevated up to 300 times in patients on diet (Krabbi et al., 2011). Studies have reported galactitol elevations in the brains of neonatal and pediatric CG patients (Quan-Ma et al., 1966; Berry et al., 2001; Otaduy et al., 2006; Rossi-Espagnet et al., 2021). Galactitol is poorly diffusible and highly osmotic, and can lead to cell swelling and brain edema. *In vivo* elevation of brain galactitol was associated with diffuse white matter abnormalities in a newborn with CG and encephalopathy (Berry et al., 2001). Furthermore, increased T2 signal in white matter and areas of restricted diffusion involving the cortex and deep grey matter nuclei, consistent with cytotoxic edema, was observed in 3 patients during neonatal illness and confirmed galactitol accumulation (Rossi-Espagnet et al., 2021).

Little attention has been paid to the possible role of galactonate in CG pathophysiology. Although the metabolite is excreted in urine or used in the pentose phosphate pathway, its toxicity cannot be ruled out completely and requires further study (Berry et al., 1998).

3.2 Aberrant glycosylation

Aberrant glycosylation has been hypothesized to be a major mechanism of disease (Maratha et al., 2017). UDP-hexoses serve as key sugar donors for glycosylation, and deficiency of UDP-galactose and disturbance of the UDP-glucose/UDP-galactose ratio have been described in CG (Charlwood et al., 1998; Lai et al., 2003; Coss et al., 2014; Maratha et al., 2017). Furthermore, Gal-1-P may compete as substrate for other nucleotide sugar reactions.

Systemic glycan assembly defects have been documented in neonatal illness which largely resolve with galactose restriction (Charlwood et al., 1998; Quintana et al., 2009). However, there is evidence of continuing glycan processing abnormalities (Coss et al., 2012; Coss et al., 2014; Maratha et al., 2017). Of interest, in a CG sibling study, marked differences in outcomes of the second born siblings were noted, with early onset cerebellar and cerebral atrophy in 2 sibling pairs (Hughes et al., 2009), and significant differences in N-glycosylation in later life (Coman et al., 2010).

While differences in glycosylation can be identified in CG individuals at older age, with differing tolerances to moderate galactose intake liberalization (Coss et al., 2012; Knerr et al., 2015), the significance of these findings is unknown. Polymorphic glycan modifier genes (*MGAT3*, *FUT8* and *ALG9*) can influence glycan chain bisecting and fucosylation, and subsequent cell signaling and adhesion (Wahl et al., 2018).

Myelin may be especially vulnerable to disturbed glycosylation, as it is rich in galactocerebrosides (Barnes-Vélez et al., 2023). Low levels in autopsy brain tissue of an untreated patient raised the question of aberrant glycosylation of galactocerebrosides (Haberland et al., 1971; Koch et al., 1992; Lebea and Pretorius, 2005). Glycosylation also plays an important role in the neuromuscular junction (NMJ) (Dani and Broadie, 2012), and GALT was identified as a potent regulator of NMJ structure in *Drosophila melanogaster* (Jumbo-Lucioni et al., 2014).

3.3 Myo-inositol deficiency

Myo-inositol serves a dual role in human physiology. It is a precursor of membrane phospholipids that are important for calcium- and protein kinase C signaling, and serves as a buffer of osmotic balance (Berry et al., 1995b; Berry, 2011). Brain content of myo-inositol peaks prenatally and continues to decline until a postnatal baseline is reached, which is maintained up to a second decline at middle age (Kreis et al., 2002; Buccafusca et al., 2008). Reduction in intracellular myo-inositol has been associated with impaired integrated stress response signaling and ER stress (Wells and Remy, 1965; Slepak et al., 2007; Hagen-Lillevik et al., 2022). The first reports of myo-inositol deficiency in the brain of CG children date back to 1965 (Wells et al., 1965) and 1966 (Quan-Ma et al., 1966). High levels of Gal-1-P may sequester myo-inositol as inositol monophosphate by inhibition of inositol monophosphatase (Slepak et al., 2007). In addition, galactitol accumulation may lead to poor myo-inositol transport into the cell, further decreasing myo-inositol availability (Berry, 2011).

3.4 Endoplasmic reticulum stress, oxidative stress and signaling pathway alterations

ER stress (Slepak et al., 2007; De-Souza et al., 2014) and oxidative stress (Slepak et al., 2007; Jumbo-Lucioni et al., 2012; Tang et al., 2014) are two other pathological mechanisms. In fibroblasts derived from CG patients (Slepak et al., 2007) and *GalT* gene-trapped mice (Balakrishnan et al., 2016; Balakrishnan et al., 2017), evidence was found for activation of the unfolded protein response and ER stress. Interestingly, salubrinal (an eIF2 α phosphatase inhibitor) administration in these mice reversed the downregulation of PI3K/Akt signaling pathway and significantly slowed down the loss of Purkinje cells in the cerebellum (Balakrishnan et al., 2017). Additionally, administration of purple sweet potato color (PSPC) and myo-inositol, two compounds hypothesized to rescue aberrant signaling pathways in CG partly due to their antioxidant properties, ameliorated dysregulation of cellular pathways in this model (Hagen-Lillevik et al., 2022).

3.5 Structural impairments of GALT

The fundamental biochemical cause of the disease is a severe decrease in enzymatic activity. Some of the pathogenic variants result in a less stable protein that is unable to reach a correct folding,

and so has an increased propensity to aggregation and proteolysis (McCorvie et al., 2013; Coelho et al., 2014).

3.6 Potential epigenetic effects and genetic modifiers

The role of epigenetics and modifier genes needs to be studied more extensively. Genetic modifiers are genetic variants that can influence the phenotypic outcome of a disease-causing variant in another gene, and have repeatedly been postulated to explain the phenotypic variability seen in CG (see also subsection aberrant glycosylation). It is well recognized that genetic modifiers can affect glycosylation pathways in Congenital Disorders of Glycosylation, rendering what was considered to be single gene abnormalities as 'multifactorial' (Quelhas et al., 2023). Several genetic modifiers have already been discovered for other rare Mendelian disorders (Rahit and Tarailo-Graovac, 2020).

4 Time of damage

Intra-uterine toxicity of galactose metabolites has been postulated an important pathogenic factor (Holton, 1995; Segal, 1995). Gal-1-P was elevated in the liver of galactosemic fetuses at 20 weeks gestation, as well as in the cord blood of galactosemic infants born to mothers who abstained from galactose consumption during pregnancy (Gitzelmann, 1995; Holton, 1995).

GALT activity measured in several animal models throughout development (Shin-Buehring et al., 1977; Rogers et al., 1989a; Rogers et al., 1989b; Rogers et al., 1992; Daude et al., 1996) was particularly higher in the early postnatal period relative to adulthood, which has been attributed to the high galactose ingestion and physiological needs during the suckling period (Rogers et al., 1989a). GALT mRNA and protein are already weakly expressed during late embryonic and postnatal development of the brain and peripheral nerve of the rat, with a peak of expression concomitant with myelogenesis (Daude et al., 1996). GALT activity in the late prenatal stage in various organs of a sheep model (Coelho et al., 2017) showed that galactosemia acute target organs—liver, small intestine and kidney—had the highest late prenatal activity, whereas the chronic target organs—brain and ovary—did not exhibit a noticeable pre- or postnatal different activity, in line with the notion that some organs/cells have a greater susceptibility to impaired galactose metabolism.

Supporting an early life injury, disruptions of fiber tracts and brain nuclei formed during embryogenesis and early fetal brain development were reported in ten adult patients (Ahtam et al., 2020). Moreover, a recent study that used retinal neuro-axonal imaging as a surrogate of brain pathology to assess neuronal integrity and monitor neurodegenerative disease progression pointed towards early brain damage (Lotz-Havla et al., 2023).

Some movement disorders, e.g., tremor, are more frequently seen at an older age (Kuiper et al., 2019). It is not clear whether disease-related mechanisms continue to damage structures (striatum/cerebellum) or whether this is the result of a prenatal/perinatal hit with a dying back phenomenon. Vasogenic edema might play a role in the delayed myelination later in life (Rossi-Espagnet et al., 2021). However, disturbances in myelination are also

found in children without neonatal illness, suggesting the implication of other disease mechanisms.

5 Follow-up/treatment current and future perspectives

Dietary galactose restriction is currently the cornerstone for treatment but does not prevent long-term complications. In 2016, the members of the Galactosemia Network (GalNet) developed an evidence-based and internationally applicable guideline for diagnosis, treatment and follow-up of CG patients (Welling et al., 2017b). The guideline recommends a galactose-restricted diet that eliminates sources of galactose from dairy products but permits galactose from non-milk sources. The natural history study showed that patients with a liberalized diet did not have a worse outcome neurologically (Rubio-Gozalbo et al., 2019). Moderate liberalization of galactose intake improved IgG glycosylation in a small number of patients (Coss et al., 2014; Knerr et al., 2015). The guideline also offers guidance for testing various neurocognitive and psychosocial domains to facilitate tailored interventions as part of the treatment plan.

In search of new therapeutic approaches, extensive research has been performed to limit accumulation of toxic metabolites or increase levels of deficient metabolites (Simard-Duquesne et al., 1985; Ng et al., 1989; Mizisin and Powell, 1993; Tang et al., 2012; Ji et al., 2017; Hu et al., 2019; Mackinnon et al., 2021). GALK1 inhibitors were shown to prevent accumulation of Gal-1-P in cellular models, but remain to be studied *in vivo* (Tang et al., 2012; Hu et al., 2019; Mackinnon et al., 2021). Uridine supplementation to increase levels of UDP-Glc and UDP-Gal was not able to rescue the biochemical and clinical phenotype (Ng et al., 1989). Safety and effectiveness of the AR inhibitor AT007 is currently being investigated (NCT04902781; NCT05418829).

Furthermore, to improve GALT activity, chaperone therapy and nucleic acid therapy have been studied. Supplementation of the amino acid arginine as a chaperone had a mutation-specific effect with rescue of human GALT in an *E. coli* model (Coelho et al., 2015b), but failed to exhibit positive effects in four c.563A>G; p.Gln188Arg homozygous patients (Haskovic et al., 2018). Whether other pathogenic variants are amenable has not been studied. *hGALT* mRNA therapy and GALT gene therapy restored GALT activity in cellular and animal models of CG (Balakrishnan et al., 2020; Brophy et al., 2022; Daenzer et al., 2022; Delnoy et al., 2022), but many unknowns remain to be answered before these therapies can be applied. Other treatment options could be compounds that target the integrated stress response such as PSPC and *myo*-inositol (Balakrishnan et al., 2016), which improved brain tissue structures in *GalT* gene-trapped mice (Hagen-Lillevik et al., 2022). An advantage is their favorable safety profile in humans, which could hasten their application in clinical practice.

6 Brain function through adulthood

In CG, brain function is affected in 85% of the patients, with significant individual variability in severity and symptoms (Rubio-

Gozalbo et al., 2019). Since Komrower (Komrower and Lee, 1970) in 1970 reported on physical and mental development in the first cohort of 60 dietary treated CG patients, numerous studies have been performed to shed more light on brain effects in CG (summarized in Supplementary Table S1). While these have expanded our knowledge on the neurocognitive, neuropsychological, neuropsychiatric, social emotional and neurological difficulties associated with the disease, as well as the abnormalities seen in neuroimaging and electrophysiological assessments, information about the disease course in adulthood is still scarce. The majority of studies are cross-sectional, or retrospective using cross-sectional data from different age groups. The few longitudinal studies that have been performed are usually based on small sample sizes, with relatively young patients and limited follow-up time. Although the results from these studies should be treated cautiously, they provide us with the first valuable insights into CG brain function over time.

Nelson et al. (Nelson et al., 1992) performed MRI imaging in 63 CG patients (1 month–42 years of age). Of the 24 patients who underwent follow-up MRI after 1–4 years, abnormal peripheral white matter and ventricle enlargement remained unchanged. One patient showed progression of cerebellar atrophy. Schadewaldt et al. (Schadewaldt et al., 2010) reported TIQ, PIQ and VIQ scores in 23 patients, with the first tests performed at a mean age of 11 ± 5 years and the second tests at a mean age of 26 ± 5 years. The mean TIQ and PIQ did not change significantly over time, whereas the mean VIQ score showed a variable but significant decline at follow-up. However, no consistent changes were found, as a number of participants showed significant increases and other patients decreases of these scores with age. In line with these results, neurocognitive function did not deteriorate in a cohort of 35 patients aged 1 week – 16 years, but the follow-up time was only 2–5 years (Manis et al., 1997). A recent study in a robust dataset of CG patients (mean age of 18 years) concluded that speech/voice/language, cognitive, motor, and psychosocial outcomes are not progressive in most patients, but also here the time between testing was limited (Smith et al., 2023). A pilot study with 10 adult patients (mean age 33 years) and a mean time interval of 3 years and 9 months reported cognitive stability (Hermans et al., 2024).

In addition to the longitudinal studies, Lotz-Havla et al. (Lotz-Havla et al., 2023) studied retinal neuroaxonal function as marker for neurodegeneration in 11 CG patients and 60 controls, and did not find evidence for retinal neuroaxonal degeneration. Moreover, specialist teams within the GalNet that treat CG patients and take part in this review observe improvements in language performance (scores on verbal tests), and absence of cognitive decline. Patients, nevertheless, do complain about motor and social function, and at older ages complaints about tremor, memory issues, anxiety and depression are reported more often.

Although there might be progression concerning signs of early aging, memory issues and depression, “growing into deficits” can play a role. Adult life is often more stressful than childhood, so the features of anxiety and depression (financial worries, loneliness) may be more pronounced with time. There is also a subset of patients that experience neurological worsening,

which are very often patients who already had significant neurological issues in childhood. Patients with early onset cerebral or cerebellar atrophy can also show progressive natural senescence effects. The pathophysiological mechanisms therefore seem multifactorial, with individual susceptibility as one of the most important determinants. Studies with sensitive tests for the different affected domains and follow-up of decades in larger cohorts need to be performed to adequately delineate the disease course through adulthood.

7 Conclusion

In this review, we describe the role of impaired galactose metabolism on brain dysfunction. Our conclusion is that, based on the current data and insights, the majority of patients do not exhibit cognitive decline. A subset of patients experiences neurological worsening, often those patients with early onset cerebral and cerebellar volume loss. At older ages complaints about memory issues, anxiety and depression are seen more often, but are likely multifactorial in origin.

Author contributions

BP: Writing–original draft, Writing–review and editing. EV: Writing–original draft, Writing–review and editing. IB: Writing–review and editing. ABo: Writing–review and editing. MB: Writing–review and editing. ABu: Writing–review and editing. DCa: Writing–review and editing. DCo: Writing–review and editing. MC: Writing–review and editing. AD: Writing–review and editing. DD: Writing–review and editing. AE: Writing–review and editing. MG: Writing–review and editing. OG: Writing–review and editing. SG: Writing–review and editing. SK: Writing–review and editing. IK: Writing–review and editing. EL-T: Writing–review and editing. DM: Writing–review and editing. EM: Writing–review and editing. KÖ: Writing–review and editing. AP: Writing–review and editing. SP: Writing–review and editing. RP: Writing–review and editing. IR: Writing–review and editing. SS-B: Writing–review and editing. IS: Writing–review and editing. TS: Writing–review and editing. LS: Writing–review and editing. AS: Writing–review and editing. KS: Writing–review and editing. ET: Writing–review and editing. SW: Writing–review and editing. GB: Conceptualization, Writing–original draft, Writing–review and editing. MR-G: Conceptualization, Writing–original draft, Writing–review and editing.

Funding

The author(s) declare that no financial support was received for the research, authorship, and/or publication of this article.

Conflict of interest

The authors declare that the research was conducted in the absence of any commercial or financial relationships that could be construed as a potential conflict of interest.

The author(s) declared that they were an editorial board member of Frontiers, at the time of submission. This had no impact on the peer review process and the final decision.

Publisher's note

All claims expressed in this article are solely those of the authors and do not necessarily represent those of their affiliated organizations, or those of the publisher, the editors and the

reviewers. Any product that may be evaluated in this article, or claim that may be made by its manufacturer, is not guaranteed or endorsed by the publisher.

Supplementary material

The Supplementary Material for this article can be found online at: <https://www.frontiersin.org/articles/10.3389/fgene.2024.1355962/full#supplementary-material>

References

- Ahtam, B., Waisbren, S. E., Anastasoia, V., Berry, G. T., Brown, M., Petrides, S., et al. (2020). Identification of neuronal structures and pathways corresponding to clinical functioning in galactosemia. *J. Inherit. Metab. Dis.* 43 (6), 1205–1218. doi:10.1002/jimd.12279
- Antshel, K. M., Epstein, I. O., and Waisbren, S. E. (2004). Cognitive strengths and weaknesses in children and adolescents homozygous for the galactosemia Q188R mutation: a descriptive study. *Neuropsychology* 18 (4), 658–664. doi:10.1037/0894-4105.18.4.658
- Arn, P. H. (2003). Galactosemia. *Curr. Treat. Options Neurol.* 5 (4), 343–345. doi:10.1007/s11940-003-0040-x
- Aydin-Ozemer, Z., Tekturk, P., Uygur, Z. O., and Baykan, B. (2014). Galactosemia and phantom absence seizures. *J. Pediatr. Neurosci.* 9 (3), 253–256. doi:10.4103/1817-1745.147581
- Balakrishnan, B., An, D., Nguyen, V., DeAntonis, C., Martini, P. G. V., and Lai, K. (2020). Novel mRNA-based therapy reduces toxic galactose metabolites and overcomes galactose sensitivity in a mouse model of classic galactosemia. *Mol. Ther.* 28 (1), 304–312. doi:10.1016/j.ymthe.2019.09.018
- Balakrishnan, B., Chen, W., Tang, M., Huang, X., Cakici, D. D., Siddiqi, A., et al. (2016). Galactose-1 phosphate uridylyltransferase (GalT) gene: a novel positive regulator of the PI3K/Akt signaling pathway in mouse fibroblasts. *Biochem. Biophys. Res. Commun.* 470 (1), 205–212. doi:10.1016/j.bbrc.2016.01.036
- Balakrishnan, B., Nicholas, C., Siddiqi, A., Chen, W., Bales, E., Feng, M., et al. (2017). Reversal of aberrant PI3K/Akt signaling by Salubrinal in a GalT-deficient mouse model. *Biochim. Biophys. Acta Mol. Basis Dis.* 1863 (12), 3286–3293. doi:10.1016/j.bbadis.2017.08.023
- Barnes-Vélez, J. A., Aksoy Yasar, F. B., and Hu, J. (2023). Myelin lipid metabolism and its role in myelination and myelin maintenance. *Innov. (Camb.)* 4 (1), 100360. doi:10.1016/j.xinn.2022.100360
- Belman, A. L., Moshe, S. L., and Zimmerman, R. D. (1986). Computed tomographic demonstration of cerebral edema in a child with galactosemia. *Pediatrics* 78 (4), 606–609. doi:10.1542/peds.78.4.606
- Berry, G. T. (2011). Is prenatal myo-inositol deficiency a mechanism of CNS injury in galactosemia? *J. Inherit. Metab. Dis.* 34 (2), 345–355. doi:10.1007/s10545-010-9260-x
- Berry, G. T., Hunter, J. V., Wang, Z., Dreha, S., Mazur, A., Brooks, D. G., et al. (2001). In vivo evidence of brain galactitol accumulation in an infant with galactosemia and encephalopathy. *J. Pediatr.* 138 (2), 260–262. doi:10.1067/mpd.2001.110423
- Berry, G. T., Mallee, J. J., Kwon, H. M., Rim, J. S., Mulla, W. R., Muenke, M., et al. (1995b). The human osmoregulatory Na⁺/myo-inositol cotransporter gene (SLC5A3): molecular cloning and localization to chromosome 21. *Genomics* 25 (2), 507–513. doi:10.1016/0888-7543(95)80052-n
- Berry, G. T., Moate, P. J., Reynolds, R. A., Yager, C. T., Ning, C., Boston, R. C., et al. (2004). The rate of *de novo* galactose synthesis in patients with galactose-1-phosphate uridylyltransferase deficiency. *Mol. Genet. Metab.* 81 (1), 22–30. doi:10.1016/j.ymgme.2003.08.026
- Berry, G. T., Nissim, I., Gibson, J. B., Mazur, A. T., Lin, Z., Elsas, L. J., et al. (1997). Quantitative assessment of whole body galactose metabolism in galactosemic patients. *Eur. J. Pediatr.* 156 (Suppl. 1), S43–S49. doi:10.1007/pl00014271
- Berry, G. T., Nissim, I., Lin, Z., Mazur, A. T., Gibson, J. B., and Segal, S. (1995a). Endogenous synthesis of galactose in normal men and patients with hereditary galactosaemia. *Lancet* 346 (8982), 1073–1074. doi:10.1016/s0140-6736(95)91745-4
- Berry, G. T., Wehrli, S., Reynolds, R., Palmieri, M., Frangos, M., Williamson, J. R., et al. (1998). Elevation of erythrocyte redox potential linked to galactonate biosynthesis: elimination by Tolrestat. *Metabolism* 47 (11), 1423–1428. doi:10.1016/s0026-0495(98)90317-1
- Boca, M., and Whone, A. (2017). Letter to the editor on "Evidence for dopaminergic denervation in classical galactosemia. *Mov. Disord.* 32 (12), 1797. doi:10.1002/mds.27187
- Bohles, H., Wenzel, D., and Shin, Y. S. (1986). Progressive cerebellar and extrapyramidal motor disturbances in galactosaemic twins. *Eur. J. Pediatr.* 145 (5), 413–417. doi:10.1007/BF00439251
- Bosch, A. M., Grootenhuys, M. A., Bakker, H. D., Heijmans, H. S., Wijburg, F. A., and Last, B. F. (2004). Living with classical galactosemia: health-related quality of life consequences. *Pediatrics* 113 (5), e423–e428. doi:10.1542/peds.113.5.e423
- Bosch, A. M., Maurice-Stam, H., Wijburg, F. A., and Grootenhuys, M. A. (2009). Remarkable differences: the course of life of young adults with galactosaemia and PKU. *J. Inherit. Metab. Dis.* 32 (6), 706. doi:10.1007/s10545-009-1253-2
- Brophy, M. L., Stansfield, J. C., Ahn, Y., Cheng, S. H., Murphy, J. E., and Bell, R. D. (2022). AAV-mediated expression of galactose-1-phosphate uridylyltransferase corrects defects of galactose metabolism in classic galactosemia patient fibroblasts. *J. Inherit. Metab. Dis.* 45 (3), 481–492. doi:10.1002/jimd.12468
- Buccafusca, R., Venditti, C. P., Kenyon, L. C., Johanson, R. A., Van Bockstaele, E., Ren, J., et al. (2008). Characterization of the null murine sodium/myo-inositol cotransporter 1 (Smit1 or Slc5a3) phenotype: myo-inositol rescue is independent of expression of its cognate mitochondrial ribosomal protein subunit 6 (Mrps6) gene and of phosphatidylinositol levels in neonatal brain. *Mol. Genet. Metab.* 95 (1–2), 81–95. doi:10.1016/j.ymgme.2008.05.008
- Charlwood, J., Clayton, P., Keir, G., Mian, N., and Winchester, B. (1998). Defective galactosylation of serum transferrin in galactosemia. *Glycobiology* 8 (4), 351–357. doi:10.1093/glycob/8.4.351
- Choulout, J. J., Brivet, M., Virlon, P., Sevely, A., Manelfe, C., Mensire, A., et al. (1991). Severe neurologic course of galactosemia. Default of myelination caused by deficient synthesis of UDP-galactose? *Arch. Fr. Pediatr.* 48 (4), 267–269.
- Coelho, A. I., Berry, G. T., and Rubio-Gozalbo, M. E. (2015a). Galactose metabolism and health. *Curr. Opin. Clin. Nutr. Metab. Care* 18 (4), 422–427. doi:10.1097/MCO.0000000000000189
- Coelho, A. I., Bierau, J., Lindhout, M., Achten, J., Kramer, B. W., and Rubio-Gozalbo, M. E. (2017). Classic galactosemia: study on the late prenatal development of GALT specific activity in a sheep model. *Anat. Rec. Hob.* 300 (9), 1570–1575. doi:10.1002/ar.23616
- Coelho, A. I., Trabuco, M., Ramos, R., Silva, M. J., Tavares de Almeida, I., Leandro, P., et al. (2014). Functional and structural impact of the most prevalent missense mutations in classic galactosemia. *Mol. Genet. Genomic Med.* 2 (6), 484–496. doi:10.1002/mgg3.94
- Coelho, A. I., Trabuco, M., Silva, M. J., de Almeida, I. T., Leandro, P., Rivera, I., et al. (2015b). Arginine functionally improves clinically relevant human galactose-1-phosphate uridylyltransferase (GALT) variants expressed in a prokaryotic model. *JIMD Rep.* 23, 1–6. doi:10.1007/8904_2015_420
- Coman, D. J., Murray, D. W., Byrne, J. C., Rudd, P. M., Bagaglia, P. M., Doran, P. D., et al. (2010). Galactosemia, a single gene disorder with epigenetic consequences. *Pediatr. Res.* 67 (3), 286–292. doi:10.1203/PDR.0b013e3181cbd542
- Conte, F., van Buuringen, N., Voermans, N. C., and Lefeber, D. J. (2021). Galactose in human metabolism, glycosylation and congenital metabolic diseases: time for a closer look. *Biochim. Biophys. Acta Gen. Subj.* 1865 (8), 129898. doi:10.1016/j.bbagen.2021.129898
- Coss, K. P., Byrne, J. C., Coman, D. J., Adamczyk, B., Abrahams, J. L., Saldova, R., et al. (2012). IgG N-glycans as potential biomarkers for determining galactose tolerance in Classical Galactosaemia. *Mol. Genet. Metab.* 105 (2), 212–220. doi:10.1016/j.ymgme.2011.10.018
- Coss, K. P., Doran, P. P., Owoe, C., Codd, M. B., Hamid, N., Mayne, P. D., et al. (2013). Classical Galactosaemia in Ireland: incidence, complications and outcomes of treatment. *J. Inherit. Metab. Dis.* 36 (1), 21–27. doi:10.1007/s10545-012-9507-9
- Coss, K. P., Hawkes, C. P., Adamczyk, B., Stockmann, H., Crushell, E., Saldova, R., et al. (2014). N-glycan abnormalities in children with galactosemia. *J. Proteome Res.* 13 (2), 385–394. doi:10.1021/pr4008305

- Crome, L. (1962). A case of galactosaemia with the pathological and neuropathological findings. *Arch. Dis. Child.* 37 (194), 415–421. doi:10.1136/adc.37.194.415
- Daenzer, J. M. I., Rasmussen, S. A., Patel, S., McKenna, J., 3rd, and Fridovich-Keil, J. L. (2022). Neonatal GALT gene replacement offers metabolic and phenotypic correction through early adulthood in a rat model of classic galactosemia. *J. Inherit. Metab. Dis.* 45 (2), 203–214. doi:10.1002/jimd.12471
- Dani, N., and Broadie, K. (2012). Glycosylated synaptomatrix regulation of trans-synaptic signaling. *Dev. Neurobiol.* 72 (1), 2–21. doi:10.1002/dneu.20891
- Daude, N., Ellie, E., Reichardt, J. K., and Petry, K. G. (1996). *In vivo* and *in vitro* expression of rat galactose-1-phosphate uridylyltransferase (GALT) in the developing central and peripheral nervous system. *Brain Res. Dev. Brain Res.* 94 (2), 190–196. doi:10.1016/0165-3806(96)00058-2
- Delnoy, B., Haskovic, M., Vanoevelen, J., Steinbusch, L. K. M., Vos, E. N., Knoops, K., et al. (2022). Novel mRNA therapy restores GALT protein and enzyme activity in a zebrafish model of classic galactosemia. *J. Inherit. Metab. Dis.* 45 (4), 748–758. doi:10.1002/jimd.12512
- Demirbas, D., Huang, X., Daesety, V., Feenstra, S., Haskovic, M., Qi, W., et al. (2019). The ability of an LC-MS/MS-based erythrocyte GALT enzyme assay to predict the phenotype in subjects with GALT deficiency. *Mol. Genet. Metab.* 126 (4), 368–376. doi:10.1016/j.ymgme.2019.01.016
- De-Souza, E. A., Pimentel, F. S., Machado, C. M., Martins, L. S., da-Silva, W. S., Montero-Lomeli, M., et al. (2014). The unfolded protein response has a protective role in yeast models of classic galactosemia. *Dis. Model Mech.* 7 (1), 55–61. doi:10.1242/dmm.012641
- Dubroff, J. G., Ficioglu, C., Segal, S., Wintering, N. A., Alavi, A., and Newberg, A. B. (2008). FDG-PET findings in patients with galactosaemia. *J. Inherit. Metab. Dis.* 31 (4), 533–539. doi:10.1007/s10545-008-0806-0
- Fishler, K., Koch, R., Donnell, G. N., and Wenz, E. (1980). Developmental aspects of galactosemia from infancy to childhood. *Clin. Pediatr. (Phila.)* 19 (1), 38–44. doi:10.1177/000992288001900106
- Friedman, J. H., Levy, H. L., and Boustany, R. M. (1989). Late onset of distinct neurologic syndromes in galactosemic siblings. *Neurology* 39 (5), 741–742. doi:10.1212/wnl.39.5.741
- Gitzelmann, R. (1995). Galactose-1-phosphate in the pathophysiology of galactosemia. *Eur. J. Pediatr.* 154 (7 Suppl. 2), S45–S49. doi:10.1007/BF02143803
- Göppert, F. (1917). Galaktosurie nach Milchzuckergabe bei angeborenem, familiaerem chronischem Leberleiden. *Klin. Wschr* 54, 473–477.
- Gubbels, C. S., Maurice-Stam, H., Berry, G. T., Bosch, A. M., Waisbren, S., Rubio-Gozalbo, M. E., et al. (2011). Psychosocial developmental milestones in men with classic galactosemia. *J. Inherit. Metab. Dis.* 34 (2), 415–419. doi:10.1007/s10545-011-9290-z
- Haberland, C., Perou, M., Brunngraber, E. G., and Hof, H. (1971). The neuropathology of galactosemia. A histopathological and biochemical study. *J. Neuropathol. Exp. Neurol.* 30 (3), 431–447. doi:10.1097/00005072-197107000-00009
- Hagen-Lillevik, S., Johnson, J., Siddiqi, A., Persinger, J., Hale, G., and Lai, K. (2022). Harnessing the power of purple sweet potato color and myo-inositol to treat classic galactosemia. *Int. J. Mol. Sci.* 23 (15), 8654. doi:10.3390/ijms23158654
- Hansen, T. W., Henrichsen, B., Rasmussen, R. K., Carling, A., Andressen, A. B., and Skjeldal, O. (1996). Neuropsychological and linguistic follow-up studies of children with galactosaemia from an unscreened population. *Acta Paediatr.* 85 (10), 1197–1201. doi:10.1111/j.1651-2227.1996.tb18228.x
- Haskovic, M., Coelho, A. I., Bierau, J., Vanoevelen, J. M., Steinbusch, L. K. M., Zimmermann, L. J. I., et al. (2020). Pathophysiology and targets for treatment in hereditary galactosemia: a systematic review of animal and cellular models. *J. Inherit. Metab. Dis.* 43 (3), 392–408. doi:10.1002/jimd.12202
- Haskovic, M., Derks, B., van der Ploeg, L., Trommelen, J., Nyakayiru, J., van Loon, L. J. C., et al. (2018). Arginine does not rescue p.Q188R mutation deleterious effect in classic galactosemia. *Orphanet J. Rare Dis.* 13 (1), 212. doi:10.1186/s13023-018-0954-8
- Hermans, M. E., Geurtsen, G. J., Hollak, C. E. M., and Bosch, A. M. (2024). Neuropsychological stability in classical galactosemia: a pilot study in 10 adult patients. *JIMD Rep.* doi:10.1002/jimd.12410
- Hermans, M. E., van Oers, H. A., Geurtsen, G. J., Haverman, L., Hollak, C. E. M., Rubio-Gozalbo, M. E., et al. (2023). The challenges of classical galactosemia: HRQoL in pediatric and adult patients. *Orphanet J. Rare Dis.* 18 (1), 135. doi:10.1186/s13023-023-02749-8
- Hoffmann, B., Wendel, U., and Schweitzer-Krantz, S. (2011). Cross-sectional analysis of speech and cognitive performance in 32 patients with classic galactosemia. *J. Inherit. Metab. Dis.* 34 (2), 421–427. doi:10.1007/s10545-011-9297-5
- Holton, J. B. (1995). Effects of galactosemia in *utero*. *Eur. J. Pediatr.* 154 (7 Suppl. 2), S77–S81. doi:10.1007/BF02143809
- Hu, X., Zhang, Y. Q., Lee, O. W., Liu, L., Tang, M., Lai, K., et al. (2019). Discovery of novel inhibitors of human galactokinase by virtual screening. *J. Comput. Aided Mol. Des.* 33 (4), 405–417. doi:10.1007/s10822-019-00190-3
- Hughes, J., Ryan, S., Lambert, D., Geoghegan, O., Clark, A., Rogers, Y., et al. (2009). Outcomes of siblings with classical galactosemia. *J. Pediatr.* 154 (5), 721–726. doi:10.1016/j.jpeds.2008.11.052
- Huttenlocher, P. R., Hillman, R. E., and Hsia, Y. E. (1970). Pseudotumor cerebri in galactosemia. *J. Pediatr.* 76 (6), 902–905. doi:10.1016/s0022-3476(70)80373-0
- Jan, J. E., and Wilson, R. A. (1973). Unusual late neurological sequelae in galactosaemia. *Dev. Med. Child. Neurol.* 15 (1), 72–74. doi:10.1111/j.1469-8749.1973.tb04869.x
- Ji, L., Cheng, L., and Yang, Z. (2017). Diosgenin, a novel aldose reductase inhibitor, attenuates the galactosemic cataract in rats. *J. Diabetes Res.* 2017, 7309816. doi:10.1155/2017/7309816
- Jumbo-Lucioni, P., Parkinson, W., and Broadie, K. (2014). Overelaborated synaptic architecture and reduced synaptomatrix glycosylation in a *Drosophila* classic galactosemia disease model. *Dis. Model Mech.* 7 (12), 1365–1378. doi:10.1242/dmm.017137
- Jumbo-Lucioni, P. P., Garber, K., Kiel, J., Baric, I., Berry, G. T., Bosch, A., et al. (2012). Diversity of approaches to classic galactosemia around the world: a comparison of diagnosis, intervention, and outcomes. *J. Inherit. Metab. Dis.* 35 (6), 1037–1049. doi:10.1007/s10545-012-9477-y
- Kaufman, F. R., Horton, E. J., Gott, P., Wolff, J. A., Nelson, M. D., Jr., Azen, C., et al. (1995b). Abnormal somatosensory evoked potentials in patients with classic galactosemia: correlation with neurologic outcome. *J. Child. Neurol.* 10 (1), 32–36. doi:10.1177/088307389501000109
- Kaufman, F. R., McBride-Chang, C., Manis, F. R., Wolff, J. A., and Nelson, M. D. (1995a). Cognitive functioning, neurologic status and brain imaging in classical galactosemia. *Eur. J. Pediatr.* 154 (7 Suppl. 2), S2–S5. doi:10.1007/BF02143794
- Knerr, I., Coss, K. P., Kratzsch, J., Crushell, E., Clark, A., Doran, P., et al. (2015). Effects of temporary low-dose galactose supplements in children aged 5–12 y with classical galactosemia: a pilot study. *Pediatr. Res.* 78 (3), 272–279. doi:10.1038/pr.2015.107
- Koch, T. K., Schmidt, K. A., Wagstaff, J. E., Ng, W. G., and Packman, S. (1992). Neurologic complications in galactosemia. *Pediatr. Neurol.* 8 (3), 217–220. doi:10.1016/0887-8994(92)90072-7
- Komrower, G. M., and Lee, D. H. (1970). Long-term follow-up of galactosaemia. *Arch. Dis. Child.* 45 (241), 367–373. doi:10.1136/adc.45.241.367
- Krabbi, K., Uudelepp, M. L., Joost, K., Zordania, R., and Öunap, K. (2011). Long-term complications in Estonian galactosemia patients with a less strict lactose-free diet and metabolic control. *Mol. Genet. Metab.* 103 (3), 249–253. doi:10.1016/j.ymgme.2011.03.023
- Kreis, R., Hofmann, L., Kuhlmann, B., Boesch, C., Bossi, E., and Hüppi, P. S. (2002). Brain metabolite composition during early human brain development as measured by quantitative *in vivo* 1H magnetic resonance spectroscopy. *Magn. Reson. Med.* 48 (6), 949–958. doi:10.1002/mrm.10304
- Kuiper, A., Grunewald, S., Murphy, E., Coenen, M. A., Eggink, H., Zutt, R., et al. (2019). Movement disorders and nonmotor neuropsychological symptoms in children and adults with classical galactosemia. *J. Inherit. Metab. Dis.* 42 (3), 451–458. doi:10.1002/jimd.12054
- Lai, K., Elsas, L. J., and Wierenga, K. J. (2009). Galactose toxicity in animals. *IUBMB Life* 61 (11), 1063–1074. doi:10.1002/iub.262
- Lai, K., Langley, S. D., Khwaja, F. W., Schmitt, E. W., and Elsas, L. J. (2003). GALT deficiency causes UDP-hexose deficit in human galactosemic cells. *Glycobiology* 13 (4), 285–294. doi:10.1093/glycob/cwg033
- Lebea, P. J., and Pretorius, P. J. (2005). The molecular relationship between deficient UDP-galactose uridylyl transferase (GALT) and ceramide galactosyltransferase (CGT) enzyme function: a possible cause for poor long-term prognosis in classic galactosemia. *Med. Hypotheses* 65 (6), 1051–1057. doi:10.1016/j.mehy.2005.06.025
- Leslie, N. D. (2003). Insights into the pathogenesis of galactosemia. *Annu. Rev. Nutr.* 23, 59–80. doi:10.1146/annurev.nutr.23.011702.073135
- Lo, W., Packman, S., Nash, S., Schmidt, K., Ireland, S., Diamond, I., et al. (1984). Curious neurologic sequelae in galactosemia. *Pediatrics* 73 (3), 309–312. doi:10.1542/peds.73.3.309
- Lotz-Havla, A. S., Christmann, T., Parhofer, K. G., Maier, E. M., and Havla, J. (2023). Optical coherence tomography: retinal imaging contributes to the understanding of brain pathology in classical galactosemia. *J. Clin. Med.* 12 (5), 2030. doi:10.3390/jcm12052030
- Mackinnon, S. R., Krojer, T., Foster, W. R., Diaz-Saez, L., Tang, M., Huber, K. V. M., et al. (2021). Fragment screening reveals starting points for rational design of galactokinase 1 inhibitors to treat classic galactosemia. *ACS Chem. Biol.* 16 (4), 586–595. doi:10.1021/acschembio.0c00498
- MacWilliams, J., Patel, S., Carlock, G., Vest, S., Potter, N. L., and Fridovich-Keil, J. L. (2021). Hand fine motor control in classic galactosemia. *J. Inherit. Metab. Dis.* 44 (4), 871–878. doi:10.1002/jimd.12376
- Manis, F. R., Cohn, L. B., McBride-Chang, C., Wolff, J. A., and Kaufman, F. R. (1997). A longitudinal study of cognitive functioning in patients with classical galactosaemia, including a cohort treated with oral uridine. *J. Inherit. Metab. Dis.* 20 (4), 549–555. doi:10.1023/a:1005357622551
- Maratha, A., Colhoun, H. O., Knerr, I., Coss, K. P., Doran, P., and Treacy, E. P. (2017). Classical galactosaemia and cdg, the N-glycosylation interface. A review. *JIMD Rep.* 34, 33–42. doi:10.1007/8904_2016_5

- Martins, E., Teixeira, J., Cardoso, M. L., Lima, M. R., Briones-Godino, P., and Barbot, C. (2004). Galactosemia: the genotype and phenotype of seven patients. *Rev. Neurol.* 38 (12), 1132–1135. doi:10.33588/rn.3812.2002564
- Mason, H. H., and Turner, M. E. (1935). Chronic galactemia, report of case with studies on carbohydrates. *Am. J. Dis. Child.* 50 (2), 359. doi:10.1001/archpedi.1935.01970080053005
- McCorvie, T. J., Gleason, T. J., Fridovich-Keil, J. L., and Timson, D. J. (2013). Misfolding of galactose 1-phosphate uridylyltransferase can result in type I galactosemia. *Biochim. Biophys. Acta* 1832 (8), 1279–1293. doi:10.1016/j.bbdis.2013.04.004
- Mizisin, A. P., and Powell, H. C. (1993). Schwann cell injury is attenuated by aldose reductase inhibition in galactose intoxication. *J. Neuropathol. Exp. Neurol.* 52 (1), 78–86. doi:10.1097/00005072-199301000-00010
- Nelson, C. D., Waggoner, D. D., Donnell, G. N., Tuerck, J. M., and Buist, N. R. (1991). Verbal dyspraxia in treated galactosemia. *Pediatrics* 88 (2), 346–350. doi:10.1542/peds.88.2.346
- Nelson, M. D., Jr., Wolff, J. A., Cross, C. A., Donnell, G. N., and Kaufman, F. R. (1992). Galactosemia: evaluation with MR imaging. *Radiology* 184 (1), 255–261. doi:10.1148/radiology.184.1.1319076
- Neville, S., O'Sullivan, S., Sweeney, B., Lynch, B., Hanrahan, D., Knerr, I., et al. (2016). Friedrich ataxia in classical galactosaemia. *JIMD Rep.* 26, 1–5. doi:10.1007/8904_2015_477
- Ng, W. G., Xu, Y. K., Kaufman, F. R., and Donnell, G. N. (1989). Deficit of uridine diphosphate galactose in galactosaemia. *J. Inherit. Metab. Dis.* 12 (3), 257–266. doi:10.1007/BF01799215
- Otauy, M. C., Leite, C. C., Lacerda, M. T., Costa, M. O., Arita, F., Prado, E., et al. (2006). Proton MR spectroscopy and imaging of a galactosemic patient before and after dietary treatment. *AJNR Am. J. Neuroradiol.* 27 (1), 204–207.
- Özgün, N., Celik, M., Akdeniz, O., Ozbek, M. N., Bulbul, A., and Anlar, B. (2019). Early neurological complications in children with classical galactosemia and p.gln188arg mutation. *Int. J. Dev. Neurosci.* 78, 92–97. doi:10.1016/j.ijdevneu.2019.07.004
- Papachristoforou, R., Petrou, P. P., Sawyer, H., Williams, M., and Drousiotou, A. (2014). A novel large deletion encompassing the whole of the galactose-1-phosphate uridylyltransferase (GALT) gene and extending into the adjacent interleukin 11 receptor alpha (IL11RA) gene causes classic galactosemia associated with additional phenotypic abnormalities. *JIMD Rep.* 12, 91–98. doi:10.1007/8904_2013_249
- Potter, N. L. (2011). Voice disorders in children with classic galactosemia. *J. Inherit. Metab. Dis.* 34 (2), 377–385. doi:10.1007/s10545-010-9213-4
- Potter, N. L., Lazarus, J. A., Johnson, J. M., Steiner, R. D., and Shriberg, L. D. (2008). Correlates of language impairment in children with galactosaemia. *J. Inherit. Metab. Dis.* 31 (4), 524–532. doi:10.1007/s10545-008-0877-y
- Potter, N. L., Nievergelt, Y., and Shriberg, L. D. (2013). Motor and speech disorders in classic galactosemia. *JIMD Rep.* 11, 31–41. doi:10.1007/8904_2013_219
- Quan-Ma, R., Wells, H. J., Wells, W. W., Sherman, F. E., and Egan, T. J. (1966). Galactitol in the tissues of a galactosemic child. *Am. J. Dis. Child.* 112 (5), 477–478. doi:10.1001/archpedi.1966.02090140149018
- Quelhas, D., Jaeken, J., and Azevedo, L. (2023). Genetic modifiers in glycosylation pathways: is there a link between PMM2 and PGM1? *J. Inherit. Metab. Dis.* 46 (1), 1–2. doi:10.1002/jimd.12576
- Quintana, E., Navarro-Sastre, A., Hernández-Pérez, J. M., García-Villoria, J., Montero, R., Artuch, R., et al. (2009). Screening for congenital disorders of glycosylation (CDG): transferrin HPLC versus isoelectric focusing (IEF). *Clin. Biochem.* 42 (4–5), 408–415. doi:10.1016/j.clinbiochem.2008.12.013
- Rahit, K., and Tarailo-Graovac, M. (2020). Genetic modifiers and rare mendelian disease. *Genes (Basel)*. 11 (3), 239. doi:10.3390/genes11030239
- Ridel, K. R., Leslie, N. D., and Gilbert, D. L. (2005). An updated review of the long-term neurological effects of galactosemia. *Pediatr. Neurol.* 33 (3), 153–161. doi:10.1016/j.pediatrneurol.2005.02.015
- Robertson, A., Singh, R. H., Guerrero, N. V., Hundley, M., and Elsas, L. J. (2000). Outcomes analysis of verbal dyspraxia in classic galactosemia. *Genet. Med.* 2 (2), 142–148. doi:10.1097/00125817-200003000-00005
- Rogers, S., Heidenreich, R., Mallee, J., and Segal, S. (1992). Regional activity of galactose-1-phosphate uridylyltransferase in rat brain. *Pediatr. Res.* 31 (5), 512–515. doi:10.1203/00006450-199205000-00021
- Rogers, S. R., Bovee, B. W., Saunders, S. L., and Segal, S. (1989a). Galactose as a regulatory factor of its own metabolism by rat liver. *Metabolism* 38 (8), 810–815. doi:10.1016/0026-0495(89)90072-3
- Rogers, S. R., Bovee, B. W., Saunders, S. L., and Segal, S. (1989b). Activity of hepatic galactose-metabolizing enzymes in the pregnant rat and fetus. *Pediatr. Res.* 25 (2), 161–166. doi:10.1203/00006450-198902000-00017
- Rossi-Espagnet, M. C., Sudhakar, S., Fontana, E., Longo, D., Davison, J., Petengill, A. L., et al. (2021). Neuroradiologic phenotyping of galactosemia: from the neonatal form to the chronic stage. *AJNR Am. J. Neuroradiol.* 42 (3), 590–596. doi:10.3174/ajnr.A7016
- Rubio-Agusti, I., Carecchio, M., Bhatia, K. P., Kojovic, M., Parees, I., Chandrashekar, H. S., et al. (2013). Movement disorders in adult patients with classical galactosemia. *Mov. Disord.* 28 (6), 804–810. doi:10.1002/mds.25348
- Rubio-Gozalbo, M. E., Haskovic, M., Bosch, A. M., Burnyte, B., Coelho, A. I., Cassiman, D., et al. (2019). The natural history of classic galactosemia: lessons from the GalNet registry. *Orphanet J. Rare Dis.* 14 (1), 86. doi:10.1186/s13023-019-1047-z
- Schadewaldt, P., Hoffmann, B., Hammen, H. W., Kamp, G., Schweitzer-Krantz, S., and Wendel, U. (2010). Longitudinal assessment of intellectual achievement in patients with classical galactosemia. *Pediatrics* 125 (2), e374–e381. doi:10.1542/peds.2008-3325
- Schadewaldt, P., Kamalanathan, L., Hammen, H. W., and Wendel, U. (2004). Age dependence of endogenous galactose formation in Q188R homozygous galactosemic patients. *Mol. Genet. Metab.* 81 (1), 31–44. doi:10.1016/j.ymgme.2003.10.007
- Schweitzer, S., Shin, Y., Jakobs, C., and Brodehl, J. (1993). Long-term outcome in 134 patients with galactosaemia. *Eur. J. Pediatr.* 152 (1), 36–43. doi:10.1007/BF02072514
- Segal, S. (1995). *In utero* galactose intoxication in animals. *Eur. J. Pediatr.* 154 (7 2), S82–S86. doi:10.1007/BF02143810
- Shah, P. A., and Kuchhai, F. A. (2009). Galactosemia with chorea—an unusual presentation. *Indian J. Pediatr.* 76 (1), 97–98. doi:10.1007/s12098-009-0037-x
- Shin-Buehring, Y. S., Beier, T., Tan, A., Osang, M., and Schaub, J. (1977). The activity of galactose-1-phosphate uridylyltransferase and galactokinase in human fetal organs. *Pediatr. Res.* 11 (10 Pt 1), 1045–1051. doi:10.1203/00006450-197710000-00004
- Simard-Duquesne, N., Greselin, E., Dubuc, J., and Dvornik, D. (1985). The effects of a new aldose reductase inhibitor (tolrestat) in galactosemic and diabetic rats. *Metabolism* 34 (10), 885–892. doi:10.1016/0026-0495(85)90133-7
- Slepek, T. I., Tang, M., Slepek, V. Z., and Lai, K. (2007). Involvement of endoplasmic reticulum stress in a novel Classic Galactosemia model. *Mol. Genet. Metab.* 92 (1–2), 78–87. doi:10.1016/j.ymgme.2007.06.005
- Smith, N. H., Hendrickson, E. T., Garrett, O. S., Chernoff, R. A., Orloff, D. H., Druss, J. J., et al. (2023). Long-term complications in classic galactosemia are not progressive. *Mol. Genet. Metab.* 140 (3), 107708. doi:10.1016/j.ymgme.2023.107708
- Tang, M., Odejinmi, S. I., Vankayalapati, H., Wierenga, K. J., and Lai, K. (2012). Innovative therapy for Classic Galactosemia - tale of two HTS. *Mol. Genet. Metab.* 105 (1), 44–55. doi:10.1016/j.ymgme.2011.09.028
- Tang, M., Siddiqi, A., Witt, B., Yuzyuk, T., Johnson, B., Fraser, N., et al. (2014). Subfertility and growth restriction in a new galactose-1 phosphate uridylyltransferase (GALT) - deficient mouse model. *Eur. J. Hum. Genet.* 22 (10), 1172–1179. doi:10.1038/ejhg.2014.12
- Tang, M., Wierenga, K., Elsas, L. J., and Lai, K. (2010). Molecular and biochemical characterization of human galactokinase and its small molecule inhibitors. *Chem. Biol. Interact.* 188 (3), 376–385. doi:10.1016/j.cbi.2010.07.025
- Timmers, I., Jansma, B. M., and Rubio-Gozalbo, M. E. (2012). From mind to mouth: event related potentials of sentence production in classic galactosemia. *PLoS One* 7 (12), e52826. doi:10.1371/journal.pone.0052826
- Timmers, I., van den Hurk, J., Di Salle, F., Rubio-Gozalbo, M. E., and Jansma, B. M. (2011). Language production and working memory in classic galactosemia from a cognitive neuroscience perspective: future research directions. *J. Inherit. Metab. Dis.* 34 (2), 367–376. doi:10.1007/s10545-010-9266-4
- Timmers, I., van den Hurk, J., Hofman, P. A., Zimmermann, L. J., Uludağ, K., Jansma, B. M., et al. (2015a). Affected functional networks associated with sentence production in classic galactosemia. *Brain Res.* 1616, 166–176. doi:10.1016/j.brainres.2015.05.007
- Timmers, I., van der Korput, L. D., Jansma, B. M., and Rubio-Gozalbo, M. E. (2016). Grey matter density decreases as well as increases in patients with classic galactosemia: a voxel-based morphometry study. *Brain Res.* 1648, 339–344. doi:10.1016/j.brainres.2016.08.005
- Timmers, I., Zhang, H., Bastiani, M., Jansma, B. M., Roebroek, A., and Rubio-Gozalbo, M. E. (2015b). White matter microstructure pathology in classic galactosemia revealed by neurite orientation dispersion and density imaging. *J. Inherit. Metab. Dis.* 38 (2), 295–304. doi:10.1007/s10545-014-9780-x
- van Erven, B., Jansma, B. M., Rubio-Gozalbo, M. E., and Timmers, I. (2017). Exploration of the brain in rest: resting-state functional MRI abnormalities in patients with classic galactosemia. *Sci. Rep.* 7 (1), 9095. doi:10.1038/s41598-017-09242-w
- von Reuss, A. (1908). Sugar excretion in infancy. *Wien Med. Wschr* 58, 799–804.
- Waggoner, D. D., Buist, N. R., and Donnell, G. N. (1990). Long-term prognosis in galactosaemia: results of a survey of 350 cases. *J. Inherit. Metab. Dis.* 13 (6), 802–818. doi:10.1007/BF01800204
- Wahl, A., van den Akker, E., Klaric, L., Štambuk, J., Benedetti, E., Plomp, R., et al. (2018). Genome-wide association study on immunoglobulin G glycosylation patterns. *Front. Immunol.* 9, 277. doi:10.3389/fimmu.2018.00277
- Waisbren, S. E., Norman, T. R., Schnell, R. R., and Levy, H. L. (1983). Speech and language deficits in early-treated children with galactosemia. *J. Pediatr.* 102 (1), 75–77. doi:10.1016/s0022-3476(83)80292-3

- Waisbren, S. E., Potter, N. L., Gordon, C. M., Green, R. C., Greenstein, P., Gubbels, C. S., et al. (2012). The adult galactosemic phenotype. *J. Inherit. Metab. Dis.* 35 (2), 279–286. doi:10.1007/s10545-011-9372-y
- Welling, L., Bernstein, L. E., Berry, G. T., Burlina, A. B., Eyskens, F., Gautschi, M., et al. (2017b). International clinical guideline for the management of classical galactosemia: diagnosis, treatment, and follow-up. *J. Inherit. Metab. Dis.* 40 (2), 171–176. doi:10.1007/s10545-016-9990-5
- Welling, L., Meester-Delver, A., Derks, T. G., Janssen, M. C. H., Hollak, C. E. M., de Vries, M., et al. (2019). The need for additional care in patients with classical galactosaemia. *Disabil. Rehabil.* 41 (22), 2663–2668. doi:10.1080/09638288.2018.1475514
- Welling, L., Waisbren, S. E., Antshel, K. M., Colhoun, H. O., Gautschi, M., Grunewald, S., et al. (2017a). Systematic review and meta-analysis of intelligence quotient in early-treated individuals with classical galactosemia. *JIMD Rep.* 37, 115–123. doi:10.1007/8904_2017_22
- Wells, I. C., and Remy, C. N. (1965). Choline metabolism in normal and choline-deficient rats of different ages. *Arch. Biochem. Biophys.* 112 (1), 201–206. doi:10.1016/0003-9861(65)90030-5
- Wells, W. W., Pittman, T. A., Wells, H. J., and Egan, T. J. (1965). The isolation and identification of galactitol from the brains of galactosemia patients. *J. Biol. Chem.* 240, 1002–1004. doi:10.1016/s0021-9258(18)97527-7
- Welsink-Karssies, M. M., Ferdinandusse, S., Geurtsen, G. J., Hollak, C. E. M., Huidekoper, H. H., Janssen, M. C. H., et al. (2020a). Deep phenotyping classical galactosemia: clinical outcomes and biochemical markers. *Brain Commun.* 2 (1), fcaa006. doi:10.1093/braincomms/fcaa006
- Welsink-Karssies, M. M., Oostrom, K. J., Hermans, M. E., Hollak, C. E. M., Janssen, M. C. H., Langendonk, J. G., et al. (2020b). Classical galactosemia: neuropsychological and psychosocial functioning beyond intellectual abilities. *Orphanet J. Rare Dis.* 15 (1), 42. doi:10.1186/s13023-019-1277-0
- Welsink-Karssies, M. M., Schrantee, A., Caan, M. W. A., Hollak, C. E. M., Janssen, M. C. H., Oussoren, E., et al. (2020c). Gray and white matter are both affected in classical galactosemia: an explorative study on the association between neuroimaging and clinical outcome. *Mol. Genet. Metab.* 131 (4), 370–379. doi:10.1016/j.ymgme.2020.11.001



OPEN ACCESS

EDITED BY

Generoso Andria,
University of Naples Federico II, Italy

REVIEWED BY

Vincenza Gragnaniello,
University Hospital of Padua, Italy
Rossella Parini,
IRCCS San Gerardo dei Tintori Foundation,
Italy
Thomas Spentzas,
University of Tennessee Health Science Center
(UTHSC), United States

*CORRESPONDENCE

A. D. Dornelles
✉ alidorneles@gmail.com

RECEIVED 09 October 2023

ACCEPTED 16 January 2024

PUBLISHED 15 February 2024

CITATION

Dornelles AD, Junges APP, Krug B,
Gonçalves C, de Oliveira Junior HA and
Schwartz IVD (2024) Efficacy and safety of
enzyme replacement therapy with
alglucosidase alfa for the treatment of
patients with infantile-onset Pompe disease:
a systematic review and meta-analysis.
Front. Pediatr. 12:1310317.
doi: 10.3389/fped.2024.1310317

COPYRIGHT

© 2024 Dornelles, Junges, Krug, Gonçalves,
de Oliveira Junior and Schwartz. This is an
open-access article distributed under the
terms of the [Creative Commons Attribution
License \(CC BY\)](#). The use, distribution or
reproduction in other forums is permitted,
provided the original author(s) and the
copyright owner(s) are credited and that the
original publication in this journal is cited, in
accordance with accepted academic practice.
No use, distribution or reproduction is
permitted which does not comply with these
terms.

Efficacy and safety of enzyme replacement therapy with alglucosidase alfa for the treatment of patients with infantile-onset Pompe disease: a systematic review and metanalysis

A. D. Dornelles^{1,2,3*}, A. P. P. Junges⁴, B. Krug⁵, C. Gonçalves⁵,
H. A. de Oliveira Junior⁶ and I. V. D. Schwartz^{1,4,5,7}

¹Faculty of Medicine, Universidade Federal do Rio Grande do Sul, Porto Alegre, Brazil, ²Pediatric Service, Hospital de Clínicas de Porto Alegre, Porto Alegre, Brazil, ³Faculty of Medicine, Universidade Federal do Rio Grande do Sul, Porto Alegre, Brazil, ⁴Medical Genetics Service, Hospital de Clínicas de Porto Alegre, Porto Alegre, Brazil, ⁵Nuclimed, Clinical Research Centre, Hospital de Clínicas de Porto Alegre, Porto Alegre, Brazil, ⁶Health Technology Assessment Unit, Hospital Alemão Oswaldo Cruz, São Paulo, Brazil, ⁷Department of Genetics, Universidade Federal do Rio Grande do Sul, Porto Alegre, Brazil

Introduction: Pompe disease (PD) is a glycogen disorder caused by the deficient activity of acid alpha-glucosidase (GAA). We sought to review the latest available evidence on the safety and efficacy of recombinant human GAA enzyme replacement therapy (ERT) for infantile-onset PD (IOPD).

Methods: We systematically searched the MEDLINE (via PubMed) and Embase databases for prospective clinical studies evaluating ERT for IOPD on pre-specified outcomes. Meta-analysis was also performed.

Results: Of 1,722 articles identified, 16 were included, evaluating 316 patients. Studies were heterogeneous and with very low certainty of evidence for most outcomes. A moderate/high risk of bias was present for most included articles. The following outcomes showed improvements associated with alglucosidase alfa, over natural history of PD/placebo, for a mean follow-up of 48.3 months: left ventricular (LV) mass {mean change 131.3 g/m² [95% confidence interval (CI) 81.02, 181.59]}, time to start ventilation (TSV) [HR 0.21 (95% CI: 0.12, 0.36)], and survival [HR 0.10 (95% CI: 0.05, 0.19)]. There were no differences between the pre- and post-ERT period for myocardial function and psychomotor development. Adverse events (AEs) after ERT were mild in most cases.

Conclusion: Our data suggest that alglucosidase alfa potentially improves LV mass, TSV, and survival in IOPD patients, with no important safety issues.

Systematic Review Registration: PROSPERO identifier (CRD42019123700).

KEYWORDS

enzyme replacement therapy, alglucosidase alfa, Pompe disease, glycogen storage disease type II, systematic review, meta-analysis

1 Introduction

Pompe disease, also known as type II glycogenosis or acid maltase deficiency (OMIM 232300), is a rare lysosomal storage disorder that presents with a progressive neuromuscular involvement and is often fatal in the most severe forms. It is caused by the deficient activity of acid alpha-glucosidase (or acid maltase; EC 3.2.1.20), an enzyme responsible for glycogen degradation in the lysosomes (1). Deficient activity of this enzyme leads to an accumulation of glycogen within the lysosomes and cytoplasm of smooth, skeletal, and cardiac muscle. This accumulation ends up damaging cellular functioning and destroying cells, due to hypertrophy and rupture of lysosomes (2–7).

Infantile onset PD (IOPD), originally described by Pompe in 1932, involves patients with total acid alpha-glucosidase deficiency, with symptom onset at an average of between 1.6 and 2 months of life, which may even manifest in the uterus (8, 9). It is characterized by the presence of severe disease symptoms (3), such as generalized muscle weakness, cardiomegaly, and cardiac hypertrophy. The global incidence of PD is estimated at 1/40,000 new-borns (NBs), with 1/138,000 NBs for IOPD and 1/57,000 NBs for the late form. An ethnic influence is identified, as there is a high incidence of the disease in African American (1/12,000 NBs) and Chinese (1/40,000–1/50,000 NBs) patients (2, 4). Additionally, studies from newborn screening programs demonstrate higher incidence than reported previously: 1/25,200 NBs (IOPD and LOPD combined) in California, USA, as an example (10).

There is no curative treatment for PD. Currently, available treatment options are designed to address the mutant protein and consist of enzyme replacement therapy (ERT) with alglucosidase alfa (MyozymeTM), a form of human acid alpha-glucosidase (GAA) produced by recombinant DNA technology in Chinese hamster ovary cells (3) or with avalglucosidase alfa-ngpt (Nexvzyme[®]). The recommended dosage regimen of alglucosidase alfa is 20 mg/kg body weight, administered every 2 weeks by intravenous (IV) infusion (11), although dosage can vary accordingly to each patient. Furthermore, a new generation of rhGAA, cipaglucoaldase alfa co-administered with an enzyme stabilizer, miglustat (12, 13), as well as gene therapy can be new alternatives for the treatment of these patients soon (14).

A previous systematic review (SR) on IOPD has already been published (15), without meta-analysis, and included only the study from Kishnani et al. (16). The authors concluded that this small trial provided no robust evidence about which dosing schedule of ERT is more effective and reinforces the need of a large RCT comparing different dosing schedules. They also affirm the need of standardizing the main clinical outcomes. Therefore, the impact of alglucosidase alfa treatment on key outcomes, such as cardiomyopathy and time to start ventilatory support (TSV), is still unclear. Within this context, the present SR with meta-analysis was designed to evaluate the effects of alglucosidase alfa ERT in IOPD.

2 Methodology

2.1 Information sources and search strategy

This study aimed to review the latest available evidence on the efficacy and safety of alglucosidase alfa ERT in IOPD. To guide the literature search, a structured “Patient, Intervention, Comparison and Outcome” (PICO) question was formulated as follows: “Is the use of alglucosidase alfa effective and safe as ERT in patients with IOPD?”. The MEDLINE (via PubMed) and Embase databases were searched for studies published before 25 April 2022, including terms for glycogen storage disease type II and alpha glucosidase (Supplementary Table S1), complemented by a manual search. The SR is reported as proposed by the PRISMA guidelines (17) and has been previously registered in the PROSPERO database (CRD42019123700).

2.2 Eligibility criteria and study selection

We planned to include only randomized clinical trials (RCT) and observational comparative studies in which ERT with alglucosidase alfa was used for the treatment of patients with IOPD. Other prospective study designs would be included (open-label and non-randomized trials, controlled or otherwise, including quasi-experimental designs) if the sample size was ≥ 5 . *In vitro* studies or animal models, reviews, expert opinions, and retrospective studies were excluded. Unpublished work was covered by the identification of conference abstracts containing data deemed to be of interest. The final published articles were then included when available.

Studies that did not evaluate at least one of the eight outcomes of interest, defined *a priori* by a team of experts, were excluded. These outcomes were left ventricular (LV) mass, myocardial function [evaluated through LV ejection fraction (EF)], quality of life (QOL), survival, TSV in months, psychomotor development, decreased muscle tone, swallowing, and safety.

The selection stage was performed independently by two investigators (APPJ and CG), who assessed the abstracts retrieved during the search for eligibility. Decisions were compared, and articles deemed relevant were forwarded to two other investigators (ADD and BK) who independently extracted information on the characteristics of these studies (design, randomization methods, population of participants, interventions, and outcomes) using a standardized data collection form. The two investigators then took part in a consensus meeting. Any disagreement that remained was addressed by the intervention of a third investigator (HAOJ or IVDS). Finally, the references of the selected articles were hand-searched for potentially relevant studies not identified by the previous search strategies. When such information could not be retrieved, an email was sent to authors requesting non-reported data.

2.3 Data collection

Studies with data from the same population were excluded from meta-analyses. In these cases, the study with the largest

sample (or, if both studies had the same sample size, that with the longest follow-up) was retained for analysis.

2.4 Statistical analysis

We summarized results using mean changes from baseline with 95% confidence intervals (CIs) for continuous outcomes. To incorporate follow-up time, we used incidence rates (IRs) with 95% CIs to summarize events. When not directly reported, the mean change from baseline and standard error estimates were approximated based on reported statistics (95% CI, *p*-values, median, and interquartile range). If needed, data conversion (e.g., confidence interval to standard deviation) would be performed (18).

Pairwise meta-analyses for dichotomous outcomes were analyzed using the Mantel-Haenszel method, with random model, and the DerSimonian-Laird estimator of τ^2 . Continuity correction of 0.5 in studies with zero cell frequencies were employed in all analyses. Quantitative assessment of time-dependent outcomes consisted of meta-analyses of studies reporting the hazard ratio (HR). Pooled analyses were performed on unadjusted HR with reported 95% confidence intervals (CIs) using an inverse of variance, random-effects model.

In addition to the qualitative analysis of methodological and clinical similarity of the studies, statistical analysis of heterogeneity was performed considering Higgins inconsistency analyses (I^2) (19). Cochran's *Q* was considered statistically significant for heterogeneity if $P < .10$ (20). No threshold for statistical significance was used for the evaluation of clinical variables. Analyses were performed with R (version 3.2.3, R Core Team, The R Foundation, Vienna, Austria) and Review Manager (version 5.3.5 Copenhagen: The Nordic Cochrane Centre, The Cochrane Collaboration, 2014.).

2.5 Risk of bias of included studies

The risk of bias of included studies was evaluated with tools appropriate for each study designs: the Risk of Bias tool (RoB) 2.0 for RCTs and Risk of Bias in Non-randomized Studies of Interventions tool (ROBINS-I) for non-randomized studies of interventions (NRSI) (21, 22).

2.6 Certainty of evidence

Certainty of evidence of outcomes defined *a priori* was evaluated according to Grading of Recommendation, Assessment, Development and Evaluation (GRADE) criteria (23–25). Assessment of certainty of the evidence for outcomes was performed independently by two investigators (ADD and HAOJ).

3 Results

The broad search strategy retrieved 1,722 references (797 from MEDLINE and 925 from Embase), of which 250 were duplicated.

The titles and abstracts of 1,472 references were read, and 33 publications were selected for full-text evaluation. Of these, 16 were selected for eligibility, and 18 were excluded (the reason for deletion has been recorded and it is available in [Supplementary Table S2](#)). A PRISMA flow diagram of evidence selection is shown in [Figure 1](#). Ultimately, 15 studies were identified for IOPD.

Among the included studies, there is one phase II open clinical trial (26), one open clinical trial (16) and its extension study (27), one case-control study, and all the others are NRSI. Studies that evaluated the outcomes defined *a priori* are described in [Table 1](#). Our search did not retrieve any articles evaluating QOL, hypotonia, or swallowing disorder that matched the inclusion criteria; therefore, these outcomes could not be evaluated.

3.1 Characteristics of included studies

All included studies and their characteristics are described in [Table 2](#). A total of 16 studies containing data from 316 patients were evaluated, for a mean follow-up time of 48.3 months. The mean age of starting ERT was 6.3 months, ranging from 0.1 to 43.1.

3.2 Left ventricular mass

The LV mass was described in 11 studies, as shown in [Table 1](#). The results of the included studies are detailed in [Supplementary Table 2](#). There were three reports for the same study (16, 26, 27). Therefore, we only considered the first to be published as its data were completed (26). Kishnani et al. (16), Nicolino et al. (28) and Zhu et al. (29) showed the beneficial effect of ERT, with reductions in LV mass as follows: -106.6 g/m^2 (16), -62.7% (28) and $-227.60 \pm 155.99 \text{ g/m}^2$ (29), after ERT respectively.

Furthermore, two studies with smaller samples showed stabilization of LV mass after treatment: Barker et al. ($n = 5$) (30) and van Gelder et al. ($n = 8$). Van Gelder et al. mentioned that one patient normalized LV mass after treatment, but the data were not detailed (31). For meta-analysis, we included 5/10 studies with comparable data and the results are shown in [Figure 2](#), showing a significant reduction in LV mass after ERT, suggesting a benefit for LV mass, although with a high statistical heterogeneity ($I^2 = 88\%$), mainly due to clinical heterogeneity of patients included.

3.3 Myocardial function

As an indicator of myocardial function, the ejection fraction (EF) was considered in four studies ([Table 1](#)). Nicolino et al. was the study with the largest sample to evaluate this outcome ($n = 21$) and showed improvement in myocardial function in 30.4% after ERT. However, comparison with other included studies should be cautious as authors used shortening fraction instead of EF (28). Data from other included studies showed stabilization of EF, with no significant differences before and after ERT ([Supplementary Table S4](#)).

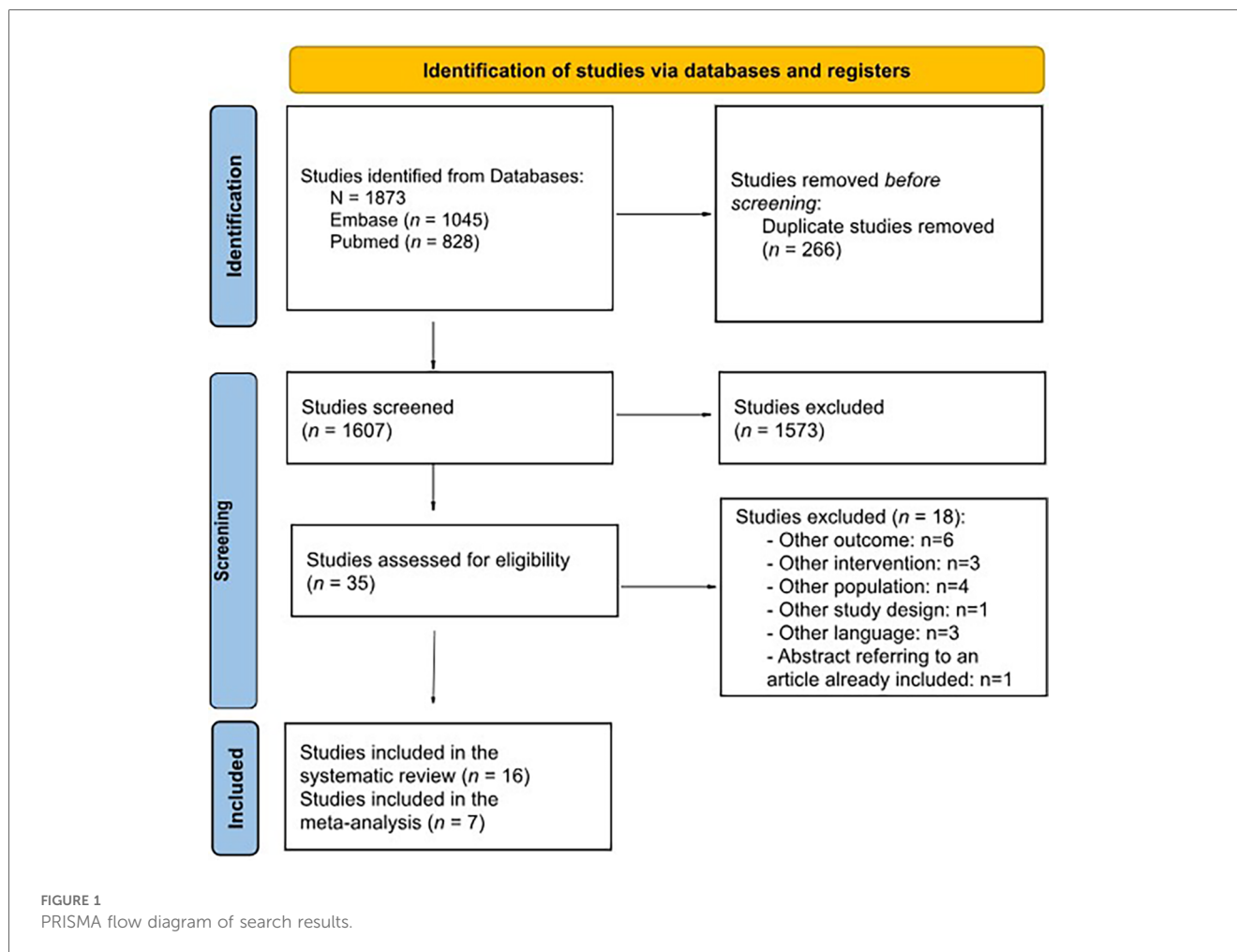


TABLE 1 Outcomes of interest defined *a priori* and studies that met the inclusion criteria.

Outcome	Number of articles	References
Left ventricular mass	11	(3, 16, 26–34)
Safety	9	(16, 26–30, 32, 35, 36)
Survival	9	(16, 26–29, 32, 35, 37, 38)
Time to start ventilatory support	8	(16, 26–29, 32, 34, 37)
Myocardial function	5	(16, 28, 30, 33, 37)
Psychomotor development	2	(16, 39)
Quality of life	0	
Hypotonia	0	
Swallowing disorder	0	

3.4 Time to start ventilatory support

TSV was evaluated in eight studies (Table 1). Meta-analysis of 2/8 studies which described the time free of mechanical ventilation (MV) as hazard ratios was performed. Data are described in Figure 3. Complete data for TSV were described for 4/8 studies and suggest that ERT increases the time to start ventilation (Supplementary Table S5).

Chien et al. showed (37) and confirmed the finding with a follow-up study in 2015 (32) that time to start ventilation is prolonged after starting ERT in comparison to untreated cases ($P < .001$) (Supplementary Table S5). These studies also showed that the newborn screened population that started ERT earlier than the clinical cases population start ventilation even later ($P < .001$). Zhu et al. (29) showed that only 1/9 subjects used an invasive ventilator during the study. At the end of the study (13 months), all nine survivors were free from the use of any ventilators.

The study from Kishnani et al. (16) was not included in meta-analysis because its follow-up was included (27). The authors grouped the risk of death or invasive MV and this was reduced by 92% (HR 0.08, 95% CI: 0.03–0.21, $P = .001$) with ERT. Risk of death or any type of ventilation was reduced by 88% (HR 0.12, 95% CI: 0.05–0.29, $P = .001$). Three patients required MV before 18 months of age, with a survival rate without invasive MV of 88.9% (95% CI: 74.4%–100%). Non-invasive ventilation was required for another three patients, with a survival rate at 18 months without any type of ventilatory support of 66.7% (95% CI: 44.9%–88.4%). The follow-up study (27) corroborated its findings: 3/18 patients required MV at 18 months, 6/18 at 24 months, and 9/18 at 36

TABLE 2 Included studies and their characteristics.

Author	Patients (n; female)	Design	Age of onset of ERT -months— μ or median (range)	Intervention (alglucosidase alfa IV) and follow-up duration	Comparison	Follow-up (mean in months)	Patients on ventilation (n)	CRIM status (n of positive/total)
Barker et al. (30)	10; 2	NRSI	4 (1–10)	Unspecified dose for 36 months	–	36	–	8/10
Chen et al. (33)	9; 3	NRSI	1.8 (0.4–4.2)	20–40 mg/kg/2 weeks for 27.6 months (median)	–	27.6 (median)	–	N/A
Chien et al. (37)	6; 3	Case control	2.9 (0.4–14) (cases)	20 mg/kg/2 weeks for up to 40 months diagnosed with NBS	Alglucosidase alfa IV 20 mg/kg/2 weeks with clinical diagnosis (n = 10)	40	I = 0; C = 3 invasive	6/6
Chien et al. (32)	10; N/A	NRSI	0.5 (0.2–1.1)	20 mg/kg/2 weeks for up to 63 months (median)	Alglucosidase alfa IV 20 mg/kg/2 weeks with clinical diagnosis	63 (median)	Invasive = 5; non-invasive = 1	14/18
Ditters et al. (38)	116 cases, 8 controls; 58 cases, 2 controls	NRSI	3.3 (0.03–11.8)	20 mg/kg/2 weeks for up to 60.1 months	Alglucosidase alfa IV other doses	60.1	N/A	72/96 (controls N/A)
Kishnani et al. (26)	8; 4	Phase II open clinical trial and extension study	4.7 (2.7–14.6)	Initial phase 12.7 months: 10 mg/kg/wk.; Extension phase up to 38.2 months: 10–20 mg/kg/wk. or 20 mg/kg/2 weeks		38.2	Invasive = 1; deceased = 2	6/8
Kishnani et al. (16)	18; 7	Open ECR	5.3 (1.2–6.1)	20–40 mg/kg/2 weeks for 12.7 months	Untreated historical cohort	18	Invasive = 3; non-invasive = 3	15/18
Kishnani et al. (27)	18; 7	NRSI (extension study by Kishnani et al.; 2007)	5.3 (1.2–6.1)	20–40 mg/kg/2 weeks for 36 months	Untreated historical cohort	27.6 (median)	Invasive = 9	14/18
Levine et al. (3)	8; N/A	NRSI	4.7 (2.7–14.6)	10 mg/kg weekly for 12.7 months	–	13	N/A	N/A
Nagura et al. (35)	10; N/A	NRSI	13.9 (0.4–36.9)	20 mg/kg/2 weeks for 9 years	–	108	N/A	N/A
Nicolino et al. (28)	21; N/A	NRSI	13 (3.7–43.1)	20–40 mg/kg/2 weeks for 12.7 months	Untreated reference cohort	30 (median)	Invasive = 8; non-invasive = 0; deceased = 6	19/21
Spiridigliozzi et al. (39)	17; N/A	NRSI	5.2 (0.4–7.1)	20–40 mg/kg/2 weeks for 13 months	–	13	N/A	14/17
van Capelle et al. (34)	14; 7	NRSI	2.7 (0.1–8.3)	20 mg/kg/2 weeks or 40 mg/kg weekly for 57.6 months (median)	–	57.6 (median)	Invasive = 5	12/14
van Gelder et al. (31)	8; 4	NRSI	1.8 (0.1–4.6)	20 mg/kg/2 weeks for 63 months (median)	Alglucosidase alfa IV 40 mg/kg/week	43.6	I = 1/4; C = 0/4 (all invasive)	8/8
van Kooten et al. (36)	5; 3	NRSI	26.4 (13.2–40.8)	20–40 mg/kg/2 weeks for 12.4 years (median)	–	148.8 (median)	Invasive = 1; non-invasive = 3	N/A
Zhu et al. (29)	10; 6	NRSI	4.2 (1–6)	20 mg/kg every 2 weeks for up to 52 weeks		13		9/10
Total	316	–	6.3 (0.1–43.1)	–	–	48.3	–	197/244

ERT, enzyme replacement therapy; μ , mean; IV, intravenous; I, intervention; C, control; NBS, newborn screening; N/A, not available; NRSI, non-randomized study of intervention. Mean or median were used, as described in the included article.

months, at the time of death or at the end of the study, whichever came first. The Kaplan–Meier ventilation-free survival rates at different ages were as follows: 66.7% (95% CI: 44.9%–88.4%) at 24 months and 49.4% (95% CI: 26%–72.8%) at 36 months. Thus, alglucosidase alfa reduced the risk of invasive ventilation or death by 91% (hazard ratio 0.09, 95% CI: 0.04–0.22), when compared to the historical control group (Figure 3).

3.5 Survival

Nine studies evaluated survival in IOPD and two were included in a meta-analysis (Figure 4). There was an increase in survival in all studies that evaluated this outcome. Meta-analysis suggests that the effect of ERT is potentially beneficial in patients’ survival. However, there is uncertainty due to high statistical heterogeneity ($I^2 = 78\%$).

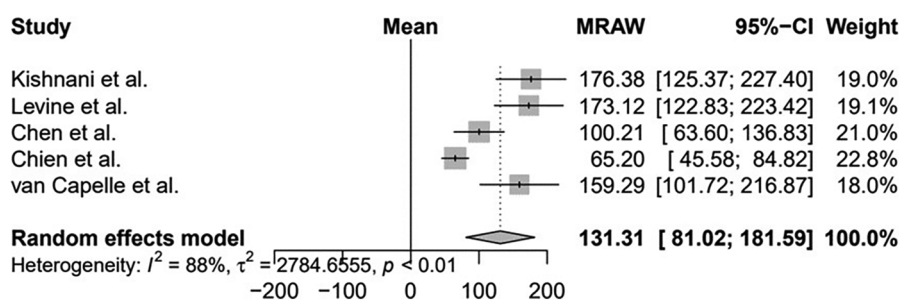


FIGURE 2

Evaluation of the left ventricular mass of patients with infantile-onset Pompe disease on enzyme replacement therapy with alglucosidase alfa. Weights are inverse-variance weights and are proportional to the contribution of each study to the summary estimate. I^2 is the fraction of variance that is due to statistical heterogeneity and not chance. τ^2 denotes the between-study variance.

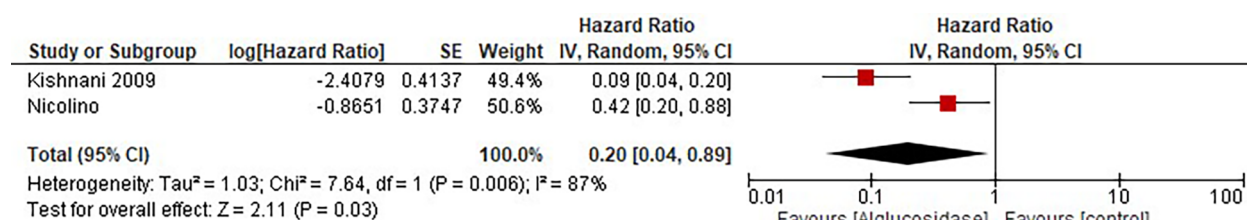


FIGURE 3

Evaluation of the time free of ventilation of patients with infantile-onset Pompe disease on enzyme replacement therapy with alglucosidase alfa. Weights are inverse-variance weights and are proportional to the contribution of each study to the summary estimate. I^2 is the fraction of variance that is due to statistical heterogeneity and not chance. τ^2 denotes the between-study variance.

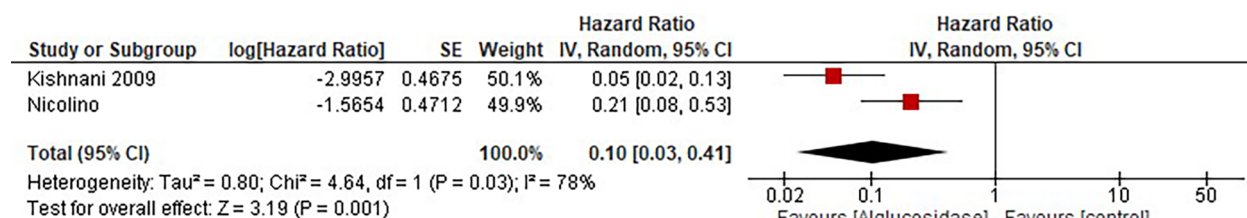


FIGURE 4

Evaluation of survival time of patients with infantile-onset Pompe disease on enzyme replacement therapy with alglucosidase alfa. Weights are inverse-variance weights and are proportional to the contribution of each study to the summary estimate. I^2 is the fraction of variance that is due to statistical heterogeneity and not chance. τ^2 denotes the between-study variance.

Chien et al. (32) described a 100% survival rate (10/10) for patients treated for 63 months on average. This study was not included in the meta-analysis due to the incomplete reporting of data. Kaplan–Meier analysis indicated that the survival of patients diagnosed by newborn screening test was significantly better than untreated patients ($P < .001$) and late diagnosis patients ($P = .03$), data not shown. Kaplan–Meier analysis was also performed in the study by Chien et al. (37), with similar results: greater survival in patients from the early diagnosis (newborn screening) group (up to 40 months of follow-up, without deaths) compared to the untreated cohort (100% of deaths after 35 months of follow-up; $P = .001$) and without significant difference compared to patients treated with late diagnosis (65% mortality with a follow-up of 80 months; $P = 0.48$).

Nicolino et al. (28) compared the survival of patients starting treatment before and after 12 months of age with the survival of a historical control cohort without treatment, described in Kishnani et al. (26). Patients starting treatment before 12 months had a survival rate of 50% after 104 weeks of treatment (95% CI: 19%–81%; $n = 10$), against a survival rate of 9.2% (95% CI: 1.5 to 16.8%; $n = 59$) in the control cohort. Patients starting treatment after 12 months showed treatment survival of 91% (95% CI: 74%–100%; $n = 11$), against a survival rate of 45.5% (95% CI: 16%–75%; $n = 11$) after 104 weeks of follow-up. The reduction in the risk of death in treated patients compared to the historical cohort was 79% ($P < .01$).

In the study conducted by Kishnani et al. (26), two patients died, respectively, at 14.7 and 18.3 months, after 43 and 16

weeks of treatment, both due to respiratory failure. Kishnani et al. (16) evaluated 15 patients when they turned 18 months of age and compared them with a historical untreated cohort described in Kishnani et al. (40), in which only 1/61 patients reached this age. ERT reduced the risk of death by 99% (HR = 0.01; $P = .001$). Finally, Kishnani et al. (27), in 2009, presented data from 18 patients, of whom 17 reached 24 months of age, with a survival rate of 94.4% (95% CI: 83.9% to 100%) at this time and of 72% (95% CI: 47.9% to 96%) at 36 months. In Kishnani et al. (27), 7/18 patients reached 36 months of age. These data were also compared to the same historical controls, with survival at 24 and 36 months of 1.9% (95% CI: 0%–5.5%). Finally, the survival rate of Zhu et al. (29) was 100% ($n = 9$, 95% CI: 66.4%–100%).

3.6 Psychomotor development

As shown in Table 1, only two studies described this outcome. As an indicator of psychomotor development, the mental development index (MDI) was evaluated. MDI was considered for assessment because it was the sole measure which could be compared between studies and with data availability after the intervention (ERT). The results were evaluated in a very heterogeneous way and are described in Supplementary Table S6. However, like the study by Kishnani et al. (16), it did not present pre-treatment data. Therefore, it was not possible to assess its effect.

3.7 Safety

3.7.1 Adverse events

The summary of safety results is described in Supplementary Table S7. Data for Nagura et al. (35) was not described as authors mixed IOPD and late-onset patients' data. Kishnani et al. (27) reported safety data for 18 patients undergoing treatment with ERT, of which 11 had 224 AEs, all mild or moderate in intensity, managed with reduced infusion speed or pause. The most common AEs were urticaria ($n = 47$ events), fever ($n = 27$), and desaturation ($n = 24$ events) and were most commonly reported in the 40 mg/kg dose group. Similar preliminary results had already been reported by Kishnani et al. in 2007 (16).

In Kishnani et al. (26), ERT was well tolerated, with all patients presenting at least one AE, mostly mild or moderate. The AEs described were as follows: skin rash, fever, changes in blood pressure or heart rate, and bronchospasm, all resolved with symptomatic treatment and by slowing or pausing the infusion. Nicolino et al. (28) described 42 AEs in 11 patients (52%), the most common being skin changes (13 events), vascular changes (10 events), and changes in vital signs (7 events), which were also resolved with symptomatic treatment and by slowing or pausing the infusion. The data, therefore, suggests that alglucosidase alfa is potentially safe as ERT in patients with IOPD, since most AEs are mild to moderate.

Zhu et al. (29) had at least one AE reported for each participant. All AEs identified in this study were treatment-emergent AE

(TEAEs), and at least one serious TEAE (SAE) was reported for nine subjects (90%). The most frequently reported SAEs ($\geq 20\%$) were pneumonitis (60%; $n = 6$), followed by pneumonia (30%; $n = 3$), respiratory tract infection (20%; $n = 2$), gastroenteritis rotavirus (20%; $n = 2$), and bronchitis (20%; $n = 2$).

3.7.2 Anti-alglucosidase alfa antibodies

Nicolino et al. (28) reported that 19/20 patients (95%) developed anti-alglucosidase alfa antibodies (Ab), but none of these patients showed inhibitory activity during the entire follow-up. In the study by Kishnani et al. (27), 16/18 patients had high titers of Ab, but only 3/16 had levels above 20% of neutralizing Ab. Similar preliminary results had already been reported by Kishnani et al. in 2007 (16). Chien et al. (32) described the development of Ab in 9/10 patients, with no description of neutralizing Ab. In Kishnani et al. (26), all patients developed Ab during treatment, also without description of neutralizing Ab. Finally, in Barker et al. (30), there was also development of Ab in all patients, and one patient, who had high and sustained Ab titers, showed neutralizing Ab, with increased ventricular mass despite treatment. Cross reactive immunologic material (CRIM) status was available for 197/244 patients in included studies (Table 2). However, this status was very heterogeneously described for each outcome and, therefore, could not be assessed. Only Zhu et al. (29) described that an immune tolerance induction (ITI) regimen was used.

3.8 Risk of bias and quality of included studies

The risk of bias of the included NRSI is shown in Figure 5. Most included articles showed a moderate to serious risk of bias, independently of the study design, mainly due to confounding. Only one RCT was included (16) which was evaluated with serious risk of bias according to the R.o.B. 2.0, presenting some concerns in almost all domains but domain 3.

3.9 Certainty of evidence by outcomes

All outcomes were assessed for certainty of evidence, with low certainty for TSV and survival. All other outcomes had very low certainty of evidence, mainly due to the uncontrolled observational design of the included studies, with data from secondary outcomes. A full analysis is available in the Supplementary Table S8.

4 Discussion

IOPD is a rare, serious disease with no specific treatment available other than ERT. To the best of our knowledge, this is the first SR with meta-analysis to evaluate the effect of ERT on IOPD and included a total of 15 studies containing data from 316 patients. Patients were followed for a mean time of 48.3 months and the mean age of starting ERT was 6.3 months,



FIGURE 5
Risk of bias of included studies evaluated through the ROBINS-I tool. D6—The studies were not blinded. D1 Kishnani et al. (26)—Did not have an appropriate analysis method. D5 Kishnani et al. (6)—Outcome data were not available for all participants. D1 Kishnani et al. (27)—Patients with cardiac insufficiency were excluded. D1 Levine et al. (3)—Most patients had onset of symptoms after 1 year of age. D1 Nicolino—A patient was excluded due to discrepant cognitive function. D1 Spiridigliozzi et al. (39)—Patients with cardiac HF were excluded from the intervention group, but not from the control group. D1 Van Capelle—The duration of treatment was very discrepant between the groups. D1 Van Gelder—There was no statistical analysis and the two groups had different doses. D1 Van Kooten e Nagura—Did not differentiate between early and late forms in the analysis of outcomes (some patients started with symptoms after 1 year of age).

ranging from 0.1 to 43.1. Among the outcomes evaluated for IOPD, a benefit for LV mass, TSV, and survival were seen in meta-analysis. Alglucosidase alfa appears to be safe in the population studied. Although the occurrence of AEs related to

treatment or infusion are frequent, they are, in most cases, mild and easily treatable.

All studies had different ages, stages, durations of disease burden prior to start of ERT, and phenotypic manifestations.

CRIM status was available in 12/16 included studies; however, it was very heterogeneously described for each outcome. However, CRIM status is known to have a big impact on outcomes and determines if an immune tolerance induction regimen is recommended concomitantly with ERT. Therefore, this needs to be taken into considerations while interpreting the results.

An SR on IOPD has already been published (15) and SR data for juvenile onset PD are available (41); none of them conducted a meta-analysis. The SR by Chen et al. (15) only included randomized trials and, therefore, included only Kishnani et al. (16), also considered in this SR. The authors concluded that this small trial provided no robust evidence for which dosing schedule of ERT is more effective and reinforced the need of a large RCT comparing different dosing schedules. They also affirmed the need of standardizing the main clinical outcomes, a limitation found in our SR as well (15).

Our results confirm a previously published study (42) and its follow-up (43) that evaluated cardiomyopathy, also indicating the beneficial effect of ERT with 4,000 L alglucosidase alfa for cardiac outcomes. Our study also indicates a beneficial effect of ERT on TSV, showing a reduction of 80% on the risk of being ventilated, with follow-up data up to 40 months, which can be considerable for this infantile form, in comparison with no treatment. A previous SR by our group for LOPD patients showed a beneficial effect of ERT on reducing time on ventilation (44).

Concerning survival, our study showed a beneficial effect of ERT for IOPD, indicating a reduction of 90% on the risk of death. A previous SR on juvenile patients (41) was not able to show any ERT effect for this population, as well as the previous SR by our group for LOPD patients (44), despite some effect on reducing mortality being reported by us. Recent data on IOPD included in this SR (38) showed that this improvement in survival can be even higher when patients are treated with high dosage ERT (40 mg/kg per week) when compared with patients treated with the standard dosage (20 mg/kg every other week); both studies included in meta-analysis (27, 28) did not separate data from different dosages, and therefore the effect described could be higher.

Regarding limitations, the included studies were highly heterogeneous, enrolling patients with different disease severities, and these are small, underpowered studies, with a high risk of bias. The certainty of the evidence was low, meaning the findings should be interpreted with caution, and it suggests that larger and more robust studies are encouraged. In addition, most included studies were non-randomized studies of interventions, with low methodological quality, no comparison group, or comparison with a historical cohort. Another challenge is incompletely reported data, as mentioned. Therefore, the findings of this review and meta-analysis should be interpreted with caution. Usually, data from secondary outcomes were poorly reported, as studies were not designed to measure them. In most cases, however, conclusions were made without showing full data and results. Proper reporting of data is essential.

Moreover, evaluating hypotonia, swallowing disorder, and pediatric quality of life, which are important outcomes for daily

pediatric practice, must be addressed in future primary studies. Concerning psychomotor development, despite mentioned in few studies, the data suggest that the efficacy of ERT needs to be better evaluated for this outcome. One strength of the present study was that we included only prospective trials to avoid memory and selection bias. Prospective trials also have the advantage of collecting data according to the predefined outcomes of interest, which does not happen in retrospective trials. Also, of our best knowledge, this is the first SR with meta-analysis to evaluate the effect of ERT on IOPD and included a total of 15 studies containing data from 316 patients.

In conclusion, alglucosidase alfa potentially increases the survival rate, improves cardiac functioning, and may delay the start of ventilatory support in treated patients. The treatment is safe in the studied population, with generally mild adverse events. Further studies could evaluate the impact of the duration of follow-up, taking into consideration that the efficacy of ERT may present some secondary decline after 3 to 5 years of treatment (data for LOPD) (45).

Data availability statement

The original contributions presented in the study are included in the article/[Supplementary Material](#), further inquiries can be directed to the corresponding author.

Author contributions

AD: Conceptualization, Data curation, Investigation, Methodology, Project administration, Writing – original draft. AJ: Resources, Visualization, Writing – original draft. BK: Methodology, Resources, Supervision, Writing – review & editing. CG: Methodology, Resources, Supervision, Writing – review & editing. HO: Conceptualization, Data curation, Formal Analysis, Investigation, Methodology, Project administration, Resources, Supervision, Validation, Writing – review & editing. IS: Conceptualization, Methodology, Project administration, Resources, Supervision, Validation, Writing – review & editing.

Funding

The author(s) declare financial support was received for the research, authorship, and/or publication of this article.

This research was funded by the Hospital de Clínicas de Porto Alegre Research Funding and Incentives (FIPE/HCPA), grant number (protocol code) 2019-0495, by the Pro-BIC HCPA/CNPq Undergraduate Research Program, by Casa dos Raros, Center for Comprehensive Care and Training in Rare Diseases, and by Casa Hunter. The authors thank to Research Funding and Incentives (FIPE/HCPA) for the financial support.

Conflict of interest

The authors declare that the research was conducted in the absence of any commercial or financial relationships that could be construed as a potential conflict of interest.

The author(s) declared that they were an editorial board member of Frontiers, at the time of submission. This had no impact on the peer review process and the final decision.

Publisher's note

All claims expressed in this article are solely those of the authors and do not necessarily represent those of their

affiliated organizations, or those of the publisher, the editors and the reviewers. Any product that may be evaluated in this article, or claim that may be made by its manufacturer, is not guaranteed or endorsed by the publisher.

Supplementary material

The Supplementary Material for this article can be found online at: <https://www.frontiersin.org/articles/10.3389/fped.2024.1310317/full#supplementary-material>

References

- Adeva-Andany MM, González-Lucán M, Donapetry-García C, Fernández-Fernández C, Ameneiros-Rodríguez E. Glycogen metabolism in humans. *BBA Clin.* (2016) 5:85–100. doi: 10.1016/j.bbacli.2016.02.001
- Llerena JC, Horowitz DM, Marie SK, Porta G, Giugliani R, Rojas MV, et al. The Brazilian consensus on the management of Pompe disease. *J Pediatr.* (2009) 155(4 Suppl):S47–56. doi: 10.1016/j.jpeds.2009.07.006
- Levine JC, Kishnani PS, Chen YT, Herlong JR, Li JS. Cardiac remodeling after enzyme replacement therapy with acid alpha-glucosidase for infants with Pompe disease. *Pediatr Cardiol.* (2008) 29(6):1033–42. doi: 10.1007/s00246-008-9267-3
- Slonim AE, Bulone L, Goldberg T, Minikes J, Slonim E, Galanko J, et al. Modification of the natural history of adult-onset acid maltase deficiency by nutrition and exercise therapy. *Muscle Nerve.* (2007) 35(1):70–7. doi: 10.1002/mus.20665
- Geel TM, McLaughlin PM, de Leij LF, Rutgers MH, Niezen-Koning KE. Pompe disease: current state of treatment modalities and animal models. *Mol Genet Metab.* (2007) 92(4):299–307. doi: 10.1016/j.ymgme.2007.07.009
- Winchester B, Bali D, Bodamer OA, Caillaud C, Christensen E, Cooper A, et al. Methods for a prompt and reliable laboratory diagnosis of Pompe disease: report from an international consensus meeting. *Mol Genet Metab.* (2008) 93(3):275–81. doi: 10.1016/j.ymgme.2007.09.006
- Bembi B, Cerini E, Danesino C, Donati MA, Gasperini S, Morandi L, et al. Diagnosis of glycogenosis type II. *Neurology.* (2008) 71(23 Suppl 2):S4–11. doi: 10.1212/WNL.0b013e31818da91e
- Hamdan MA, El-Zoabi BA, Begam MA, Mirghani HM, Almalik MH. Antenatal diagnosis of Pompe disease by fetal echocardiography: impact on outcome after early initiation of enzyme replacement therapy. *J Inher Metab Dis.* (2010) 33(Suppl 3):S333–9. doi: 10.1007/s10545-010-9179-2
- Cohen JL, Chakraborty P, Fung-Kee-Fung K, Schwab ME, Bali D, Young SP, et al. In utero enzyme-replacement therapy for infantile-onset Pompe's disease. *N Engl J Med.* (2022) 387(23):2150–8. doi: 10.1056/NEJMoa2200587
- Tang H, Feuchtbauer L, Sciortino S, Matteson J, Mathur D, Bishop T, et al. The first year experience of newborn screening for Pompe disease in California. *Int J Neonatal Screen.* (2020) 6(1):9. doi: 10.3390/ijns6010009
- Llerena Junior JC, Nascimento OJ, Oliveira AS, Dourado Junior ME, Marrone CD, Siqueira HH, et al. Guidelines for the diagnosis, treatment and clinical monitoring of patients with juvenile and adult Pompe disease. *Arq Neuropsiquiatr.* (2016) 74(2):166–76. doi: 10.1590/0004-282X20150194
- Shosher B, Roberts M, Byrne BJ, Sitaraman S, Jiang H, Laforêt P, et al. Safety and efficacy of cipaglucosidase alfa plus miglustat versus alglucosidase alfa plus placebo in late-onset Pompe disease (PROPEL): an international, randomised, double-blind, parallel-group, phase 3 trial. *Lancet Neurol.* (2021) 20(12):1027–37. Erratum in: *Lancet Neurol.* 2023 Oct;22(10):e11. doi: 10.1016/S1474-4422(21)00331-8
- Fiege L, Duran I, Marquardt T. Improved enzyme replacement therapy with cipaglucosidase alfa/miglustat in infantile Pompe disease. *Pharmaceuticals (Basel).* (2023) 16(9):1199. doi: 10.3390/ph16091199
- Unnisa Z, Yoon JK, Schindler JW, Mason C, van Til NP. Gene therapy developments for Pompe disease. *Biomedicines.* (2022) 10(2):302. doi: 10.3390/biomedicines10020302
- Chen M, Zhang L, Quan S. Enzyme replacement therapy for infantile-onset Pompe disease. *Cochrane Database Syst Rev.* (2017) 11:CD011539. doi: 10.1002/14651858.CD011539.pub2
- Kishnani PS, Corzo D, Nicolino M, Byrne B, Mandel H, Hwu WL, et al. Recombinant human acid [alpha]-glucosidase: major clinical benefits in infantile-onset Pompe disease. *Neurology.* (2007) 68(2):99–109. doi: 10.1212/01.wnl.0000251268.41188.04
- Page MJ, McKenzie JE, Bossuyt PM, Boutron I, Hoffmann TC, Mulrow CD, et al. The PRISMA 2020 statement: an updated guideline for reporting systematic reviews. *Int J Surg.* (2021) 88:105906. doi: 10.1016/j.ijsu.2021.105906
- Int'Hout J, Ioannidis JP, Borm GF. The Hartung-Knapp-Sidik-Jonkman method for random effects meta-analysis is straightforward and considerably outperforms the standard DerSimonian-Laird method. *BMC Med Res Methodol.* (2014) 14:25. doi: 10.1186/1471-2288-14-25
- Higgins J, Green S. *Cochrane Handbook for Systematic Reviews of Interventions* Version 5.1.0 (updated March 2011) The Cochrane Collaboration (2011).
- Pereira TV, Patsopoulos NA, Salanti G, Ioannidis JP. Critical interpretation of Cochran's Q test depends on power and prior assumptions about heterogeneity. *Res Synth Methods.* (2010) 1(2):149–61. doi: 10.1002/jrsm.13
- Sterne JAC, Savović J, Page MJ, Elbers RG, Blencowe NS, Boutron I, et al. Rob 2: a revised tool for assessing risk of bias in randomised trials. *Br Med J.* (2019) 366:14898. doi: 10.1136/bmj.14898
- Sterne JA, Hernán MA, Reeves BC, Savović J, Berkman ND, Viswanathan M, et al. ROBINS-I: a tool for assessing risk of bias in non-randomised studies of interventions. *Br Med J.* (2016) 355:i4919. doi: 10.1136/bmj.i4919
- Balshem H, Helfand M, Schünemann HJ, Oxman AD, Kunz R, Brozek J, et al. GRADE Guidelines: 3. Rating the quality of evidence. *J Clin Epidemiol.* (2011) 64(4):401–6. doi: 10.1016/j.jclinepi.2010.07.015
- Guyatt GH, Oxman AD, Vist GE, Kunz R, Falck-Ytter Y, Alonso-Coello P, et al. GRADE: an emerging consensus on rating quality of evidence and strength of recommendations. *Br Med J.* (2008) 336(7650):924–6. doi: 10.1136/bmj.39489.470347.AD
- Guyatt GH, Oxman AD, Schünemann HJ, Tugwell P, Knottnerus A. GRADE guidelines: a new series of articles in the journal of clinical epidemiology. *J Clin Epidemiol.* (2011) 64(4):380–2. doi: 10.1016/j.jclinepi.2010.09.011
- Kishnani PS, Nicolino M, Voit T, Rogers RC, Tsai AC, Waterson J, et al. Chinese Hamster ovary cell-derived recombinant human acid alpha-glucosidase in infantile-onset Pompe disease. *J Pediatr.* (2006) 149(1):89–97. doi: 10.1016/j.jpeds.2006.02.035
- Kishnani PS, Corzo D, Leslie ND, Gruskin D, Van der Ploeg A, Clancy JP, et al. Early treatment with alglucosidase alfa prolongs long-term survival of infants with Pompe disease. *Pediatr Res.* (2009) 66(3):329–35. doi: 10.1203/PDR.0b013e3181b24e94
- Nicolino M, Byrne B, Wraith JE, Leslie N, Mandel H, Freyer DR, et al. Clinical outcomes after long-term treatment with alglucosidase alfa in infants and children with advanced Pompe disease. *Genet Med.* (2009) 11(3):210–9. doi: 10.1097/GIM.0b013e31819d0996
- Zhu D, Zhu J, Qiu W, Wang B, Liu L, Yu X, et al. A multi-centre prospective study of the efficacy and safety of alglucosidase alfa in Chinese patients with infantile-onset Pompe disease. *Front Pharmacol.* (2022) 13:903488. doi: 10.3389/fphar.2022.903488
- Barker PC, Pasquali SK, Darty S, Ing RJ, Li JS, Kim RJ, et al. Use of cardiac magnetic resonance imaging to evaluate cardiac structure, function and fibrosis in children with infantile Pompe disease on enzyme replacement therapy. *Mol Genet Metab.* (2010) 101(4):332–7. doi: 10.1016/j.ymgme.2010.07.011

31. van Gelder CM, Poelman E, Plug I, Hoogeveen-Westerveld M, van der Beek NAME, Reuser AJ, et al. Effects of a higher dose of alglucosidase alfa on ventilator-free survival and motor outcome in classic infantile Pompe disease: an open-label single-center study. *J Inherit Metab Dis.* (2016) 39(3):383–90. doi: 10.1007/s10545-015-9912-y
32. Chien YH, Lee NC, Chen CA, Tsai FJ, Tsai WH, Shieh JY, et al. Long-term prognosis of patients with infantile-onset Pompe disease diagnosed by newborn screening and treated since birth. *J Pediatr.* (2015) 166(4):985–91.e1–2. doi: 10.1016/j.jpeds.2014.10.068
33. Chen CA, Chien YH, Hwu WL, Lee NC, Wang JK, Chen LR, et al. Left ventricular geometry, global function, and dyssynchrony in infants and children with Pompe cardiomyopathy undergoing enzyme replacement therapy. *J Card Fail.* (2011) 17(11):930–6. doi: 10.1016/j.cardfail.2011.07.011
34. van Capelle CI, Poelman E, Frohn-Mulder IM, Koopman LP, van den Hout JMP, Régál L, et al. Cardiac outcome in classic infantile Pompe disease after 13 years of treatment with recombinant human acid alpha-glucosidase. *Int J Cardiol.* (2018) 269:104–10. doi: 10.1016/j.ijcard.2018.07.091
35. Nagura H, Hokugo J, Ueda K. Long-term observation of the safety and effectiveness of enzyme replacement therapy in Japanese patients with Pompe disease: results from the post-marketing surveillance. *Neurol Ther.* (2019) 8(2):397–409. doi: 10.1007/s40120-019-00157-4
36. van Kooten HA, Ditters IAM, Hoogeveen-Westerveld M, Jacobs EH, van den Hout JMP, van Doorn PA, et al. Antibodies against recombinant human alpha-glucosidase do not seem to affect clinical outcome in childhood onset Pompe disease. *Orphanet J Rare Dis.* (2022) 17(1):31. doi: 10.1186/s13023-022-02175-2
37. Chien YH, Lee NC, Thurberg BL, Chiang SC, Zhang XK, Keutzer J, et al. Pompe disease in infants: improving the prognosis by newborn screening and early treatment. *Pediatrics.* (2009) 124(6):e1116–25. doi: 10.1542/peds.2008-3667
38. Ditters IAM, Huidekoper HH, Kruijschaar ME, Rizopoulos D, Hahn A, Mongini TE, et al. Effect of alglucosidase alfa dosage on survival and walking ability in patients with classic infantile Pompe disease: a multicentre observational cohort study from the European Pompe consortium. *Lancet Child Adolesc Health.* (2022) 6(1):28–37. doi: 10.1016/S2352-4642(21)00308-4
39. Spiridigliozzi GA, Heller JH, Case LE, Jones HN, Kishnani PS. Early cognitive development in children with infantile Pompe disease. *Mol Genet Metab.* (2012) 105(3):428–32. doi: 10.1016/j.ymgme.2011.10.012
40. Kishnani PS, Hwu WL, Mandel H, Nicolino M, Yong F, Corzo D, et al. A retrospective, multinational, multicenter study on the natural history of infantile-onset Pompe disease. *J Pediatr.* (2006) 148(5):671–6. doi: 10.1016/j.jpeds.2005.11.033
41. Joanne M, Skye N, Tracy M. The effectiveness of enzyme replacement therapy for juvenile-onset Pompe disease: a systematic review. *J Inherit Metab Dis.* (2019) 42(1):57–65. doi: 10.1002/jimd.12027
42. Hahn SH, Kronn D, Leslie ND, Pena LDM, Tanpaiboon P, Gambello MJ, et al. Efficacy, safety profile, and immunogenicity of alglucosidase alfa produced at the 4,000-liter scale in US children and adolescents with Pompe disease: ADVANCE, a phase IV, open-label, prospective study. *Genet Med.* (2018) 20(10):1284–94. doi: 10.1038/gim.2018.2
43. Byrne BJ, Colan SD, Kishnani PS, Foster MC, Sparks SE, Gibson JB, et al. Cardiac responses in paediatric Pompe disease in the ADVANCE patient cohort. *Cardiol Young.* (2022) 32(3):364–73. doi: 10.1017/S1047951121002079
44. Dornelles AD, Junges APP, Pereira TV, Krug BC, Gonçalves CBT, Llerena JC, et al. A systematic review and meta-analysis of enzyme replacement therapy in late-onset Pompe disease. *J Clin Med.* (2021) 10(21):4828. doi: 10.3390/jcm10214828
45. Harlaar L, Hogrel JY, Perniconi B, Kruijschaar ME, Rizopoulos D, Taouagh N, et al. Large variation in effects during 10 years of enzyme therapy in adults with Pompe disease. *Neurology.* (2019) 93(19):e1756–e67. doi: 10.1212/WNL.00000000000008441



OPEN ACCESS

EDITED BY

Luigia De Falco,
Centro Polidiagnostico Strumentale, Italy

REVIEWED BY

Claudia Gonzaga-Jauregui,
Universidad Nacional Autónoma de México,
Mexico
Steven Erdman,
Nationwide Children's Hospital, United States

*CORRESPONDENCE

Sara Guillén-Lopez
✉ sara_guillen@hotmail.com

RECEIVED 28 August 2023

ACCEPTED 02 February 2024

PUBLISHED 19 February 2024

CITATION

López-Mejía L, Guillén-Lopez S, Vela-Amieva M, Santillán-Martínez R, Abreu M, González-Herrera MD, Díaz-Martínez R and Reyes-Magaña JG (2024) Importance of genetic sequencing studies in managing chronic neonatal diarrhea: a case report of a novel variant in the glucose–galactose transporter SLC5A1.
Front. Pediatr. 12:1284671.
doi: 10.3389/fped.2024.1284671

COPYRIGHT

© 2024 López-Mejía, Guillén-Lopez, Vela-Amieva, Santillán-Martínez, Abreu, González-Herrera, Díaz-Martínez and Reyes-Magaña. This is an open-access article distributed under the terms of the [Creative Commons Attribution License \(CC BY\)](https://creativecommons.org/licenses/by/4.0/). The use, distribution or reproduction in other forums is permitted, provided the original author(s) and the copyright owner(s) are credited and that the original publication in this journal is cited, in accordance with accepted academic practice. No use, distribution or reproduction is permitted which does not comply with these terms.

Importance of genetic sequencing studies in managing chronic neonatal diarrhea: a case report of a novel variant in the glucose–galactose transporter SLC5A1

Lizbeth López-Mejía¹, Sara Guillén-Lopez^{1*},
Marcela Vela-Amieva¹, Rosalía Santillán-Martínez²,
Melania Abreu^{2,3}, María Dolores González-Herrera⁴,
Rubicel Díaz-Martínez⁵ and Juan Gaspar Reyes-Magaña⁴

¹Laboratorio de Errores Innatos del Metabolismo y Tamiz, Instituto Nacional de Pediatría, Mexico City, Mexico, ²Laboratorio de Biología Molecular, Genos Medica, Mexico City, Mexico, ³Centro de Cáncer, Centro Médico ABC, Mexico City, Mexico, ⁴Servicio de Medicina Interna, Hospital del Niño Dr. Rodolfo Nieto Padrón, Villahermosa, Mexico, ⁵Servicio de Genética, Hospital del Niño Dr. Rodolfo Nieto Padrón, Villahermosa, Mexico

Introduction: Congenital glucose–galactose malabsorption (CGGM) is a rare autosomal recessive disorder that primarily causes chronic intractable diarrhea. This study aims to describe the clinical history, laboratory profile, diagnostic workflow, and management of the first patient reported with CGGM in Mexico.

Methods: The case involves a Mexican female infant with recurrent admissions to the emergency room since birth due to chronic diarrhea.

Results: The infant was born at term by C-section with a birth weight of 3.120 kg and height of 48 cm for consanguineous parents. She had been breastfed until day 5 of her life when she presented lethargy, diarrhea, abdominal discomfort, and jaundice. During the first evaluation at the emergency room, the significant laboratory finding was blood tyrosine elevation; afterward, amino acid and succinylacetone determinations were obtained, discarding tyrosinemia. When admitted to the hospital, an abdominal ultrasound detected a duplex collecting system. At this time, rice formula was introduced to the patient. She was discharged with jaundice improvement, but diarrhea persisted. Several formula changes had been made from rice to extensively hydrolyzed casein protein to whey-based, with no clinical improvement; the patient still had 10–12 excretions daily. In the second hospitalization, the patient presented anemia, severe dehydration, hyperammonemia, and renal tubular acidosis. A next-generation sequencing panel for inborn errors of metabolism and congenital diarrhea was performed, identifying a homozygous variant in *SLC5A1* (c.1667T>C). The diagnosis of CGGM was made at 3 months of age. The infant was initially treated with a modular galactose–glucose-free formula with oil, fructose, casein, minerals, and vitamins until a commercial fructose-based formula was introduced. This led to a complete resolution of diarrhea and improved nutritional status.

Discussion: Diagnosing CGGM is challenging for clinicians, and next-generation sequencing is a valuable tool for providing appropriate treatment. More detailed information on patients with this condition might lead to possible phenotype–genotype correlations. This case’s primary clinical and biochemical findings were chronic diarrhea, anemia, jaundice, renal tubular acidosis, hyperammonemia, and initial hypertyrosinemia. Symptoms were resolved entirely with the fructose-based formula.

KEYWORDS

glucose–galactose malabsorption, infantile diarrhea, *SLC5A1*, SGLT-1, sodium/glucose cotransporter, inborn errors of metabolism, case report

1 Introduction

Diarrhea in neonates is defined by a stool volume of more than 20 ml/kg/d and a chronic one that lasts more than 14 days. One of the causes of chronic non-bloody diarrhea could be explained by an osmotic process of unabsorbed or partially absorbed nutrients, leading to an increased intraluminal solute load. Carbohydrate malabsorption is the most frequent finding related to osmotic diarrhea (1). Monogenic intestinal epithelial disorders or congenital diarrheas and enteropathies are a heterogeneous group of diseases characterized by neonatal or infantile-onset diarrhea and malabsorption. They are classified as defects in epithelial transport, epithelial enzymes and metabolism, epithelial structure, trafficking, polarity, enteroendocrine function, and epithelial stem cell function. The sodium-dependent glucose transporters could be responsible for congenital diarrhea; different genes are associated with this dysfunction: *SLC26A3* (MIM 126650), *SLC10A2* (MIM 601295), *SLC5A1* (MIM 182380), *SLC7A7* (MIM 603593), *SLC39A4* (MIM 607059), *GUCY2C* (MIM 601330), *SLC9A3* (MIM 182307), and *SLC51B* (MIM 612085) (2).

Congenital glucose–galactose malabsorption (CGGM) is an autosomal recessive genetic disorder (CIE-10 74.3, CIE-11 5C61.0) caused by pathogenic variants in *SLC5A1* (OMIM #606824, <https://www.omim.org/entry/606824>) encoding for the sodium-dependent glucose transporter-1 (SGLT-1) (3). SGLT-1 is the primary transporter of monosaccharides in the small intestine and is responsible for moving glucose and galactose across the intestinal brush border using active transport (4). A defect in the SGLT-1 results in the non-absorption of glucose, galactose, and sodium, leading to clinical manifestations that begin in the neonatal period (5).

The most common symptoms include severe hyperosmotic diarrhea, dehydration, abdominal distension, vomiting, failure to thrive, and weight loss (6). Other complications reported are kidney injury, hypernatremia, hypercalcemia, nephrolithiasis, polyuria, and hematuria (7). Diagnosis should be suspected based on clinical symptoms and confirmed by genetic testing (5). Treatment consists of a long-term particular dietary therapy that avoids foods containing glucose and galactose (8). Older children may show improved glucose tolerance as they age (9). In this study, we report a homozygous likely pathogenic variant in *SLC5A1* and describe the clinical and biochemical characteristics and management of the first patient with CGGM reported in Mexico.

2 Case presentation

The proband is an 8-month-old female, a child of second pregnancy, for consanguineous parents from a small endogamic region in Tabasco, Medellín de Madero, a town of nine thousand inhabitants. She was the second offspring in the family, with a previous healthy sibling. The patient’s mother had prenatal care with four ultrasounds and five doctor visits during her pregnancy. The proband was born by C-section due to oligohydramnios. At birth, a weight of 3.120 kg (Z-score: −0.25) and a height of 48 cm (Z-score: −0.62), weight for length 0.52, were reported, Apgar 9. She was exclusively breastfed with adequate suction for 5 days when she presented with abdominal distension and diarrhea that gradually increased to 10–12 liquid stools daily. At 1 month of age, she was admitted to the hospital for 8 days for jaundice, lethargy, and severe diarrhea. During her first evaluation at the emergency room, coprological and coproparasitoscopic methods were performed without finding any alterations in the reported samples, and fecal-reducing substances were reported negative. Viral infections were also discarded. Because of the hepatic alterations, antibodies IgM and IgG against CMV and EBV were also tested, with negative results. C-reactive protein, thyroid function test, and coagulation parameters showed no alterations. Severe dehydration was immediately corrected with IV fluids, so a trial of oral rehydration solution was not performed. A metabolic screening showed elevated blood concentrations of tyrosine (6.57 mg/dl, normal range <4.98 mg/dl) and alpha-fetoprotein (184 ng/ml, normal range: 0–20 ng/ml) but average blood concentrations of succinylacetone. Afterward, tyrosine 46 µmol/L (normal range 26–155 µmol/L) and succinylacetone were repeated and were in the normal ranges, ruling out the diagnosis of tyrosinemia type 1. Relevant biochemical studies during treatment are depicted in Table 1. When admitted to the hospital, an abdominal ultrasound revealed a duplex kidney collecting system and a clubfoot was diagnosed. At this time, breastfeeding was suspended, and she was given a partially hydrolyzed formula based on rice protein. However, jaundice improved over time; there was no change in the number of bowel movements, so the formula was changed to extensive casein hydrolyzed, and then she was discharged.

After several formula changes, the patient continued to have 10–15 excretions per day, causing her severe dehydration, vomiting,

TABLE 1 Relevant biochemical studies during treatment of a CGGM patient.

Biochemical studies	Age			
	1 month	8 months	9 months	10 months
Glucose (mg/dl)	75	102	95	76
Urea (mg/dl)	39	28	17.3	
Blood nitrogen urea (mg/dl)	18.4	13	8.1	
Creatinine (mg/dl)	0.6	0.2	0.4	0.3
Uric acid (mg/dl)		3.1	4.8	
Sodium (mmol/L)	145	137		
Potassium (mmol/L)	3.5	5.4		
Chlorine (mmol/L)	118	106		
Calcium (mg/dl)	12.2	10.6		
Phosphorus (mg/dl)	5	7		
Magnesium (mg/dl)	2.1	1.9		
Triglycerides (mg/dl)	80	86	86	77
Total cholesterol (mg/dl)	138	142	134	210
HDL cholesterol (mg/dl)		67		74
LDL cholesterol (mg/dl)		57.8		113
VLDL cholesterol (mg/dl)		17.2		15.4
Total bilirubin (mg/dl)	11.2	0.3		
Direct bilirubin (mg/dl)	0.6	0.1		
Indirect bilirubin (mg/dl)	10.6	0.2		
Serum albumin (g/dl)	4.1	4.3		
Aspartate aminotransferase (U/L)	30.3	34		
Alanine transaminase (U/L)	24	26		
Hemoglobin (g/dl)	6.6	12.2	11	12.4
Hematocrit (%)	19.6	36.8	34	37.6
Platelet (×10 ³ /μl)	641	541	545	367
pH	7.1			
HCO ₃ (mmol/L)	3.8			
Lactate (mmol/L)	2.5			
Ammonium (μmol/L)	213	29		

anorexia, and inadequate weight gain, requiring a second hospitalization at 2 months of age that lasted 80 days. During this hospitalization, another coprological study was done; this time, an acid stool pH of 5 and positive reducing substances were reported. The patient presented anemia (hemoglobin 9.6 g/dl, hematocrit 32.2%), hyperammonemia (213 μg/dl), hyponatremia with sodium levels initially at 145 mmol/L, increasing up to 152.8 mmol/L, and hypercalcemia of 8.9 mg/dl. The patient was diagnosed with severe malnutrition, and an ultrasound was performed with evidence of nephrocalcinosis. The nephrology department started sodium bicarbonate at 7 mEq/kg/d due to hyperchloremic metabolic acidosis, elevated urinary pH, and hypokalemia. Parenteral nutrition with IV glucose/kg/minute of 6.5 was initiated through a central line because the patient experienced hypoglycemia (69 mg/dl) even with enteral formula infusion through a nasogastric tube. The patient had two previous transfusions. The hematology department started erythropoietin at 2,000 IU per week and 1,000 IU twice weekly, along with iron, folic acid, and complex B vitamin supplementation to treat anemia. A positive blood culture for *Klebsiella pneumoniae* was also detected and treated with meropenem.

At this point, a monogenic disease was suspected due to the heterogeneous phenotype, and a next-generation sequencing

panel was considered the first genetic test. Genomic DNA was extracted from peripheral blood using the Gentra Puregene Kit (Qiagen®). Clinical Exome Solution V3 Panel (Sophia Genetics, Saint-Sulpice, Switzerland) was used for in-solution hybridization to enrich target sequences, which covers the coding regions (±5 bp of intronic regions) of 4,728 genes, the entire mitochondrial genome, and ~200 non-coding variants with known pathogenicity in deep introns/enhancer/promoter genes. The primers were by design (Primer3 v. 0.4.0) as follows: Chr22:32104691: Fw 5'-TTCCCTTCCTTGATGCATATCT-3' Rv 5'-TTAACTTCCCCAAACCCACTT-3'. The DNA sample was sequenced on the Illumina NextSeq 500 (Illumina, Inc., San Diego, CA, United States). The average coverage depth was 113×, with over 99.8% of the target regions covered by at least 20 reads. Sequence quality control was performed with FastQC; BWA mapped reads, variant calling was done with GATK4, and verification of the effects of these variants using SnpEff, inspection of selected variants through IGV, and sequenced reads were compared with the reference human genome version (GRCh38/hg38).

The bioinformatic analysis was done in the Sophia DDM platform (Sophia Genetics, Saint-Sulpice, Switzerland) with a virtual gene panel of 1,125 genes associated with inborn errors of metabolism, 260 of congenital diarrhea and 100 with both phenotypes; 1,485 genes in total were analyzed (Supplementary Table S1).

This panel allowed the identification of the NM_000343.4 (SLC5A1):c.1667T>C (p.Leu556Pro) variant. This missense mutation replaces leucine residue by proline at position 556 of the coding region of the *SLC5A1* gene (exon 14 of 15) located in the single intramembrane position of the protein. It was classified as likely pathogenic according to the ACMG criteria (10) as it has extremely low frequencies in population databases and is not present in Clinvar, LOVD, or disease-related databases (PM2), for a missense variant in a gene that has a low rate of benign missense variation and in which missense variants are a common mechanism of disease (PP2). Several lines of computational evidence support a potential pathogenic effect (PP3, REVEL 0.875 score as pathogenic moderate, PolyPhen: possibly damaging, MetaRNN: pathogenic strong). The segregation analysis by Sanger sequencing confirmed the heterozygous state of both parents (PM3) (Figure 1), and the patient's phenotype history is highly specific for a disease with a single genetic etiology (PP4). CGGM was diagnosed at 3 months of age with the clinical phenotype and the likely pathogenic variant detected.

Specific dietary treatment for CGGM was started after diagnostic confirmation at the Pediatrics Hospital in Tabasco with the support of the National Pediatrics Institute in Mexico City. Since the fructose-based commercial formula (Galactomin 19® Nutricia, Germany) was not available in Mexico, a modular galactose-glucose-free formula containing oil, fructose, casein, vitamins, and minerals was introduced initially. When Galactomin 19® became available, it replaced the modular diet. Significant clinical improvement was observed, with a decrease in the number of bowel movements and improved nutritional status. The patient was discharged at 3 months of age. Over 2 months, from 4 to

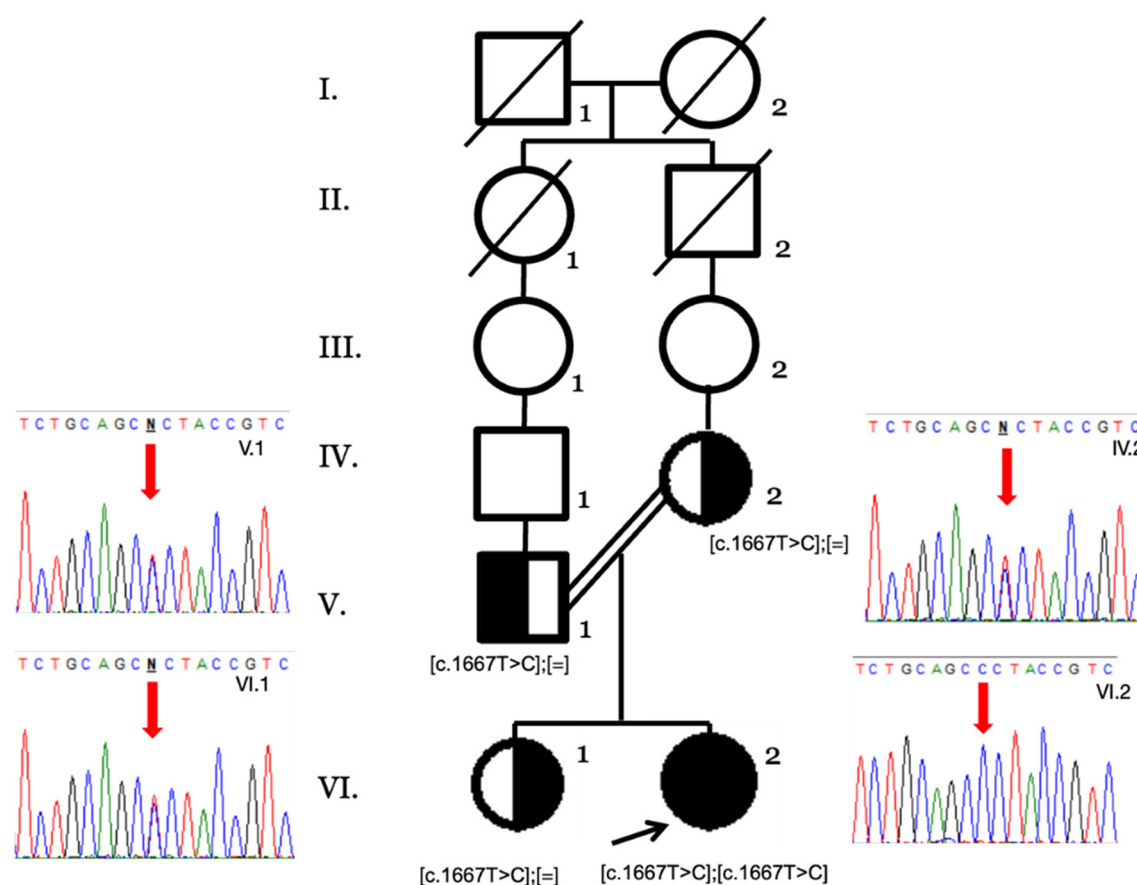


FIGURE 1

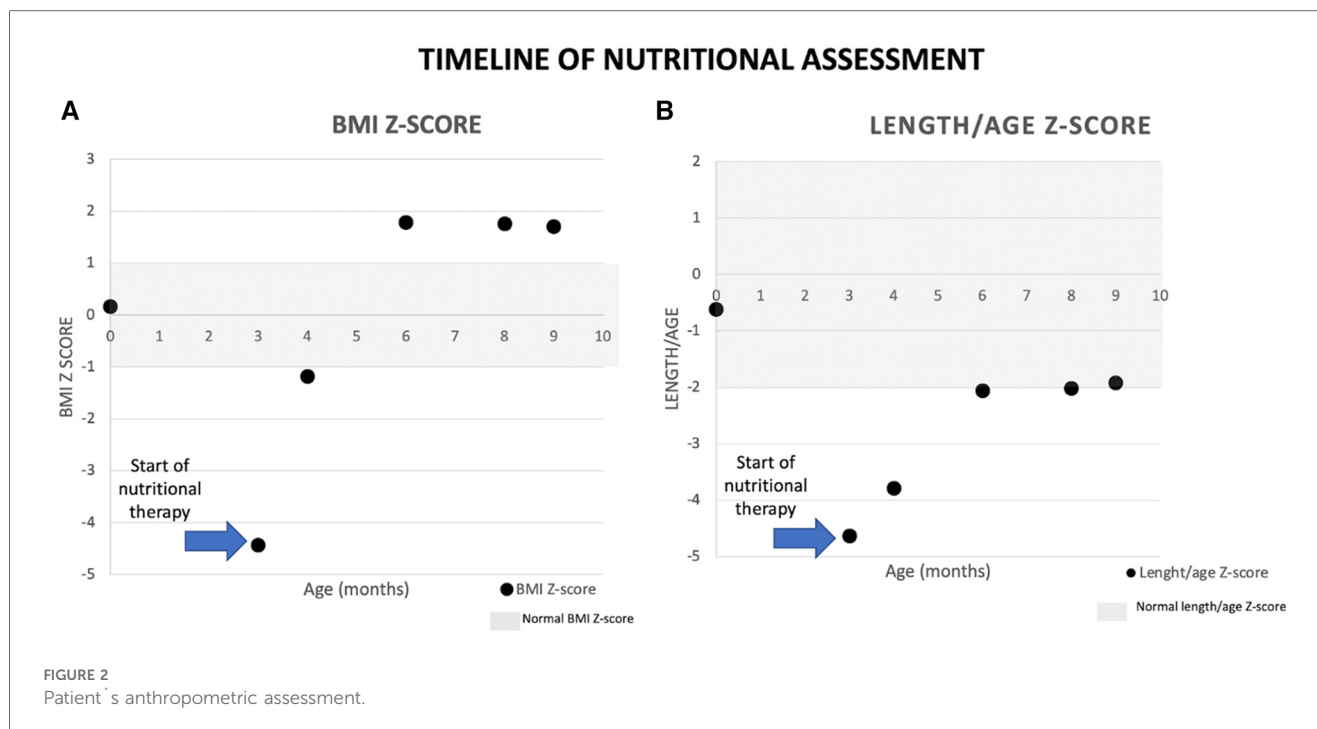
Family pedigree by Sanger sequencing of the available family members. The heterozygous genotypes of the nuclear family (V.1, IV.2, and VI.1) and the homozygous variant in the index case (VI.2) are shown with the red arrows.

6 months, the patient's mother chose to increase the consumption of fructose formula without following the prescribed guidelines. Consequently, the patient experienced a significant increase in weight and triglyceride levels (271 mg/dl). When the patient reached 6 months of age, medical follow-up was re-established and provided a specific prescription to reduce the amount of formula intake. Furthermore, we counseled the patient and her family about the potential adverse effects of consuming excessive fructose in her diet.

Complementary feeding was started at 6 months of age, and a 1-month meal plan was given to the family to enhance adherence; the diet included fruit, vegetables, meat, and some small amounts of cereals. Currently, the patient presents one to two depositions per day, and constipation has also been reported but less frequent; she has a normal developmental milestone for her age. Renal function tests were normalized after the second hospitalization, and a citrate solution was prescribed until she was 6 months old. After that, the nephrologist prescribed hydrochlorothiazide 1.5 mg once a day to treat nephrocalcinosis. Nephrological follow-up will continue in Tabasco, and nutritional follow-up is ongoing at the National Institute of Pediatrics in Mexico City (Figure 2).

3 Discussion

The diagnosis of CGGM can be challenging to suspect for clinicians because the symptoms are not specific (6). Reaching the correct diagnosis in neonates starts by discarding general causes of chronic diarrhea. A key point is the timing, mainly if it occurs soon after birth, because it could be related to congenital anomalies and enteropathies (1, 2). At the beginning of diagnosis, an important point to consider is to distinguish whether there is blood in the stools so inflammatory and allergic causes can be discarded. In this case, non-bloody diarrhea can be due to malabsorption. Medernach and Middleton suggest performing a 24–48 h fasting to differentiate between osmotic and secretory diarrhea. A stool pH < 5 suggests carbohydrate malabsorption because of its fermentation and the subsequent production of short-chain fatty acids. Stool-reducing substances greater than 0.5% is indicative of monosaccharide malabsorption. In the first hospitalization, the patient did not show a decreased pH in stools or positive reducing substances to suspect carbohydrate malabsorption, and it was until the second hospitalization that the patient manifested these alterations. Even though an esophagogastroduodenoscopy with biopsy could differentiate a deficiency among the disaccharidases,



in this case, a biopsy cannot help establish the diagnosis of CGGM (11) nor the breath hydrogen testing. In some local hospitals, these procedures are not available. Figure 3 describes an algorithm for the differential diagnosis of diarrhea in neonates. As mentioned, several genes could be related to defects in epithelial transport, and some differences might lead to the diagnosis; for example, *GUCY2C*, *SLC9A3*, and *SLC26A3* are early-onset watery secretory diarrheas, unlike *SLC5A1* (2). However, establishing the diagnosis based on the clinical and biochemical findings might take a long time. Initial history and symptoms, serum laboratories, stool and dietary evaluation, endoscopic biopsy, and genetic testing should be performed (2, 11). In the patient reported in this case, the main symptom observed was severe osmotic diarrhea that began in the first days of life after feeding exclusively with breast milk. Because of the late treatment, she developed nephrolithiasis. In a recent literature review of CGGM, complications such as kidney injury, hypercalcemia, and nephrolithiasis were found in 18.7% of the studied patients, and hypernatremia (found in 53.3%) was also shown in our case (7).

Diarrhea led to severe dehydration, anemia, jaundice, renal tubular acidosis, hyperammonemia, and malnutrition. These symptoms are like those reported in the literature (6). Dietary treatment that consists of glucose and galactose elimination from the diet resulted in an essential clinical improvement and in the cessation of symptoms (8). The initial hand-crafted formula recipe is described in Supplementary Table S2. The diet should include a metabolic formula with fructose, fruits and vegetables, animal protein sources, legumes, oils, and fats. A more detailed list of allowed and restricted food is described in Table 2 (8, 12).

Early diagnosis is essential to improve symptoms and avoid complications such as kidney injury and nephrolithiasis. Health personnel must know about this metabolic disease to consider

CGGM a possible diagnosis in newborns presenting severe osmotic refractory diarrhea, metabolic acidosis, and dehydration that do not respond to standard therapy (5).

As it has been previously described (13), patients with congenital diarrheal disorders benefit from genetic testing as the first diagnostic approach because they provide not only the specific diagnosis but also the rapid implementation of target therapies. In this case, a next-generation sequencing panel identified a homozygous missense variant in *SLC5A1* (c.1667T>C). *SLC5A1* (Gene/locus MIM number: 182380) is located on the long arm of chromosome 22 in the region 22q12.3. This gene encodes a member of the GLT family in epithelial cell membranes of the intestine that co-transporters sodium ion(s) and monosaccharides into the cell using the sodium concentration gradient. *SLC5A1* is predominantly expressed in the small intestine, characterized by its strict selectivity and binding affinity to D-glucose (1.74 mM) and D-galactose (3.12 mM) substrates (14). This gene comprises 15 exons extending over 69.8 kb and encodes 664 amino acids. Fifty-six different missense, non-sense, frame shift, and splice site variants have been described in *SLC5A1* associated with CGGM; most are private coding variants that produce abnormal or truncated proteins. Family cases reported of CGGM with missense variants in *SLC5A1* have shown loss of the transporter activity that impairs trafficking to the plasma membrane (15). The variant c.1667T>C (p.Leu556Pro) affects the C-terminal part of the transporter (residues 407–664 containing trans-membrane helices 10–14), which determines sugar selectivity and affinity; this may explain the accumulation of unabsorbed glucose and galactose observed clinically in this patient.

In the first genetic assessment, the family was not self-aware of any consanguinity, only that they were coming from a small town (endogamy). Until the detection of the homozygous variant, a six-

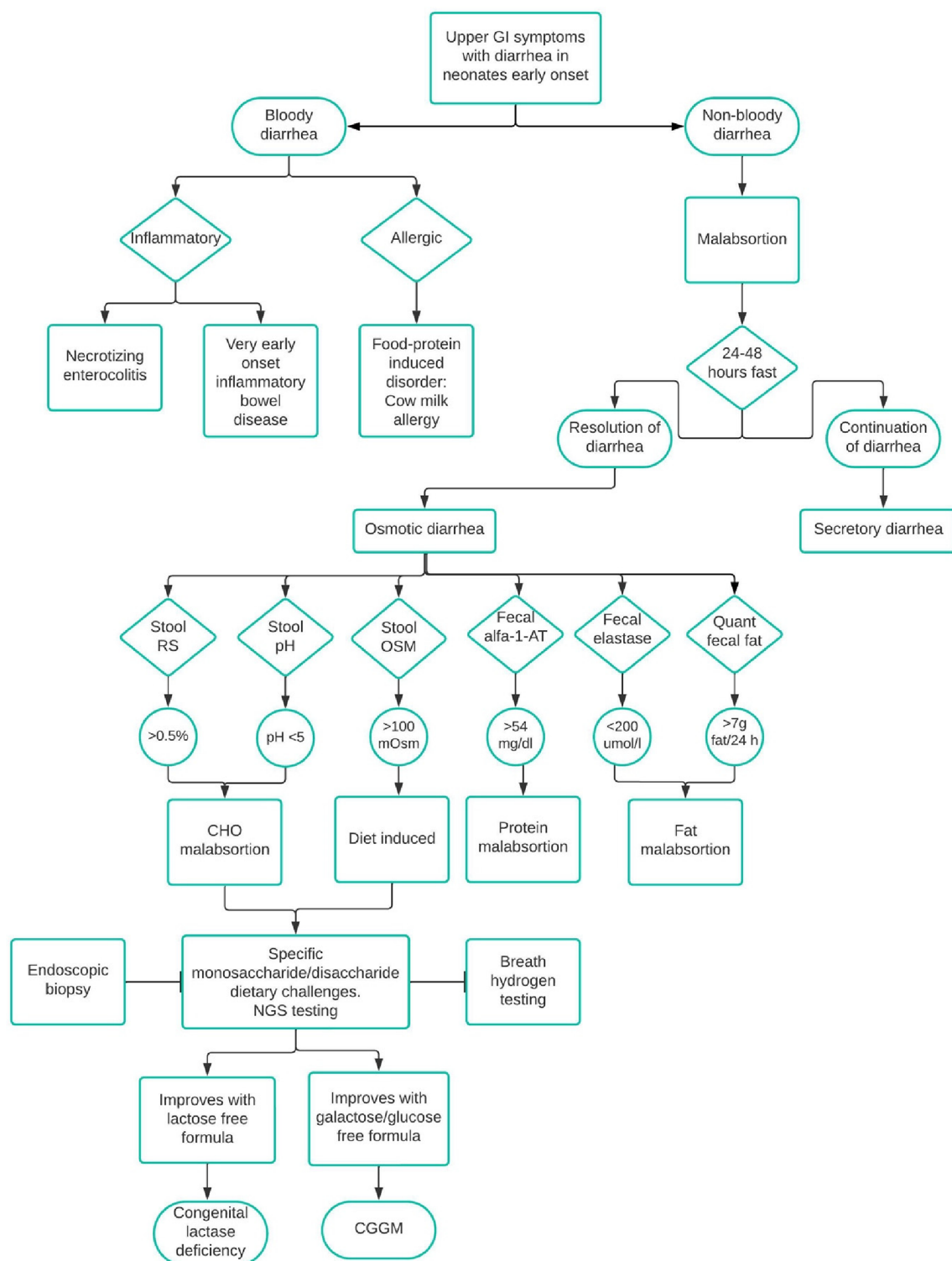


FIGURE 3

Differential diagnosis of diarrhea in neonates. CHO, carbohydrate; alfa-1-AT, alfa-1-antrypsin; OSM, osmolality; RS, reducing substances; Quant, quantitative; NGS, next-generation sequencing.

generation pedigree confirmed the relationship and genetic counseling as an autosomal recessive disorder was given to the family. Among 65.2%–76.7% of the CGGM cases reported are homozygous, such as this case, supporting the observation that

this is a disease with high morbidity in countries or regions with high endogamy or inbreeding (6).

The variant c.1667T > C (rs1049516620) has an extremely low frequency reported in population databases (4/264,690, TOPMED;

TABLE 2 Allowed and restricted food in congenital glucose–galactose transporter deficiency.

Group of food	Allowed	Restricted
Dairy products	None	All: milk, human milk, formulas with lactose, butter, yogurt, cheese, ice cream, industrialized food with lactose, condensed milk, cream, all sorts of dairy products
Fruits	All kinds: banana, apple, peach, strawberry, oranges, pear, watermelon, unsweetened juice	Fruits with added sugar, fruits in syrup, fruit juice with sucrose, marmalade, jellies
Cereals	Rice, noodles, potato, quinoa, wheat, unsweetened cereal, bread with fructose, oats, and whole grain without sugary coating	Sweetened cereal, biscuits, bread with sucrose and milk, all desserts made with sugar and milk, commercial cookies, and cakes
Vegetables	All kinds	None
Animal protein	All sorts: fish (salmon, tuna, catfish), egg, chicken, beef, turkey, duck, pork, lamb, goat, seafood (shrimp, crab, clams, lobster, scallops, oysters, mussels)	None
Legumes	Beans, soybeans, chickpeas, lentils, peas	None
Nuts	All: Cashews, peanuts, almonds, hazelnuts, walnuts, Brazil nuts, pecans, pine nuts, pistachios	Praline nuts with sugar
Fats and oils	All vegetable oils	Frostings, meringue with sugar
Sweeteners and flavorings	Fructose, honey, cocoa, sugar-free marmalade	Glucose, dextrose, dextrin, glucose polymers, maltodextrin, maltose, corn syrup, lactose, stevia, sugar (sucrose), candies, chocolate, ketchup with sugar

3/140,234, GnomAD). One of the main disadvantages of contrasting low-frequency variants in public databases is that not all populations are well represented; however, in the internal records of the laboratory, which has more than 2,000 clinical exomes of Mexican patients and in the 79,656 clinical exomes from the Sophia Community, the variant was not detected either; this along with the segregation analysis suggest it as associated with the disease. There are only 107 documented CGGM cases from 2001 to 2019 worldwide (6). This rare variant probably has a founder effect in this Tabasco community, and the healthcare providers of the region must be aware of this metabolic disease presenting as chronic osmotic refractory diarrhea and treated promptly to avoid unnecessary prolonged hospitalizations, morbidity, and mortality.

It is essential to highlight the benefit of the next-generation sequencing panel performed on this patient, which allowed the correct diagnosis of a rare disease difficult to suspect clinically, especially in the neonatal period when presentation tends to be more severe with life-threatening episodes. Next-generation sequencing is now proposed also as a first-line test for diagnosing inborn errors of metabolism; this panel type has favorable diagnostic rates as high as 60% (16). Once the diagnosis was confirmed, the specific treatment saved this patient's life. Diagnosing an inborn error of metabolism is a medical challenge, particularly considering that CGGM does not appear in any newborn screening program, and this disease does not have a specific blood or urine biomarker.

A proper follow-up should remain throughout the duration of treatment. Excess fructose leads to obesity and hypertriglyceridemia, which can be preventable with a closer follow-up. Fructose promotes *de novo* hepatic lipogenesis with an overproduction of acetyl-CoA and glycerol-3-phosphate and is linked with postprandial hypertriglyceridemia, leading to hepatic steatosis, insulin resistance, and hyperuricemia (17). The biochemical follow-up in these patients should consider regular insulin, glucose, hemoglobin A1C, uric acid, lipid

profile, and liver function test. Medical–nutritional assessments should prevail throughout the patient's life to prevent complications.

In conclusion, clinicians should consider CGGM in patients with chronic diarrhea or renal tubular acidosis. Early diagnosis through next-generation sequencing approaches can save lives by initiating specific treatments promptly and avoiding a diagnostic odyssey. Regular follow-up and dietary management are essential to prevent complications and ensure better long-term outcomes for patients with CGGM. Healthcare professionals' awareness of this metabolic disorder is critical to improving patient care.

Data availability statement

The datasets for this article are not publicly available due to concerns regarding participant/patient anonymity. Requests to access the datasets should be directed to the corresponding author.

Ethics statement

The studies involving humans were approved by Research, Biosecurity and Ethics Committees of the National Institute of Pediatrics (Instituto Nacional de Pediatría, Secretaría de Salud, México), approval number 2022/051. The studies were conducted in accordance with the local legislation and institutional requirements. Written informed consent for participation was not required from the participants or the participants' legal guardians/next of kin in accordance with the national legislation and institutional requirements. Written informed consent was obtained from the individual(s), and minor(s)' legal guardian/next of kin, for the publication of any potentially identifiable images or data included in this article.

Author contributions

LL-M: Investigation, Writing – original draft, Writing – review & editing. SG-L: Conceptualization, Data curation, Investigation, Project administration, Supervision, Validation, Writing – original draft, Writing – review & editing. MV-A: Formal Analysis, Supervision, Validation, Writing – review & editing. RS-M: Formal Analysis, Software, Writing – review & editing. MA: Conceptualization, Data curation, Formal Analysis, Writing – review & editing. MG-H: Supervision, Validation, Visualization, Writing – review & editing. RD-M: Investigation, Supervision, Validation, Writing – review & editing. JR-M: Data curation, Investigation, Writing – review & editing.

Funding

The authors declare financial support was received for the research, authorship, and/or publication of this article.

This research was funded by the National Institute of Pediatrics (Recursos Fiscales 2018–2023, Programa E022 Investigación y Desarrollo Tecnológico en Salud, Secretaría de Salud, México). Project number 2022/051.

References

- Younis M, Rastogi R, Chugh A, Rastogi S, Aly H. Congenital diarrheal diseases. *Clin Perinatol*. (2020) 47(2):301–21. doi: 10.1016/j.clp.2020.02.007
- Babcock SJ, Flores-Marin D, Thiagarajah JR. The genetics of monogenic intestinal epithelial disorders. *Hum Genet*. (2023) 142(5):613–54. doi: 10.1007/s00439-022-02501-5
- Lostao MP, Loo DD, Hernell O, Meeuwisse G, Martin MG, Wright EM. The molecular basis of glucose galactose malabsorption in a large Swedish pedigree. *Function*. (2021) 2(5):zqab040. doi: 10.1093/function/zqab040
- Koepsell H. Glucose transporters in the small intestine in health and disease. *Pflugers Arch*. (2020) 472(9):1207–48. doi: 10.1007/s00424-020-02439-5
- Akduman H, Dilli D, Ceylaner S. A case of congenital glucose galactose malabsorption with a new mutation in the *SLC5A1* gene. *J Pediatr Genet*. (2020) 11(4):317–9. doi: 10.1055/s-0040-1719161
- Wang W, Wang L, Ma M. Literature review on congenital glucose-galactose malabsorption from 2001 to 2019. *J Paediatr Child Health*. (2020) 56(11):1779–84. doi: 10.1111/jpc.14702
- Alruwaili NW, Alshdayed F. Fructose metabolism and its effect on glucose-galactose malabsorption patients: a literature review. *Diagnostics*. (2023) 13(2):294. doi: 10.3390/diagnostics13020294
- Ma M, Long Q, Chen F, Zhang T, Lu M, Wang W, et al. Nutrition management of congenital glucose-galactose malabsorption: case report of a Chinese infant. *Medicine*. (2019) 98(33):e16828. doi: 10.1097/MD.00000000000016828
- National Center for Biotechnology Information (US). Genes and disease. Bethesda (MD) (1998-). Glucose galactose malabsorption. Available online at: <https://www.ncbi.nlm.nih.gov/books/NBK22210/> (accessed July 28, 2023).
- Richards S, Aziz N, Bale S, Bick D, Das S, Gastier-Foster J, et al. Standards and guidelines for the interpretation of sequence variants: a joint consensus recommendation of the American College of Medical Genetics and Genomics and the Association for Molecular Pathology. *Genet Med*. (2015) 17(5):405–24. doi: 10.1038/gim.2015.30
- Medernach J, Middleton JP. Malabsorption syndromes and food intolerance. *Clin Perinatol*. (2022) 49(2):537–55. doi: 10.1016/j.clp.2022.02.015
- Canani Berni R, Pezzella V, Amoroso A, Cozzolino T, Di Scala C, Passariello A. Diagnosing and treating intolerance to carbohydrates in children. *Nutrients*. (2016) 8(3):157. doi: 10.3390/nu8030157
- Cakir M, Sag E, Guven B, Akbulut F, Issi B, Cebi AH, et al. Early onset congenital diarrheas; single center experience. *Pediatr Neonatol*. (2021) 62(6):612–9. doi: 10.1016/j.pedneo.2021.05.024
- Kamitori K, Shirota M, Fujiwara Y. Structural basis of the selective sugar transport in sodium-glucose cotransporters. *J Mol Biol*. (2022) 434(5):167464. doi: 10.1016/j.jmb.2022.167464
- Martín MG, Turk E, Lostao MP, Kerner C, Wright EM. Defects in Na⁺/glucose cotransporter (SGLT1) trafficking and function cause glucose-galactose malabsorption. *Nat Genet*. (1996) 12(2):216–20. doi: 10.1038/ng0296-216
- Barbosa-Gouveia S, Vázquez-Mosquera ME, González-Vioque E, Álvarez JV, Chans R, Laranjeira F, et al. Utility of gene panels for the diagnosis of inborn errors of metabolism in a metabolic reference center. *Genes*. (2021) 12(8):1262. doi: 10.3390/genes12081262
- Dugic A, Kryk M, Mellenthin C, Braig C, Catanese L, Petermann S, et al. Fructose-induced severe hypertriglyceridemia and diabetes mellitus: a cautionary tale. *Endocrinol Diabetes Metab Case Rep*. (2021):21–110. doi: 10.1530/EDM-21-0110

Conflict of interest

The authors declare that the research was conducted in the absence of any commercial or financial relationships that could be construed as a potential conflict of interest.

Publisher's note

All claims expressed in this article are solely those of the authors and do not necessarily represent those of their affiliated organizations, or those of the publisher, the editors and the reviewers. Any product that may be evaluated in this article, or claim that may be made by its manufacturer, is not guaranteed or endorsed by the publisher.

Supplementary material

The Supplementary Material for this article can be found online at: <https://www.frontiersin.org/articles/10.3389/fped.2024.1284671/full#supplementary-material>



OPEN ACCESS

EDITED BY

Ashutosh Pandey,
Baylor College of Medicine, United States

REVIEWED BY

Mónica Lopes-Marques,
University of Porto, Portugal
Miguel Angel Alcántara-Ortigoza,
National Institute of Pediatrics, Mexico

*CORRESPONDENCE

Ivan Martínez Duncker,
✉ duncker@uaem.mx
Gildardo Zafra de la Rosa,
✉ gzafradelarosa@gmail.com

RECEIVED 31 December 2023

ACCEPTED 08 April 2024

PUBLISHED 06 May 2024

CITATION

Martínez Duncker I, Mata-Salgado D,
Shammas I, Ranatunga W, Daniel EJP,
Cruz Muñoz ME, Abreu M, Mora-Montes H,
He M, Morava E and Zafra de la Rosa G (2024),
Case report: Novel genotype of ALG2-CDG and
confirmation of the heptasaccharide glycan
(NeuAc-Gal-GlcNAc-Man2-GlcNAc2) as a
specific diagnostic biomarker.
Front. Genet. 15:1363558.
doi: 10.3389/fgene.2024.1363558

COPYRIGHT

© 2024 Martínez Duncker, Mata-Salgado,
Shammas, Ranatunga, Daniel, Cruz Muñoz,
Abreu, Mora-Montes, He, Morava and Zafra de
la Rosa. This is an open-access article
distributed under the terms of the [Creative
Commons Attribution License \(CC BY\)](#). The use,
distribution or reproduction in other forums is
permitted, provided the original author(s) and
the copyright owner(s) are credited and that the
original publication in this journal is cited, in
accordance with accepted academic practice.
No use, distribution or reproduction is
permitted which does not comply with these
terms.

Case report: Novel genotype of ALG2-CDG and confirmation of the heptasaccharide glycan (NeuAc-Gal-GlcNAc-Man2-GlcNAc2) as a specific diagnostic biomarker

Ivan Martínez Duncker^{1*}, Denisse Mata-Salgado¹,
Ibrahim Shammas², Wasantha Ranatunga²,
Earnest James Paul Daniel³, Mario E. Cruz Muñoz⁴,
Melania Abreu⁵, Héctor Mora-Montes⁶, Miao He³, Eva Morava²
and Gildardo Zafra de la Rosa^{7*}

¹Laboratorio de Glicobiología Humana y Diagnóstico Molecular, Centro de Investigación en Dinámica Celular, Instituto de Investigación en Ciencias Básicas y Aplicadas, Universidad Autónoma del Estado de Morelos, Cuernavaca, Mexico, ²Department of Clinical Genomics, Department of Laboratory Medicine and Pathology, Mayo Clinic, Rochester, MN, United States, ³Palmieri Metabolic Disease Laboratory, Children's Hospital of Philadelphia, Philadelphia, PA, United States, ⁴Laboratorio de Inmunología Molecular, Facultad de Medicina, Universidad Autónoma del Estado de Morelos, Cuernavaca, Mexico, ⁵Genos Médica, Ciudad de México, Mexico, ⁶Departamento de Biología, División de Ciencias Naturales y Exactas, Campus Guanajuato, Universidad de Guanajuato, Guanajuato, Mexico, ⁷Genetics Service, Cancer Center Tec100, Querétaro, Mexico

This report outlines the case of a child affected by a type of congenital disorder of glycosylation (CDG) known as ALG2-CDG (OMIM 607906), presenting as a congenital myasthenic syndrome (CMS) caused by variants identified in ALG2, which encodes an α 1,3-mannosyltransferase (EC 2.4.1.132) involved in the early steps of N-glycosylation. To date, fourteen cases of ALG2-CDG have been documented worldwide. From birth, the child experienced perinatal asphyxia, muscular weakness, feeding difficulties linked to an absence of the sucking reflex, congenital hip dislocation, and hypotonia. Over time, additional complications emerged, such as inspiratory stridor, gastroesophageal reflux, low intake, recurrent seizures, respiratory infections, an inability to maintain the head upright, and a global developmental delay. Whole genome sequencing (WGS) revealed the presence of two ALG2 variants in compound heterozygosity: a novel variant c.1055_1056delinsTGA p.(Ser352Leufs*3) and a variant of uncertain significance (VUS) c.964C>A p.(Pro322Thr). Additional studies, including determination of carbohydrate-deficient transferrin (CDT) revealed a mild type I CDG pattern and the presence of an abnormal transferrin glycoform containing a linear heptasaccharide consisting of one sialic acid, one galactose, one

N-acetyl-glucosamine, two mannoses and two N-acetylglucosamines (NeuAc-Gal-GlcNAc-Man2-GlcNAc2), ALG2-CDG diagnostic biomarker, confirming the pathogenicity of these variants.

KEYWORDS

CDG (congenital disorder of glycosylation), congenital myasthenic syndromes (CMS), ALG2, biomarker, glycan

1 Introduction

Congenital disorders of glycosylation (CDG) are an expanding group of hereditary metabolic disorders that represent genetic defects in the synthesis of glycans and their binding to proteins, lipids, and RNA (Chang et al., 2018; Ondruskova et al., 2021). Particularly, protein glycosylation is a process that can occur through *N*-linked glycosylation and/or *O*-linked glycosylation. Pathogenic variants in over 40 genes that participate in the *N*-glycosylation pathway clinically translate into multiple phenotypes, most of which include seizures, axial hypotonia, global developmental delay/intellectual disability, cerebellar atrophy, and delayed myelination (Cossins et al., 2013; Chang et al., 2018; Francisco et al., 2023). This highlights the crucial importance of *N*-glycosylated proteins for normal neuronal development and the establishment and maintenance of appropriate cognitive functions.

In addition to their neurological manifestations, *N*-glycosylation defects are also linked to neuromuscular disorders. Notable examples associated to congenital myasthenic syndromes (CMS) include pathogenic variants in *ALG2*, *ALG14*, *DPGAT1* and *GMPPB* (Belaya et al., 2015; Paprocka et al., 2021; Francisco et al., 2023). CMS are a heterogeneous group of hereditary disorders derived from alterations in signal transmission at the neuromuscular synapse, characterized by fatigable muscle weakness. ALG2-CDG (OMIM 607906), previously known as CDG-II, is an autosomal recessive rare disorder caused by pathogenic variants in *ALG2* (OMIM 607905) that encodes the α 1,3-mannosyltransferase (EC 2.4.1.132) involved in the second and third steps of mannose addition during the early steps of *N*-glycosylation. Currently, it is recognized that ALG2-CDG exhibits a broad clinical spectrum, characterized primarily by global developmental delay and predominant muscular weakness. To date, 14 cases have been reported, including three patients from Latin America (Thiel et al., 2003; Cossins et al., 2013; Monies et al., 2014; Monies et al., 2016; Papazoglu et al., 2021; Ehrstedt et al., 2022). In addition to neurological and neuromuscular manifestations, abnormal coagulation, hepatomegaly, colobomas, and hearing loss have been reported (Thiel et al., 2003; Cossins et al., 2013; Monies et al., 2014; Monies et al., 2016; Papazoglu et al., 2021; Ehrstedt et al., 2022). This case report addresses the clinical findings and molecular diagnosis of an infant of Mexican ancestry affected by ALG2-CDG, supported by biochemical and genetic tests that evidence the deleterious effect of the identified heterozygous variants.

2 Case report and methods

The proband is a 1-year-old male of Mexican ancestry, born to non-consanguineous parents with no relevant family history of genetic alterations. He is the only child in the family, born by

cesarean section at 40.1 weeks of gestation, with a birth weight of 2,995 kg (percentile 10-25), length of 48.5 cm (percentile 25-50), and head circumference of 35.4 cm (percentile 25-50). Apgar scores were 7 at 1 minute, improving to nine at 5 minutes, requiring 1 hour after birth of bag-mask resuscitation with two cycles and nasal prongs.

During the neonatal period, the child presented with inspiratory stridor, congenital hip dislocation, absence of crying, and drooling. Neurological evaluation revealed generalized hypotonia, proximal muscle weakness, decreased tendon reflexes, and the absence of both the Moro reflex and sucking reflex. Subsequently, additional symptoms emerged, including weak crying, both proximal and distal muscle weakness, gastroesophageal reflux, inability to maintain head control, recurrent infections, contractures in proximal joints, and feeding difficulties. Due to the latter, a gastrostomy was performed at 13 months, with continuous follow-up by the gastroenterology team.

Furthermore, at 1.5 months of age, the child experienced seizures characterized by absent gaze and brief cyanosis, which were partially controlled with valproic acid and levetiracetam.

In the current clinical assessment at 1 year and 7 months, the child weighs 8,350 g (percentile <3), has a head circumference of 44.8 cm (percentile <3), and a length of 79 cm (percentile <3 for expected height based on familial growth charts). Global developmental delay has been observed, accompanied by a poor response to painful stimuli, generalized muscle weakness, generalized hypotonia, depressed osteotendinous reflexes, laxity in distal joints, and seizures that are better controlled with valproic acid and lacosamide. It is important to note that these findings occur in the context of normal creatine kinase (CPK) levels.

Dysmorphic features include a prominent forehead, metopic prominence, fan-shaped eyebrows, long eyelashes, sunken eyes, nystagmus, wide nasal bridge, full cheeks, thick nasal tip, prominent upper lip, high palate, retrognathia, pointed ears with hypoplastic helix and prominent concha (Figure 1), as well as wide-set nipples, dorsal hypertrichosis, and a congenital dermal melanocytosis (mongolian spot) over the sacral region, and non-communicating sacral dimple. Additionally, there are transverse creases on the hands, abduction of the first finger on the left hand due to a restrictive fold, mildly marked flexion creases in the phalanges, pads on the fingertips, and a thicker first toe on the left foot compared to the right. Brain imaging studies only revealed a temporal arachnoid cyst (17 × 9 mm). Renal ultrasound showed normal kidneys. The complete blood cell count, serum chemistry and coagulation tests were normal.

Genetic testing was initiated obtaining buccal samples for Whole Genome Sequencing (WGS) test by Biomegen (Querétaro, México). Libraries were sequenced from both ends in an Illumina platform reaching a depth of ~30x. An internal bioinformatic process was applied that included alignment of the reading with the Human



FIGURE 1

Dysmorphic facial features. Dysmorphic features include a prominent forehead, metopic prominence, fan-shaped eyebrows, long eyelashes, sunken eyes, nystagmus, wide nasal bridge, full cheeks, thick nasal tip, prominent upper lip, retrognathia, pointed ears with hypoplastic helix and prominent concha.

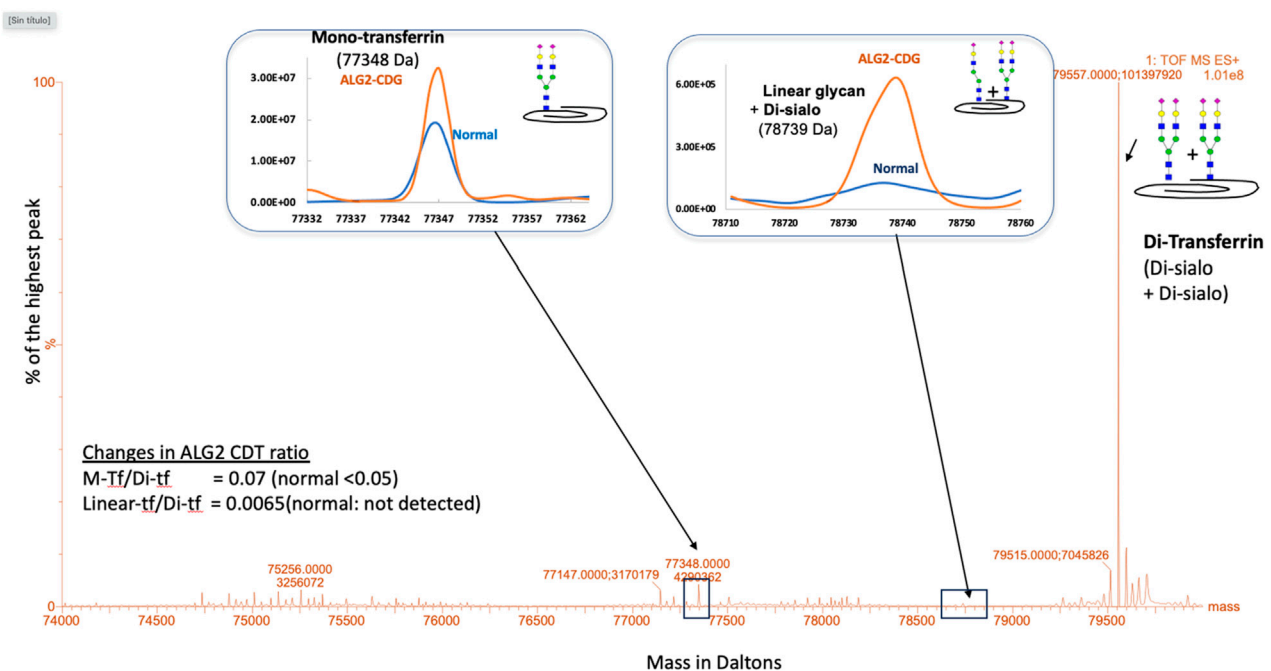









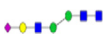


FIGURE 2

ESI-MS analysis of plasma transferrin isoforms. A type 1 CDG profile was identified with increased ratio of mono-transferrin (M-tf) to di-transferrin (Di-tf). Also, a transferrin isoform bearing a linear heptasaccharide glycan (NeuAc-Gal-GlcNAc-Man2-GlcNAc2; linear-tf) was identified.

genome assembly GRCh37/hg19 and the Revised Cambridge Reference Sequence of the Human Mitochondrial DNA (NC_012920), variant call, annotation and exhaustive filtration of variants. The DRAGEN Copy Number Variant pipeline from Illumina was applied. All variants with an allelic frequency lower to 1% in the gnomAD database as well as the disease-causing

variants annotated in HGMD and ClinVar were evaluated. Two variants in compound heterozygosity were identified in *ALG2*: NM_033087.4: c.1055_1056delinsTGA p.(Ser352Leufs*3) and NM_033087.4: c.964C>A p.(Pro322Thr). Parental testing revealed that the father carried the variant c.964C>A p.(Pro322Thr), while the mother carried the c.1055_1056delinsTGA p.(Ser352Leufs*3)

TABLE 1 N-glycan changes in child's plasma. * Predicted structure and component are shown. Simplified structure of each N-glycan is shown as pictures: lavender diamond represents sialic acid (Neu5Ac), yellow circle represents galactose (gal), green circle represents mannose (Man), red triangle represents fucose (Fic) and dark blue square represents N-acetyl-glucosamine (GlcNAc). Table: N-glycan changes in ALG2-CDG patient.

Plasma N-glycans (%total)		Proband	Reference normal (n = 60)	
*Predicted structure	Predicted glycan components		LOW	HIGH
	Man ₂ GlcNAc ₂	0.18	0.03	0.24
	Neu5Ac ₁ Gal ₁ Man ₂ GlcNAc ₃ (Linear glycan)	1.80	0.06	1.48
	Fuc ₁ Neu5Ac ₁ Gal ₁ Man ₂ GlcNAc ₃ (Linear glycan - fuc)	0.22	0.00	0.21
	Neu5Ac ₂ Gal ₂ Man ₃ GlcNAc ₄ (Disialo glycan)	49.68	25.55	55.21
Transferrin N-glycan (%total)		Proband	Reference normal (n = 60)	
			LOW	HIGH
	Neu5Ac ₁ Gal ₁ Man ₂ GlcNAc ₃ (Linear glycan)	1.26	0.58	1.17
	Fuc ₁ Neu5Ac ₁ Gal ₁ Man ₂ GlcNAc ₃ (Linear glycan - fuc)	0.10	0.00	0.10
	Neu5Ac ₂ Gal ₂ Man ₃ GlcNAc ₄ (Disialo glycan)	78.76	61.04	79.42
Tf and IgG depleted plasma fraction N-glycan (%total)		Proband	Reference normal (n = 60)	
			LOW	HIGH
	Neu5Ac ₁ Gal ₁ Man ₂ GlcNAc ₃ (Linear glycan)	1.79	0.53	1.00
	Fuc ₁ Neu5Ac ₁ Gal ₁ Man ₂ GlcNAc ₃ (Linear glycan - fuc)	0.17	0.00	0.12
	Neu5Ac ₂ Gal ₂ Man ₃ GlcNAc ₄ (Disialo glycan)	56.68	39.9	60.7

Bold values represents the abnormal values.
Italic values represents the percentage (%).

variant. To date, there have been no reports of the occurrence of these variants in individuals affected by ALG2-CDG. Variant classification followed the guidelines of the American College of Medical Genetics (Richards et al., 2015).

The variant c.964C>A p.(Pro322Thr) is classified as a VUS (ClinVar 2155640; dbSNP rs1228242180), where proline, which is neutral and non-polar, is substituted by threonine, which is neutral and polar. Algorithms such as SIFT, PolyPhen-2, and Align-GVGD suggest that this variant is likely deleterious (Ng and Henikoff, 2003; Mathe et al., 2006; Tavtigian et al., 2006; Adzhubei et al., 2013). Additionally, STRUM was employed to investigate a potential alteration in protein stability induced by the amino acid substitution, measuring the differences in Gibbs free energy (ddG) between wild-type and mutated proteins (Quan et al., 2016). This analysis revealed a ddG of −0.5, suggesting a decrease in protein stability. Simultaneously, the predictive method SAAFEC-SEQ, supported by a decision tree machine learning algorithm, was employed (Li et al., 2021). This method utilizes physicochemical properties, sequence characteristics, and evolutionary information. A ddG of −1.07 was obtained, indicating a destabilizing effect predicted by this approach (Li et al., 2021). Interestingly,

according to gnomAD exomes and genomes database (Chen et al., 2022) the variant is restricted to admixed American genetic ancestry group with a frequency of 0.00004572 or two in 43740 (gnomAD Exomes Version 4.0 as of December 2023). Interestingly, these alleles were found in one male and one female, indicating a heterozygous state.

As for the novel variant c.1055_1056delinsTGA p.(Ser352Leufs*3), it results in a premature stop codon, predicting truncation of the protein in the glycosyltransferase family one domain. The variant has the potential to impact protein function by altering the last 65 amino acids in the protein sequence. The variant is absent from gnomAD exomes and genomes database (gnomAD Exomes Version 4.0 as of December 2023). It is noteworthy that another variant p.(Ser352Tyrfs*2) is found in the same position resulting in the similar premature truncation of the protein. Interestingly, all 75 carriers of this allele are also heterozygous (dbSNP rs757837485).

The carbohydrate-deficient transferrin (CDT) analysis is the primary biochemical test available for CDG diagnosis and was performed using accurate mass analysis of affinity purified transferrin protein using a LC-ESI-TOF MS system (Li et al.,

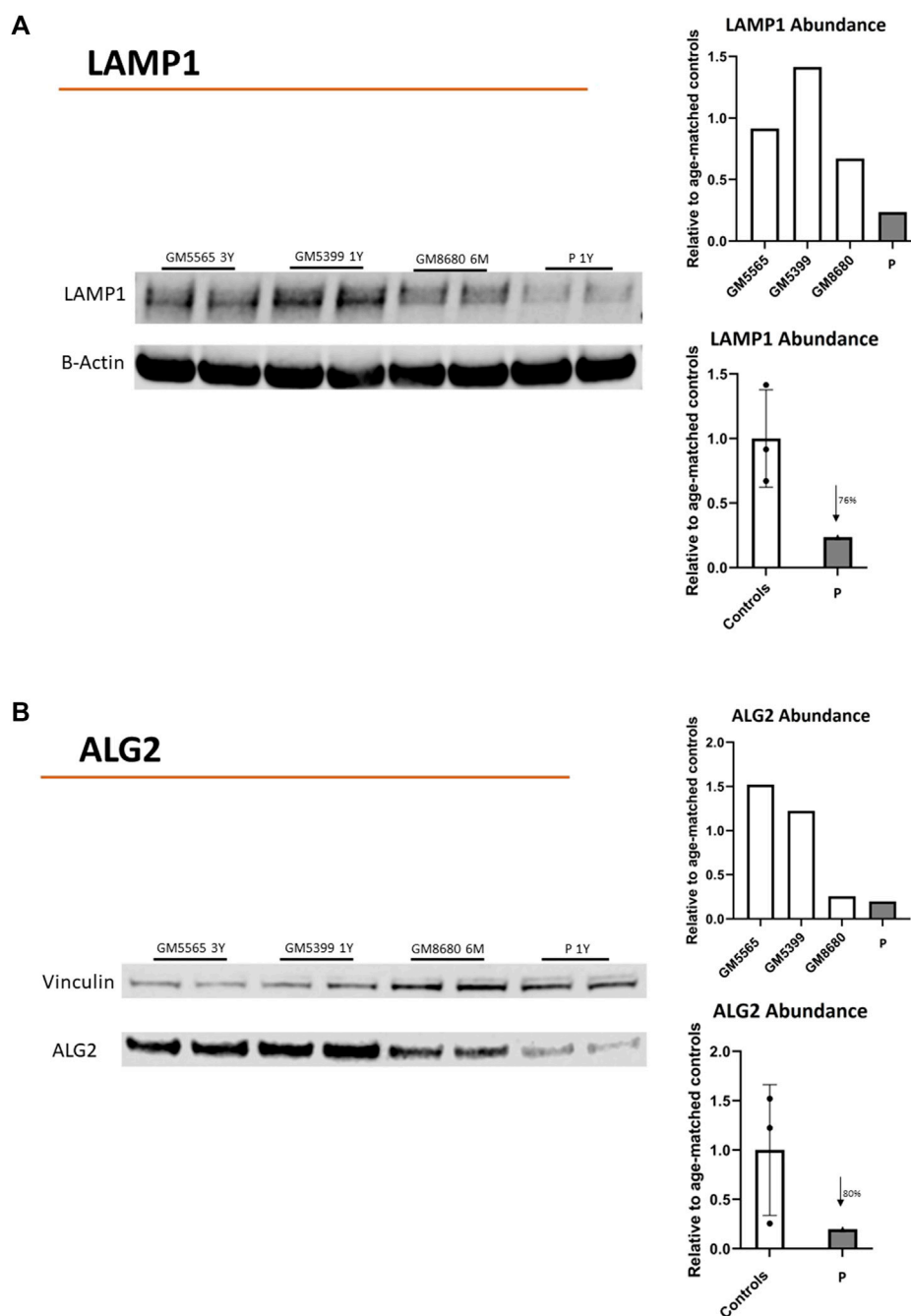


FIGURE 3

Protein abundance of LAMP1 and ALG2. Immunoblots showing LAMP-1 (A) or ALG2 (B) protein abundance in child's fibroblasts (P). Healthy Controls (GM5565, 3-year-old; GM5399, 1 year-old; GM8680 6 months-old). Beta-Actin or vinculin were used as a loading control. LAMP-1, ALG2, B-ACTIN or VINCULIN bands in the blots were quantified using Li-Cor Odyssey Image Studio (version 3.1). The quantified values for LAMP1 or ALG2 were expressed relative to quantified value of BACT or VINCULIN, respectively. The average value (relative to BACT or VINCULIN) of all controls (in duplicate) were used to express the fold change of expression for child's values (in duplicate). LAMP1: reduced 76% vs. control average. ALG2: reduced 80% vs. control average.

2015). A mild type 1 CDG pattern was identified with an increased mono-oligosaccharide/di-oligosaccharide ratio. Also, an abnormal transferrin glycoform containing one linear complex heptasaccharide glycan (NeuAc-Gal-GlcNAc-Man2-GlcNAc2) and one normal disialo glycan was found. Interestingly, this unusual glycan has also been recently reported in Argentinian ALG2-CDG patients (Papazoglu et al., 2021) (Figure 2). To

determine its presence in other plasma glycoproteins, IgG and transferrin were removed from plasma and the remaining fraction tested, both the linear and fucosylated linear glycans were found to be increased (Table 1), suggesting this is likely a generalized glycosylation abnormality in ALG2-CDG.

Additionally, we evaluated the presence of ALG2 and LAMP1 in the child's fibroblasts. LAMP1 is a common marker of cellular

TABLE 2 Clinical features of ALG2-CDG patients^a.

Main symptoms	Reported cases	This report	Total	Ref.
ALG2-CDG	14/14	+	15/15	Thiel et al. (2003), Cossins et al. (2013), Monies et al. (2014), Monies et al. (2016), Papazoglu et al. (2021), Ehrstedt et al. (2022)
Intellectual disability/global developmental delay	10/14	+	11/15	Thiel et al. (2003), Cossins et al. (2013), Monies et al. (2014), Papazoglu et al. (2021), Ehrstedt et al. (2022)
Seizures	4/14	+	5/15	Thiel et al. (2003), Papazoglu et al. (2021)
Hypotonia	9/14	+	10/15	Thiel et al. (2003), Cossins et al. (2013), Monies et al. (2014), Papazoglu et al. (2021), Ehrstedt et al. (2022)
Brain structural alterations	4/14	+	5/15	Thiel et al. (2003), Papazoglu et al. (2021)
Microcephaly	3/14	+	4/15	Papazoglu et al. (2021)
Ocular symptoms (coloboma, strabismus, nystagmus and not specified)	2/14	+	3/15	Thiel et al. (2003), Papazoglu et al. (2021)
Predominantly proximal muscle weakness	10/14	+	11/15	Cossins et al. (2013), Monies et al. (2014), Monies et al. (2016), Ehrstedt et al. (2022)
Dystonia	1/14	-	1/15	Papazoglu et al. (2021)
Joint laxity	5/14	+	6/15	Cossins et al. (2013), Papazoglu et al. (2021)
Facial weakness	4/14	-	4/15	Cossins et al. (2013)
Hearing impairment	3/14	-	3/15	Papazoglu et al. (2021)
Gastrointestinal disorders (difficulty feeding, gastroesophageal reflux, diarrhea or hepatomegaly)	5/14	+	6/15	Thiel et al. (2003), Papazoglu et al. (2021), Ehrstedt et al. (2022)
Facial dysmorphism	2/14	+	3/15	Papazoglu et al. (2021)

^a+, present; -, absent.

glycosylation that has been previously shown to decrease in CDG fibroblasts (Ligezka et al., 2023). LAMP1 abundance was decreased by 76% compared to control cells (Figure 3A). The abundance of ALG2 was also reduced 80% compared to control cells (Figure 3B).

3 Discussion

This report provides a detailed analysis of the clinical and molecular characteristics of the first child of Mexican ancestry diagnosed with ALG2-CDG, an extremely rare autosomal recessive disorder, of which only 14 cases have been documented in the literature to date (Table 2). Consistent with previous cases, the child exhibits a congenital myasthenic syndrome manifesting with muscular weakness, perinatal asphyxia, and feeding-related complications stemming from suction issues. Additionally, the fatigue experienced during the feeding sessions led to inadequate nutrition. Neurological manifestations were also observed, including seizures, global developmental delay, hypotonia, and structural brain alterations in agreement with previous ALG2-CDG reports (Thiel et al., 2003; Cossins et al., 2013; Monies et al., 2014; Monies et al., 2016; Papazoglu et al., 2021; Ehrstedt et al., 2022). Also, no dystonia, facial weakness or hearing loss reported in some ALG2-CDG patients was identified in the child (Table 2).

Dysmorphic facial features were identified in the child, including a prominent forehead, metopic prominence, fan-shaped eyebrows, long eyelashes, sunken eyes, full cheeks, thick nasal tip, wide nasal bridge, prominent upper lip, high palate, retrognathia, pointed ears

with hypoplastic helix and prominent concha (Figure 1). It is important to note that, until now, facial dysmorphism has only been described in two previous cases, characterized by upward-slanting palpebral fissures, wide nasal bridge, and bilateral epicanthic folds (Papazoglu et al., 2021). Therefore, dysmorphic facial characteristics emerge as an additional distinctive feature of ALG2-CDG, emphasizing the importance of considering this phenotypic variability in future reports and studies on the disease.

Both the identified VUS c.964C>A p.(Pro322Thr) as well as the novel variant c.1055_1056 delinsTGA p.(Ser352Leufs*3) are predicted to be pathogenic through different bioinformatic tools. Additionally, the Pro322Thr variant has a low frequency in the population and is carried in a heterozygous state, also suggesting pathogenicity. In regard to the c.1055_1056 delinsTGA p.(Ser352Leufs*3) novel variant, it was absent from population databases and its characteristics support its classification as “likely pathogenic” according to ACMG standard and guidelines, considering criteria PVS1 and PM2 (Richards et al., 2015).

The CDT and plasma N-glycan analysis revealed the presence of a linear heptasaccharide glycan (NeuAc-Gal-GlcNAc-Man2-GlcNAc2) recently reported in Argentinian ALG2-CDG patients, further confirming the diagnosis and the relevance of this biomarker as specific for ALG2-CDG. This linear heptasaccharide would result because of impaired ALG2 function causing a deficiency in the branching of the biantennary N-glycan during lipid-linked oligosaccharide synthesis, with only one branch being fully synthesized. The transference of truncated glycans from the lipid-linked oligosaccharide to nascent N-glycoproteins during the first

stage of *N*-glycan synthesis has been identified in other CDGs. For example, a tetrasaccharide biomarker has been identified for the diagnosis of ALG1-CDG (Bengtson et al., 2016; Zhang et al., 2016; González-Domínguez et al., 2021).

Deficient glycosylation was further confirmed with a substantial decrease in the expression of LAMP1, a cellular marker associated with glycosylation (Figure 3). Also, the decreased abundance of ALG2 is consistent with the predicted instability of the mutated proteins establishing the connection between altered glycosylation, reduced ALG2 abundance, and the observed clinical phenotype.

The integration of clinical, biochemical, and genetic findings reinforces the association between the identified genetic variants in ALG2 and the specific clinical presentation of this ALG2-CDG case. In the future, detailed phenotypic reports of new cases and the identification of additional pathogenic mutations will contribute to defining the spectrum and progression of the disease more precisely. These contributions will not only enhance the understanding of the syndrome but also facilitate the recognition of genotype-phenotype correlations for the various characteristics of this disorder.

Data availability statement

The raw data supporting the conclusion of this article will be made available by the authors, without undue reservation.

Ethics statement

The studies involving humans were approved by the Comité de Ética en Investigación, Facultad de Medicina, Universidad Autónoma del Estado de Morelos. The studies were conducted in accordance with the local legislation and institutional requirements. Written informed consent for participation in this study was provided by the participants' legal guardians/next of kin. Written informed consent was obtained from the minor(s)' legal guardian/next of kin for the publication of any potentially identifiable images or data included in this article.

Author contributions

IM: Conceptualization, Data curation, Formal Analysis, Funding acquisition, Investigation, Methodology, Project administration, Resources, Software, Supervision, Validation, Visualization, Writing–original draft, Writing–review and editing. DM-S: Data

curation, Investigation, Writing–original draft, Writing–review and editing, Software. IS: Investigation, Methodology, Writing–original draft, Writing–review and editing. WR: Investigation, Writing–original draft, Writing–review and editing, Methodology. EP: Investigation, Methodology, Writing–original draft, Writing–review and editing. MC: Writing–original draft, Writing–review and editing. MA: Investigation, Writing–original draft, Writing–review and editing. HM-M: Investigation, Writing–original draft, Writing–review and editing, Data curation. MH: Methodology, Validation, Writing–original draft, Writing–review and editing, Data curation, Funding acquisition. EM: Investigation, Supervision, Validation, Writing–original draft, Writing–review and editing, Funding acquisition. GZ: Conceptualization, Data curation, Investigation, Methodology, Supervision, Validation, Writing–original draft, Writing–review and editing.

Funding

The author(s) declare financial support was received for the research, authorship, and/or publication of this article. This work was partially funded by the grant titled Frontiers in Congenital Disorders of Glycosylation (1U54NS115198) from the National Institute of Neurological Diseases and Stroke (NINDS) and the National Center for Advancing Translational Sciences (NCATS), and the Rare Disorders Clinical Research Network (RDCRN), at the National Institute of Health (EM, WR, IS and MH). IM was supported by grants 293399 Red Temática Glicociencia en Salud–CONAHCYT. DM-S is recipient of a scholarship from CONAHCYT.

Conflict of interest

The authors declare that the research was conducted in the absence of any commercial or financial relationships that could be construed as a potential conflict of interest.

Publisher's note

All claims expressed in this article are solely those of the authors and do not necessarily represent those of their affiliated organizations, or those of the publisher, the editors and the reviewers. Any product that may be evaluated in this article, or claim that may be made by its manufacturer, is not guaranteed or endorsed by the publisher.

References

- Adzhubei, I., Jordan, D. M., and Sunyaev, S. R. (2013). Predicting functional effect of human missense mutations using PolyPhen-2. *Curr. Protoc. Hum. Genet. SUPPL.* 76 Chapter 7, Unit7.20. doi:10.1002/0471142905.hg0720s76
- Belaya, K., Rodríguez Cruz, P. M., Liu, W. W., Maxwell, S., McGowan, S., Farrugia, M. E., et al. (2015). Mutations in GMPPB cause congenital myasthenic syndrome and bridge myasthenic disorders with dystroglycanopathies. *Brain* 138 (9), 2493–2504. doi:10.1093/brain/awv185
- Bengtson, P., Ng, B. G., Jaeken, J., Matthijs, G., Freeze, H. H., and Eklund, E. A. (2016). Serum transferrin carrying the xeno-tetrasaccharide NeuAc-Gal-GlcNAc2 is a biomarker of ALG1-CDG. *J. Inher. Metab. Dis.* 39 (1), 107–114. doi:10.1007/s10545-015-9884-y
- Chang, I. J., He, M., and Lam, C. T. (2018). Congenital disorders of glycosylation. *Ann. Transl. Med.* 6 (24), 477. doi:10.21037/atm.2018.10.45
- Chen, S., Francioli, L. C., Goodrich, J. K., Collins, R. L., Wang, Q., Alfoldi, J., et al. (2022). A genome-wide mutational constraint map quantified from variation in 76,156 human genomes. *bioRxiv*. doi:10.1101/2022.03.20.485034
- Cossins, J., Belaya, K., Hicks, D., Salih, M. A., Finlayson, S., Carboni, N., et al. (2013). Congenital myasthenic syndromes due to mutations in ALG2 and ALG14. *Brain* 136 (3), 944–956. doi:10.1093/brain/awt010
- Ehrstedt, C., Liu, W. W., Frykholm, C., Beeson, D., and Punga, A. R. (2022). Novel pathogenic ALG2 mutation causing congenital myasthenic syndrome: a case report. *Neuromuscul. Disord.* 32 (1), 80–83. doi:10.1016/j.nmd.2021.11.012
- Francisco, R., Brasil, S., Poejo, J., Jaeken, J., Pascoal, C., Videira, P. A., et al. (2023). Congenital disorders of glycosylation (CDG): state of the art in 2022. *Orphanet J. Rare Dis.* 18 (1), 329. doi:10.1186/s13023-023-02879-z

- González-Domínguez, C. A., Fiesco-Roa, M. O., Gómez-Carmona, S., Kleinert-Altamirano, A. P. I., He, M., Daniel, E. J. P., et al. (2021). ALG1-CDG caused by non-functional Alternative Splicing involving a novel pathogenic complex allele. *Front. Genet.* 12, 744884. doi:10.3389/fgene.2021.744884
- Li, G., Panday, S. K., and Alexov, E. (2021). Saafec-seq: a sequence-based method for predicting the effect of single point mutations on protein thermodynamic stability. *Int. J. Mol. Sci.* 22 (2), 606. doi:10.3390/ijms22020606
- Li, X., Raihan, M. A., Reynoso, F. J., and He, M. (2015). Glycosylation analysis for congenital disorders of glycosylation. *Curr. Protoc. Hum. Genet.* 2015, 1–17. doi:10.1002/0471142905.hg1718s86
- Ligezka, A. N., Budhraj, R., Nishiyama, Y., Fiesel, F. C., Preston, G., Edmondson, A., et al. (2023). Interplay of impaired cellular Bioenergetics and Autophagy in PMM2-CDG. *Genes* 14 (8), 1585. doi:10.3390/genes14081585
- Mathe, E., Olivier, M., Kato, S., Ishioka, C., Hainaut, P., and Tavtigian, S. V. (2006). Computational approaches for predicting the biological effect of p53 missense mutations: a comparison of three sequence analysis based methods. *Nucleic Acids Res.* 34 (5), 1317–1325. doi:10.1093/nar/gkj518
- Monies, D., Alhindi, H. N., Almuhaizea, M. A., Abouelhoda, M., Alazami, A. M., Goljan, E., et al. (2016). A first-line diagnostic assay for limb-girdle muscular dystrophy and other myopathies. *Hum. Genomics* 10 (1), 32. doi:10.1186/s40246-016-0089-8
- Monies, D. M., Al-Hindi, H. N., Al-Muhaizea, M. A., Jaroudi, D. J., Al-Younes, B., Naim, E. A., et al. (2014). Clinical and pathological heterogeneity of a congenital disorder of glycosylation manifesting as a myasthenic/myopathic syndrome. *Neuromuscul. Disord.* 24 (4), 353–359. doi:10.1016/j.nmd.2013.12.010
- Ng, P. C., and Henikoff, S. (2003). SIFT: predicting amino acid changes that affect protein function. *Nucleic Acids Res.* 31 (13), 3812–3814. doi:10.1093/nar/kgk509
- Ondruskova, N., Cechova, A., Hansikova, H., Honzik, T., and Jaeken, J. (2021). Congenital disorders of glycosylation: Still “hot” in 2020. *Biochimica Biophysica Acta - General Subj.* 1865 (Issue 1), 129751. doi:10.1016/j.bbagen.2020.129751
- Papazoglu, G. M., Cubilla, M., Pereyra, M., de Kremer, R. D., Pérez, B., Sturiale, L., et al. (2021). Mass spectrometry glycophenotype characterization of ALG2-CDG in Argentinean patients with a new genetic variant in homozygosis. *Glycoconj. J.* 38 (2), 191–200. doi:10.1007/s10719-021-09976-w
- Paprocka, J., Jezela-Stanek, A., Tylki-Szymańska, A., and Grunewald, S. (2021). Congenital disorders of glycosylation from a neurological perspective. *Brain Sci.* 11 (1), 88. doi:10.3390/brainsci11010088
- Quan, L., Lv, Q., and Zhang, Y. (2016). STRUM: structure-based prediction of protein stability changes upon single-point mutation. *Bioinformatics* 32 (19), 2936–2946. doi:10.1093/bioinformatics/btw361
- Richards, S., Aziz, N., Bale, S., Bick, D., Das, S., Gastier-Foster, J., et al. (2015). Standards and guidelines for the interpretation of sequence variants: a joint consensus recommendation of the American College of Medical genetics and Genomics and the association for molecular Pathology. *Genet. Med.* 17 (5), 405–424. doi:10.1038/gim.2015.30
- Tavtigian, S. V., Deffenbaugh, A. M., Yin, L., Judkins, T., Scholl, T., Samollow, P. B., et al. (2006). Comprehensive statistical study of 452 BRCA1 missense substitutions with classification of eight recurrent substitutions as neutral. *J. Med. Genet.* 43 (4), 295–305. doi:10.1136/jmg.2005.033878
- Thiel, C., Schwarz, M., Peng, J., Grzmil, M., Hasilik, M., Braulke, T., et al. (2003). A new type of congenital disorders of glycosylation (CDG-II) provides new insights into the early steps of dolichol-linked oligosaccharide biosynthesis. *J. Biol. Chem.* 278 (25), 22498–22505. doi:10.1074/jbc.M302850200
- Zhang, W., James, P. M., Ng, B. G., Li, X., Xia, B., Rong, J., et al. (2016). A novel N-tetrasaccharide in patients with congenital disorders of glycosylation, including asparagine-linked glycosylation protein 1, phosphomannomutase 2, and mannose phosphate isomerase deficiencies. *Clin. Chem.* 62 (1), 208–217. doi:10.1373/CLINCHEM.2015.243279

Frontiers in Genetics

Highlights genetic and genomic inquiry relating to all domains of life

The most cited genetics and heredity journal, which advances our understanding of genes from humans to plants and other model organisms. It highlights developments in the function and variability of the genome, and the use of genomic tools.

Discover the latest Research Topics

[See more →](#)

Frontiers

Avenue du Tribunal-Fédéral 34
1005 Lausanne, Switzerland
frontiersin.org

Contact us

+41 (0)21 510 17 00
frontiersin.org/about/contact

